FTD-MT-24-290-69

FOREIGN TECHNOLOGY DIVISION

ROCKET ENGINES

by

T. M. Mel'kumov, N. I. Melik-Pashayev,
P. G. Chistyakov and A. G. Shiukov

631

FTD-MT- 24-290-69

EDITED MACHINE TRANSLATION

ROCKET ENGINES

By: T. M. Mel'kumov, N. I. Melik-Pashayev,
P. G. Chistyakov and A. G. Shiukov

English pages: Cover to 620

SOURCE: Raketnyye Dvigateli. 1968, pp. 1-511.

This document is a Systran machine aided translation, post-edited for technical accuracy by:
Charles T. Ostertag and Francis T. Russell.

Insert: Chapters I-VI, pages 1-158, FTD-HT-23-1531-68.

PREPARED BY:

TRANSLATION DIVISION
FOREIGN TECHNOLOGY DIVISION
WP-AFB, OHIO.

TABLE OF CONTENTS

U. S. BOARD ON GEOGRAPHIC NAMES TRANSLITERATION SYSTEM

Block	Italic	Transliteration	Block	Italic	Transliteration
А а	*А а*	A, a	Р р	*Р р*	R, r
Б б	*Б б*	B, b	С с	*С с*	S, s
В в	*В в*	V, v	Т т	*Т т*	T, t
Г г	*Г г*	G, g	У у	*У у*	U, u
Д д	*Д д*	D, d	Ф ф	*Ф ф*	F, f
Е е	*Е е*	Ye, ye; E, e*	Х х	*Х х*	Kh, kh
Ж ж	*Ж ж*	Zh, zh	Ц ц	*Ц ц*	Ts, ts
З з	*З з*	Z, z	Ч ч	*Ч ч*	Ch, ch
И и	*И и*	I, i	Ш ш	*Ш ш*	Sh, sh
Й й	*Й й*	Y, y	Щ щ	*Щ щ*	Shch, shch
К к	*К к*	K, k	Ъ ъ	*Ъ ъ*	"
Л л	*Л л*	L, l	Ы ы	*Ы ы*	Y, y
М м	*М м*	M, m	Ь ь	*Ь ь*	'
Н н	*Н н*	N, n	Э э	*Э э*	E, e
О о	*О о*	O, o	Ю ю	*Ю ю*	Yu, yu
П п	*П п*	P, p	Я я	*Я я*	Ya, ya

* ye initially, after vowels, and after ъ, ь; e elsewhere. When written as ё in Russian, transliterate as yё or ё. The use of diacritical marks is preferred, but such marks may be omitted when expediency dictates.

BLANK PAGE

FOLLOWING ARE THE CORRESPONDING RUSSIAN AND ENGLISH

DESIGNATIONS OF THE TRIGONOMETRIC FUNCTIONS

Russian	English
sin	sin
cos	cos
tg	tan
ctg	cot
sec	sec
cosec	csc
sh	sinh
ch	cosh
th	tanh
cth	coth
sch	sech
csch	csch
arc sin	$\sin^{-1}$
arc cos	$\cos^{-1}$
arc tg	$\tan^{-1}$
arc ctg	$\cot^{-1}$
arc sec	$\sec^{-1}$
arc cosec	$\csc^{-1}$
arc sh	$\sinh^{-1}$
arc ch	$\cosh^{-1}$
arc th	$\tanh^{-1}$
arc cth	$\coth^{-1}$
arc sch	sech^{-1}
arc csch	csch^{-1}
rot	curl
lg	log

The book discusses fundamental problems in the theory and construction of liquid and solid rocket engines.

Problems pertaining to the strength of liquid rocket engines [LRE] (ЖРД) and solid rocket engines [SRE] (РДТТ) are discussed; guidance and automatic control systems of rocket engines [RE] (РД) are analyzed, and types of process instability appearing in rocket engines are considered. Material published in the foreign and Soviet literature is used as a basis for information given on RE designs, fuels, cooling systems, turbupump units, gas generators, and applications of nuclear energy in rocket engines.

The book is designed for engineers working in the aviation industry and students and graduate students attending higher aviation educational institutions.

The book contains 30 tables, 307 illustrations, and 61 bibliographic references.

PREFACE

In recent years, there have been many Soviet books and texts dealing with individual rocket-engine [RE](РД) problems: combustion processes and characteristics of liquid and solid rocket engines, design fundamentals, dynamics, and stability of RE processes. There are no books, however, that consider rocket engines in all their complexity; the sole exception is the book by D. Satton [44] published in 1952; it is outdated, however, and, what is more, each problem is discussed in extremely condensed form.

Despite the apparent simplicity of rocket-engine arrangements, the design of reliable and economical RE requires a thoroughgoing understanding of the essence of the complicated processes taking place and solution of a large set of laborious problems.

The present authors' aim was to give, within a single volume, the basic data on processes and characteristics for liquid and solid rocket engines, their construction, control fundamentals, and the application of nuclear energy in RE. The choice of material and the nature of the presentation was based on the interests of a broad group of readers. The book ought to be useful not just to engineers, but to students in higher technical educational institutions as well.

The book consists of two parts. The first part presents the theory of liquid rocket engines[LRE] (ЖРД) and solid rocket engines [SRE](РДТТ); the second discusses their construction and mechanical-strength calculations for individual RE components, together with basic data on guidance and automatic control systems for LRE and SRE.

The first two chapters give the basic arrangements, parameters, and characteristics of RE, and discuss the efficiency of rocket engines; the third chapter describes the characteristics of various liquid fuels and their components. Next consideration is given to processes occurring in the combustion chambers of LRE and SRE, problems of liquid-fuel mixing and atomization, organization of solid-fuel combustion, and the influence of various factors on RE operating stability.

Chapters 7, 8 and 9 deal with features of processes in nozzles, thermodynamic calculations for combustion and combustion-product flow, and RE characteristics as a function of the pressure in the combustion chamber and of altitude. Chapter 10 discusses heat exchange in LRE, the characteristics of combustion-product heat transfer to combustion-chamber walls, and various methods of cooling the chamber. A special chapter is devoted to the application of nuclear energy in RE. It briefly discusses the fundamentals of nuclear-reac-

tor theory, shows arrangements of possible nuclear RE, and compares rockets using chemical and nuclear energy.

The discussion of LRE chapter-component construction in Chapters 12 and 13 also covers mechanical-strength design methods with allowance for vibration loads. Chapter 14 deals with construction and mechanical-strength design of turbopump units.

The final chapters give detailed consideration to various fuel-supply systems and problems of automatic control of LRE; control systems are analyzed, their accuracy computed, and a method given for selecting controller dynamic parameters.

The book concludes with a description of SRE chamber elements, mechanical-strength calculations, and a presentation of methods for adjusting and controlling SRE.

Chapters 1, 2, 5, 6 and 11 were written by T.M. Mel'kumov; Chapters 3, 4, 7-10 by N.I. Melik-Pashayev; Chapters 12-15 and 18 by A.G. Shiukov; and Chapters 16 and 17 by P.G. Chistyakov.

The authors wish to thank the reviewer, Doctor of Technical Sciences G.B. Sinyarev, for much valuable advice.

Part 1

THEORY OF ROCKET ENGINES

Chapter 1

BASIC ROCKET-ENGINE DESIGNS AND PARAMETERS

1.1. DEFINITION AND OPERATING PRINCIPLES OF ROCKET ENGINES

By a rocket engine we mean a heat engine that transforms the energy of the working materials carried onboard the moving vehicle into the kinetic energy of the spent masses, thus producing thrust to move the vehicle in space. Consequently, for an engine to be called a rocket engine, it must satisfy two conditions: first, all working substances needed to realize the engine process, over the entire time of operation between launch and final cutoff, must be stored onboard the vehicle; second, the motor must directly create thrust to move the vehicle.

The second condition is satisfied in turbojet engines [TJE] (ТРД) and in elementary (no-compressor) air-breathing jet engines [EABJE](ПВРД). The first condition is not satisfied by TJE and EABJE, however, since these engines require air to realize their process, air taken from the atmosphere surrounding the earth; thus the engines, although of reaction type, are not rocket engines.

The above definition of a rocket engine is not associated with engine function or the type of vehicle in which the engine is installed.

The primary energy source in rocket engines may be the chemical energy of fuel, nuclear energy from fission of heavy atoms or fusion of light atoms or, finally, solar energy.

In the ensuing discussion, we shall be concerned only with motors using chemical energy. Nuclear-energy applications are discussed in Chapter 11.

Either liquid or solid materials may be used as the source of chemical energy. In rocket engineering, the combination of all materials required for the combustion process and introduced into the engine chamber, or placed within this chamber in advance, is called the fuel.

Solid-fueled reaction engines are sometimes referred to as powder-fuel engines, although the modern solid rocket fuel differs in composition and properties from ordinary powders. We shall henceforth use the more general term: solid rocket engine [SRE](РДТТ).

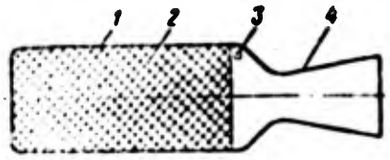

Fig. 1.1. End-burning SRE. 1) Chapter; 2) fuel charge; 3) igniter; 4) nozzle.

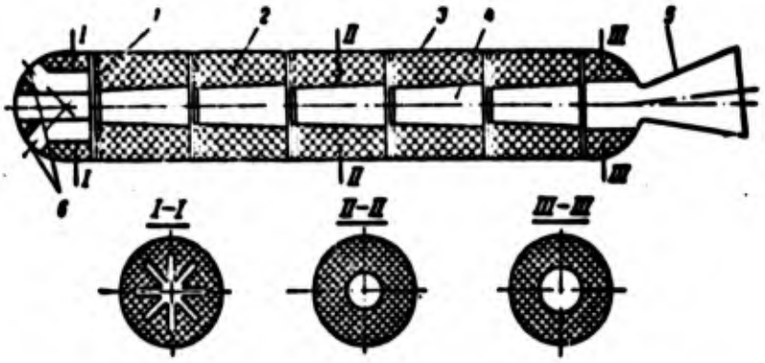

Fig. 1.2. Internal-burning SRE. 1) Partition; 2) fuel charge; 3) case; 4) internal channel; 5) nozzle; 6) motor-cutoff and thrust-reversal elements.

In solid-fuel engines, the entire charge is accommodated within a cylindrical chamber where gas generation and combustion takes place. Gas generation occurs at a preformed surface. The fuel burns gradually, layer by layer, along the normal to the combustion surface. Figure 1.1 shows an elementary SRE.

Here the fuel charge 2 takes the form of a solid cylinder inserted within chamber 1. The chamber is connected to the exhaust nozzle 4, which is a Laval nozzle. The entire surface of the fuel charge, except for the end facing the nozzle, has a special anti-ignition coating or else lies tightly (with no gap) against the chamber walls. The chamber has an igniter 3 whose function is to liberate a sufficient amount of heat within a short time period so as to set up a stable combustion process in the main fuel charge with the motor and fuel cold. Since all fuel-charge surfaces other than the end facing the nozzle are specially inhibited or restricted by the chamber walls, combustion takes place at the free end surface. As a result, gases with a specific temperature and pressure are generated in the chamber; all other conditions being equal, the pressure is influenced by the nozzle throat area. At the nozzle exit, the gases leaving the engine have a velocity w_s whose magnitude depends on the pressure drop in the chamber and at the nozzle exit, on the gas temperature and composition, and on the nozzle losses.

Solid rocket engines are simple in construction and require no mechanisms or auxiliary machinery. The high gas pressures and temperatures, and the lack of external chamber and nozzle cooling

raise several difficult problems in the design of large SRE, particularly when attempts are made to increase the burn duration.

Figure 1.2 shows a large SRE in which the fuel charge is cast directly in the case; when the fuel solidifies, it forms a tight strong bond with the case walls. Here the combustion surface is located at the center of the charge along the engine axis; its cross section is in part round and in part star-shaped. The end surface facing the nozzle is restricted, so that combustion takes place along the internal fuel surface over the entire charge length along the normal to the cross-section surface elements. This way of manufacturing SRE and this initial combustion-surface shape make it possible to obtain high absolute thrusts, as well as the required burn duration and thrust time variation.

Major successes have now been scored in designing large SRE with special fuels. They have case diameters of 3-4 m, and develop thrusts in excess of 1000 tf for more than 100 s.

The solid rocket engine has a long military history; the first published mention of military application of rockets goes back to the middle of the 9th century.

The notion of using a solid rocket engine to power a guided flying craft originated with the Russian revolutionary Nikolay Ivanovich Kibal'chich. In 1881, shortly before his execution, while in prison for an attempt on Alexander II, N.I. Kibal'chich set forth a description and diagram of a flying craft with solid rocket engine, in which the powder grains were replaced by new grains as they burned, thus providing continuous guided flight. This plan became known only after the great October revolution, when the police archives were investigated.

In 1928, the Stemmer airframe with rocket engine flew for the first time; the total flight distance was not great, amounting to 1500 m. Within the past ten years, significant successes have been scored in the manufacture of SRE and solid fueled rockets.

Rocket engines making use of liquid fuels are referred to as liquid rocket engines [LRE](ЖРД). As in SRE, the heat liberated by a chemical reaction of oxidation or a reaction involving decomposition of a single substance is converted into the kinetic energy of the combustion or decomposition products. In contrast to SRE, the liquids required for the process are carried in special tanks on board the vehicle. From the structural viewpoint, LRE are just as simple as SRE, and they have no mechanisms other than the pumps used to supply working fluids to the engine chamber and to drive the pumps themselves. In many cases, the engine installation does not even have pump units, but uses some gas under high pressure to force the working fluids out of the tank and into the engine chamber.

Many LRE use corrosive substances (nitric acid, for example), while the combustion products are at high temperatures; this makes it very difficult for the engine designer to ensure reliability and the required operating life. Basic difficulties also occur in arranging for an economical and stable operating process and in ensuring smooth transition, launch, and cutoff regimes.

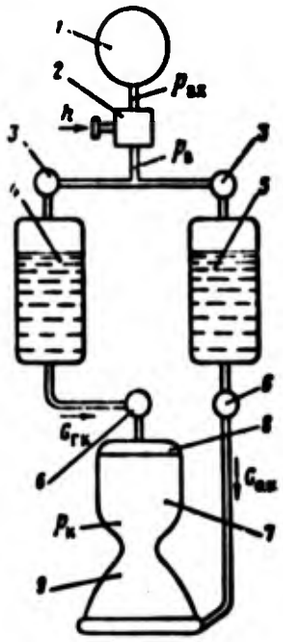

Fig. 1.3. Basic arrangement of LRE with pressure feeding of fuel components. 1) Cylinder with gas at high pressure; 2) gas pressure regulator; 3) shutoff valves; 4) combustible tank; 5) oxidizer tank; 6) main valves; 7) engine combustion chamber; 8) motor head; 9) Laval nozzle.

Owing to the high temperatures involved in the LRE process, it becomes important to arrange for adequate and economical cooling of all hot engine surfaces. The engine feed system, with all regulating and monitoring-protection devices and components must also meet several specific requirements, necessitating solution of numerous complex problems. Finally, the automation of the processes of launching, transition to operating regime, throttling, and cutoff on the basis of a prescribed control program is intimately associated with the nature of these processes in an LRE and with the particular application of the given engine.

Two initial substances, a combustible and an oxidizer, are most frequently required to realize these processes in a liquid rocket engine. Here the vehicle must carry separate tanks for the combustible and the oxidizer. The reaction between combustible and oxidizer is accompanied by release of heat and a significant rise in the temperature of the end products. Depending on the value of nozzle throat for the given per-second rate at which reaction products flow out of the engine, a specific pressure will be established in the combustion chamber; this will be considerably above the ambient pressure. The combustible and oxidizer are supplied to the engine chamber in a specific ratio of weights under a pressure somewhat exceeding the chamber pressure.

One liquid rocket engine arrangement is shown in Fig. 1.3. The engine itself consists of the chamber 7, heat 8, and Laval nozzle 9. Here the combustible from tank 4 and the oxidizer from

tank 5 are expelled by the compressed gas stored in cylinder 1, and are supplied directly to the engine, where they are atomized and mixed at the motor head in the required proportions. The combustion chamber can arbitrarily be divided into two zones: a preparation zone and a zone of reaction and parameter equalization, although there is no definite boundary between these zones in an actual chamber. The Laval nozzle forms a third zone, the zone of reaction-product expansion from the chamber pressure to the pressure at the nozzle exit; the velocity of the reaction products with respect to the engine will reach a certain value w_s at the nozzle exit.

The engine arrangement is complicated by various starting, operating, and monitoring devices and instruments; other systems may be used for combustible and oxidizer feed.

There is no fundamental change in the engine process if a single substance is introduced into the chamber rather than a combustible and an oxidizer, provided this single substance is capable of breaking down under certain conditions with liberation of heat and gaseous decomposition products. In either case, the exhaust velocity will depend on the heat released during the reaction between the combustible and oxidizer or on the heat released by the decomposition reaction for the material introduced into the engine, as well as on the properties of the gases forming in the reaction.

If the process is based on an oxidation reaction, the engine will operate at high temperatures, since high-temperature products are formed when a combustible is burned ($T > 2500°K$). If the process is based on a decomposition reaction, a low-temperature engine will usually be obtained, since for the materials employed in practice, the decomposition products form at relatively low temperatures. The overwhelming majority of modern LRE use the oxidation reaction.

With a high-temperature process, to ensure reliable engine operation, even for one-shot applications, it is necessary to cool the walls of the chamber, nozzle, and head by one or both fuel components. Small engines with a very short burn time (several seconds) are an exception.

As we have said, in the ensuing discussion we shall mean by the fuel the initial substances introduced into the chamber; by the working fluid we mean the fuel as well as the intermediate and end products of the reaction. The combustible and oxidizer are referred to as the fuel components. For an oxidation reaction, we have to do with a two-component working fluid although, in general, it might have three or more components. Conversely, we speak of a single-component, or unitary, liquid fuel if the engine makes use of the decomposition reaction or the reaction of decomposition and oxidation of combustible elements of a unitary field. For a fuel with two or more components, several processes take place in the preparation zone; atomization, evaporation, and mixing of the components as well as preignition oxidation and decomposition of the reagents; with a unitary fuel, atomization, evaporation, and partial decomposition take place in this zone.

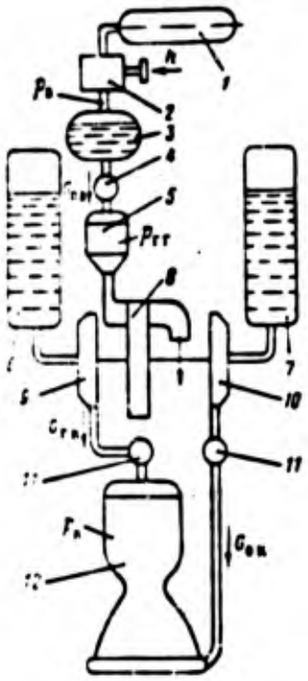

Fig. 1.4. Basic arrangement of LRE with monopropellant gas generator. 1) Cylinder with high-pressure gas; 2) gas pressure regulator; 3) tank with hydrogen peroxide; 4) hydrogen peroxide shutoff valve; 5) gas generator; 6) combustible tank; 7) oxidizer tank; 8) turbine of turbopump unit; 9) combustible pump; 10) oxidizer pump;11) main valves; 12) engine chamber.

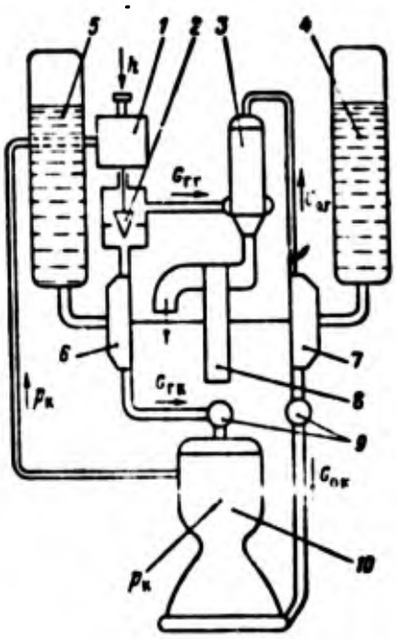

Fig. 1.5. Basic arrangement of LRE with bipropellant gas generator. 1) Thrust regulator; 2) final-control element of regulator 1; 3) bipropellant gas generator; 4) oxidizer tank; 5) combustible tank; 6) combustible pump;7) oxidizer pump; 8) turbine of turbopump unit [TPU](THA); 9) main valves; 10) motor chamber.

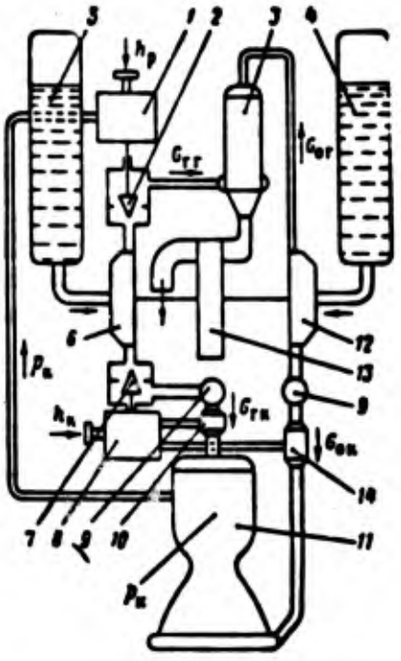

Fig. 1.6. Basic arrangement of LRE with control of thrust and of fuel-component ratio for engine. 1) Thrust regulator; 2) final-control element of regulator 1; 3) bipropellant gas generator; 4) oxidizer tank; 5) combustible tank; 6) combustible pump; 7) final-control element of regulator 8; 8) fuel-component ratio regulator; 9) control valve; 10) combustible flow-rate sensor; 11) engine chamber; 12) oxidizer pump; 13) TPU turbine; 14) oxidizer flow-rate sensor.

The products of the oxidation or decomposition reaction are directionally ejected at high speed from the chamber through nozzle 9 into the external environment; this generates the reactive force of engine thrust, which acts in the direction opposite to the velocity vector.

The LRE design of Fig. 1.3 is referred to as a forced-feed or, in the given case, cylinder-feed arrangement, since the fuel components are fed from the tank into the chamber by means of compressed gas supplied from cylinder 1 through pressure regulator 2. Various methods may be used to produce the high-pressure gas and to force the fuel components out of the tanks; some of them will be considered later.

The LRE with turbopump feed of fuel components is basically different (Fig. 1.4). In contrast to a forced-feed system, here the combustible and oxidizer tanks are under a low pressure that is not related to the pressure in the engine chamber. The turbine 8, operated by gas (or by a vapor-gas mixture) supplied by the special gas generator 5, develops adequate power to turn the combustible and oxidizer pumps 9 and 10 and to deliver the components to the engine chamber in the required amounts and under the required pressure. The gas following the turbine should be used in some way or another to produce additional engine thrust.

The turbopump-feed design of LRE is now widely employed in all powerplants except for low-thrust and short-burn engines. The turbopump unit (TPU) is a very important component of the powerplant.

Figure 1.5 shows an arrangement differing from that of Fig. 1.4 in that gas generator 3 receives the two principal components of the LRE fuel, so that the generator delivers gas having the parameters required by the turbine 8 of the TPU. The system of Fig. 1.6 makes it possible to regulate engine thrust and the ratio of the fuel component delivered to chamber 11. Figure 1.7 shows a system in which there is regulation not only of the engine thrust and the ratio of fuel components delivered to chamber 13, but also of the ratio of components delivered to gas generator 4. Figure 1.8 shows the basic arrangement of a "closed" system LRE, in which the gases leaving the TPU turbine are supplied to and used in the motor chamber.

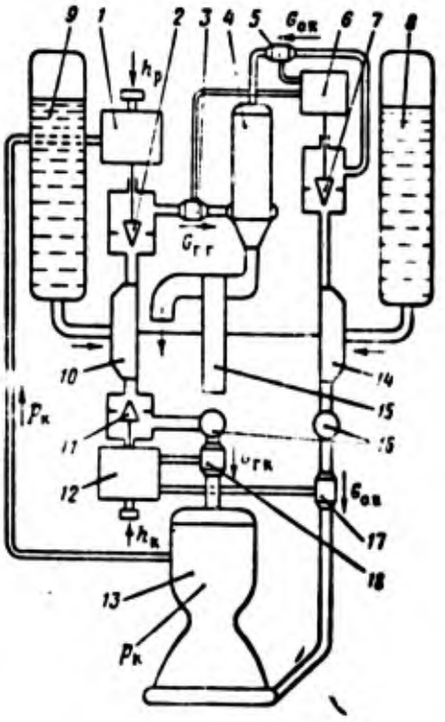

Fig. 1.7. Basic arrangement of LRE with control of thrust and fuel-component ratios for engine and gas generator. 1) Thrust regulator; 2) final-control element of regulator 1; 3) gas-generator combustible flowrate sensor; 4) bipropellant gas generator; 5) gas-generator oxidizer flowrate sensor; 6) fuel-component ratio regulator for gas generator; 7) final-control element of regulator 6; 8) oxidizer tank; 9) combustible tank; 10) combustible pump; 11) final-control element of regulator 12; 12) engine fuel-component ratio regulator; 13) motor chamber; 14) oxidizer pump; 15) TPU turbine; 16) main valve; 17) motor-chamber oxidizer flow-rate sensor; 18) motor-chamber combustible flowrate sensor.

Although the history of liquid rocket engine development has been very brief, it nonetheless has found wide practical application, particularly in rocket engineering, where its characteristics

are particularly suitable. It is precisely LRE that were used to launch the world's first(Soviet) artificial earth satellites, the lunar and interplanetary space vehicles, and the "Vostok"("East") and "Voskhod" ("Sunrise") manned vehicles.

The Soviet Union and many foreign countries have manufactured reliable and quite economical light-weight LRE using various working fluids, having thrusts ranging from low (fractions of a kgf) to very high (680-700 tf) values in a single chamber.

In Russia, utilization of the liquid rocket engine was pioneered by K.E. Tsiolkovskiy, who began theoretical studies in 1896 on utilization of rockets for spaceflights; in 1903, the journal "Scientific Survey" published his study "Investigation of Cosmic Spaces by Reaction Devices." Here K.E. Tsiolkovskiy gave diagrams of a rocket and an engine using liquid oxygen and liquid hydrogen. Without restricting his examination to this motor design, K.E. Tsiolkovskiy proposed several fuel components, one to be used to cool the motor; he indicated the desirability of using pumps to feed working fluids into the chamber, and in this initial and subsequent studies presented many other advanced engine concepts. Although his main field of interest involved interplanetary flight, K.E. Tsiolkovskiy clearly understood that it was the engine that was of fundamental significance.

The work of the Soviet engineer F.A. Tsander should also be noted. In his book "The Problem of Flight with the Aid of Reaction Craft" (1932), he considered liquid reaction engines and their working materials, including metals. The premature death of F.A. Tsander interrupted his investigation of rocket flight and his work on appropriate engines.

In the Soviet Union, M.K. Tikhonravov, S.P. Korolev, Yu.A. Pobedonostsev, L.S. Dushkin, and others carried out successful work on rocket and engine design before the Second World War. This resulted in the creation of experimental rockets and liquid rocket engines for aircraft and rocket craft. As we know, the first Soviet rocket designed by M.K. Tikhonravov, with an LRE, was successfully launched in 1933.

The first flight of the rocket craft designed by S.P. Korolev, with an LRE, took place in February 1940. In May of 1942, the aircraft designed by V.F. Bolkhovitinov, with liquid rocket engine, flew for the first time.

Rocket vehicles developed in the postwar period under the guidance of S.P. Korolev were used to launch Soviet artificial earth satellites, automatic interplanetary stations, lunar craft, and the "Vostok"and "Voskhod" manned spacecraft.

In Germany, Research was carried out by individuals (G. Obert, E. Zenger, V. Braun, etc.) and by organizations; the work culminated in 1942 with creation of the V-2 (A-4) missile. This missile was first used by the Germans against Great Britain in 1944. The missile had a range of 250-300 km with an initial weight of 13 tf and a warhead weighing 750 kgf. Maximum missile speed at the instant of engine

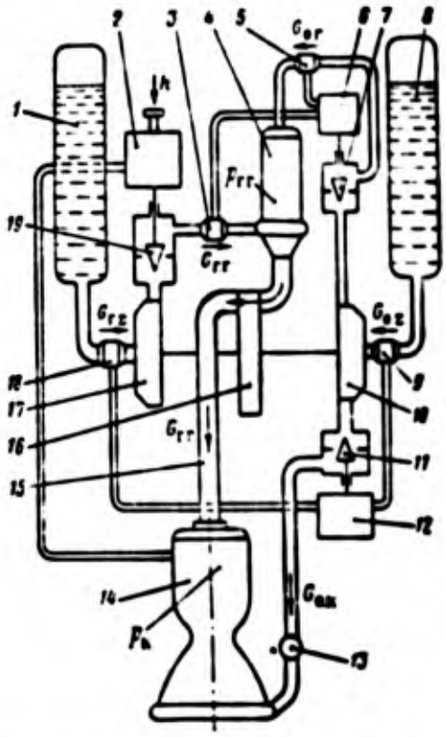

Fig. 1.8. Basic arrangement of closed-system LRE. 1) Combustible tank; 2) thrust regulator; 3) gas-generator combustible flowrate sensor; 4) gas generator; 5) gas-generator oxidizer flowrate sensor; 6) gas-generator component-ratio regulator; 7) final-control element for regulator 6; 8) oxidizer tank; 9) oxidizer total flowrate sensor; 10) oxidizer pump; 11) final-control element of regulator 12; 12) motor-chamber fuel-component ratio regulator; 13) oxidizer shutoff valve; 14) motor chamber; 15) line feeding generator gas to motor chamber; 16) TPU turbine; 17) combustible pump; 18) combustible total flowrate sensor; 19) final-control element of regulator 2.

cutoff reached 1540 m/s; the flight trajectory peaked at 82 km.

During the Second World War, LRE were used for aircraft, particularly the German Me-163; owing to process instability during throttling and defects in the starting and shutdown processes, engines and aircraft were destroyed. Research into these processes carried out in the USSR led to more reliable LRE and opened the door to investigation of terrestrial and cosmic space.

Theoretical and experimental research was carried out in other countries as well (for example, R. Goddard in the United States, R. Esno-Pel'tri [sic] in France, etc.). The USSR and the United States are now making rockets of all classes using liquid and solid rocket engines.

Rocket engines have two basic advantages: the internal process is independent of the presence or absence of an external medium (air, for example), i.e., they are independent, while it is possible

to create large thrust with a light-weight engine. These characteristics have determined the region of rocket-engine applicability: flying craft with high rates of climb, craft with high flight speeds and altitudes, and spacecraft. Such craft have enormous significance for peaceful scientific purposes and as powerful means of defense and attack. Thus following the Second World War, many countries devoted enormous effort to creating various types of rocket engines. Major successes in rocketry were scored by the USSR.

Rocket engines are used:

- for short-,medium-, and long-range (intercontinental or global) "surface to surface" missiles for delivery of atomic and hydrogen warheads or other destructive military devices to any point on the surface of the earth;

- for "air to air" and "air to surface" guided missiles launched from aircraft or other flying craft to destroy relatively small moving or fixed objects;

- for antiaircraft and antimissile missiles operating against aircraft and missiles to protect the nation and individual important targets against attack from the air or from space;

- for aerodynamic rockets (rocket gliders) designed to reach any point on the earth's surface at a speed approaching that of a ballistic missile, and for converting a rocket glider into a short-mission artificial satellite returning to earth (there still is no such rocket glider);

- for meteorological rockets used in deep atmospheric probes to study atmospheric properties; for high-altitude research rockets to study terrestrial magnetism, the ionosphere, the radiation belts around the earth, the solar corpuscular radiation, etc.;

- for space vehicles designed to launch artificial earth satellites and interplanetary space stations;

- on board medium- and long-ranged rockets, satellites, and interplanetary space stations as on-board units for correcting rocket courses, satellite orbits, and space-station motion;

- on board aircraft as takeoff boosters and for short-term increase in maximum flight speed or altitude;

- on board experimental aircraft to study the behavior of men and instruments under high accelerations, high speeds, and high altitude;

- for special moving surface devices.

As this list shows, rocket engines are already in wide and varied use for both peaceful and military purposes.

1.2. BASIC REQUIREMENTS FOR ROCKET ENGINES

To formulate the basic requirements for a rocket motor, we use the K.E. Tsiolkovskiy formula, derived for free rocket flight, neglecting the influence of the gravitational force and the resistance of the medium. Let:

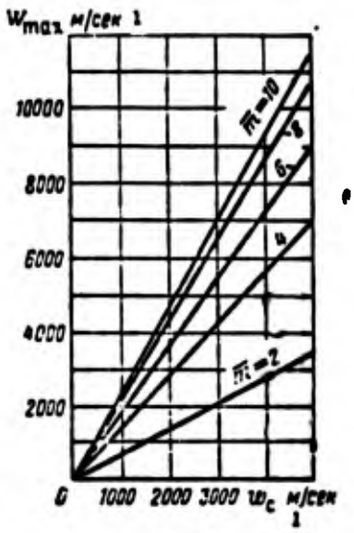

Fig. 1.9. Maximum speed of single-stage rocket as function of engine gas exit velocity and of rocket mass number. 1) m/s.

M_n and M_k are, respectively, the initial and final masses of a simple-stage rocket;

w_s is the time-invariant gas nozzle-exit velocity;

w_{max} is the rocket speed at the end of engine operation, when all of the fuel has been expended; the fuel mass is $M_t = M_n - M_k$.

Under these conditions, the rocket acceleration will be proportional to the thrust, while the latter, as will be shown later, is proportional to the exit velocity w_s and the fuel flowrate per unit time. On this basis, the Tsiolkovskiy formula yields the following relationship between the rocket speed w_{max} at the end of motor operation (at the end of boost or at the end of the active section of the rocket path) on the exit velocity and the initial and final rocket masses:

$$w_{max} = w_c \ln \frac{M_n}{M_k}. \qquad (1.1)$$

The ratio $M_n/M_k = \bar{m}$ is called the mass number; it depends on the rocket design and the quality with which it was manufactured.

The final mass (or weight) of the rocket includes the payload, for example, the pod with instruments and other components of the data recording and transmission system, the rocket body, the guidance units, and the engine plant. The higher the mass number m, the greater the maximum speed. Thus one problem in rocket design is to reduce the structural weight, including the weight of the motor and all associated systems.

It follows directly from Formula (1.1) that for a constant mass number the maximum rocket speed will be directly proportional to the gas exit velocity. The latter depends on the type of fuel and the quality of the process taking place in the chamber and the nozzle, as well as on the engine structural and thermodynamic parameters.

Formula (1.1) is valid, as has been shown, only if the rocket is traveling with no resistance of the medium and with no gravitational force acting. The problem can be made more complicated by including the influence of the earth's gravitational force and the atmospheric resistance; there is no need for this, however, since there would be no change in the formulation of the basic requirements for the engine. These reduce to two main requirements:

1. The engine gas exit velocity should be increased as much as possible.

2. The engine plant should have the least possible weight for a specified thrust, i.e., the minimum specific weight.

Figure 1.9 shows the change in maximum rocket velocity according to Formula (1.1) as a function of gas exit velocity for various values of the mass number. The maximum velocity can be used to attain maximum altitude in vertical flight of the rocket or to obtain maximum range. The effective maximum attainable height or maximum range of the rocket will be determined not only by w_s and $\bar{m}$, but also by the values selected for the accelerations (or the engine thrust) in the gravitational field and in the environmental resistance.

Under the actual conditions of rocket-engine utilization, manufacturing and storage defects may impair the engine process, and the design value of exit velocity may not be attained. It can also happen that flaws in the system supplying fuel to the LRE will leave some of the fuel unused in the tanks, with the motor having already been cut off; this increases the final rocket mass or decreases the mass number. Analogous conditions can arise in an SRE if the combustion process is halted before the fuel has been completely burned up. In an SRE, when the process has concluded, the residual fuel charge may also break down and leave the chamber without liberating chemical energy. This reduces the engine burn time, but has no influence on the gas exit velocity or the final rocket mass. In an LRE, one component may be fully expended while the other is underutilized; this occurs if the engine and engine system are not regulated so as to ensure the design proportional component consumption. In such case, the gas exit velocity will not equal the design value, and the final rocket mass will be greater owing to the mass of the component left in the tanks.

Let us consider the influence of fuel underutilization when

ω_s = const, and the influence of process imperfections or inaccurate maintenance of the component ratio in an LRE on the maximum rocket speed according to Formula (1.1).

Fig. 1.10. Influence of underutilization of fuel supply on maximum rocket speed. 1) Percent unused fuel.

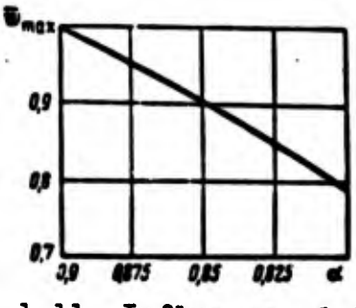

Fig. 1.11. Influence of inaccurate control of combustible flowrate on maximum speed.

Figure 1.10 shows the influence of fuel underutilization on maximum rocket speed for the case in which the mass number $\bar{m}$ = 5, i.e., when the fuel weight amounts to 80% of the initial rocket weight. As the graph shows, even a 2% underutilization of the entire fuel reserve will reduce the maximum rocket speed by almost 5% under these conditions.

If the actual engine process is imperfect, so that it differs from the design process, the gas exit velocity will be below the design value. When all fuel is fully utilized, a reduction in gas exit velocity, as Formula (1.1) implies, will lead to a proportional reduction in maximum rocket speed at the end of powered flight.

If inaccurate manufacture and regulation of the feed system causes the component ratio for the actual process to differ from the design ratio, there will be a change in the gas exit velocity, and the component remaining unexpended will increase the final rocket mass. Both these factors reduce the maximum rocket speed, but the increase in final mass owing to the unused component plays the decisive role.

Figure 1.11 shows the influence of inaccurate control of fuel-component flowrates to the LRE on maximum rocket speed when kerosene

and nitric acid are used as the fuel. The design regime corresponds to a mass number $\bar{m} = 5$ and a 10% excess of combustible above the stoichiometric ratio, i.e., $\alpha = 0.9$. It is clear from the graph that additional enrichment of the fuel with combustible amounting to 5% above the design ratio will reduce the maximum rocket speed by nearly 10%. Here the chief influence is exerted by the increase in final rocket mass, i.e., by the reduction in the mass number below the design value; the change in exit velocity is of secondary importance.

The above examples show that still another important operating requirement must be imposed on the rocket engine and engine system: the engine process must be maintained as close as possible to the design process for each specific object; to do this it is necessary to have stable fuel properties, precision manufacture of the engine and all its components and, in addition, for LRE exact regulation of the entire feed system, so as to ensure utilization of the design store of combustible and oxidizer in the required ratio.

1.3. ENGINE THRUST. SPECIFIC PARAMETERS

Thrust. By the thrust force, or thrust, of an engine we mean the resultant of all forces acting on the engine, produced by the engine process and the pressure of the undisturbed medium. This resultant force is responsible for motion of the vehicle carrying the engine. In steady horizontal motion, engine thrust is balanced by the external drag forces. In unsteady motion, the engine thrust is also used to accelerate the vehicle and to overcome the gravitational force if the flight altitude is increased.

On the basis of the definition of thrust, we can compute its value for steady engine operation at a given altitude (Fig. 1.12) from the expression

$$P = \int_{F_{vn}} p\,dF\cos\alpha - \int_{F_{nar}} p_n\,dF\cos\alpha, \qquad (1.2)$$

where p is the variable gas pressure within the engine, acting normal to the surface element dF;

α is the angle between the normal to dF and the positive direction of the x axis (i.e., between vector pdF or $p_n dF$ and the direction in which the P vector acts);

F_{vn} is the inside surface of the engine;

F_{nar} is the outside surface of the engine;

p_n is the pressure on the external surfaces of the engine, which can be assumed to be constant.

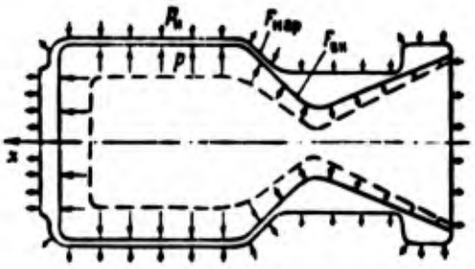

Fig. 1.12. Distribution of pressure forces on inside and outside surfaces of engine.

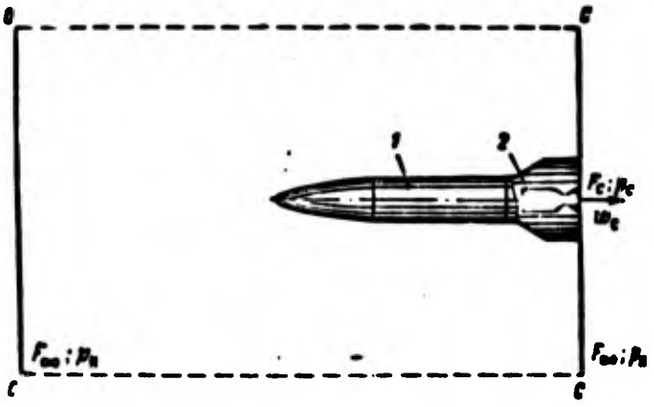

Fig. 1.13. Determining the thrust.

In solid rocket engines, F_{vn} is a variable in the general case, while in LRE, the surface F_{vn} = const.

Even for a very simple LRE, Formula (1.2) cannot be used to determine the thrust with the required accuracy. For an LRE, all cylindrical sections of the inside and outside surfaces parallel to the x axis should be eliminated from both terms on the right side of Expression (1.2); for example, only the base, the nozzle, and the transition surfaces should be considered. Determination of the thrust by this method is complicated and not accurate enough, since we must know the law governing the pressure variation along the entire nozzle. But this law will not always be known, particularly for the converging section of the nozzle, i.e., between the end of the chamber and the throat. It is still more complicated to use Formula (1.2) for an SRE, where the inside surface of the engine is a variable.

It is simpler and more convenient to calculate the engine thrust by using the impulse theorem (the momentum law). For a steady process, the impulse per unit time (1 s) is numerically equal to the thrust. In this case, the algebraic sum of the projections onto the given direction of all forces acting on the body equals the change in the momenta of the body in this direction during 1 s.

Let the vehicle 1 (Fig. 1.13) be moving at a certain constant altitude H with an absolute (i.e., relative to the earth) steady speed w_0 m/s. The engine 2 on board the vehicle has a nozzle exit area F_s cm^2; the gas pressure at the nozzle exit equals p_s kgf/cm^2; the velocity with respect to the engine is w_s m/s, while the absolute velocity is $w_a = w_s - w_0$.

We take two reference planes perpendicular to the direction of flight: plane OO far ahead of the vehicle, and plane CC at the nozzle exit. In practice, the area F_∞ of each of these planes, bounded by a certain cylindrical surface $\breve{O}C$, is infinitely greater than the area F_s. In this case, we have no interest in the external friction forces or any other forces resisting the motion of the vehicle, since in steady motion they will equal the thrust, as we have already mentioned. Thus we can assume that within the isolated volume the pressure p_n is the same everywhere except at the surface F_s.

The working fluid has an initial absolute velocity w_0 in the direction of flight, but leaving the engine it obtains a final absolute velocity w_a in the direction opposite to the flight direction. Consequently, in the earth-referenced coordinate system considered, an elementary change in momentum will equal

$$(w_a + w_0)\,dM = w_c\,dM;$$

here dM is the elementary mass quantity of gas leaving the engine within time $d\tau$. Within 1 s, the change in momentum will be

$$\int_{\tau=0}^{\tau=1} w_c\,dM = \frac{G_{\Sigma sek}}{g} w_c \qquad (1.3)$$

where $G_{\Sigma sek}$ is the per-second weight flowrate of working fluid, kgf/s;

g is the gravitational acceleration at the given altitude, m/s^2.

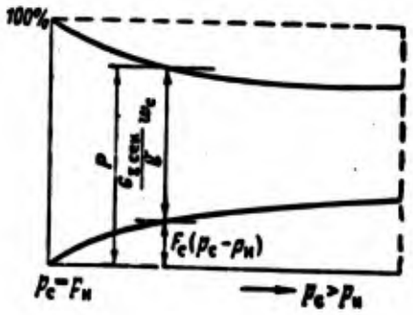

Fig. 1.14. Variation in thrust, momentum thrust, and pressure thrust with increase in pressure at nozzle exit.

The algebraic sum of all forces acting on the engine in the direction of flight will be

$$\int_{O} p_n dF - \int_{C} p\, dF + P;$$

(the + sign is used for forces represented by vectors pointing in the direction of flight).

Here the indices on the integration signs indicate that summation is carried out over the *OO* and *CC* planes; the forces acting on surface *OC* are omitted for obvious reasons. This expression can be rewritten as

$$p_n F_a - p_n (F_a - F_c) - p_c F_c + P$$

or

$$P - F_c (p_c - p_n). \qquad (1.4)$$

Equating Expression (1.3) and (1.4), we obtain an expression for the engine thrust force under steady-state conditions for a specified flight altitude,

$$P = \frac{G_{\Sigma sek}}{g} w_c + F_c (p_c - p_n). \qquad (1.5)$$

With the dimensions used above for the right side, the thrust force is expressed in kgf.

The first term on the right side of Expression (1.5), namely $(G_{\Sigma sek}/g)w_s$, is called the momentum thrust, while the second term $F_s(p_s - p_n)$ is called the pressure thrust.

If $p_s = p_n$, i.e., if in the nozzle there is complete expansion (to the design value for the nozzle) of the gases from the chamber pressure p_k^* to the pressure p_n of the environment, then the pressure thrust is

$$F_c (p_c - p_n) = 0$$

and the thrust is

$$P = \frac{G_{\Sigma sek}}{g} w_c. \qquad (1.6)$$

For different nozzles, providing different gas expansion ratios, for the same per-second flowrate, from a certain constant chamber pressure p_k^* to a variable pressure $p_s \geq p_n$ at the nozzle exit, the ratio of the values of the first and second terms on the right side of Expression (1.5) will vary. The momentum thrust reaches a maximum at $p_s = p_n$, while the pressure thrust is numerically equal to zero. When $p_s > p_n$ and p_s increases, the momentum thrust decreases while, conversely, the pressure thrust increases; the thrust force

as a whole diminishes, however (Fig. 1.14). From this it follows that proper nozzle design, allowing for all vehicle flight regimes and trajectories for the powered segment, i.e., for the segment over which the engine operates, is of great importance.

A rocket engine is capable of developing high thrust. The thrust value depends on the per-second flowrate of gas and the velocity at which the gas leaves the nozzle. In certain countries, liquid rocket engines with per-chamber thrusts of 450-680 tf are in series production, while thrusts of 1000 tf or more are obtained from solid rocket engines. There is no other engine type [turbojet engine TJE](ТРД) or ramjet engine [RJE](ПВРД) that can develop such a thrust. Thus there is no competition for rocket engines where great thrust is required, for hypervelocity or cosmic-velocity flight.

It is important to note that, as follows from Expression (1.5), rocket-engine thrust is independent of flight speed (provided the latter does not influence the pressure p_s at the nozzle exit).

Specific thrust (specific impulse). The specific thrust or specific impulse P_{ud} of an engine is defined as the thrust referred to the weight flowrate of working fluid per unit time, i.e.,

$$P_{уд} = \frac{P}{G_{сек}}. \qquad (1.7)$$

This definition gives the dimensions of specific thrust, kgf·s/kgf; in the literature, the dimensions of P_{ud} are sometimes given as s.

For an LRE, the engine thrust and fuel flowrate can be measured quite accurately in steady and unsteady operation. For the general case of unsteady operation, if P is the instantaneous thrust over a time $d\tau$ and dG_Σ is the fuel flowrate over the same time interval, then

$$P_{уд} = \frac{P\,d\tau}{dG_\Sigma}. \qquad (1.8)$$

In SRE, it is usual to determine the average specific thrust, or specific impulse, over the entire engine burn time. If $\overline{P}$ is the average thrust over the time τ s of engine operation, during which all G_Σ kgf of fuel is expended, then the average impulse of the SRE will equal

$$P_{уд} = \frac{\overline{P}\tau}{G_\Sigma}. \qquad (1.9)$$

With improved test methods, the instantaneous specific thrust of an SRE can be determined by Formula (1.7) for steady operation and from Formula (1.8) for unsteady operation.

An expression is easily obtained for the specific thrust if we substitute the value of P from Formula (1.5) into Eq. (1.7); then

$$P_{уд} = \frac{w_c}{g} + F_c \frac{p_c - p_н}{G_{сек}}.$$

But

$$G_{\text{сек}} = \mu_c F_c w_c \gamma_c,$$

where μ_s is the nozzle discharge coefficient, referred to the exit section F_s, the velocity w_s, and the weight density γ_s of the gases in this section; consequently,

$$P_{уд} = \frac{w_c}{g} + \frac{p_c - p_н}{\mu_c w_c \gamma_c}. \qquad (1.10)$$

when $p_s = p_n$, i.e., for complete expansion of the gases in the nozzle, the specific thrust will equal

$$P_{уд} = \frac{w_c}{g}. \qquad (1.11)$$

If $p_s \neq p_n$, we can also use Formula (1.11) to find the specific thrust, replacing the actual velocity w_s by a certain arbitrary effective gas exit velocity w_{eff}, found from the formula

$$w_{эфф} = w_c + \frac{g(p_c - p_н)}{\mu_c w_c \gamma_c}. \qquad (1.12)$$

Consequently, in the general case

$$P_{уд} = \frac{w_{эфф}}{g}; \qquad (1.13)$$

for the special case in which $p_s = p_n$, the velocity $w_{eff} = w_s$, and the specific thrust is found from Formula (1.11).

The greater the specific thrust, the greater the absolute thrust of the engine for a specified per-second working-fluid flowrate, or the lower the per-second flowrate for a specified engine thrust. All other conditions being equal, the greater the specific thrust, the greater the vehicle flight range for the same total consumption of working fluid.

The value of specific thrust depends on the type of fuel and on the engine-process parameters, and is characterized by the stability for each fuel type and the engine process level.

Depending on the type of fuel and the process parameters, in modern engines the specific thrust at the earth's surface for LRE is

$$P_{уд} = 240\text{--}420 \text{ kgf·s/kgf or more;}$$

for an SRE it is

$$P_{уд} = 200\text{--}250 \text{ kgf·s/kgf or more.}$$

Higher values of specific thrust can be expected for LRE and SRE when fuels of the future are used and future process parameters employed.

Specific consumption. By the specific consumption we mean the fuel consumed to develop 1 kgf of thrust during one hour. Consequently,

$$c_{ya} = \frac{3600\, G_{sec}}{P} \tag{1.14}$$

or

$$c_{ya} = \frac{3600}{P_{ya}} \text{ kgf/kgf·h.} \tag{1.15}$$

The specific consumption is inversely proportional to the specific thrust.

For modern engines, the specific consumption at the earth's surface is: for LRE,

$$c_{ya} \approx 9\text{—}15 \text{ kgf/kgf·h;}$$

for SRE,

$$c_{ya} \approx 15\text{—}18 \text{ kgf/kgf·h.}$$

In practical computations, it is convenient to use the specific fuel consumption in 1 s for 1 kgf or 1 tf of thrust, rather than the per-hour specific consumption. From Expression (1.15), the per-second specific consumption is

$$c_{ya.sec} = \frac{1}{P_{ya}} \text{ kgf/kgf·s}$$

or, refering the specific consumption to 1 tf of thrust,

$$c_{ya.sec} = \frac{1000}{P_{ya}} \text{ kgf/tf·s.} \tag{1.16}$$

Thus if P_{ud} = 250 kgf·s/kgf, it is then necessary to expend 4 kgf of fuel in 1 s for each 1 tf of absolute thrust developed.

The specific consumptions of rocket engines are extremely high; they are many times the specific consumptions of TJE or EABJE. This is explained primarily by the fact that for all types of engines using air, the specific consumption refers solely to the consumption of combustible carried on board the craft, while for rocket engines, the specific consumption refers to all fuel consumed on board the vehicle, which carries not only the combustible but the oxidizer as well (whether separately or in combined form). The oxidizer consumption is usually considerably greater than the consumption of combustible, so that the specific fuel consumptions are large for rocket engines. Thus it is clear that rocket engines must be used for brief operation, or else the dimensions of the vehicle will rise excessively and the engine thrust may prove inadequate to impart the required velocity to the vehicle.

As an illustration, we give the general formula for the possible duration of engine operation in the system of a rocket (or other

vehicle).

Let M_k be the final rocket mass and

$\bar{m}$ the mass number.

Then the mass of the fuel in the rocket will be

$$M_т = M_к(\bar{m}-1) = M_к\bar{m}_т = M_н\frac{\bar{m}_т}{\bar{m}}.$$

where $\bar{m} - 1 = \bar{m}_t$ is the ratio of the fuel mass to the final rocket mass, while $\bar{m}_t/\bar{m}$ is the fuel as a fraction of the initial mass M_n or initial weight G_n of the rocket.

When the motor thrust P and specific fuel consumption c_{ud} are constant in magnitude, the duration of engine operation will be

$$\tau = \frac{G_н\bar{m}_т}{Pc_{уд}\bar{m}} \text{ h}.$$

The ratio of engine thrust to initial rocket weight is called the thrust-to-weight ratio,

$$\beta = P/G_н.$$

Introducing this parameter, we obtain the duration of engine operation under the above condition,

$$\tau = 3600\frac{\bar{m}_т}{\bar{m}\beta c_{уд}} \text{ s} \qquad (1.17)$$

or on the basis of Expression (1.15)

$$\tau = \frac{\bar{m}_т}{\bar{m}}\frac{P_{уд}}{P}. \qquad (1.18)$$

Thus the duration of rocket-engine duration in a rocket system when P = const and c_{ud} = const is proportional to the proportion, by mass or by weight, of fuel in the rocket and to the specific engine thrust, and inversely proportional to the rocket thrust-to-weight ratio.

It is important to note that Formulas (1.17) or (1.18) do not contain the rocket dimensions explicitly; they appear implicitly in the fuel ratio $\bar{m}_t$, which depends to a certain degree on the rocket dimensions. A somewhat larger mass number can be attained for large rockets than for small ones.

Let P_{ud} = 300 kgf s/kgf, $\bar{p}$ = 1.5, $\bar{m}$ = 10 and, consequently, $\bar{m}_t$ = 9; then with thrust of constant magnitude, the engine operating time will be

$$\tau = 0{,}9\frac{300}{1{,}5} = 180 \text{ s}.$$

Rocket-engine operating periods are short not only as a result of the high specific consumption, but also owing to the restricted motor life owing to the high temperatures, corrosiveness of several fuel components, and the need to make the structure as light as possible. In SRE, there is an additional restriction on engine operating time associated with the lack of cooling for such important parts as the engine exhaust nozzle.

Specific weight $\gamma_{d.u}$ of engine plant. This parameter is defined as the ratio of the weight $G_{d.u}$ of the entire plant as a whole to the thrust developed by the engine, i.e.,

$$\gamma_{d.u}=\frac{G_{d.u}}{P}.$$

The weight of the engine plant includes the weight of the entire system except for the weight of the fuel. In a SRE, this includes the chamber, nozzle, igniter and its associated system, and the thrust regulating system (when there is one). For a LRE, this includes tanks, lines, valves, pumps and drive motors (turbopump units), the starting and regulating system, and auxiliary system (gas generators for the turbine, etc.).

For rockets in particular, the specific weight of the engine plant is of great importance since, all other conditions being equal, it influences the maximum speed and, consequently, the range of the vehicle. The lower the initial weight of the rocket, the greater the influence of engine-plant weight.

Liquid rocket engines have specific weights of 0.008-0.04 kgf/ /kgf. Lower values are associated with engines having greater thrust and higher values with low-thrust LRE.

For solid-fuel engines, the specific weight depends in great measure on the engine design, the type and dimensions of the fuel charge, and the chamber material. If the fuel is cast directly in the chamber and the chamber walls are made of thin metal or plastic, without heat insulation, the SRE will weigh less, with the engine weighing 5-7% of the fuel weight. With a pressed fuel charge installed within the chamber with a gap, which makes it necessary to increase chamber wall thickness and to employ heat insulation, the weight of the SRE increases, reaching 5-10% or more of the fuel-charge weight.

The compactness (over-all dimensions) of the powerplant is of enormous importance, since for specified values of thrust and motor burn time, the plant dimensions, together with the fuel volume, determine the dimensions of the entire rocket. The specific frontal thrusts of rocket engines considerably exceed the specific frontal thrusts of all other engine types, reaching 80-100 T or more for 1 m^2 of front.

The following basic conclusions can be drawn from the nature of the process in a rocket engine and the process parameters:

1. The rocket engine develops thrust by using materials carried onboard the flying craft itself; thus the engine is completely independent, i.e., it can develop thrust at any altitude whether or not there is air in the environment; all other engine types require external air, since oxygen is needed to oxidize the combustible used in the engine and carried by the craft.

2. A rocket engine can develop a large absolute thrust; this requires ejection of considerable masses of reaction products at high speed; in this respect, the rocket engine has a substantial advantage over other types of reaction engines;

3. The need for the flying craft to carry the entire reserve of initial substances required for the engine process represents a very great limitation on the operating duration; in this respect, rocket engines are considerably inferior to all other types of reaction engines.

Manuscript Page No.	Transliterated Symbols
4	c = s = soplo = nozzle
6	вх = vkh = vkhodnyy = input
6	к = k = kamera = chamber
6	в = v = vytecnitel'nyy = forced
6	г.к = g.k = goryuchiy komponent = combustible component
6	о.к = o.k = okislyayushchiy komponent = oxidizing component
8	пв = pv = perekis' vodoroda = hydrogen peroxide
8	г.г = g.g = gazogenerator = gas generator
8	г.г = g.g = generatornoye goryucheye = generator combustible
9	г.о = g.o = generatornyy okislitel' = generator oxidizer
12	о = o = okislitel' = oxidizer
12	г = g = goryucheye = combustible
14	н = n = nachal'nyy = initial
14	к = k = konechnyy = final
14	т = t = toplivo = fuel
17	вн = vn = vnutrenniy = inside

17 нар = nar = naruzhnyy = outside

19 сек = sek = sekundnyy = per-second

22 эфф = eff = effektivnyy = effective

22 уд = ud = udel'nyy = specific

25 д.у = d.u = dvigatel'naya ustanovka = engine plant

Chapter 2

ROCKET-ENGINE CYCLE AND EFFICIENCIES

2.1. IDEAL CYCLE. THERMAL EFFICIENCY AND MAXIMUM GAS EXIT VELOCITY

A rocket engine organically combines devices for producing the kinetic energy of gases from the chemical energy of the fuel introduced into the chamber, and for obtaining thrust as a result of the conversion process. The rocket-engine process takes place continuously at constant chamber pressure. Although other process conditions are possible, we shall henceforth be concerned solely with the process involving heat supplied at p = const.

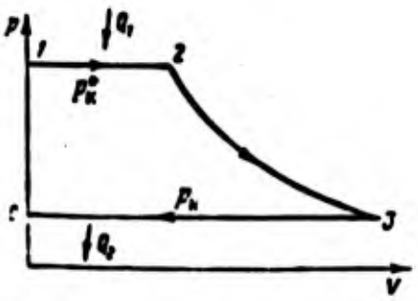

Fig. 2.1. Ideal rocket-engine cycle.

Even though the rocket engine does not have all the elements in which the individual thermodynamic processes of the cycle take place, it is still quite legitimate to represent its thermodynamic cycle graphically and to carry out a general investigation to establish and understand the basic relationships and factors determining the cycle properties.

In a liquid rocket engine [LRE] (ЖРД) there is an increase in the pressure of the fuel components delivered to the combustion chamber in the liquid or gaseous state. If we neglect the work done to compress the components delivered in the liquid state, we can represent the ideal cycle of such a liquid rocket engine as the graph shown in Fig. 2.1. The isobar 1-2 represents the segment on which heat Q_1 is supplied; the chamber pressure p_k^* for the ideal cycle is taken equal to the pressure of the decelerated gases in the actual cycle; in the ideal cycle considered here, the adiabatic curve 2-3 corresponds to the process of isentropic expansion of the gases in the nozzle from the initial pressure p_k^* to the final pressure $p_s = p_n$, where p_n is the external pressure; line 3-0 arbitrarily represents the isobar closing the cycle with removal of heat Q_2 from the cycle; line 0-1 shows the increase in the pressure of the liquid working fluids introduced into the engine; the volume of these fluids can be neglected as being negligibly small as compared with the volume of the gaseous products.

The ideal cycle of a solid rocket engine [SRE](РДТТ) will evidently be quite analogous to the cycle of an LRE with liquid compon-

ents at the chamber entrance, since the solid fuel is at a pressure p_k^* in the chamber, and its volume is also quite negligible. On the isobar 1-2, the fuel is gasified and burned to release the heat Q_1.

Like the initial pressure p_k^*, the final cycle pressure p_s is selected for a given fuel with allowance for the rocket efficiency. When they have been selected, these values determine the cycle pressure-reduction ratio

$$\pi = \frac{p_k^*}{p_s}.$$

If we let h_u, kcal/kgf, represent the working (lower) heating value, or the heat of the decomposition reaction, for 1 kgf of fuel, then

$$Q_1 = h_u = i_2 - i_1$$

or

$$Q_1 = h_u \approx c_p T_2; \qquad (2.1)$$

here i_2 and i_1 are the respective enthalpies of the working fluid for the final and initial temperatures at points 2 and 1;

c_p is the constant heat capacity of the ideal process or the average heat capacity of the reaction products in the range between the temperature at point 1 and T_2°K;

T_2 is the theoretical temperature of the gases at point 2, on the assumption that no heat is lost in the chamber and that the gases have zero velocity.

The thermal effect produced by the reaction of a unitary fuel will always be a definite value equaling h_u. For an oxidizing reaction, the thermal effect of the reaction will depend on the ratio of combustible and oxidizer. If there is less oxidizer in the component ratio than is required by the stoichiometric equation, then in place of h_u, we should use $h_a < h_u$ in Formula (2.1) and in the rest of the discussion, since some of the heat may not be released owing to a lack of oxidizer. In the general case,

$$Q_1 = h_a \approx c_p T_a \qquad (2.2)$$

For the ideal cycle, the work done is numerically equal to the kinetic energy of the combustion products at point 3, i.e., at the end of the adiabatic expansion process; it is represented as

$$AL_{ad} = A\frac{k}{k-1}RT_a\left[1-\left(\frac{p_3}{p_a}\right)^{\frac{k-1}{k}}\right]. \qquad (2.3)$$

where

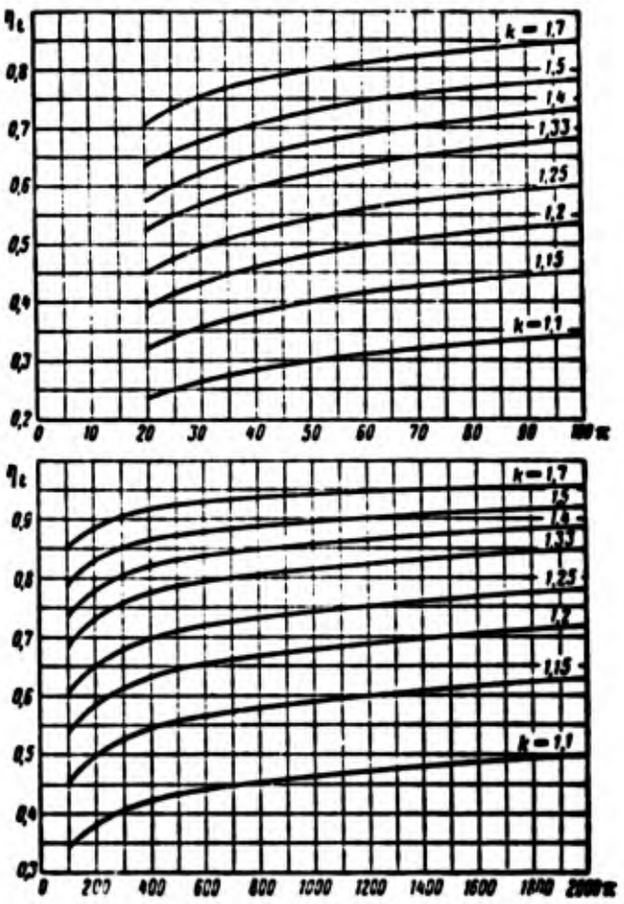

Fig. 2.2. Thermal efficiency as function of gas pressure reduction ratio in nozzle and of exponent k

$$A\frac{k}{k-1}R=c_p, \qquad (2.4)$$

Here k is the constant exponent in the ideal adiabatic process;

R is the reaction-product gas constant.

The ideal-cycle thermal efficiency is

$$\eta_t=\frac{AL_{ad}}{Q_1}.$$

On the basis of Expressions (2.1) or (2.2) and (2.4),

$$\eta_t=1-\left(\frac{p_2}{p_1}\right)^{\frac{k-1}{k}}=1-\frac{1}{\pi^{\frac{k-1}{k}}}. \qquad (2.5)$$

The thermal efficiency of an ideal rocket engine depends solely on the gas pressure reduction ratio π and on the composition k of the reaction products; Figure 2.2 shows η_t as a function of π for various

values of k. The less the heat capacity of the gas, the greater the thermal efficiency. From this viewpoint, an increase in the content of polyatomic gases in the combustion products is undesirable. The thermal efficiency approaches unity as $p_n \to 0$. This case corresponds to an ideal lossless cycle and to total gas expansion in vacuum regardless of the initial pressure.

Depending on the characteristic of the working fluid for the ideal cycle, the values of cycle thermal efficiency will differ for the same value of the pressure ratio π. If we take a real working fluid (reaction products, for example) for the ideal cycle and make allowance for dissociation and for the relationship between the heat capacity and the temperature, then the maximum temperature T_z and the thermal efficiency η_t will be lower than for the case in which c_p = const, as we know from thermodynamics.

In the calculations, it is desirable to take as the ideal cycle a cycle with an actual working fluid characterized by variable composition, variable heat capacity, and dissociation, since such a cycle permits more exact evaluation of how closely the real process in the engine approximates the theoretically possible process. In this case, the factor c_p in Formula (2.1) will allow not only for the composition of the working fluid and the way in which the heat capacity depends on the temperature, but also the dissociation of combustion products at the temperature T_z. The method used to determine T_z will be discussed in Chapter 8. The actual temperature T_k^* of the decelerated gases in the chamber will differ under this approach from the temperature T_z of the reaction products at the end of the chamber only as a result of the incompleteness of the reaction and the thermal losses in the chamber wall.

The work L_{id} of the ideal cycle in a rocket engine (with p_s = p_n) is utilized completely to produce the kinetic energy of the jet of gases leaving the nozzle. The gas exit velocity ω_{id} for the nozzle of an ideal engine is found from the equation

$$\frac{w_{id}^2}{2g} = L_{id}.$$

Thus, taking Eq. (2.3) into account, we can write

$$w_{id} = \sqrt{2g\frac{k}{k-1}RT_z\left[1-\left(\frac{p_n}{p_k}\right)^{\frac{k-1}{k}}\right]} \qquad (2.6)$$

or

$$w_{id} = \sqrt{2g\frac{k}{k-1}RT_z\eta_t} \qquad (2.7)$$

or, with allowance for (2.2) and (2.4):

$$w_{вх} = \sqrt{2g\frac{h_t}{A}\eta_t}. \qquad (2.8)$$

Formula (2.8) shows that the maximum gas exit velocity in an ideal rocket engine depends on the reaction heat of 1 kgf of fuel and on the thermal efficiency.

The specific thrust of an ideal rocket engine is

$$P_{уд.вх} = \frac{w_{вх}}{g}. \qquad (2.9)$$

2.2. CHARACTERISTICS OF ACTUAL PROCESS. EFFICIENCIES

The actual rocket-engine process differs from the ideal process in that there are losses in the chamber and the nozzle.

The chamber losses are determined by the following two factors:

1) the reaction (oxidation or decomposition) is not fully completed in the chamber, so that a portion Δh_1 of the heat is not released (incompleteness of the reaction, neglecting dissociation);

2) a portion Δh_2 of the oxidation-reaction heat is expended on dissociation of the reaction products; dissociation plays a significant role in high-temperature engines, since the combustion temperature in rocket engines reaches 3000-3500°K or more. The dissociation losses are accounted for by the following factors: the heat going for combustion-product dissociation is expended at high temperature in the chamber, and is returned fully or in part during the process of expansion in the nozzle while the gas temperature is being lowered and recombination is taking place. Although dissociation is a fully reversible reaction, the removal of heat during its liberation in the chamber at p_k^* and the return of this same heat at lower values of p leads to a reduction in efficiency.

In an LRE, the first loss is caused by the imperfection of the mixing process, and by the nonuniformity of mixture composition over the chamber cross section. In many cases, this nonuniformity is necessary to reduce the thermal stresses in the chamber walls. If the reaction-product parameters do not become equalized at the end of the chamber, there will be an additional loss of heat as compared with the ideal process in which for a given value of α the gas parameters are assumed to be identical over the entire cross section.

In an LRE, a portion Δh_3 of the heat is transferred from the gases to the walls; this amount of heat is not large, and with the exception of experimental engines and certain engines that are not cooled or that are cooled by flowing water or other liquid, this portion of heat is again returned to the engine chamber together with the working-mixture component used to cool the engine walls. For uncooled engines and for engines using external cooling by a liquid that does not participate in the process of heat release in the chamber, the heat Δh_3 represents a loss, since the gas temperature in the engine system decreases. The situation is different for engines cooled by one of the components, particularly for diergolic fuels, where heat must be supplied to vaporize the components and

to bring about all the intermediate preignition processes. For uncooled chambers, this heat is taken completely and directly from the combustion zone with the aid of radiant heat and "reverse flows" (see Chapter 4); for cooled chambers, it is also supplied from the combustion zone, but with part coming directly from the reverse flows and radiant heat and part coming through the walls by heating of the component that cools the engine. Here, consequently, the heat Δh_1 does not represent a loss in the actual process, since the thermal effect of the reaction, determined expermentally, allows for the heat expended on evaporation and on the intermediate reaction.

In certain engines, the cooling component, or both components, are vaporized and initially used to drive the turbine in the turbopump unit [TPU](THA), and are then introduced into the chamber; here some of the energy is lost from the viewpoint of the process in the engine chamber, although it is used for the engine plant as a whole.

In low-temperature motors where the process is based on a decomposition reaction, the main loss involves only the first type of loss.

As we have said, like the variable heat content of the gases, the heat expended on dissociation should be taken into account beforehand as part of the ideal-cycle thermal efficiency realized by the actual reaction products. Then the actual process in the chamber of the actual engine will deviate less from the ideal, and will be completely determined just by the incompleteness of the reaction and the difference in the gas parameters at the chamber exit section.

In rocket-engine process calculations, we always determine the actual composition and actual properties of the gases in the chamber.

If Δh allows for the heat lost owing to incomplete combustion and the heat lost in the chamber wall, we can find the chamber efficiency η_k from the relationship

$$\eta_k = \frac{h_k - \Delta h}{h_k}. \qquad (2.10)$$

In manufactured chambers $\eta_k = 0.92\text{-}0.98$.

As a result of the chamber heat losses, the actual gas temperature at the end of the chamber $T_k^* < T_k$. As we have said, we define the actual temperature as the temperature of the adiabatically decelerated gases.

Clearly,

$$c_p T_k^* = h_k - \Delta h. \qquad (2.11)$$

The average heat capacities can be assumed to be identical for the ideal and actual processes. This is quite acceptable provided the ideal process allows for the variable heat capacity and if the gas composition is the same for the actual and ideal processes. Here, using Eqs. (2.1) and (2.11) from (2.10) we obtain an expression for the chamber efficiency:

$$\eta_c = \frac{T_c^*}{T_c}. \qquad (2.12)$$

If the nozzle expansion process is assumed to be isentropic with allowance for molecular recombination, then the resulting exit velocity may be referred to as the theoretical velocity. When $p_s = p_n$, it is computed from the formula

$$w_t = \sqrt{2g\frac{k}{k-1}RT_c^*\left[1-\left(\frac{p_n}{p_c^*}\right)^{\frac{k-1}{k}}\right]}. \qquad (2.13)$$

Here k is the isentropic index, allowing for molecular recombination during the expansion process.

The coefficient φ_k, which allows for the reduction in the ideal velocity resulting from the presence of losses in the actual chamber that are neglected in the ideal cycle, may be used to establish a relationship between w_t and w_{id}:

$$w_t = \varphi_k w_{id}. \qquad (2.14)$$

On the basis of (2.6), (2.12) and (2.13)

$$\eta_c = \sqrt{\eta_c^*} \qquad (2.15)$$

or

$$\eta_c = \varphi_k^2. \qquad (2.16)$$

The theoretical work corresponds to the theoretical velocity:

$$L_t = \frac{k}{k-1}RT_c^*\left[1-\left(\frac{p_n}{p_c^*}\right)^{\frac{k-1}{k}}\right]. \qquad (2.17)$$

Clearly,

$$L_t = \frac{w_t^2}{2g}. \qquad (2.18)$$

The following processes take place in an actual nozzle:

1) expansion of gases with a reduction in temperature and pressure and an increase in gas velocity along the nozzle;

2) liberation of heat owing to the incompleteness of the reaction in the chamber and in high-temperature engines, in addition, owing to recombination (association) of dissociation products when the gas temperature in the nozzle decreases;

3) removal of a portion of the heat from the gases to the walls;

4) gas-wall friction and internal friction in the gas itself.

In virtue of the above factors, the actual nozzle process will not be adiabatic, but will follow a complicated law, differing for different nozzle sections, and with the gas composition varying along the nozzle.

In calculations for the gas expansion process in the nozzle, molecular recombination at lower temperatures is taken into account by some given method, for example, on the assumption that the gas in each nozzle section is in the equilibrium state corresponding to the mean gas temperature in this section. Here the deviation between the actual and ideal processes will result solely from friction and from heat transfer to the walls.

The actual expansion process can be replaced by an equivalent polytropic process (for example, on the basis of the exit velocity attained) having a certain constant index n. In such case, the actual gas velocity at the nozzle exit will be

$$w_a = \sqrt{2g\frac{n}{n-1}RT_k^*\left[1-\left(\frac{p_a}{p_k^*}\right)^{\frac{n-1}{n}}\right]}, \qquad (2.19)$$

while the actual internal real-cycle work will be

$$L_i = \frac{n}{n-1}RT_k^*\left[1-\left(\frac{p_a}{p_k^*}\right)^{\frac{n-1}{n}}\right]. \qquad (2.20)$$

Clearly,

$$L_i = \frac{w_a^2}{2g}. \qquad (2.21)$$

The nozzle efficiency η_s shows the influence of the deviation between the actual nozzle process and the theoretical process on the efficiency of the rocket-engine cycle for identical initial gas parameters (p_k^*, T_k^*) and for an identical degree of expansion π. In realized designs, η_s has had a value of 0.90-0.96. The higher values are attained in high-thrust engines and engines with special nozzle profiles.

It follows from (2.13) and (2.19) that the nozzle efficiency is

$$\eta_s = \frac{w_a^2}{w_t^2}. \qquad (2.22)$$

If we let

$$w_a = \varphi_s w_t, \qquad (2.23)$$

where φ_s is the nozzle velocity coefficient, then

$$\eta_s = \varphi_s^2. \qquad (2.24)$$

Under bench conditions ($\omega_1 = 0$), the internal efficiency η_i of

the actual rocket-engine process can be found as the ratio of the actual or internal work L_i or the real process, expressed in calories, to the heat Q_1 expended to produce this work. Consequently,

$$\eta_i = \frac{AL_i}{Q_1} = \frac{A\frac{w_e^2}{2g}}{h_\alpha}. \tag{2.25}$$

With the aid of (2.7), we can determine the actual exit velocity from (2.25):

$$w_e = \sqrt{2g\frac{k}{k-1}RT_\alpha\eta_i} \tag{2.26}$$

or, with allowance for (2.6), (2.14), and (2.23),

$$w_e = \varphi_\kappa\varphi_c w_{max} \tag{2.27}$$

and

$$w_e = \varphi_c\sqrt{2g\frac{k}{k-1}RT_\alpha^*\left[1-\left(\frac{p_\alpha}{p_\alpha^*}\right)^{\frac{k-1}{k}}\right]}. \tag{2.28}$$

2.3. EFFICIENCIES OF ENGINE IN FLIGHT

For the powered segments of the path, i.e., the segments for which the engine operates and develops thrust, the vehicles in which rocket engines are installed usually do not have a steady flight regime or (for aircraft and for aviation rockets), the regime is brief. Thus, generally speaking, the efficiencies of an engine in flight will vary; the values will depend on the flight conditions.

It is necessary to consider two flight cases: 1) the flight speed is relatively small and the kinetic energy of the fuel can be neglected in comparison with the chemical energy; this case applies, for example, to launching of a rocket and to an aircraft booster; 2) the flight speed is high and the fuel kinetic energy is commensurate with the chemical energy; this case applies to all rocket stages (with the exception of the first in isolated cases). The second case is more general; we shall consider it first.

The external resultant effect of engine operation in flight will be the work done in moving the vehicle.

Let P be the instantaneous engine thrust and dS the path, or path projection, for the flying craft in the direction of the thrust over the time $d\tau$; then the external useful (effective) work done by the engine will be

$$dL_e = PdS. \tag{2.29}$$

In addition to the chemical energy h_α, during flight the working fluid will also possess an initial kinetic energy corresponding, in

general, to the time-varying speed w_0 at which the vehicle flies. If the flight speed is great, in determining the efficiency we cannot neglect the initial kinetic energy of the fuel; its value becomes quite commensurate with the thermal effect of the reaction. Naturally, the kinetic energy of the fuel at a given time results from the chemical energy of the spent fuel masses expended prior to this time on the vehicle motion path. Nonetheless, considering an arbitrary time during motion of the vehicle, we must reckon with the kinetic energy that the remaining fuel has acquired as of the given time. Thus, for example, when h_α = 1500 kcal/kgf and w_0 = = 200, 600, 1000, 1500, 3000, and 6000 m/s, the ratio $Aw_0^2/2gh_\alpha$ will have the respective approximate values 0.003, 0.028, 0.075, 0.17, 0.68, and 2.8. As we see, when the flight speeds are very great, it is necessary to allow for the initial external kinetic energy of the fuel when we determine the running value of the entire amount of energy expended and the running efficiency values. Consequently, the total energy obtained from 1 kgf of fuel will equal $(h_\alpha/A)+(w_0^2/2g)$; here w_0 is the instantaneous flight speed.

If the consumption of working fluid over time $d\tau$ is dG, then the instantaneous value of energy expended on flight will be

$$dG\left(\frac{h_\alpha}{A}+\frac{w_0^2}{2g}\right). \tag{2.30}$$

The effective (total) efficiency η_e of the engine in flight is the ratio of the useful work done in moving the vehicle owing to engine operation to the total energy expended in the engine to accomplish this motion.

On the basis of Eqs. (2.29) and (2.30), the instantaneous effective (total) efficiency of the engine will be

$$\eta_e=\frac{P\,dS}{dG\left(\frac{h_\alpha}{A}+\frac{w_0^2}{2g}\right)}. \tag{2.31}$$

Since

$$dS=w_0\,d\tau$$

while in steady flight

$$\frac{dG}{d\tau}=G_{\text{sec}} \text{ and } \frac{P}{G_{\text{sec}}}=P_{\text{ud}},$$

the effective efficiency will be represented by the expression

$$\eta_e=\frac{P_{\text{ud}}w_0}{\frac{h_\alpha}{A}+\frac{w_0^2}{2g}} \tag{2.32}$$

or in the general case, when $P_{\text{ud}} = w_{\text{eff}}/g$,

$$\eta_e = \frac{w_{\text{эф}} w_0}{g\left(\frac{h_a}{A} + \frac{w_0^2}{2g}\right)}. \qquad (2.33)$$

The internal efficiency η_i of an engine in flight is the ratio of the internal work done by the engine, equaling the work done to move the vehicle plus the kinetic energy remaining in the gases after they leave the engine, to the total energy expended in the engine. The absolute velocity of the gases leaving the engine with respect to the fixed spatial coordinates (earth-referenced coordinates, for example) equals $w_a = w_c - w_0$ for complete expansion of the gases in the nozzle; for incomplete expansion, $w_a = w_{\text{эф}} - w_0$; thus in the general case, the unused kinetic energy in 1 kgf of gases will equal

$$\frac{w_a^2}{2g} = \frac{(w_{\text{эф}} - w_0)^2}{2g}. \qquad (2.34)$$

By definition, the instantaneous value of internal efficiency during flight will be

$$\eta_i = \frac{P\,dS + dG\,\frac{(w_{\text{эф}} - w_0)^2}{2g}}{dG\left(\frac{h_a}{A} + \frac{w_0^2}{2g}\right)}. \qquad (2.35)$$

If the flight speed $w_0 = \text{const}$ for a certain segment of the path, then

$$\eta_i = \frac{P_{уд} w_0 + \frac{(w_{\text{эф}} - w_0)^2}{2g}}{\frac{h_a}{A} + \frac{w_0^2}{2g}}. \qquad (2.36)$$

or

$$\eta_i = \frac{\frac{w_{\text{эф}} w_0}{g} + \frac{(w_{\text{эф}} - w_0)^2}{2g}}{\frac{h_a}{A} + \frac{w_0^2}{2g}},$$

or, finally,

$$\eta_i = \frac{\frac{w_{\text{эф}}^2}{2g} + \frac{w_0^2}{2g}}{\frac{h_a}{A} + \frac{w_0^2}{2g}}. \qquad (2.37)$$

The thrust efficiency, or propulsive efficiency, η_p is the ratio of the useful work done in moving the vehicle to the useful work plus the remaining kinetic energy of the gases, which equals

$(w_{эфф}-w_0)^2/2g$ for 1 kgf. The propulsive efficiency shows the fraction of the effective kinetic energy of the exhaust gases is used under the given flight conditions for external useful work done to move the vehicle.

On the basis of this definition, the instantaneous value of η_p equals

$$\eta_p = \frac{P\,dS}{P\,dS + dG\,\dfrac{(w_{эфф}-w_0)^2}{2g}}. \qquad (2.38)$$

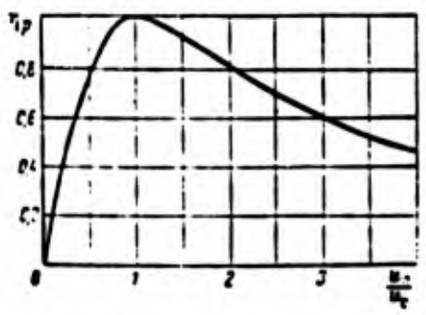

Fig. 2.3. Instantaneous propulsive efficiency as function of ratio w_0/w_s.

TABLE 2.1

$\alpha=p_н^*/p_н$	25				50				100			
w_0, m/s	300	1000	2000	3000	300	1000	2000	3000	300	1000	2000	3000
η_i	0.389	0.434	0.541	0.651	0.46	0.499	0.595	0.691	0.508	0.544	0.630	0.719
η_p	0.265	0.775	0.997	0.945	0.255	0.729	0.991	0.967	0.243	0.701	0.975	0.919
η_e	0.103	0.336	0.539	0.615	0.117	0.363	0.590	0.668	0.123	0.382	0.613	0.708

TABLE 2.2

$\alpha=p_н^*/p_н$	800			1000		
w_0, m/s	1000	3000	6000	1000	3000	6000
η_i	0.376	0.57	0.79	0.388	0.58	0.794
η_p	0.714	0.974	0.686	0.705	0.978	0.698
η_e	0.268	0.555	0.542	0.273	0.565	0.551

If w_0 = const for a certain flight segment, then

$$\eta_p = \frac{P_{уд} w_0}{P_{уд} w_0 + \frac{(w_{эф} - w_0)^2}{2g}}$$

or

$$\eta_p = \frac{\frac{w_{эф} w_0}{g}}{\frac{w_{эф} w_0}{g} + \frac{(w_{эф} - w_0)^2}{2g}}. \qquad (2.39)$$

or, finally,

$$\eta_p = 2 \frac{w_0 / w_{эф}}{1 + \left(\frac{w_0}{w_{эф}}\right)^2}. \qquad (2.40)$$

The product of (2.37) and (2.40) gives the total flight efficiency

$$\eta_e = \eta_i \eta_p = \frac{w_{эф} w_0}{g\left(\frac{h_\alpha}{A} + \frac{w_0^2}{2g}\right)}. \qquad (2.41)$$

With total expansion of the gases in the nozzle, the effective velocity w_{eff} in the formulas for η_i, η_p, and η_e should be replaced by the exit velocity w_s.

Formula (2.40) is shown graphically in Fig. 2.3. The maximum value $\eta_p = 1$ occurs when $w_0 = w_s$. This is understandable, since when $w_c \geq w_0$, the gases leaving the engine possess an unused residual kinetic energy $(w_c - w_0)^2/2g$; it is only when $w_s = w_0$ that all of the gas kinetic energy obtained owing to the internal engine process will be converted into useful work done to move the vehicle.

Table 2.1 shows values of η_i, η_p, and η_e as functions of flight speed for three values of $\pi = p_k^*/p_n$, with T_g = 3000° abs. and h_α = 1400 kcal/kgf. It is clear from the table that at low flight speeds, η_e is small; accordingly, at high flight speeds, the effective efficiency of a rocket engine reaches very high values. Table 2.2 shows the same quantities for larger values of π and w_0, and for h_α = 2000 kcal/kgf.

If the flight velocity is not great and the fuel kinetic energy is negligible as compared with the chemical energy, then on the basis of (2.33), we obtain the following expression for the effective efficiency:

$$\eta_e = \frac{w_{эф} w_0}{g \frac{h_\alpha}{A}},$$

while the internal efficiency from Formula (2.37), in analogy with (2.25), will be

$$\eta_i = \frac{\frac{w_{эфф}^2}{2g}}{\frac{A_e}{A}},$$

while the thrust (propulsive) efficiency will be

$$\eta_p = \frac{\eta_e}{\eta_i} = 2\frac{w_0}{w_{эфф}}.$$

This last expression can be obtained from (2.40) when $w_{эфф} \gg w_0$, if we neglect the square of the ratio $w_0/w_{эфф}$ in the denominator.

For an engine operating on a test bench, $w_0 = 0$, so that $\eta_e = 0$ and $\eta_p = 0$, but $\eta_i \neq 0$. It is clearly impossible for the external useful work done during flight to exceed the available effective kinetic energy of the gases.

When a rocket engine is employed for a rocket or a missile, it is possible to determine the mean effective (total) efficiency $\bar{\eta}_e$ for the entire powered-flight segment, and the mean thrust (propulsive) efficiency $\bar{\eta}_p$ on this segment, on the basis of the following considerations. As a result of engine operation over the entire period of powered flight, the speed of the rocket or missile will vary from the initial value $w_1 = 0$ to some final value w_2; the mass of the rocket (missile) will vary from the initial value M_n to the final value M_k. The difference $M_n - M_k$ represents the total mass M_t of all fuel expended for the powered segment.

At the end of the powered segment, the entire vehicle will have accumulated a kinetic energy $M_k(w_2^2/2)$. Moreover, if the altitude has changed from the initial value H_1 (for example, at the level of the earth) to a certain final value H_2, then the vehicle will also have accumulated a potential energy of

$$M_k \int_{H_1}^{H_2} g\,dH = M_k \int_{R_1}^{R_1+H_2} g\,dR,$$

where R_1 is the initial distance between the launch site and the center of the earth;

H_2 is the radial change in this distance;

g is the local gravitational acceleration.

As we know,

$$g = g_1 \frac{R_1^2}{R^2},$$

where g_1 is the acceleration on the radius R_1; thus at the end of the powered flight segment, the vehicle will have accumulated a po-

tential energy

$$M_k g_1 R_1^2 \int_{R_1}^{R_1+H_2} \frac{dR}{R^2} = M_k g_1 R_1 \frac{H_2}{R_1+H_2}. \qquad (2.42)$$

If the beginning of flight corresponds to $R_1 = R_0$ (sea level), then $g_1 = g_0 = 9.81$ m/s, and the expression for the potential energy will be

$$M_k g_0 R_0 \frac{H_2}{R_0+H_2}.$$

Up to an altitude of 100 km, it is quite permissible to determine the potential energy from the simplified formula

$$M_k g_1 (H_2 - H_1), \qquad (2.43)$$

where H_1 and H_2 are the initial and final vehicle flight altitudes above sea level, m.

If $H_1 = 0$, the formula becomes still simpler:

$$M_k g_0 H_2.$$

At an altitude of 100 km, the difference in the numerical values found from Formulas (2.42) and (2.43) does not exceed 0.3%.

The change in the potential energy of the vehicle's vertical position becomes great for a segment of 50 km or more. For example, with a final vehicle speed of 1000 m/s, the potential energy at an altitude of 50 km will amount to ~100% of the kinetic energy, while it will be nearly 4 times the kinetic energy at 200 km.

The total useful effect of engine work over the entire period of powered rocket flight from the earth will be

$$M_k \frac{w_2^2}{2} + M_k g_0 R_0 \frac{H_2}{R_0+H_2}.$$

The energy expended equals

$$(M_0 - M_k) g_0 \frac{h_0}{A},$$

so that the effective (total) efficiency, averaged over the entire powered-flight segment, will be

$$\bar{\eta}_e = \frac{M_k}{M_0 - M_k} \frac{\frac{w_2^2}{2} + g_0 R_0 \frac{H_2}{R_0+H_2}}{g_0 \frac{h_0}{A}},$$

or

$$\bar{\eta}_e = \frac{1}{m-1} \frac{\frac{w_2^2}{2g_0} + R_0 \frac{H_2}{R_0 + H_2}}{\frac{h_0}{A}}.$$

The mean internal efficiency during flight will equal

$$\bar{\eta}_i = \frac{\int_{M_1}^{M_2} \frac{w_c^2}{2} dM}{(M_2 - M_1) g_0 \frac{h_0}{A}},$$

where w_s is the actual relative speed at which the gases leave the engine nozzle; in general, it will differ for different elementary gas masses dM. If we assume w_s = const or, more accurately, if we assume the arbitrary effective gas exit velocity w_{eff} found from (1.12) to be constant, then

$$\eta_i = \frac{\frac{w_{eff}^2}{2g}}{\frac{h_0}{A}},$$

i.e., we obtain Formula (2.25), as we might have expected.

The mean values of η_e and η_i can also be determined for individual sections of the powered-flight segment.

The internal efficiency does not depend on the characteristics of the flying craft, but is determined solely by the quality of the process in the engine, while the instantaneous and mean values of effective and propulsive efficiency also depend on the dimensions, shape, and construction of the vehicle. The vehicle dimensions and construction actually determine the fraction of the initial weight that remains at the end of the powered segment, as well as the work done against the force of gravity; the dimensions and shape determine the vehicle resistance to motion and, consequently, the flight speed, all other conditions being equal.

The material presented in this section also implies that the propulsive and effective efficiencies of the same engine, installed in different aircraft, rockets, or missiles, will differ in value. Even for the same vehicle, depending on its application (with respect to w and H), the instantaneous and mean values of η_e and η_p will differ.

2.4. TOTAL IMPULSE. SPECIFIC IMPULSE OF CHAMBER

It follows from Expression (2.32) that the effective rocket-engine efficiency is proportional to the specific thrust or the specific impulse. The instantaneous value of specific thrust or specific impulse can be found if we know the instantaneous value of the effective speed; from Expression (1.8), the instantaneous absolute thrust equals

$$P = P_{yд} \frac{dG}{d\tau}.$$

If a specified flight is to be realized, the vehicle must be given a certain total impulse

$$I_\Sigma = \int_0^\tau P\,d\tau \qquad (2.44)$$

or

$$I_\Sigma = \int_0^{G_т} P_{yд}\,dG \qquad (2.45)$$

over the powered segment of the path.

In these formulas, P_{ud} and P will in general be variable.

The altitude and maximum speed for range of the rocket depend on the accuracy with which the variation law $P = f(\tau)$ and the absolute total impulse I_Σ are maintained. The thrust value at each particular time will depend on the amount of fuel supplied to the engine (dG) and the efficiency with which it is used to develop the thrust (P_{ud}). As a consequence, the rocket must have a system capable of regulating engine thrust and cutting off the engine when a specified speed has been reached at the end of the powered segment. For ballistic missiles, the accuracy with which a specified region on the earth's surface can be hit depends directly on the $P = f(\tau)$ law and on I_Σ, unless there are special energy sources and guidance systems to correct or change the path immediately before the instant of impact. If they are to land on the earth or other planets or satellites, spacecraft must have energy-developing (rocket) means of braking before landing. Here the time at which these devices are turned on, the thrust-time relationship, and the total impulse are also of importance. These quantities are also important for maneuvering in space.

As we have already mentioned, maximum utilization of the fuel supply carried onboard the craft is of great significance in the flight performance of the vehicle, so that engine control and cutoff must be very accurate with respect to both magnitude and time. To this end, engines must be manufactured with rigid tolerances on all dimensions important from the viewpoint of the process and the fuel consumption; the flowrates of combustible and oxidizer (in LRE) must be regulated with high accuracy; the fuel must possess specific physical-chemical properties, with parameters varying within narrow limits. Moreover, when the engine is installed in the rocket, it is important that its geometric axis be exactly positioned with respect to the rocket axis; for example, in a single-stage rocket with one engine, the engine and rocket axes must coincide, or else there will be an additional constant load on the rocket flight-control elements.

It can be shown that the total impulse is proportional to the product of the specific thrust by the weight density of the fuel.

If we let P_{ud} = const in Formula (2.45) or bring the mean value of specific impulse during the engine burn time out from behind the integral sign, then

$$I_\Sigma = P_{yд} G_т,$$

where

$$G_т = V_т \gamma_т$$

when the fuel supply has been fully exhausted; here V_t is the working volume of the liquid-fuel tanks, or the solid-fuel volume in an SRE; γ_t is the weight density of a solid fuel or of a unitary liquid fuel, or the specific weight density of the fuel for a bipropellant or a multicomponent liquid fuel (see Chapter 3).

Substituting the value of G_t into the formula for the total impulse, we find

$$I_\Sigma = V_т P_{yд} \gamma_т. \qquad (2.46)$$

For a specific design, V_t will be a constant, so that the total impulse is proportional to the product $P_{ud}\gamma_t$.

Another quantity, called the specific chamber thrust, is also of importance. It is found from the expression

$$\beta = \frac{P_к^* F_{кр}}{G_{т_{сек}}} \qquad (2.47)$$

and represents the engine thrust referred to 1 kgf of fuel if there were no diverging section of the nozzle and if the chamber pressure were everywhere equal to p_k^*. The product $p_k^* F_{kr}$ clearly represents the engine thrust for this case under the specified conditions, while β is the specific thrust. When the nozzle has a diverging section, the quantities $p_k^* F_{kr}$ and β will naturally be less than the thrust P and the specific thrust P_{ud}; they will be smaller the greater the degree of gas expansion in the nozzle.

The specific chamber thrust, the pressure impulse in the chamber or, as it is frequently called, the number β has a special physical meaning. Since the per-second gas flowrate in the throat equals

$$G_{т_{сек}} = F_{кр} w_{кр} \gamma_{кр},$$

while

$$\gamma_{кр} = \gamma_к \left(\frac{2}{k+1}\right)^{\frac{1}{k-1}} = \left(\frac{2}{k+1}\right)^{\frac{1}{k-1}} \frac{P_к^*}{RT_к^*}$$

and

$$w_{kp} = \sqrt{gkRT_{kp}} = \sqrt{gkRT_k^* \frac{2}{k+1}},$$

then

$$G_{sec} = F_{kp} \frac{p_k^*}{\sqrt{T_k^*}} m, \qquad (2.48)$$

where

$$m = \sqrt{\frac{gk}{R}\left(\frac{2}{k+1}\right)^{\frac{k+1}{k-1}}}. \qquad (2.49)$$

On the basis of (2.48), the specific chamber thrust, or the number β will be

$$\beta = \frac{\sqrt{T_k^*}}{m}. \qquad (2.50)$$

Since the temperature T_k^* depends on the type of fuel and, to a slight extent, on the fuel utilization in the chamber (η_k), while the quantity m, which is a function of the combustion-product composition (k, R), also depend chiefly on the fuel (and to a slight extent on p_k^*), the number β can serve as a thermodynamic characteristic of the fuel.

For an ideal lossless chamber

$$\beta_{id} = \frac{\sqrt{T_k}}{m} = \frac{\beta}{\varphi_k}, \qquad (2.51)$$

which permits us to establish the value of φ_k and, consequently, the level of losses in the actual chamber by computing β_{id} and determining β experimentally.

The value of β can be found for various fuels (with allowance for η_k and p_k^*); then Expression (2.48) can be used to find the per-second fuel consumption

$$G_{sec} = \frac{F_{kp} p_k^*}{\beta} \qquad (2.52)$$

for various values of nozzle throat area and chamber pressure. It follows from Formula (2.52) that for a given fuel the chamber pressure (for F_{kr} = const) is proportional to the per-second consumption.

Manuscript Page No.

Footnotes

31 [1]This does not contradict the second law of thermodynamics, since if $p_s = p_n = 0$, then $T_n = 0$ as well and in this case $\eta_t = 1$ for a Carnot cycle. In actuality, p_s never equals 0, while it is always the case that $\eta_t < 1$.

Manuscript Page No.

Transliterated Symbols

28 к = k = kamera = chamber

28 н = n = naruzhnyy = external

28 с = s = soplo = nozzle

29 ид = id = ideal'nyy = ideal

32 уд = ud = udel'nyy = specific

37 сек = sek = sekundnyy = per-second

37 эфф = eff = effektivnyy = effective

41 н = n = nachal'nyy = initial

41 к = k = konechnyy = final

45 т = t = toplivo = fuel

45 кр = kr = kriticheskiy = critical

Chapter 3

LIQUID ROCKET FUELS

3.1. GENERAL CONCEPTS

In liquid and solid rocket engines, energy is released as a result of a chemical reaction.

Energy can be released as a result of the following chemical reactions:

a) oxidation-reduction (oxidation) reaction, where the energy is released during a reaction between oxidizing and combustible elements; here the fuel consists of at least two substances, the oxidizer and the combustible;

b) a decomposition reaction, where the heat is released during the decomposition of a complex substance into simpler materials; here the fuel may consist of just a single substance;

c) a recombination (combination) reaction, where the heat is released when like atoms or radicals are combined into molecules.

Rocket-engine fuels can be divided into the following four groups: separately supplied liquid fuels; unitary liquid fuels; solid fuels; mixed-aggregate-state fuels.

For a separately supplied liquid fuel, energy is released as a result of an oxidation-reduction reaction. The oxidation reaction can be arbitrarily represented as an exchange of electrons at the outer electron shell of the atoms participating in the process. Here the atoms of combustible elements yield electrons, while the atoms of oxidizer elements acquire electrons.

The combustible elements include carbon C, hydrogen H, boron B, aluminum Al, lithium Li, beryllium Be, etc.

The oxidizer elements include fluorine F, oxygen O, chlorine Cl, and bromine Br. Fluorine and oxygen are considerably more effective than the other oxidizing elements.

In the general case, the oxidizer and combustible are complex compounds whose compositions may include both oxidizing and combustible elements.

A combustible is a substance that requires an external oxidizer

for complete oxidation of its combustible elements, whether or not it contains oxidizing elements.

Thus, in addition to combustible elements (C and H), ethyl alcohol C_2H_5OH contains an oxidizing element, oxygen, but not nearly enough for complete oxidation of the combustible components of the alcohol; thus ethyl alcohol is a combustible.

An oxidizer is a substance that may contain combustible elements, but which has a considerable excess of oxidizing elements, so that when its intrinsic combustible elements have been completely oxidized, a free quantity of oxidizing components is left that can be used to oxidize some other combustible. For example, nitric acid HNO_3 or hydrogen peroxide H_2O_2 contain a combustible, hydrogen, but the oxidizing component (oxygen) is present in sufficient quantity that when the oxygen of nitric acid or hydrogen peroxide has been fully oxidized, there is a residue of oxygen that can be used to oxidize a combustible; thus HNO_3 and H_2O_2 are oxidizers.

The proportions of oxidizer and combustible in a fuel are determined by a quantity called the mixture ratio.

The theoretical (stoichiometric) mixture ratio κ_0 is also defined as the minimum amount of oxidizer required for complete oxidation of 1 kgf of combustible. In other words, the theoretical mixture ratio is the ratio of oxidizer and combustible flowrates for which the oxidizer completely oxidizes the combustible while leaving no excess.

The actual mixture ratio κ is defined as the actual ratio of the rates at which oxidizer and combustible are supplied to the chamber; it can differ from the theoretical value. Ordinarily, $\kappa < \kappa_0$.

The ratio

$$\alpha = \frac{\kappa}{\kappa_0}$$

is called the excess-oxidizer coefficient. The excess-oxidizer coefficient at which maximum specific thrust occurs is called the optimal coefficient.

Separately supplied fuel can be hypergolic or diergolic. The hypergolic fuels include fuels whose oxidation and ignition reactions commence spontaneously when the oxidizer and combustible come into contact under the conditions obtaining in the chamber during launching, with no additional intervention. Diergolic fuels require some firing device for ignition (when the engine is started).

In general, a mixture of oxidizer and combustible presents an explosion hazard. Thus all factors that prevent accumulation of such a mixture in the engine tend to increase engine reliability. From this viewpoint, it is better to use hypergolic fuels, since the high chemical activity of the components in such a fuel makes it almost impossible for an oxidizer-combustible mixture to accumulate.

The high chemical activity of hypergolic fuels is often an important condition for ensuring engine operating stability.

Separately supplied liquid fuels are widely employed, since they provide quite high specific engine parameters with fairly acceptable operating properties.

By a unitary (single-component) fuel, we mean a substance or previously prepared mixture of substances that will release heat under certain conditions as a result of chemical reactions of decomposition or oxidation; in the latter case, all components required for oxidation are contained within the unitary fuel itself.

The greater structural simplicity of engines using unitary liquid fuels represents an undoubted advantage over separately supplied liquid fuels. Just a single supply-system line is required. These fuels have not found wide application in liquid rocket engines [LRE](ЖРД), and they are chiefly used for auxiliary purposes, for example, to drive turbines in turbopump units, and for auxiliary low-thrust engines designed to control and stabilize the flying craft The reason is that unitary liquid fuels having acceptable operating properties are relatively inefficient as compared with the widely employed separately supplied fuels. Unitary liquid fuels are known that possess fairly high efficiency, but they are unacceptable for operating purposes, basically owing to their great tendency to explode.

Solid rocket fuels are naturally unitary fuels, since they contain within themselves all substances required for the chemical reaction. Materials capable of an exothermal decomposition reaction, or oxidizer-combustible mixtures, can serve as a basis for solid rocket fuels.

Solid fuels are widely employed in rocket technology. They make it possible to use an engine of simpler design, which needs little preparation for launching. The known solid fuels have lower specific thrust than the liquid fuels, however.

Mixed-aggregate-state (hybrid) fuels consist of components that are in different aggregate states, such as a liquid-solid fuel, in which one of the components is solid and the other liquid. In this case, the solid component is placed within the chamber, while the liquid is carried in a tank and supplied in some way or another to the chamber, where a chemical reaction takes place between the oxidizer and combustible, with the formation of gaseous combustion products.

Liquid-solid fuels have certain advantages over both liquid and solid fuels. Such a hybrid fuel may have a certain advantage over a separately supplied liquid fuel in that the engine structure is simpler, since just one line is required to feed fuel to the engine. The hybrid fuel may be better than a solid fuel in that longer uninterrupted engine operation is possible, more flexible control can be used, and more efficient component pairs can be selected.

Liquid fuels are discussed in this chapter.

3.2. ROCKET-FUEL REQUIREMENTS

The type of fuel used for an engine and its properties to a considerable degree determine the characteristics (parameters) of the rocket engine and the flying craft, and markedly influence the construction, weight characteristics, and operating conditions.

TABLE 3.1

Molecular Heat Content c_{p_m} kcal/kgf·deg of Certain Gases at Various Temperatures, °K

Одноатомные газы [1]	2000	3000	4000	Двухатомные газы [2]	2000	3000	4000	Многоатомные газы [3]	2000	3000	4000
H	4,968	4,968	4,968	H_2	8,195	8,989	9,345	H_2O	12,008	12,913	13,308
B	4,968	4,968	4,968	B_2	8,852	8,901	8,923	CO_2	14,502	14,043	15,355
				N_2	8,602	8,861	8,989	BF_3	19,381	19,649	19,745
N	4,969	5,01	5,214	O_2	9,029	9,551	9,932	B_2O_3	25,159	25,534	25,663
O	4,977	5,004	5,091	F_2	8,881	8,915	8,927	Al_2O_3	25,159	25,534	25,663
F	5,001	4,983	4,977	HF	8,143	8,700	9,045				

1) Monatomic gases; 2) diatomic gases; 3) polyatomic gases.

Specific requirements are imposed on fuels. Although in most cases, they cannot be fully satisfied, nonetheless it is important to formulate these requirements so that a comparative evaluation of fuels can be made.

The fuel is primarily the factor responsible for such an important engine parameter as the specific thrust. Since the specific thrust of a rocket engine also depends on the parameters and quality of the engine process, to eliminate the influence of engine characteristics in a comparative evaluation of fuels, we proceed on the basis of the ideal specific thrust $P_{ud.id}$ (i.e., the specific thrust computed with no engine losses), determined for identical gas pressure reduction ratios in the nozzle.

The magnitude of the specific thrust depends on the amount of heat released during the chemical reaction, i.e., on the heating value of the fuel and the degree to which this heat is converted into the kinetic energy of the combustion products, i.e. ,the thermal efficiency.

The degree to which heat is converted into kinetic energy of the combustion products depends on the properties of the combustion products. It was shown in Chapter 2 that the thermal efficiency will be greater the higher the exponent k, i.e., the lower the molecular heat capacity c_{p_m} of the combustion products. As we know, the molecular heat capacity of gases depends principally on the number of atoms

in the molecule; it increases as the number of atoms goes up (Table 3.1).

The degree of conversion of the heat released in the chamber into kinetic energy is influenced by the dissociation of the combustion products. The greater the degree of dissociation, the lower the thermal efficiency. Different gases dissociate to different degrees. Thus, for example, most fluorides dissociate less than oxides. The dissociation of combustion products depends in great measure on the temperature, increasing as the temperature goes up. An increase in pressure reduces the degree of dissociation.

For a given heating value, the combustion-product temperature will be lower the higher the weight heat capacity of the products. For a given atomicity of the gases, the weight heat content of the gas will rise as the molecular weight decreases,

$$c_p = \frac{c_{p_m}}{\mu}.$$

The degree to which heat is converted into the kinetic energy of directed combustion-product motion also depends on the aggregate state. The expansion process that leads to such a conversion is completed only in gases. The thermal efficiency drops when the combustion products contain condensed substances. The greater the proportion of condensed substances in the combustion products, the lower the thermal efficiency.

Thus for a comparative qualitative evaluation of rocket fuels, where the specific thrust is not calculated, it is necessary to consider not only the heating value, but also the properties of the combustion products. From this viewpoint, they must satisfy the following basic conditions:

- high heating value;
- few atoms in the combustion-product molecules;
- low molecular weight of combustion products;
- maximum proportion of gases in combustion products.

Sometimes fuels are only compared for heating value in such an evaluation. In certain cases, such an approach can lead to an erroneous result, particularly if fuels differing in chemical nature are compared.

Let us look at an example. An oxygen + hydrazine fuel has a heating value h_u = 1940 kcal/kgf, less than for an oxygen + kerosene fuel (h_u = 2270 kcal/kgf). The first fuel provides greater specific thrust than the second, however (see Table 3.9). This is associated with the fact that the combustion products of the oxygen + hydrazine fuel have better thermodynamic properties (lower molecular weight and fewer atoms in the molecules) than the combustion products of the oxygen + kerosene fuel.

A comparison on the basis of heating value is permissible only for fuels of similar chemical compositions and, naturally, the evaluation can only be qualitative.

Rocket characteristics are influenced by the fuel density. An increase in density reduces the required tank capacity and, consequently, decreases the dimensions and relative weight of the vehicle structure.

For a liquid bipropellant, the oxidizer and combustible may differ in density. Then to characterize the fuel, we consider a certain arbitrary value of weight density, equaling the ratio of oxidizer and combustible weight to their total volume:

$$\gamma_т = \frac{G_{ок} + G_т}{V_{ок} + V_т}.$$

It is easily found that

$$\gamma_т = \frac{1 + \alpha}{\frac{1}{\gamma_т} + \frac{\alpha}{\gamma_{ок}}}.$$

Fuels should be stable, and their physical-chemical properties should not change during operation, storage, or transportation. To preserve the aggregate state, liquid-fuel components should have high boiling points and low freezing points, while solid fuels should have high melting points.

Fuels should present no explosion hazard, should not be harmful to personnel, and should be relatively uncorrosive or not corrosive at allfor the structural materials encountered in storage, transportation, and operation.

The physical-chemical properties of fuels should ensure stable engine operation over a wide range of regimes. It is important for liquid fuels that their components be usable as engine coolants.

The fuel selected should have an adequate industrial base for extraction and processing, so that the required amounts of fuel will be available at the lowest possible price.

3.3. EFFECTIVENESS OF ELEMENTS AS ROCKET-FUEL COMPONENTS

Let us consider oxidizing processes occurring between elements on the assumption that under normal conditions they are in a stable state. This means that under these conditions certain elements are in the molecular state (H_2, F_2, O_2, etc.), while others are in the atomic state (C, Al, B, Be, etc.).

Tables 3.2-3.4 show the parameters of the principal combustible and oxidizer elements, their total combustion (oxidation) products, as well as the energy characteristics of the oxidation reaction: the heating value and ideal specific thrust. Some of the values are approximate.

The heating-capacity values for oxidation products with high boiling and melting points are given for two cases: in the first case, the oxidation products have been brought to the solid or liquid state (higher heating value h_0); in the second case, they have been brought to the gaseous state (working heating value h_u).

TABLE 3.2

Properties of Combustible and Oxidizing Elements

1 Наименование элемента	2 Формула	3 Молекулярный вес	4 Температура плавления °С	5 Температура кипения °С	6 Весовая плотность кГ/л	7 Фаза, соответствующая весовой плотности*
8 Водород	H_2	2.016	—257	—253	0.0709	ж
9 Литий	Li	6.941	186	1400	0.537	тв
10 Бериллий	Be	9.02	1280	—	1.85	тв
11 Бор	B	10.82	2300	—	1.73	тв
12 Углерод	C	12.01	3500	4200	2.17—2.3	тв
13 Натрий	Na	22.997	97.5	880	0.97	тв
14 Магний	Mg	24.32	650	1120	1.74	тв
15 Алюминий	Al	26.97	658	2000	2.7	тв
16 Кремний	Si	28.06	1414	2400	2.35	тв
17 Калий	K	39.096	62.5	760	0.86	тв
18 Кальций	Ca	40.08	809.6	1240	1.55	тв
19 Кислород	O_2	32	—218	—183	1.14	ж
20 Фтор	F_2	38	—223	—182	1.51	ж
21 Хлор	Cl_2	70.914	—101.6	—34.6	1.56	ж

*Ж) liquid; ТВ) solid.

1) Element; 2) formula; 3) molecular weight; 4) melting point, °C; 5) boiling point, °C; 6) weight density, kgf/l; 7) phase corresponding to weight density*; 8) hydrogen; 9) lithium; 10) beryllium; 11) boron; 12) carbon; 13) sodium; 14) magnesium; 15) aluminum; 16) silicon; 17) potassium; 18) calcium; 19) oxygen; 20) fluorine; 21) chlorine.

The tables confirm that the most effective oxidizing elements are fluorine and oxygen. Thus oxidizers based on these elements are also effective. Hydrogen is very effective among the combustible elements. Oxidation reactions with several metals, silicon, etc., are accompanied by a large thermal effect. The parameters of the oxides (the products resulting from combustion of these elements in oxygen) are not always favorable, however. These oxides have a high boiling point, so that condensed phase can be present in the combustion products of some of them (BeO, Al_2O_3, for example). The thermal effect of the oxidation reaction for these elements, referred to the

TABLE 3.3

Basic Parameters for Reactions of Combustible Elements and Liquid Oxygen

1 Горючий элемент	2 Химическая формула окисла	3 Параметры окисла: 4 молекулярный вес	$t_{пл}$ °C	$t_{кип}$ °C	π_0	h_0 ккал/кГ 5	h_u ккал/кГ 6	$P_{уд.т}$ кГ·сек/кГ при π=100 7
H_2	H_2O	18,016	0	100	7,95	—	3030	400
Li	Li_2O	29,88	1300	1700	1,16	4700	3400	370
Be	BeO	25,02	2500	3900	1,78	5300	—	—
B	B_2O_3	69,64	450	2150	2,21	4340	3100	290
C	CO_2	44,01	—	—78	2,66	—	2070	300
Na	Na_2O	61,99	—	1275	0,348	1600	—	—
Mg	MgO	40,32	2800	3000	0,66	3600	—	
Al	Al_2O_3	101,94	2050	2980	0,855	3800	2440	270
Si	SiO_2	60,06	1470	2600	1,19	3400	2000	290
K	K_2O	94,19	800	1500	0,205	900	—	—
Ca	CaO	56,08	2570	2850	0,4	2700	—	—

1) Combustible element; 2) chemical formula of oxide; 3) oxide parameters; 4) molecular weight; 5) h_0, kcal/kgf; 6) h_u, kcal/kgf; 7) $P_{ud.id}$, kgf·s/kgf at π = 100.

case in which the oxides are in the gaseous state, is not very great. The oxides of several elements have a high molecular weight and many atoms (Al_2O_3, B_2O_3, for example), which explains the relatively moderate thermal efficiency and, therefore, the relatively low specific thrust for high heating values. Such methods can be effectively utilized in conjunction with other combustible elements (hydrogen in particular, whose oxidation products possess favorable thermodynamic characteristics, so that they successfully combine high heating values and good thermal efficiency, and can give high specific thrust, on the whole.

Following hydrogen in effectiveness when combined with oxygen are lithium, carbon, and boron. Carbon and hydrogen are the most common combustible components in rocket-engine fuels.

It is clear from Tables 3.3 and 3.4 that for most of the combustible elements considered, it is more effective to combine them with fluorine than with oxygen. In certain cases, this is explained by the more favorable parameters of fluorides as compared with oxides (fewer atoms and lower boiling point), and in others by the greater thermal effect. Hydrogen, lithium, beryllium, boron, magnesium, and aluminum are particularly effective with fluorine.

Table 3.5 shows certain oxidation processes for several elements that take the form of atoms in the initial state.

TABLE 3.4

Basic Parameters for Reaction of Combustible Elements with Liquid Fluorine

1 Горючий элемент	2 Формула фторида	Параметры фторида: молекулярный вес 4	$t_{кд}$ °C	$t_{кип}$ °C	α_0	h_0 ккал/кГ 5	h_u ккал/кГ 5	$P_{уд.им.}$ кГ·сек/кГ при π=100 6
H_2	HF	20,008	−[illegible]	19,5	18,9	—	3030	420
Li	LiF	25,94	842	1670	2,74	5000	3170	420
Be	BeF_2	47,02	800	—	4,22	5600	3800	380
B	BF_3	67,82	−127	−100	5,26	—	3700	350
C	CF_4	88,01	−183	−128	6,3	—	2500	—
Na	NaF	42	990	1700	0,825	—	1800	—
Mg	MgF_2	62,32	1270	2240	1,56	4200	3080	340
Al	AlF_3	83,97	1040	1290	2,12	3700	2800	310
Si	SiF_4	104,06	—	−95	2,71	—	3400	300
K	KF	58,1	880	1500	0,486	—	1400	—
Ca	CaF_2	78,06	1400	2500	0,95	3700	2600	330

1) Combustible element; 2) fluoride formula; 3) fluoride parameters; 4) molecular weight; 5) kcal/kgf; 6) kgf·s/kgf at.

TABLE 3.5

Oxidation Processes Between Atoms

1 Реакция	2 Молекулярный вес продуктов реакции	3 Тепловой эффект реакции ккал/кГ
$2O+C=CO_2$	44,00	4850
$O+2H=H_2O$	18,06	12200
$H+F=HF$	20,01	7730

1) Reaction; 2) molecular weight of reaction products; 3) reaction thermal effect, kcal/kgf.

TABLE 3.6

Recombination Reaction

1 Реакции	2 Молекулярный вес продуктов реакции	3 Тепловой эффект реакции ккал/кГ
$H+H=H_2$	2,016	51 600
$D+D=D_2$	4,03	25 900
$N+N=N_2$	28,02	6 110
$O+O=O_2$	32,00	3 800
$NH+NH=N_2+H_2$	15,00	5 300

1) Reactions; 2) molecular weight of reaction products; 3) reaction thermal effect, kcal/kgf.

It follows from the table that if all of the initial elements for the reactions considered are in the atomic state the fuel will be more effective in virtue of the higher thermal effect.

Combination reactions between certain like elements and radicals are accompanied by large thermal effects. Some of these recombination reactions are shown in Table 3.6.

From Tables 3.5 and 3.6 we can conclude that by using recombination reactions of atoms and radicals in rocket engines, as well as oxidation reactions between atoms, it is possible to obtain high specific thrust. Many atoms, however (H, N, O, etc.) and radicals of interest from this viewpoint cannot exist for any length of time under ordinary conditions, and in practice combine instantaneously to form molecules. To make practical utilization in engines of recombination or oxidation reactions of elements in the atomic state it is necessary to find methods for keeping these atoms and radicals in the free state so that the molecular-generation reactions take place only within the engine chamber.

Atomic oxygen and nitrogen have been obtained in "frozen" form at a temperature of 4°K. When this "frozen" system is heated to 20-30°K, the atoms recombine actively, releasing much heat.

3.4. SEPARATELY SUPPLIED LIQUID FUELS

On the basis of storage and operating conditions, liquid fuels can be divided into conveniently storable (long shelf life) and nonconveniently storable. The first group includes substances that can be stored for long periods at ordinary ambient temperatures with no perceptible loss, and with no need for special measures complicating operation with the substances. Utilization of such materials means that the craft can be maintained for long periods in fueled condition, and thus rapidly readied for launching. The nonconveniently storable group chiefly includes the so-called cryogenic substances (liquefied gases), which have low boiling points and low critical temperatures. Liquid oxygen is an example.

All liquefied gases are ordinarily stored at a temperature close to the boiling point. This means that there is continuous evaporation, and it is necessary to use special heat-insulated tanks to reduce the evaporation losses.

Chemically unstable substances also present storage difficulties.

Petroleum-base combustibles can be stored for long periods, for example. The long-shelf-life components include nitrogen tetroxide, in particular. Although its boiling point is not high, a slight increase in tank pressure eliminates this drawback.

Table 3.7 and 3.8 show the basic physical parameters of oxidizers and combustibles for separately supplied liquid fuels. The properties of the pure substances are indicated. Both oxidizers and combustibles frequently include various additives resulting from processing techniques and introduced to improve various character-

TABLE 3.7

Physical Parameters of Oxidizers

1 Окислитель	2 Формула	3 Молекулярный вес	4 Весовая плотность кГ/л	$t_{пл}$ °C	$t_{кип}$ °C
5 Кислород	O_2	32	1,14*	−218	−183
6 Перекись водорода	H_2O_2	34,02	1,44	−1	150
7 Азотная кислота	HNO_3	63,02	1,52	−41,2	85
8 Четырехокись азота	N_2O_4	92,02	1,46	−11	21
9 Тетранитрометан	$C(NO_2)_4$	196	1,65	13,6	127
10 Фтор	F_2	38	1,51*	−223	−182
11 Озон	O_3	48	1,45*	−252	−112
12 Окись фтора	OF_2	54	1,53*	−223	−144
13 Трехфтористый хлор	ClF_3	92,46	1,7	−82,6	−12,1
14 Пятифтористый бром	BrF_5	175	2,5	−61,3	40,5
15 Перхлорил фтора	ClO_3F	102,5	1,89	−110	−46,8

*Weight density for liquefied gases is given for a temperature close to the boiling point.

1) Oxidizer; 2) formula; 3) molecular weight; 4) weight density, kgf/l; 5) oxygen; 6) hydrogen peroxide; 7) nitric acid; 8) nitrogen tetroxide; 9) tetranitromethane; 10) fluorine; 11) ozone; 12) fluorine oxide; 13) chlorine trifluoride; 14) bromine pentafluoride; 15) perchloryl fluorine.

TABLE 3.8

Physical Parameters of Combustibles

[1] Горючее	[2] Формула	Молекулярный [3] вес	Весовая плотность кГ/л [4]	$t_{пл}$ °C	$t_{кип}$ °C
[5] Керосин	—	—	0,79—0,83	—60	130—150*
[6] Анилин	$C_6H_5NH_2$	93,13	1,02	—6,2	184,4
[7] Триэтиламин	$N(C_2H_5)_3$	101,2	0,728	—115	89,5
[8] Ксилидин	$C_6H_3(CH_3)_2NH_2$	121,2	0,98	—20	210
[9] Тонка (50% ксилидина +50% триэтиламина)	—	—	0,85	<—70	87*
[10] Анилин + фурфуриловый спирт	—	—	1,08	—	—
[11] Метиловый спирт	CH_3OH	32,04	0,796	—94,8	64,6
[12] Этиловый спирт	C_2H_5OH	46,07	0,789	—112,0	78,3
[13] Изопропиловый спирт	C_3H_7OH	60,09	0,786	—85,8	82,3
[14] Аммиак	NH_3	17,03	0,68	—77	—33
[15] Гидразин	N_2H_4	32,05	1,01	2	113,5
[16] Несимметричный диметилгидразин	$N_2H_2(CH_3)_2$	60,10	0,83	—57,2	63,1
[17] Монометилгидразин	$CH_3N_2H_3$	46,07	0,8	—52,0	88,0
[18] Пентаборан	B_5H_9	63,17	0,63	—47,0	50,0

*Initial boiling point.

1) Combustible; 2) formula; 3) molecular weight; 4) weight density, kgf/l; 5) kerosene; 6) aniline; 7) triethylamine; 8) xylidine; 9) Tonka (50% xylidine + 50% triethylamine); 10) aniline + furfuryl alcohol; 11) methyl alcohol; 12) ethyl alcohol; 13) isopropyl alcohol; 14) ammonia; 15) hydrazine; 16) unsymmetrical dimethyl hydrazine; 17) monomethyl hydrazine; 18) pentaborane.

istics. Naturally, the parameters of such substances will differ somewhat from the parameters of the pure materials. The properties of several oxidizers and combustibles are briefly described below.

Oxidizers

Liquid oxygen is widely employed in technology, and has an advanced industrial processing base, with unlimited supplies of raw material.

Many materials become brittle at the temperature of liquid oxygen (steel, cast iron, rubber, etc.). Copper and aluminum and their alloys are stable in this respect, as well as alloy steels, for example, chrome-nickel steel.

Liquid oxygen presents no explosion hazard in pure form; if oil or other organic compounds enter liquid oxygen, however, explosive mixtures will form. For this reason, all parts in contact with liquid oxygen must be cleaned and degreased. Liquid oxygen is nontoxic and noncorrosive.

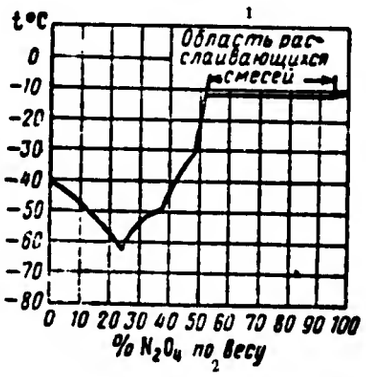

Fig. 3.1. Melting point of mixture of nitrogen tetroxide and nitric acid. 1) Region of mixture separation; 2) by weight.

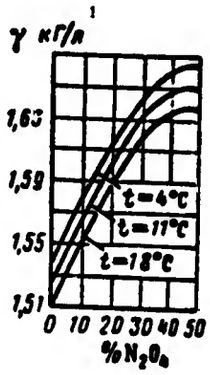

Fig. 3.2. Weight density of mixtures of nitric tetroxide and nitric acid. 1) kgf/l.

Special heat-insulated tanks are used to reduce liquid-oxygen losses during storage and transportation.

Nitric acid is widely employed in various industries, has an extensive industrial base, and is an inexpensive product.

Technical nitric acid contains 2-4% of impurities, chiefly water, as well as nitric tetroxide; thus its physical parameters differ somewhat from the values shown in Table 3.7.

Chemically pure nitric acid is colorless; technical nitric acid is light yellow owing to the presence of the nitrogen tetroxide.

Nitric acid is a quite stable compound, and can be stored with

no special complications for long periods of time. Nitric acid attacks most structural materials. Chrome-nickel and chrome steels, aluminum, and aluminum alloys have the greatest corrosion resistance to nitric acid. The corrosiveness of nitric acid can be reduced by adding special substances (inhibitors). Certain compounds of fluorine, phosphorous, and iodine are used as inhibitors.

Nitric acid is harmful to the human organism. Burns result when it comes into contact with the skin; contact with the eye is particularly dangerous. Nitric acid vapors are poisonous; breathing of air containing large amounts of nitric acid vapors may lead to poisoning. Special clothing and protection must be employed in work with nitric acid.

Nitric acid is not explosive by itself, but like other oxidizers, with organic compounds it forms explosive mixtures. Thus nitric acid cannot come into contact with the combustible during operation.

Nitrogen tetroxide is a yellow liquid at ordinary temperatures. As the temperature increases, it dissociates to form the dioxide, while absorbing heat. The increased percentage of nitrogen dioxide imparts a brown color, while the endothermal thermal effect results in increased heat capacity. Nitric tetroxide is considerably less corrosive for structural materials than nitric acid.

Nitrogen tetroxide mixes with nitric acid, but not in all concentrations; mixtures containing between 52 and 98% N_2O_4 will separate.

An increased N_2O_4 content of the mixture will improve the mixture properties: the freezing point drops (to an N_2O_4 content of the order of 40%, see Fig. 3.1), the weight density increases (Fig. 3.2), the specific thrust of nitrogen tetroxide base fuels rises, the corrosiveness drops for structural materials; there is some reduction in boiling point, however (Fig. 3.3).

Hydrogen peroxide (anhydrous) is a colorless transparent liquid having a bluish hue in large quantities.

In LRE, it is used in water solutions of 80-90% or greater concentration.

Hydrogen peroxide, when anhydrous or with low water content, is an unstable chemical compound, and can break down to form water and oxygen, with release of heat:

$$H_2O_2 = H_2O + {}^1/_2O_2.$$

Chemically pure hydrogen peroxide and its water solutions break down slowly even at somewhat elevated temperatures, but many factors facilitate more rapid decomposition (heat, certain metals, various contaminants, etc.).

This property of hydrogen peroxide makes it necessary to take special measures in operation. These include: the addition of stabilizers (substances retarding decomposition); selection of special structural materials having no influence on breakdown and not cor-

roding in hydrogen peroxide (pure aluminum, certain aluminum alloys, and certain types of stainless steels); and satisfaction of special storage conditions (tank cleanliness, moderate temperatures, etc.). Stabilized pure hydrogen peroxide is a relatively stable product, and when specified rules are observed, it can be stored for long periods without noticeable decomposition (about 1% per year).

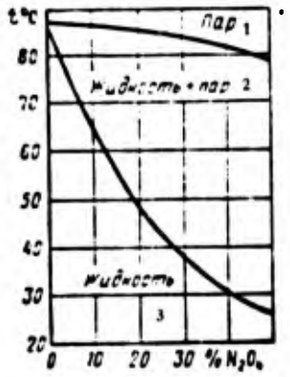

Fig. 3.3. Boiling points for mixtures of nitrogen tetroxide and nitric acid. 1) Vapor; 2) liquid + vapor; 3) liquid.

Liquid fluorine is a liquid gas. It is an extremely active oxidizer, and reacts energetically with many substances even at ordinary temperatures.

Fluorine is very toxic, and has a harmful effect on the organism. The low boiling point in conjunction with the toxic characteristics makes it very difficult to operate with fluorine. Liquid fluorine is mixed with oxygen. Like pure fluorine, these mixtures form inflammable combinations with many combustibles.

Combustibles

Petroleum-based combustibles, a group that includes combustibles made from products of petroleum refining, are mixtures of hydrocarbons with various chemical structures and various molecular weights. Different petroleum-based combustibles (kerosene, gasoline, etc.) when paired with the same oxidizer yield similar values of specific thrust. The weight density of petroleum combustibles fluctuates between 0.7 and 0.9 kgf/l. Since the combustible represents the smaller fraction of the fuel, however, this range of variation in combustible density has comparatively little influence on the change in the relative density of the fuel as a whole.

Kerosene is often used in LRE. This is a result of its favorable physical properties and the existence of a broad extraction and processing industry. In many cases, selection of petroleum-based combustibles containing specific hydrocarbons can provide better conditions for the combustion process and more stable engine operation.

Petroleum-based combustibles will not ignite upon contact with ordinary oxidizers. Thus engines using such combustibles ordinarily have a special ignition source.

Alcohols (isopropyl, ethyl, and methyl) are used in LRE owing to their availability, stability, and other physical-chemical properties.

Alcohols do not ignite upon contact with oxidizers. They are somewhat less efficient combustibles than kerosene, i.e., alcohol-burning engines will have somewhat lower specific thrust, all other conditions being equal, so that alcohols are finding fewer and fewer applications, as they give way to more effective combustibles.

Amines are a group that includes ammonia derivatives in which individual hydrogen atoms are replaced by hydrocarbon radicals. Aniline, triethylamine, xylidine, etc., are employed in LRE. These substances ignite easily whencombined with many common oxidizers, in particular, with nitric acid, nitrogen tetroxide, and their mixtures. Many of these materials (xylidine, aniline, triethylamine, etc.) are poisonous; they will poison the organism upon coming into contact with the skin or when the vapors are breathed.

For the sake of better physical parameters or increased chemical activity, amines are often used not in the pure form, but as mixtures with other substances, including other amines. For example, a mixture of triethylamine and xylidine (so-called "Tonka"), a mixture of aniline with furforyl alcohol, and other mixtures are employed. Amines and amine-based combustibles are close to petroleum-product combustibles in effectiveness.

Ammonia and hydrazine contain hydrogen as the combustible element. This provides favorable thermodynamic parameters for the combustion products (low atomicity and low molecular weight). They are very effectively used with fluorine and its derivatives. Ammonia and hydrazine are poisonous. Under certain conditions, their vapors mix with air to form explosive combinations. When hydrazine is used as a combustible, it is ordinarily mixed with other combustibles (ammonia, dimethyl hydrazine, etc.).

Hydrazine derivatives are obtained by replacing hydrogen atoms in the hydrazine by hydrocarbon radicals, for example, as in monomethyl hydrazine or dimethyl hydrazine. Unsymmetrical dimethyl hydrazine [UDMH](НДМГ) is used in LRE; it has a lower melting point than the symmetrical modification. Metals are not corroded by UDMH, and it can be stored for long periods.

Hydrogen as we have already mentioned, combines with oxygen and fluorine to yield very large values of specific thrust. Hydrogen has an extremely low boiling point, however (−253°C) and is low in density. The low boiling point raises certain difficulties in operation and storage, while the low weight density requires large tank volume. It is necessary to prevent air from entering the hydrogen tanks, since air freezes at the boiling point of hydrogen and, moreover, a hydrogen-air mixture can ignite over a wide range of concentrations. Published data, accumulated experience and special research show, however, that hydrogen is no

more dangerous to handle than many other fuel components, although certain operating rules must be observed. Hydrogen is now successfully employed in rocket technology.

Hydrogen can exist in two modifications, one called ortho hydrogen and the other para hydrogen. A definite equilibrium concentration of these two modifications corresponds to each temperature. Thus at the boiling point (20.2°K), only 0.2% will be represented by the ortho modification. At normal temperature and above, 75% will be ortho and 25% para. Hydrogen having this composition is called **normal hydrogen.**

It must be remembered that the transition from one state to another is accompanied by a thermal effect; the transition from the ortho to the para state involves the release of heat. Without catalysts, the transition is extremely slow, so that if normal hydrogen is cooled and liquefied, while in the liquid state it will also contain 75% ortho and 25% para modification. The ortho hydrogen will gradually be transformed to para hydrogen, with the release of heat. As a result, some of the hydrogen will gradually evaporate and be lost, so that liquid hydrogen should be used in the para modification.

Metals are difficult to use in pure form as LRE combustibles, since under normal conditions they are in the solid phase; thus they are best used as suspensions in liquid combustibles or as chemical compounds with other elements. It follows from what we have said previously (§3.3), that it is very effective to use suspensions of metals in hydrogen-containing combustibles; compounds of metals and hydrogen, the metal hydrides, should also be effective. Calculations have confirmed this. The outstanding hydrides from the viewpoint of physical properties and amount of research are boron hydride and pentaborane, which is a liquid under ordinary conditions. Like the other hydrides of boron, pentaborane is toxic; it breaks down when heated.

In addition to the metal hydrides, other metal compounds such as certain organometallic compounds can be considered as combustibles.One such material is triethyl aluminum $Al(C_2H_5)_3$ ($t_{pl} = -47°C$; $t_{kip} = 186°C$), which ignite spontaneously with oxygen. There is some indication that it is used for ignition of certain American oxygen engines.

Separately Supplied Liquid Fuels

Table 3.9 shows the energy characteristics of certain combinations of oxidizer and combustible, and the values of relative fuel density.

Of the fuels shown, those using nitrogen oxidizers and liquid oxygen are now in wide use. Fuels based on hydrogen peroxide are also employed occasionally.

Fuels based on liquid oxygen provide the greatest specific thrust of all presently employed fuels. The low oxidizer boiling

TABLE 3.9

Parameters of Separately Supplied Fuels

1 Окислитель	2 Горючее	3 h_u, ккал/кГ	4 $P^{\circ}_{уд.пл}$ кГ·сек/кГ	5 $\gamma_т$, кГ/л
O_2	H_2	3030	400	0,35
O_2	6 Керосин	2270	310	1,01
O_2	C_2H_5OH	2020	300	1,1
O_2	$N_2H_2(CH_3)_2$	2230	320	1,01
O_2	N_2H_4	1940	325	1,07
O_2	B_5H_9	—	335	0,9
HNO_3	6 Керосин	1440	265	1,32
HNO_3	7 Тонка	1460	267	1,32
HNO_3	$N_2H_2(CH_3)_2$	—	275	1,3
N_2O_4	6 Керосин	1700	285	1,27
N_2O_4	$N_2H_2(CH_3)_2$	—	295	1,24
N_2O_4	N_2H_4	—	300	1,22
N_2O_4	B_5H_9	—	315	1,12
F_2	H_2	3030	420	0,65
F_2	N_2H_4	2420	370	1,32
F_2	NH_3	2300	365	1,18
F_2	B_5H_9	—	365	1,27
OF_2	N_2H_4	—	355	1,25
OF_2	6 Керосин	—	350	1,32
O_3	6 Керосин	3000	335	1,25
$C(NO_2)_4$	6 Керосин	1720	285	1,42
90% H_2O_2	6 Керосин	—	275	1,29
H_2O_2	6 Керосин	—	285	1,31
H_2O_2	N_2H_4	—	295	1,27
H_2O_2	B_5H_9	—	325	1,02
ClF_3	N_2H_4	—	300	1,48

*The specific-thrust values are given for π = = 100 and total expansion in the nozzle.

1) Oxidizer; 2) combustible; 3) kcal/kgf; 4) kgf·s/kgf; 5) kgf/l; 6) kerosene; 7) Tonka.

point is a drawback, making liquid oxygen difficult to use for craft that must spend relatively long periods in a state of complete preparedness.

At present, liquid oxygen is used in the main with petroleum-based combustibles (chiefly kerosene), as well as combustibles based on dimethyl hydrazine and several other substances. Hydrazine and pentaborane provide somewhat greater specific thrust with oxygen (see Table 3.9).

Oxygen-hydrogen fuels occupy a special position. They yield 25-45% more specific thrust than other fuels.

Oxygen-hydrogen fuel is used in the United States for engines used to launch artificial satellites and spacecraft, where the specific thrust is of utmost importance, and the inconveniences resulting from the properties of these components (particularly hydrogen) are not decisive.

Fuels based on nitric acid, nitrogen tetroxide, and their mixtures are inferior to liquid-oxygen based fuels in specific thrust. They have an advantage in their high weight density and in the fact that the components of these fuels are high-boiling substances with long shelf life; thus craft can be held for long periods in a state of full readiness. The corrosiveness of nitric acid represents a certain restriction, since it results in gradual corrosion of feed-system tanks and fittings.

Nitric acid oxidizers are used in combination with petroleum-based combustibles, and with combustibles based on amines (Tonka, for example). They can also be coupled with more effective combustibles: dimethyl hydrazine, hydrazine, etc. For example, the Titan-2 rocket uses a fuel consisting of nitric tetroxide and aerozine, which permits the missile to be kept in the fueled state for long periods. Aerozine is a mixture of equal amounts of dimethyl hydrazine and hydrazine. The addition of UDMH to hydrazine improves the thermal stability of the combustible, while lowering its melting point (t_{pl} = -8°C for aerozine).

Aerozine has some advantage in density and specific thrust over UDMH.

Table 3.9 shows specific-thrust values for a fuel based on HNO_3 and N_2O_4; as we can see, nitrogen tetroxide provides greater specific thrust. Fuels using a mixture of HNO_3 + N_2O_4 have 2-5% greater specific thrust than for nitric acid alone (depending on the N_2O_4 content). It has been shown that the addition of N_2O_4 to nitric acid also increases the density of the oxidizer and, consequently, of the fuel. Figure 3.4 illustrates the influence of the N_2O_4 content of nitric acid on the specific thrust of a fuel using kerosene as the combustible.

Nitrogen oxidizers form hypergolic fuels in conjunction with combustibles based on amines, dimethyl hydrazine, and certain other substances.

Hyperbolic fuels should have a short ignition delay $\tau_{з0}$ when the engine is started. By the delay period, we mean the time between the instant at which the oxidizer and combustible come into contact and the time at which they ignite during a launch. If this time is long, a relatively large amount of fuel may accumulate in the combustion chamber during the starting period, and ignition and combustion will be accompanied by a sharp rise in pressure. When $\tau_{з0}$ is very long, experience shows that explosive combustion may occur rather than normal ignition.

Thus a requirement is imposed on hypergolic fuels to the effect that the ignition delay not exceed a specified value,

$$\tau_{з0} < 0{,}03 \text{ с}.$$

The value of $\tau_{з0}$ depends on the oxidizer and combustible types, on their temperature, and on many other factors. As the temperature goes up, $\tau_{з0}$ decreases (Fig. 3.5).

Fuels based on hydrogen peroxide deliver specific thrusts almost equaling the values obtainable from fuels based on nitrogen oxidizers. Since its operating characteristics are less favorable, H_2O_2 is less often used as an oxidizer.

Calculations show that high specific thrust values can be obtained from fuels with hydrogen peroxide if certain metal-based compounds are used as combustibles, in particular, the hydrides of metals. This results from a favorable combination of heating value and combustion-product composition.

Fuels made up of hydrogen peroxide and liquid hydrides of metals are one of the most efficient fuels with high-boiling components.

Fuels based on low-boiling fluorine oxidizers (liquid fluorine and liquid fluorine oxide) are very efficient. It is best to use fluorine with combustibles containing no carbon, since the product resulting from combustion of carbon in fluorine (CF_4) has high atomicity and high atomic weight, which somewhat impairs the combustion-product characteristics. These combustibles primarily include hydrogen, hydrazine, and ammonia. Certain metal-containing combustibles are also effective with fluorine. Certain carbon-containing combustibles such as dimethyl hydrazine are also effective with oxygen fluoride, owing to its oxygen content.

Despite the very unfavorable physical properties of fluorine oxidizers, their use in rocket fuels makes it possible to increase engine specific thrust considerably, which is particularly important for long-range and space vehicles.

High-boiling fluorine-containing oxidizers (ClF_3, BrF_5) provide less specific thrust since they contain the inefficient oxidizing elements Cl, Br, but they have high density.

Ozone-based fuels are explosive. The breakdown of ozone to form oxygen is accompanied by heat release (720 kcal/kgf), so that when combustibles are burned in ozone, more heat is released, and

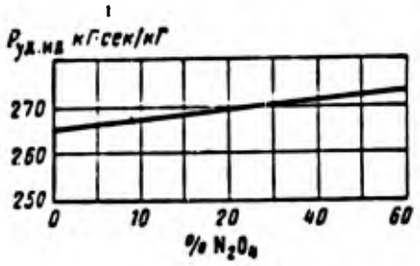

Fig. 3.4. Specific thrust of fuel (HNO_3 + N_2O_4 oxidizer and kerosene combustible) as function of weight content of N_2O_4 in oxidizer at π = 100. 1) kgf·s/kgf.

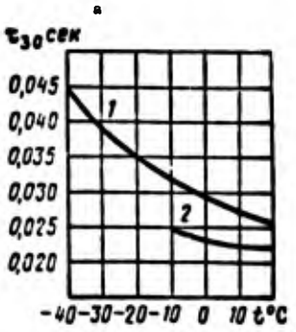

Fig. 3.5. Delay in ignition of "Tonka" with oxidizers as function of temperature. 1) HNO_3; 2) N_2O_4. a) s.

the specific thrust with ozone can be roughly 10% greater than for oxygen; it will only be possible to use ozone in LRE when methods can be found to eliminate the explosion hazard.

3.5. LIQUID UNITARY FUELS

We have previously noted that individual liquid substances capable of an exothermal decomposition reaction as well as previously prepared oxidizer-combustible mixtures can be used as liquid unitary fuels.

A common property of many liquid unitary fuels is a tendency to knocking as well as to direct detonation when certain factors (shock, heating, etc.) act. This tendency depends on the nature of the material.

It is known that a positive reaction thermal effect is a necessary condition for explosive transformation of a system. Thus the tendency to explosive transformation and the explosive force is often higher for substances with identical chemical natures the higher the heating value (the heat of decomposition). In part, this accounts for the fact that unitary fuels presenting no explosion hazard possess a relatively small heating value and thus provide a relatively small specific thrust for the engine.

TABLE 3.10

Parameters of Nitro Compounds and Complex Esters of Nitric Acid

1 Название	2 Формула	Молекулярный вес	$t_{пл}$ °C	$t_{кип}$ °C	4 γ кГ/л	a_{O_2}	5 Теплота разложения ккал/кГ
6 Нитроглицерин	$C_3H_5(ONO_2)_3$	227	13,5	—	1,60	1,06	1485
7 Нитрогликоль	$C_2H_4(ONO_2)_2$	152	—	85	1,50	1,0	1580
8 Нитрометан	CH_3NO_2	61	– 29	101	1,13	0,572	1040
9 Нитроэтан	$C_2H_5NO_2$	76	—	103	1,05	0,307	680
10 Метилнитрат	CH_3ONO_2	77	—	65	1,21	0,857	1490
11 Этилнитрат	$C_2H_5ONO_2$	91	—112	87	1,12	0,46	713
12 Пропилнитрат	$C_3H_7ONO_2$	105	—	110,5	1,06	0,315	550
13 Изопропилнитрат	$C_3H_7ONO_2$	105	—60	101	1,02	0,315	550

1) Name; 2) formula; 3) molecular weight; 4) kgf/l; 5) heat of decomposition, kcal/kgf; 6) nitroglycerine; 7) nitroglycol; 8) nitromethane; 9) nitroethane; 10) methyl nitrate; 11) ethyl nitrate; 12) propyl nitrate; 13) isopropyl nitrate.

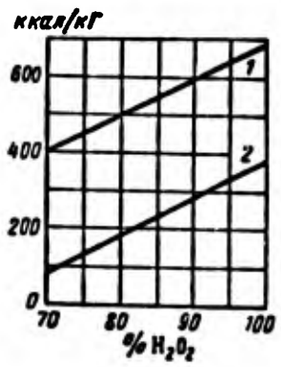

Fig. 3.6. Heat of decomposition of hydrogen peroxide as function of content in water mixture. 1) Higher heating value; 2) lower heating value.

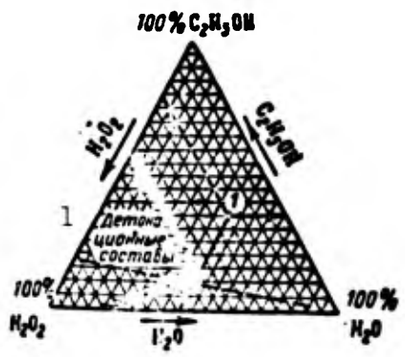

Fig. 3.7. Diagram for mixtures of hydrogen peroxide with ethyl alcohol and water. 1) Detonation compositions.

Let us consider individual groups of possible unitary fuels.

Nitro compounds and complex esters of nitric acid are organic compounds containing nitro (NO_2) and nitrate (ONO_2) groups. Many of these substances can sustain exothermal decomposition reactions, and are widely employed as explosives. These compounds contain both combustible (C, H) and oxidizer (O) elements.

The decomposition (combustion) reaction of these substances can be represented as their decomposition into atoms and subsequent oxidation of the combustible elements to form oxides. For example, the decomposition of methyl nitrate takes place as follows:

$$CH_3-ONO_2=CO_2+H_2O+\frac{1}{2}H_2+\frac{1}{2}N_2.$$

Many properties of such substances, primarily the heat of decomposition, depend on the proportions of oxidizing and combustible lements contained. In the theory of explosives, the proportion of oxidizer and combustible elements in a substance is characterized by a quantity called the oxygen balance. The oxygen balance is defined as the excess (positive oxygen balance) or defect (negative oxygen balance) of oxygen in the substance as compared with the amount needed for total oxidation of the combustible elements contained by the substance.

We shall characterize the oxygen balance quantitatively in terms of a quantity analogous to the excess-oxidizer coefficient: the oxygen-excess coefficient α_{O_2}, the ratio of the amount of oxygen contained in the given compound to the amount required for total oxidation of its combustible elements.

Table 3.10 shows the parameters of certain nitro compounds and nitric acid esters. Since the decomposition products of these substances have roughly identical properties, only the heats of decomposition are given for a comparative qualitative evaluation of their effectiveness. It is clear from Table 3.10 that the closer α_{O_2} is to unity, the higher the heat of decomposition of the substance will be in the general case. This law also holds, in approximation, for explosives. The least explosive substances considered have a considerable oxygen defect as compared with the amount required for total oxidation, so that they do not release enough heat. Isopropyl nitrate is one such compound [43].

It should be noted that unitary fuels with negative oxygen balances ($\alpha_{O_2}<1$) can be used as combustibles in bipropellants. Conversely, unitary fuels with a large oxygen excess ($\alpha_{O_2}>1$) can be used as oxidizers (tetranitromethane, hydrogen peroxide, etc.).

The most effective substances shown in Table 3.10 (nitroglycerine, methyl nitrate, etc.) are explosive, and thus cannot be used in pure form for rocket engines.

Hydrogen peroxide can decompose with release of heat and formation of vapor (a mixture of H_2O and O_2); thus it can be used as a unitary fuel.

Decomposition of 100% hydrogen peroxide releases 680 kcal/kgf. Some of this heat goes to heat and evaporate the water forming upon decomposition, so that the working heating value is 385 kcal/kgf. Figure 3.6 shows the way in which the higher and lower heating values of hydrogen peroxide depend on the concentration. As the data show, the lower heating value of 80-90% hydrogen peroxide is 180-280 kcal/kgf, which permits a total specific thrust of 100-140 kgf·s/kgf to be obtained in an engine.

Of the other unitary fuels based on individual substances, definite interest is presented by substances investigated, like hydrogen peroxide, as components of separately supplied fuels, while possessing the ability to decompose with the release of heat (for example, dimethyl hydrazine, hydrazine, etc.). This permits them to be used as unitary fuels to drive the turbine in an engine turbopump unit TPU, when this material is used as the combustible in the main fuel.

Mixtures of oxidizers and combustibles, as we have already noted, are explosive over a wide range of concentrations. The explosive characteristics of such mixtures can be eliminated by adding inert materials that do not participate in combustion, such as water, or by preparing these mixtures with a large excess of combustible. Either approach naturally reduces the mixture heating value. As an example, Fig. 3.7 shows the results of an investigation into the explosive characteristics of a $H_2O_2+H_2O+C_2H_5OH$ mixture; the arrows indicate the direction in which the diagram is to be read. Thus, for example, the mixture represented by point 1 contains 45% H_2O, 35% C_2H_5OH and 20% H_2O_2. The dashed line represents the locus of points for the stoichiometric mixtures. It is clear that for mixtures with no added inert material (water) (left side of triangle), the explosion-safe concentrations correspond to a considerable excess of combustible. For the stoichiometric mixtures (dashed line), explosion-safe concentrations are possible only when an inert material (water in the given case) is added.

Considering the liquid unitary fuels, we can conclude that the explosion-safe fuels suitable for utilization in engines are substantially less efficient than separately supplied fuels. This is why they are used for auxiliary purposes, to drive TPU turbines, and for low-thrust auxiliary engines designed to stabilize and control vehicles.

Manuscript Page No.	Transliterated Symbols
51	уд = ud = udel'nyy = specific
51	ид = id = ideal'nyy = ideal
52	ок = ok = Okislitel' = oxidizer
52	г = g = goryucheye = combustible
54	ж = zh = zhidkost' = liquid
54	тв = tv = tverdaya = solid
54	пл = pl = plaveniye = melting
54	кип = kip = kipeniye = boiling

Chapter 4

PROCESSES IN COMBUSTION CHAMBERS OF LIQUID ROCKET ENGINES [LRE](ЖРД)

4.1. GENERAL PATTERN OF COMBUSTION-CHAMBER PROCESS

The oxidizer and combustible are supplied to the combustion chamber by the feed system through atomizers located on the head. In some engines, both components are delivered to the combustion chamber in liquid form, while in others one part of the fuel is delivered as a liquid and the other part as a gas. Such a combustion chamber can be used in engines using afterburning of generator gas,

TABLE 4.1

[1] Горючее	[2] Температура термического самовоспламенения °С
[3] Триэтиламин	300
[4] Фурфуриловый спирт	325
[5] Легкое масло пиролиза	430
[6] Крекинг-керосин	425
[7] Керосин прямой гонки	506

1) Combustible; 2) temperature of thermal self-ignition, °C; 3) triethylamine; 4) furforyl alcohol; 5) light pyrolysis oil; 6) cracking kerosene; 7) straight-run kerosene.

and in many other cases.

To ensure process continuity, it is necessary to set up the conditions required for sequential occurrence of a complex set of physical and chemical events. These include preparation of the mixture for combustion, which involves breaking liquid components down into drops, heating, vaporization, and mixing; this is followed by mixture ignition and combustion.

The total reaction time, or the time required to convert the initial liquid products into the final gaseous products, equals the sum of the times required for all the sequential stages; it is determined principally by the time taken by the slowest stages of the process.

At temperatures above 1800-2000°K, where the time taken by chemical reactions is very short, the physical processes will be controlling. The slowest of these are vaporization and mixing of the gaseous products. Consequently, to speed up heat release and to attain more complete combustion the physical processes should be improved. In particular, heat release is accelerated significantly if the liquid components are mixed in advance and if they are more finely dispersed. The evaporation rate, which depends on the conditions under which heat is supplied to the liquid, can be increased by intensifying gas exchange for the high-temperature zones.

The physical processes also play a role after the basic heat-release process has terminated if the mixture composition is nonuniformly distributed over the chamber cross section. In such case, the combustion-product composition will be equalized owing to turbulent diffusion.

In addition, the total time taken by the process and its nature will be affected by chemical factors, chiefly in the zone near the head, where the temperature is not very high. Certain portions of fuel will ignite in this very zone. The heat liberated here following ignition will directly affect the rate of heating and evaporation of the remaining unignited portion of fuel. Clearly, the greater the chemical activity of the components in the low-temperature region, the greater the heat-release rate and thus the shorter the heating and evaporation time.

Thus it is better to use hypergolic components igniting spontaneously in the liquid phase as a result of surface contact; the heat liberated facilitates heating and evaporation of the still unignited portion of the fuel.

Ignition occurs above 200°C in the vapor state; the vapors of diergolic components ignite at higher temperatures than those of hypergolic components. Spontaneous ignition of hot vapors is called thermal ignition, and the minimum temperature at which this can occur is called the thermal selfignition temperature. Table 4.1 shows values of the thermal selfignition temperature for certain combustibles combined with nitric acid.

The lower the thermal selfignition temperature, the earlier ignition will occur in the low-temperature zone, which will ultimately shorten the total time required by the processes in the combustion chamber.

The combustion chamber (see Chapter 1) can be arbitrarily divided into two basic zones. The first is located directly at the head. At the beginning of the zone, liquid drops predominate; the drops are nonuniformly distributed over the head cross section: there are differences not only in the local value of the excess oxidizer coefficient, but also in the number of drops per unit volume. The number of drops vaporizing is still not great; preliminary drop heating takes place in this zone, and only the smallest drops vaporize. In the second part of the first zone there is intense evaporation, and the initial combustion sites form; these promote a further acceleration in the dispersion, heating, and evaporation processes

for the drops, and in combustion. At the end of the first zone there is vigorous combustion of the main part of the fuel mixture. The products of incomplete oxidation burn in the second zone, and the gas composition is equalized by turbulent diffusion.

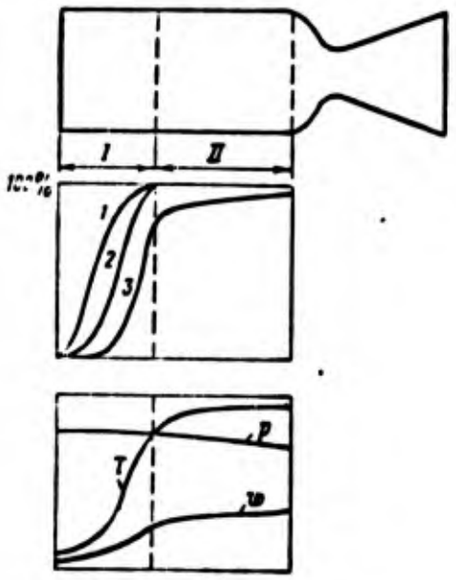

Fig. 4.1. Processes taking place along combustion chamber. 1) Atomization; 2) vaporization; 3) combustion.

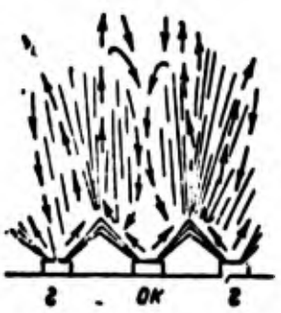

Fig. 4.2. Reverse flows.

Figure 4.1 illustrates the processes of atomization 1, vaporization 2, and combustion 3 in the separate zones; the change in temperature T, velocity w, and gas pressure p along the chamber length are shown.

Let us look in more detail at the heating, vaporization, and ignition processes occurring in the first zone. The drops leaving the injectors are retarded by the gas; the gas itself then begins to move, entraining the liquid. As a result, the gases flow away from the head; at sites with low drop density, there is a compensatory inflow of gas from the combustion zone. Thus at the head,

together with the concordant flows, reverse gas flows will form, directed from the combustion zone toward the head.

The reverse flows bring in heat for initial warming and vaporization of the drops and ignition of the fuel vapors; these flows play a major role in stabilizing the combustion-chamber process. Figure 4.2 shows the formation of reverse flows. These flows, entering a region with low drop density, rapidly heat and vaporize the available drops; the vapors formed then ignite. Next the flow of burning gases at the head turns and enters a zone with denser drop flow, where the drops are heated and vaporized, and the vapors ignited. An important condition for formation of the reverse flows is a certain nonuniformity in distribution of the liquid over the head cross section.

As vaporization and combustion progress, the gas velocity increases, while the drops are decelerated. When the drop velocity becomes equal to the gas velocity, the reverse flows vanish. Heat for subsequent warming and vaporization of the drops is provided by combustion, which takes place simultaneously with vaporization.

The process intensifies significantly with an increase in distance from the head; owing to the growth in total drop surface and the greater rate of supply, the vaporization rate increases; thus the heat-release rate rises, and the initial fuel is converted more rapidly into combustion products. As a result, the main fuel mass vaporizes and burns within a very short section of the combustion chamber (Fig. 4.1), forming a sort of "flame front."

The first zone is not very long; in the flow core it is usually no more than 100 mm in length. In the layer near the wall, where the values of excess oxidizer coefficient may be low, the combustion-product temperature will be relatively low; as a result, the heating, vaporization, and combustion products will take place over a considerable extent, sometimes occupying the entire length of the combustion chamber to the nozzle. Despite the relative shortness of the first zone, the processes taking place within it have a decisive influence on the course of the entire combustion-chamber process for an LRE. First, a specific distribution of component proportions over the combustion-chamber cross section, including the wall layer, is established in the first zone; second, turbulence is generated in the first zone, ensuring that the combustion products will be mixed and that their composition will be equalized in the rest of the combustion chamber, which is important if high specific thrust is to be obtained; third, the time required for the liquid components to be converted into gaseous products, the so-called conversion time, is determined by the time taken by the first-zone processes. The conversion time greatly influences the stability of the process in an LRE chamber.

As we have noted above, fuel combustion in the flow core basically terminates within the first zone; in the wall layer, if the values of the excess oxidizer coefficient are low, the combustion process may extend for a considerable length. In the general case, the combustion products will not have uniform composition over the combustion-chamber cross section at the end of the first zone; accordingly, the temperature will also vary. Nonuniformities can

also occur along the chamber diameter (core and wall layer) and, to a smaller degree, between adjacent injectors. If there is a significant difference in gas composition over the combustion-chamber cross section, there will be a loss in exit velocity and specific thrust, since some of the chemical energy contained in the fuel will remain unused.

In the second chamber zone, the composition and temperature of the combustion products are equalized over the cross section, in the main by natural means, turbulent and molecular diffusion. Turbulent mass transport is of fundamental importance.

The uniformity of gas composition at the end of the chamber depends on the mixture uniformity(in composition and in flow density) at the beginning of the chamber, on the intensity of turbulence, and on the chamber length.

4.2. INJECTORS OF LRE

Liquid components are dispersed by injectors, through which they are supplied to the combustion chamber under a certain gauge pressure. Atomization of the fluid is accompanied by breakdown of the jet and by drop formation. The set of flying drops forms the dispersed spray.

Two types of injector are used in LRE, jet and swirl.

Jet injectors are simple in construction; they are illustrated in Fig. 4.3.

To design a jet injector, we determine the diameter d of the injector nozzle aperture for a known flowrate G_f through it, and a pressure drop Δp_f across the injector.

The calculations are based on the flow-rate equation

$$G_\phi = \mu_\phi f_\phi \sqrt{2g\Delta p_\phi \gamma}, \qquad (4.1)$$

where μ_ϕ is the flow coefficient;

γ is the weight density of the liquid;

f_f is the area of the injector nozzle.

The flow coefficient ranges from 0.65 to 0.9, and depends on the ratio l/d where l is the length of the injector nozzle), the absolute diameter d, and the shape of the nozzle-channel entrance.

For LRE injectors, the value of the diameter d lies in the 0.5-3.0 mm range. An increase in injector diameter impairs the fineness of atomization; when d is very small, the chamber may be obstructed. The spray angle α is not large for jet injectors, amounting to 5-20°.

Swirl injectors combine a fine spray at low pressure drops with a large spray angle (α = 60-100°) (Fig. 4.4). The injector consists of the swirl chamber a, entrance channels with radii r_{vkh},

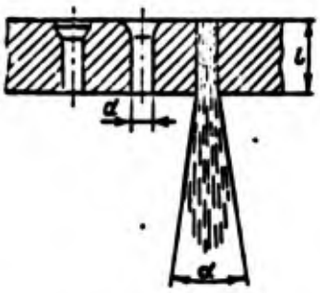

Fig. 4.3. Jet injectors.

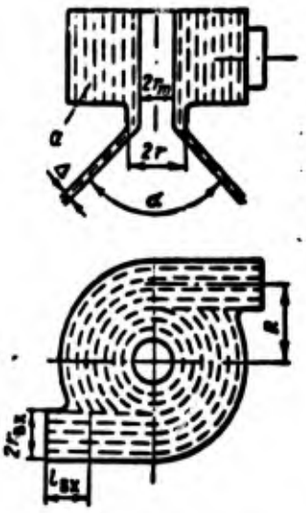

Fig. 4.4. Swirl injector.

and a nozzle with radius r. The rotary motion of the liquid at the nozzle entrance is the principal difference between this injector and the jet injector. The liquid is delivered over several (rarely over one) tangential channels to the swirl chamber where it is rotated. The central portion of the injector is filled with gas from the chamber, which entrains the liquid and is also placed into rotation, forming a gas vortex of radius r_m

The liquid flows out only within the area of the ring adjacent to the nozzle wall, so that the liquid only fills the nozzle-area fraction

$$f_m = \varepsilon f_\phi = \varepsilon \pi r^2;$$

where ε is the useful jet cross-section coefficient, or the fill factor.

The thickness Δ of the liquid sheet will evidently be less the greater the vortex radius for a given f_f.

The liquid in a swirl injector can be set into rotary motion not only by supplying it through tangential entrance channels, but in other ways as well, for example, by passing the liquid through a swirler having a helical notch on the outside surface, through which the liquid moves.

The flow coefficient μ_f in Eq. (4.1) can be represented as

$$\mu_\phi = \varepsilon \varphi_c,$$

where f_s is a velocity factor allowing for the reduction in axial velocity owing to twisting of the liquid and to hydraulic losses.

The coefficients, ε, φ_s, and μ_f obviously depend on the intensity with which the liquid rotates in the injector. The intensity of liquid rotation can be characterized by the ratio of peripheral velocity w_u near the wall of the injector nozzle to the arbitrary mean axial velocity, expressed in terms of the per-second liquid flowrate G_f and the nozzle exit area f_f,

$$A=\frac{w_u}{G_\phi}\gamma f_\phi.$$

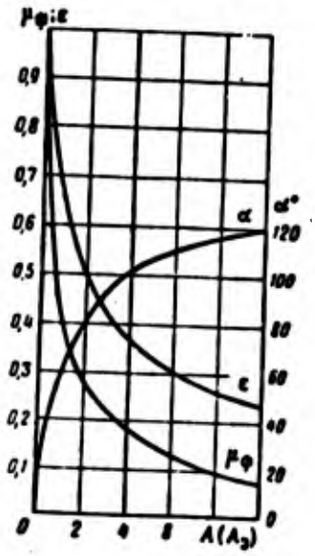

Fig. 4.5. Parameters of swirl injector as function of injector geometric characteristic.

An increase in A means that the intensity of rotation in the injector will increase owing to a rise in the moment of momentum; this reduces the flow coefficient μ_f. The coefficient A is expressed in terms of the injector geometry, and is called the injector geometric characteristic.

The injector geometric characteristic for an ideal fluid (without friction) can be represented as

$$A=\frac{\pi Rr}{nf_{vkh}}, \qquad (4.2)$$

where R is the distance between the injector axis and the entrance-channel axis;

n is the number of entrance channels;

f_{vkh} is the entrance-channel cross-sectional area.

If the entrance channels are not perpendicular to the injector axis, the expression for the geometric characteristic takes the form

$$A=\frac{\pi Rr}{nf_{вх}}\sin\beta, \qquad (4.3)$$

where β is the angle between the entrance-channel axis and the injector-nozzle axis (see Fig. 12.15).

Leaving the swirl injector, the liquid takes the form of a hollow cone or,more accurately, of a single-sheeted hyperboloid of revolution, along whose generatrices the liquid particles move. The paths of the particles leaving the injector are determined by the relationship between the peripheral component w_u and axial component w_a of the velocity at the nozzle-channel exit; the spray angle α at the injector exit is determined by the relationship

$$\operatorname{tg}\frac{\alpha}{2}=\frac{w_u}{w_a}.$$

Like the flow factor μ_f, the angle α depends on the intensity of liquid rotation, i.e., on the geometric characteristic A.

Figure 4.5 shows a graph representing the quantities, ε, μ_f, and α as functions of A for flow of an ideal liquid. It follows from the graph that when A increases, the spray angle α becomes greater, while the quantities ε and μ_f decrease. This is so since when A increases, it means that the peripheral component of velocity in the nozzle also increases. Despite the approximate nature of the relationships for ε, α, and μ_f, they can be utilized in preliminary calculations for swirl injectors of LRE.

An experimental check supports the basic concepts of swirl-injector theory for an ideal fluid. In many cases, however, there is a discrepancy between the experimental and theoretical values of μ_f and α. It has been established that when an actual viscous liquid is atomized, friction influences the flowrate and shape of the jet. Friction ahead of the injector nozzle reduces the moment of momentum of the fluid at the entrance to the injector nozzle, so that for an actual liquid, the angle α is less and μ_f is greater than for an ideal liquid. It follows from the theory that the coefficients ε and μ_f, and the angle α can be found with allowance for friction from the formulas or curves obtained for an ideal liquid (see Fig. 4.5), if we replace the characteristic A with the equivalent geometric characteristic

$$A_э=A\left[1+\frac{\xi}{2}\left(\frac{\pi R^2}{nf_{вх}}-A\right)\right]^{-1}, \qquad (4.4)$$

where ξ is the coefficient of friction for the injector; the latter can be found from the approximate formula

$$\xi = 2\frac{0{,}316}{\mathrm{Re}^{0{,}25}}. \qquad (4.5)$$

Here the Reynolds number is found from the entrance condition,

$$\mathrm{Re} = \frac{w_{vkh} d_e}{\nu}, \qquad (4.6)$$

where d_e is the equivalent hydraulic diameter of the entrance channels;

ν is the kinematic viscosity coefficient for the liquid;

w_{vkh} is the velocity at the entrance channel.

The ratio A_e/A shows the reduction in moment of momentum owing to the action of the friction forces.

4.3. ATOMIZATION

Evaluation of injector operation and, consequently, of atomization quality makes use of various characteristics: the dimensions of the resulting drops, their uniformity, the range of the jet, and the shape of the spray.

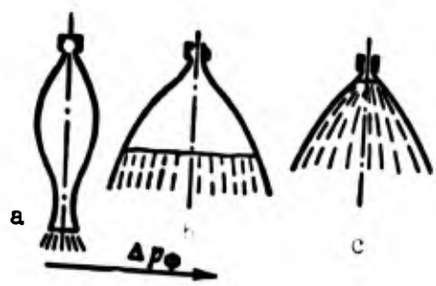

Fig. 4.6. Spray shapes.

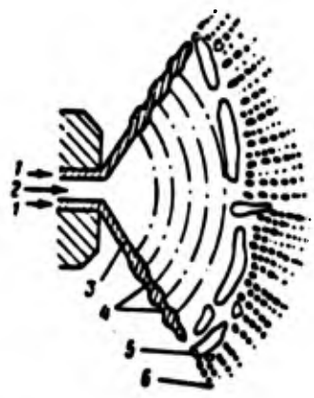

Fig. 4.7. Mechanism for atomization of liquid by swirl injector. 1) Jet; 2) gas vortex; 3) reduction in sheet thickness; 4) formation of bridges; 5) breakup into parts; 6) drop formation.

To speed up the vaporization process, the spray should be fine (the mean drop diameter should be small). In this case, the total evaporation surface will be greater and the time required for evaporation less.

Chamber processes are influenced by the shape of the spray and the liquid distribution over the spray cross section. For easier vaporization of the liquid, there should not be an excessive concentration of liquid phase in individual combustion-chamber zones.

The liquid distribution over the spray surface also influences the range, i.e., the depth to which the liquid travels in the medium after leaving the injector. All other conditions being equal, the more compact the longer the range. The range requirements depend on the mixture-formation conditions. It is usual to attempt to decrease the range, since dispersion takes place closer to the head and the preparatory processes are completed within a shorter length of the combustion chamber. In certain cases, it is desirable to extend the primary zone along the combustion-chamber length. It is then necessary to use injectors with differing ranges. Liquid sprayed from a swirl injector has less range than for a jet injector. This results from the very large surface of the spray ejected from the swirl injector. Here the external resistance forces reducing the range act on both the inside and outside surfaces of the cone. Moreover, the sheet of the cone produced by a swirl injector is considerably less stable than the solid jet from a jet injector. Thus the cone breaks up closer to the injector nozzle, and at a lower pressure drop, which reduces the range.

In the atomization process, the jet leaving the injector nozzle breaks down in successive stages, and large drops are broken up into finer particles. The factors causing the jet to break up can be divided into factors external to the jet and internal factors.

The external factors include aerodynamic drag forces and forces appearing upon collision of the jet and individual drops or upon collision with an obstacle. These factors will have a greater influence the higher the relative velocity of the liquid and the medium or of the impinging jets. The aerodynamic forces also depend on the density of the medium; they increase as the density goes up.

The internal factors facilitating breakup of the jet include the inertial forces resulting from turbulent pulsations in the liquid jet, and increasing as the liquid velocity increases.

The molecular attraction forces appear as viscosity forces in internal layers of the liquid and as surface-tension forces at the interface; they oppose breakup of the liquid into drops. The temperature of the liquid influences the molecular forces. As the temperature increases, their action becomes weaker; at the critical temperature, the surface-tension forces vanish.

The spray shape and fineness depend on the pressure drop under which the fluid leaves the injector nozzle. As the pressure drop Δp_f increases, the influence of both the internal and external factors becomes stronger, and the jet breaks down into finer drops,

since the velocity at which the liquid leaves the injector exit increases. For example, when a swirl injector is used at very low pressure drop, the surface of the exiting spray clearly shows the helical particle trajectories. As the pressure drop at the nozzle exit increases, a cavity develops; its continuous surfaces takes the form of a "bubble" (Fig. 4.6a); the bubble is constricted a certain distance from the nozzle by the surface-tension forces. With a further increase in the drop, the "bubble" opens, becoming a "tulip" (Fig. 4.6b). At a certain distance from the nozzle, the "tulip" breaks up into isolated rings, which then form into clumps of liquid, filaments, and individual drops. The intact portion of the "tulip" is called the sheet. As the pressure drop increases, the length of the intact section of the sheet decreases until atomization takes place almost at the nozzle (Fig. 4.6c). Figure 4.7 shows the mechanism for atomization of the liquid by a swirl injector.

Drops of varying size are formed during atomization. Atomization quality is evaluated on the basis of experimental data. For this purpose, the drops of atomized liquid are trapped in some way or another, and grouped on the basis of diameter. The atomization fineness characteristics are then constructed as curves representing the drop distribution by diameter. For example, the total weight curves are constructed; here the results obtained by weighing all drops of a specified diameter or less are successively plotted along the axis of ordinates (Fig. 4.8). Some average drop diameter is used to evaluate the fineness of atomization. The diameter $d_{0.5}$ corresponding to a relative weight $\bar{G} = 0.5$ on the curve of Fig. 4.8 is often taken as this average diameter.

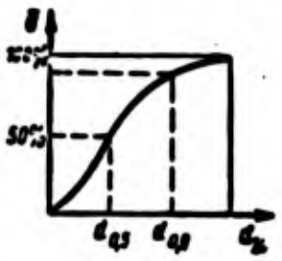

Fig. 4.8. Distribution curve for atomized liquid.

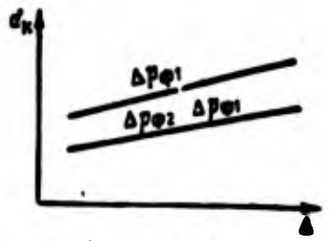

Fig. 4.9. Average drop diameter as function of sheet thickness.

In addition to estimates based on average drop diameter, atomization quality can also be judged from the dimensional uniformity of the drops obtained. Since the minimum drop diameter equals the molecular size, the uniformity can be characterized by the maximum drop diameter or, for example, by the $d_{0.9}$ diameter on the distribution curve (Fig. 4.8), which corresponds to 90% of the total drop weight. The smaller $d_{0.9}$, the more uniform the atomization.

Atomization fineness depends on the drop Δp_f. When Δp_f = 3-6 kgf/cm^2, swirl injectors deliver a $d_{0.5}$ average diameter of the order of 50-200 μm. Drop diameter decreases with increasing pressure drop; this relationship is quite weak for high pressure drops.

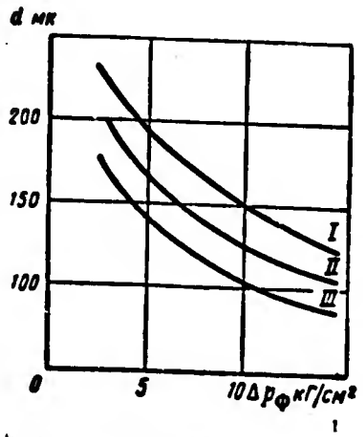

Fig. 4.10. Average drop diameter as function of pressure drop across injector. 1) kgf/cm².

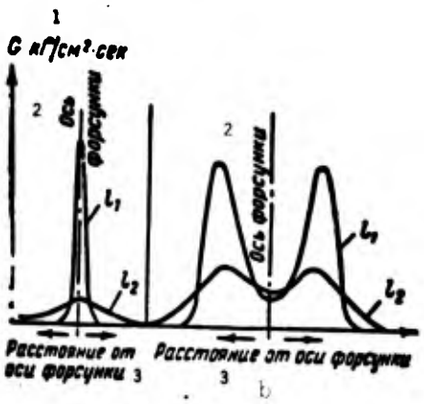

Fig. 4.11. Curves representing distribution of per-second flowrate along radius for two distances from nozzle ($l_2 > l_1$). a) Jet injector; b) swirl injector. 1) kgf/cm²·s; 2) injector axis; 3) distance from injector axis.

Atomization fineness also depends on the shape and state of the liquid jet surface at the injector exit. The thicker the liquid jet at the exit, the more compact it is, since the smaller the surface-to-volume ratio, the less the effect of the aerodynamic forces and, all other conditions being equal, the poorer the atomization. Figure 4.9 shows the change in drop diameter as a function of sheet thickness Δ for the liquid at the exit from a swirl injector. Atomization is degraded as the sheet becomes thicker. The value of Δ will be higher the higher the flow coefficient and the smaller the angle α (for a given injector nozzle diameter).

All other conditions being equal, an increase in nozzle size will increase Δ and thus impair atomization.

This situation is illustrated in Fig. 4.10, which shows three curves for the average drop diameter d as a function of the pressure drop across the injector. These curves apply to three swirl

injectors with the following flowrates, in kgf/s: I, 240; II, 120; III, 60 (at a pressure drop of 7 kgf/cm^2); the apertures and liquid jets will consequently also differ in diameter. Clearly, the smaller the jet, the finer the atomization.

Owing to the high temperatures and pressures in the combustion chambers of LRE, and the vigorous heat exchange between drops and gases, there is no need for excessively fine atomization or, consequently, for a great pressure drop across the injectors. In practice, the minimum drop across LRE injectors lies in the 1-4 kgf/cm^2 range.

As a rule, the liquid in the jet is nonuniformly distributed over both the cross section and the length of the spray.

Figure 4.11 shows curves representing the distribution of fluid flowrate along the radius of the jet for two distances from the nozzle. The curves show that both jet and swirl injectors are characterized by flow-rate nonuniformity over the cross section. With increasing distance from the injector nozzle, the fluid distribution over the jet cross section becomes more uniform.

4.4. MIXING OF COMPONENTS

The oxidizer and combustible must be brought into contact if they are to react chemically. There will always be an improvement in the degree of heat release when the quality of preliminary mixing improves, regardless of the type of fuel components employed.

The components can be mixed by the interaction of jets in the combustion chamber during atomization or by preliminary mixing of the liquids followed by spraying through one injector. The best results, from the viewpoint of degree of combustion, should be obtained with preliminary mixing, since this makes it easier to ensure that the proportions of the components remain the same over the combustion-chamber cross section. It is safer to mix the components after they have left the injectors; this type of mixing predominates in existing engines.

By a mixing element or mixer, we mean the smallest number of injectors used to mix the components in the specified proportions. Then the entire head may include several elementary mixing elements, each consisting of several injectors in the general case. The mixing elements influence one another, but the quality of the head is determined, in the main, by mixing quality and by the conditions set up for subsequent vaporization by the individual mixing elements.

When jet injectors are used, mixers consisting of triple- or double-jet injectors are found (Fig. 4.12). Since the spray angle is relatively small for a jet injector, to promote better contact and mixing of the components, the injectors for unlike components are often set in the mixer at an angle with respect to one another (Fig. 4.12a and Fig. 4.12b). Jet mixers with parallel injector axes are also employed (Fig. 4.12c). Good contact of the components in the liquid phase is of particular importance for hypergolic fuels. Triple-jet mixers (Fig. 4.12a), consisting of two oxidizer injectors and one combustible injector, are better than double-jet devices,

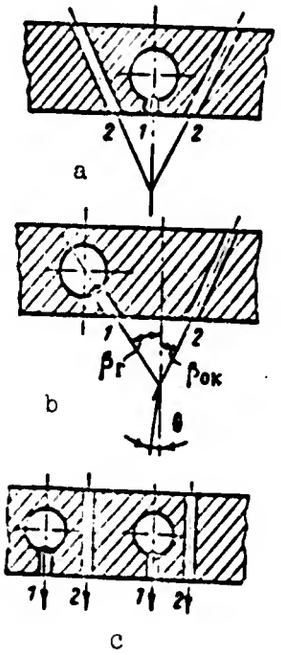

Fig. 4.12. Jet mixers. 1) Combustible; 2) oxidizer.

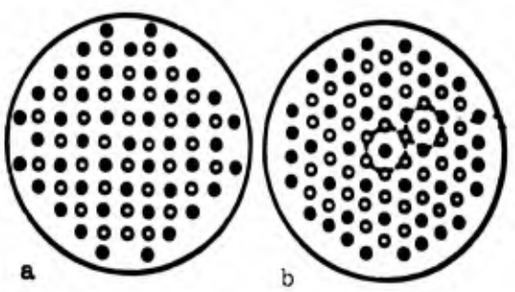

Fig. 4.13. Injector configurations. a) Staggered arrangement; b) honeycomb arrangement. black circle) combustible injectors; open circle) oxidizer injectors.

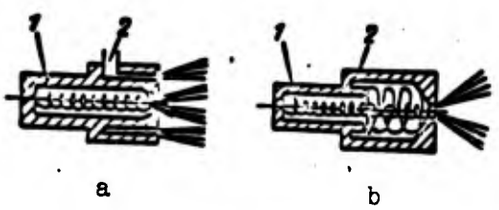

Fig. 4.14. Diagrams of two-component injectors. a) Injector with external mixing; b) injector with internal mixing. 1) Supply of first component; 2) supply of second component.

since the volume flowrate of oxidizer is often 2-3 times that of the combustible. Thus an increase in the number of oxidizer apertures reduces the size of the oxidizer jet and ensures better atomization and better mixing of combustible and oxidizer. In a symmetric triple-jet mixer, the resultant jet moves along the axis of the center injector.

When two jets collide, the resultant jet will deviate through a certain angle, which may vary when the operating regime changes. On the assumption that the total momentum of the streams remains constant when they collide, we can find the direction of the resultant jet (the angle θ between the chamber axis and the jet direction).

If w_{ok} and w_g are, respectively, the velocities of the oxidizer and combustible jets at the injector exit, we arrive at the expression

$$\operatorname{tg}\theta = \frac{\varkappa \frac{w_{ok}}{w_r}\sin\beta_{ok} - \sin\beta_r}{\varkappa \frac{w_{ok}}{w_r}\cos\beta_{ok} + \cos\beta_r}, \qquad (4.7)$$

where $\varkappa$ is the ratio of components.

By specifying the angle θ (for example, $\theta = 0$), we can find the required positions of the oxidizer and combustible injectors (β_{ok}, β_g).

The geometric interaction of the jets must be taken into account when a head is designed if we are to prevent liquid from striking the walls or from clumping together in individual chamber zones.

A head using jet injectors, ordinarily include many identical mixers positioned uniformly over the cross section. There may be an exception near the wall, where mostly combustible injectors are installed to improve cooling conditions.

When swirl injectors are employed, the designer also attempts to locate them uniformly over the head to produce a uniform cross-sectional distribution of components. Since a swirl injector produces a large-angle spray, jets of unlike components will collide even when the injector axes are parallel. Combustible and oxidizer injectors ordinarily alternate, and the jets from neighboring injectors intersect or merge.

When swirl injectors are used, staggered, honeycomb, or other injector configurations are used (Fig. 4.13). As with jet injectors, combustible injectors predominate in the outer ring of the head to improve engine cooling conditions. This also prevents oxidizer from striking the wall, thus protecting the wall material against corrosion.

If the peripheral nozzles are neglected, then with a staggered injector array, one oxidizer injector is used for each combustible

injector; for a honeycomb array, two oxidizer injectors are used for each combustible injector; as we have noted, this is a positive feature.

We have so far considered single-component injectors, where each separate injector is used to atomize just one component. Two-component injectors can be used; both components are supplied through these devices; here the injector in essence represents an elementary mixer.

Two-component injectors may use external or internal (preliminary) mixing. In the first case, the injector consists of coaxially positioned oxidizer and combustible injectors (two-nozzle injector) (Fig. 4.14a). The conical component jets intersect at the injector exit. The injector is so designed that the combustible and oxidizer cones intersect near the injector nozzle; this requires that the spray angle be larger for the inside nozzle. With internal premixing (emulsion injector) (Fig. 4.14b), the components are mixed within the injector, which ensures good mixing of oxidizer and combustible. Two-component injectors are structurally more complicated than single-component devices, but they permit better mixing to be obtained with fewer injectors in the head.

When two-component injectors with internal mixing are used, it should be remembered that the mixture components may ignite or explode within the injector. If this is to be prevented, the time spent by the oxidizer and combustible mixture in the injector must be less than the ignition delay period under these conditions.

Fuel is distributed over the head cross section owing to the atomization and mixing of the liquid component (Fig. 4.15). The local values of the excess oxidizer coefficient α_i may differ from the average chamber value α_{sr} even when the injectors are located uniformly over the head. Several factors are responsible: nonuniform flowrates from individual injectors, incomplete mixing of components within one mixer, nonuniform positioning of injectors on the head, and contact of some fuel with the walls. Since the injectors are arranged in definite groups on the head, the average values α_{isr} will be roughly identical for individual jets with transverse dimension close to the value t_f of the injector spacing. The layer at the wall ordinarily represents an exception, since the excess oxidizer coefficient decreases here owing to the need for enrichment with combustible.

The part of the fuel (or gas) flow at the center of the combustion chamber, where α_{isr} varies little, is often called the flow core, while the flow at the wall, which has a significantly lower excess oxidizer coefficient, is referred to as the wall layer.

Roughly 15-30% of the fuel is located at the wall (in the wall layer). As the chamber dimensions increase and the injector spacing decreases, a smaller proportion of the fuel will be at the wall.

If the oxidizer and combustible vaporize at different rates, one of the components will vaporize before the other, and the lateral flow of its vapors may redistribute the components over the cross section, changing the distribution that obtained in the liquid phase at the injector exits. Thus the distribution of α, calculated from the combustion-product composition at the end of the 1st zone may differ from the distribution in the liquid phase at the head.

Differences in drop sizes or in physical properties may result in differing vaporization rates for the components. Thus, for example, for an engine operating on nitric acid and kerosene, since the flow-rate through the oxidizer injector is ordinarily greater than through the combustible injector, the oxidizer drops will be larger. Since the weight density of nitric acid is nearly double that of kerosene, here the oxidizer drops will be considerably greater in mass than the combustible drops; all other conditions being equal, correspondingly more heat and more time will be required for vaporization.

As we have already noted, following the first zone the combustion-product composition will be equalized by turbulent mixing.

The turbulence that mixes the combustion products in the second zone appears in the first zone owing to gas flowing from regions with higher drop density into regions with lower density during evaporation, and also as a result of longitudinal velocity differences in individual gas streams.

The degree of combustion-product mixing depends on the turbulence intensity, which can be measured in terms of the pulsation velocities.

For the turbulence intensities occurring in practice in LRE, and for the combustion-product mixing lengths usual for combustion chambers, the nonuniformities in distribution of composition and temperature between the zones of individual injectors will be smoothed out.

Consequently, if at the end of the first zone the distribution of α over the chamber cross section, determined from the combustion-product composition, has the form shown in Fig. 4.16 by the dashed line, for example, then at the end of the combustion chamber, i.e., at the end of the second zone, this distribution will have roughly the form shown by the solid line. This is an important fact: the smaller the nonuniformity created by the head, the shorter the section required for equalization of combustion-product composition.

If we take an ideal engine for which the mixture composition at the beginning of the combustion chamber is identical everywhere over the cross section, the combustion chamber of this engine will have the shortest length. It is determined, in the main, by the length of the preliminary-mixing and vaporization zone and the length of the combustion zone. From this viewpoint, a reduction of the spacing between injectors for a given head size, i.e., an increase in the number of injectors, is desirable. Utilization of two-component injectors should also have a positive influence.

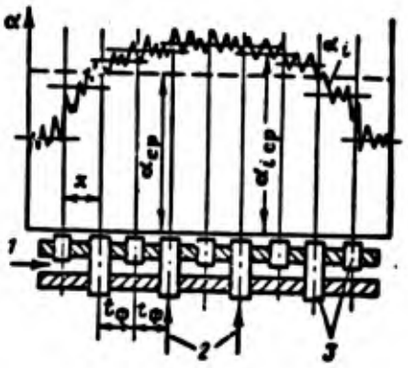

Fig. 4.15. Distribution of excess oxidizer coefficient (component ratio) over head diameter. 1) Combustible; 2) oxidizer; 3) injectors.

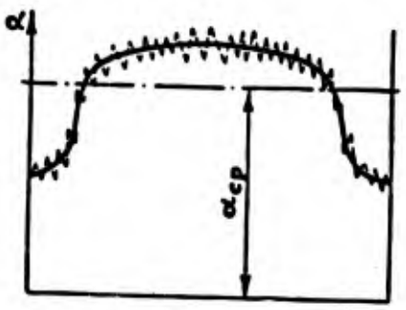

Fig. 4.16. Distribution of excess oxidizer coefficient (component ratio) at beginning and end of second zone.

4.5. DIMENSIONS OF HEAD AND COMBUSTION CHAMBER

The transverse head dimensions depend on the number of injectors and their spacing.

To reduce engine size, we should attempt to decrease the head diameter, i.e., to reduce injector spacing and decrease the number of injectors; the number and spacing of injectors influence the process, however, and thus cannot be selected arbitrarily.

A reduction in injector spacing below a certain limit, for a given number of injectors, may impair heat-supply conditions, since the relationship between the liquid and gaseous parts of the medium that fill the chamber at the head will change unfavorably. At the same time, mixing conditions improve for the components when the spacing is decreased, since the nonuniformity in component distribution over the cross section decreases in inverse proportion to the injector spacing. The spacing reduction may also be restricted by the conditions governing injector positioning on the head.

The choice of spacing must be coordinated with the flowrate through a single injector. As this increases, the injector spacing must be increased, or else the normal course of the combustion process will be disturbed. The disturbance results from considerable thickening of the liquid jets in individual zones of the head, and impairment of vaporization conditions. An increase in the spacing, with a corresponding increase in the injector-nozzle diameter, i.e., in the injector output, above a certain value may also impair mixing and atomization conditions; thus there are restrictions on both the maximum spacing and the maximum rate of flow through one injector.

When the chamber pressure rises, the density of the gases at the head rises. This improves the supply of heat for warming and vaporizing the components, and should make it possible either to reduce the injector spacing for a specified number of injectors, or to reduce the number of injectors for a constant spacing, thus decreasing head dimensions somewhat.

Head dimensions are frequently characterized by the discharge intensity q_g, which is the ratio of the fuel per-second flowrate $G_{\Sigma sek}$ to the head area F_g:

$$q_r = \frac{G_{\Sigma сек}}{F_r}. \tag{4.8}$$

Like the injector spacing, the discharge intensity indirectly characterizes the conditions under which heat is supplied to the liquid mixture. The larger this quantity and the smaller the head area, the greater the concentration of liquid at the head and the more difficult it is to organize a supply of heat to the fuel.

In selecting a value of discharge intensity for a head, it is necessary to take account of the same factors as for the choice of injector spacing. Improvement in mixture-formation and evaporation conditions makes it possible to increase head discharge intensity; just as an increase in chamber pressure improves drop vaporization conditions, an increase in p_k^* should make it possible to increase q_g. The ratio

$$\bar{q}_r = \frac{q_r}{p_k^*} \tag{4.9}$$

is called the relative discharge intensity of the head. On the average, for existing engines $\bar{q}_g = (0.6\text{-}2.5)10^{-3}$ kgf/s·m²·atm (abs). Higher values are found in certain engines.

All otherconditions being equal, the required volume of the first chamber zone is less for hypergolic and low-boiling fuels. This volume can be reduced by improving the mixture-forming systems. All other conditions being equal, an increase in discharge intensity will lengthen the first zone. The length of the second zone, i.e., the section within which the combustion-product composition is equalized over the chamber cross section is relatively large in virtue of the low rate at which the processes take place in this zone.

The combustion-chamber volume determines the time spent by

the fuel and the combustion products; this time should be sufficient for total completion of all processes taking place in the combustion chamber. The better the process is organized, the less time need be spent.

The combustion-chamber volume required to produce the necessary degree of combustion can be determined exactly only by experiment. The chamber volume can be selected in approximation by using statistical values for the time τ_n spent by the gases in the chamber and for the characteristic (reduced) length L_n of the chamber.

The mean time spent by the gas can be represented as the ratio of the weight G_k of the gas in the combustion chamber to the per-second gas flow rate:

$$\tau_n = \frac{G_k}{G_{sec}}. \tag{4.10}$$

If we arbitrarily assume that the weight density of the gas in the chamber is constant, and equal to the value at the end of the chamber, and if we neglect the volume occupied by the liquid phase, then

$$\tau_n = \frac{V_k \gamma_k}{G_{sec}}. \tag{4.11}$$

Assuming further that

$$\gamma_k \approx \frac{p_k^*}{RT_k^*}, \tag{4.12}$$

on the basis of Eq. (2.48), we obtain

$$\tau_n = \frac{1}{mR\sqrt{T_k^*}} \cdot \frac{V_k}{F_{sp}}. \tag{4.13}$$

The combustion-chamber volume can be determined if we know τ_n from prototype data.

The ratio $L_n = V_k/F_{kr}$ is the characteristic length of the chamber. The greater L_n, the longer the gas spends in the chamber, and the higher, up to a certain limit, the degree of heat release and the specific thrust.

The time required and the reduced length will differ for different fuels, and will depend on mixing and evaporation conditions in the first combustion-chamber zone. These quantities will be smaller for hypergolic fuels; as preliminary mixing improves, the required values of τ_n and L_n drop.

For most existing engines, τ_n = 0.0020-0.0045 s, while L_n = = 1.5-3.5 m.

If, like the head discharge intensity, the value of L_n is

selected on the basis of statistical data when the engine is designed, it is necessary to consider engines using the same fuel (or one with similar properties), and the same process organization. Here allowance must be made for the type and spacing of injectors, the flow-rate through one injector, and the head shape.

We also note that, as statistics show, the combustion-chamber volume (all other conditions being equal) is ordinarily decreased by reducing the transverse dimensions. We can thus assume in approximation that lower values of L_n go with higher values of q_g and vice versa.

The combustion-chamber volume is sometimes estimated from the heat release rate q_k of the combustion chamber, which is determined by the expression

$$q_k = \frac{Q}{V_k P_k^2} \text{ kcal/(m}^3\cdot\text{h}\cdot\text{atm abs)}. \qquad (4.14)$$

Here Q is the amount of heat released in unit time, kcal/h (for complete combustion). It is not difficult to show that the value of q_k is connected with L_n and τ_n. In fact, since $Q = 3600\, G_{\Sigma sek} h_\alpha$, then with allowance for Eq. (2.48), we can obtain

$$q_k = \frac{3600 A_0}{\sqrt{T_k^2}} \frac{m}{L_n}. \qquad (4.15)$$

4.6. COMBUSTION-CHAMBER SHAPE

In the main, two shapes are employed for combustion chambers: cylindrical and spherical (or nearly spherical).

Cylindrical chambers are widely employed for many types of engine. The transverse dimensions of such a chamber are determined principally by the mixing conditions. There is a specific relationship between the relative head area and the relative discharge intensity.

The quantity $\bar{q}_g$ can be associated with the relative head area:

$$\bar{f}_r = \frac{F_r}{F_{sp}}.$$

Since the rate at which fuel flows through the head equals the rate at which gas flows through the nozzle, we can substitute Expressions (4.8) and (2.48) into Formula (4.9); then

$$\bar{q}_r = \frac{1}{\bar{f}_r} \frac{m}{\sqrt{T_k^2}}. \qquad (4.16)$$

For cylindrical combustion chambers,

$$\bar{f}_r = \bar{f}_k,$$

where $\bar{f}_k = F_k/F_{sp}$ and F_k is the cross-sectional area of the combustion chamber.

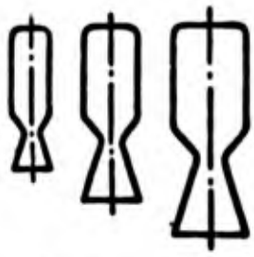

Fig. 4.17. Change in chamber configuration with increasing thrust.

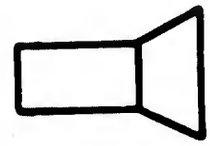

Fig. 4.18. Semithermal nozzle.

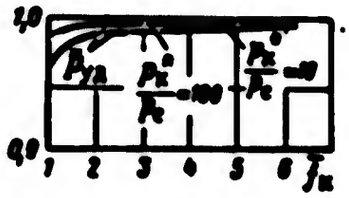

Fig. 4.19. Relative specific thrust as function of $\bar{f}_k$.

Thus $\bar{f}_k$ depends on $\bar{q}_g$, with the latter being determined by the engine mixing condition.

Figure 4.17 shows schematically how the combustion-chamber and nozzle configurations change as the thrust increases with constant pressure p_k^* and the same method of organizing the process. The head discharge intensity and the nozzle expansion ratio are assumed to remain constant. As the thrust increases, the engine becomes longer, basically owing to an increase in nozzle dimensions; there is little change in the length of the cylindrical combustion-chamber section.

A decrease in combustion-chamber transverse dimensions is associated with a reduction in the relative area $\bar{f}_k$. In the modification with the maximum degree of forcing ($\bar{f}_k = 1$), the combustion-chamber diameter equals the nozzle throat diameter (Fig. 4.18). A combustion chamber of this type is called a "semithermal nozzle" in the literature. The gas velocity equals the speed of sound at the end of the cylindrical portion of such a chamber.

A reduction in the relative combustion-chamber area $\bar{f}_k$ increases the gas velocity in the chamber and, consequently, reduces the total (stagnation) pressure at the end of the combustion chamber owing to an increase in thermal resistance.[1] The drop in total pressure in turn reduces the specific thrust somewhat.

Figure 4.19 shows the reduction in specific thrust when $\bar{f}_k$ decreases as a result of the influence of thermal resistance. In parti-

cular, the graph shows that when $\bar{f}_k \geq 3$, there is almost no thermal resistance, and its influence on the specific thrust can be neglected.

Forced operation of LRE combustion chambers by a reduction in $\bar{f}_k$ means a simultaneous increase in the head discharge intensity $\bar{q}_g$ and, as a consequence, possible impairment of the conditions for heat supply to the fresh fuel mixture. Thus forced-operation combustion chambers with low $\bar{f}_k$ can only be used if the mixing systems give good results with high values of discharge intensity. Where this is not the case, utilization of such chambers may lead to a reduction in the degree of combustion and to unstable operation.

Manuscript Page No.

Footnotes

94 [1]By the thermal resistance, we mean the stagnation-pressure reduction effect produced when fuel is supplied to a moving gas flow.

Manuscript Page No.

Transliterated Symbols

77 ф = f = forsunka = injector

77 вх = vkh = vkhodnoy = entrance

77 с = s = skorost' = velocity

78 ж = zh = zhidkost' = liquid

80 э = e = ekvivalentnyy = equivalent

84 к = k = kaplya = drop

87 г = g = goryucheye = combustible

87 ок = ok = okislitel' = oxidizer

88 ср = sr = sredniy = average

88 г = g = golovka = head

88 сек = sek = sekundyy = per-second

88 к = k = kamera = chamber

92 кр = kr = kriticheskiy = critical

Chapter 5

FUNDAMENTALS OF PROCESS IN SOLID ROCKET ENGINES

In recent years, interest in solid rocket engines [SRE](РДТТ) has risen significantly. This is so since solid rocket engines permit:

1) great simplification of rocket construction;

2) substantial reduction in time required to prepare rocket for launching;

3) long-term storage of fueled rockets, ready to launch;

4) simplified operation and a reduction in attendant personnel.

Thus solid-fueled engines are of great military interest (reserves of ready-to-use weapons can be accumulated; the missiles are in an advanced state of preparedness; and a rocket spends less time on the launching pad, so that it is less vulnerable on the ground).

In addition, the possibilities for making engines with thrusts of 1000-1200 T or more in a single chamber are very good, and SRE are very reliable owing to their simplicity.

There are drawbacks to SRE: they develop less specific thrust than liquid rocket engines [LRE](ЖРД), burn time is often shorter, and it is more difficult to control the thrust.

5.1. FUELS

Solid rocket fuels can be classified into two groups: double-base(colloidal) and composite.

Double-base fuels. These fuels are based on guncotton (nitrocellulose). Nitrocellulose is a substance that can decompose explosively when acted on in various ways; thus it is not employed in pure form. Nitrocellulose consists of cellulose {with formula $[C_6H_7O_2(OH)_3]_n$ } in which certain OH groups are replaced by ONO_2 nitrate groups through treatment with nitric acid. The properties of cellulose nitrates depend on the number of groups involved or, what is the same, the per cent nitrogen content. Nitrocellulose has a negative oxygen balance (α_{O_2} = 0.57-0.67). The higher the nitration

of the cellulose, the more favorable the balance; an increase in the per cent nitrogen content (i.e., in the number of ONO_2 groups) increases the heat of decomposition, but impairs the ability of gun cotton to dissolve in solvents. The heat of decomposition fluctuates between 700 and 1000 kcal/kgf for nitrocellulose, and depends on the amount of nitrogen, which is usually contained in amounts of 11.5-13.8%.

When nitrocellulose is dissolved in appropriate substances, it is less liable to explode, and more capable of normal combustion. Nitroglycerin is most frequently used as a relatively nonvolatile solvent in rocket fuels. Other solvents are also introduced on occasion. The nitroglycerin content of the solution generally exceeds 40%, which is why a fuel based on nitrocellulose and nitroglycerin is called a double-base propellant.

An increase in the per cent content of nitroglycerin increases the heating value of the fuel and, consequently, the specific thrust, since the heat of decomposition exceeds that of nitrocellulose. Moreover, nitroglycerin has a positive oxygen balance, so that some of the combustible components of nitrocellulose are oxidized by the oxygen in the nitroglycerin; the oxygen excess of nitroglycerin is about 35 gf for each 1 kgf.

A stoichiometric mixture of nitroglycerin and nitrocellulose should contain 89.5% of the first component. The nitroglycerin content of double-base propellants seldom exceeds 43%, however; the limitation on the nitroglycerin content is associated with the grain properties, since a further increase in the nitroglycerin reduces grain strength and impairs stability.

In addition to the basic components, double-base propellants include certain additives that function to increase grain stability during storage (stabilizers such as centralite or diphenyl amine), to reduce or increase the combustion rate (dephlegmatizers and catalysts), to improve manufacturing qualities, for coloring, etc.

With double-base propellants, SRE develop specific thrusts in the 200-240 kgf·s/kgf range; higher values refer to fuels with higher content of nitroglycerin and with nitrocellulose having a higher degree of nitration. Table 5.1 shows the content of individual components in a double-base fuel.

After the nitrocellulose has been dissolved and the additives introduced, the double-base fuel takes the form of a viscous homogeneous mass which is pressed or cast in the required shape. The surface at which combustion is not to occur is restricted by a thin coating of inert material (for example, a thin layer of acetyl cellulose, ethyl cellulose, etc.).

Composite fuels. This group includes fuels in the form of mechanical mixtures of solid combustibles and oxidizers; various additives are also employed.

Inorganic salts that are solid under normal conditions are employed as oxidizers for such fuels; they contain a high percentage of free oxygen. These are usually perchlorates or nitrates: calcium

perchlorate $KClO_4$, ammonium perchlorate NH_4ClO_4, sodium nitrate $NaNO_3$, and certain others. Ammonium perchlorate is now the most commonly used oxidizer.

TABLE 5.1

Composition of Certain Double-Base Fuels (in % by weight), and Their Characteristics

A Состав и свойства / B Топливо	JPN баллистит C	JP	HES 4016	SC Кордит D	Кордит D	M—7
1. Нитроцеллюлоза	51,5	52,5	54,0	49,5—50,0	56,5	54,5
E Содержание в ней азота в %	13,25	13,25	13,25	12,2	12,2	
2. Растворитель						
F нитроглицерин	43,0	43,0	43,0	41,0	28,0	35,5
G динитротолуол	—	—	—	—	11,0	—
3. Добавки						
H этилцентралит	1	—	—	9,0	4,5	0,9
I диэтилфталат	3,25	3,0	3,0	—	—	—
J дифениламин	—	0,6	—	—	—	—
K сульфат калия	1,25	—	—	—	—	—
L нитрат калия	—	1,2	—	—	—	—
M газовая сажа	0,2*	—	—	—	—	1,2
N воск	0,08*	—	—	0,07*	—	—
O краситель	—	0,1*	—	—	—	—
KCl_4	—	—	—	—	—	7,8*
P Теплотворная способность ккал/кГ	1230	1230	1260	965	980	
Q Температура горения °K	3160	3160	3080	2500	2340	
R Скорость горения в см/сек при 70 кГ/см²	1,65	1,7	1,4	0,8	—	
S при 140 кГ/см²	2,50		2,29	1,24	1,19	
T Показатель n	0,69—0,73	0,71	0,75	0,69	0,73	
U Весовая плотность кГ/дм³	1,61	1,6				

*Contents shown exceed 100%.

1) Nitrocellulose; 2) solvent; 2) additives. A) Composition and properties; B) fuel; C) ballistite; D) cordite; E) nitrogen content, %; F) nitroglycerin; G) dinitrotoluene; H) ethyl centralite; I) diethyl phthalate; J) diphenyl amine; K) calcium sulfate; L) calcium nitrate; M) gas black; N) wax; O) dye; P) heating value, kcal/kgf; Q) combustion temperature, °K; R) combustion rate, cm/s at 70 kgf/cm²; S) at 140 kgf/cm²; T) index *n*; U) weight density, kgf/dm³.

In composite fuels, the combustible also acts as a binder. Substances with high heating value, capable of serving as binders, are used as combustibles in these fuels. The materials ordinarily employed are high molecular weight synthetic compounds of the rubber or plastic type (for example, polysulfides or thiokols, polyurethanes, polybutadienes, etc.), as well as heavy hydrocarbons (asphalt, for example).

Solid composite fuels are manufactured by introducing finely ground particles of oxidizer into the molten combustible, the binder. The resulting mass can either be used to produce grains which are then placed into the combustion chamber or it can be poured directly into the combustion chamber where it hardens and makes a strong bond with the walls. Here the fuel charge must be sufficiently elastic to prevent formation of cracks by the thermal stresses produced by the differing coefficients of linear expansion for the materials used in the fuel and the chamber. Grains bonded strongly to the case make better utilization of the chamber volume; moreover, if the grain burns from the center to the periphery, there is no need to protect the combustion-chamber walls by heat-insulating materials.

For the majority of combinations of solid fuels and oxidizers, the oxidizer forms 85-90% or more of the stoichiometric mixture. When the oxidizer content is considerable, however, the mechanical properties of the grains are impaired, since there is such a low proportion of the combustible binder. In composite fuels, therefore, the excess oxidizer coefficient is ordinarily less than unity, and less than the optimal value. From this viewpoint, it is better to use combinations having a fairly low value of κ_0.

Composite fuels without additives provide specific thrusts of the same order as double-base fuels. The specific thrust can be increased by introducing a certain amount of metallic combustible. At present, composite fuels are in use that contain added aluminum powder, which increases the fuel heating value. In this case, in fact, the combustion products contain the monotonic oxide of aluminum (Al_2O_3), much of which condenses; nonetheless, there is a gain in specific thrust. Aluminum added in amounts of up to 5-15% increases the specific thrust by 10-20 kgf·s/kgf. Other methods have been developed for improving the specific thrust of solid fuel, in particular, the synthesis of combustibles in which the metallic elements are chemically bonded to the other components. The specific thrust can also be increased by using more efficient oxidizers. This applies in particular to lithium perchlorate $LiClO_4$. An increase in the proportion of oxidizer in solid composite fuels up to a certain limit should also tend to increase the specific thrust.

Composite fuels offer several advantages over double-base propellants. They are less expensive, easier to manufacture, and can be used to make grains forming an intimate contact with the case; with metallic additives, they provide higher specific thrust; finally, by varying the proportions it is possible to obtain a broader range of variation in the propellant characteristics.

Mixed-type solid fuels are sometimes used; they include elements of both composite and double-base propellants. An example is

TABLE 5.2

Composite Fuels and Their Characteristics (γ_t = 1.77 gf/cm³)

Состав топлива*		$P_{уд_{70}}$ кГ·сек/кГ	T_s °K
Окислитель	Горючее-связка		
Перхлорат аммония	Полиуретан	244—248	3300
Перхлорат аммония	Сополимер бутадиена+акриловая кислота	248—252	3530
Перхлорат аммония	Сополимер бутадиена+акрилнитрат	245	3200
Перхлорат аммония	Полибутадиен с конечной карбоксильной группой	251—255	3900

*All of these fuels contain added aluminum powder.

1) Fuel composition*; 2) oxidizer; 3) combustible-binder; 4) kgf·s/kgf; 5) ammonium perchlorate; 6) polyurethane; 7) copolymer of butadiene plus acrylic acid; 8) copolymer of butadiene + acryl nitrate; 9) polybutadiene with terminal carboxyl.

one ballistic-missile engine propellant: ammonium perchlorate, nitroglycerin, nitrocellulose, and aluminum powder.

The composite fuels include Alt-161 (76.5% calcium perchlorate by weight and 23.5% asphalt-bitumen with lubricating oil), GALCIT (based on calcium perchlorate and asphalt-petroleum products). These fuels have low specific impulse, 185 and 195 kgf·s/kgf, respectively, for a chamber pressure of 70 kgf/cm². One modification of the second stage for the American intercontinental "Minuteman" missile uses a composite fuel of the following composition: oxidizer, 74-76% ammonium perchlorate by weight; combustible-binder, about 10% polyurethane; about 15% of aluminum powder; combustion-rate catalyst, Fe_2O_3; plasticizer, dibutyl sebacinate. This fuel has a specific thrust of about 250 kgf·s/kgf for a chamber pressure of 70 kgf/cm².

Table 5.2 gives data for certain widely used composite fuels.

New composite solid propellants have recently appeared that develop higher specific thrust while multiplying burn duration. In addition, the new composite fuels yield a stable combustion process at lower chamber pressures, which is impossible with double-base fuels. The decrease in pressure makes it possible to reduce the weight of the engine structure.

Solid fuels reach 1.8 gf/cm³, while the relative weight density of LRE fuels is less than 1.4 gf/cm³, with still lower values for high heating value liquid fuels. On the average, the weight density of solid fuels is 15-25% greater than for liquid fuels.

Solid-fueled engines are now employed very extensively. While at the beginning of the Second World War, engines had specific impulses of 60-70 kgf·s/kgf, ran on standard powders, with burn times of 5-15 s; now composite-fuel SRE have appeared with specific impulses reaching 240-250 kgf·s/kgf or more, with burn times reaching 2-3 min for side burning and 10 min or more with end burning.

New methods are in use for manufacturing fuel to be directly cast in high-strength light-weight combustion chambers with no special heat insulation; high-temperature nozzles (molybdenum, for example) are in use; chamber pressures have been reduced; all these measures have sharply decreased structural weight and have increased the proportion of fuel charge in the total weight of a present-day SRE to 0.93, a value that had been significantly lower as recently as 1950-1951.

Solid rocket engines are widely employed in devices ranging from small rockets of the jet-projectile type to large vehicles carrying payloads into space. Liquid fuels have recently appeared that permit long-term storage (up to several years) of a fully fueled ready-to-launch rocket with an LRE. These include, for example, kerosene and N_2O_4 (nitrogen tetroxide) and unsymmetrical dimethyl hydrazine. Such liquid fuels still deliver less specific thrust than the best modern liquid fuels. This gives SRE additional advantages in the competition with LRE.

As we have already said, a drawback to the SRE is the low specific impulse as compared with the LRE. At the same time, the SRE requires no piping or valves, no turbopump unit [TPU](THA), gas generators, or other feed-system components used in LRE; thus the specific weight of an engine plant using an SRE may prove no greater than the specific weight of an engine plant with an LRE; moreover, as has been pointed out, a solid fuel has higher weight density.

Let γ_1 and γ_2 be the specific weights of engine plants with LRE and SRE, respectively; $\gamma_1 \geqslant \gamma_2$; $P_{уд1}$ и $P_{уд2}$ are the specific thrusts; $P_{уд1} > P_{уд2}$; $\gamma_{т1}$ и $\gamma_{т2}$ are the weight densities of the liquid and solid fuels; $\gamma_{t1} < \gamma_{t2}$; for LRE, γ_{t1} is the relative weight density of the fuel, unless it is a unitary fuel.

We find the relationship between the specific thrusts of liquid and solid rocket engines under the following conditions:

1) the weight of the payload, nosecone, and vehicle guidance elements is the same; 2) the fuels occupy equal volumes; 3) both rockets are of the single-stage type, with identical maximum speeds at the end of powered flight.

Let M_a be the mass of the payload, nosecone, and guidance elements. Then the final rocket mass will be

$$M_к = M_a + M_{д.у}. \qquad (5.1)$$

Here $M_{d.u}$ is the mass of the engine plant, equaling

$$M_{д.у}=\frac{P\gamma}{g},$$

where P is the thrust and γ is the specific weight of the engine plant.

The initial mass of the rocket is

$$M_{ц}=M_{к}+M_{д.у}+M_{т},$$

where the fuel mass is

$$M_{т}=\frac{V_{т}\gamma_{т}}{g}; \tag{5.2}$$

here V_t is the volume occupied by the fuel.

We can write

$$M_{д.у}+M_{т}=M_{т}k, \tag{5.3}$$

where k is a coefficient used to convert from the mass (or weight) of the fuel to the mass (or weight) of the entire engine plant together with the fuel. Thus

$$M_{к}=M_{к}+\frac{V_{т}\gamma_{т}}{g}k. \tag{5.4}$$

On the basis of (5.1) and (5.3), the final mass of the nose-zone will equal

$$M_{к}=M_{к}+\frac{V_{т}\gamma_{т}}{g}(k-1). \tag{5.5}$$

On the basis of Eqs. (5.4) and (5.5), we can write Eq. (1.1) for the maximum speed of the rocket with the LRE:

$$w_{max1}=P_{уд1}g\ln\frac{M_{к}+\frac{V_{т}\gamma_{т1}}{g}k_1}{M_{к}-\frac{V_{т}\gamma_{т1}}{g}(k_1-1)}$$

or

$$w_{max1}=P_{уд1}g\ln\frac{1+\frac{V_{т}}{G_{к}}\gamma_{т1}k_1}{1+\frac{V_{т}}{G_{к}}\gamma_{т1}(k_1-1)}. \tag{5.6}$$

Similarly, for the rocket with the SRE,

$$w_{max2}=P_{уд2}g\ln\frac{1+\frac{V_{т}}{G_{к}}\gamma_{т2}k_2}{1+\frac{V_{т}}{G_{к}}\gamma_{т2}(k_2-1)}. \tag{5.7}$$

Since by hypothesis V_t = const and $w_{max1} = w_{max2}$, on the basis of Expressions (5.6) and (5.7), we can write

$$\frac{P_{y2}}{P_{y1}} = \frac{\ln \dfrac{1 + \dfrac{V_т}{G_e} \gamma_{т1} k_1}{1 + \dfrac{V_т}{G_e} \gamma_{т1} (k_1 - 1)}}{\ln \dfrac{1 + \dfrac{V_т}{G_e} \gamma_{т2} k_2}{1 + \dfrac{V_т}{G_e} \gamma_{т2} (k_2 - 1)}}. \qquad (5.8)$$

From Eq. (5.8) we can determine the ratio of solid- and liquid-fuel specific thrusts that is required if identical maximum speeds are to be attained at the end of powered flight; here the fuels have weight densities γ_{t_1} and γ_{t_2} and different weight proportions $1/k_2$ and $1/k_1$ for the fuel with respect to the total weight of engine plant and fuel; the weights of the payload, nosecone, and guidance elements are assumed to be the same, as are the volumes occupied by the fuel.

If we simplify the problem and assume that the specific weights of the engine plants are identical, with only the weight densities of the fuels differing, we then obtain the following expression from the basic equation (1.1):

$$\frac{P_{y2}}{P_{y1}} = \frac{\ln \dfrac{M_{п1}}{M_{к1}}}{\ln \dfrac{M_{п2}}{M_{к2}}} = \frac{\ln \bar{m}_1}{\ln \bar{m}_2}.$$

It is quite obvious that the quantities $\bar{m}_1$ and $\bar{m}_2$ are of decisive significance. For the rocket with the LRE, let the mass ratio, or the mass number, equal 6; as a consequence, the ratio of the fuel mass to the final rocket mass will be 5. If the weight density of the solid fuel is 20% greater than the weight density of the liquid fuel, while the fuels occupy identical volumes, then for the rocket with the SRE, the ratio $M_{т2}/M_{к2} = 5.2$, while the mass number equals 6.2. It is assumed that the final rocket masses are the same in both cases, i.e., $M_{к_1} = M_{к_2}$. Thus

$$\frac{P_{y2}}{P_{y1}} = \frac{\ln 6}{\ln 6.2} \approx 0{,}96.$$

If the initial mass number for the rocket with the LRE is less than 6, while the weight density of the solid fuel is higher than was assumed, then P_{ud_2} will be still smaller than P_{ud_1}. For a properly designed rocket with SRE, it is evidently possible to obtain almost the same initial weight for specified payload and final powered-flight speed of the vehicle as for an LRE using storable propellants.

5.2. PROCESS DIAGRAM FOR ELEMENTARY SRE

An elementary SRE is illustrated schematically in Fig. 1.1. Since all propellant grain surfaces, except for the end facing the nozzle, are restricted by walls, combustion appears at the free end surface. If we assume the fuel to be homogeneous (and this must be ensured by the manufacturing process), we can represent the combustion process in the following manner, without dwelling on details. Combustion takes place from the end surface facing the nozzle. This surface F_{gor} moves to the left at a certain rate w_{gor} toward the cap. The quantity w_{gor} is called the combustion rate, and is measured in cm/s or mm/s.

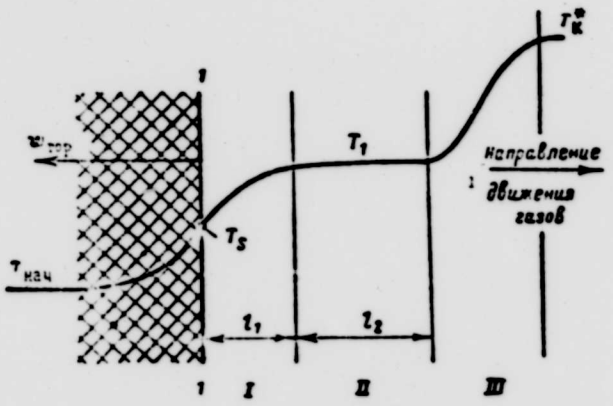

Fig. 5.1. Solid-fuel combustion diagram.
1) Direction of gas motion.

If the grain has a length L cm along the engine axis, while $\bar{w}_{gor}$ is the mean fuel combustion rate, cm/s, then the total engine burn time will equal

$$\tau = \frac{L}{\bar{w}_{гор}}. \qquad (5.9)$$

The combustion process is represented in the following form.

The ignition source releases a certain amount of heat to initiate the combustion process, which is subsequently selfsustaining. The propellant at the end surface breaks down and vaporizes, softening or passing through the liquid phase. The reaction in the solid fuel (pyrolysis sublimation) is usually exothermal in this stage, so that the temperature of the decomposition products rises. In Fig. 5.1, the vertical line 1 corresponds to the arbitrary boundary of the solid surface. The fuel a short distance behind surface 1 actually becomes included gradually in the decomposition process. Calculations and experiment have shown that since the propellant thermal conductivity is low, only a very thin fuel layer, about 0.1 mm or even less, participates in the gas-generating reaction. As a conse-

quence, the main fuel mass maintains its initial temperature T_{nach}, and it is only in the thin layer at the combustion chamber that this temperature gradually rises to T_s, the arbitrary temperature at surface 1, which is taken as the solid-phase boundary.

Zone I touches surface 1; within this zone, the fuel decomposes and is converted from the solid to the liquid and vapor phases. Thus in zone I, there are substances whose aggregate states and temperatures are variable. This zone has length l_1. The product temperature rises to T_1 owing to the heat released during the decomposition reaction.

Beyond zone I, there is a zone II of length l_2; preparation for combustion takes place within this zone. Here active products are formed without liberation of heat; thus in zone II, the temperature $T_1 \approx$ const. The rate of gas generation depends on the fuel properties, on the chamber pressure, and on the combustion-product temperature. Zones I and II are not luminous.

Finally, where a sufficient concentration of active products has formed in zone II, we reach zone III, the combustion zone. The temperature at the end of zone III reaches the maximum value T_k^*, whose value depends on the type of fuel. Zone III is the flame zone or the luminous zone.

The decomposition of fuel at the surface and formation of the combustible gas mixture represents the basic stage in the process, the stage determining the combustion rate. The fuel decomposition rate is heavily influenced by the heat transferred from the flame zone although, as has been indicated, decomposition itself is an exothermal process. More heat is transferred to the fuel surface from the flame zone the greater the chamber pressure p_k^* and temperature T_k^*.

Experiment has shown that the total length of the nonluminous zones I and II depends in great measure on the pressure:

$$l_1 + l_2 \approx \frac{K}{p_k^*}. \qquad (5.10)$$

where K is a constant differing for different fuels. For example, K = 8825 for double-base fuels (nitroglycerin, nitrocellulose, and additives). In Formula (5.10), the length $l_1 + l_2$ is in cm, the pressure is in kgf/cm^2. Consequently, having the pressure increase reduces the length of zone I and II by a factor of 8, and brings the flame zone closer to the surface of the solid fuel.

When p_k^* and T_k^* are small, the gas-formation rate depends little on the heat flowing in from the combustion zone, while with a further reduction in p_k^*, the flame zone moves so far away from the solid-fuel surface that the external inflow of heat becomes almost negligible; at a certain pressure, combustion ceases, since the exothermal decomposition reaction proves inadequate by itself to sustain the

process.

At high pressures, the flame zone approaches the combustion surface, and the heat flowing to the fuel surface rises.

In this case, particularly for high T_k^*, the fuel combustion rate rises, since the rate of fuel decomposition and gas generation increases. Thus for high p_k^*, the combustion rate is determined in great measure by the value of T_k^*, i.e., by the heat supplied by the combustion zone to the fuel surface. With lower chamber pressures, the flame front goes still further from the solid-fuel surface; thus the combustion rate depends little on T_k^*.

The heat radiated from the flame zone influences the fuel decomposition rate. This effect must be properly used, however, or else there may be a harmful selective influence of the radiant energy on individual fuel components. This may result in the formation of cracks, increasing the combustion surface, raising the chamber pressure, and destroying the grain. To prevent this, substances opaque to radiant energy are introduced into solid fuel (gas black, for example).

5.3. SOLID-FUEL COMBUSTION RATES

In the general case, the solid-fuel combustion rate is measured by the displacement of the combustion surface along the normal to the surface in unit time. The combustion rate is influenced by the chamber pressure and the initial temperature of the fuel, since the fuel temperature and the chamber gas pressure determine the conversion rates and the widths of zones I and II.

As we have already mentioned, the chamber pressure determines the amount of heat arriving at the fuel surface from the flame zone.

The equation for the combustion rate of solid composite fuels is obtained theoretically in the form

$$\frac{1}{u_{rop}} = \frac{a}{p} + \frac{b}{p^c}, \qquad (5.11)$$

where a and b have a physical interpretation associated with the gas-phase reaction time and the diffusion time; for fuels based on ammonium perchlorate, c has a value of 0.33. The values of a, b and c are obtained experimentally, and depend not only on the oxidizer, but also on the ratio of oxidizer and binder masses; these values are also affected by which factor predominates, depending on the chamber pressure, diffusion mixing of fuel decomposition products in the zone near the surface or mixing of gaseous components in the narrow combustion zone and the zone immediately ahead.

Empirical equations are most frequently used to determine the combustion rates of specific fuels. The empirical relationship between the combustion rate and the pressure and the initial temperature is written in the following form, for the general case:

$$u_{r.p} = k_t p_k^{*n}; \qquad (5.12)$$

here k_t depends on the initial temperature and the type of fuel;

n is the pressure exponent, depending on the fuel properties and, to a lesser extent, on p_k^*.

Relationship (5.12) is valid only beginning with a certain minimum value p_{kmin}^*, below which the combustion rate drops sharply and combustion soon ceases altogether. The minimum pressure differs for different fuels, and depends on the initial fuel temperature. It is determined by the condition requiring that for this pressure the amount of fuel supplied by the flame zone to the fuel surface be adequate to maintain a steady combustion process.

The temperature coefficient, which also differs for different fuels, indicates the change in combustion rate for a 1°C change in fuel temperature; it has a value of 0.001-0.007 for each 1°C; as a consequence,

$$k_t = k_{t_0} \div (1 \div 7) \cdot 10^{-3}(t - t_0),$$

where t is the temperature at which k_t is determined, while t_0 is the temperature at which we know the value of k_{t_0} for the given fuel.

At low pressure values, k_t depends considerably on the pressure; this is associated with the reduced influence of the external supply of heat to the fuel from the flame zone.

For most solid fuels, the combustion rate increases by 0.1-0.35% when the initial temperature goes up by 1°C. A change from $t_{nach} = -40$ to $t_{nach} = +40$°C increases the combustion rate by 10-25%, and by more in isolated cases.

The temperature coefficient is found from the expression

$$\left(\frac{\partial \ln u_{r.p}}{\partial T_{nach}}\right)_p,$$

when we have an analytic or graphical relationship for the combustion rate.

The temperature coefficient is higher for double-base fuels than for complex composite fuels. Thus, for example, for JPN ballistite, the temperature coefficient is 0.0038 for each 1°C, while for GALCJT, it is 0.0015 for each 1°C.

The pressure exponent n differs for different fuel, ranging from 0.1 to 0.8. The value of n also depends on the pressure, decreasing as p_k^* decreases.

Figure 5.2 shows the combustion rate as a function of chamber pressure for one value of solid-fuel initial temperature.

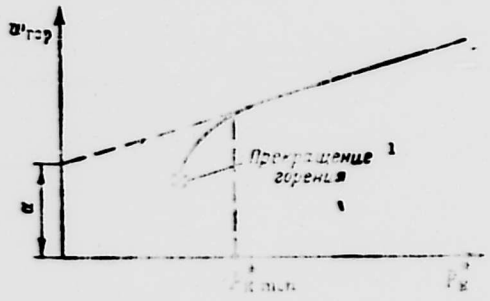

Fig. 5. . Combustion rate as a function of pressure. 1) Combustion chamber.

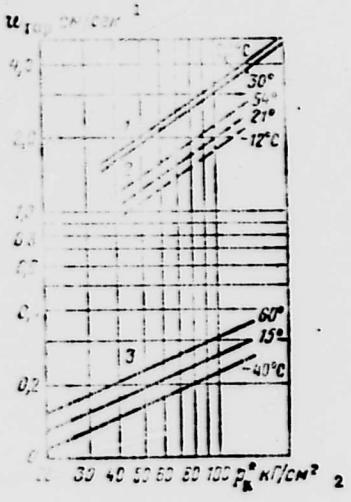

Fig. 5.3. Change in combustion rate as a function of chamber pressure and initial fuel temperature. 1) Asphalt-perchlorate; 2) JPN; 3) composite fuel based on ammonium nitrate. 1) cm/s; 2) kgf/cm^2.

Fig. 5.4. Combustion rate of certain fuels as a function of pressure. 1) JP; 2) German ATO; 3) composite fuel based on $KClO_4$. 1) cm/s; 2) kgf/cm^2.

When the combustion-rate equation is written in the form of (5.12), the origin is placed at the point on the $w_{gor} = f(p_k^*)$ curve where the abscissa value is p^*_{kmin}, with an ordinate value $w_{gor} > 0$.

The combustion-rate equation is sometimes written in the form

$$w_{rel} = a + k_1 p_k^{*n}, \qquad (5.13)$$

where a is the arbitrary or actual combustion rate for a certain initial standard pressure value.

Figure 5.3 shows the combustion rate as a function of pressure for three fuels at various initial temperature values.

The value of the pressure exponent n is of great significance to the engine process. If n is sufficiently large (0.7-1.0), then the combustion rate will depend heavily on the chamber pressure; as a consequence, process stability can easily be lost when various random disturbances act on the pressure. If n is small, the pressure has less influence on the combustion rate, and the chamber process is very stable. With $n = 0$, the pressure will have no influence whatsoever on the process. As a consequence, to obtain a stable process it is desirable to use a fuel with a low value of n. Double-base propellants have relatively high values of n (0.7-0.8 or more). Composite fuels based on perchlorates have lower values of n (0.1-0.4). The smaller n, the lower the chamber pressure at which a stable combustion process is possible for solid fuel, since the combustion rate depends little on p_k^*. In this sense, composite fuels based on perchlorates and nitrates (potassium, ammonia, etc.) are superior to double-base propellants (based on nitroglycerin and nitrocellulose).

Figure 5.4 shows the combustion rate of certain double-base fuels as a function of pressure (curves 1 and 2); the same figure gives curve 3 for a composite fuel based on potassium perchlorate. Although curve 3 lies above curves 1 and 2, we should not conclude that composite fuels always have higher combustion rates than double-base fuels.

A change in initial temperature influences the fuel combustion rate; thus for a given SRE construction and the same nozzle throat area, the chamber pressure, engine thrust, and engine burn time will change. Figure 5.5 shows the thrust as a function of time for the same engine, with three different values of initial grain temperature. The higher initial temperatures correspond to greater values of thrust and chamber pressure, but a shorter engine burn time.

The temperature sensitivity of a fuel can be estimated not only from the temperature coefficient discussed previously, but also from the relative increase in chamber pressure resulting from a 1°C change in initial fuel temperature. For double-base fuels, the chamber pressure increase amounts to 1.17-1.25% for each 1°C, while for composite fuels it is only 0.5% or less for each 1°C. One problem in the development of composite fuels is the need to ensure that the combustion rate will not depend on the fuel temperature.

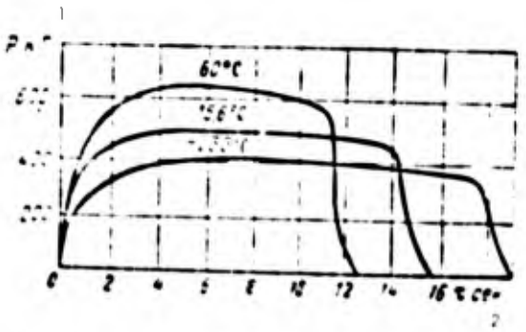

Fig. 5.5. Time variation in SRE thrust for various initial fuel temperatures. 1) kgf; 2) s.

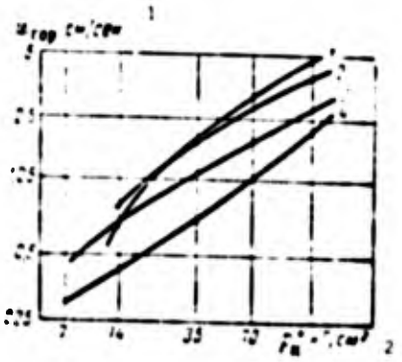

Fig. 5.6. Influence of potassium perchlorate particle size on combustion rate of composite fuel. 1) Up to 2 μm; 2) 12 μm; 3) 35 μm; 4) no potassium perchlorate (38% nitroglycerin, 60% nitrocellulose, 2% ethyl centralite).

The combustion rate of composite solid fuels also depends on the dimensions of the oxidizer grains. Experience has shown that the larger the oxidizer grain size, the slower the combustion rate, all other conditions being equal (Fig. 5.6). The reason is that when composite solid fuels have a heterogeneous structure, the gas flows in the preparation zones are not strictly homogeneous with respect to the combustible and oxidizer concentrations; the larger the oxidizer grains, the less uniform the composition ahead of the combustion reaction zone.

5.4. EROSIVE COMBUSTION

By erosive combustion we mean a process in which the combustion products move toward the nozzle along patns parallel to the combustion surface with a certain, usually variable, velocity v. Figure 5.7 clearly illustrates erosive combustion; here we see a cylindrical annular internal-burning grain. To prevent combustion of the end and external cylinder surfaces (when there is a gap between the grain and the engine case), these surfaces are protected, i.e., restricted by means of inert materials (for example, as we have already noted, a layer of acetyl cellulose, ethyl cellulose, etc.). In an annular cylindrical internal-burning grain, the gas velocity will have its greatest value at the grain exit aperture.

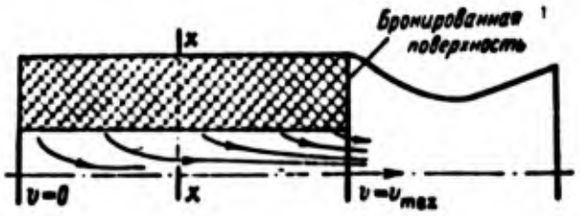

Fig. 5.7. Erosive combustion of annular cylindrical grain. 1) Restricted surface.

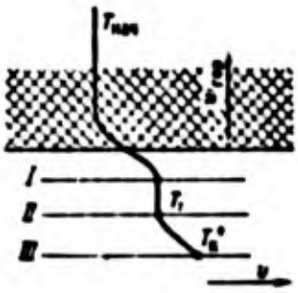

Fig. 5.8. Erosive combustion.

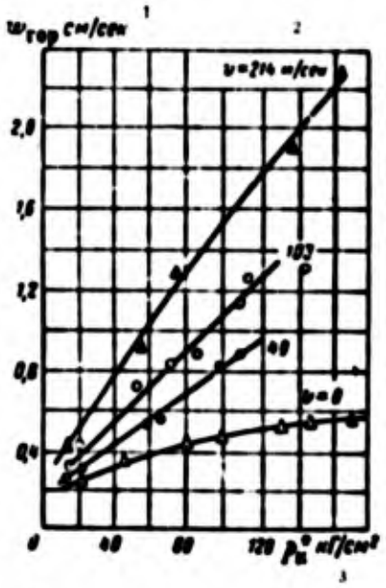

Fig. 5.9. Influence of gas pressure and velocity on combustion rate. 1) cm/s; 2) m/s; 3) kgf/cm^2

As calculations and experiment have shown, v_{max} = 200-400 m/s.

When the gases move parallel to the combustion surface, a turbulent boundary layer appears or becomes intensified; the burning rate along the surface creates turbulence in the flows within the decomposition and preparation zones. Thus there is a noticeable drop in the heat transferred from the combustion zone to the solid-fuel surface, while the fuel combustion rate becomes greater. At large values of gas velocity it is not impossible for erosion to occur in the literal sense owing to removal by the gases of solid, softened, or liquid particles from the surface.

The actual diagram of the erosive-burning process (Fig. 5.8) remains the same for an arbitrary section x-x (Fig. 5.7) as for end combustion of the grain. The greater the gas velocity, the more heat transferred from the combustion zone and the higher the fuel combustion rate ω_{gor}.

For erosive combustion, experience shows that

$$\omega_{гор} = \omega_{гор_{v=0}}(1 + k_v v). \qquad (5.14)$$

where v is the gas velocity along the combustion surface, m/s;

$\omega_{gor_{v=0}}$ is the combustion rate, m/s, when v = 0;

k_v is a constant for the given fuel, s/m.

The value of k_v is nearly independent of the pressure and equals $32.8 \cdot 10^{-4}$ for cordite and $9.8 \cdot 10^{-4}$ for ballistite, for example.

The "cooler" the fuel, i.e., the lower the temperature of the combustion products, the wider the entire reaction zone, and thus the stronger the erosion effect. For "hot" fuels (high T_k^*), the reaction zone is narrow, and the velocity v has less influence. This explains why k_v is lower for ballistite than for cordite.

If we use Expression (5.12) for the combustion rate when v = 0, then in the general case the solid-fuel combustion rate is written as

$$\omega_{гор} = k_1 p_к^{*n}(1 + k_v v). \qquad (5.15)$$

Figure 5.9 shows the way in which the gas velocity influences the combustion rate of a composite fuel consisting of ammonium perchlorate (NH_4ClO_4), a polyester, and binders, with a mean oxidizer particle size of 24-30 μm.

Since T_{nach}, p_k^* and v influence the burning rate, special measures must be taken to see that the process develops in the required direction. One important option is the choice of combustion-surface shape.

As has been pointed out, when burning takes place along the

internal surfaces of fuel-grain channels, the rate of gas motion gradually rises, reaching a maximum at the end of the grain facing the nozzle. The open channel cross sections are increased so as to limit the velocity effect to the required degree. For example, instead of a round cylindrical hole, the channel can be made completely conical or partially cylindrical and particially conical (Fig. 5.10). In this case, the process will clearly begin with an increase in chamber pressure and engine thrust; then when the position indicated by the dashed line is reached, the combustion surface will begin to diminish, and the engine thrust will continuously drop. This also aids in reducing the influence of gas velocity, particularly during the second phase of the combustion process, when the channel cross sections increase considerably.

Figure 5.11 shows another example of an internal-burning fuel grain with channel in the form of a six-pointed star; here the cross sections increase from the closed end to the nozzle, as shown at sections 1-1, 2-2, and 3-3. Here also, as the process develops, the combustion surface is first constant and then begins to diminish, while the open cross sections continously increase.

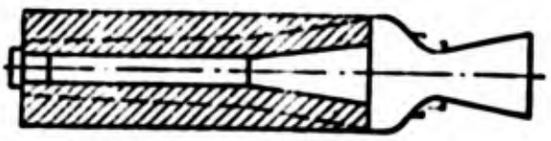

Fig. 5.10. Fuel grain with cylindrical and conical internal combustion surfaces.

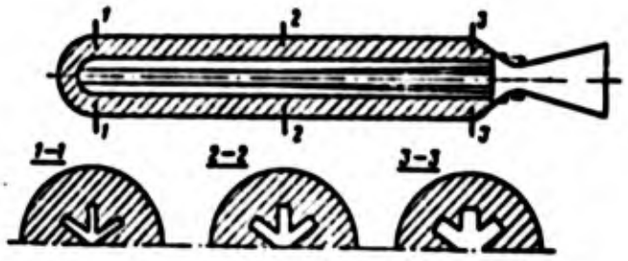

Fig. 5.11. Change in internal-channel cross section along length of engine, with allowance for erosion effect.

5.5. EQUILIBRIUM CHAMBER PRESSURE

Let the instantaneous fuel combustion rate be w_{gor}, cm/s, the instantaneous combustion surface F_{gor}, cm^2, and the fuel weight density γ_t, gf/cm^3.

The quantity of gases, gf, forming in 1 s will be

$$G_{t_{сек}} = F_{гор} w_{гор} \gamma_t 10^{-3} \text{ kгf/s}.$$

or, substituting Expression (5.15),

$$G_{\text{газ сек}} = F_{\text{кр}} \gamma_т k_t (p_к^*)^n (1 + k_\varphi v) 10^{-3}. \qquad (5.16)$$

If F_{kr} is the exhaust-nozzle throat area, m^3;

ω_{kr} is the gas velocity in the throat, m/s, and

γ_{kr} is the gas weight density, kgf/m^3, then the amount of gas leaving the engine will equal, by Expression (2.48),

$$G_{\text{газ}} = F_{\text{кр}} \frac{p_к^*}{\sqrt{T_к^*}} m. \qquad (5.17)$$

For a stationary process, clearly

$$G_{\text{газ сек}} = G_{\text{газ}}.$$

Equating Expressions (5.16) and (5.17), we obtain

$$F_{\text{кр}} \gamma_т k_t (p_к^*)^n (1 + k_\varphi v) 10^{-3} = F_{\text{кр}} \frac{p_к^*}{\sqrt{T_к^*}} m.$$

From this we obtain an expression for the equilibrium pressure in the chamber or the pressure for a stationary engine process,

$$p_к^* = \left[\frac{\gamma_т k_t (1 + k_\varphi v)}{z} \frac{F_{\text{кр}}}{F_{\text{кр}}} \right]^{\frac{1}{1-n}}. \qquad (5.18)$$

Here, taking Eq. (2.49) into account,

$$z = 10^3 \sqrt{\frac{kg}{RT_к^*} \left(\frac{2}{k+1} \right)^{\frac{k+1}{k-1}}}.$$

As we see, the chamber pressure depends on the fuel properties $(\gamma_т, k_t, n, k, T_к^*, k_\varphi)$, on the grain structure (v), and on the ratio of the fuel combustion surface to the nozzle throat area, $\bar{f}_{gor} = F_{gor}/F_{kr}$, which has a great influence on the way in which the chamber pressure varies during burning of the grain. Knowing the fuel characteristics and grain shape, and selecting a value for $\bar{f}_{gor}$, we can determine the chamber pressure.

While the fuel is burning, depending on the shape of the grain and the combustion surfaces, the magnitude of combustion surface and burning rate can vary; this influences the chamber pressure.

5.6. SOLID-FUEL COMBUSTION PATTERNS

Depending on the grain shape and its initial combustion surface, three basic patterns can be distinguished for combustion of solid fuels, according to the nature of the time variation in thrust:

1) combustion with constant thrust magnitude;

2) regressive combustion, where the thrust gradually diminishes during burning;

3) progressive combustion, where the thrust gradually increases during burning, reaching a maximum at the end of the combustion process.

Figure 5.12 illustrates these three basic combustion patterns.

If the thrust is to remain constant, the per-second gas flow rate and the exit velocity must remain constant, i.e., F_{gor}, p_k^*, and T_k^* must remain constant for F_{kr} = const. This case is most simply realized for end burning of a solid cylindrical grain. Here, in fact, F_{gor} = const, while p_k^* and T_k^* are also constant.

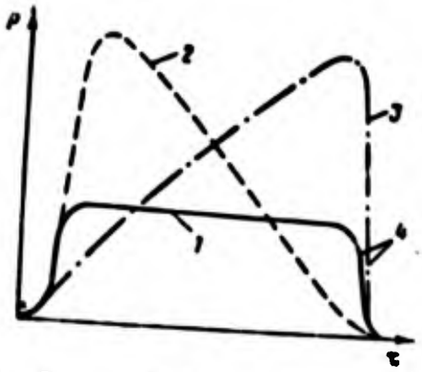

Fig. 5.12. Basic combustion patterns. 1) Constant thrust; 2) regressive combustion; 3) progressive combustion; 4) free exhaust section.

An example of regressive combustion is burning of the outside surface of a cylindrical charge with restricted ends, or of an annular cylindrical charge restricted on the inside surface and the ends. Here as the combustion process develops, the combustion surface diminishes continually, the amount of gases generated decreases, and the chamber pressure falls. The thrust is reduced owing to the reduced per-second gas flowrate and the drop in exit velocity.

An example of progressive combustion is burning of the inside cylindrical surface of a hollow cylindrical grain restricted at the ends and on the outside surface. Here the combustion surface increases during the fuel burning process, while there is a continuous increase in the per-second quantity of gases generated, which increases the chamber pressure. As a result, as the fuel is burned, the thrust rises owing both to the increased per-second gas flowrate and the increased effective exhaust velocity.

If an annular cylindrical grain is restricted only at the end

surfaces and, consequently, there is regressive combustion at the outside cylindrical surface and progressive combustion at the inside surface, it is possible to obtain constant thrust over the entire burning process.

The actual combustion process may be more complicated in nature.

The fuel grains shown in Figs. 5.10 and 5.11 will initially burn progressively owing to the increase in F_{gor} and then regressively owing to the reduction in F_{gor} and ω_{gor}. The combustion rate will diminish owing to the reduction in the gas velocity v, since the open cross sections continuously increase.

The shape of the combustion surface has a great influence on the process in an SRE. This affects the chamber pressure (for F_{kr} = const), the total burn time, the time variation in engine thrust, the thermal effect at the chamber walls, the structural weight, etc. For example, for a solid cylindrical grain with external burning, during the entire time that the fuel is burning, the chamber walls will take up the gas pressure and the heat produced by the combustion products. For a hollow internal-burning cylindrical cylinder, the fuel itself insulates the chamber walls from the thermal effects of the gases; moreover, to a certain extent the fuel grain takes up the load of the gas-pressure forces (particularly for a case-bonded grain). In the first case, special thermal insulation must be used for the chamber walls. Thus the weight of the structure, equaling the initial weight of the fueled SRE less the weight of the fuel, will be greater for an engine with cylindrical external-burning grain and less for an engine with annular cylindrical internal-burning grain.

Modern techniques for casting composite fuels in a chamber with a strong bond between the solidified fuel and the wall makes it possible to avoid using steel as a structural material for the engine combustion chamber, and to use fiberglas or other plastics instead, greatly reducing the structural weight.

For a given chamber diameter, an end-burning propellant grain offers three advantages: a very simple way of ensuring constant thrust, increased burn time for a specified grain length, and burnup of almost all the fuel, with no residue. This combustion method has its drawbacks: relatively low engine thrust, together with direct and long-duration influence of gas pressure and temperature on the combustion-chamber surface. It should also be remembered that in this case as the fuel burns up, the engine center of gravity shifts toward the rear cap. All of this restricts application of end-burning grains to large engines. At present, most rocket engines use fuel grains with surface burning along internal channels of various shapes.

The absolute engine thrust also plays a role in the development of combustion-surface shapes; if this thrust value is of decisive importance, the combustion surface should be as extensive as possible. If the grain length is limited for any reason (strength, manufacturing simplicity, rocket configuration, etc.), then exten-

sion of the combustion surface will reduce the burn time, all other conditions being equal. Figure 5.13 shows arrangements in which the combustion surface consists chiefly of the external grain surface; the restricted surfaces are indicated by the heavy lines. Figure 5.14 shows examples of cylindrical fuel grains restricted along the outside surface and having internal combustion surfaces of various shapes. By manipulating the shape of the grain and the combustion surface, we can obtain the desired type of engine-thrust time variation.

In many cases, grains are not restricted along the entire surface length, but for just a part of the length. Combining restricted and unrestricted sections in various ways, we can also influence the fuel burnup law and, consequently, the time dependence of the engine thrust.

The fraction of fuel remaining at the end, and thus not participating in combustion or creation of thrust, is of great significance in selection of the shape of a grain and its internal channels. The larger this residue, the smaller the total impulse. Figure 5.15 shows successive positions of the combustion surface and the residue for two cylindrical grains with internal combustion surface in the form of a star (Fig. 5.15a) and in the form of a "cross" (Fig. 5.15b). Owing to the sharp reduction in combustion surface at the end, the pressure drops below the permissible value, and combustion ceases. In certain cases determined by the shape of the grain and the channels, the residual grain breaks up and is expelled through the nozzle.

The proportion of fuel left unburned can be estimated from the so-called residue coefficient, which for internal burning gives the ratio of the grain cross-sectional area after burning to a depth l_{min} to the cross-sectional area of the chamber. The smaller this coefficient, the greater the useful per-unit-weight output of the SRE.

If for Fig. 5.15 we let f_{ost} be the cross-sectional area of a single residual deposit, and let i be the number of deposits, which depends on the internal-channel configuration, then the residue coefficient for these arrangements will be

$$k_{ост} = \frac{if_{ост}}{F_t}, \qquad (5.19)$$

where F_t is the initial grain cross-sectional area.

In well-made grains, k_{ost} should not exceed 0.03. For an annular cylindrical grain with external and internal burning, the fuel wall thickness will decrease as burning advances, and at a certain time the wall will be destroyed, with the fragments leaving through the nozzle; the residual losses are relatively high for such a grain. For specified combustion-chamber diameter and length, the maximum possible amount of fuel can be accommodated by the engine if it takes the form of a solid cylindrical grain, with end burning or burning along the external cylindrical surface. In all other cases,

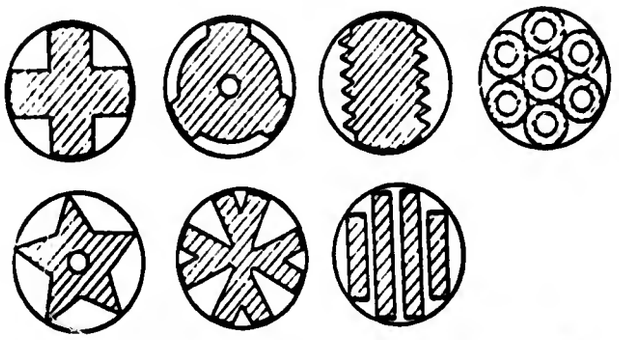

Fig. 5.13. Certain grain shapes with external side burning.

Fig. 5.14. Certain grain shapes with internal burning.

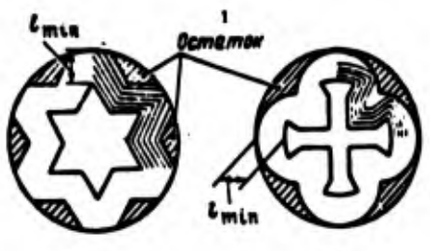

Fig. 5.15. Formation of fuel residues. 1) Residue.

a specified engine-chamber volume will accommodate less fuel or, as it is said, the missile or rocket will be less densely fueled.

Figure 5.16 shows the influence of grain combustion-surface shape on the relative change in engine thrust and on engine burn time. The fuel is the same in all cases, the engine dimensions do not change, and the initial chamber pressure is identical. Grains 8 and 9 give regressive combustion with the longest burn time; grains 1, 2, 3, and 4 give sharply progressive combustion with reduced burn time; grains 6 and 7 provide constant thrust, while grain 5 initially gives a thrust increase, followed by a decrease to constant thrust, with progressive combustion at the end.

The amount of fuel G_t (or its volume V_t) that the engine must contain depends on the fuel burn time τ_{gor}, on the required type of relationship $P = f(\tau)$, and on the residue coefficient k_{ost}.

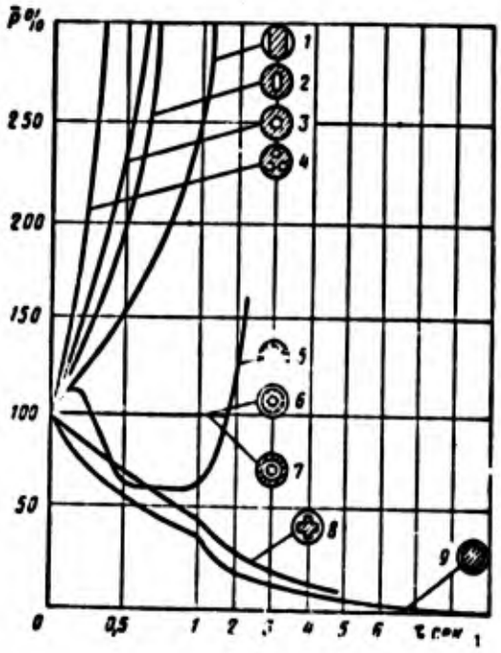

Fig. 5.16. Influence of grain shape on time variation in thrust and on engine burn time. 1) s.

For a given fuel and a specified initial temperature, the combustion rate will depend on the chamber pressure and the gas velocity along the combustion surface; the combustion surface varies in time as a function of grain construction and combustion rate; the specific impulse depends on the gas properties, the pressure drop in the nozzle, and on the nozzle back pressure (i.e., the effective gas velocity). In the general case, therefore, the total engine impulse is

$$I_2 = \int_0^{\tau_{rop}} P_{ya} w_{rop} F_{rop} \gamma_T d\tau.$$

The fuel weight density γ_t can always be removed from the integrand. If we specify the initial combustion surface (grain shape) and determine $w_{gor} = f_1(\tau)$ with the required reliability, we can find $F_{gor} = f_2(\tau)$ and then $P_{ud} = f_3(\tau)$, and consequently the mean integral value $\overline{P}_{ud}$. Then a formula resembling (2.46) can be used to find the volume of fuel charge that participates in creating the total impulse:

$$V_t' = \frac{I_2}{\gamma_T \overline{P}_{ya}(1 + k_{ost})}. \qquad (5.20)$$

For the special case in which combustion takes place at the end surface, $w_{gor} = \text{const}$, $F_{gor} = \text{const}$, and $P_{ud} = \text{const}$; therefore

$$I_2 = \gamma_T w_{rop} F_{rop} P_{ya} \tau_{rop}.$$

Determining the required fuel volume $V_t = V_t'(1 + k_{ost})$, the outside diameter D_{nar} or the grain length L_t can be determined on the basis of considerations pertaining to structure (engine or vehicle), strength or ease of manufacturing.

5.7. THRUST CONTROL. REVERSAL

From the viewpoint of thrust control, LRE are better than SRE. In an LRE, it is possible to reduce the component flowrate and, consequently, the engine thrust. There are single-chamber models of LRE in which the ratio of maximum to minimum thrust reaches 10:1 or better. Here SRE require special design and control methods, since the fuel is contained completely within the engine.

To a certain degree, thrust can be controlled by opening small additional nozzle apertures. This increases the total critical cross section, reduces the $\overline{f}_{gor}$ ratio, and decreases p_k^* in accordance with Formula (5.18), which reduces the thrust. The drop in chamber pressure reduces the combustion rate (5.15), which in turn decreases p_k^* and the thrust. A certain time after the additional apertures have been opened, the chamber pressure and the thrust take on the new steady values.

Thrust can also be controlled by varying the throat area of the main nozzle. This method has a drawback: it is difficult to control the nozzle throat area when there are uncooled structures such as the case of the SRE and its nozzle; thus application of this control method is limited to relatively small engines designed for short burns.

The thrust can be controlled by using two types of fuel in one chamber, with one type burning at a rapid rate. There are many versions of this type of control; the particular modification is determined by the desired type of thrust time variation. Figure 5.17 shows an elementary arrangement using two types of cylindrical end-burning grains; there is one exhaust nozzle with a constant throat area. With such an arrangement, experience has shown that properly

selected grains can provide a launching thrust 10 times greater than the thrust delivered by the second grain during midcourse flight of the vehicle. Sometimes a single common chamber is not used for the two fuel types; two chambers with separate nozzles are used, combined in a single structure to save weight. Figure 5.18 shows two arrangements of double-chamber multinozzle SRE, with the chambers containing different types of fuel charges.

In contrast to LRE, where thrust can be smoothly controlled, in SRE, the thrust varies in steps, unless the nozzle has a central element that can be moved. A separately manufactured launch engine can be jettisoned after its charge has burned. When a design is selected, allowance must also be made for the stability of the engine center of gravity.

In modern large SRE it is better to use concentrically positioned two-fuel charges with differing characteristics. By a proper combination of combustion-surface shape and fuel characteristics it is possible to obtain the desired type of time variation in thrust. Figure 5.19 shows a single-chamber SRE in which the inner fuel has a complex combustion surface with a lower combustion rate than the second fuel, which is case earlier in the chamber as a hollow cylinder. Owing to these characteristics of the combustion-surface shape and the fuels, a unique relationship is obtained between the thrust and the time, with high impulses at the beginning and end of the process, and relatively constant thrust in between.

High targeting accuracy of missiles requires, in addition to thrust control, the use of thrust cutoff and thrust reversal. Cutoff and reversal can be used to correct the total impulse and the rocket speed at the end of powered flight. The thrust can be cut off when the required speed is reached, even when the fuel has not been fully expended, by rapidly opening additional large apertures. This sharply reduces the pressure; the rarefaction wave sharply expands the first and second zones of fuel decomposition and preparation, with a sharp reduction in the heat supplied to the fuel surface; combustion ceases.

Thrust reversal is used when the rocket speed at the end of powered flight exceeds the required value; in this case, thrust reversal can be used to increase the accuracy with which the vehicle accomplishes its mission. Figure 5.20 shows two thrust-reversal schemes. With the first arrangement, lateral apertures are made at the entrance section of the main nozzle; they are capped. The caps are separated fromthe hot gases by heat-insulating materials. These side apertures are directed at a certain angle away from the main nozzle. At the required time, special charges with a separate electric control system free the caps; thus some of the gases are directed through the reversing nozzle. The gases from the reversing nozzle should not have a harmful influence on the vehicle or, more important, on the remaining engine fuel charge.

Here we shall not go into detail on methods for controlling the direction of the thrust vector (introduction of liquids or gases on one side of the nozzle, control surfaces, various types of rotary heads, rotary nozzles, rocking engines, vernier engines), since the problems are common to SRE and LRE, although the particu-

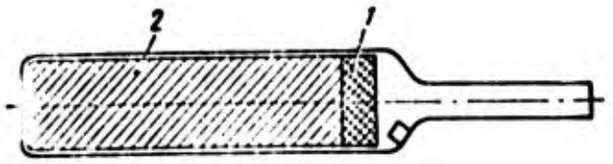

Fig. 5.17. Single-chamber SRE with two fuels. 1) launch fuel; 2) midcourse fuel.

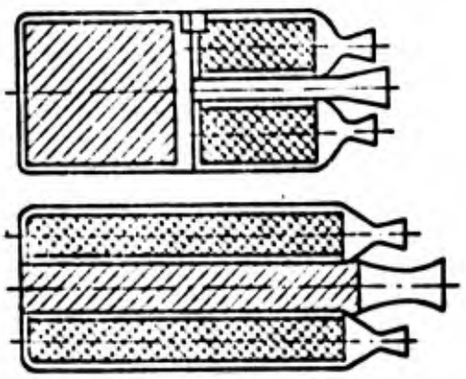

Fig. 5.18. Double-chamber multinozzle SRE with two fuels.

Fig. 5.19. Single-chamber engine with two fuels.

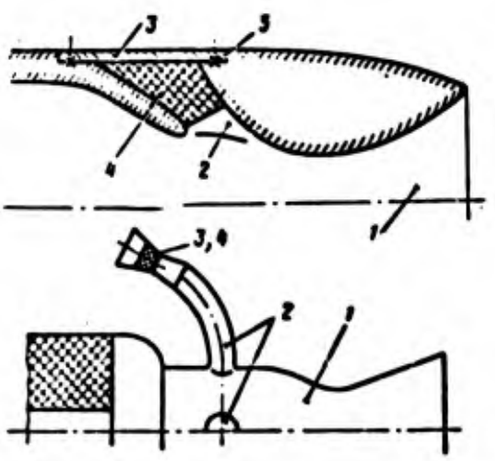

Fig. 5.20. Two thrust-reversible arrangements. 1) Main nozzle; 2) additional reversal nozzle; 3) caps; 4) heat insulation; 5) breakaway charge.

lar design (rotary nozzles, for example) will have its characteristic features for the SRE.

5.8. ABNORMALITIES OF ENGINE OPERATION

Abnormal processes can occur in an SRE during ignition, during stationary combustion, and when the engine is cut off.

Abnormal ignition can be caused both by an inadequate total energy reserve and a low rate of energy release or, conversely, by an excessive rate of igniter energy release. When igniter energy is low, the process may be stifled at the very beginning, and never reach the stationary regime. The igniter should consequently have adequate thermal power and the required amount of energy to ensure stable combustion of the main fuel charge. If, conversely, the ignition source has a considerable excess of power over the required amount, there will be a pressure peak at the beginning of the process (Fig. 5.21); this is dangerous to the structural integrity of the fuel grain (particularly one manufactured by compression) and to the chamber walls.

Several factors can produce abnormalities in the established combustion process of the main fuel charge: cracks in the fuel grain, erosive combustion, nonuniform composition of the fuel or its macrostructure. We shall discuss the unstable combustion process separately.

To keep the discussion simple, we consider a solid cylindrical end-burning grain. When the combustion surface reaches a crack as the fuel burns (Fig. 5.22a), the hot gases enter the slit, and the combustion surface gradually increases (Fig. 5.22b); thus the chamber pressure and engine thrust exceed the expected values, while the fuel burn time is shortened. Depending on the grain shape and the location of the cracks, the grain may be broken up, with increasing mechanical losses of fuel and cessation of combustion. Even hairline cracks may cause this type of disturbance in the normal process.

With erosive combustion, an abnormal process can appear, usually in the initial phase of combustion, if the final channel cross section for gas flow is made too small, so that the gas velocities at the end of the channel become great. The high velocities produce significant erosion of the final combustion-surface sections, thus increasing the combustion rate. As a result, an erosive pressure peak and thrust peak appear (Fig. 5.23). With intensified burning of the channel end sections, however, the open cross sections for the gases increase, the erosion effect diminishes, the combustion rate decreases, while the chamber pressure and engine thrust drop to the normal values. An erosion peak is undesirable not only since it increases the chamber pressure, but also since it distorts the necessary relationship between the thrust and the time and reduces the engine burn time. The erosion pressure and thrust peaks can be eliminated by changing channel and grain shapes as shown by the dashed line for the two grains. A distinction should be made between design pressure peaks (see Fig. 5.19), required for rocket operation by various factors, and additional unforeseen erosion peaks of the

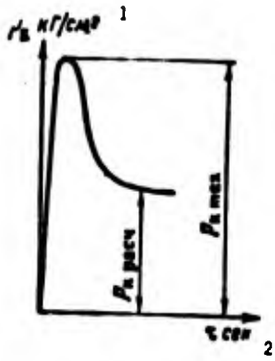

Fig. 5.21. Pressure peak resulting from excessive igniter power. 1) kgf/cm^2; 2) s.

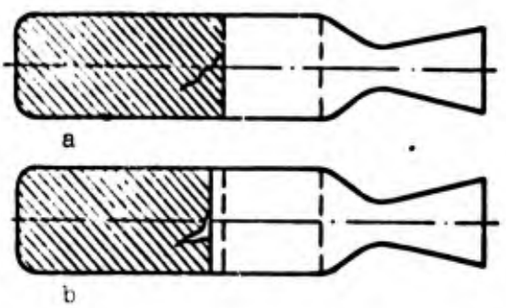

Fig. 5.22. Influence of crack in fuel on increase in combustion surface.

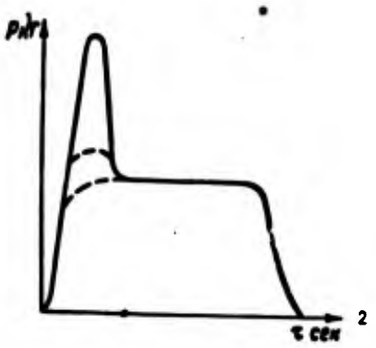

Fig. 5.23. Abnormal thrust (pressure) peak for erosive combustion. 1) kgf; 2) s.

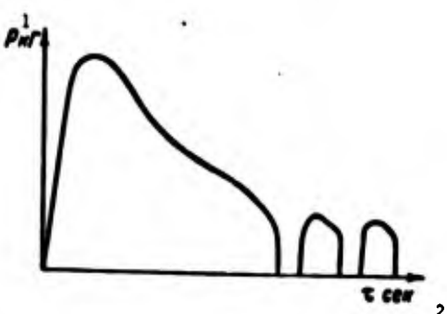

Fig. 5.24. Repeated ignition at cutoff. 1) kgf; 2) s.

type described.

The process abnormalities introduced by substantial structural nonuniformity of the fuel are obvious, so that there is no need to dwell on them here.

Abnormal operation can occur at the end of the engine burn both with forced cutoff and with natural completion of the process (particularly with a regressive process), when the fuel store is exhausted. When the pressure drops below a certain value, combustion may cease. The fuel surface is hot, and the exothermal decomposition and gasification reactions still continue; moreover, the hot engine components radiate heat to the fuel surface; this combination of factor may reignite the fuel, increase the pressure, and produce thrust. As the gases exit, the pressure will again drop and combustion will again cease. This process may repeat several times (Fig. 5.24).

5.9. BASIC SOLID-FUEL REQUIREMENTS

By studying the characteristics of the SRE process, it is possible to formulate the basic requirements to be met by a solid fuel for reliable operation and process stability, as well as for improved rocket performance. These requirements reduce to the following:

1. The fuel must release as much heat as possible as it burns, with formation of light combustion products, so as to increase the exit velocity and, consequently, the specific impulse.

2. The fuel must have a high weight density; all other conditions being equal, this makes it possible to reduce engine dimensions. This is particularly important for an SRE, where all the fuel is located within the engine chamber.

3. The chamber pressure at which stable combustion of the fuel is possible should be relatively small; this reduces the structural weight and increases process reliability.

4. The fuel combustion rate should be relatively small; for a given charge, this will increase the combustion time and improve the stability of the combustion process.

5. The combustion rate should depend little on the chamber pressure, i.e., the pressure exponent n should be as small as possible, since this tends to increase the combustion-process stability.

6. The initial fuel temperature should have as little influence as possible on the combustion rate; this increases process stability and missile targeting accuracy for all possible initial fuel temperatures.

7. For modern solid fuels to be used in medium- and long-range vehicles, the specific impulse should be quite high.

8. When the fuel is cast in the chamber case, it should form a strong bond with the engine-chamber walls, and the bond should be

influenced by neither transportation nor combustion conditions.

9. When solid-fueled rockets are in long-term storage, wide variations in ambient temperature should not disrupt the fuel-case bond owing to differences in expansion coefficients or to changes in the structure or physical-chemical properties of the fuel, in particular.

Let us look at some examples illustrating certain of the above situations.

According to United States Army specifications, the solid fuel used in the engine of the Nike-Ajax missile must operate satisfactorily: after three days in −40°C temperatures, after one day at +50°C, and after four hours of maximum sunlight. The fuel should be storable for at least a year with no change in physical-chemical properties; it must operate satisfactorily at fuel temperatures between −45 and +65°C.

Double-base fuels using nitroglycerin and nitrocellulose require high chamber pressures (70-140 kgf/cm^2 or more). As a rule, the specific impulse of these fuels does not exceed 200 kgf·s/kgf. In fact, calculations have shown that for a 2:1 ratio of nitroglycerin to nitrocellulose and a 13-14% of nitrogen in the nitrocellulose, with 5% of stabilizer (centralite), the maximum specific thrust may reach 240-250 kgf·s/kgf. It has as yet not been possible to realize such specific thrusts, however. For this optimal composition, the combustion rate is 2 cm/s. The heat of detonation or the heating value of double-base fuels is 650-1400 kcal/kgf, depending on the composition.

For modern and prospective composite fuels, the pressure in the engine chamber is 40-70 kgf/cm^2; the specific impulse reaches 240 kgf·s/kgf at sea level; in the future, it may reach 270-280 kgf·s/kgf or more. The heating value is 1200-1800 kcal/kgf, while for promising lithium perchlorate base fuels, it is 2500 kcal/kgf or more.

For HES-4016 double-base fuel, consisting of 54% by weight of nitrocellulose (containing 13.25% nitrogen), 43% nitroglycerin, and 3% centralite, near the combustion surface the processes in the fuel itself lead to the release of about 140 kcal/kgf of heat; where the fuel layer has a heat capacity of 0.35 kcal/kgf °C, this yields a temperature of ~700°K at the fuel surface when t_{nach} = 27°C. In the gasification zone, about 140-280 kcal/kgf is also released, with the temperature reaching T_1 = 1100-1400°K. At the end of the combustion zone, about 700 kcal/kgf more is released, with the temperature reaching 3370°K.

The combustion rate for this fuel can be represented by the formula

$$w_{rop} = 0{,}158 + 0{,}0379\, p_k^{0{,}821},$$

which holds in the 10 to 340 kgf/cm^2 pressure range. In the p_k^* = = 50-200 kgf/cm^2 range, the temperature coefficient equals roughly 0.004 for each 1°C.

For Alt-161 cast potassium perchlorate base fuel (76.5% and 23.5% a mixture of asphalt bitumen and lubricating oil), the temperature at the end of the combustion zone is $T_k^* = 2040°K$ at $p_k^* = 136$ kgf/cm^2; $k = 1.27$ and $\gamma_t = 1.77$ gf/cm^3. The combustion rate of this fuel is expressed by the formula

$$w_{rop} = 0{,}103\, p_k^{*0{,}745},$$

which holds for pressures of 100-200 kgf/cm^2. The temperature coefficient equals ~0.0013 for each 1°C.

For a composite fuel consisting of polystyrene + ammonium nitrate with 3% by weight of added $(NH_4)_2Cr_2O_7$, for a particle size of 10 μm, we have the following empirical equation for the combustion rate,

$$w_{rop} = 0{,}092 + 0{,}002\, p_k^* \quad \text{cm/s}.$$

For a composite fuel based on polystyrene + ammonium perchlorate with an 80:20 ratio of oxidizer and binder masses, and oxidizer particle sizes of 60 and 8 μm, the following empirical equations have been obtained for the combustion velocity:

$$\frac{1}{w_{rop}} = \frac{3{,}62}{p_k^*} + \frac{4{,}39}{p_k^{*0{,}33}} \quad \text{cm/s}.$$

and

$$\frac{1}{w_{rop}} = \frac{4{,}99}{p_k^*} + \frac{2{,}64}{p_k^{*0{,}33}} \quad \text{cm/s}.$$

Manuscript Page No.	Transliterated Symbols
100	т = t = toplivo = fuel
100	уд = ud = udel'nyy = specific
101	к = k = konechnyy = final
102	ду = du = dvigatel'naya ustanovka = engine plant
102	н = n = nachal'nyy = initial
104	гор = gor = goreniye = combustion
104	нач = nach = nachal'nyy = initial
113	сек = sek = sekundnyy = per-second

114 кр = kr = kriticheskiy = critical

114 газ = gaz = gaz = gas

117 ост = ost = ostatok = residue

Chapter 6

UNSTABLE PROCESSES

6.1. GENERAL CONCEPTS

Experience has shown that in both liquid rocket engines [LRE] (ЖРД) and in solid rocket engines [SRE](РДТТ) under certain conditions that depend on the engine operating regime, the fuel properties, the chamber geometry, and other factors, the process becomes unstable. The process instability consists in the following: the pressure at an arbitrary point in the chamber (and the temperature, consequently) is not constant, but fluctuates with larger or smaller amplitude and frequency about a certain mean value. Small fluctuations in process parameters, primarily the pressure, will always occur during engine operation, but they have almost no influence on operating economy and reliability, and are not transmitted to the vehicle; such microfluctuations do not disturb process stability. Only when the amplitude of the pressure fluctuations becomes sufficiently large and the fluctuations become periodic in nature does the process become unstable. Depending on the amplitude and frequency of pressure fluctuations, the process goes over to an unstable operating regime, which under certain conditions will rapidly destroy the engine.

In a LRE, we observe two types of instability, two characteristic types of oscillation, low-frequency and high-frequency. With low-frequency oscillations, the pressure in the entire chamber is the same at every given instant. The oscillations range in frequency from dozens to hundreds of Hertz, and are distinguished by the fact that the oscillatory process most often encompasses not only the gas in the combustion chamber, but the entire fuel-supply system as well; these fluctuations appear when the chamber is operating at low pressure (low thrust), and in this case do not present any great danger to engine strength. High-frequency oscillations with frequencies of several hundred or thousands of Hertz are observed with high chamber pressures and are localized within the combustion chamber; their appearance leads to very rapid destruction of the engine, however. These fluctuations are acoustical oscillations in a gas medium; consequently, the pressure varies in time and will not be identical over the chamber volume at any given instant.

In SRE, where there is no fuel-supply system, no low-frequency oscillations are observed; here we find only high-frequency pressure fluctuations at 500-50,000 Hz. High-frequency oscillations are the same in nature for LRE and SRE, but in LRE the sources sustaining the oscillations are distributed widely over the chamber volume,

while in SRE they are concentrated within a shorter section near the fuel combustion surface.

When an unstable process appears, the following defects can arise in the engine system and the craft as a whole: 1) large fluctuations in thrust and, consequently, additional (often unacceptable) loads on the engine and craft controls that ensure craft motion along the specified path; 2) large fluctuations in pressure (and temperature) in the chamber, leading to increased mechanical and thermal loads on the engine walls, and to burnout and failure; 3) vibrations in the entire system, capable of loosening joints and causing other defects. Thus in LRE and SRE, the process should be brought to a degree of perfection such that no instability will appear for any possible steady or transient engine operating regimes. This is one of the most important tasks in the practical design of rocket engines.

There are many published studies dealing with the theoretical and experimental investigation of unstable processes in LRE and SRE. Theoretical analysis is complicated, and usually based on various rough assumptions; nonetheless, such analysis yields qualitative and, often, good quantitative results.

6.2. LOW-FREQUENCY INSTABILITY OF LRE PROCESS

As has been indicated, low-frequency instability of an LRE process is primarily characterized by pressure fluctuations in the chamber at frequencies of the order of dozens or hundreds of Hertz. Such fluctuations can be produced by random disturbances in pressure, in total fuel flowrate or in the flowrate of one of the components, by vibration of the vehicle in flight caused by control systems, etc. Low-frequency oscillations do not arise instantaneously, but result from gradual intensification of relatively small oscillations when conditions are favorable for such intensification. It has been established that an engine whose process is completely stable at normal thrust (and, consequently, normal chamber pressure) tends to go into an unstable process when the thrust is decreased (together with the chamber pressure).

As a rule, low-frequency pressure oscillations in the chamber are transmitted through the injectors to the fuel mains, where pressure fluctuations appear at the same frequency, but with lower amplitude and with a phase shift. Pressure fluctuations in the entire engine plant (chamber and fuel mains), as in a single system, can themselves excite oscillations in the vehicle as a whole.

Low-frequency instabilities in the engine plant are produced by the following factors. With constant fuel pressure (in the tanks or beyond the pumps), a change in chamber pressure leads to a change in the drop Δp_f across the injectors and, consequently, to a change in the flowrate and velocity at which the fuel components are injected. The combustible and oxidizer lines differ in length and structure; through these lines, the disturbance from the injector nozzle travels against the flow at the speed of sound (about 1200 m/s), as does the reflected wave going with the flow toward the nozzle; thus the drops Δp_f may differ for the oxidizer and the combustible; moreover, there can be phase shifts between the maximum and minimum component flow-

rates, also leading to fluctuations in the relationship of fuel components in the chamber. If the chamber pressure fluctuations become periodic in nature, then so will the fluctuations in component flowrates, in injection velocities, and in the component ratio. In fact, owing to fluctuations in the fuel flowrate, the amount of heat energy released during the reaction will also fluctuate. If the fluctuations in the amount of heat released are in phase with the chamber pressure fluctuations, then pressure fluctuations appearing for any reason will be sustained, will become stable, and the engine process will become unstable. Conversely, if the fluctuations in the amount of heat released are not in phase with the chamber pressure fluctuations, the oscillatory process will be damped, and the engine process will again become stable. Consequently, maintenance of an unstable process requires that the fluctuations in the energy released by the reaction be in phase with the chamber pressure fluctuations, i.e., the maximum value of p_k^* must correspond to the maximum energy release and vice versa.

For a low-frequency instability, a pressure disturbance appearing for any reason in the chamber is transmitted through the injector nozzle, which acts as a resistance, into the fuel line. The wave traverses the entire line, end-to-end, and upon returning to the injector increases the drop Δp_f. The fuel main has its own natural relaxation time τ_m, i.e., disturbance damping time. This time differs for different systems and is of the order of 0.001-0.01 s. A change in the drop across the injectors changes the component flowrate and injection velocity and, consequently, also changes the fineness and range of dispersion, the mixing conditions, and the local mixture compositions.

A certain time τ_{zap}, the delay time, elapses between arrival of the liquid fuel at the chamber and the time at which it is converted into gaseous combustion products. The delay time (0.03-0.05 s) significantly exceeds the fuel-main relaxation time. Thus between the time at which a signal appears in the chamber (the pressure disturbance) and the time at which the fuel system responds to this signal, a time of the order of $\tau_m + \tau_{zap}$ elapses. In the chamber itself, a certain time τ_k, the chamber relaxation time, is required for the influence of the heat-release variation to make itself felt. This time is of the same order as for the fuel mains, although the range of possible values is narrower τ_k.

If we let τ_p represent the period of the chamber pressure oscillations, then in the general case the condition for phase coincidence of the pressure and heat-release oscillations in the chamber can be written as

$$\tau_k + \tau_{zap} + \tau_m = k\frac{\tau_p}{2},$$

where k is any odd integer.

Here τ_m and τ_{zap} play the principal role, since τ_k is small.

Since the delay time τ_{zap} for a given fuel is a function of the chamber pressure (and temperature), of the injection velocity (fineness and range of dispersion), and of the component ratio, this time will not remain constant over a cycle of chamber pressure fluctuation. It has been established experimentally that the shorter the delay time, the higher the fluctuation frequency.

The fuel mains, injectors, and their chosen parameters have a large influence on the low-frequency oscillations. It is not difficult to see that when provision is made for a fairly large pressure drop across the injectors ($\Delta p_f > 10$ kgf/cm^2), it is possible to ensure that chamber pressure fluctuations will be damped, since they will not be maintained by noticeable oscillations in the fuel mains. This explains the fact that the engine process, while stable under normal conditions, becomes unstable when the thrust is reduced, i.e., when the fuel flowrate decreases and, consequently, when Δp_f is decreased, since in an LRE the injectors are of the open type with constant nozzle area. For low-frequency oscillations, it is not so much the absolute value of the injector pressure drop that is important as it is the ratio $\Delta p_f/p_k^*$. When the injector nozzle cross section is constant, Δp_f will decrease roughly in proportion to the square of the fuel (or component) flowrate, while for a constant engine nozzle throat area, the pressure p_k^* decreases in proportion to the fuel flowrate. Thus the ratio $\Delta p_f/p_k^*$ decreases as the flowrate decreases.

There are various methods for eliminating the influence of the fuel-main system. In particular, introduction into the fuel mains of accumulators capable of damping liquid pressure fluctuations will promote stability of the fuel flowrate. Another method consists in employing a controller responding to the chamber pressure and regulating the fuel feed so as to extinguish any pressure oscillations that appear, thus returning the engine to the equilibrium regime. It is possible to preserve a specified high drop Δp_f by disconnecting an injector group in throttling regimes.

Figure 6.1 gives a simplified sequence diagram for the physical-chemical processes; for the conditions indicated, this reduces to maintaining the pressure oscillation. The horizontal lines correspond to the mean values of the variables; the curves represent the oscillations in the values. In this case, as we can see, when $k = 1$ the oscillations in the heat release Q are in phase with the pressure oscillation, according to the formula given above.

It should be noted that the low-frequency oscillations are complex, since in addition to the fundamental oscillations, they also contain oscillations at higher frequencies. Improving the entire fuel system is one way of contending with low-frequency instability.

When we are concerned with the low-frequency oscillations, we must reckon with such an important factor as the time delay. All other conditions being equal, in the general case

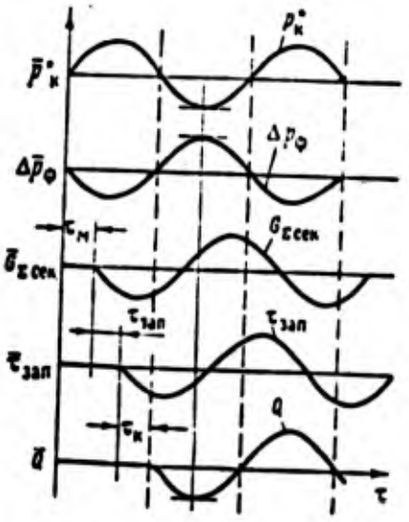

Fig. 6.1. Assorted variables as functions of time during low-frequency pressure oscillations.

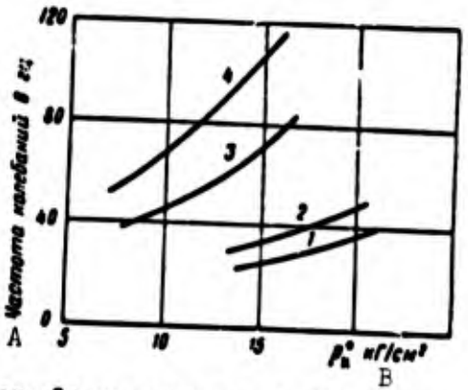

Fig. 6.2. Oscillation frequency as a function of chamber pressure for two fuels and two values of L^*. 1, 2) HNO_3 + octane; 3, 4) HNO_3 + furforyl alcohol; 1, 3) $L^* = 3.55$ m; 2, 4) $L^* = 2.35$ m. A) Oscillation frequency, Hz; B) kgf/cm^2.

$$\tau_{зап} = f(p_к^*, T_к^*),$$

so that this by itself can maintain the oscillations that appear. In fact, when p_k^* decreases, τ_{zap} increases, so that even when $\tau_m = 0$ and $\tau_k = 0$ conditions can be created such that the heat-release fluctuations will be in phase with the pressure oscillation. This type of low-frequency instability has come to be called chamber internal instability, since in this case the characteristics of the fuel system do not play any great role. With internal chamber instability, the oscillation frequency is usually higher than in the previously considered general case of low-frequency instability, where the oscillations involve the entire engine system.

If the delay time were infinitesimal, there would be no low-frequency instability. In such case, a change in chamber pressure an increase, for example, should lead to a change in the drop across the injectors and, in our case, to a reduction in the instantaneous pressure drop and fuel flowrate. As a result (with $\tau_{zap} = 0$), the amount of heat released decreases, and the chamber process becomes stable. This hypothetical example serves to illustrate the fact that in maintenance of a low-frequency instability, an important role is played by the delay time, or the time required to convert the liquid components into the gaseous reaction products; this, of course, is in addition to the role played by the characteristics of the fuel mains.

Experience has shown that the frequency of the low-frequency oscillations rises with increasing chamber pressure, and with decreasing characteristic chamber length L^*. Figure 6.2 illustrates this relationship for two fuels and two values of L^*. The influence of p_k^* is connected with the variation in τ_{zap}, and the influence of L^* with the variation in τ_k and the time spent by the gases in the chamber. As a consequence, a low-frequency instability can also be eliminated by raising the chamber pressure, provided the structure permits this.

For a low-frequency instability, the fuel distribution over the volume and, consequently, the site at which energy is released will not be of decisive importance, since the rate at which a disturbance propagates in the chamber is large (in excess of 1000 m/s), while the chamber dimensions are relatively small, so that disturbances produced at individual points, for example, by nonuniform combustion, are transmitted almost instantaneously throughout the entire volume.

The factors resulting in attenuation of the oscillations are the hydraulic losses in the fuel-main system, various types of oscillation dampers, and nonlinear effects, for example, the exponential relationship between the reaction rate and the temperature (or pressure).

The operation of any element in the closed loop is also of importance particularly, in systems with forced feed, the operation of the pressure reducer.

We have so far assumed that the initial disturbance resulting in instability appears in the combustion chamber. It has been shown that an unstable process in the engine plant can produce longitudinal oscillatory motion of the vehicle as a whole with respect to the path. There can be another source for the initial disturbance, however. When the vehicle moves with acceleration, the fuel can shift throughout the fuel system, particularly onboard large vehicles. This may result in flowrate fluctuations for one or both components, resulting in fluctuations in energy release and pressure oscillations in the chamber. If the system has no capability for selfregulation, i.e., for restoration of exit equilibrium for chamber pressure, the process will become unstable.

6.3. HIGH-FREQUENCY INSTABILITY OF LRE PROCESS

Within an enclosed object bounded by rigid walls and filled with a homogeneous gas, acoustical oscillations at the natural frequencies can arise.

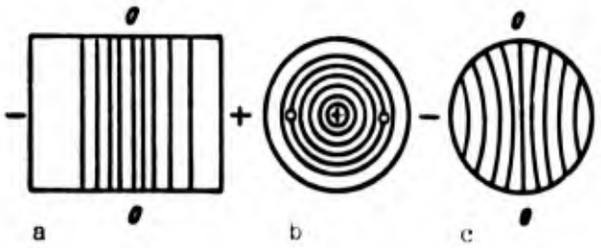

Fig. 6.3. Forms of oscillation in closed cylindrical vessel. a) Longitudinal; b) transverse; c) tangential.

In an engine chamber, acoustical oscillations can also appear at frequencies that depend on the chamber geometric dimensions and the properties of the fluid. The engine chamber differs from a closed vessel, however, first in the presence of a nozzle through which the gases escape and, second, in the inhomogeneity of the medium, since in addition to the gases in the chamber, there is a liquid phase and fuel vapors; a chemical reaction also takes place. The basic difference between an engine chamber and a closed volume lies in the exit nozzle. In the absence of decelerating effects, in a closed vessel no energy need be expended to maintain acoustical oscillations; when there is a Laval nozzle through which gases escape the engine, however, the acoustical oscillations in the chamber can only be maintained if energy is expended, even where all other factors (friction, etc.) are absent. The sources of this energy are evidently the fuel and the heat released in the combustion zone. If the oscillations in the strengths of the heat-release sources are in phase with one of the natural resonant frequencies for the gases in the chamber, a new type of internal chamber instability appears, high-frequency LRE instability (at hundreds or thousands of Hertz).

For high-frequency oscillations, the disturbance propagation time in the chamber becomes commensurate with the pressure-oscillation period; thus in contrast to a low-frequency instability, the parameters at different points within the chamber (pressure, temperature) will differ at any given instant. This nonuniformity of parameters within the chamber volume makes it necessary to consider the spatial and temporal distribution of energy sources. Almost none of the high-frequency pressure oscillations are transmitted to the fuel system.

Longitudinal, transverse (radial), and tangential oscillations can exist in chambers. Figure 6.3 shows examples of these three types of acoustical oscillations in a closed cylindrical vessel; the figure shows isobars at a certain specific instant. For longi-

tudinal oscillations in a homogeneous medium, the gas parameters are identical for each chamber cross section, but they vary from section to section. For transverse oscillations, the gas parameters vary radially. The transverse oscillations are greatest near the head, gradually becoming weaker toward the nozzle. The source of transverse oscillations is the cross-sectional nonuniformity of the mixture composition, caused by the discrete nature of the combustible and oxidizer jets and the variations in the characteristics of the injectors themselves. Transverse oscillations can also appear for a monopropellant owing to the discrete distribution of the flowrate over the head cross section. Acoustical oscillations produced by various factors generate and intensify transverse oscillations; these acoustical oscillations lead to transverse disturbances in the combustible and oxidizer jets and to variation in the jet mixing conditions and, consequently, to variations in heat release. If the transverse pressure oscillations are in phase with the heat-release oscillations, the process becomes resonant at a high frequency. Upon reaching the walls, the compression waves set up additional mechanical loads unforeseen by design calculations and, just as important, impart additional heat to the walls owing to the increased gas density and temperature. These two factors, acting simultaneously, usually cause the engine to fail. Transverse oscillations most frequently appear in large chambers with a high diameter-to-length ratio.

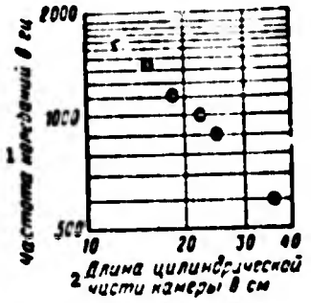

Fig. 6.4. Oscillation frequencies as a function of chamber length. 1) Oscillation frequency, Hz; 2) length of cylindrical portion of chamber, cm.

Longitudinal oscillations are observed in relatively long chambers; the longer the chamber, however, the lower the oscillation frequency (Fig. 6.4). The intensity of longitudinal oscillations is strongly influenced by the shape of the subsonic section of the nozzle. A reduction of the cone angle in the nozzle converging section weakens the effect of longitudinal-oscillation reflection; consequently, in this way it is possible to completely eliminate or noticeably attenuate a high-frequency instability produced by longitudinal oscillations. This has been established experimentally and confirmed theoretically. For a semithermal nozzle, where the minimum cross-sectional area equals the chamber area, longitudinal oscillations will naturally not be reflected from the nozzle.

For the same head structure and, consequently, for identical mixture-formation conditions, longitudinal high-frequency oscillations can be generated or absorbed by varying the chamber length; for specified gas-medium properties, this influences the frequency of resonance acoustical oscillations. Experience has shown that for each chamber diameter there exist minimum and maximum lengths below and above which longitudinal oscillations at a given frequency will not become stabilized. Thus by varying the chamber length we can avoid longitudinal oscillations at a dangerous frequency.

Tests on models have also shown that as the steady-state pressure p_k^* in the chamber increases, all other conditions being the same, the oscillation frequencies and amplitudes also rise. Thus in one investigation, with $p_k^* = 3.6$ kgf/cm^2, the pressure-oscillation frequency was 920 Hz and the maximum amplitude 1.4 kgf/cm^2, while at $p_k^* = 9.1$ kgf/cm^2, the corresponding values were 1000 Hz and 2.45 kgf/cm^2. The increasing oscillation amplitude with rising p_k^* is explained by the greater amount of unburned fuel included in the reaction when the compression wave passes through the mixture [34].

Rigid walls need not be present for transverse oscillations and a subsonic nozzle section need not be present for longitudinal oscillations for maintenance of the oscillatory process. The basic influence is exerted by the synchronization between the intensity fluctuations of the energy sources and the pressure oscillations. The reflected waves can only intensify the oscillation amplitudes.

If the chamber walls reflect pressure waves, the oscillations (transverse or longitudinal) can become shock-type oscillations, and can exert a powerful influence on the course of the chemical reaction, to the point of detonation which, in turn, intensifies the oscillatory process. All forms of acoustical oscillation are characterized by standing waves; here the pressure remains constant at node points (or surfaces), while the pressure oscillates between them; the peak oscillation amplitude is reached at the section where the standing-wave antinode is established. Under engine conditions, naturally, node surfaces and antinode regions will not be strictly fixed in space; nonetheless, the standing-wave model is applicable in practice to engines. In this case, if the combustion front is narrow and coincides with a node surface, or is located near such a surface, the oscillations will not be stable, since when $G_{\Sigma sek} = \text{const}$ and $p_k^* = \text{const}$, the amount of energy released will also be constant and, consequently, there will be no energy sources to maintain the oscillations. Conversely, if the flame front (assumed to be narrow) is located near an antinode, where the pressure-oscillation amplitude is at a maximum, an oscillatory heat-release process can occur, since with variation in p_k^* (and the temperature) there will be variation in the delay time and the chemical reaction rate and, consequently, in the amount of energy released. Given this model of the high-frequency oscillatory process, we can conclude that the wider the combustion zone, the less the heat released in an antinode region, and the smaller the amount of energy used to sustain the oscillations. Distribution of fuel over a significant fraction of the chamber volume can promote process stability.

The delay time plays a significant role in all cases of high-frequency oscillation (longitudinal, transverse, and mixed). Since for a given fuel the gas temperature also varies during pressure fluctuations, we can assume, in general, that

$$\tau_{zap} = f(p_k^*)$$

and, moreover,

$$v_r = f_1(p_k^*),$$

where v_g is the chemical reaction rate.

It is precisely the dependence of the delay time and the reaction rate on the pressure that produces fluctuations in the heat released when p_k^* oscillates. Thus one possible method for contending with high-frequency instability is to vary the chemical activity of the fuel, i.e., to act on τ_{zap} and v_g. These quantities can be influenced by introducing various additives into the fuel, and by using a fuel atomization method that will produce mixtures with varying delay times in different chamber zones.

Another way of contending with high-frequency instability, based on published data, consists in increasing the chamber pressure considerably. In this case, on the one hand, the fuel delay time decreases sharply for steady-state operation, and becomes less sensitive to fluctuations in the pressure and temperature of the fluid; on the other hand, the chamber dimensions are reduced, affording better coverage of the chamber volume by the fuel components.

It should be noted that there still is no rigorous theory of high-frequency instability in LRE processes, although there are many important practical observations that have been described in the periodical and special literature.

6.4. PROCESS INSTABILITY IN SRE

Experience shows that high-frequency pressure oscillations appear in SRE. As in LRE, there always are microfluctuations in pressure, although the cause is still not completely clear; there also is no definite idea as to the degree to which their generation is influenced by such factors as fuel structure, combustion-surface

Fig. 6.5. Diagram of combustion process. 1) Stable process; 2) unstable process. A) kgf/cm²; B) s[illegible]

variations, changes in gas velocities within channels in the course of the process, etc. In many cases, however, chamber pressure oscillations appear with a high amplitude that may be commensurate with the average pressure for normal combustion. These fluctuations definitely have the nature of resonance acoustical oscillations.

Figure 6.5 shows two curves, one referring to normal combustion and the other to unstable, resonance combustion. As we see, in the second case the maximum pressure is nearly twice the normal value; in addition, there is a noticeable reduction in total fuel burn time. Unstable, resonance combustion not only reduces the engine burn time, but can also result in destruction of the grain, followed by explosion. Even if combustion takes place without explosion, the useful effect of the grain will still be reduced by 10-15% in small engines, since in the presence of a nozzle energy is expended to maintain the oscillations in the chamber gas column, heat transfer will rise, and friction will increase. We have already indicated that there are energy losses in a rocket engine chamber during an unstable process; the presence of the exhaust nozzle was held responsible, in the main, for these losses.

The physical pattern for generation and maintenance is basically the same for oscillations in an SRE as for internal high-frequency chamber instabilities in LRE, for all types of oscillation.

As we have already pointed out, for a stationary process in a chamber, there will always be pressure microfluctuations. A pressure increase (a disturbing factor produced by random causes, for example, by nonuniformity in fuel structure) generates a wave which upon moving toward the combustion surface compresses the gas layer near the surface and reduces the width of the gasification and preparation zones to a greater or lesser extent, depending on the intensity of the wave.

The pressure increase and the reduction in the widths of zones I and II (see Figs. 5.1 and 5.8) speed up the processes of decomposition, gasification and preparation, thus increasing the combustion rate. Following the pressure wave, a reflected wave appears, however, and after a certain time interval, the next pressure wave arrives at the combustion surface. If the intensification produced by the first wave in the processes of fuel decomposition and preparation for combustion has been completed by the time the next pressure wave arrives, the excess energy freed will act as a source supplying and maintaining the oscillations. If the time interval between the disturbing factor (the pressure variation here) and its result (the change in combustion rate here) are equal to or a multiple of the period of oscillation for the disturbing factor, the oscillations will be sustained and will become resonant in nature, since we will have a synchronous release of excess energy, in phase with the pressure oscillations. We can therefore assume with full justification that it is precisely the existence of the time interval between the instant at which the gas disturbance occurs and the instant at which this disturbance acts on the combustion rate and the amount of heat liberated that is the factor responsible for maintenance of the unstable combustion process.

Since the chamber pressure oscillations are acoustical in nature, it is clear that the process instability depends on the geometric dimensions and configuration of the channel, as well as on the properties of the medium; the maintenance of this process depends primarily on the physical-chemical properties of the fuel. Thus in contrast to an LRE, initially stable combustion may become unstable, and vice versa, as the geometric dimensions of the channels and the chamber vary during the course of combustion.

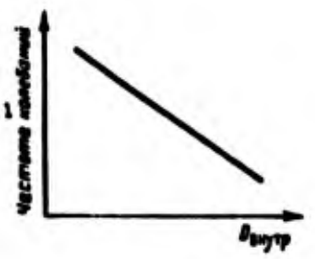

Fig. 6.6. Oscillation frequency as a function of inside diameter of hollow cylindrical grain. 1) Oscillation frequency.

The oscillation frequency depends on the gas temperature and the geometric dimensions of the chamber and channels. Experience has shown, for example, that unstable combustion is most often observed for a cylindrical annular internal-burning grain; the oscillation frequency is lower the greater the channel diameter (Fig. 6.6). In such a grain, unstable combustion can become more stable, or completely stable, as the fuel is burned. Variations in channel shape can also lead to stable combustion owing to a change in the rate of erosive combustion (the influence of v) and as a result of a change in the resonant frequency. Friction and heat exchange are the only internal factors tending to damp any oscillations that appear. Thus individual experiments have shown that combustion is stabilized if special rods are introduced, holes are drilled, or special local radial apertures are made during manufacturing.

Fuels with a high value of pressure index n and with greater sensitivity to initial grain temperature have a greater tendency to unstable resonance combustion. Fuels with a high heating value, for which the reaction-product temperature T_k^* is greater, have more of a tendency toward an unstable process. More uniform combustion is exhibited by fuels with low heating value, a low combustion rate, and little dependence of ω_{gor} on p_k^*, i.e., with a low value of the index n.

Investigations have also shown that when the proportion of oxidizer by weight remains the same, a reduction in oxidizer grain size will increase the combustion rate and promote a tendency toward unstable combustion.

The initial fuel temperature has a twofold influence on process stability. The higher the initial temperature, the less the

influence of external factors (for a given pressure) on the combustion rate, so that the process becomes more stable. On the other hand, an increase in the initial temperature decreases the activation energy which, as experiments have shown, has a strong influence on process stability: a reduction in activation energy increases the tendency of the process toward instability.

An increase in chamber pressure increases the combustion rate and, consequently, reduces the conversion period; this favors process stability. In addition, a pressure increase will change the properties of the gaseous medium and, consequently, the frequency of the resonant acoustical oscillations. A reduction in the time required to convert the fuel into gaseous reaction products, accompanied by an increase in p_k^*, is of very great significance.

For erosive combustion, an increase in the average combustion rate $\overline{\omega}_{gor}$ results not only from chamber pressure oscillations, but also from an increase in the longitudinal velocity gradient. For an unstable process, all of these oscillations coincide in phase.

In an SRE, a very great process instability will also occur if the oscillating combustion zone is located near an antinode of the pressure standing wave. In contrast to an LRE, here there are no means for broadening the volume distribution of energy sources, which would weaken or eliminate the instability.

Both theory and experiment indicate certain methods for contending with process instability in an SRE [54]:

1) acoustical interference, consisting in specially selected chamber geometry, grain shape, and grain working-channel shapes;

2) oscillation damping by increased friction and heat transfer; this includes, in particular, radial apertures in the grain perpendicular to the working channels, and special rods in the working channel; this method increases engine losses;

3) variation in fuel properties by addition of carbon black, aluminum, aluminum oxide, etc., so as to increase combustion stability, thus effecting the combustion rate, the index n, and the conversion period.

Manuscript Page No.

Transliterated Symbols

130 ф = f = forsunka = injector

131 к = k = kamera = chamber

131 зап = zapazdyvaniye = delay

133 сек = sek = sekundnyy = per-second

138 г = g = goreniye = combustion

140 внутр = vnutr = vnutrenniy = inside

138 гор = gor = goreniye = combustion

Chapter 7

PROCESS IN ROCKET-ENGINE NOZZLES

In the nozzle section, the enthalpy of the fuel combustion products is converted into kinetic energy. In rocket engines, the pressure drop in the nozzle considerably exceeds the critical value, so that supersonic nozzles are employed in these engines to attain high efficiencies and, consequently, high exhaust velocities.

The actual flow process in a nozzle is extremely complex. It is accompanied by friction and heat exchange between the working fluid and the walls. The flow is not uniform, since the gas parameters and composition may differ over a cross section.

The temperature reduction along the nozzle produces a decrease in heat capacity and leads to recombination of atoms and radicals if the gas ahead of the nozzle has dissociated. Owing to the high velocities, the working fluid spends little time in the nozzle (10^{-4}-10^{-5} s); this in turn results in a very rapid change of state. The following problem thus arises: to what degree is the nozzle flow process an equilibrium process or, in other words, during the time involved, is it possible to complete the processes of change in all types of internal molecular energy and in the chemical composition in accordance with the temperature and pressure variations (here the oscillatory components of the internal energy are of decisive significance).

The correspondence between the energy of molecular motion and the temperature indicates that there is an energy equilibrium, while the correspondence between the chemical composition of the combustion products and the pressure and temperature shows that there is chemical equilibrium.

For a flow of gaseous combustion products, we can assume in most cases that the process in a rocket-engine nozzle takes place with chemical and energy equilibrium, for all practical purposes. This means that in each nozzle cross section the gas composition and the internal-energy value can be established that correspond to the pressure and temperature in the given section. Here very short nozzles may represent an exception, since the gas spends little time so that the internal energy and chemical composition cannot change with the temperature and pressure variations. Where condensed phase is present, additional conditions influencing nozzle process equilibrium will appear (see below, §7.4).

For the purposes of analysis and computation, we often idealize the nozzle flow process, neglecting friction and heat exchange, and assuming chemical and energy equilibrium. Corrections are used to convert from the characteristics of such an ideal full-equilibrium isentropic process to the parameters of the actual process.

Since the combustion-product composition and heat content vary along the nozzle, so does the expansion-process index. When necessary, therefore, we consider a certain average constant value of the process index in flow-process calculations and analysis.

7.1. VARIATION IN GAS PARAMETERS ALONG NOZZLE

A nozzle is said to be in design operation if the pressure p_s of the gas in the exit section equals the external pressure p_n. Regimes in which the pressure p_s deviates from the external value are

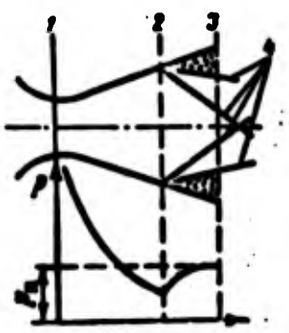

Fig. 7.1. Flow separation at nozzle walls and variation in pressure along nozzle with separation. 1) Throat section; 2) separation section; 3) exit section; 4) pressure shock.

said to be nondesign regimes. The case in which $p_s > p_n$ is called underexpansion, while when $p_s < p_n$, it is called overexpansion.

Experiment has shown that for underexpansion the flow conditions within the nozzle are not violated, but resemble those in design nozzle operation ($p_s = p_n$). Final expansion of the gas jet to the outside pressure takes place beyond the nozzle, and has no influence on the nature of the flow within the nozzle.

In overexpansion, up to a certain pressure ratio p_s/p_n, the flow conditions within the nozzle also do not depart from the design conditions. The increase in the jet gas pressure at the nozzle exit (from p_s to p_n) takes place in a system of shocks located beyond the nozzle. Beginning at a certain value of p_s/p_n, however,

where the pressure difference $(p_n - p_c)$ is great and, consequently, there is a large positive pressure gradient, the boundary layer separates from the nozzle walls, and the shock system extends within the nozzle. Separation results in a change in the internal pressure distribution at the nozzle walls. The pressure increases at the separation site, approaching the external atmospheric pressure (Fig. 7.1). The limiting value of p_s/p_n at which flow separation from the nozzle wall commences will depend on several factors, the Mach number M and Reynolds number, and the nozzle geometry. On the average, this value will equal

$$\left(\frac{p_s}{p_n}\right)_{sep} = 0{,}2 - 0{,}4.$$

We note that rocket engines basically operate under conditions such that $p_s/p_n > (p_s/p_n)_{pred}$, and it is extremely rare for gas to flow with separation at the nozzle walls in such engines; thus in the ensuing discussion we shall be concerned, in the main, in nozzle gas flow without separation.

With an above-critical pressure drop and unseparated isentropic gas flow, external factors (variations in external atmospheric pressure, for example) have no influence on the type of flow in the nozzle. Under these conditions, the ratios of gas parameters (pressure p, temperature T) in any nozzle section to the same gas parameters ahead of the nozzle (at the end of the combustion chamber) will depend solely on the relative area of the given section and on the process index k:

$$\frac{p}{p_n^*} = \varphi_1(\bar{f}, k); \quad \frac{T}{T_n^*} = \varphi_2(\bar{f}, k).$$

Here $\bar{f} = F/F_{kr}$ is the relative area of the given nozzle section;

F is the area of the given nozzle section.

For one-dimensional isentropic flow, the pressure ratio p/p_k^* is associated with $\bar{f}$ in the following manner:

$$\bar{f} = \frac{\sqrt{\left(\frac{2}{k+1}\right)^{\frac{k+1}{k-1}}}}{\sqrt{\frac{2}{k-1}\left[(p/p_n^*)^{2/k} - (p/p_n^*)^{\frac{k+1}{k}}\right]}}.$$

Figure 7.2 shows $\bar{f}$ as a function of p_k^*/p.

The gas velocity in any cross section is determined by the value of p/p_k^* and by the gas parameters ahead of the nozzle:

$$w = \sqrt{2g\frac{k}{k-1}RT_n^*\left[1 - \left(\frac{p}{p_n^*}\right)^{\frac{k-1}{k}}\right]}. \qquad (7.1)$$

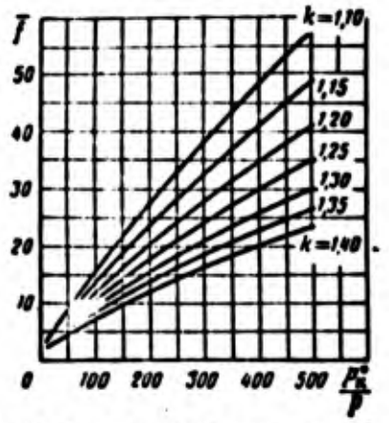

Fig. 7.2. Dependence of $\bar{f}$ on p_k^*/p.

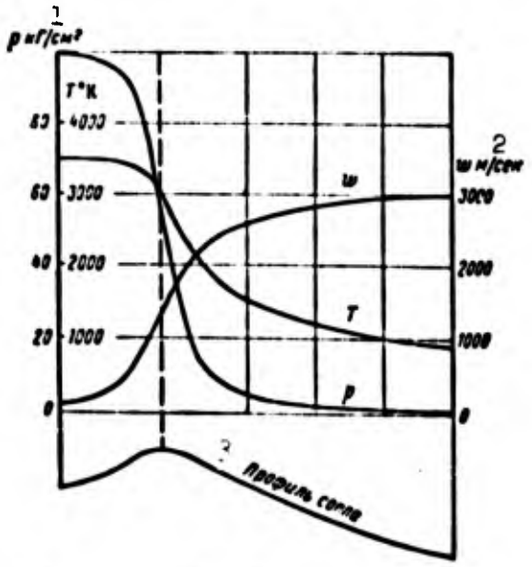

Fig. 7.3. Variation in gas parameters along nozzle. 1) kgf/cm^2; 2) m/s; 3) nozzle profile.

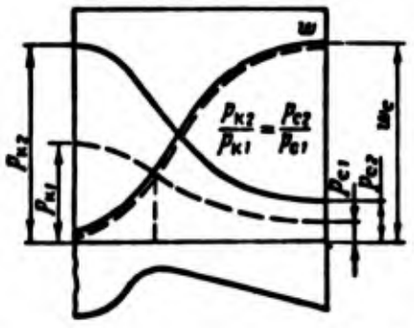

Fig. 7.4. Variation in gas parameters along nozzle for various chamber pressures.

Figure 7.3 shows the nature of variation and order of magnitude of the pressure, temperature, and gas velocity along the nozzle.

The relative nozzle exit area

$$\overline{f}_c = \frac{f_c}{f_{cr}}$$

is called the nozzle expansion ratio. Consequently,

$$\frac{p_c}{p_k^*} = \varphi_1(\overline{f}_c;\ k); \quad \frac{T_c}{T_k^*} = \varphi_2(\overline{f}_c;\ k).$$

For nozzles with constant geometry ($\overline{f}$ = const, an uncontrolled nozzle), the operating regimes remain similar when the flow parameters change at the nozzle entrance, provided k = const. In other words, if in this case the temperature, pressure, or flow velocity vary at the nozzle entrance, the ratios of like flow parameters in any two nozzle cross sections will remain constant; such relative quantities as the Mach number M, the reduced velocity, etc., will also remain unchanged. In particular, for the entrance and exit sections we can write

$$\frac{p_c}{p_k^*} = \text{const}; \quad \frac{T_c}{T_k^*} = \text{const}.$$

For a fixed-area nozzle with k = const, the gas parameters in the nozzle exit section (as in any other section) and the gas exit velocity are determined solely by the gas parameters in the chamber. If the pressure p_k^* is increased, then the pressure in each nozzle section, including the exit section, varies in direct proportion to p_k^*. If in this case the temperature and composition of the gas in the combustion chamber remain constant, then the gas velocity in any nozzle section, including the exit section, will also remain unchanged (Fig. 7.4).

Above we have considered ideal isentropic flow of a gas in a nozzle. Qualitatively speaking, however, all of the material presented above also applies to a real flow (with the exception of a flow with separation at the nozzle walls).

7.2. LOSSES IN NOZZLE

The axial component of the exit velocity participates in creation of thrust. Thus as the actual exhaust velocity we take the average value of the axial projection of the exhaust velocity. Here the averaging should be based on the condition requiring conservation of impulse along the axis. This is less than the ideal velocity for an isentropic equilibrium process in the nozzle, owing to energy dissipation resulting from the fact that the process is not in energy and chemical equilibrium, from friction, and from pressure shocks, where the latter take place within the nozzle. The deviation of the exhaust velocity vector from the nozzle axis also diminishes the actual exhaust velocity (as compared with the ideal value).

The actual flow process in the nozzle is also influenced by heat exchange between the gas and the walls; heat exchange influences

both friction and process thermodynamics, in particular, the process index.

The reduction in exhaust velocity as compared with the ideal value is called the nozzle loss. The nozzle coefficient φ_s is used to allow for the influence of the losses on the exhaust velocity; this factor equals the ratio of the actual velocity to the exhaust velocity with an equilibrium isentropic exhaust process. For rocket-engine nozzles, $\varphi_s = 0.95\text{-}0.98$.

When we consider nozzle losses, we can arbitrarily divide them into the losses resulting from the lack of energy and chemical equilibrium (nonequilibrium losses); friction losses (losses to friction); losses caused by pressure shocks (wave losses); and losses caused by the lack of parallelism of the flow at the nozzle exit (nonparallelism losses).

As has already been noted, when there is no condensed phase in the combustion products, in most cases the flow process in a nozzle takes place with energy and chemical equilibrium. What is more, if the nozzle profile is properly designed, there will ordinarily be no pressure shocks within the nozzle (we are speaking of flow without separation).

In the ensuing discussion, therefore, we shall only consider the losses caused by friction and the lack of parallelism. To analyze these losses, we represent the nozzle coefficient as the following product.[1]

$$\varphi_s = \varphi_r \varphi_a$$

where φ_r and φ_a are coefficients allowing for the exhaust velocity reduction caused by friction and by the fact that the velocity vector is not parallel to the nozzle axis.

The friction losses depend on the condition of the surface (roughness), and decrease somewhat as the Reynolds number goes up. The magnitude of these losses is influenced by the heat exchanged between the gases and the wall; heat transfer from the gas to the wall increases the friction losses. All other conditions being equal, the friction losses rise as the nozzle surface becomes greater, so that these losses increase as the cone angle of the exit transcritical section decreases. For smooth nozzles, the value of φ_r averages 0.97-0.99.

Let us consider the losses caused by lack of parallelism. In the ideal case, and with special profiles in the diverging zone of the nozzle, there will be axial flow at the nozzle exit; the specific-thrust losses caused by departure from one-dimensional flow equal zero and $\varphi_a = 1$ (Fig. 7.5a). For an axisymmetric conical nozzle, the vectors representing the velocities of all elementary streams other than the central stream are inclined to the axis at a certain angle that depends on the nozzle divergence angle α_2 and on the distance between the stream and the axis (Fig. 7.5b). Only the axial velocity component participates in the creation of thrust.

[1]/158

The larger α_2, the greater the losses produced by lack of parallelism. The value of φ_a can be found, in approximation, from the formula

$$\varphi_a = \frac{w_z}{(w_z)_{\alpha_1=0}} = 0{,}5\left(1+\cos\frac{\alpha_1}{2}\right).$$

In the derivation of this formula it is assumed that the velocities of the individual streams at the nozzle exit are identical in magnitude and directed along straight lines emanating from the cone vertex.

TABLE 71.

α_2	0	8	12	16	20	24	28	32	36	40
φ_a	1,000	0,999	0,997	0,995	0,992	0,989	0,985	0,981	0,976	0,970

Table 7.1 shows the values of φ_a for various divergence angles.

The divergence angle α_2 has an opposite influence on the friction losses and on the lack of flow parallelism; thus the nozzle coefficient φ_s has a maximum at some optimal divergence angle (Fig. 7.6).

The value of the optimal angle α_2 depends on the shape of the transcritical nozzle zone, i.e., on the profiling method and the expansion ratio $\bar{f}_s$. As the nozzle expansion ratio decreases, the optimal value of the angle α_2 diminishes, while the value of the coefficient φ_s becomes somewhat larger, since the friction losses have less influence.

Simple conical and profiled nozzles differ in the profile of the diverging section. In the first case, the cone angle of the transcritical zone is constant along the length, and for such nozzles the optimal angle α_2 lies in the 18-25° range. Such nozzles are simple to manufacture, but for optimal angles α_2 they are relatively long; it is always acceptable to increase the value of α_2 for such nozzles, since here the increase in losses owing to lack of parallelism reduces the specific engine thrust.

A relatively short nozzle can be obtained with no increase in α_2 if the angle of the nozzle exit zone is made variable, increasing toward the throat. It should be kept in mind, however, that here the nozzle profile cannot be arbitrary, since a sharp change in direction of the supersonic gas flow may produce pressure shocks within the nozzle. The aim of profiling is to provide the most uniform possible flow at the exit of the nozzle, with the elementary streams directed axially. Profiles of such nozzles are designed by special methods of gasdynamics (the method of characteristics). The nozzle is relatively long at $\alpha_2 = 0$, however. For rocket engines

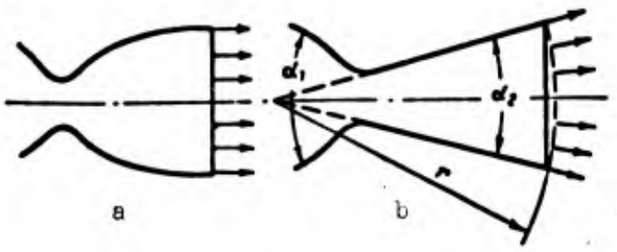

Fig. 7.5. Determining losses caused by lack of parallelism. a) Profiled nozzle with axial flow at exit; b) simple conical nozzle.

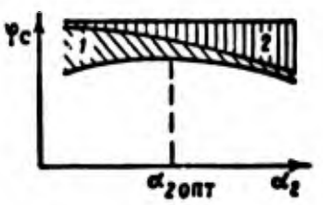

Fig. 7.6. Dependence of φ_s on angle α_2. 1) Friction losses; 2) losses caused by lack of parallelism.

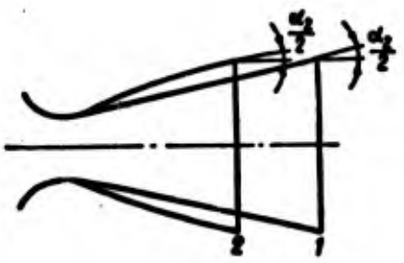

Fig. 7.7. Comparison of nozzles with identical angle α_2. 1) Simple conical nozzle; 2) profiled nozzle.

there is no need to provide strictly axial flow at the nozzle exit, since for $\alpha_2 < 15\text{-}20°$, the reduction in specific thrust caused by the losses introduced by lack of parallelism amount to less than 1% (see Table 7.1), while the flow nonuniformity is negligible in this case. Thus $0 < \alpha_2 < 20°$ for profiled rocket-engine nozzles; this noticeably shortens the nozzle as compared with simple conical nozzles (Fig. 7.7), and somewhat reduces the hydraulic losses. The value of φ_s is somewhat greater for profiled nozzles (by 1-2%) than for simple conical nozzles.

7.3. THRUST AND SPECIFIC THRUST FOR VARIOUS NOZZLE OPERATING REGIMES

If the nozzle expansion ratio is increased, the exhaust velocity will rise and, consequently, the first term in the thrust formu-

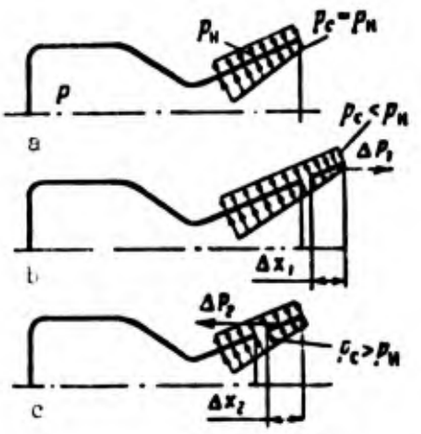

Fig. 7.8. Determination of optimal nozzle operating regime.

la (1.5) will become greater; the pressure p_s will also be reduced, resulting in a simultaneous reduction in the second term; if $\bar{f}_s$ is decreased, we will obviously have the opposite result.

Letus find the optimal nozzle exit area (or, what is the same thing, the optimal pressure p_s) for which the engine thrust will be greatest. We consider the forces acting on the nozzle walls, neglecting friction forces; these will be the forces of internal gas pressure and external pressure of the environment.

The pressures will be distributed along the nozzle as shown in Fig. 7.8a under design conditions. For the same pressure p_k^*, a nozzle operating with overexpansion ($p_s < p_n$) should have a larger expansion ratio. Consequently, to the basic nozzle we should add the section Δx_1 (Fig. 7.8b) to which the force ΔP_1 is applied, the force balancing the forces of internal and external pressure, and directed so as to oppose the thrust. Consequently, the engine thrust, as well as the specific thrust in overexpansion operation, will be less than the design thrust:

$$\Delta P_{уд} = P_{расч} - \Delta P_1.$$

A nozzle operating with underexpansion ($p_s < p_n$) must be shorter than the design length by a certain segment Δx_2 (Fig. 7.8c).

It is not difficult to see that the force ΔP_2 acting on this deleted section will have the same direction as the engine thrust. Consequently, with underexpansion, the engine thrust will be less than the thrust in design nozzle operation:

$$P_{уд} = P_{расч} - \Delta P_2.$$

Thus for a specified chamber pressure, a rocket engine will develop maximum thrust and specific thrust when the nozzle is operating in

the design regime, i.e., when the gas is expanded to the external environmental pressure.

An increase or decrease in the nozzle expansion ratio with respect to the optimal value will result in specific-thrust losses.

The result obtained is illustrated by Fig. 7.9. The data of Fig. 7.9 were obtained with no allowance for flow separation from the nozzle walls, which can occur when there is significant overexpansion. When there is overexpansion, the flow increases the thrust and, consequently, the specific thrust of the engine. It is not difficult to see this if we compare the diagrams for the pressure at the wall (Fig. 7.10).

The results of an analysis of nozzle operation in various regimes are used to select a nozzle for an engine. If the engine is operated at constant altitude (p_n = const) and with a constant regime (p_k^* = const), there is no difficulty in selecting the nozzle so as to produce maximum specific thrust; here the best nozzle is the one calculated to produce the optimal expansion ratio. Where there is a large available pressure drop p_k^*/p_n, the required value of $\bar{f}_s$ and, consequently, the nozzle dimensions may prove very large. In such case, the exit section is often made smaller than the optimal size, since for large p_k^*/p_s a certain reduction in $\bar{f}_s$ from the optimal value will at most decrease the specific thrust negligibly. This is clear, for example, from the data of Fig. 7.9. Thus if the available pressure drop is p_k^*/p_n = 200, and we halve the nozzle exit area (or what is the same thing, the value of $\bar{f}_s$) as compared with the optimal value, the specific thrust will be reduced by less than 2%. If there is an available pressure drop of 20 and we halve the optimal nozzle exit area, the specific thrust will be reduced by roughly 6%.

As a rule, a rocket engine operates with variable regimes and at different altitudes, so that the best nozzle will ensure the greatest total economy over the entire vehicle flight segment with allowance for motor size and weight. Here it is a complicated matter to perform exact computations for the best nozzle. The designer should know the range of altitudes within which the engine is to operate and the burn time at the different altitude segments.

Statistical data are often used for rough estimates. For example, for engines of single-stage rockets, a pressure p_s = 0.4-0.8 atm (abs) is used, depending on the maximum altitude for powered flight. Lower pressure values are used for nozzles in upper-stage engines.

7.4. CHARACTERISTICS OF HETEROGENEOUS MIXTURE OF COMBUSTION PRODUCTS FLOWING IN NOZZLES

When a fuel contains metallic elements, the combustion products, in addition to gases, may also contain condensed material (solid or liquid), products of oxidation of the metals (for example, Al_2O_3,

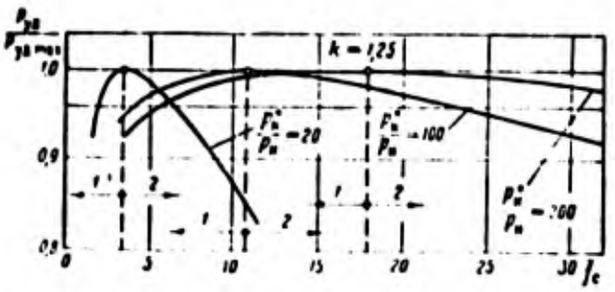

Fig. 7.9. Influence of f_c on specific thrust. 1) Underexpansion; 2) overexpansion.

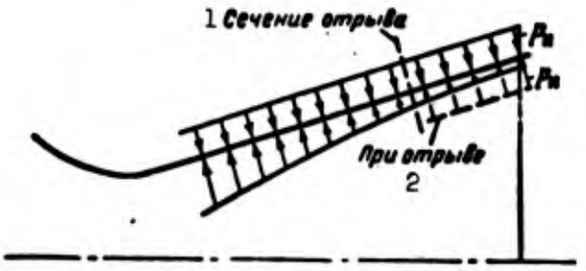

Fig. 7.10. Diagram for pressures on nozzle wall with and without separation of flow from nozzle walls. 1) Separation section; 2) with separation.

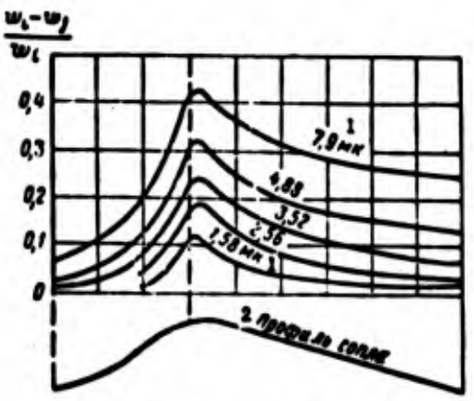

Fig. 7.11. Lag in velocity of condensed particles. 1) μm; 2) nozzle profile.

MgO, BeO, etc.).

In this case, the gas stream flowing through the nozzle will contain suspended condensed particles. As it moves along the nozzle, the gas expands and accelerates; its pressure and temperature drop. The condensed particles are entrained by the gas and are thus accelerated; their temperature drops owing to heat exchange with the gas.

In the general case, the temperature and velocity of the gas and condensed particles need not be the same. The relationships among the velocities and temperatures affect the parameters of the nozzle process. It must be remembered that if the velocities of the two phases differ, proper evaluation of engine efficiency, i.e., computation of thrust and specific thrust, require that consideration be given to the mean mass exit velocity, which equals

$$w_c = \frac{w_{ci}G_i + w_{cj}G_j}{G_i + G_j},$$

where w_{si}, G_i are the gas exhaust velocity and weight flowrate;

w_{sj}, G_j are the same quantities for the condensed particles.

We let g_j represent the proportion by weight of condensed particles:

$$g_j = \frac{G_j}{G_i + G_j}.$$

Then

$$w_c = (1 - g_j)w_{ci} + g_j w_{cj}. \qquad (7.2)$$

We can now deal with the two extreme cases for the nozzle flow process of a heterogeneous working fluid:

1. There is total thermal and dynamic equilibrium between the gaseous and condensed phases; here the velocities and temperatures of the two phases are identical in every cross section. This case can only be realized when the condensed particles are extremely small, so that there is vigorous heat exchange between the particles and the gas, while the particles are small in mass.

2. The condensed particles exchange neither heat nor momentum with the gas, so that their velocity is nearly zero, while the temperature is constant along the nozzle and equals the chamber temperature; this case, in which there is no thermal or dynamic equilibrium whatsoever between the phases is possible when the particles are very large.

In actuality, a certain intermediate case is realized; depending on the size of the condensed particles, the actual process will approach the first or second limiting cases. The latter is illustrated in Fig. 7.11, which shows the variation of the lag in

velocity of condensed particles $\left(\frac{w_i - w_j}{w_i}\right)$ along the nozzle length as a function of particle size [22].

The data of Fig. 7.12 [22] give some idea of the possible dimensions of condensed particles obtained upon combustion of solid fuels with added aluminum.

Let us consider one-dimensional flow of a heterogeneous working fluid. For simplicity, we neglect friction and heat exchange with the walls; the chemical composition and heat capacity of the two phases are taken to be constant along the nozzle, while the proportion by weight of condensate is also constant. The energy equation for a flow of heterogeneous working fluid with constant g_j and no heat exchange with the walls has the form

$$(1-g_j)I_{ki}+g_jI_{kj}=(1-g_j)\left(A\frac{w_{ci}^2}{2g}+I_{ci}\right)+g_j\left(A\frac{w_{cj}^2}{2g}+I_{cj}\right). \qquad (7.3)$$

Here I_{ki}, I_{kj} are the enthalpies of the gas and the condensed particles ahead of the nozzle (at the end of the combustion chamber);

I_{si}, I_{sj} are the same, for the nozzle exit section.

For equilibrium outflow, $w_i=w_j=w$; $T_i=T_j=T$. Thus when there is thermal and dynamic equilibrium between the phases,

$$w_c=\sqrt{\frac{2g}{A}[(1-g_j)c_{pi}+g_jc_j](T_k^*-T_c)},$$

where c_{pi}, c_j are the heat capacities of the gaseous and condensed phases.

After certain manipulations (when there is no friction and the chemical composition and heat capacity do not change), we can convert the preceding formula to the form

$$w_c=\sqrt{2g\frac{k_{эф}}{k_{эф}-1}R(1-g_j)T_k^*\left[1-\left(\frac{p_c}{p_k^*}\right)^{\frac{k_{эф}-1}{k_{эф}}}\right]}, \qquad (7.4)$$

where $k_{эф}=\frac{(1-g_j)c_{pi}+g_jc_j}{(1-g_j)c_{vi}+g_jc_j}$ is the effective value of the process index for expansion of a heterogeneous working fluid;

R is the gas constant, calculated from the composition of the gaseous phase.

Using Formula (7.4), let us see how the presence of the condensed phase influences the exhaust velocity when there is equilibrium between the phases. To do this, we consider the quantity $\bar{w}_c$, which equals the ratio of the exhaust velocity of the heterogeneous mixture to the exhaust velocity of a homogeneous gas mixture at equal temperatures in the combustion chamber and for equal nozzle pressure ratios. From the way in which this quantity depends on the weight proportion g_j of condensed phase (Fig. 7.13), it is

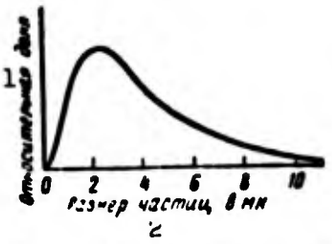

Fig. 7.12. Measured size distribution of condensed particles. 1) Relative proportion; 2) particle size, μm.

clear that the presence of the condensed phase has a negative effect on the exhaust velocity even for an equilibrium process; from this we should not derive the erroneous conclusion, however, that it is altogether undesirable to use metallic elements that produce condensed oxides. As we have previously noted (Chapter 3), in many cases their introduction into a fuel raises the fuel heating value so much that this effect prevails over the drop in thermal efficiency produced by impairment of combustion-product characteristics, including the influence of the condensed phase.

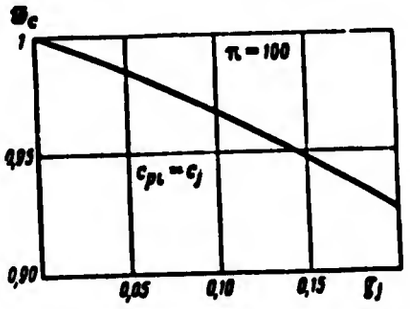

Fig. 7.13. Dependence of $\bar{w}_s$ on g_j.

Let us consider the second limiting case: there is no heat exchange or momentum exchange between the phases; the condensed particles have zero velocity, while their temperature is constant and equal to the chamber temperature. This means that the condensed particles do not leave the combustion chamber and do not give up their energy to the gas. Only the gas stream leaves the nozzle, and its exhaust velocity will be the same in this case as for a homogeneous mixture of combustion products. The mean mass exhaust velocity is represented by the formula

$$w_c = (1 - g_j)\sqrt{2g\frac{k}{k-1}RT_c^*\left[1 - \left(\frac{p_c}{p_c^*}\right)^{\frac{k-1}{k}}\right]}. \qquad (7.5)$$

Let us consider one more case for the nozzle process; we as-

sume that both phases have equal velocities (dynamic equilibrium), but that there is no heat exchange between the phases, while the temperature of the condensed phase is constant and equal to the chamber temperature (there is no thermal equilibrium whatsoever). For this case, we can obtain the following expression from Eq. (7.3)

$$w_c = \sqrt{(1-g_j)\,2g\,\frac{k}{k-1}\,RT_c^*\left[1-\left(\frac{p_c}{p_c^*}\right)^{\frac{k-1}{k}}\right]}. \qquad (7.6)$$

In the absence of process equilibrium, as we have already noted, the exhaust velocity will be less than the equilibrium-process velocity. Thus if there is neither dynamic nor thermal equilibrium in the heterogeneous combustion-product mixture, while both substances differ in velocity and temperature in the nozzle, there will be additional losses in the exhaust velocity and, consequently, lowered specific thrust. The losses caused by lack of process equilibrium (here we have in mind thermal and dynamic equilibrium between the phases) are characterized by the coefficient φ_n, which equals the ratio of the exhaust velocities for nonequilibrium and equilibrium processes.

Where there is a total lack of either dynamic or thermal equilibrium, the coefficient φ_n will equal the ratio of the velocities, computed from Formulas (7.5) and (7.4), respectively, while when there is a complete lack of thermal equilibrium alone, it will equal the ratio of the velocities computed from Formulas (7.6) and (7.4) (Fig. 7.14). Depending on the particle dimensions, the actual value of φ_n will lie between unity and a value determined by the lower curve of Fig. 7.14; it can be determined from experimental data. According to certain investigations of solid rocket engines using fuel with aluminum additives, the losses caused by lack of equilibrium between the phases amount to 2-4% [22]. In this case, consequently, when the actual exhaust velocity is determined from the known exhaust velocity for the isentropic process, the nozzle coefficient φ_s found for a nozzle with a homogeneous gas flow (see §7.2) should be reduced by 2-4%.

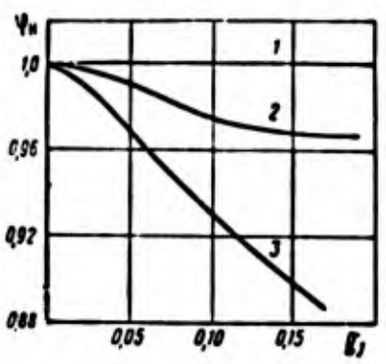

Fig. 7.14. Dependence of φ_n on g_j. 1) Flow with complete equilibrium; 2) identical phase velocities, constant temperature of condensed phase; 3) no thermal or dynamic equilibrium between phases whatsoever.

Footnotes

Manuscript Page No.	
148	[1]This method is acceptable since the individual losses are so small.
152	[2]We obtained this result by neglecting the friction forces. When allowance is made for these forces, the optimal nozzle will operate with a certain degree of underexpansion. The reason is that shortening of the nozzle designed for complete expansion decreases the friction force.

Transliterated Symbols

Manuscript Page No.	
144	с = s = soplo = nozzle
144	н = n = naruzhnyy = external
145	прел = pred = predel'nyy = limiting
145	кр = kr = kriticheskiy = critical
150	опт = opt = optimal'nyy = optimal
151	пер = per = pererasshireniye = overexpansion
151	нед = ned = nedorasshireniye = underexpansion
151	расч = rasch = raschetnyy = design
155	эфф = eff = effektivnyy = effective
157	н = n = neravnovesnost' = nonequilibrium

C H A P T E R VIII

THERMODYNAMIC CALCULATION OF COMBUSTION AND OUTFLOW IN JET ENGINES

8.1. General Positions

For calculation of the process in a jet engine and determination of its specific parameters and geometric dimensions it is necessary to know the composition, temperature, pressure, and rate of combustion products in the combustion chamber and in various sections of the nozzle. These values are determined with help of thermochemical and thermodynamic dependences, i.e., by means of thermodynamic calculation of combustion and outflow.

Components of rocket fuels generally can contain various elements: C, H, Li, B, O, F, and others. These elements can also be contained and in monopropellants which are capable of exothermic reactions of decomposition or recombination.

Reactions of oxidation, as was noted, can be represented conditionally as an exchange by electrons on the outermost electron shell of atoms.

During the formation of products of complete oxidation combustible elements give off all their outer electrons, and the oxidizing elements supplement the number of outer electrons to eight. The number of electrons given off or received by an element during a chemical reaction determines its valence. Thus the valence of combustible elements in products of complete oxidation $i_г$ is equal

to the number of their electrons n, and the valence of oxidizing elements i_{OH} is equal to 8-n, where n – number of electrons in the outer electron shell.

For a number of elements the number of electrons n is given in Table 8.1.

Table 8.1. Number of electrons on outer shell and valence of certain elements.

Element	H	Li	Mg	Be	B	Al	C	Si	O	F	Cl
Number of electrons	1	1	2	2	3	3	4	4	6	7	7
Valence of oxidizing element	1	1	2	2	3	3	4	4	2	1	1

Using the shown determinations, it is not difficult to find the products of complete oxidation for different combinations of oxidizing and combustible elements, considering $i_r = i_{OH}$. Some of these are given in Table 8.2.

Table 8.2. Products of complete combustion.

Combustible element / Oxidizing element	H	Li	K	Mg	Be	B	Al	C
O	H_2O	Li_2O	K_2O	MgO	BeO	B_2O_3	Al_2O_3	CO_2
F	HF	LiF	KF	MgF_2	BeF_2	BF_3	AlF_3	CF_4

In the event of deficiency of oxidizing element products of incomplete oxidation will be formed. Thus, with a deficiency of oxygen, besides CO_2 CO will be formed. In a number of cases with a deficiency of oxidizer a portion of the combustible element is oxidized into a product of incomplete oxidation, and the remaining share is present in a unoxidized form. Thus, with a deficiency of

oxygen, hydrogen partially forms H_2O and partially remains in the form of H_2; lithium with fluorine with a deficiency of fluorine will form LiF and Li.

For fuels consisting of elements H, C, N and O, the products of complete oxidation will be H_2O and CO_2. Nitrogen is oxidized by oxygen only at high temperatures, where the reaction of its oxidation is endothermal, i.e., is accompanied by absorption of heat. Under usual conditions nitrogen does not enter into the reaction and in products of complete combustion is present in a molecular state N_2.[1]

8.2. Elementary Composition. Conditional Chemical Formula

The composition of a substance in weight fractions of separate elements is called elementary composition. The general formula for weight fraction of an individual (k) element in a substance has the form

$$b_k = \frac{a_k A_k}{\mu},$$

here b_k – weight fraction of k element; a_k – number of atoms of given element in molecule of compound being considered; A_k – atomic weight of this element.

If one were to be limited yet to the elements H, C, N, and O, then in general the chemical formula of the substance has the form

$$C_m H_n O_p N_q.$$

Then the elementary composition will be

$$b_C = \frac{12m}{\mu}; \quad b_H = \frac{n}{\mu}; \quad b_O = \frac{16p}{\mu}; \quad b_N = \frac{14q}{\mu}; \tag{8.1}$$

here $\mu = 12m + n + 16p + 14q$ -- molecular weight of substance; b_C, b_H, b_O, b_N – weight fraction of carbon, hydrogen, oxygen, and nitrogen.

---

[1] An exception are certain fuels, the reaction products of which include nitrides of a number of elements, for example, of boron nitride BN.

If the fuel or its component constitutes a combination of several substances, then the weight fraction of a separate (k) element will be found thus:

$$b_k = \sum g_i b_{k_i},$$

where b_k – weight fraction of k element in the mixture; g_i – weight fraction of separate (i) substance in mixture; b_{k_i} – weight fraction of k element in i substance.

For a mixture of substances, consisting of elements H, C, O, and N, the elementary composition is found in the following way:

$$b_C = \sum g_i b_{C_i}; \quad b_H = \sum g_i b_{H_i};$$
$$b_O = \sum g_i b_{O_i}; \quad b_N = \sum g_i b_{N_i};$$

here $b_{C_i}, b_{H_i}, b_{O_i}, b_{N_i}$ – weight fractions of elements in separate (i) substance; g_i – weight fraction of separate (i) substance in mixture.

If the fuel consists of an oxidizer and fuel and the relationship of components κ and elementary composition of both components are known then the weight fraction of separate (k) element in the fuel is found thusly:

$$b_k = \frac{b_{k_г} + \alpha b_{k_{ок}}}{1+\alpha}. \qquad (8.2)$$

For fuel consisting of elements H, C, O, and N, the elementary composition of fuel is determined by the following equations:

$$\left.\begin{aligned} b_C &= \frac{b_{C_г} + \alpha b_{C_{ок}}}{1+\alpha}; & b_H &= \frac{b_{H_г} + \alpha b_{H_{ок}}}{1+\alpha}; \\ b_O &= \frac{b_{O_г} + \alpha b_{O_{ок}}}{1+\alpha}; & b_N &= \frac{b_{N_г} + \alpha b_{N_{ок}}}{1+\alpha}. \end{aligned}\right\} \qquad (8.3)$$

When the components constitute a mixture of individual substances, then for certain calculations it is convenient to use a conditional chemical formula for the given component. Such a formula can be constructed in various ways. For example, it is convenient to determine it, proceeding from the number of atoms of various elements

which are present per 100 weight units of examined component. Then the conditional chemical formula will have the form:

$$C_mH_nO_pN_q\ldots,$$

where

$$m=\frac{100b_C}{12};\quad n=\frac{100b_H}{1};\quad p=\frac{100b_O}{16};\quad q=\frac{100b_N}{14},$$

and b_C, b_H, b_O, b_N — weight factions of corresponding elements in the given component.

8.3. Theoretical Relationship of Components κ_0

Calculation formula for determination of κ_0 can be written on the basis of the following.

Let us assume that $i_г^г$ — sum of valences of combustible elements in a molecule of fuel; $i_г^{ок}$ — sum of valences of oxidizing elements in molecule of fuel; then $i_г^г - i_г^{ок}$ — number of free valences of combustible elements in a molecule of fuel; $\frac{i_г^г - i_г^{ок}}{\mu_г}$ — number of free valences of combustible elements in 1 kgf of fuel.

Further let us assume that $i_{ок}^{ок}$ — sum of valences of oxidizing elements in molecule of oxidizer and $i_{ок}^г$ — sum of valences of combustible elements in molecule of oxidizer; then $\frac{i_{ок}^{ок} - i_{ок}^г}{\mu_{ок}}$ — number of free valences of oxidizing elements in 1 kgf of oxidizer. Since

$$\kappa_0\frac{i_{ок}^{ок} - i_{ок}^г}{\mu_{ок}} = \frac{i_г^г - i_г^{ок}}{\mu_г}, \tag{8.4}$$

then

$$\kappa_0 = \frac{i_г^г - i_г^{ок}}{i_{ок}^{ок} - i_{ок}^г}\frac{\mu_{ок}}{\mu_г} \tag{8.5}$$

If the component constitutes a mixture of individual substances, then during determination of sums of valences it is convenient to originate from a conditional chemical formula.

Value κ_0 for a number of fuels is given in Table 8.3.

Table 8.3. Theoretical relationship of components.

Oxidizer	Fuel	κ_0	Oxidizer	Fuel	κ_0
HNO_3	[illegible]	5.34	O_2	N_2H_4	1.0
96% HNO_3	kerosene	5.57	O_2	H_2	7.95
HNO_3	tonka	4.67	F_2	kerosene	8.05
HNO_3	N_2H_4	1.97	F_2	NH_3	3.35
HNO_3	B_5H_9	4.8	F_2	N_2H_4	2.37
N_2O_4	kerosene	4.88	F_2	B_5H_9	7.24
N_2O_4	tonka	4.26	OF_2	kerosene	5.75
N_2O_4	N_2H_4	1.44	OF_2	N_2H_4	1.68
$C(NO_2)_4$	[illegible]	6.92	OF_2	$N_2H_2(CH_3)_2$	3.6
O_2	75% C_2H_5OH	1.55	OF_2	B_5H_9	5.13
O_2	C_2H_5OH	2.072	ClF_3	N_2H_4	2.88
O_2	kerosene	3.39	ClF_3	B_5H_9	6.76
H_2O_2	kerosene	7.18	$KClO_4$		7.0
90% H_2O_2	kerosene	7.98	NH_4ClO_4	heavy oil products	9.5
80% H_2O_2	kerosene	8.9	$NaNO_3$		6.7

Frequently for determination of value κ_0 they use a formula founded on the weight fractions of elements. However, this is convenient when the number of possible elements in the fuel is limited.

If the oxidizing element is oxygen and chemical formulas of oxidizer and fuel are known

$$C_{m_г}H_{n_г}O_{p_г}N_{q_г} \quad \text{and} \quad C_{m_{ок}}H_{n_{ок}}O_{p_{ок}}N_{q_{ок}},$$

then

$$\begin{aligned} b_г' - b_г'' &= 4m_г + n_г - 2p_г; \\ b_{ок}'' - b_{ок}' &= 2p_{ок} - 4m_{ок} - n_{ок}; \\ \kappa_0 &= \frac{4m_г + n_г - 2p_г}{2p_{ок} - 4m_{ок} - n_{ок}} \frac{\mu_{ок}}{\mu_г}. \end{aligned} \tag{8.6}$$

Considering that

$$\frac{4}{\mu}m = \frac{b_C}{3}, \quad \frac{n}{\mu} = b_H, \quad \frac{2p}{\mu} = \frac{b_O}{3},$$

Formula (8.6) can be written in the form

$$\alpha_0 = \frac{\frac{8}{3} b_{C_r} + 8 b_{H_r} - b_{O_r}}{b_{O_{ox}} - \frac{8}{3} b_{C_{ox}} - 8 b_{H_{ox}}}. \qquad (8.7)$$

For characteristics of certain monopropellants, as was mentioned above, there is interest in the value of coefficient of surplus of oxygen α_{O_2}, equal to the ratio of actual content of oxygen to that necessary for complete oxidation of combustible elements.

If the elementary composition of a substance is known (for example, b_C, b_H, b_N and b_O), then α_{O_2} is not difficult to find. Actual content of oxygen in 1 kgf of fuel is equal to b_O. Necessary quantity of oxygen for complete oxidation of combustible elements is equal to $\frac{8}{3} b_C + 8 b_H$. then

$$\alpha_{O_2} = \frac{b_O}{\frac{8}{3} b_C + 8 b_H}. \qquad (8.8)$$

8.4. Composition of Products of Combustion

Composition of combustion products of a concrete fuel depends on temperature and pressure.

Influence of temperature has an effect on dissociation of combustion products, which in turn leads to a decrease of temperature of combustion and lowers thermal efficiency and discharge velocity of gases from the nozzle.

Dissociation is practically perceptible, starting from temperatures of an order of 2000°K.

At very high temperatures (T > 5000°K) ionization of gases can also occur, i.e., breakaway of electrons from atoms; in this case besides neutral atoms and molecules, ions and electron gas are also present in the products of combustion.

Dissociation leads to an increase in the number of moles, and consequently also the volume of products of combustion, therefore the increase of pressure, preventing an increase of volume, lowers the degree of dissociation of combustion products and leads to an increase of temperature of combustion. With those same values of pressure, which are encountered in the combustion chamber of jet engines, the influence of pressure on dissociation is not great (see, for example, Fig. 8.6).

The composition of combustion products depends also on the degree of completeness of the reaction (combustion efficiency). Thermodynamic calculation is conducted on the assumption that the composition of products is chemically an equilibrium at a given temperature and pressure.

At relatively low temperatures the composition of combustion products will include products of complete oxidation (H_2O, CO_2, HF, and others) and incomplete oxidation (for example, CO) which are stable under these conditions, and also molecules (or atoms) of other elements (H_2, N_2, O_2, Li, B, and others).

Concrete composition is determined by the initial composition of fuel. For example, for fuel consisting of elements H, C, O, and N, at low temperatures the composition of combustion products includes the following gases:

with $\alpha=1$—H_2O, CO_2, N_2; with $\alpha>1$—H_2O, CO_2, N_2, O_2;

with $\alpha<1$—H_2O, CO_2, N_2, H_2, CO.

Furthermore, with a considerable deficiency of oxygen the lowest hydrocarbons (CH_4, C_2H_6) and also free carbon can be formed.

The composition of combustion products at high temperatures is different from their composition at low temperatures due to dissociation. If one were to examine fuels consisting of elements H, C, O, and N, then besides the above-indicated gases, as calculations and experiment show, at temperatures higher than 2000°K the products of

combustion will also include the following gases: OH, O, H, NO, and N. At very high temperatures the appearance of free carbon is possible. The appearance of these gases (H, C, O, N, and others) is the result of dissociation of complex compounds into simpler one:

$$\left.\begin{aligned} CO_2 &\rightleftarrows CO + \tfrac{1}{2}O_2 \\ H_2O &\rightleftarrows H_2 + \tfrac{1}{2}O_2 \\ H_2O &\rightleftarrows OH + \tfrac{1}{2}H_2 \\ O_2 &\rightleftarrows 2O \\ H_2 &\rightleftarrows 2H \\ N_2 &\rightleftarrows 2N \\ N_2 + O_2 &\rightleftarrows 2NO \end{aligned}\right\}. \qquad (8.9)$$

Although the last reaction is not a reaction of dissociation in a full sense, it is accompanied by absorption of heat and with a temperature rise is displaced to the right.

From reactions (8.9) it follows that at high temperatures the products of incomplete oxidation (CO and H_2) and oxygen (O_2) can be obtained both with $\alpha < 1$ and with $\alpha > 1$. Relative content of separate gases depends on excess-oxidant ratio and is changed with temperature.

The change of equilibrium composition of combustion products with temperature is shown in Fig. 8.1.

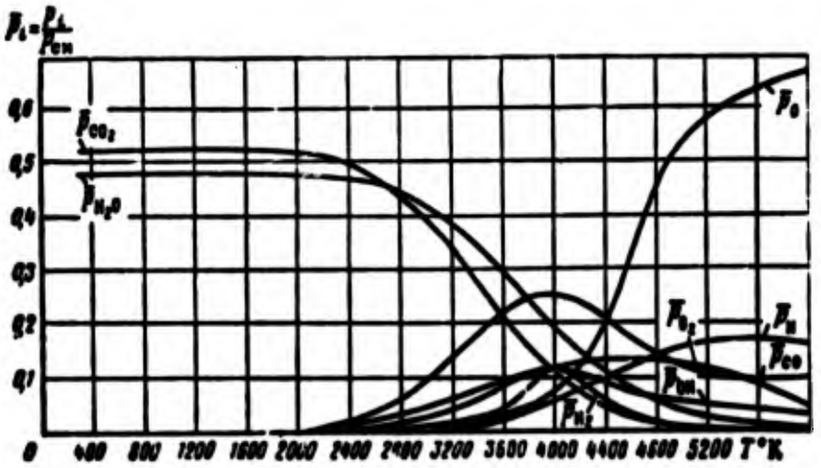

Fig. 8.1. Composition of combustion products for oxygen-kerosene fuel at $\alpha = 1$ and $p_{CM} = 40$ atm(abs.).

In a state of chemical equilibrium the quantities of separate gases in a reacting mixture are found in a strictly definite relationship, emanating from the equation for chemical equilibrium (equations of constant of equilibrium). Thus, for the reaction

$$aA+bB\rightleftarrows mM+nN,$$

where A, B, M, N – reacting substances; a, b, m, n – stoichiometric coefficients, the equation of chemical equlibrium has the form:

$$K_p=\frac{p_M^m p_N^n}{p_A^a p_B^b}. \qquad (8.10)$$

Here K_p – constant of equilibrium; p_M, p_N, p_A, p_B – partial pressures of corresponding substances.

In a complex mixture of gases several chemical reactions can flow simultaneously. Every chemical reaction is described by its own equation of chemical equilibrium. However, inasmuch as separate gases can participate simultaneously in several reactions, then the quantity of one or another gas will be determined by the totality of equations of chemical equilibrium describing those reactions in which the given compound participates. The quantity of independent equations, describing the chemical equilibrium of a complex mixture of gases, as is known, equals

$$Z=X-Y, \qquad (8.11)$$

where X – number of separate gases; Y – number of chemical elements, from which these gases are composed.

For example, if the composition of combustion products includes the gases CO_2, H_2O, CO, H_2, O_2, N_2, OH, NO, O, H, N, then X = 11, Y = 4, Z = 7.

For a mixture consisting only of CO_2, H_2O, N_2, and O_2, the number of equations of equilibrium Z = 0.

Calculation of composition has the purpose of determining the quantity of separate gases in the mixture of combustion products. The number of unknown is equal to the number possible gases X.

For resolution of problem equations of chemical equilibrium and material balance are used. The number of equations of chemical equilibrium. as shown above, is equal to X - Y.

Equations of material balance express the law of conservation of matter and determine the equality of quantity of separate elements in the initial fuel and in end products of combustion.

The equation of material balance in a general case has the form

$$b_k = A_k \sum a_{ki} n_i, \tag{8.12}$$

where b_k – weight fraction of k element in fuel, is determined by the formula (8.2); A_k – atomic weight of given element; a_{ki} – number of atoms of k element in i component of mixture of combustion products; n_i – number of moles of given component. Obviously the number of equations of material balance is equal to the number of elements Y. Consequently, the system of equations of chemical equilibrium and material balance includes X equations and is sufficient for resolution of the problem.

If in the products of combustion the same compound is present both in a gaseous and also in a condensed form (heterogeneous system), then for determination of the composition of combustion products it is necessary to have one more equation, since an additional unknown appears – the fraction of substance in a condensed form. Such an equation is the equation for the dependence of pressure of saturated vapor p_s of the given compound on temperature:

$$p_s = f(T). \tag{8.13}$$

The composition of gaseous products of combustion can be expressed in moles n_i of separate gases per 1 kgf of combustion products

(mole/kilogram-force), in weight fractions g_i, or in partial pressures p_i atm(abs.).

Transition from these values to others can be performed by the known equations

$$\frac{p_i}{p_{см}} = \frac{n_i}{n_{см}}; \tag{8.14}$$

$$\frac{p_i}{p_{см}} = \frac{\frac{g_i}{\mu_i}}{\sum \frac{g_i}{\mu_i}}. \tag{8.15}$$

Here $p_{см} = \sum p_i$; $n_{см} = \sum n_i$; μ_i — molecular weight of i gas.

Apparent molecular weight $\mu_{см}$ is equal to the weight of the mixture of gases, divided by their total number of moles; if the numbers of moles $n_{см}$ are referred to a unit of weight of the mixture of gases, then

$$\mu_{см} = \frac{1}{n_{см}}.$$

If the composition of the mixture of gases is assigned by partial pressures, then it is convenient to use the formula for $\mu_{см}$, expressed through p_i. Inasmuch as

$$\mu_{см} = \frac{\sum n_i \mu_i}{n_{см}},$$

then taking into account equation (8.10) we obtain

$$\mu_{см} = \frac{\sum p_i \mu_i}{\sum p_i} = \frac{\sum p_i \mu_i}{p_{см}}. \tag{8.16}$$

8.5. Calculation of Composition of Combustion Products

The problem is reduced to a determination of equilibrium composition of combustion products at an assigned temperature and pressure. In a general case the composition of combustion products

is very complex and can include up to 10-20 components and more. The problem somewhat is simplified, if on the basis of calculation or experimental data the list of compounds entering into the composition of combustion products is known and it is possible to disregard certain of them. Otherwise one has to be concerned with all possible (expected) compounds.

The initial system of equations, necessary for determination of quantities of separate components of a mixture of combustion products, as was noted, includes the equations of chemical equilibrium and material balance. The equations of chemical equilibrium describe the corresponding chemical reactions – in this case reactions of the dissociation type (8.9). It is necessary to consider that in general the system of equations of dissociation can be composed arbitrarily, but in such a manner that it completely describes mixture ratio of products of combustion and the chemical interaction between separate components of the mixture. Frequently they originate from equations of dissociation of molecular components into atomic. For example, for fuel consisting of the elements H and O, the equations of dissociation on the basis of equations (8.9) can be presented in the form

$$\left.\begin{aligned} &H_2O \rightleftarrows H_2 + \tfrac{1}{2}O_2 \\ &H_2O \rightleftarrows OH + \tfrac{1}{2}H_2 \\ &O_2 \rightleftarrows 2O \\ &H_2 \rightleftarrows 2H \end{aligned}\right\}. \qquad (8.17)$$

Instead of this system it is possible to write its equivalent system of chemical equations of dissociation of molecules and radicals into atoms:

$$\left.\begin{aligned} &H_2O \rightleftarrows 2H + O \\ &OH \rightleftarrows O + H \\ &O_2 \rightleftarrows 2O \\ &H_2 \rightleftarrows 2H \end{aligned}\right\}. \qquad (8.18)$$

For the first system of chemical reactions the equations of chemical equilibrium have the form:

$$\left.\begin{aligned} K_{p_{H_2O}} &= \frac{p_{H_2} \cdot p_{O_2}^{1/2}}{p_{H_2O}}; \\ K'_{p_{H_2O}} &= \frac{p_{OH} \cdot p_{H_2}^{1/2}}{p_{H_2O}}; \\ K_{p_{O_2}} &= \frac{p_O^2}{p_{O_2}}; \\ K_{p_{H_2}} &= \frac{p_H^2}{p_{H_2}}, \end{aligned}\right\} \qquad (8.19)$$

and for the second system

$$\left.\begin{aligned} K''_{p_{H_2O}} &= \frac{p_H^2 \cdot p_O}{p_{H_2O}}; \\ K_{p_{OH}} &= \frac{p_O \cdot p_H}{p_{OH}}; \\ K_{p_{O_2}} &= \frac{p_O^2}{p_{O_2}}; \\ K_{p_{H_2}} &= \frac{p_H^2}{p_{H_2}}. \end{aligned}\right\} \qquad (8.20)$$

However, such a system of reactions (decomposition of molecular compounds into atoms) sometimes can turn out to be not very convenient, in particular in those cases when in the products of combustion there is an absence of any of the elements in an atomic state, although it is included in the composition of other compounds (for example, in the combustion products of fuels consisting of elements H, C, O, and N there is practically no free carbon, although it is included in the composition of other gases such as CO_2, CO).

Equilibrium constants for ideal gases depend on temperature and are cited in special literature.[1]

It should be borne in mind that if in the tables the constants of equilibrium corresponding to the accepted system of reactions are absent, then these necessary constants can be obtained by a combination of those available in tables.

---

[1]Very detailed data are given in the reference book "Thermodynamic Properties of Individual Substances," vol. 1 and 2. Publishing house for the Academy of Sciences, USSR, 1962. See also [21].

We will examine example: in the tables there are equilibrium constants applicable to the second system (decomposition of molecules into atoms); it is required to find constants for the first two reactions of the first system ($K_{p_{H_2O}}$ and $K'_{p_{H_2O}}$).

$$K_{p_{H_2O}} = \frac{p_{H_2} \cdot p_{O_2}^{\frac{1}{2}}}{p_{H_2O}} = \frac{p_{H_2}}{p_H^2} \frac{p_H^2 p_O}{p_{H_2O}} \left(\frac{p_{O_2}}{p_O^2}\right)^{\frac{1}{2}} = \frac{K'_{p_{H_2O}}}{K_{p_{H_2}} K_{p_{O_2}}^{\frac{1}{2}}};$$

$$K'_{p_{H_2O}} = \frac{p_{OH} p_{H_2}^{\frac{1}{2}}}{p_{H_2O}} = \frac{p_{OH}}{p_H p_O} \frac{p_H^2 p_O}{p_{H_2O}} \left(\frac{p_{H_2}}{p_H^2}\right)^{\frac{1}{2}} = \frac{K'_{p_{H_2O}}}{K_{p_{OH}} K_{p_{H_2}}^{\frac{1}{2}}}.$$

We will compose the initial system of the equation for calculation of equilibrium composition of dissociated combustion products in an example of fuel consisting of elements H and O.

The composition of combustion products includes gases H_2O, O_2, H_2. OH, H, and O. This composition is described by four equations of chemical equilibrium and two equations of material balance. Equations of chemical equilibrium are presented above, for example, (8.19) or (8.20). Equations of material balance on the basis of equation (8.12) can be written as:

$$b_O = 16(n_{H_2O} + 2n_{O_2} + n_{OH} + n_O);$$
$$b_H = 1(2n_{H_2O} + 2n_{H_2} + n_{OH} + n_H);$$

or in partial pressures:

$$b_O = 16(p_{H_2O} + 2p_{O_2} + p_{OH} + p_O)\frac{n_{CM}}{p_{CM}};$$

$$b_H = (2p_{H_2O} + 2p_{H_2} + p_{OH} + p_H)\frac{n_{CM}}{p_{CM}}.$$

For exclusion of cofactor n_{CM}/p_{CM} in the last equations it is convenient to switch to relative equations of material balance:

$$\frac{b_O}{b_H} = \frac{16(p_{H_2O} + 2p_{O_2} + p_{OH} + p_O)}{2p_{H_2O} + 2p_{H_2} + p_{OH} + p_H}. \qquad (8.21)$$

Inasmuch as in this case the number of equations is decreased then the system should be augmented with one more equation. Usually equation of the law of Dalton is used:

$$p_{см} = \sum p_i$$

or for the given fuel

$$p_{см} = p_{H_2O} + p_{O_2} + p_{H_2} + p_{OH} + p_O + p_H. \qquad (8.22)$$

Thus, for determination of six unknown partial pressures there are six equations (8.20), (8.21), (8.22), with the help of which it is possible to find the composition of combustion products if the elementary composition of initial substances, pressure, and temperature of products of combustion are known.

At relatively low temperatures the number of products of dissociation decreases. Thus, at T < 2500°K practically atomic gases of H and O are absent, and if with this $\alpha < 1$, then molecular oxygen O_2 is also absent. In this case the number of unknowns also decreases, which simplifies the calculation. At T < 2000°K, as was shown above, products of dissociation are practically absent.

The composition of combustion products for fuels which also include other elements besides H and O is determined likewise. The initial system of equations includes Z = X - Y equations of chemical equilibrium, Y - 1 equations of material balance, written in a relative form, and one equation of the law of Dalton, i.e., there is always an identical number of equations and unknowns.

For an illustration we will also compose a system of equations for fuel, in which the fuel is H_2 and oxidizers is F_2. The products of combustion of this fuel contain the gases: HF, F_2, H_2, F, H; consequently, here X = 5 and Y = 2. The composition of combustion products is described by three equations of chemical equilibrium (Z = 3):

$$K_{p_{HF}} = \frac{p_H p_F}{p_{HF}}; \quad K_{p_{H_2}} = \frac{p_H^2}{p_{H_2}}; \quad K_{p_{F_2}} = \frac{p_F^2}{p_{F_2}};$$

one equation of material balance in relative form

$$\frac{b_H}{b_F} = \frac{1}{19} \frac{p_{HF} + 2p_{H_2} + p_H}{p_{HF} + 2p_{F_2} + p_F}.$$

and the equation

$$p_{см} = p_{HF} + p_{H_2} + p_{F_2} + p_H + p_F.$$

We will compose further a system of equations, describing the composition of combustion products of a heterogeneous system. Let us consider for an example a fuel, where the combustible is magnesium and the oxidizer – oxygen. In the products of combustion in this case there can be the gases MgO, Mg, O_2, O, and liquid $(MgO)_ж$. The weight fraction of $(MgO)_ж$ we will designate by g_{MgO}. Five unknowns are subject to determination.

For the given case X = 4 and Y = 2.

Composition of combustion products is described by two equations of chemical equilibrium (Z = 2):

$$K_{p_{MgO}} = \frac{p_{Mg} p_O}{p_{MgO}}; \quad K_{p_{O_2}} = \frac{p_O^2}{p_{O_2}}; \tag{8.23}$$

one equation of material balance:

$$\frac{b_{Mg} - \frac{24,3}{40,3} g_{MgO}}{b_O - \frac{16}{40,3} g_{MgO}} = \frac{24,3}{16} \frac{p_{MgO} + p_{Mg}}{2p_{O_2} + p_O + p_{MgO}} \tag{8.24}$$

and the equation

$$p_{см} = p_{MgO} + p_{O_2} + p_O + p_{Mg}. \tag{8.25}$$

The last equation, supplementing the system of equations to five, is the dependence of pressure of saturated vapors of MgO on temperature:

$$p_{s_{MgO}} = f(T). \tag{8.26}$$

In the equation of material balance (8.24) the members 16/40.3 and 24.3/40.3 represent the weight fractions of oxygen and magnesium present for $(MgO)_ж$ (24.3 – atomic weight of Mg; 40.3 – molecular weight MgO).

The solution of these five equations gives, at the assigned p_{CH} and T, the values of g_{MgO} and all partial pressures.

If as a result of calculation a negative value of weight fraction of the condensed phase is obtained, then this means that the condensed phase is absent; in this case the calculation should be conducted by the usual method for gas. Conversely, if the calculation was conducted neglecting the condensed phase and partial pressures of separate gases are obtained which are larger than the pressure of saturated vapors of the corresponding substances at the given temperature, this means that there is a condensate and the method of calculation should be modified.

8.6. Enthalpy of Parent Substances and Products of Combustion

For calculations there is no necessity to know the absolute value of enthalpy, but it is important to be able to find the change in it during a change of state of the substance. In the area of moderate pressures the change of enthalpy of a substance of constant chemical composition is connected only with a change of temperature. Therefore in this case we examine values $i_{T_0}^{T}$, equal to a change of enthalpy of a substance in the interval of temperatures from a certain T_0, accepted as initial, to T.

Change of enthalpy in the temperature interval from T_1 to T_2 is found here in the following way:

$$i_{T_1}^{T_2} = i_{T_0}^{T_2} - i_{T_0}^{T_1} \qquad (8.27)$$

The heat of formation ΔH of any substance is the name given to the thermal effect of the reaction of its formation from simple substances. Here the simple substances are examined in such states and allotropic modifications, which for them during normal conditions are stable: H_2 – gas; O_2 – gas; F_2 – gas, C – beta-graphite, Li – solid, B – solid, etc. The heat of formation of a substance at standard conditions (t = 20°C and p = 1 atm(abs.)) is called the standard heat of formation ΔH_{T_0}.

Heat of formation is considered positive, if the formation of a given substance from simple ones occurs with the absorption of heat (increase of enthalpy), and negative if the formation of a substance takes place with the liberation of heat.

In Table 8.4 are given the values of heat of formation of certain substances.

Table 8.4. Standard values of heat of formation of certain substances.

Gas	H	O	N	F	H_2	N_2	F_2	OH	NO
Heat of formation cal/kgf·mole	52000	59150	85550	0	0	0	0	10000	21600

Table 8.4. (Continued)

Gas	CO	HF	CO_2	H_2O	CF_4	$(H_2O)_m$
Heat of formation cal/kgf·mole	−26420	−64200	−94050	−57798	−231000	−68360

From Table 8.4 one can see for example, that the standard heat of formation of water is equal to 68360 cal/kgf·mole of water.

Complete enthalpy I, besides heat $i_{T_0}^{T}$, also considers chemical energy i_x. For the chemical energy of a substance it is accepted to use the change of enthalpy of a system during its formation from initial substances, the chemical energy of which is accepted as zero. In other words, for chemical energy we accept the thermal effect of the reaction of formation of the given substance from initial; thus

$$I_T = i_{T_0} + i_{xT_0}. \tag{8.28}$$

Here i_{xT_0} – change of enthalpy during formation of a given substance from initial at T_0.

Complete enthalpy at a temperature of T can also be written in the form

$$I_T = (i_{T_0}^T)_{исх} + i_{x_T},$$

where $(i_{T_0}^T)_{исх}$ – change of enthalpies of initial substances in the interval of temperatures $T-T_0$; i_{x_T} – change of enthalpy during formation of the given substance from initial at a temperature T.

The numerical value of complete enthalpy I_T depends on the selection of the beginning of reading, i.e., on the selection of initial substances, the chemical energy of which is accepted as equal to zero, and on the selection of the value of initial temperature T_0.

Widely distributed in the theory of jet engines is the system of reference, in which $T_0 = 293^\circ$ K, and as initial simple substances are accepted which are examined, as was indicated, in that state which under the given circumstances is stable for them. In this case for simple substances

$$i_x = 0; \quad I_{T_0} = 0; \quad I_T = i_{T_0}^T.$$

For any other substances with the given system of reference it is easy to see that

$$i_{x_{T_0}} = \Delta H_{T_0}.$$

Consequently, in general for any substance

$$I_T = \Delta H_{T_0} + i_{T_0}^T. \tag{8.29}$$

If the fuel (or component) constitutes a mixture of several substances, then its enthalpy is equal to

$$I = \sum g_i I_i + \Delta H_{раст}; \tag{8.30}$$

here g_i I_i – weight fraction and enthalpy of separate substances included in the mixture; $\Delta H_{раст}$ – thermal effect of dissolution.

Enthalpy of fuel of separate supply during relationship of components κ is equal to

$$I = \frac{\alpha}{1+\alpha} I_{ок} + \frac{1}{1+\alpha} I_{г} \qquad (8.31)$$

Enthalpy of products of combustion, constituting a mixture of gases, is found from equation (8.30), where $\Delta H_{раст} = 0$. If the composition is assigned through partial pressures, then entahlpy of the mixture of gases is equal to

$$I = \frac{1}{P_{см} r_{см}} \sum I_{iP_i} P_i. \qquad (8.32)$$

8.7. Determination of Temperature of Combustion

For determination of actual temperature of combustion it is necessary to have a calculation heat losses in the combustion chamber of the engine at the expense of incompleteness of combustion and heat transfer into the wall. Two methods of calculation of these losses are possible. In one case of loss are considered in the overall heat balance, and thus during a determination of combustion temperature only that heat, which goes to increasing the enthalpy of combustion products is taken into account. In the second case during a determination of combustion temperature losses are not considered at all and the theoretical temperature obtained thusly is then corrected with the help of special coefficients. In the theory of jet engines the second method is used.

Let us work out an equation of energy for a working substance in an engine. Let us consider a liquid propellant rocket engine (ZhRD) with a pump system of feeding, in which the working substance after the turbine is burned out in the main chamber. The equation, written for sections 0-0 and K-K (Fig. 8.2), in the absence of heat exchange, will have the form:

$$I_{ок0} G_{ок} + I_{г0} G_{г} + A L_{в ок} G_{ок} + A L_{в г} G_{г} - A L_{г} (G_{ок_{гг}} + G_{г_{гг}}) = I_{к}^{*} (G_{ок} + G_{г}). \qquad (8.33)$$

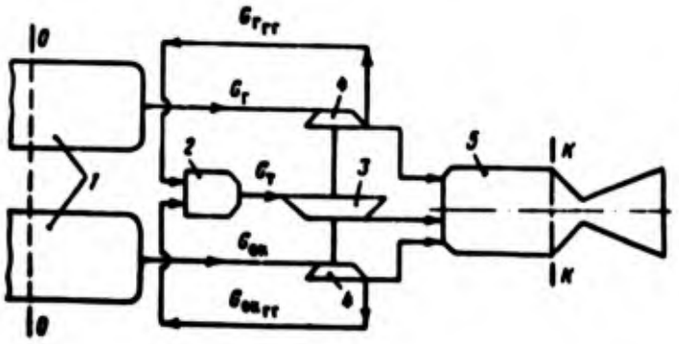

Fig. 8.2. For compilation of equation of energy: 1 – tanks; 2 – gas generator; 3 – turbine; 4 – pumps; 5 – chamber.

Here $G_{ок}$, $G_г$ – complete consumption of oxidizer and fuel in the engine; $G_{ок\,гг}$, $G_{г\,гг}$ – consumption of oxidizer and fuel in the gas generator; $I_{ок0}$, $I_{г0}$ – initial enthalpies of oxidizer and fuel in the tank (secton 0-0); $I_к^*$ – adiabatic enthalpy (isentropically) of inhibited flow of products of combustion at the end of the combustion chamber (section K-K). $L_т$ – effective operation of turbine, i.e., work, transmitted to the shaft of the turbine by one kilogram of working substance; $L_т = L_{ад.т}\eta_т$, where $L_{ад.т}$ – adiabatic work, $\eta_т$ – effective efficiency of turbine (see below §9.4); $L_н$ – effective work of pump, i.e., work from pump spindle for 1 kgf of pumped liquid; $L_н = H/\eta_н$, where H – actual pressure of pump; $\eta_н$ – complete efficiency of pump (see §9.4). Inasmuch as

$$L_{т\,ок} G_{ок} + L_{т\,г} G_г = L_т (G_{ок\,гг} + G_{г\,гг}),$$

then from equation (8.33) it is not difficult to obtain

$$I_{ок0} \frac{\alpha}{1+\alpha} + I_{г0} \frac{1}{1+\alpha} = I_к^*. \qquad (8.34)$$

By designating through I_0 the enthalpy of initial fuel at initial temperature

$$I_0 = \frac{\alpha}{1+\alpha} I_{ок0} + \frac{1}{1+\alpha} I_{г0},$$

we obtain

$$I_0 = I_к^*. \qquad (8.35)$$

If complete heat liberation is examined, i.e., complete combustion in the absence of heat transfer in the wall, then

$$T_z = T_z; \quad I_z = I_z$$

and

$$I_0 = I_z. \tag{8.36}$$

Thus, in the stated case complete enthalpy of products of combustion at temperature T_z is equal to enthalpy of the initial fuel in the tank at the starting temperature.

For a ZhRD with an open feeding system, when the working substance of the turbine is not used in the main chamber, it is possible to obtain:

$$I_0 + A\left(\frac{\alpha}{1+\alpha} L_{0\text{ок}} + \frac{1}{1+\alpha} L_{0\text{г}}\right) = I_z. \tag{8.37}$$

However, the increase of enthalpy of fuel in the pumps, which is equal to the member in parentheses of the last equation, is small and usually comprises less than 0.5% of its calorific value. Therefore even in this case for the calculations of combustion temperature an equation in the form (8.36) is used with sufficient accuracy. The same equation is also true for a ZhRD with pressurized feeding system and for solid propellant rocket engines.

Thus, the initial equation in the determination of combustion temperature in rocket engines is equation (8.36), according to which in the absence of losses of heat complete enthalpy of products of combustion with a temperature at the end of burning T_z is equal to enthalpy of the initial fuel at a temperature T_0.

Enthalpy of combustion products depends both on temperature, and also on their composition; composition of combustion products in turn depends on temperature. For substances consisting of elements H, C, O, and N, an exception are products of combustion at low temperatures, if $\alpha \geq 1$; in this case temperature does not influence the composition of combustion products.

In a general case the determination of temperature of combustion should be conducted simultaneously with the calculation of composition of products of combustion in the chamber. The sequence for calculation of composition and temperature of products of combustion is the following. Initial data for calculation are pressure p in the combustion chamber and chemical composition of fuel. Knowing the composition of fuel, they determine its elementary composition and enthalpy I_0 at initial temperature. Further they assign several (usually three) values of temperatures (T'_z, T''_z, and T'''_z) of combustion products and for each temperature they determine the composition of combustion products. Knowing the composition of combustion products, their enthalpies I', I" and I"' are determined for selected values of temperatures and graphs of dependence of enthalpy on temperature are constructed (Fig. 8.3). Value I_T for different substances in function of temperature is cited in special literature.[1]

Fig. 8.3. For determination of temperature of combustion.

Using relationship (8.36) and the graph of Fig. 8.3, it is not difficult to find an unknown temperature.

Having calculated T_z, once can determine the actual temperature $T^*_к$ with the help of experimental coefficients (see Chapter II).

At the same time if follows to keep in mind that usually due to the relationship of components which is variable by section the temperature of gases by section of the combustion chamber is also variable. Therefore in this case the discussion concerns mean value of temperature $T^*_к$. If it is necessary to determine distribution of

---

[1]See footnote on p. 172.

temperature of combustion by section, then one should conduct the corresponding calculations for the necessary range α.

Determination of composition and temperature of combustion products in general is connected with the solution of a system which includes up to ten and more equations, which constitutes a quite laborious process. The use of electronic computers for these purposes essentially simplifies the problem.

As was noted in Chapter III, in separate cases for a comparative appraisal of fuels which are close in chemical composition, their calorific value is examined.

By calorific value of fuel we understand the amount of heat given off during combustion of 1 kgf of fuel under the condition that products of combustion are cooled to the initial temperature of fuel. Usually this standard temperature is taken equal to 20°C, and pressure – equal to one atmosphere.

Calorific value, which is a thermal effect, is obviously equal to the difference of enthalpy of end products of combustion ($I_{пр}$) and enthalpy of fuel ($I_т$). Inasmuch as the reaction of combustion of fuel is exothermal, then for giving a positive value to calorific value we will consider

$$h_\alpha = I_т - I_{пр}.$$

The sequence of determination of h_α is the following. The composition of products of combustion of fuel at a standard temperature is found; inasmuch as this temperature is low (20°C), then products of combustion are not dissociated. Further based on the known composition enthalpy of products of combustion at standard temperature is determined by the formula (8.30) or (8.32). If working (lowest) calorific value (h_α or h_u) is examined, then all the products of combustion are taken in a gaseous state. If, however, the highest calorific value (h_0) is examined, then compounds included in the composition of combustion products and having boiling or melting point higher than 20°C should be taken in a condensed form (in liquid or solid), which is considered the value of enthalpy.

Enthalpy of fuel is determined by the enthalpy of components; bipropellant – by the formula (8.31). In general their enthalpy is taken at 20°C. If any of the components is a liquified gas, then its enthalpy should be taken at the temperature of boiling.

8.8. Thermodynamic Calculation of the Process of Outflow from the Nozzle

Calculation of the process in the nozzle is usually conducted under the assumption of its isentropic nature and then the necessary corrections are introduced for determination of actual values.

During an isentropic process in the nozzle

$$S_к = S_c \tag{8.38}$$

where $S_к$ and S_c – entropy of products of the reaction at the end of the combustion chamber and in the nozzle exit section.

Equation (8.38) is initial. For calculation of an isentropic process in the nozzle it is necessary to know the values of entropy of the various compounds included in the composition of combustion products. Values of entropies are cited in special tables at the standard pressure p^0 = 1 atm(abs.) (usually in physical atmospheres).

For gases it is known from thermodynamics that

$$\left(\frac{\partial S}{\partial p}\right)_T = -\frac{AR}{p},$$

whence[1]

$$S = S^0 - \frac{1.986}{\mu} \ln \frac{p}{p^0} \ \frac{\text{Cal}}{\text{kgf} \cdot \text{deg}}. \tag{8.39}$$

Here S^0 – entropy of gas at standard pressure p^0 and given

[1]In this chapter the formulas for enthalpy and entropy are constructed proceeding from the fact that enthalpy and entropy of separate components are given for 1 kilogram-force of substance. Frequently in information tables these values are relative to a mole; this should be considered in the calculations.

temperature;[1] S – entropy of gas at arbitrary pressure p and the same temperature.

Inasmuch as $p^0 = 1$, then

$$S = S^0 - \frac{1{,}986}{\mu} \ln p. \tag{8.40}$$

For a mixture of gases

$$S = \sum g_i S_i,$$

or

$$S = \frac{1}{\mu_{см} g_{см}} \sum g_i (S_i^0 \mu_i - 1{,}986 \ln p_i) \frac{\text{Cal}}{\text{kgf} \cdot \text{deg}}. \tag{8.41}$$

Usually during calculation the composition of fuel, pressure in the chamber, and pressure in the nozzle exit section are assigned. The basic problem of calculation is determination of exit velocity, and also through sections of the nozzle.

Calculation of isentropic outflow is carried out in the following order:

1) for a specific composition of fuel at an assigned pressure the composition and temperature of products of combustion in the combustion chamber are found;

2) based on known composition and temperature the entropy of gases in the chamber is calculated;

3) for assigned pressure p_c several (usually three) values of temperatures T_1, T_2, and T_3 are selected in the region of expected temperature of gases in nozzle exit section, and for each value the composition of combustion products is found by methods expounded in this chapter; further for every value T entropy is found by the formula (8.41) and the graph $S = f(T)$ is constructed (Fig. 8.4):

[1]Data on S^0 see the literature shown on p. 172.

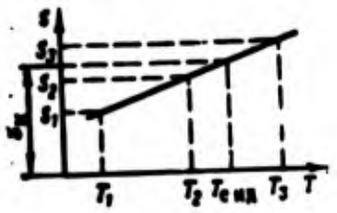

Fig. 8.4. For determination of temperature in nozzle exit section.

4) from condition (8.38) by known value $S_н$ the value is found for temperature $T_{с.ид}$ – temperature of combustion products of an ideal process in the nozzle exit section; for the value of temperature found the composition of gases and enthalpy of the mixture are determined on the basis of equation (8.32):

$$I_c = \frac{1}{\text{знам}} \sum I_i p_i (\text{знам}_i).$$

where I_i for each gas is taken at a temperature T_c;

5) ideal exit velocity is determined; this value can be found from the equation of energy, written for the entrance and nozzle exit section:

$$w_{ид} = \sqrt{\frac{2g}{A}(I_z - I_c)}.$$

Considering that $I_z = I_0$,

$$w_{ид} = 91{,}53\sqrt{I_0 - I_c}. \qquad (8.42)$$

For determination of parameters of flow and area of section in an arbitrary site along the length of nozzle it is necessary to know p and T along the nozzle. Exact determination of these values is possible by the above-stated method. The problem is facilitated, if the actual process of expansion of gases in the nozzle is replaced by a process having an average constant index, although in this case the solution obtained is approximate.

Accepting that the process of expansion in the nozzle is subordinate to equation $pv^k = \text{const}$, we determine index k from the expression

$$k=\frac{\lg\frac{p_н}{p_c}}{\lg\frac{v_c}{v_н}},$$

where $v_н$, v_c – specific volumes of gas accordingly at the beginning and at the end of the nozzle.

Average index of isentropic process, proceeding with a change of composition and heat capacity of gases, is less than the adiabatic index with a constant composition and heat capacity of gases. This is normal, since the process of equilibrium expansion of combustion products due to recombination is accompanied by the transformation of chemical energy into thermal, which is equivalent to the supply of heat to a gas of contant composition. The more strongly the gas is dissociated before the nozzle, with other things being equal, then the less is the average index k.

Let us turn to a determination of actual values of a real process of flow. Exit velocity and specific thrust for rated nozzle conditions are equal to

$$w_c=\varphi_c\sqrt{w_{ад}};$$
$$P_{уд}=\frac{w_c}{g}.$$

Average index of actual process should differ from average index of isentrope k due to the influence of hydraulic losses, heat exchange with the walls, and heterogeneity of composition along the section of flow. Individuals of these factors influence in various ways the value of index of the process (for example, heat transfer in the walls and hydraulic losses). We will consider that index of the actual process is equal to average index of isentrope k. Temperature of gas in the outlet section is equal to

$$T_c=T_c^*\left(\frac{p_c}{p_c^*}\right)^{\frac{k-1}{k}}\frac{R_c}{R_c}=\varphi_c^2T_c\left(\frac{p_c}{p_c^*}\right)^{\frac{k-1}{k}}\frac{R_c}{R_c}. \qquad (8.43)$$

Consequently:

$$T_c = \varphi_c^2 T_{c.ид}. \qquad (8.44)$$

Area of nozzle exit section

$$F_c = \frac{G_{\text{газа}}}{\gamma_c w_c}, \qquad (8.45)$$

where

$$\gamma_c = \frac{p_c}{RT_c}.$$

Nozzle throat area will be found from formula (2.52)

$$F_{кр} = \frac{G_{\text{газа}} \beta}{p_к^*}. \qquad (8.46)$$

On the basis of numerous calculations values have been established for index of isentropy k for many fuels (see below §8.10).

Using these values of index k, it is possible to calculate approximately the process of outflow if the parameters of the gas are known ($p_к^*$, T_z, R). Temperature of gas in this case is found by the formula (8.43), considering $R_к = R_c$, and exit velocity w_c – by the formula (2.27). Through sections are determined by the formulas (8.45) and (8.46).

When using the I-S diagram for dissociated products of combustion the volume of calculation is reduced considerably, however, it is necessary to have a previously prepared diagram for a given fuel of a fully definite composition, i.e., definite excess-oxidant ratio. Construction of such diagrams assumes the carrying out of a series of preliminary calculations, the expediency of which can be justified only for standard fuels. Maximum value of enthalpy on an I-S diagram is limited by its value for initial substances and constitutes the initial enthalpy of fuel I_0.

If pressure in the chamber $p_к^*$ is known (Fig. 8.5), then the initial point k, corresponding to state of combustion products in the chamber at $w_к = 0$ in an assumption of absence losses of heat,

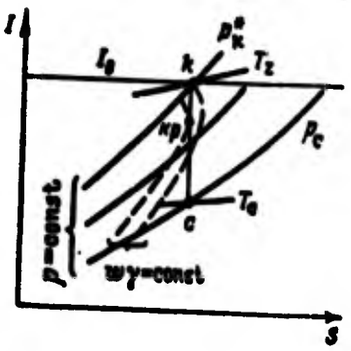

Fig. 8.5. For using the I-S diagram.

is determined by the intersection of lines $p_н^* = \text{const}$ and $I_0 = \text{const}$. At point k with the help of the diagram one can determine the temperature of gases T_z. Line k-c will be a graphic image of the process of isentropic flow in the nozzle; point c is found on isobar $p_c = \text{const}$, corresponding to pressure on a nozzle section. At point c one can determine I_c, $T_{c.ид}$. Exit velocity is determined from equation (8.42). Through sections at the exit from the nozzle and along its length are determined from the equation of consumption. For convenience on the I-S diagram lines of constant current density $w\gamma$ are plotted. Using these lines, one can also determine the critical section of the nozzle (point kp) and parameters of the state of gas in it. In a critical section the current density attains maximum value; therefore curves $w\gamma = \text{const}$ will touch isentropes k-c at point kp.

8.9. Peculiarities of Thermodynamic Calculation in the Presence of the Condensed Phase in Products of Combustion

Basically, all the above-stated position of thermodynamic calculation pertain also to a heterogeneous mixture of combustion products. The only difference lies in the necessity for calculation of properties of the condensed phase.

During determination of temperature of combustion the initial equation is the equation of energy (8.36). However, during determination of enthalpy of combustion products it is also necessary to consider enthalpy of the condensed phase, i.e.:

$$I = \sum g_i I_i + \sum g_j I_j.$$

Here g_i, I_i – weight fractions and enthalpies of gaseous products;
g_j, I_j – the same for condensed products.

If, as usually, the gaseous products are assigned in partial pressures, and condensed – in weight fractions, then

$$I=\frac{1-\sum g_j}{p_{см}\mu_{см}}\sum p_i\mu_i I_i+\sum g_j I_j. \tag{8.47}$$

The initial equation for calculation of equilibrium process of flow in a nozzle is equation (8.38), and during a determination of entropy of combustion products one should consider entropy of the condensed phase, i.e.,

$$S=\sum g_i S_i+\sum g_j S_j$$

or

$$S=\frac{1-\sum g_j}{p_{см}\mu_{см}}\sum p_i(S_i^0\mu_i-1{,}986\ln p_i)+\sum g_j S_j. \tag{8.48}$$

Values of partial pressures of gaseous products and weight fractions of condensed in heterogeneous mixture are determined from a calculation of composition of combustion products (see §8.5).

It is necessary to consider that the fraction of condensed products along the nozzle can change, due to a change of temperature and pressure.

Just as also for homogeneous products, in the case of a heterogeneous mixture it is possible to calculate the process of outflow by simply using the average index of the process. Here it is possible to use the position of §7.5. These materials can be used for calculations of outflow in the absence of equilibrium between phases in the process of flow in the nozzle.

8.10. Results of Thermodynamic Calculations and Their Analysis

In Fig. 8.6 are presented the results of a calculation of the composition of combustion products, from which it is clear that with

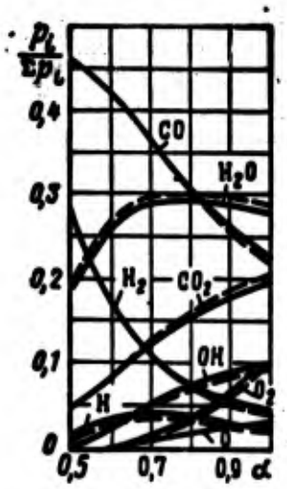

Fig. 8.6. Composition of combustion of nitric acid-kerosene fuel; - - - - $p_{см}$ = = 40 atm(abs.); —— $p_{см}$ = = 20 atm(abs.).

a decrease of excess-oxidant ratio there is a decrease in the fraction of products of complete oxidation (due to a deficiency of oxygen) and the fraction of products of dissociation. Decrease in the fraction of products of dissociation is explained, on the one hand, by a decrease of temperature of combustion due to lowering of the calorific value of fuel, and on the other hand – by an increase in the share of products of incomplete oxidation; the latter dissociate to a lesser degree than products of complete oxidation. Increase of pressure somewhat decreases the fraction of products of dissociation.

In Figs. 8.7-8.11 are shown the dependences of $P_{уд}$, $\mu_к$, T_z and k on excess-oxidant ratio for certain liquid fuels during separate feeding at a pressure in the chamber $p_к^*$ = 40 atm(abs.) and $p_c = p_н$ = = 1 atm(abs.). In the absence of dissociation maximum of temperature T_z should coincide with maximum of thermal effect, which corresponds to α = 1. An example is fuel, consisting of oxidizer – 80% H_2O_2 + + 20% H_2O and fuel – 50% $N_2H_4H_2O$ + 50% CH_3OH (Fig. 8.7); combustion temperature of this fuel is not great and products of combustion are not dissociated.

In the presence of dissociation the maximum of temperature is usually displaced in the direction of α < 1. Certain displacement of maximum value of temperature in the direction of rich mixtures is explained by a lowering in the degree of dissociation with a decrease of excess-oxidant ratio.

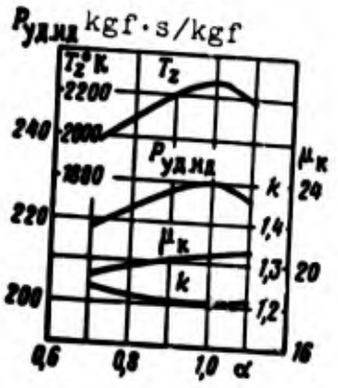

Fig. 8.7. Dependences of $P_{уд}$; $\mu_к$; T_z and k on α: oxidizer – 80% hydrogen peroxide + + 20% water; fuel – 50% hydrazine – hydrate ($N_2H_4H_2O$) + 50% methyl alcohol.

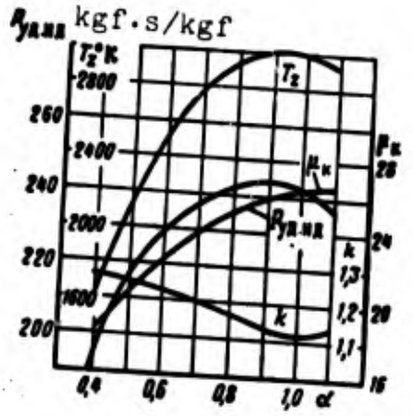

Fig. 8.8. Dependences of $P_{уд}$; $\mu_к$; T_z and k on α: oxidizer – liquid oxygen; fuel – kerosene.

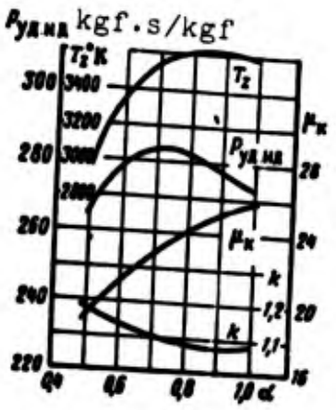

Fig. 8.9. Dependences of $P_{уд}$; $\mu_к$; T_z and k on α: oxidizer – liquid oxygen; fuel – kerosene.

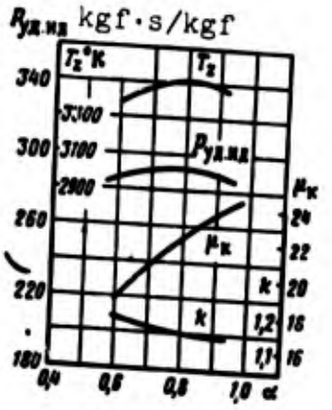

Fig. 8.10. Dependences of $P_{уд}$; $\mu_к$; T_z and k on α: oxidizer – liquid oxygen; fuel – dimethyl-hydrazine.

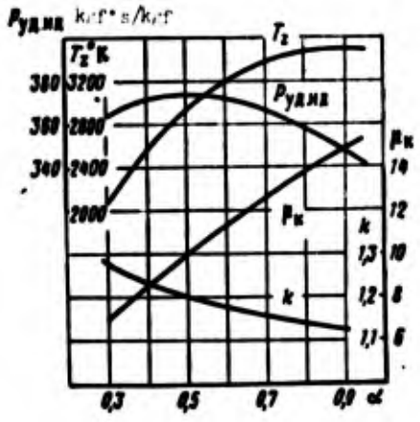

Fig. 8.11. Dependences of $P_{уд}$; $\mu_к$; T_z and k on α: oxidizer – liquid oxygen; fuel – liquid hydrogen.

Increase of pressure somewhat increases temperature due to a lowering of the degree of dissociation of combustion products (Fig. 8.12). The less dissociated the products of combustion, then the weaker the influence of pressure on temperature.

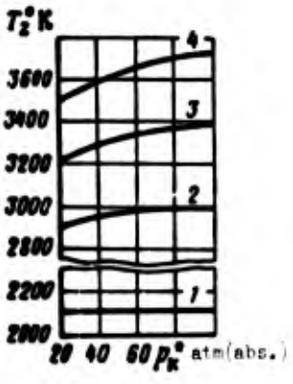

Fig. 8.12. Dependence of T_z on pressure in the chamber (α = 0.8): 1 – 80% H_2O_2 + + 20% H_2O – 50% $N_2H_4H_2O$ + + 50% CH_3OH; 2 – HNO_3 – kerosene; 3 – liquid oxygen – C_2H_5OH; 4 – liquid oxygen – kerosene.

Let us consider the influence of α on average molecular weight of products of combustion in the combustion chamber. With a decrease of α there is an increase in the fraction of lighter products of incomplete oxidation, in consequence of which $\mu_к$ drops. With an increase of pressure molecular weight increases somewhat (Fig. 8.13) due to the decrease of the share of products of dissociation.

Average index of isentrope k depends on α (see Figs. 8.7-8.11), since the composition and temperature of combustion products change. With a decrease of α (at $\alpha < 1$) temperature decreases and, consequently, also the degree of dissociation, which leads to a

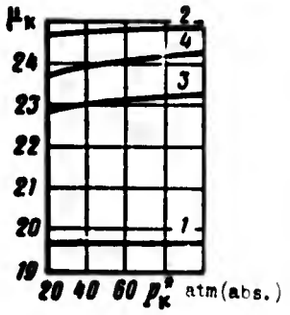

Fig. 8.13. Dependence of $\mu_к$ on pressure in chamber at $\alpha = 0.8$; (numbers of curves based on Fig. 8.12).

decrease of heat capacity and therefore to an increase of index k. Decrease of excess-oxidant ratio of α leads to an increase in the share of gases with a lesser number of atoms, which also promotes an increase of k. With an increase of pressure in the chamber value k increases somewhat due to a decrease in the degree of dissociation. At a given $p^*_к$ with an increase in the degree of lowering of pressure in the nozzle, i.e., with a decrease of p_c, value k also increases somewhat, since here there is a lowering of the influence of dissociation on the process of expansion of gas in the nozzle.

Change of specific thrust (or, just the same, exit velocity) with a change of α is determined by the influence of excess-oxidant ratio on calorific value of fuel and thermal efficiency. With a decrease of α ($\alpha < 1$) h drops, but η_t grows, since index k increases. Due to this the maximum of specific thrust is obtained usually with the excess-oxidant ratio differing from a unit, and for the majority of fuels with $\alpha < 1$. With an increase of $p^*_к$ specific thrust increases (Figs. 8.14-8.16) due to an increase of thermal efficiency, and value $\alpha_{опт}$ approaches a unit. In Figs. 8.15 and 8.16 the dotted line connects points corresponding to $\alpha_{опт}$.

In Figs. 8.17 and 8.18 the calculation values of complex $\beta_{ид}$ are given for a number of fuels. It is clear that $\beta_{ид}$ practically does not depend on pressure in the chamber; its value is determined mainly by the composition of the fuel, i.e., the type of components and value of excess-oxidant ratio.

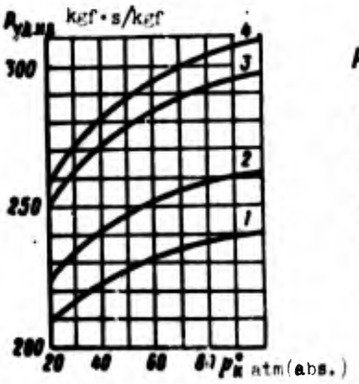

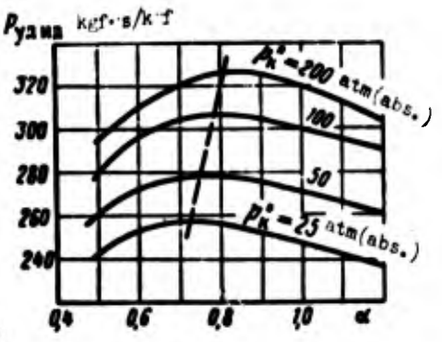

Fig. 8.14. Fig. 8.15.

Fig. 8.14. Dependence of specific thrust on pressure in the chamber at $\alpha = 0.8$; $p_c = p_н =$ = 1 atm(abs.) (numbers of curves based on Fig. 8.12).

Fig. 8.15. Specific thrust of conditional fuel $O_2 - C_nH_{2n}$ at $p_c = p_н = 1$ atm(abs.).

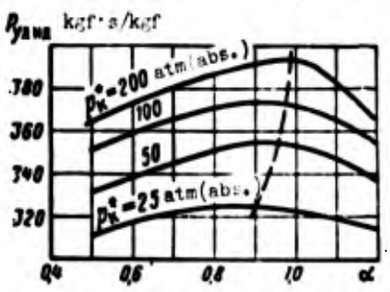

Fig. 8.16. Specific thrust of conditional fuel $F_2 - N_nH_{2n}$ at $p_c = p_н = 1$ atm(abs.).

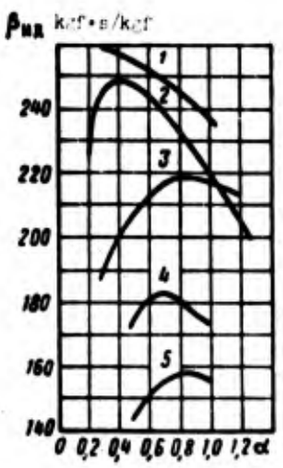

Fig. 8.17. Dependence of complex $\beta_{ид}$ on excess-oxidant ratio: 1 – $F_2 - H_2$; 2 – $O_2 - H_2$; 3 – $F_2 - NH_3$; 4 – O_2 – kerosene; 5 – HNO_3 – kerosene.

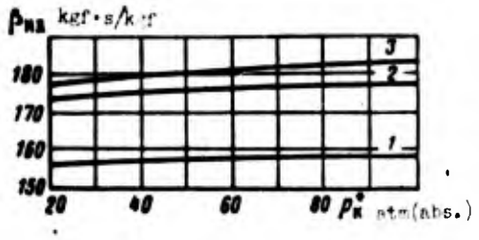

Fig. 8.18. Dependence of complex $\beta_{ид}$ on pressure in the chamber: 1 – HNO_3 – kerosene; 2 – O_2 – C_2H_3OH; 3 – O_2 – kerosene.

In Figs. 8.19 and 8.20 and in Table 8.5 the results of thermodynamic calculations for solid rocket propellants are given.

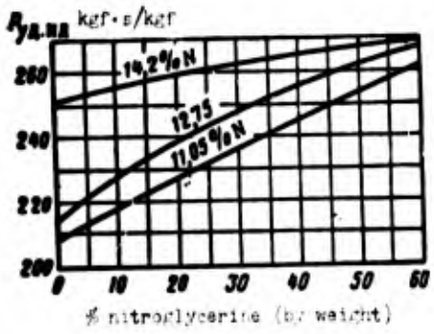

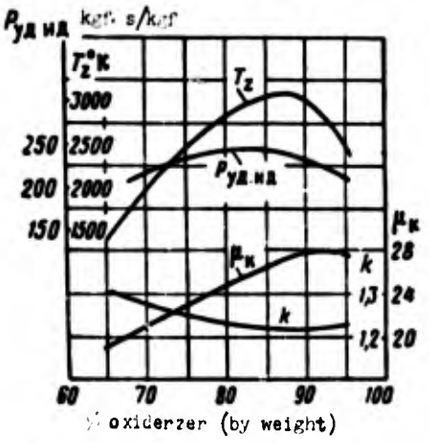

Fig. 8.19. Fig. 8.20.

Fig. 8.19. Specific thrust of dibasic fuel nitroglycerine – nitrocellulose with a various percentage of nitrogen in nitrocellulose ($p_к$ = 100 atm(abs.); $p_с = p_н$ = 1 atm(abs.)).

Fig. 8.20. Dependences of $P_{уд}$; $\mu_к$; T_z and k on share of oxidizer – ammonium perchlorate; fuel – polyestor ($p^*_к$ = 70 atm(abs.)).

It is clear from Fig. 8.19 that in dibasic fuel with an increase in the content of nitroglycerine and with an increase of share of nitrogen in nitrocellulose the specific thrust increases (mainly due to an increase of k_α). In Table 8.5 other data pertaining to this fuel are given.

The influence of share of oxidizer in mixture fuel on specific thrust and parameters of products of combustion are shown in Fig. 8.20.

Table 8.5. Parameters of products of combustion of dibasic fuels at $p_к^* = 100$ kgf/cm^2 and $p_c = 1$ kgf/cm^2.

Content of nitrogen in nitro-cellulose	% nitro-glycerine in fuel	$T_г^°$ K	$M_к$	k
11,05%	0	1750	19	1,26
	20	2420	20,3	1,25
	40	3000	22,3	1,22
	60	3215	24,6	1,18
12,75%	0	2640	21,0	1,22
	20	2960	22,5	1,19
	40	3180	23,8	1,18
	60	3310	26,2	1,15
14,12%	0	3090	23,0	1,21
	20	3230	24,3	1,19
	40	3340	25,6	1,16
	60	3380	27,3	1,12

C H A P T E R IX

CHARACTERISTIC OF ROCKET ENGINES

In process of work of a rocket engine its thrust can change. At a constant altitude this change is caused by a change in the flow rate of combustion products from the nozzle. In a liquid propellant rocket engine [ZhRD] the change of flow rate of combustion products from the nozzle is caused by a fuel change in the feeding of fuel into the chamber from the feeding system. In an RDTT [solid propellant rocket engine] the consumption of combustion products during operation of the engine can change due to a change of burning surface of charge or burning rate. Thrust and specific thrust of the engine also depend on pressure of the environment.

For a more complete appraisal of the characteristics of liquid propellant rocket engines, which have a turbopump system of feeding, one should examine the total thrust and effective specific thrust, i.e., thrust and specific thrust taking into account consumption of working substance on the turbine and additional thrust, created beyond the TNA [turbopump unit]. However, this considerably complicates the consideration of engine performance, inasmuch as the law of change of consumption of working substance depends on the method of control of the feeding system. Consideration of such characteristics has meaning for concrete constructions. In the theory of rocket engines for an exposure of main regularities usually they examine the characteristic of a liquid propellant rocket engine without considering the flow rate of working substance on

the turbine. Such dependences constitute the characteristics of only the chamber. For liquid propellant rocket engines with afterburning of generator gas in the main combustion chamber, and also for engines with pressurized feeding systems the characteristics of chamber and propulsion system coincide.

Engine characteristics in general will be the name given to dependences of thrust and specific thrust on factors affecting them and determined by external conditions or operating conditions of the engine.

In this chapter we will examine characteristics based on pressure in the chamber and altitude characteristics of a rocket engine; here the nozzle of the engine will be considered unregulated.

9.1. Characteristics of a Rocket Engine Based on Pressure in the Chamber

The given characteristics constitute the dependence of thrust and specific thrust on pressure in the chamber at a constant altitude of flight, and in the case of a liquid propellant rocket engine on bipropellant fuel also with a constant excess-oxidant ratio. For a liquid propellant rocket engine this characteristic is also called throttle. Sometimes throttle characteristics are constructed based on expended fuel, however, the value of pressure in the chamber is measured more simply and therefore more frequently it is exactly this parameter which is taken as an independent variable.

It is necessary to consider that for the separate chamber fuel consumption and pressure in chamber with sufficient accuracy are directly proportional to each other in a wide range of change of p_K^* value. Therefore characteristics based on pressure in the chamber and based on expended fuel for a single-chamber engine are practically similar to each other. This position also pertains to multichamber liquid propellant rocket engines, for which there are no separate turning off of separate chambers and pressure p_K^* in separate chambers changes to an identical degree.

If in multichamber liquid propellant rocket engines for definite conditions it is possible to turn off separate chambers and the pressure in different chambers is changed to a various degree, then in this case change of fuel consumption for the entire engine is not proportional to the change of pressure in the chambers. In such engines the characteristics for pressure in the chamber are of interest only for separate chambers. However, having the characteristics of separate chambers for pressure and value p_K^* in them for certain conditions, it is not difficult to find thrust and specific thrust of the whole engine for given conditions.

Characteristics of liquid propellant rocket engines for pressure in the chamber can be obtained by means of bench tests; in this case it is necessary to measure thrust, pressure in the chamber, and fuel consumption. Instantaneous consumption in a RDTT is not measured directly during testing. Therefore for these engines by means of testing directly it is possible to obtain only thrust and pressure in the chamber. Earlier it was noted that in reference to RDTT usually the current (instantaneous) value of specific thrust is not considered, but its average value during time of operation is used.

Characteristics of rocket engines can also be determined by the analytic method, if geometric dimensions of nozzle, parameters of gas in the chamber, and also coefficients, considering losses in the combustion chamber and nozzle, are known.

Let us consider change of thrust with change of pressure in the chamber. We will consider that the engine is operating with each p_K^* on steady-state operation, but the outflow of products of combustion from the nozzle occurs with a supercritical drop; the last assumption is quite exact in the practical range of change of pressure in the chamber. Subcritical drop of outflow can exist with $p_K^*/p_H < (1.7\text{-}1.9)$; such conditions take place only during starting and stopping of engines. Let us also accept outflow as occurring without breakaway of gas from the walls of the nozzle,

and index k constant. Thrust of the engine can be represented in the form

$$P = P_{\text{п}} - F_c p_{\text{н}}. \tag{9.1}$$

Here

$$P_{\text{п}} = \frac{G_{\text{сек}}}{g} w_c + F_c p_{\text{п}}$$

constitutes the thrust of an engine in a vacuum, when external pressure $p_H = 0$. Thrust in vacuum is equal to resultant forces of internal pressure and friction, and $F_C p_H$ – resultant forces of external pressure.

Let us consider how engine thrust in a vacuum is changed depending on pressure in the chamber. In Chapter VII it was shown that with a change of pressure in the chamber the pressure of gas in any point of the nozzle is changed directly proportional to change of p_K^*. Consequently, one may assume also that engine thrust in a vacuum also will be changed directly proportional to pressure in the chamber.

Actually, taking into account equations (2.48) and (2.28), the last expression can be reduced to the following form:

$$P_{\text{п}} = p_к^* F_{\text{кр}} \left\{ \varphi_c m \sqrt{\frac{2}{g} R \frac{k}{k-1} \left[1 - \left(\frac{p_c}{p_к^*} \right)^{\frac{k-1}{k}} \right]} + \bar{f}_c \frac{p_c}{p_к^*} \right\}.$$

According to what was said earlier, value

$$m \sqrt{\frac{2}{g} R \frac{k}{k-1} \left[1 - \left(\frac{p_c}{p_к^*} \right)^{\frac{k-1}{k}} \right]} = \varphi'(\bar{f}_c)$$

does not depend on pressure in the chamber and is determined only by the geometric characteristics of the nozzle; since a variable-area nozzle is examined, then $\varphi'(\bar{f}_c)$ = const. For the same reason

$$\bar{f}_c \frac{p_c}{p_к^*} = \varphi''(\bar{f}_c) = \text{const}.$$

Consequently:

$$P_п = K_п F_{кр} p_к^*, \tag{9.2}$$

where

$$K_п = \varphi_c \varphi'(\bar{f}_c) + \varphi''(\bar{f}_c). \tag{9.3}$$

Value $K_П = P_П/F_{кр}p_к^*$ is called coefficient of thrust in a vacuum. Value $K_П$ shows the ratio of resultant internal forces in the chamber to resultant forces of pressure which have an effect on a section of the front wall of the chamber with an area equal to $F_{кр}$, and depends on index k, geometry of nozzle ($\bar{f}_c$), and coefficient φ_c. For an engine with a fixed-area propelling nozzle $K_П$ is a constant value. Dependence of coefficient of thrust in vacuum on $\bar{f}_c$ with φ_c = 1 is shown in Fig. 9.1. Using this value, it is not difficult to estimate engine thrust in a vacuum, if geometric dimensions of nozzle ($\bar{f}_c$ and $F_{кр}$) and pressure in the chamber are known.

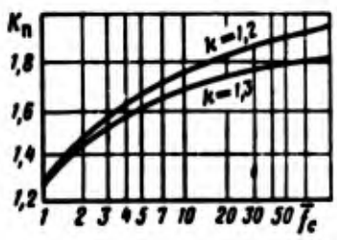

Fig. 9.1. Dependence of coefficient of thrust in a vacuum on $\bar{f}_c$.

Thus, in the examined case $P_П$ changes directly proportional to pressure in the chamber.

As a result the expression for engine thrust acquires the form:

$$P = K_п F_{кр} p_к^* - F_c p_н. \tag{9.4}$$

It follows from formula (9.4) that with the assumptions made the dependence of thrust on pressure in the chamber constitutes a straight line passing through point 0' with coordinates $p_к^*$ = 0

and $P = -F_c P_H$. It is obvious that this dependence is true only as long as the assumptions made are true, i.e., up to the moment of breakaway of gases from the walls of the nozzle. With a lowering of p_K^*, p_c also decreases; therefore, at a certain p_K^* pressure on a nozzle section p_c will be less than maximum, and breakaway of gas from the walls of the nozzle will occur; starting with the moment of breakaway the curve will deviate from straight (Fig. 9.2). With a continuous lowering of pressure engine thrust would gradually arrive at zero value with $p_K^* = p_H$. However, there is a certain minimum pressure in the chamber (greater than p_H), below which normal operation of the engine ceases.

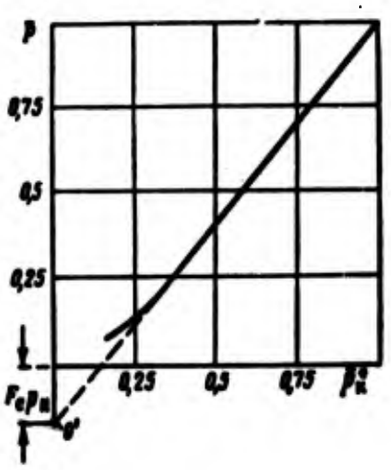

Fig. 9.2. Dependence of thrust on pressure in the chamber.

Usually the range of change of pressure in the chamber is such that the engine operates mainly on the rectilinear section of the curve; this pertains especially to engine operation at high altitudes. An exception are the conditions of starting and stopping the engine. It is necessary to note that in spite of the fictitious nature of point O', it is convenient for construction of the characteristic curve. Actually it is sufficient to have only one reliable point on the rectilinear section of the characteristic curve in order to construct it on this rectilinear section if p_H and F_c are known.

Characteristic curves based on pressure in the chamber, constructed for various altitudes, will have the form shown in Fig. 9.3.

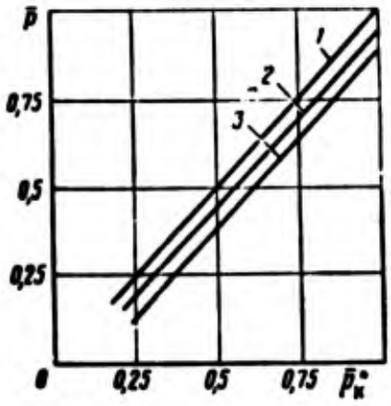

Fig. 9.3. Dependence of thrust on pressure in the chamber at various altitudes: 1 — in a vacuum; 2 — at altitude H_2; 3 — at altitude $H_1 < H_2$.

We will examine the dependence of flow rate of combustion products from the nozzle on pressure in the chamber. In a liquid propellant rocket engine flow rate through the nozzle on steady-state operation is equal to the quantity of fuel, burning in a unit of time, and also flow rate of fuel from the feeding system into the chamber. In an RDTT the flow rate through the nozzle is not strictly equal to the second quantity of combustible fuel, since in the process of operation of the engine there is a change in the quantity of gases in the chamber itself due to an increase of free volume of the chamber and a change of pressure in it. However, if the conditions of ignition of charge and termination of operation are not considered, then for remaining conditions, when pressure in the chamber is not changed strongly, these two values (flow rate through nozzle and second quantity of burning fuel — fuel expenditure) can be considered as equal with sufficient accuracy.

If one were to disregard the dependence of $\varphi_к$ and $\beta_{ид}$ on $p_к^*$, then the dependence of $G_{\Sigma сек}$ on $p_к^*$ presents a straight line coming out of the origin of the coordinates (Fig. 9.4); only at very small pressures in the chamber, at subcritical drops which do not have a practical value for rocket engines, this dependence will deviate from a straight line.

Let us turn to determination of dependence of specific thrust on pressure in the chamber, taking the same assumption as when examining thrust.

Fig. 9.4. Dependence of flow rate on pressure in the chamber.

The expression for specific thrust can be written:

$$P_{уд} = \frac{P_п}{G_{\Sigma сек}} - \frac{f_c p_п}{G_{\Sigma сек}}. \qquad (9.5)$$

The ratio $P_п G_{\Sigma сек}$ constitutes specific thrust of the engine in vacuum $P_{уд.п}$. This value does not depend on pressure in the chamber, since thrust in a vacuum and flow rate are directly proportional to pressure $p_к^*$. In the second member of formula (9.5) the numerator does not depend on pressure in the chamber, but the denominator is directly proportional to $p_к^*$.

Therefore it is possible to write

$$P_{уд} = P_{уд.п} - B\frac{p_п}{p_к^*}, \qquad (9.6)$$

where

$$P_{уд.п} = \varphi_п \beta_{ид} K_п; \quad B = \bar{f}_c \varphi_п \beta_{ид}.$$

Taking into account the assumptions made above and with constant $\beta_{ид}$ and $\varphi_к$ one may assume that values $P_{уд.п}$ and B do not depend on pressure in the chamber; then dependence of specific thrust on $p_к^*$ constitutes a hyperbola, determined by equation (9.6).

It is clear from Fig. 9.5 that with a pressure drop in the chamber specific thrust decreases; the greater the altitude of flight, the weaker the influence. Specific thrust of a rocket engine in a vacuum depends on type of fuel, on geometric characteristics of the nozzle $\bar{f}_c$, or, which is the same, on ratio of pressure $p_к^*/p_c$ and coefficients φ_c and $\varphi_к$. On Fig. 9.6 is shown, as an example, the dependence of $P_{уд.п}$ on degree of lowering of pressure in nozzle $p_к^*/p_c$ for oxygen fuel – kerosene at $\varphi_c = \varphi_к = 1$.

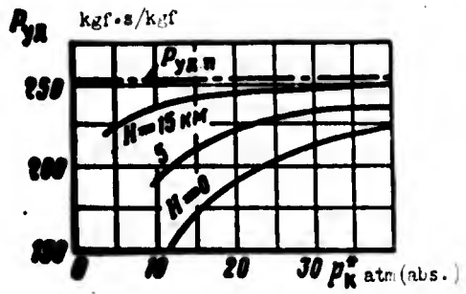

Fig. 9.5.

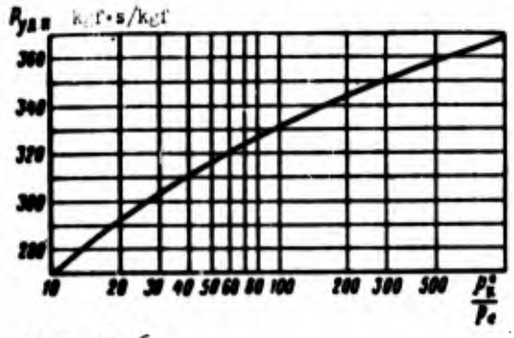

Fig. 9.6.

Fig. 9.5. Dependence of specific thrust on pressure in the chamber.

Fig. 9.6. Specific thrust in a vacuum for oxygen fuel — kerosene ($\alpha = 0.8$; $\varphi_к = \varphi_c = 1$).

We will examine the influence of degree of nozzle expansion on the flow of characteristics based on pressure in the chamber. Let us assume that for the given chamber with a nozzle, having a degree of expansion $\overline{f}_{c1}$, the characteristic curve has the form shown on Fig. 9.7 line 1. Calculation operating conditions for the nozzle will exist only at a definite pressure in the chamber; we will take: $p^*_{к.p1} = 40$ atm(abs.). If with other things being equal there is an increase of nozzle exit section, i.e., expansion area ratio is increased to $\overline{f}_{c2} > \overline{f}_{c1}$, then pressure in the chamber $p^*_{к.p2}$, corresponding to calculation conditions in the second case, will be greater than $p^*_{к.p1}$; let us assume that $p^*_{к.p2} = 100$ atm(abs.) Here $p^*_{к.p1}$ — pressure in chamber at which nozzle with expansion ratio $\overline{f}_{c1}$ works on calculation conditions, i.e., ensures complete expansion; $p^*_{к.p2}$ — the same for nozzle with expansion ratio $\overline{f}_{c2}$.

Inasmuch as at the given pressure in the chamber the greatest thrust is developed by an engine with a nozzle which ensures complete expansion, then at pressure $p^*_{к.p1}$ greater thrust will be ensured by a nozzle with an expansion ratio $\overline{f}_{c1}$, and at pressure $p^*_{к.p2}$ — a nozzle with an expansion ratio $\overline{f}_{c2}$.

Taking into account what was said the flow of characteristic curve at $\overline{f}_{c2}$ will be as shown by line 2 in Fig. 9.7. In this

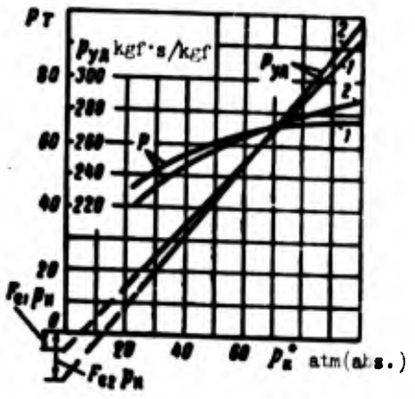

Fig. 9.7. Influence of degree of nozzle expansion on the flow of characteristics based on pressure in the chamber.

way relative flow of curves of specific thrusts at various $\bar{F}_c$ is explained.

9.2. Altitude Characteristics

Altitude characteristics of a rocket engine is what is called the dependence of thrust and specific thrust on altitude of flight with a constant value of pressure in the chamber, and for a liquid propellant rocket engine, furthermore, with a constant excess-oxidant ratio (if the fuel is bicomponent). Flow rate here is considered constant, inasmuch as pressure in the chamber is accepted as constant, and the change of external pressure cannot exert an influence on the flow rate of gas through the nozzle, since drop in the nozzle is always supercritical.

Rated altitude of nozzle H_p is the altitude, at which with a given pressure in the chamber the nozzle works on calculation conditions ($p_c = p_H$).

In the case of continuous flow of gas through the nozzle the dependence of engine thrust on altitude of flight is determined by formula (9.4). Inasmuch as $p_k^* = \text{const}$, then also $P_п = \text{const}$ and the change of thrust with altitude of flight will have the form shown in Fig. 9.8. If rated altitude of the nozzle is great, then at low altitudes due to the strong overexpansion of gas there can be a separation of flow from the walls of the nozzle. This circumstance should be considered during construction of altitude characteristic curves.

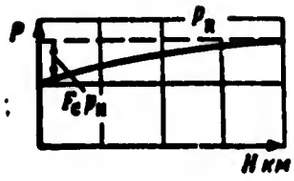

Fig. 9.8. Dependence of thrust on altitude of flight.

Dependence of specific thrust on altitude of flight with continuous flow in the nozzle is determined by formula (9.6) and, as it is easy to see, has a form similar to the dependence of thrust on altitude of flight.

We will compare the altitude characteristic curves of an engine with various pressures in the chamber. Increase of pressure in the chamber, other things being equal, leads to an increase of thrust in a vacuum, and also to a decrease of rated altitude of nozzle (since a fixed-area nozzle is examined – $F_{кр}$ = const, F_c = const).

In contrast to thrust, specific thrust of an engine in a vacuum, as this was shown above, does not depend on pressure in the chamber. Therefore the dependence of specific thrust on altitude at various $p_к^*$ has the form shown in Fig. 9.9, from which, in particular, it is clear that the higher the pressure in the chamber, the less that specific thrust depends on altitude of flight.

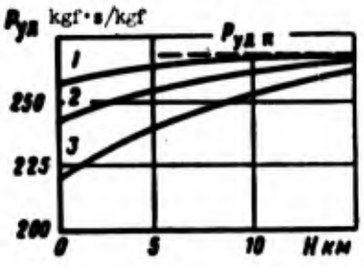

Fig. 9.9. Dependence of specific thrust on altitude of flight: 1 – $p_к^*$ = 100 atm(abs.); 2 – $p_к^*$ = 40 atm(abs.); 3 – $p_к^*$ = 20 atm(abs.).

Let us consider relative flow of altitude characteristic curves of an engine at various values of $\bar{F}_c$. Inasmuch as the nature of flow of thrust and specific thrust by altitude is identical, we will examine only specific thrust. Let us assume that for a

chamber with a nozzle, the geometric characteristic of which is equal to $\overline{f}_{c1}$, the altitude performance curve has the form shown in Fig. 9.10 (curve 1); for this nozzle rated altitude $H_{p1} = 0$. If one were to increase nozzle exit section at a constant $F_{кр}$, i.e., make $f_{c2} > f_{c1}$, then rated altitude of the nozzle will be higher, i.e., $H_{p2} > H_{p1}$. Inasmuch as for calculation conditions specific thrust of an engine has the greatest value, then, consequently, for altitude H_{p1} specific thrust $P_{уд1} > P_{уд2}$, and for altitude H_{p2} – just the opposite: $P_{уд2} > P_{уд1}$. Therefore the dependence of specific thrust on altitude for a nozzle with f_{c2} will have the form shown by curve 2. For a nozzle for which $\overline{f}_{c3} > \overline{f}_{c2}$, dependence of specific thrust on altitude is shown there by curve 3. Curve 4 shows the flow of characteristic curve for $\overline{f}_{c3}$ at low altitudes neglecting the breakaway of gas from the walls of the nozzle. It is clear from Fig. 9.10 that the greater the degree of expansion of nozzle $\overline{f}_c$, i.e., the higher the rated altitude of the nozzle, then the steeper the dependence of specific thrust on altitude. From the chart also follows the necessity for selection of degree of nozzle expansion at a definite altitude of flight. In the case of flight at various altitudes it is necessary to select a certain "compromise nozzle," considering the nature of the flight path. From a condition of maximum economy it would be desirable to have a variable-area nozzle, with which at each altitude rated conditions would be attained; for the case $p_к^*$ = const and $G_{\Sigma сек}$ = const it is sufficient to have adjustment only of the nozzle exit section. For such an "ideal" nozzle altitude performance would represent an envelope of altitude performance curves for an engine which are constructed at various $\overline{f}_c$ (curve 5).

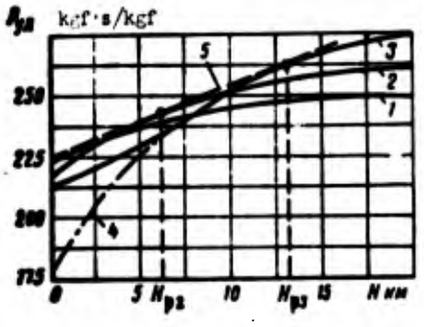

Fig. 9.10. Influence of degree of nozzle expansion on flow of altitude characteristic curve.

9.3. Peculiarities of Throttling the Thrust of Liquid Propellant Rocket Engines

Above it was indicated that change of thrust of a liquid propellant rocket engine is produced by a change of fuel consumption. In case of a single-chamber liquid propellant rocket engine at $F_{кр}$ = const there are also changes of pressure in the chamber and specific thrust. Dependence of specific thrust on thrust under these conditions is shown in Fig. 9.11. Throttling of a single-chamber engine leads to a decrease of specific thrust, i.e., to a reduction of its economy. At higher altitudes this influence is small, and in a vacuum is completely absent.

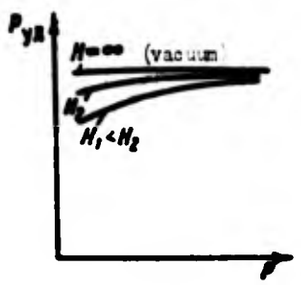

Fig. 9.11. Dependence of specific thrust on thrust.

The most desirable method of throttling an engine is such, in which specific thrust of the engine remains constant. In the case of a single-chamber engine for this it is necessary to have control of through sections of the nozzle $F_{кр}$ and F_c (this is important when working at low altitudes). However, regulation of through sections of the nozzle of a liquid propellant rocket engine encounters considerable construction difficulties.

Development of single-chamber liquid propellant rocket engines with a great range of change of thrust is complicated mainly due to the following circumstances. Decrease of fuel consumption, i.e., consumption of oxidizer and fuel, leads to a decrease of pressure drop $\Delta p_ф$ on the injectors. Drop $\Delta p_ф$ changes in conventional injectors proportional to the square of consumption. Consequently, if the drop for maximum operating conditions of the engine is selected in the usual limits, then at low ratings it will be insufficient,

which can lead to impairment of the process of combustion and to disturbance of the steady operation of the engine. Disturbance of steady operation occurs due to impairment of conditions for combustion of fuel, and also due to a decrease of the damping influence of injectors.

If, however, Δp_{Φ} for minimum conditions is made relatively high, then for maximum conditions with a large range of control of thrust the drop on injectors can turn out to be very large, which will lead to a considerable increase of feeding pressure and to loading of the engine.

One of methods for ensuring a considerable degree of change of thrust is the development of multichamber engines; in this case different methods of changing thrust are possible.

One of the possible methods for changing thrust for multichamber rocket engines is the turning off of separate chambers without adjustment of every chamber. In this case with a change of engine thrust pressure $p_{к}^{*}$ and drop Δp_{Φ} of the working chambers remain constant. Another method is not only turning off of separate chambers, but also regulation of every chamber. It is obvious that the degree of throttling of each chamber will be less than in the case of a single-chamber liquid propellant rocket engine with the same range of change of engine thrust; consequently, pressure in the chamber and pressure drop in the injectors will be changed to a lesser degree.

It is necessary to note that creation of multichamber liquid propellant rocket engines can be expedient not only due to the condition of its adjustment. In certain cases multichamber conditions are fulfilled by engines with a constant thrust. Thus, multichamber construction of high-thrust engines can facilitate experimental finishing, inasmuch as finishing of chamber of small thrust is simpler than for a chamber with great thrust. Furthermore, the application of several small chambers, instead of one large one, can lead to a decrease of weight and length of the

engine and to more favorable conditions from the point of view of steady operation.

Small changes of pressure drop on the injectors at a relatively great range of change of thrust (and, consequently, fuel consumption) can also be ensured in a single-chamber liquid propellant rocket engine. This is possible to obtain, for example, by switching off some of the injectors to conditions with a lowered flow rate. In this case flow rate through a separate injector will be changed to a lesser degree and, consequently, pressure drop will be changed to a lesser degree. However, switching off of some of the injectors in a number of cases can lead to impairment of the process in the combustion chamber due to a disturbance in the distribution of fuel over a section of chamber. Application of special adjustable swirlers is possible. For these with a decrease of fuel consumption there is a decrease of area $f_{ф}$ of a section of injector nozzle or discharge coefficient $\mu_{ф}$. Decrease of discharge coefficient is usually ensured by switching off of several entrance channels, which leads to an increase of geometric characteristics of injectors A, and, consequently, to a decrease of $\mu_{ф}$ (see Fig. 4.5).

9.4. Effective Specific Thrust of Liquid Propellant Rocket Engines

Effective specific thrust of a liquid propellant rocket engine rates the effectiveness of the propulsion system on the whole; in general it is equal to

$$P_{уд.эф}=\frac{P+P_{доп}}{G_{\Sigma сек}+G_{т}}, \qquad (9.7)$$

where P – thrust of main chambers of engine; $P_{доп}$ – additional thrust of exhaust ducts of turbopump unit; $G_{т}$ – flow rate of working substance on turbine; $G_{\Sigma сек}$ – fuel consumption in combustion chamber.

Flow rate of working substance on turbine. Pressure of pump equals

$$H=\frac{\Delta p_н}{\gamma}, \qquad (9.8)$$

where $\Delta p_н = p_{под} - p_{вх}$ – increase of pressure of liquid in pump; $p_{под}$ – feed pressure, equal to pressure of liquid at exit from pump; $p_{вх}$ – pressure of liquid at entrance to pump.

Power $N_н$, necessary for the pump for creation of pressure H at flow rate G, is equal to

$$N_н=\frac{GL_н}{75}=\frac{G\Delta p_н}{75\cdot\gamma\cdot\eta_н}. \qquad (9.9)$$

Here $\eta_н$ – full efficiency of pump.

Power of turbine

$$N_т=\frac{G_т L_т}{75}=\frac{G_т L_{ад.т}}{75}\eta_т, \qquad (9.10)$$

where $\eta_т$ – effective efficiency of turbine; $L_{ад.т}$ – adiabatic work of expansion of gas in turbine, equal to

$$L_{ад.т}=\frac{k}{k-1}RT_1^*\left[1-\left(\frac{p_2}{p_1^*}\right)^{\frac{k-1}{k}}\right].$$

Here T_1^*, p_1^* – temperature and pressure of working substance before nozzle box of turbine; p_2 – pressure behind the turbine.

Dependence of adiabatic work on drop $\pi_т = p_1^*/p_2$ is shown in Fig. 9.12. The turbine drives the pumps for the oxidizer and fuel; in certain cases it conveys power to the accessories, in particular the pump for supply of working substance to the turbine, if the latter is not a component of the basic fuel. Usually the main share of power is consumed by the pumps for the combustible $N_{н_г}$ and oxidizer $N_{н_{ок}}$; therefore subsequently we will disregard the power of accessories. Then

$$N_т=N_{н_г}+N_{н_{ок}}. \qquad (9.11)$$

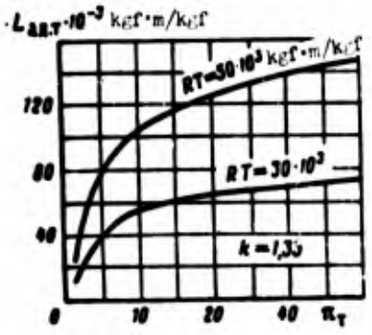

Fig. 9.12. Adiabatic work of turbine.

Putting value N_T and N_H in expression (9.11) and solving relative to G_T, we obtain:

$$G_т = \frac{1}{L_{ад.т}\eta_т}\left(\frac{G_{ок}\Delta p_{п_{ок}}}{\gamma_{ок}\eta_{п_{ок}}} + \frac{G_г\Delta p_{п_г}}{\gamma_г\eta_{п_г}}\right). \qquad (9.12)$$

For appraisal of the effectiveness of the system of feeding there is considerable value in the relative consumption of working substance $g_T = G_T/\Sigma G$, where $\Sigma G = G_{\Sigma сек} + G_T$ — total fuel consumption in engine.

For simplification of analysis we will take

$$\Delta p_{п_г} = \Delta p_{п_{ок}} = \Delta p_п \text{ and } \eta_{п_г} = \eta_{п_{ок}} = \eta_п.$$

Then

$$G_т = \frac{\Delta p_п \sum G}{L_{ад.т}\eta_{ТНА}\gamma_т}, \qquad (9.13)$$

where $\eta_{ТНА} = \eta_T\eta_H$ — efficiency factor of turbopump assembly; γ_T — conditional weight density of fuel. Relative consumption will then equal

$$g_т = \frac{\Delta p_п}{L_{ад.т}\eta_{ТНА}\gamma_т}. \qquad (9.14)$$

Thus, relative flow rate of working substance g_T depends on pressure of the pump, the value of which is determined mainly by pressure in the chamber, the efficiency factor of the turbopump assembly [THA], $L_{ад.т}$ and γ_T. For increasing the economy of the

turbopump assembly it is necessary to increase $L_{ад.т}$ and $\eta_{ТНА}$. Value $L_{ад.т}$ depends on parameters of working substance and pressure drop in the turbine $\pi_т$.

In engines with open systems usually $\pi_т$ = 15-30, where pressure beyond the turbine is equal to 1.5-2 atm(abs.). Outlet pressure from the turbine is increased somewhat relative to atmospheric in order to obtain a pressure drop in the exhaust duct of turbine which is close to critical and thus develop operation of the turbine independent of change in external conditions. This circumstance, furthermore, makes it possible to obtain a little additional thrust.

In engines with afterburners of generating gas the pressure drop on the turbine can be accepted approximately equal to

$$\pi_т \approx \frac{p^*_{гг}}{p_н},$$

where $p^*_{гг}$ – pressure of gas in gas generator. In these engines on the force of high outlet pressure from the turbine (equal to approximately $p_к$) the application of high drop (more than 1.5-2) on the turbine is inexpedient, since this will demand great pressures in the gas generator. Therefore in these engines the value $L_{ад.т}$ will be relatively small, and flow rate of working substance on the turbine will be high, and even greater, the greater the pressure in the chamber. However this does not lead to impairment of economy of the propulsion system, inasmuch as the working substance beyond the turbine enters the main chamber and subsequently participates in the creation of thrust. At very large pressures in the chamber it can turn out to be expedient to feed to the turbine one of components completely; if the turbine works on products of combustion of fuel (bicomponent gas generator), then into the gas generator a second component is fed in such a quantity that would ensure the required temperature of working substance of the turbine.

Highest possible consumption of working substance on the

turbine, if it works on products of decomposition (single-component gas generator) or evaporation and heating of one of the components, is equal to

$$G_{T\,max} = G_{ok} \quad \text{or} \quad G_{T\,max} = G_{r}.$$

As an example it is possible to cite an engine which uses hydrogen peroxide as an oxidizer. In such liquid propellant rocket engines hydrogen peroxide can initially enter the gas generator; products of decomposition from the ГГ [gas generator] reach the turbine and subsequently the combustion chamber; it is obvious that in this case $G_{Tmax} = G_{OK}$. Another example can be a liquid propellant rocket engine using hydrogen as the fuel. Hydrogen is used for cooling the chamber. Vaporized and heated, it can be used further as the working substance of the turbine, if the temperature of hydrogen after cooling the jacket is sufficient for production of the necessary power of the turbine. After the turbine H_2 enters the chamber; in the given example $G_{Tmax} = G_{Г}$.

If a two-component gas generator with a surplus of combustible is used, then

$$G_{T\,max} = G_{r} + G_{ok\,гг} = (1 + \varkappa_{гг}) G_{r}.$$

Here $G_{Г}$ – complete consumption of combustible in the engine; $G_{ОК\,ГГ}$ – consumption of oxidizer in gas generator; $\varkappa_{ГГ}$ – relationship of components in gas generator.

In this case all the combustible and a certain portion of oxidizer are fed to the gas generator. Gas after the turbine and the oxidizer are fed to the main chamber.

If the gas generator works with surplus of oxidizer, then

$$G_{T\,max} = G_{ok} + G_{r\,гг} = \left(1 + \frac{1}{\varkappa_{гг}}\right) G_{ok},$$

where $G_{ок}$ – complete consumption of oxidizer in engine; $G_{г_{гг}}$ – flow rate of combustible to gas generator.

Since the maximum flow rate of working substance through the turbine is limited by value G_{Tmax}, then there is a certain maximum pressure in the chamber which it is possible to realize in the engine. It is true that in most cases this ultimate pressure is essentially higher than the usual level of pressures in the chamber of a liquid propellant rocket engine.

Effective specific thrust. If one disregards the value $P_{доп}$ in equation (9.7), then for open systems of feeding $P_{уд.эфф}$ will be equal to

$$P_{уд.эфф} = \frac{P_{уд}}{1 + g_т \frac{G_{конс}}{\sum G}},$$

where $P_{уд}$ – specific thrust of main chambers of engine.

Considering that in the case of open systems of feeding the value $g_т$ is small, it is possible to accept

$$P_{уд.эфф} = \frac{P_{уд}}{1 + g_т}.$$

For engines with afterburning after the turbine the working substance is fed to the main combustion chamber and is used effectively. In this case $\Sigma G = G_{\Sigma сек}$. Therefore for propulsion systems with afterburning

$$P_{уд.эфф} = P_{уд}.$$

In Figs. 9.13 and 9.14 are shown the dependences $g_т$, $P_{уд}$ and by the dotted line $P_{уд.эфф}$ on pressure in the chamber for an installation with an open feeding system. With an increase of pressure in the chamber effective specific thrust increases more slowly than specific thrust of the main chamber due to an increase of

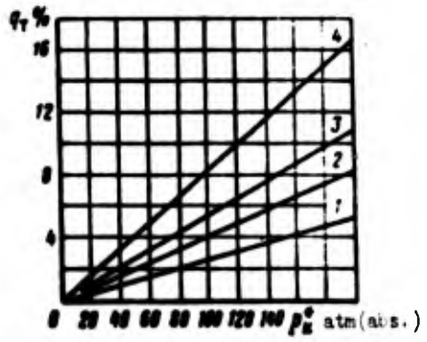

Fig. 9.13.

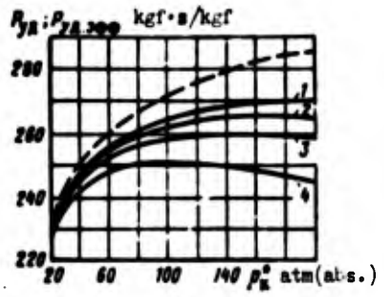

Fig. 9.14.

Fig. 9.13. Relative consumption of working substance of turbine: ($\Delta p_H = 1.3p_K^*$ and $\gamma_T = 1000$ kgf/m^3) 1 — $L_{ад.т} = 120 \cdot 10^3$ kgf·m/kgf, $\eta_{THA} = 0.4$; 2 — $L_{ад.т} = 120 \cdot 10^3$ kgf·m/kgf, $\eta_{THA} = 0.25$; 3 — $L_{ад.т} = 60 \cdot 10^3$ kgf·m/kgf, $\eta_{THA} = 0.4$; 4 — $L_{ад.т} = 60 \cdot 10^3$ kgf·m/kgf, $\eta_{THA} = 0.25$.

Fig. 9.14. Dependence of specific and effective thrust on pressure in the chamber: ($\Delta p_H = 1.3p^*$; $\gamma_T = 1000$ kgf/m^3; p_c = const) (number of curves same as Fig. 9.13).

consumption of working substance of the turbine. The higher the effectiveness of the turbopump assembly (η_{THA}, $L_{ад.т}$), the less this influence. Starting from a certain pressure p_K, effective specific thrust practically does not increase and further, especially at small η_{THA}, even starts to drop. Increase of pressure in the chamber higher than 70-100 atm(abs.), as one can see from Fig. 9.14, either in general does not lead to an increase of effective specific thrust, or produces such a small growth of $P_{уд.эфф}$ that the latter does not compensate for loading of the engine which is induced by increase of pressure. Therefore an increase of pressure in the chamber of a liquid propellant rocket engine with an open pump system of feeding higher than 70-100 atm(abs.) is not expedient.

For afterburners, inasmuch as $P_{уд} = P_{уд.эфф}$, the dotted line on Fig. 9.14 characterizes simultaneously also their effective

specific thrust. As can be seen, the advantage of engines with afterburning is especially noticeable at great pressures in the chamber (higher than 60 atm(abs.). The advantage of these systems in economy is the result, on the one hand, of the fact that here there is no ejection of unused (or little-used) working substance and, on the other – the possibilities of using great pressures in the chamber. For these systems there is no limitation of pressure in the chamber from the point of view of economy. This limitation can be superimposed by conditions of cooling and weight of the engine and, furthermore, by available consumption of working substance on the turbine ($G_{T max}$).

CHAPTER X

HEAT EXCHANGE IN LIQUID PROPELLANT ROCKET ENGINES

10.1. Heat Exchange Between Gas and Walls of the Engine

Transmission of heat from hot gases to the walls of the combustion chamber and nozzle takes place by means of convection heat exchange and radiation.

Convection heat exchange. Convection heat exchange in liquid propellant rocket engines is characterized by a turbulent state of flow of gas. In this case heat in the main part of the flow is transferred due to the disorderly shift of small volumes of gas. Close to the walls, where the thin laminar sublayer is found, heat is transmitted by means of molecular thermal conduction. Convection heat exchange between gases and the wall is described by the equation

$$q_{\text{конв}} = \alpha_г (T_г^* - T_{ст_г}), \qquad (10.1)$$

where $q_{\text{конв}}$ – specific convection heat flow from gas to wall; $\alpha_г$ – coefficient of heat transfer from gas to wall; $T_г^*$ – temperature of adiabatic inhibited flow of gas; $T_{ст_г}$ – temperature of surface of wall washed by gas.

If along a section of chamber the relationship of components is variable (see Fig. 4.15), then heat exchange is determined also by the temperature and composition of gas in the wall layer. In this case $\alpha_г$ and $T_г^*$ pertain to the wall layer. What was said is true under the condition that the thickness of the wall layer is

greater than the thickness of the boundary layer (see Fig. 10.8). This condition in a liquid propellant rocket engine is usually maintained.

In a liquid propellant rocket engine the temperature $T_г^*$ on the initial section of the combustion chamber increases due to combustion of fuel, attaining maximum value by the section where combustion is practically completed. On the further length of the chamber, including the nozzle, temperature $T_г^*$ practically remains constant.

Ccefficient of heat transfer $\alpha_г$ can be determined from the criterial equation of convection heat exchange. For a turbulent flow in a channel on a stabilized section with constant physical properties this equation has the form

$$Nu = A Re^m Pr^n. \qquad (10.2)$$

Here $Nu = \frac{\alpha_г D}{\lambda}$ – criterion of Nusselt; $Re = \frac{wDy}{\eta}$ – criterion of Reynolds; $Pr = \frac{c_p \eta}{\lambda}$ – Prandtl number; λ, η, c_p – accordingly thermal conduction, dynamic viscosity, and heat capacity of products of combustion; A – constant, determined from experiment; D – diameter of section.

For m and n during turbulent flow it is possible to take the following value: m = 0.8; n = 0.4.

In the case of liquid propellant rocket engines the physical properties of combustion products on a section of the boundary layer cannot be considered constant due to the considerable change of temperature on the section (from temperature of flow $T_г$ to temperature of wall $T_{ст_г}$).

The influence of changeability of properties on intensity of convection heat exchange is considered by various methods. For this frequently in equation (10.2) the coefficient K_t (coefficient is introduced).

For gases, as is known, the influence of alternating field of physical properties can be considered the temperature factor equal to T_{cr}/T_r^*. Then the criterial equation has the form

$$Nu = A\,Re^m\,Pr^n K_t, \tag{10.3}$$

where

$$K_t = \left(\frac{T_r^*}{T_{cr}}\right)^p.$$

It is necessary to note that turbulent flow is completely stabilized on a length of channel L (counted off from the beginning of the channel) equal to 40D. The nozzle is a channel of variable section, but combustion chamber of a liquid propellant rocket engine usually has L/D ≤ 3-5; therefore the flow of gas in a liquid propellant rocket engine cannot be completely stabilized; as a result the coefficient of heat transfer and specific heat flow will be higher. This circumstance can be considered if one were to take into account coefficient A in formulas (10.2) and (10.3) as variables in length of chamber of the engine, i.e.,

$$A = A(L/D). \tag{10.4}$$

Calculations based on ordinary formulas of convection heat exchange of the type (10.1) and (10.3), even taking into account the variability of coefficient A, sometimes give considerably smaller values of specific convection heat flow than this follows from experiments, where divergence of calculation with the experiment increases with an increase of temperature of gas and decrease of pressure. As investigations showed, the main cause of this lies in the presence of dissociated products of combustion. Due to a large gradient of temperatures in the wall layer (temperature of wall in a liquid propellant rocket engine is 3-5 times less the temperature of gas) in particles of gas, arriving from a region of high temperatures into a region of low temperatures at the wall, there occurs a recombination of earlier dissociated molecules and accordingly chemical energy is liberated. Therefore particles of gas, arriving at the wall from the region of high temperatures, transfer there not

only heat, determined by the sum of enthalpy and kinetic energy, but also energy which is liberated during cooling of the gas as a result of its recombination, which increases heat transfer to the wall.

Heat capacity of dissociated gas during recombination is higher than heat capacity, calculated in an assumption of constant composition of gas (i.e., absence of recombination), due to the presence of a thermal effect, accompanying this process (so-called full or equilibrium heat capacity).

In Fig. 10.1 is shown the change of full heat capacity of dissociated products of combustion of oxygen – heptane fuel; in the same place is shown the heat capacity, calculated in an assumption of the absence of recombination.

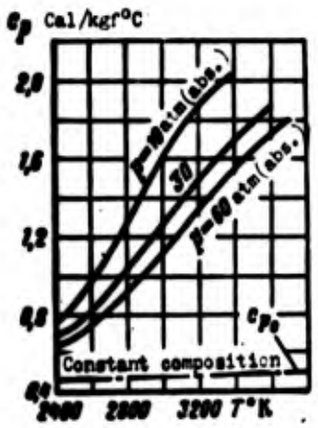

Fig. 10.1. True heat capacity of combustion products of oxygen – heptane fuel at $\alpha = 1$.

On this base it is possible to consider roughly that quantity of heat brought to the wall proportional to value $c_p T_r^*$, where T_r^* – real temperature of gas, calculated taking into account dissociation.

If one were to conditionally consider that in the process of combustion the gases do not dissociate, then it is obvious that heat capacity of such a gas c_{p_0} will be less than c_p. As a result of such a conditional process the temperature of gas T_{r_0} will be greater than the real temperature T_r due to lesser heat capacity.

Since in both cases the same expenditure of heat is examined, then it is possible to consider

$$c_p T_r^* \approx c_{p_0} T_{r_0}^*. \qquad (10.5)$$

Consequently, the influence of dissociation on the process of heat exchange can be considered, if in corresponding equations of heat exchange c_p and T_r^* or c_{p_0} and $T_{r_0}^*$ are substituted.

However, in those frequent cases, when in the wall layer there are lowered values of excess-oxidant ratio, and consequently low temperatures also, the gas in this layer is not dissociated and the given additional effect does not take place.

Theoretical calculation of specific heat flow in a rocket engine, founded on methods of the theory of the boundary layer, is very labor-consuming. Therefore frequently for the determination of $q_{\text{конв}}$ and α_r in a liquid propellant rocket engine the method of conversion is used. Besides it is assumed that for a certain initial engine the distribution of specific convection heat flow along the chamber is known. It can be obtained from a detailed theoretical calculation or from experiment. Furthermore, its geometric dimensions are known, and also pressure, temperature, and composition of gases. It is required to determine the distribution $q_{\text{конв}}$ for a projected engine, for which not only its geometric dimensions are known, but also pressure, temperature, and composition of gases.

For conversion we will use an equation of the type (10.3).

In developing the values of Re and Nu, we obtain

$$\alpha_r = A \left(\frac{\eta}{D}\right)^{1-m} c_p (\gamma w)^m \left(\frac{T_r^*}{T_{cr_r}}\right)^p \mathrm{Pr}^{n-1}. \qquad (10.6)$$

In the last formula it is convenient to make the substitution

$$w\gamma = w_{\text{кр}} \gamma_{\text{кр}} \frac{F_{\text{кр}}}{F} = \frac{\dot{G}_{\text{к}}}{f\bar{h}};$$

then

$$\alpha_r = \frac{A}{D_{\text{кр}}^{1-m}} \frac{c_p \eta^{1-m}}{\mathrm{Pr}^{1-n} \beta^m} \frac{\dot{G}_{\text{к}}^m}{\bar{f}^{\frac{m+1}{2}}} \left(\frac{T_r^*}{T_{cr_r}}\right)^p. \qquad (10.7)$$

We will designate the values pertaining to initial data by index 1, and to unknown – by index 2.

Dividing α_{r1} in α_{r2}, considering $Pr_1 = Pr_2$,[1] and considering that in both cases similar sections are examined ($A_1=A_2$; $\bar{j}_1=\bar{j}_2$), we obtain:

$$\alpha_{r2}=\alpha_{r1}\left(\frac{D_{ap1}}{D_{ap2}}\right)^{1-m}\left(\frac{\rho^*_{g_1}}{\rho^*_{g_1}}\right)^{m}\frac{s_2}{s_1}, \tag{10.8}$$

where

$$s=\frac{c_p\eta^{1-m}}{\beta^m}\left(\frac{T^*_r}{T_{cr_r}}\right)^{\beta}.$$

Inasmuch as m = 0.8, then

$$\alpha_{r2}=\alpha_{r1}\left(\frac{D_{ap1}}{D_{ap2}}\right)^{0.2}\left(\frac{\rho^*_{g2}}{\rho^*_{g1}}\right)^{0.8}\frac{s_2}{s_1}. \tag{10.9}$$

It is simple to see that the formula for conversion of specific convection flows will have the form:

$$q_{kon2}=q_{kon1}\left(\frac{D_{ap1}}{D_{ap2}}\right)^{0.2}\left(\frac{\rho^*_{g2}}{\rho^*_{g1}}\right)\frac{S_2}{S_1}, \tag{10.10}$$

where

$$S=s(T^*_r-T_{cr_r}).$$

Value S for a given fuel depends on excess-oxidant ratio, in as much as with a change of it there is a change of T^*_r, β, c_p, η, and also on temperature of the wall. With an increase of excess-oxidant ratio (in region $\alpha < 1$), value S increases mainly due to temperature increase of gas; with an increase of T_{cr_r} value S drops (Fig. 10.2).

Consequently, specific heat flow q_{kon} depends on type of fuel, excess-oxidant ratio, pressure in the chamber, temperature T_{cr_r} and to a certain degree on absolute dimensions of engine (D_{ap}).

---

[1]This is permissible, since the Prandtl number depends on atomicity (number of atoms in molecule) of gases, but average atomicity of products of combustion of different fuels is approximately identical. On the average it is possible to take Pr = 0.8.

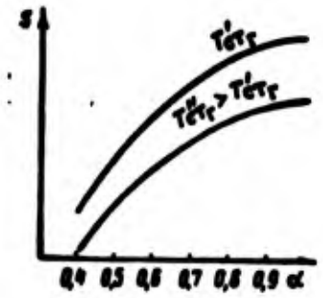

Fig. 10.2. Dependence of complex S excess-oxidant ratio.

When initial data, necessary for the determination of $q_{пов}$ by the method of conversion are absent, it is possible to use the method recommended in work [60]. Here for the initial they take an equation analogous to equation (10.7):

$$q_r = \frac{0{,}026}{D_{кр}^{0.2}} \frac{c_p \eta^{0.2}}{p_r^{0.6} \beta^{0.6}} \frac{\left(\rho_r^*\right)^{0.8}}{f^{0.9}} \sigma, \tag{10.11}$$

where

$$\sigma = \frac{1}{\left[0{,}5 \frac{T_{ст_r}}{T_r^*}\left(1 + \frac{k-1}{2} M^2\right) + 0{,}5\right]^{0.8 - \frac{\omega}{2}} \left(1 + \frac{k-1}{2} M^2\right)^{\frac{\omega}{2}}}; \tag{10.12}$$

here ω – exponent in temperature function of viscosity; it is possible to accept $\omega = 0.6$.

Physical properties in equation (10.11) are taken at a temperature of T_r^*. Coefficient σ considers the influence of variability of physical properties on intensity of heat exchange and a change of them along the length of the nozzle. Change σ along the length of the nozzle depending upon temperature factor $T_{ст_r}/T_r^*$ is shown in Fig. 10.3.

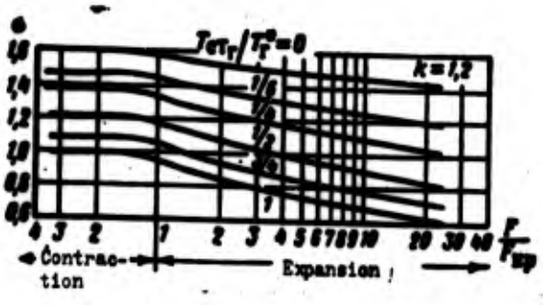

Fig. 10.3. Change of σ along length of nozzle.

Heat exchange by radiation. On the force of high temperatures in the chamber of a liquid propellant rocket engine, the energy, radiated by products of combustion on the wall, is sufficiently great and it is necessary to consider. Products of combustion of conventional fuels for a liquid propellant rocket engine, which do not contain metallic elements, practically do not have any solid particles, and their radiation is gaseous. During radiant heat exchange between the gas and the solid wall the specific heat flow can be determined from equation

$$q_л = \varepsilon_{пр} c_0 \left[\left(\frac{T_г}{100}\right)^4 - \left(\frac{T_{ст_г}}{100}\right)^4\right], \qquad (10.13)$$

where $\varepsilon_{пр}$ – given degree of blackness, depending on degree of blackness of wall and gas; $c_0 = 4.9$ Cal/m^2·h·°K^4 – radiation factor of ideal black body.

Inasmuch as temperature of combustion products in liquid propellant rocket engines reaches values of 3000°C and higher, and the temperature of the walls does not usually exceed 1000°C, then the second member of the expression in brackets in formula (10.13) comprises no more than 3-5% of the first. Considering that in a liquid propellant rocket engine, especially in the nozzle, to the share of radiant heat flow belongs the smaller share of total heat flow, it is possible to disregard the value $(T_{ст_г}/100)^4$ in formula (10.13).

In this case

$$q_л = \varepsilon_г \varepsilon'_{ст} c_0 \left(\frac{T_г}{100}\right)^4, \qquad (10.14)$$

where $\varepsilon'_{ст}$ – effective degree of blackness of wall approximately equal to $0.5\,(\varepsilon_{ст}+1)$.

Radiation of combustion products in contemporary liquid propellant rocket engines is determined practically by the radiation of H_2O and CO_2. In this case with sufficient accuracy it is possible to accept

$$\varepsilon_г = \varepsilon_{CO_2} + \varepsilon_{H_2O}. \qquad (10.15)$$

Degree of blackness of a gas depends on the product $p_i \ell$ and temperature:[1]

$$\varepsilon_г = f(p_i \ell, T_г); \tag{10.16}$$

here p_i – partial pressure of gas; ℓ – effective length of ray.

Experience shows that for CO_2 the degree of blackness indeed depends on the product $p_i \ell$, and not on each value separately. Regarding vapor, then for it the dependence (10.16) it not completely correct; in this case it is necessary to introduce another correction $\delta_{p_{H_2O}}$ for pressure, i.e.,

$$\varepsilon_{H_2O} = \varepsilon^0_{H_2O} \cdot \delta_{p_{H_2O}}. \tag{10.17}$$

Calculation of radiant heat flow in liquid propellant rocket engines is conducted by the formula (10.14), for which it is necessary to have knowledge of three values ($T_г$, $\varepsilon_г$ and $\varepsilon_{ст}$). Degree of blackness of the wall depends on the material, and also on the treatment and state of its surface, presence of an oxide film, carbon black, etc. Degree of blackness of a gas is determined by formula (10.15). Values ε_{CO_2} and ε_{H_2O}, entering into this formula, are determined from experiments, the results of which are usually given in the form of graphs [26]. If such data in the necessary range of parameters are absent, then in first approximation it is possible to use the following dependence:

$$\varepsilon_{CO_2} = 0{,}715 (p_{CO_2} \ell)^{0{,}33} \left(\frac{T_г}{100}\right)^{-0{,}5}; \tag{10.18}$$

$$\varepsilon_{H_2O} = 0{,}715 (p_{H_2O})^{0{,}8} \ell^{0{,}6} \left(\frac{T_г}{100}\right)^{-1}; \tag{10.19}$$

here p_{H_2O} and p_{CO_2} – in kgf/cm^2; ℓ – in m.

---

[1]Radiation of gases depends not only on partial pressure, but also on absolute pressure of a mixture of gases. However, source material concerning this question is inadequate.

Partial pressures p_{H_2O} and p_{CO_2}, necessary for finding ε_{H_2O} and ε_{CO_2}, are determined from a thermodynamic calculation.

Value $q_л$ on the last section of the combustion chamber and in the initial section of nozzle is determined by the parameters of products of combustion in the combustion chamber which are obtained from a thermodynamic calculation. On the section of the nozzle radiant heat flow is determined by the parameters of gas in the given section of the nozzle.

It is necessary to consider that part of the radiant flow from the combustion chamber falls on the subcritical segment of the nozzle. Therefore on the initial section of the subcritical sector of the nozzle the radiant flow is higher than that calculated by the parameters of gas in the given section.

Change of specific heat flow along the combustion chamber and nozzle. From what was stated above it is easy to see that a change of $q_{пол}$ along the engine is determined by change of temperature of gas, coefficient of heat transfer $\alpha_г$ and temperature of the wall $T_{ст_г}$. For simplicity of reasonings we will take the temperature of the wall from the side of gas along engine as identical; in reality it is not the same; a change of it depends on organization of cooling of the engine, where it usually has the greatest value in the region of critical section of the nozzle. The assumption made does not affect the nature of distribution of convection specific heat flow.

Let us trace the change of $\alpha_г$ along the engine. Its change is determined mainly by the change of current density $w\gamma$ (10.6) and (10.7); therefore $\alpha_г$ along the combustion chamber changes little; along the nozzle $\alpha_г$ increases up to the critical section (due to increase of current density), and then drops. Temperature $T_г^*$ along the combustion chamber increases initially due to development of the process of combustion, and then remains practically constant, since heat withdrawal in the wall is small as compared to the complete heat content of the gas. As a result the distribution of $q_{пол}$ over the length of the engine has the form shown in Fig. 10.4. On the

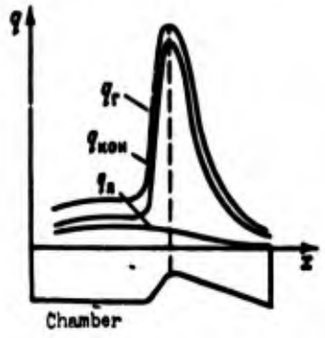

Fig. 10.4. Distribution of specific heat flows along the combustion chamber and nozzle.

initial section $q_{конв}$ increases due to temperature rise of gas and then up to the nozzle remains almost constant. On the subcritical section of the nozzle value $q_{конв}$ increases sharply due to an increase of coefficient of heat transfer. On the supercritical section of the nozzle specific heat flows decrease mainly due to a lowering of α_r.

Let us consider change of radiant heat flow along the chamber of a liquid propellant rocket engine. Value $q_л$ is determined mainly by the temperature of the gas and degree of blackness ε_r. Temperature of the gas on the initial section of the combustion chamber increases, and in the nozzle drops. Degree of blackness of the gas also decreases along nozzle due to pressure drop of gas. As a result the distribution of specific radiant heat flows along the engine has the form shown in Fig. 10.4. On the initial section of the combustion chamber $q_л$ increases due to a temperature rise of gas, then along the combustion chamber and on the initial section of the nozzle radiant heat flow remains practically constant; on the remaining section of the nozzle $q_л$ decreases, due to decrease of temperature and degree of blackness of the gas.

Full specific thermal flow from gas to the wall q_r is equal to

$$q_r = q_{конв} + q_л.$$

Specific heat flows in rocket engines can attain very large values. Thus, in liquid propellant rocket engine specific heat flows have approximately the following order of values: in the combustion chamber $1 \cdot 10^6$-$5 \cdot 10^6$ Cal/m^2·h and more, here the share of convection heat flow is up to 60-80%; in the critical section of the nozzle – $5 \cdot 10^6$-$30 \cdot 10^6$ Cal/m^2·h and more, of these the share of convection is more than 90%; in the nozzle exit section the share

of convection flow is still a greater portion (usually more than 95%).

If the total amount of heat, given by gas to the wall of the engine in a unit of time is examined, then it turns out that radiant flow comprises approximately 10-25% of the total. The share of radiant flow depends on the composition of fuel, and also on the relationship of dimensions of the combustion chamber and nozzle and absolute dimensions of the engine.

Thus, the main role in heat exchange between gas and the wall in a liquid propellant rocket engine is played by convection heat exchange. The role of radiant heat flow is relatively great in the combustion chamber. In the supercritical section of the nozzle it is small and is comparable with value of accuracy of determination of heat flows. Maximum of full specific heat flow belongs to the region of the critical section of the nozzle, therefore this part of the engine is the most strained in a thermal respect.

Influence of various factors on heat flow from a gas to the wall. With a rise in temperature of combustion products there is an increase of convection and also radiant heat flows. Thus, during the application of liquid oxygen and kerosene specific heat flows are 60-70% higher than during the application of nitric acid and kerosene.

Excess-oxidant ratio through the temperature of the gas and partly through its composition also exerts an influence on value of heat flows. In Fig. 10.5 is shown the approximate dependence of specific heat flow on excess-oxidant ratio; in the same place is given the change of specific thrust.

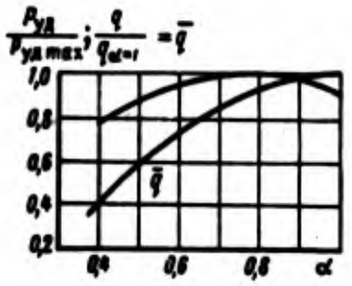

Fig. 10.5. Dependence of specific heat flow on excess-oxidant ratio.

With an increase of pressure in the combustion chamber heat flows increase. Growth of convection heat flows is connected with an increase of coefficient of heat transfer due to an increase of density of the gas. From formula (10.10) it follows that coefficient of heat transfer is proportional to $(p_г^*)^{0.8}$.

If here it is considered that $T_{ст_г}$ = const, then heat flows can also be accepted as proportional to $(p_г^*)^{0.8}$.

Radiant heat flow also changes with a change of pressure due to a change in the degree of blackness of the gas, however, to a lesser degree than convection.

Value of temperature of wall from the side of gas exerts a lesser influence on heat flow than the temperature of the gas, inasmuch as it can change in smaller limits. Though not exerting practically any influence on radiant heat flow, $T_{ст_г}$ somewhat affects convection heat flow. This is more strongly, the less the temperature of the gas, as this is easy to see from formula (10.1). If the engine operates with an excess-oxidant ratio close to optimum value, and has equal distribution of the relationship of components by section, then usually $T_{ст_г}$ makes up 0.2-0.3 of the temperature of gas, and its influence on heat flow is relatively small: change of $T_{ст_г}$ by 10% changes heat flow all told by 3-4%. If, however, the engine operates at lowered values of α or has nonuniform distribution of components by section with small values of α, and consequently also of temperature $T_г$ in the wall layer, then the influence of $T_{ст_г}$ on heat flow is stronger (Fig. 10.6). This circumstance can be used, for example, in the event of external cooling of the engine, when for a decrease in the amount of heat given off to the liquid coolant there is an increase in the temperature of the wall (if the material of the wall allows this).

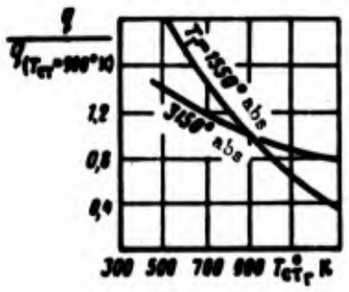

Fig. 10.6. Influence of temperature of wall $T_{ст_г}$ on specific heat flow from gas to the wall.

10.2. Methods of Cooling a Liquid Propellant Rocket Engine

The basic problem of cooling an engine lies in the fact that in the process of operation the temperature of the walls is not higher than a certain permissible limit, determined by the properties of the material of the wall and the resource of the engine.

Removal of heat from the wall of the combustion chamber and nozzle is carried out usually by the oxidizer or fuel. Such method for cooling the engine is called external flow-through cooling.

Chambers with external flow-through cooling are equipped with a cooling jacket. In the clearance between the wall of the chamber ard the jacket flows one of components of the fuel, which then proceeds through the head into the combustion chamber.

For cooling a liquid can also be used which is unnecessary directly for the process in the chamber, but possesses good cooling properties, water for example (especially under bench conditions).

If specific heat flows are small, then heat removal from the wall can be ensured by radiation of the latter into external space (radiation cooling). Such conditions (low specific heat flows) take place on the final sections of the nozzle at small pressures of gas on a section. Specific heat flow, given off from the wall to the external medium by radiation, is equal to

$$q = \varepsilon_{cr} c_0 \left(\frac{T_{ст}}{100}\right)^4.$$

The higher the permissible temperature of the wall and the degree of its blackness, then the greater the heat flow removed by means of radiation (Fig. 10.7).

If there is no constant heat removal from the wall which is equal in value to the influx of heat from the gas, then the temperature of the wall does not remain constant and is increased in process of operation of the engine. Heat, proceeding from the gas to the wall, in such case is absorbed by the material of the

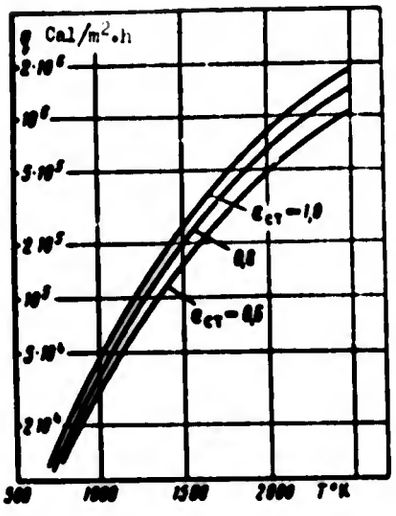

Fig. 10.7. Dependence of specific heat flow, removed from the wall by radiations on temperature and degree of blackness of the wall.

walls. Since here the accumulating capacity of the material of the walls is used, i.e., its thermal capacity, then such method of cooling is called capacity. Duration of work of the engine, determined by the condition of heating of the walls, in this case depends on the dimensions and assignment of the engine, permissible temperature of the walls, and accumulating capacity of the material of the walls.

In a liquid propellant rocket engine internal cooling is also used. By internal cooling is understood different methods for lowering the specific heat flow from gas to the wall by means of creation on its internal surface of a protective layer of liquid or a layer of gas (vapor) with a reduced temperature. It is natural that a lowering of heat flow in all cases facilitates resolution of the problem of cooling the engine. Used most extensively in liquid propellant rocket engines is external flow-through cooling, usually used in combination with internal.

For increasing the effectiveness of shielding the walls of rocket engines from the influence of high temperatures heat-resistant refractory materials are used. They are used to cover the internal surfaces of the walls in the sections of the engine which receive the most thermal stress.

For thermal shielding of the walls it is also possible to use the so-called ablating coverings, which are applied on the fire

surface of the walls. In this case the flow of gas, exerting an influence on the covering, phase transitions (fusion, evaporation, sublimation) or endothermal reactions in it; products of these transformations are carried away by gas. Heat which is supplied to the wall is expended mainly in these transformations, in consequence of which heat flow, driven deep into the wall, is not great.

The effect, ensuring shielding of the walls of constructions at the expense of phase and chemical transformations with subsequent removal of the products of these transformations from the surface of the covering during the influence of gas flow on it, is called ablation, and the corresponding coverings – ablating.

10.3. Internal Cooling

Internal cooling is used widely in liquid propellant rocket engines and is the basic method for lowering of specific heat flow. In principle, with the corresponding constructive realization, with the help of internal cooling it is possible to reduce specific heat flow practically to zero and thus to maintain the temperature of the wall on necessary level without additional measures. But at present internal cooling is usually used in combination with other forms of shielding for the walls, in particular, in combination with external flow-through cooling. Most frequently for lowering the specific heat flow from gas to the wall a curtain of low-temperature gas is created at the wall. This leads to a decrease of convection heat flow.

The low-temperature wall layer also absorbs part of the radiant energy coming from the burning gases in the nucleus of flow, thus also decreasing radiant heat flow. Diagram of a gas curtain is shown in Fig. 10.8.

The low-temperature wall layer is usually created by means of feeding an excess quantity of combustible to the wall, which leads to an excess-oxidant ratio which is variable across the section of the chamber with a minimum value at the wall (see Fig. 4.15). Such

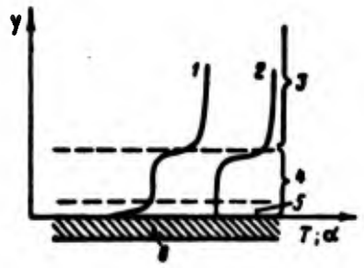

Fig. 10.8. Diagram of gas curtain: 1 – profile of temperature along a section of flow; 2 – change of excess-oxidant ratio along a section of flow; 3 – nucleus of flow of gas; 4 – wall layer; 5 – boundary layer; 6 – wall.

a wall layer can be created by special location of injectors on the head; in this case the fuel injectors are disposed mainly on periphery of head at the wall. A role of additional injectors of combustible can be played by a gap in the wall near the head.

On the initial section of the chamber near the head the wall is covered by film of liquid which is enriched with combustible. With further movement toward the nozzle the film is gradually vaporized and burns, and at the wall a layer of gas is formed with a low value of excess-oxidant ratio ($\alpha_{ст}$), and therefore – with reduced temperature. The process of combustion in the wall layer, as was noted, occurs more slowly than in the nucleus of flow due to the lower temperatures and therefore is protracted on a large length of the chamber.

Combustible for the curtain is also supplied through the wall. In this case it is introduced through a slot or holes which are made in definite sections of the combustion chamber or nozzle. The film forming on the wall, by absorbing heat from combustible gases, gradually vaporizes; the vapors mix with products of combustion and form the wall gas layer with a low excess-oxidant ratio and therefore with a low temperature.

In the examined methods of organization of internal cooling it is possible to distinguish sections. First – the section near the point of supply of the liquid;[1] here the wall is covered by a liquid

[1]In certain cases a gas (vapor) and not a liquid, can be introduced into the curtain, for example, in a hydrogen liquid propellant rocket engine, in which in a cooling cavity hydrogen is reduced to a gaseous state.

film. Temperature of the wall on this section is close to the boiling point of the liquid, inasmuch as heat, given off by the gases, is absorbed in the basic film. Only part of the radiant flow (rays with wavelengths for which the film is transparent), goes through the film and reaches the wall. Therefore on this section heat flows on the wall are insignificant under the condition that the wall is evenly covered by the liquid. Second is the section after vaporization and burning out of the film, where the wall is washed by a low-temperature wall layer – a gas curtain (see Fig. 10.8). Here heat flow is determined by the temperature and composition of gas of this layer. Knowing the excess-oxidant ratio of the wall layer $\alpha_{ст.}$, it is possible to estimate the value of heat flows on this section (see Fig. 10.5).

At a considerable distance from the point of entry of excess combustible to examined section the wall layer, as a result of mixing with the nucleus of flow, is eroded and its temperature is increased. This lowers the effect of internal cooling. Therefore the point of entry of excess fuel should be selected in such a manner that the low-temperature curtain is preserved up to the most thermally stressed parts of the engine (in particular, up to the critical section of the nozzle). In some engines this is limited by the organization of cooling with the help of the head; in others additional inlets through the wall are established, for example, before the nozzle.

The curtain, being an effective method for lowering of heat flows, at the same time leads to certain losses in specific thrust, inasmuch as exit velocity of gases, corresponding to excess-oxidant ratio in the wall layer $\alpha_{ст.}$ is lower than at $\alpha_{сопт.}$ In the designing of engines one should aspire to decrease these losses. At a given value of $\alpha_{ст}$ this can be attained by decreasing the quantity of substance, giving into the gas curtain, i.e., by decrease the layer of gas which has a lower excess-oxidant ratio. However, in this respect there are limitations, since the thinner this layer, the more rapidly it is mixed with the nucleus of flow and the earlier it ceases to exist.

Losses in specific thrust $\Delta P_{уд}$, connected with the curtain, can be estimated, in an assumption of the absence of mixing between gas the curtain and nucleus of flow and complete combustion of the mixture both in the nucleus of flow and also in the wall layer, in the following way:

$$\Delta P_{уд} = P_{уд.опт} - P_{уд},$$

where $P_{уд.опт}$ – specific thrust of engine with value $\alpha = \alpha_{опт}$; identical everywhere; $P_{уд}$ – specific thrust of engine with curtain.

Is considering that the excess-oxidant ratio in the nucleus of flow is equal to optimum value $\alpha_{опт}$, and in the wall layer – $\alpha_{ст}$, we obtain:

$$\Delta P_{уд} = g_з (P_{уд.опт} - P_{уд.ст}),$$

or in relative values

$$\overline{\Delta P}_{уд} = \frac{\Delta P_{уд}}{P_{уд.опт}} = g_з \left(1 - \frac{P_{уд.ст}}{P_{уд.опт}}\right). \qquad (10.20)$$

Here $g_з = \frac{G_з}{G_{з.опт}}$ – relative quantity of gases forming the curtain; G_3 – fuel consumption on gas curtain; $G_{з.опт}$ – total fuel consumption.

If one were to take $\alpha_{опт} = 0{,}9$, then with the accepted assumptions the losses in specific thrust will have the values shown in Fig. 10.9.

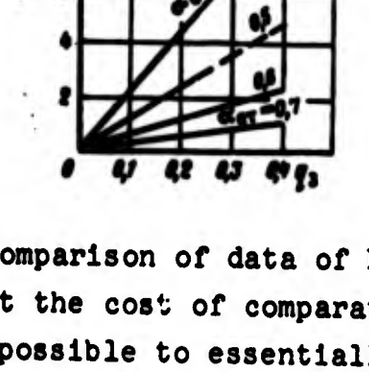

Fig. 10.9. Dependence of losses in specific thrust on the parameters of the gas curtain at $\alpha_{опт} = 0{,}9$.

Comparison of data of Fig. 10.9 with data of Fig. 10.5 shows that at the cost of comparatively small losses in specific thrust it is possible to essentially lower heat transfer from gas to the wall of the engine. It is necessary, however, to consider that the

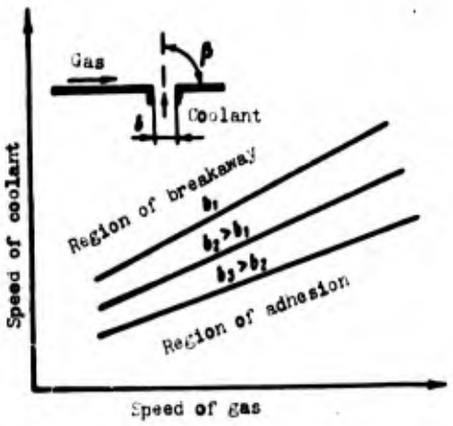

Fig. 10.10. Regions of breakaway and adhesion of film.

data in Fig. 10.9 were obtained at a specific fuel consumption on the curtain. The problem of constructive realization is to ensure the necessary level of lowering of specific heat flows at possibly smaller flow rates on the curtain.

The effectiveness of internal cooling is influenced greatly by the nature of movement of the film along the wall. The more stable the movement of the film, the more prolonged its existence and more effective the internal cooling. For stable movement the film should adhere to the wall. The influence of certain factors on the nature of movement of the film is shown in Fig. 10.10, on which limiting lines are plotted, thus dividing the plane into regions of breakaway and adhesion. The greater the width of slot b, through which the liquid is fed to the wall, then the lower the boundary curve is disposed, and the narrower the region of adhesion.

At a given speed of circumventing gas for ensuring the adhesion of the film to the wall it is necessary to lower the rate of feeding the liquid and to decrease the width of slot b. It is obvious that the smaller angle β is, the more favorable the condition for adhesion.

But even in the presence of adhesion the film can lose its stability due to disturbances which appear during its movement. It was established that with an increase of flow rate of the coolant the length of the film at first is increased, and then, starting with a certain critical flow rate, this increase is slowed down or is ceased due to a loss of stability. The most favorable conditions

for the stable movement of the film are while its thickness does not exceed the thickness of laminar sublayer of gas flow. Therefore an increase of expediture on film is effective only up to certain limits. With a further increase of expenditure the conditions of cooling are no longer improved, since here there is a lessening of stability of the film and the additional expenditure of liquid is carried away by gases. This can be seen from the graph in Fig. 10.11, which is constructed according to the results of experiments.

The necessary flow rate of liquid through the openings in the wall $G_{ж}$ for lowering of specific heat flows by a given value depends on the structure for admitting liquid to the wall, on the properties of the liquid, and also on the parameters of gas flow and are usually found experimentally. It is always necessary to aspire to decrease this value for the purpose of lowering losses in specific thrust.

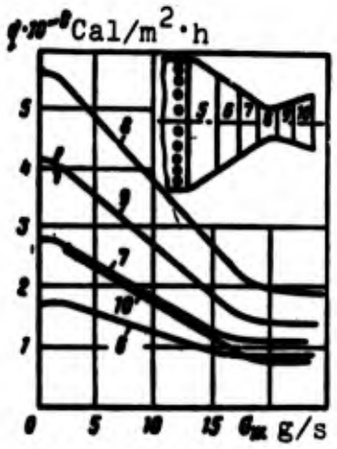

Fig. 10.11. Influence of internal cooling on specific heat flow.

In a liquid propellant rocket engine losses in specific thrust, connected with the organization of internal cooling, are found on the average within the limits of 1-5%; for engines with large thrusts they should be less (other things being equal). This is connected first of all with the fact that the perimeter of the section of combustion chamber and nozzle with an increase of engine thrust increases to a lesser degree than fuel consumption. Therefore the relative expenditure of coolant for the curtain decreases, inasmuch as for engines of various thrusts one may assume that necessary expenditure of liquid per unit of length of perimeter is approximately identical.

During a calculation of specific thrust these losses are considered by the value $\phi_к$ and comprise the basic share of losses in the chamber.

Transpiration cooling. The greatest lowering of heat transfer to the wall can be secured if the entire internal surface is completely covered by a film of liquid. For this it is necessary to connect the slots (apertures) by increasing the number of them and lowering the flow rate in each of them (Fig. 10.12). Such a method of cooling is called film. Close to this method is the so-called transpiration cooling. The wall in this case is prepared from porous material, the coolant is pressed through the pores from the external surface to the internal, which circumvents the hot gas, and thus lowers heat flow from the gas to the wall; heat which penetrates to the wall is absorbed by the coolant which is passing through its pores (Fig. 10.13).

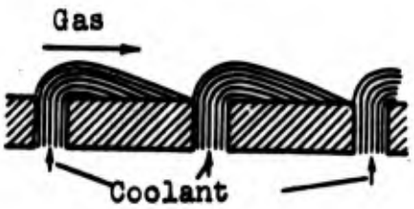

Fig. 10.12.

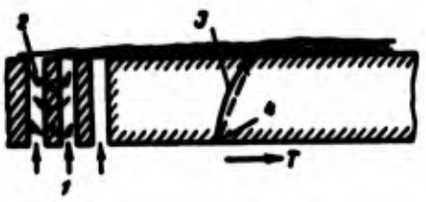

Fig. 10.13.

Fig. 10.12. Diagram of film cooling.

Fig. 10.13. Diagram of transpiration cooling: 1 – coolant; 2 – heat; 3 – temperature of coolant; 4 – temperature of wall.

The temperature of the wall during transpiration cooling essentially depends on the flow rate of coolant through it. If the coolant is a liquid, then there is a certain critical flow rate, at which the temperature of the wall becomes equal to the boiling point of the liquid. In this case, at large flow rates the liquid passing through the wall does not succeed in vaporizing and, consequently, the wall on the side of the gas is washed by the liquid. With a flow rate lower than critical due to an increase of heat per unit of expenditure of coolant the liquid which is passing through the

wall vaporizes and the internal surface of the wall is no longer washed by the liquid layer, which leads to an increase of $T_{ст_г}$. Such conditions of cooling, although connected with an increase of temperature of the wall, are not more suitable, inasmuch as in this case there is a decrease in the expenditure of liquid. At a specific flow rate vaporization will occur already on the external surface of the wall and through the pores of the wall vapor will pass. In this case a decrease of heat flow from gas to wall occurs at the expense of blasting relatively cold vapor into the boundary layer of gas. Heat which reaches the wall goes for heating of vapors which are passing through the wall and for heating and vaporization of liquid on the external surface of the wall. Such operating conditions ensures the uniform and economic cooling of the wall.

One of the main difficulties in the use of transpiration cooling is the obtaining of materials of high strength and with uniform porosity. Nonfulfillment of the last condition leads to the nonuniform expenditure of liquid coolant through the surface of the wall and to nonuniform temperature fields for the wall.

Well orgainzed transpiration cooling can ensure reliable shielding of the walls from high temperatures with very small expenditures of coolant without external cooling.

10.4. External Flow-Through Cooling

External flow-through cooling of an engine is also called regenerative, inasmuch as here practically all the heat given off to the wall returns back to the combustion chamber. External flow-through cooling of an engine is used more frequently in combination with internal.

During external flow-through cooling heat flow from the gas to the wall is equal to heat flow through the wall and to heat flow from the wall to the liquid coolant. If one were to disregard the difference between values of internal and external surfaces of the wall, then it is possible to also consider specific heat flows as equal:

$$q_г = q_{ст} = q_ж = q, \tag{10.21}$$

where $q_г$, $q_{ст}$, $q_ж$ — specific heat flows accordingly from gas to wall, in the wall, and from wall to liquid coolant.

It is known that

$$q_г = \alpha'_г (T^*_г - T_{ст_г}); \tag{10.22}$$

$$q_{ст} = \frac{\lambda_{ст}}{\delta}(T_{ст_г} - T_{ст_ж}); \tag{10.23}$$

$$q_ж = \alpha_ж (T_{ст_ж} - T_ж). \tag{10.24}$$

Here $\alpha'_г$ — certain effective coefficient of heat transfer, considering in addition to convection also radiant heat flow:

$$\alpha'_г = \alpha_г + \frac{q_л}{T^*_г - T_{ст_г}};$$

δ — thickness of walls; $\alpha_ж$ — coefficient of heat transfer from wall to liquid coolant; $T_{ст_ж}$ — temperature of surface of wall from the side of liquid coolant.

Solving these equations jointly, we obtain:

$$q = \frac{T_{ст_г} - T_{ст_ж}}{\frac{1}{\alpha_ж} + \frac{\delta}{\lambda_{ст}} + \frac{1}{\alpha'_г}}.$$

Value $\left(\frac{1}{\alpha_ж} + \frac{\delta}{\lambda_{ст}} + \frac{1}{\alpha'_г}\right)$ is frequently called thermal resistance. Consequently, thermal resistance is made up of resistance of gas $1/\alpha'_г$, resistance of wall $\delta/\lambda_{ст}$ and resistance of liquid coolant $1/\alpha_ж$. It is necessary to note that the basic value is the thermal resistance of gas. Actually, for a liquid propellant rocket engine the following order of values, included in formula (10.25) are characteristic:

$$\alpha'_г = 10^3 \div 10^4 \text{ Cal/m}^2 \cdot \text{h} \cdot \text{deg};$$

$$\alpha_ж = 10^4 \div 10^5 \text{ Cal/m}^2 \cdot \text{h} \cdot \text{deg};$$

$$\lambda_{ст}/\delta = 10^4 \div 2 \cdot 10^5 \text{ Cal/m}^2 \cdot \text{h} \cdot \text{deg}.$$

Change of temperatures during transmission of heat in a liquid propellant rocket engine from the gas through the wall to the liquid

coolant is shown in Fig. 10.14. Also shown there are the approximate values of temperatures.

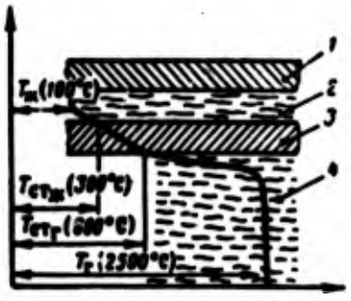

Fig. 10.14. Nature of change of temperature during transmission of heat through the wall from the gas to the liquid coolant: 1 – wall of jacket; 2 – liquid coolant; 3 – wall of chamber; 4 – gases.

Temperature of coolant on emergence from the jacket will be found from condition

$$(I_{ж\,вых} - I_{ж\,вх}) + A\frac{c^2_{ж\,вых} - c^2_{ж\,вх}}{2g} = \frac{Q}{G_ж}, \qquad (10.26)$$

where $I_{ж\,вх}$, $I_{ж\,вых}$, $c_{ж}$, $c_{ж\,вых}$ – enthalpy and speed of cooler on entry into and exit from the cooling jacket; $G_ж$ – expenditure of coolant; Q – total quantity of heat, transmitted from wall to liquid coolant (overall heat removal).

Usually the change of kinetic energy is small as compared to change of enthalpy and it can be disregarded. Inasmuch as heat flows along the engine are variable, then for convenience of calcualtion the surface of the engine is split along the length into sections, then

$$I_{ж\,вых} - I_{ж\,вх} = \frac{1}{G_ж}\sum F_i q_i. \qquad (10.27)$$

Here q_i, F_i – average specific heat flow and surface of wall of separate i section.

If the coolant does not change its aggregate state in jacket and dependence of heat capacity on pressure can be disregarded, then it is possible to write

$$T_{ж\,вых} - T_{ж\,вх} = \frac{1}{C_ж G_ж}\sum q_i F_i, \qquad (10.28)$$

where $T_{ж\,вх}$, $T_{ж\,вых}$ – temperature of coolant at inlet to and exit from jacket; $C_ж$ – average heat capacity of coolant.

Heat transfer from wall to liquid coolant. During external cooling of the engine it is necessary to ensure that value of coefficient of heat transfer $\alpha_ж$ from the wall to the liquid, at which the temperature of the wall on the side of the gas would not exceed permissible limits. It is not difficult to see that for this temperature of the wall on the side of the liquid $T_{ст_ж}$ should have a fully specific value:

$$T_{ст_ж} = T_{ст_г} - \frac{\delta}{\lambda_{ст}} q. \qquad (10.29)$$

In its turn provision of the necessary value $T_{ст_ж}$ amounts to obtaining a fully specific value of $\alpha_ж$:

$$\alpha_ж = \frac{q}{T_{ст_ж} - T_ж}. \qquad (10.30)$$

If value of the coefficient of heat transfer from the wall to the liquid coolant is less than necessary, then this will entail an increase of $T_{ст_ж}$, and consequently also of $T_{ст_г}$.

Conditions of heat exchange between the wall and liquid coolant depend to a considerable degree on temperature of the surface of the wall which is washed over by the liquid. During stabilized turbulent flow in rectilinear channels, when there is no boiling on the wall, the coefficient of heat transfer $\alpha_ж$ can be found from the criterial equation

$$Nu = 0{,}023\,Re^{0{,}8} Pr^{0{,}4} K_t. \qquad (10.31)$$

In this equation physical properties during determination of criteria are taken at the temperature of the coolant $T_ж$, coefficient K_t, as was noted, considers the influence of variability of physical properties on intensity of heat exchange.

By expanding the criterion of similarity in the last equation we obtain:

$$\frac{\alpha_ж d_{экв}}{\lambda} = 0{,}023 \left(\frac{c\gamma d_{экв}}{\eta}\right)^{0{,}8} \left(\frac{\eta \cdot C_ж}{\lambda}\right)^{0{,}4} K_t;$$

here c, γ, λ, η, $C_ж$ – respectively rate, density, thermal conductivity, viscosity, and heat capacity of coolants; $d_{экв}$ – equivalent diameter.

Solving the last expression relative to $\alpha_{ж}$ and considering dimensions

$\alpha_{ж}$ in Cal/m^2·h·deg; γ in kgf/m^3; η in kgf/m·s;
c in m/s; $d_{экв}$ in m; $C_{ж}$ in Cal/kgf·deg; λ in Cal/m·h·deg,

we obtain:

$$\alpha_{ж}=0{,}615\frac{(c\gamma)^{0{,}8}}{d_{экв}^{0{,}2}}K_{ж}K_{t}, \qquad (10.32)$$

where

$$K_{ж}=\left(\frac{C_{ж}}{\eta}\right)^{0{,}4}\lambda^{0{,}6};\quad d_{экв}=\frac{4f}{\Pi};$$

f – area of cross section of channel; Π – perimeter of section of channel.

Thus, coefficient of heat transfer $\alpha_{ж}$ depends on mass velocity $c\gamma$, properties of the coolant, and geometry of the channel. Dependence of $K_{ж}$ on temperature for certain liquids is presented in Fig. 10.15.

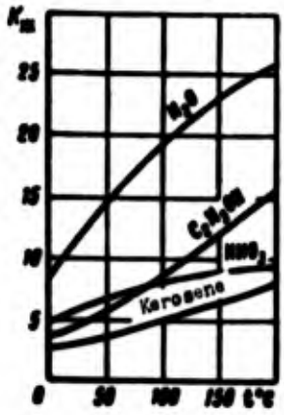

Fig. 10.15. Dependence of complex $K_{ж}$ on temperature.

The nature of influence of variability of physical properties on intensity of heat exchange, and consequently also on value K_t depends on a whole number of factors (pressure, temperature, properties of coolant, etc.). For drop liquids at subcritical pressures and in the absence of boiling on the wall ($T_{ст_ж} < T_{кип}$) it is possible to take

$$K_l = \left(\frac{\eta_{ж}}{\eta_{ст}}\right)^{0.14}, \qquad (10.33)$$

where $\eta_{ж}$ – dynamic viscosity of coolant at $T_{ж}$; $\eta_{ст}$ – the same at $T_{ст_{ж}}$. If the coolant is in a gaseous state, then, as was noted, the influence of variability of physical properties is described by the temperature factor $T_{ст}/T_{ж}$; for case of addition of heat to gas it is possible to take

$$K_l = \left(\frac{T_{ж}}{T_{ст}}\right)^{0.5}. \qquad (10.34)$$

It is necessary to consider that for certain liquids the maximum permissible temperature $T_{ст_{ж}}$ is limited. Thus, for certain petroleum fuels experience shows that, starting with a certain temperature $T_{ст_{ж}}$, in the layer of liquid adjacent to the wall solid compounds start to form and are deposited on the wall in the form of carbon. The layer of carbon increases thermal resistance, thereby worsening conditions for cooling of the engine. According to experiments on kerosene at a pressure of 35 atm(abs.) carbon formation takes place at a wall temperature of 430-480°C.

Peculiarities of heat transfer during boiling of a liquid on the wall. The layer of liquid adjacent to the wall has temperature exceeding the temperature of liquid in the main part of the flow $T_{ж}$. Therefore a situation can occur when $T_{ж}$ is lower than the boiling point of the liquid, and $T_{ст_{ж}} > T_{кип}$, i.e., in the absence of boiling of liquid in the main part of flow at the wall the liquid boils. The process of convection heat exchange here differs from case, when there is no boiling at the wall. It is known that if in this case specific heat flows do not exceed the critical value $q_{кр}$, then bubble boiling appears: on the wall bubbles of vapor will be formed which, by being torn from the wall, are directed to the nucleus of flow and are condensed. Transverse movement of bubbles causes mixing of the boundary layer, which intensifies the process of heat withdrawal from the wall and, consequently, leads to an increase of coefficient of heat transfer. The more intense the vaporization of liquid with the formation of separate bubbles of vapor, which are mixing the boundary layer, then the more intense is heat removal from the wall

of the liquid; therefore with an increase of heat flow the intensity of heat exchange between the wall and the liquid increases and the coefficient of heat transfer increases. However, this holds true only to a certain limit; when specific heat flow exceeds $q_{кр}$, the number of bubbles created becomes so large that they merge and form a solid vapor film, insulating the liquid from the wall. Conditions of film boiling develop; heat withdrawal from the wall drops here.

If at a constant speed of liquid in the channel and constant temperature of liquid $T_{ж}$ the specific heat flow is changed, the coefficient of heat transfer $\alpha_{ж}$ (Fig. 10.16) with an increase of q to a definite limit will change little (a certain increase of it is caused by increase of $T_{ж}$). Temperature pressure $(T_{ст_ж} - T_ж)$ and temperature of the wall $T_{СТ_ж}$ will be increased in accordance with equation (10.24). When the temperature of the wall exceeds the value of boiling point, bubble boiling will start, which intensifies heat exchange. With a further increase of q the coefficient of heat transfer increases intensively, and the temperature of the wall is changed little.

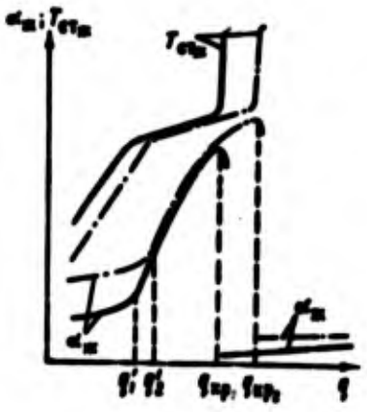

Fig. 10.16. Dependence of $\alpha_{ж}$ and $T_{СТ_ж}$ on specific heat flow during boiling on the wall: —— c_1; - - - - $c_2 > c_1$

The presence of organized flow of a liquid influences heat exchange during bubble boiling as long as disturbances introduced by the process of vaporization, do not start to play a decisive role. This role of bubble boiling sets in according to the value of specific heat flow. The greater the velocity c of liquid in the channel, the later this is.

Even if specific heat flow is increased further, then upon achievement of critical value of heat flow $q_{кр}$ conditions of film boiling appear. Coefficient of heat transfer drops strongly and temperature of the wall increases sharply. A very possible result of this circumstance can be burnout of the wall. The higher the velocity of the liquid, the greater the value $q_{кр}$. In Fig. 10.16 a picture is given for two values of speed of liquid c_1 and c_2.

Critical heat flow in general depends on properties of the liquid, pressure, rate of movement, on the value of underheating of liquid up to boiling point ($T_{\text{кип}}-T_{\text{ж}}$) and several other factors.

From what was said it follows that if heat transfer to the liquid coolant occurs during boiling on the wall, then it is necessary to exclude the possibility of transition to film boiling. For this the specific heat flow should be less than critical by a value, knowingly covering the irregularity of heat flow over the perimeter of a section of chamber, and also the influence of changes of operating conditions of the engine.

Peculiarities of heat exchange at supercritical pressure. If the pressure of liquid exceeds critical pressure $p_{кр}$, then boiling is impossible. If, however, $T_{ст_{ж}}$ is less than critical temperature, then conditions of heat exchange are the same as without boiling on the wall during subcritical pressure, and coefficient of heat transfer $\alpha_{ж}$ can be found from equations (10.31) and (10.33). If, however, temperature of the wall exceeds critical temperature $T_{кр}$, then heat exchange between the wall and the liquid has its own peculiarities. Physical properties along a section of flow in this case change monotonically from values, peculiar to a liquid, to values which are characteristic for gas; fluid flow is separated from the wall by a thin gaseous layer with increased thermal resistance. Therefore with an increase of $T_{ст_{ж}}$ at $T_{ст_{ж}} > T_{кр}$ the intensity of heat exchange and, consequently, also the coefficient of heat transfer drop. Investigations show that value K_t in these conditions is a function of given temperature $\tau_{ж}$ and $\tau_{ст}$ and given pressure π.

Here

$$\tau_{ж}=\frac{T_{ж}}{T_{кр}};\quad \tau_{ст}=\frac{T_{ст_{ж}}}{T_{кр}};\quad \pi=\frac{p}{p_{кр}}.$$

For definite parameters value K_t can be determined approximately from Fig. 10.17.[1]

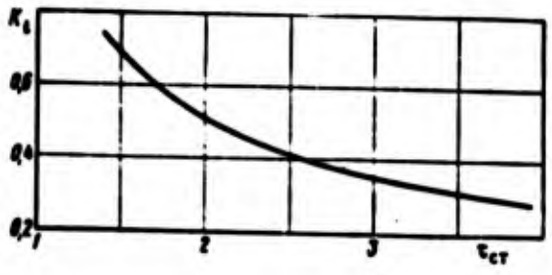

Fig. 10.17. Dependence of K_t on temperature of wall at supercritical pressure ($\tau_ж<1$; $\pi\approx1{,}5$–2).

Under certain conditions, as experiments show, the process of heat transfer to a liquid at supercritical pressure and $T_{ст_ж}>T_{кр}$ is accompanied by fluctuation phenomena, which essentially changes the nature of the process. However, source material from investigations of heat exchange under these conditions is still insufficient.

Factors affecting the conditions of external flow-through cooling. Intensity of cooling should be such that the temperature of the wall on the side of gas would be lower than the permissible temperature for the given material of the wall, i.e., $T_{ст_г}<T_{доп}$.

In specific cases there can be limitations on the temperature of the coolant at the outlet from the jacket, for example: $T_{ж_{вых}}<T_{ж_{кип}}$. However, this condition is not always obligatory. There may be limitations, connected with temperature $T_{ст_ж}$. Thus, at subcritical pressures it is necessary to exclude the possibility of bubble boiling on the wall. For liquids which are capabl of carbon formation the temperature $T_{ст_ж}$ should be lower than the temperature of carbon formation.

---

[1]Calculation of heat exchange during supercritical pressure, see in work [31].

Let us place in equation (10.23) the value $T_{CT_{ж}}$ from equation (10.24) and solve it relative to $T_{CT_{г}}$:

$$T_{ст_г}=T_ж+q\left(\frac{1}{\alpha_ж}+\frac{\delta}{\lambda_{ст}}\right). \qquad (10.35)$$

From equation (10.35) it is clear that temperature $T_{CT_{г}}$ at a given temperature of liquid and specific heat flow depends on coefficient of heat transfer $\alpha_{ж}$, thickness of wall δ, and its coefficient of thermal conduction λ_{CT}.

Decrease of temperature $T_{CT_{г}}$ can be attained by intensification of heat removal from the walls, i.e., by an increase of coefficient of heat transfer $\alpha_{ж}$, which depends to a considerable degree on mass flow rate of the coolant. If the coolant is a liquid, then the density is a value which is practically constant, and in this case it is possible to influence the coefficient of heat transfer $\alpha_{ж}$ just by changing the rate of movement of the liquid in the coolant passage. The higher the rate the greater the coefficient of heat transfer and the less the temperature of the wall.

The flow rate of liquid coolant at its assigned expenditure depends on the area of section of the channel for coolant passage. If the required flow rate of liquid at a given expenditure is great and therefore the area of a section of channel is small, then the necessary height of channel or clearance between jacket and internal wall of the chamber Δ, can turn out to be very small. To produce an engine with a very small height of channel is technologically difficult. Usually it is made no less than 1-1.5 mm. When the flow of liquid is not sufficient, then in order to obtain the required flow of liquid at an acceptable value of clearance, the jacket is sometimes made up of helical channels, since with a helical direction of channel and the same altitude Δ the area of its section is less than during longitudinal (along the axis of the engine). Actually, if it is considered that expenditures of liquid coolant in both cases are equal, then

$$\frac{c_в}{c_{вр}}=\frac{f_{вр}}{f_в},$$

where $c_в, f_в$ — speed of coolant and area of channel during helical movement; $c_{вр}, f_{вр}$ — speed of coolant and area of channel during longitudinal movement.

It is not difficult to see, if thickness of ribs forming the channels is disregarded that $f_{вр}=\pi D\Delta$ and $f_в=\pi D\Delta\sin\varphi$, where ϕ — angle of ascent of helical thread; therefore

$$c_в=\frac{c_{вр}}{\sin\varphi}.$$

However, it is inexpedient to increase considerably the flow of coolant in the jacket, since this increase loss of pressure of liquid (proportional to the square of flow) which can cause a strong increase in the required value of feed pressure.

Inasmuch as the greatest values of specific heat flow belong to area of critical section of the nozzle, then in this place it is necessary to have the greatest expenditures of liquid coolant. Flow of liquid in the area of critical section of the nozzle is equal to 10-50 m/s and higher. Losses of liquid pressure in the cooling jacket on the average are equal to 5-20 kgf/cm^2. In separate cases, in the event of the necessity to remove high specific heat flows, it is necessary to considerably increase the flow of liquid coolant, and with it losses of pressure which can attain several tens of atmospheres.

A combination of change of specific heat flows and coefficient $\alpha_м$ along the chamber determines the distribution of temperature of wall in length. In general the greatest values of wall temperature are found in the area of critical section of the nozzle. In Fig. 10.18 is shown an approximate picture of change of wall temperature along the chamber and other parameters during external cooling of liquid propellant rocket engines.

Considerable influence on value $T_{ст_г}$ is exerted by pressure in the chamber. With an increase of pressure in the chamber there is

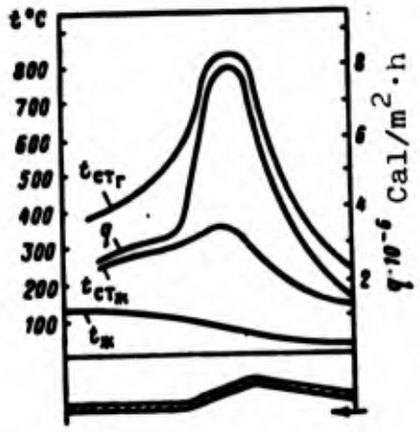

Fig. 10.18. Change of parameters during external flow-through cooling

an increase of specific heat flows approximately proportional to power 0.8. If change of pressure in the chamber of a specific engine ($F_{кр}$ = const) is examined, then approximately to the same degree coefficent $\alpha_ж$ will be changed. Change of $\alpha_ж$ in this case is caused by a change of expenditure and flow of liquid coolant, if cooling is carried out by one of the components.

Inasmuch as thermal resistance of the wall $\delta/\lambda_{ст}$ does not change here, then from equation (10.35) it follows that temperature of the wall $T_{ст_г}$ should be increased with an increase of pressure in the chamber.

To a still greater degree will be the increase of $T_{ст_г}$ with an increase of $p_к^*$, if pressure in the chamber is increased at the expense of decreasing the critical section with a constant expenditure of gas, and consequently also of liquid coolant; in this case various engines, having various $F_{кр}$ and equal fuel consumption, are compared. The greater increase of $T_{ст_г}$ will be due to the fact that with a change of pressure in the chamber to thermal resistance remains constant, not only of the wall, but also of the liquid coolant, if clearances in cooling jackets at various $p_к^*$ are identical. Thus an increase of pressure in the chamber hampers cooling of the engine from the point of view of value $T_{ст_г}$ (Fig. 10.19).

Change of $p_к^*$ at $F_{кр}$ = const leads to a proportional change of expenditure of liquid coolant, which is one of the components. The

Fig. 10.19. Dependence of temperature $T_{ст_г}$ on pressure in the chamber ($\lambda_{ст}$ = 40 Cal/m·h·deg and δ = 1 mm).

amount of heat, given off through the wall to the liquid coolant (general heat removal Q), is changed to a lesser degree. Therefore the amount of heat, belonging to 1 kgf of fuel (specific heat removal Q_0), and consequently also to 1 kgf of liquid coolant, decreases (at a constant excess-oxidant ratio). Therefore with an increase of pressure in the chamber the temperature of the liquid coolant at the outlet from the jacket is decreased. In Fig. 10.20 is shown the dependence on pressure in the chamber of overall heat removal Q (Cal/s), specific heat removal Q_0 (Cal/kgf), and value of preheating of coolant $\Delta T_ж = T_{ж_{вых}} - T_{ж_{вх}}$.

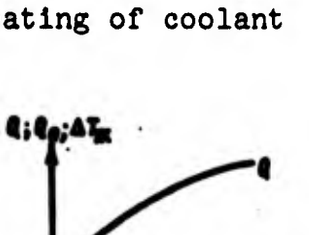

Fig. 10.20. Influence of pressure in the chamber on overall heat removal Q, specific heat removal Q_0, and on preheating of liquid in the jacket.

Increase of wall thickness leads to an increase of thermal resistance of the wall, and consequently also to a certain lowering of specific heat flows. However, here there is increased temperature drop on the wall and accordingly of value $T_{ст_г}$ (Fig. 10.21). The latter is not difficult to see from formula (10.35), if one considers that change of thickness of wall has little effects on q. An increase of coefficient of thermal conductivity of the wall material decreases $T_{ст_г}$. Consequently, the application of better heat-conducting materials and a decrease of wall thickness during external flow-through cooling furthers the improvement of conditions of cooling of an engine from the point of view of $T_{ст_г}$. However, there is an

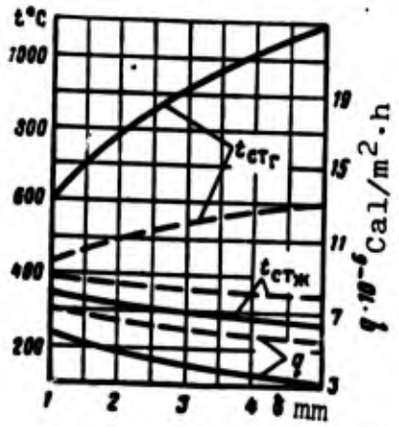

Fig. 10.21. Influence of thickness and thermal conductivity of the wall on temperature of the wall and heat flow:
——$\lambda_{ст}$ = 30 Cal/m·h·deg;
----$\lambda_{ст}$ = 150 Cal/m·h·deg.

increase in the amount of heat given off to the liquid coolant, since specific heat flow increases; therefore at a constant $\alpha_{ж}$ temperature $T_{ст_{ж}}$ is increased.

A positive influence on conditions of cooling of an engine can be exerted by the application of refractory thermal insulation coverings, possessing a low coefficient of thermal conductivity and high permissible temperature of heating. If the internal surface of the wall is covered with such a material, then overall thermal resistance of the wall will be increased, which will decrease specific heat flow and therefore also the values of wall temperature. In Fig. 10.22 is shown the distribution of temperatures in the wall in the presence and absence of thermal insulation, where the conditions of heat exchange on the part of gas and liquid are taken as identical.

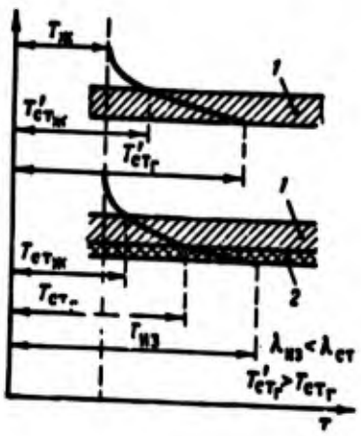

Fig. 10.22. Influence of heat insulating coverings on conditions of cooling: 1 – wall; 2 – thermal insulation.

The application of ribs. Certain constructions, the walls are equipped with ribs for increasing rigidity and improving the cooling

of the engine. Improvement of cooling is connected with the fact that due to an increase of external surface of the chamber wall the same heat flow from the wall to the liquid coolant will be transmitted in case of a ribbed wall with a smaller difference of temperatures $T_{ст_г}-T_ж$. Therefore the temperature of the wall at the given value $\alpha_ж$ will be lower. However, heat transfer from the wall to the liquid coolant does not increase proportionally to the increase of external surface of a ribbed wall, but to a lesser degree. This is explained by the fact that temperature of the rib for height does not remain constant (Fig. 10.23), but decreases due to heat removal from its edges. Therefore a noticeable improvement of conditions of cooling of an engine is observed only at a specific height of rib.

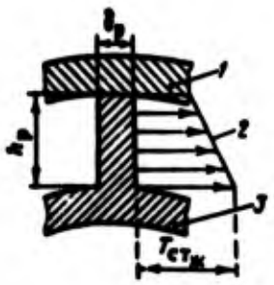

Fig. 10.23. Change of temperature of wall with height of rib: 1 – external wall; 2 – profile of temperature; 3 – internal wall.

The greater the coefficient of thermal conductivity of wall material, the more even the temperature profile for height of rib and, consequently, the greater the effect of ribbing. For this reason the relative improvement of cooling of an engine with ribbing will be even greater, the less the value of coefficient of heat transfer $\alpha_ж$.

Decrease of thickness $\delta_р$ of the rib also promote an increase of its effectiveness, since here there is an increase in the number of ribs and, consequently, the overall surface of the wall which is washed by the liquid.

Let us consider a ribless wall, having a surface F and temperatures $T_{СТ_ж}$, which is washed by a liquid coolant with temperature $T_ж$. Heat flow from the wall to the liquid coolant in this case is equal to

$$Q=\alpha_ж F(T_{ст_г}-T_ж).$$

Let us assume that a portion F_2 of the surface of the examined wall is covered with ribs. Then the heat flow from the wall to the liquid coolant can be presented as the sum:

$$Q' = Q_1 + Q_2,$$

where Q_1 – heat flow from surface $F_1 = F - F_2$ of the wall not occupied by ribs; Q_2 – heat flow from share F_2 of the wall, covered by ribs.

Let us accept that in the case of a ribbed wall the value T_{CT_M} is the same as for a ribless wall. Then

$$Q_1 = \alpha_ж F_1 (T_{ст_ж} - T_ж);$$
$$Q_2 = \alpha_р F_2 (T_{ст_ж} - T_ж);$$

here α_p – certain effective coefficient of heat transfer, considering the increase of heat transfer on a surface having a rib.

General heat flow is equal to

$$Q' = (\alpha_ж F_1 + \alpha_р F_2)(T_{ст_ж} - T_ж).$$

Effectiveness of application of ribs can be evaluated by the relationship

$$\eta_р = \frac{Q'}{Q} = \frac{\alpha_р F_2}{\alpha_ж F} + \frac{F_1}{F}. \qquad (10.36)$$

It is obvious that the higher the value η_p, the more effective ribbing is.

For a flat rib of constant thickness, in the assumption that temperature based on its thickness is constant and heat removal from the upper end is negligible, the value of α_p can be determined from expression:

$$\alpha_р = \alpha_ж \sqrt{\frac{2}{Bi_р}} \operatorname{th}\left(\frac{h_р}{b_р}\sqrt{2Bi_р}\right). \qquad (10.37)$$

where $Bi_р = \frac{\alpha_ж b_р}{\lambda_{ст}}$ – Biot criterion, calculated for width of rib.

In Fig. 10.24 are given the results of calculation by the formulas (10.36) and 10.37), showing the dependence of η_p on height of rib and influence on this value of the coefficient of thermal conductivity of the wall and coefficient of heat transfer $\alpha_м$. It is clear that ribbing is most effective when using high-heat-conducting materials; the higher the coefficient $\alpha_м$, the less the effectiveness of ribs. It is necessary to consider that with a definite combination of parameters the application of ribs can give a negative effect (small $\lambda_{ст}$, large $\alpha_м$), i.e., $\eta_p < 1$.

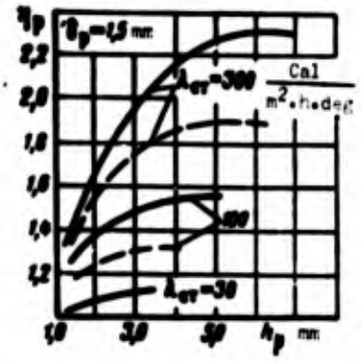

Fig. 10.24. Dependence of η_p on height of rib (with $F_1 = F_2$):
—— $\alpha_м = 30 \cdot 10^4$ Cal/m^2·h·deg;
---- $\alpha_м = 50 \cdot 10^4$ Cal/m^2·h·deg.

CHAPTER XI

THE USE OF NUCLEAR ENERGY IN ROCKET ENGINES

11.1. Basic Information

At present there are two basic methods for releasing of nuclear energy: 1) the method of fission of certain heavy nuclei under the influence of bombardment by neutrons and 2) the method of nuclear fusion of light substances under the influence of very high temperatures. In both cases a huge amount of energy is liberated.

The method of fission (splitting) of heavy nuclei has already gained practical application at industrial power and military installations (electric power station, submarines, surface ships). This turned out to be possible only with the development of a controlled, calm process of fission of heavy nuclei. This method will be the subject of further examination.

The method of synthesis is based on fusion of hydrogen nuclei with the formation of helium; this process carries the name of thermonuclear reaction. In nature thermonuclear reactions are carried out on the sun and other stars. For realization of a thermonuclear reaction heavy hydrogen is useful, but here extraordinarily high temperatures are necessary so that kinetic energy of approaching light nuclei exceeds the energy of forces of mutual repulsion. For deuterium D_1^2[1] a thermonuclear reaction requires temperatures of

[1] Figure below indicates the number of protons in the nucleus (charge), figure above – total number of nucleons (protons and neutrons).

(300-400)·10^6 deg. If one were to take mixture from equal parts of D_1^2 and tritium T_1^3, then a thermonuclear reaction can be carried out already at (40-50) × 10^6 deg. Energy given off in the process of synthesis is equal to the difference of binding energy of nuclei of end and initial products. For example,

$$D_1^2 + T_1^3 \rightarrow He_2^4 + n_0^1 + \text{energy},$$

where n – symbol for neutron.

Energy liberated during a thermonuclear reaction is very great – it is greater than the energy during fission of heavy nuclei.

For utilization of the energy of thermonuclear reactions on stationary and transport propulsion systems it is necessary to be able to control the course of these reactions. At present this goal has still not been achieved. In USSR, in England, and in the United States research is being conducted on the creation of instruments and installations for control of thermonuclear reactions.

In contemporary electrical power nuclear systems the energy of fission of heavy nuclei is used for preheating the working substance of the propulsion system instead of the chemical energy of fuel or for direct conversion of heat into electrical energy.

"Nuclear fuel" is the name for substances, which as a result of fission or fusion liberate energy. The instrument, in which a calm controlled nuclear reaction takes place is called a reactor. The name "nuclear fuel" has a conditional nature and is connected with the role which is fulfilled by fissionable material in contemporary power systems by replacing chemical fuel.

In reactors for carrying out the controlled process of fission the fissionable materials are the isotopes of uranium U_{92}^{235} (or U-235), plutonium Pu_{94}^{239} (or Pu-239), and the isotope of uranium U_{92}^{233} (or U-233) with half-lives of $8.8 \cdot 10^8$, $2.6 \cdot 10^4$, and $1.6 \cdot 10^5$ years respectively.

The isotope of uranium U-235 is contained in natural uranium in a quantity of 0.712%.

Plutonium Pu-239 is formed through a chain of transformations from natural uranium U-238 under the influence of neutrons. Isotope U-238 is contained in natural uranium in a quantity of 99.282%. Consequently, all natural uranium, with the exception of isotope U-234 (~0.006%) can be used for obtaining the energy of nuclei fission either directly (U-235) or through plutonium (U-238).

Isotope U-233 is formed through a chain of transformations from natural thorium Th_{90}^{232} (or Th-232) under the influence of neutrons. Thus the initial raw material for production of fuel for fission reactors are natural uranium and thorium.

In nuclear engineering for calculation of work the measure electron volt (eV) is used, and not the unit erg. By electron volt is understood energy content received by one electron during passage of a potential difference of one volt. Consequently,

$$1 \text{ eV} = 1.6 \cdot 10^{-19} \text{ coulomb-volt} = 1.6 \cdot 10^{-12} \text{ erg};$$

here the value $1.6 \cdot 10^{-19}$ coulomb represents the charge of an electron. Mass of an electron is equal to $9.11 \cdot 10^{-28}$ g; it is 1837 times lighter than the mass of an atom of hydrogen. In view of smallness of the eV unit in a description of nuclear processes most frequently the value MeV is used – million electron volts (or megaelectron volt):

Energy, liberated during fission of heavy nuclei, can be determined by the decrease of mass of the end products, comparatively with initial by using the Einstein equation

$$E = mc^2,$$

where m – decrease of mass or mass defect;

$c \approx 3 \cdot 10^{10}$ cm/s – speed of light.

If in 1 kgf of U-235 all the atomic nuclei are subjected to the process of fission, then the decrease of mass will be $m \approx 1$ g; consequently:

$$E = 1 \cdot 3^2 \cdot 10^{20} = 9 \cdot 10^{20} \text{ erg} \approx 21 \cdot 10^9 \text{ Cal.}$$

During fission of heavy nuclei under the influence of a neutron two fragments of unequal weight are obtained. Up to 80 different forms of fragments have been recorded from products with a mass number of 71 to products with a mass number of around 160. Most frequently the ratio of weights of two fragments comprises approximately 2:3.

For example:

$$U_{92}^{235} + n_0^1 \rightarrow Sr_{38}^{94} + Xe_{54}^{140} + 2n_0^1$$

In Fig. 11.1 is given a graph of the relative quantity of fission products of U-235, Pu-239, and U-233. The majority of these products are radioactive and acquire stability through γ-radiation or a series of successive β-disintegrations with the transformation of excess neutrons into protons.

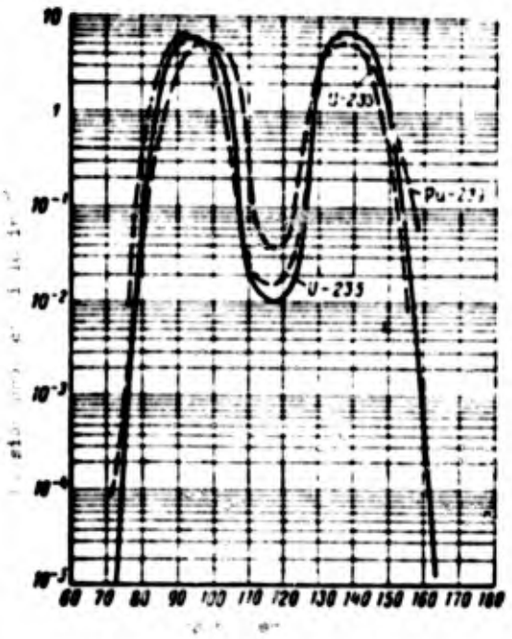

Fig. 11.1. Relative quantity of fission products of U-235, Pu-239, and U-233.

Above we pointed out a case of formation of the most probable fragments, namely - strontium and xenon with atomic numbers 38 and 54 and mass numbers 94 and 140. These mass numbers correspond to the maxima on the curve of Fig. 11.1. Relatively many of the following pairs are obtained: rubidium (Rb_{37}^{85}) and cesium (Cs_{55}^{133}); niobium (Nb_{41}^{93}) and antimony (Sb_{51}^{121}); bromine (Br_{35}^{79}) and lanthanum (La_{57}^{138}); yttrium (Y_{39}^{89}) and iodine (J_{53}^{127}), and others. These radioactive fragments (unstable due to large n/p, where n - number of neutrons, and p - number of protons of the nucleus) present unique "ashes," which change the isotopic composition of the reactor and exert a negative influence on the course of the reaction of fission with time. As it is said, as a result of nuclear reactions there occurs a gradual "poisoning" of reactor "by ashes" - fission fragments ("poisoning" by xenon, samarium, strontium, and others). Development of this process can lead to cessation of fission in the reactor, and consequently to cessation of liberation of energy in it. Due to accumulation of fission products in the reactor and change of its properties due to this, it is possible to use for fission only an insignificant share of the fissionable material (for example, uranium) which is embodied in the reactor.

Investigations showed that the greatest amount of nuclear energy is liberated in the form of kinetic energy of electrically charged fission fragments, possessing tremendous speeds due to electrostatic repulsion. Furthermore, it is necessary to consider the energy of newly formed neutrons, γ-radiation, and the energy of β-particles.

According to experimental data energy, liberated during the splitting of one nucleus of U-235, comprises 190 + 5 MeV and is distributed in approximately the following way in percentages:

kinetic energy of fission fragments..	86-87
kinetic energy of neutrons.....	2.5-3.0
energy of direct γ-radiation.....	3.0-3.5
energy of γ-radiation and β-particles during disintegration of fission fragments.....	6.0-7.0

energy, not liberated in the reactor, and energy unaccounted for (energy of a neutrino)..... the remainder

In contemporary reactors the kinetic energy of fragments and neutrons is completely converted into heat as a result of their deceleration in nuclear materials and in constructional elements. A significant share of the energy of γ-radiation and β-particles is also converted into heat. According to investigations around 94% of all the energy liberated in the reactor converts into heat and is subject to extraction from the reactor by some method.

Not any collision of a neutron with a nucleus of fissionable material leads to fission. For characterizing the effectiveness of nuclear reactions the concept of cross section of a nucleus is used.

During motion of neutrons in a mass of fissionable material two basic results are possible: 1) neutron scattering and 2) absorption of them by nuclei. Also possible is the passage of individual neutrons through the mass without collision ("miss"). Neutron scattering is possible only during the collision of neutrons and nuclei.

Scattering can be "elastic" and "inelastic." Elastic scattering corresponds to a case of collision with preservation of total kinetic energy and pulse of neutron and nucleus (analogous to the impact of two spheres in mechanics); elastic scattering is possible in the case when kinetic energy of a neutron (during direct collision with nucleus) is less than the excitation energy of the nucleus which is necessary for radiation of energy. Elastic scattering, leading to deceleration of neutron velocity, is important for a slow (neutron) reactor, since it plays the basic role in deceleration. Inelastic scattering, conversely, occurs in that case when kinetic energy of the neutron is greater than excitation energy of the nucleus; as a result, after collision the velocity (energy) of the scattered neutron will decrease, and part of the initial energy of

the neutron will be imparted to the nucleus, which will radiate energy, passing anew from the excited state into initial.

Not any absorption of a neutron by a nucleus leads to splitting of the latter. Absorption of a neutron by a nucleus in some cases leads to nuclear fission, and in others – to capture of a neutron by a nucleus without fission (to radiative capture). An example of the reaction of radiative capture is, for example:

$$H_1^1 + n_0^1 \rightarrow H_1^2 + \gamma.$$

Radiative capture is an example of inelastic scattering. By absorbing a neutron, the nucleus passes into an excited state and forms directly or through a chain of transformations a stable product with the simultaneous emission of γ-rays or β-particles.

Important examples of radiative capture in a practical respect are the capture of a neutron by a nucleus of U-238 with the formation of Pu-239 and the capture of a neutron by a nucleus of thorium Th-232 with the formation of U-233.

Excluding miss, elastic scattering, and radiative capture from all possible collisions, we will obtain only that number of effective absorptions which leads to nuclear fission.

Let us assume that the cross section of one target nucleus, or microscopic section, is σ cm^2/nucleus. If one were to take a cube with sides 1 cm, on the lateral surface of which a neutron flux falls uniformly (Fig. 11.2), then the full area of cross section of all the nuclei found in this volume, will be $N\sigma$ cm^2, where N – number of all nuclei in 1 cm^3. Probability of collision of neutrons with nuclei would be equal to

$$\frac{N\sigma}{1} = N\sigma.$$

In reality the number of effective collisions leading to fission exceeds this number.

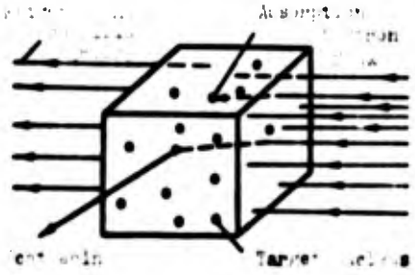

Fig. 11.2. Diagram of the interaction of neutron flux with nuclei.

Let us assume that σ_s – cross section of scattering, considering the number of collisions during elastic scattering and during passage without a collision; σ_a – cross section of absorption, considering all cases of collisions, ending in fission and radiative capture. Values σ_s and σ_a are the measure of probability of reactions of scattering and absorption. Full probability of collision

$$\sigma_t = \sigma_s + \sigma_a.$$

Values σ_s, σ_a, and σ_t pertain, as was indicated, to one nucleus and one neutron; these are microscopic sections and they correspond to one energy level of neutrons or average energy level of neutrons participating in the reaction.

Areas of nuclei have an order of 10^{-24} cm^2. For U-235 the area of the nucleus is equal to $\sigma = 2 \cdot 10^{-24}$ cm^2.

Experience shows that for U-235 the full probability of collision with slow neutrons comprises $\sigma_t \approx 698 \cdot 10^{-24}$ cm^2, i.e., a value 349 times greater than the area of the nucleus. Exactly in connection with this the remark was made concerning the conventionality of a purely geometric determination of probability of collisions.

For simplification of recording the value 10^{-24} cm^2 it is called a barn; in this case $\sigma_t \approx 698$ barns.

The value σ_a includes probable cross sections of fission σ_f and probable cross sections of radiative capture $\sigma_a - \sigma_f = \sigma_r$.

In Table 11.1 microscopic sections for slow neutrons are given for certain substances.

Table 11.1. Cross section of certain substances (slow neutrons).

-	8,2	7,73	4,22	3,51
U-235	15,0	683±3	582±4	101,0
U-238	8,3	2,75	0	2,75
U-233	8,2	576±4	525±4	53,0
Pu-239	10,0	1028±8	742±4	286
H	38,0	0,33	—	0,33
Be	7,0	0,01	—	0,01
Cd	7,0	2400	—	2400
B	4,0	750	—	750
C	4,8	0,0032	—	—
	7,0	0,00046	—	0,00046

If from one neutron and one target nucleus we switch to N nuclei, then $N\sigma = \Sigma$ pertains already to 1 cm^2 and represents a macroscopic section. Accordingly Σ_s, Σ_a, Σ_f – macroscopic cross sections of scattering, absorption, and fission.

For a different energy level of neutrons and for various media (target nuclei) values σ_s, σ_a, and σ_f (and accordingly Σ_s, Σ_a, and Σ_f) will be various. For example, for fast neutrons in uranium U-235 based on experiments the cross section of scattering is equal to $\sigma_s = 3.97$ barns; cross section of absorption $\sigma_a = 0.33$ barns, where fission cross section is equal to $\sigma_f = 0.29$ barns and radiative capture cross section $\sigma_r = 0.04$ barns.

For uranium in a mixture with other substances these values will be different.

Since 1 mole of substance contains $N_a = 6.023 \cdot 10^{23}$ atoms (Avogadro number), then the number of nuclei in 1 cm^3 will be

$$N = \frac{\gamma N_a}{m},$$

where γ – weight density of gf/cm^3; m – atomic or molecular weight.

For example, for U-235 (γ = 18.7 gf/cm^3 and m = 235) the value

$$N = 0{,}05 \cdot 10^{24}\ 1/c.м^3.$$

In this case macroscopic absorption cross section for slow neutrons will be

$$\sum = N\sigma_a = 0.05 \cdot 10^{24} \cdot 683 \cdot 10^{-24} = 34{,}15\ 1/c.м.$$

Cross sections σ_s and σ_a (or Σ_s and Σ_a) are the most important characteristics of nuclear and structural materials in nuclear engineering.

During nuclear fission neutrons are liberated. For each neutron, absorbed by a target nucleus of fissionable material, 2-3 neutrons are liberated; exactly this circumstance makes it possible to carry out both the valuable fast-flowing fission reaction (bomb), and also the calm, stationary fission reaction by means of removal of superfluous neutrons (reactor).

Statistical investigations show that on one initial neutron during one splitting the number of completely liberated neutrons comprises:

for U-235.....ν = 2.43 ± 0.02
" Pu-239.....ν = 2.89 ± 0.03
" U-233.....ν = 2.51 ± 0.02

Part of the liberated neutrons vanishes as a result of radiative capture by the fissionable material itself. Based on experimental data for every one splitting taking into account radiative capture free neutrons are emitted:

for U-235.....η = 2.07 ± 0.01
" Pu-239.....η = 2.08 ± 0.02
" U-233.....η = 2.28 ± 0.02
" natural uranium.....η = 1.34

Consequently, radiative capture lowers the free number of neutrons in a system. Statistically per splitting of U-235 by means of radiative capture 2.43 - 2.07 = 0.36 neutrons vanish from the system; the ratio of effective cross section of radiative capture to effective cross section of division for U-235 will be

$$\alpha=\frac{0,36}{2,07}\approx 0,175.$$

The bond between ν, η, and α is determined by the formula

$$\eta=\nu\frac{1}{1+\alpha}. \qquad (11.1)$$

The majority (>99%) of neutrons is emitted by fragments approximately in the period 10^{-12} s after division; these neutrons are called prompt. Less than 1% of all neutrons is emitted from certain fragments during the period 0.5-60.0 s after division; these are delayed neutrons.

Prompt neutrons have a various energy level. Distinguished are fast neutrons with tremendous energy (>1000 eV) and slow or thermal neutrons (<1 eV). In the last case their energy is comparable with the kinetic energy of molecules of gas. The energy of fast neutrons is most frequently >1 MeV, while the energy of thermal neutrons most frequently is $\leq$0.025 eV. Between thermal and fast neutrons there are neutrons with various intermediate levels of energy (from 1 to 1000 eV). Velocity distributions (energies) of neutrons have a similarity with the function of Maxwell distribution. Although there are many neutrons with an energy of 2-8 MeV, the most probable energy level is ~1 MeV.

Fast neutrons through a series of collisions with nuclei of certain substances (moderators) lose their speed and can become slow neutrons. In many nuclear processes namely slow neutrons are needed. For slow or thermal neutrons the correctness of velocity distribution based on Maxwell is also assumed. The most probable velocity comprises around 2200 m/s; this speed corresponds to a temperature of +25°C of neutron gas and energy

$$E=\frac{1}{2}M_n v^2=\frac{1}{2}1{,}66\cdot10^{-24}(2{,}2\cdot10^5)^2=4\cdot10^{-14}\ \text{erg},$$

or

$$E=0{,}025\ \text{eV};$$

here $M_n = 1.66\cdot10^{-24}$ – mass of neutron.

Delayed neutrons have important value for controlling the reactor; their energy comprises 0.25-0.70 MeV, depending on source (fission fragment). Six groups of delayed neutrons with a various time of yield have been established.

Slow neutrons divide the nucleus of U-235, Pu-239, and U-233, although these nuclei can also be divided under the influence of fast neutrons. Nuclei of U-238 and Th-232 are more capable of being divided under the influence of fast neutrons with considerable energy (>1 MeV). Thus, for example, for natural uranium fission cross section comprises ~0.015 barns at an energy level of neutrons of 1 MeV, while for thermal neutrons the cross section of fission is equal to 4.22 barns.

By converting fast neutrons in thermal with the help of moderators, it is possible to essentially decrease radiative capture of slow neutrons U-238.

A substance, which is able with a small number of collisions to lower the speed of fast neutrons to the level of thermal, is called, as was indicated, a moderator. As moderators substances are used which have no capacity for absorption of neutrons or, as far as possible, have a very small cross section of absorption. The main problem is to lower speed with the help of the process of elastic scattering.

Let us assume that M_n and M – masses of neutron and nucleus of moderator; v_0 – initial neutron velocity; speed of moderator nucleus will be considered equal to zero. During central impact (head-on collision), if V and v – speed of nucleus and neutron after impact,

it is possible to write the equations of conservation of energy and conservation of momentum and obtain:

$$v = -v_0 \frac{M - M_n}{M + M_n}. \qquad (11.2)$$

If E_0 and E – energy of neutron before and after impact, then the ratio of these values after central impact will be

$$\frac{E}{E_0} = \frac{M_n v^2}{M_n v_0^2} = \left(\frac{M - M_n}{M + M_n}\right)^2,$$

or

$$\frac{E}{E_0} = \left(\frac{\frac{M}{M_n} - 1}{\frac{M}{M_n} + 1}\right)^2. \qquad (11.3)$$

The mass of a neutron is close to a unit. The closer the value M to M_n, i.e., the lighter the nucleus of the moderator, the less the ratio (11.3) and, consequently, the greater the energy lost by a neutron during one collision. For example, for graphite

$$\frac{E}{E_0} = \left(\frac{12 - 1}{12 + 1}\right)^2 \approx 0{,}72;$$

for hydrogen

$$\frac{E}{E_0} = \left(\frac{1 - 1}{1 + 1}\right)^2 = 0,$$

i.e., a neutron can lose all its energy during one central collision with a nucleus of hydrogen. Thus the lighter the moderator, then with other things being equal the more effective it is.

We examined the simplest case of central impact. In reality there will be cases of impacts at an angle (lateral impacts), and also cases of flight past a nucleus ("miss"). In the last case energy of the neutron will remain constant; during lateral impact, at an angle, the neutron will lose less energy than in the case of a head-on collision. In view of this, for real process it is necessary to operate with the value of average loss of energy. This

value is statistical, considering all possible forms of encounter of a neutron with target nuclei. The value of average logarithmic decrement of energy for one collision is used, or the value of average change of natural logarithm of energy:

$$\xi = \overline{\ln \frac{E_1}{E}}.$$

For approximate calculations it is possible to consider

$$\xi = \frac{2}{M+1},$$

where M – mass of target nucleus. For light nuclei (small M) losses of energy are great. In the given moderator during each collision a neutron loses an identical portion of its energy practically independently of the energy level.

Knowing ξ, one can determine necessary average number of collisions C for decreasing the energy of a neutron to an assigned level with the help of a given moderator. Let us assume, for example, that a fast neutron has the energy $E_1 = 2$ MeV; in order to decrease this energy to value $E_2 = 0.025$ eV, it is necessary to have an average number of collisions

$$C = \frac{\ln \frac{E_1}{E_2}}{\xi}. \qquad (11.4)$$

For graphite

$$\xi \approx \frac{2}{12+1} \approx 0{,}159;$$

$$C_C = \frac{\ln \frac{2 \cdot 10^6}{0{,}025}}{0{,}159} = 114;$$

for hydrogen

$$\xi \approx \frac{2}{1+1} = 1;$$

$$C_H = 18.$$

Here C_H is much less than C_C (since $M_H < M_C$); but C_H is much greater than a unit, corresponding to a case of central impact; thus a head-on collision is realized rarely.

An ideal moderator will be that which does not absorb neutrons ($\sigma_a = 0$; $\sigma_s = \infty$) and lowers the energy of fast neutrons to the required level during one collision and with the least value of path length (diffusion) of fast neutrons. The delaying capacity of the moderator can be judged by the average logarithmic decrement ξ of energy for one collision;

- by the number of collisions C;

- by the coefficient of deceleration, presenting the relationship $k_з = \xi\Sigma_s/\Sigma_a$, i.e., the ratio of macroscopic moderating power of a substance to macroscopic absorption cross section; in other words, moderating ratio shows the number of effective (delaying) collisions for one absorption.

In Table 11.2 are given the values of magnitude ξ, C, and $k_з$ for various moderators. Value ξ by itself is insufficient, since different scattering and absorbing capacity of moderators can respond to identical values of ξ.

Table 11.2. Moderating properties of certain substances.

Substance	ξ	C	$k_з$	Substance	ξ	C	$k_з$
Hydrogen	1	18	66	Carbon	0.158	114	169
Water	0.927	19	67	[illegible]	0.1[illegible]	1[illegible]	[illegible]
Deuterium	0.725	[illegible]	> 5810	[illegible]	0.1[illegible]	150	[illegible]
Heavy water	0.510	[illegible]	[illegible]	Fluorine	0.102	1[illegible]	> [illegible]
Helium	0.525	[illegible]	64	Lithium	0.268	67	Insignificant
Beryllium	0.209	[illegible]	160				[illegible]
				Boron	[illegible]	[illegible]	[illegible]

From Table 11.2 it follows that from the point of view of dimensions of the reactor the best moderator is heavy water, for which $k_з > 5820$, and the number of collisions is small. However, it is necessary to consider that heavy water, deuterium, and water limit the maximum possible temperature of the reactor even during application of very high pressures. Selection of moderator should

be made taking into account the temperatures of working substance required in the power propulsion system, circuit of the atomic installation, and weight and dimensions of the reactor.

Let us assume that n – number of neutrons in 1 cm^3, and velocity of each neutron is identical in value and direction and is equal to v cm/s. Then the number of neutrons, intersecting in 1 s an area of 1 cm^2 in a direction perpendicular to velocity, will be

$$\phi = nv \text{ neutrons/cm}^2 \text{ s}. \qquad (11.5)$$

Value ϕ represents density of neutron flux, or simply neutron flux. In reality neutrons have various values and directions of velocity. However, in any direction an encounter of a neutron with a nucleus gives an identical result. This makes it possible to examine value ϕ as neutron flux in a concrete case, under the condition that the average velocity for neutrons is taken or that neutrons with identical velocities are considered.

If one were to take for a concrete example the neutron flux $\phi = 10^{13}$ neutrons/cm^2 s, and for velocity of slow neutrons $v = 2.2 \cdot 10^5$ cm/s, then the number of neutrons in 1 cm^3 of volume in this case will be

$$n = \frac{\phi}{v} = 4{,}5 \cdot 10^{7} \text{ neutrons/cm}^3.$$

This number seems very large, but it is $6 \cdot 10^{11}$ times less the number of molecules (or atoms) of gas in 1 cm^3 under normal conditions ($2.7 \cdot 10^{19}$).

In nuclear engineering, besides number of collisions necessary for moderation of fast neutrons, there is also interest in the average distance on a straight line, or average path length, of a fast neutron from the moment of its formation to the moment when it becomes thermal. This average distance is designated by L_f and is called length of diffusion of fast neutrons, or moderation length.

Theoretically the mean free path of a neutron between two collisions with a target nucleus is equal to

$$\lambda_s = \frac{1}{\Sigma_s}, \tag{11.6}$$

where Σ_s – macroscopic cross section of scattering for a given substance and for a given average level of energy of neutrons.

Based on the statistical theory of Fermi (theory of "age") the square of length of diffusion for fast neutrons, or the square of moderation length, is equal to

$$L_f^2 = \frac{\lambda_{tr}\lambda_s C}{3}, \tag{11.7}$$

where λ_{tr} – real ("transport") length of free path of neutron.

Value

$$L_f^2 = \tau \tag{11.8}$$

is called age of neutrons (based on Fermi). If the age of thermal neutrons is known, then from equation (11.8) the length of diffusion, or moderation length of fast neutrons to thermal is also known.

In the theory of nuclear reactors it is proven that

$$d\tau = -\frac{\lambda_{tr}\lambda_s}{3\xi}\frac{dE}{E},$$

from which, considering (for a substance with a large number of collisions)

is obtained

$$dC = \frac{1}{\xi}\frac{dE}{E},$$

$$d\tau = -\frac{\lambda_{tr}\lambda_s dC}{3}.$$

After integration from 0 to a full number of collisions C, which is necessary for moderation, expression (11.7) is obtained if λ_{tr} and λ_s are constants, and the age of neutrons at the initial moment $\tau = 0$.

In expression (11.7) the product of $\lambda_s C$ represents the rectified overall path length of a neutron from assigned level of energy (for example, at the time of division) to the energy of a thermal neutron.

By reasoning in the same way, one can determine the length of diffusion of thermal neutrons – the average distance along a straight line, or the average path length of a thermal neutron from the moment of its formation to the moment of its capture. Free path length of a thermal neutron up to its collision with a target nucleus (and absorption by it), just like expression (11.6), will be

$$\lambda_a = \frac{1}{\Sigma_a}, \qquad (11.9)$$

where Σ_a – macroscopic cross section of absorption for thermal neutron in the given medium. In the same way equation (11.7) can be written for the square of length of diffusion of thermal neutrons ($C = 1$):

$$L_t^2 = \frac{\lambda_{tr}\lambda_a}{3}$$

or, considering $\lambda_{tr} = 3\lambda_a$

$$L_t^2 = \lambda_a^2. \qquad (11.10)$$

Formulas (11.7) and (11.10) make it possible to calculate length of diffusion of fast and thermal neutrons and average time t of their life.

In Table 11.3 are given for certain media (moderators) the age of neutrons τ, length of moderation L_f, and moderation time t_f of fast neutrons, length L_t and diffusion time t_t of thermal neutrons.

Table 11.3. Age, length, and time of diffusion.

Medium	τ, cm²	L_f, cm	t_f, s	t_t, s	L_t, cm
Water	33	5.7	10^{-6}	$2.1 \cdot 10^{-4}$	2.88
Heavy water	120	11.0	$4.6 \cdot 10^{-5}$	0.15	171
Beryllium	98	9.9	$6.7 \cdot 10^{-5}$	$4.3 \cdot 10^{-3}$	24
Graphite	350	18.7	$1.5 \cdot 10^{-4}$	$1.2 \cdot 10^{-2}$	50
Beryllium oxide	143	12.0	$7.8 \cdot 10^{-5}$	$6.8 \cdot 10^{-3}$	

11.2. Basic Information About Reactors

The process of calm, controlled fission of heavy nuclei is carried out in reactors. Nuclear reactors can be classified according to the following criteria:

1. Based on energy level of neutrons utilized for division the reactors can be for fast, thermal, and intermediate neutrons.

2. According to the nature of fissionable material the reactors can be for natural uranium, for uranium enriched by isotope U-235, and for pure fissionable materials U-235, Pu-239, and U-233.

3. According to the nature of cooling substance nuclear reactors can be with water, heavy water, liquid metals (and their alloys), and gases.

4. According to the nature of moderator nuclear reactors for thermal neutrons can be aqueous, with heavy water, graphite, beryllium and its oxide, and others.

5. According to the nature of location of fissionable material and moderator reactors can be heterogeneous, when fissionable material is placed in the reactor core in the form of separate blocks, and homogeneous, when fissionable material is evenly distributed throughout the volume of the reactor.

6. Based on assignment reactors can be research (for carrying out of separate experiments), power (for production of energy), regenerative (for production of Pu-239 or U-233) and combined (for simultaneous obtaining of energy and fissionable material).

Fast-neutron reactors depending upon assignment can be with a moderator and without a moderator. Thermal-neutron reactors always have a moderator.

If the internal volume of the reactor is occupied by fissionable material and moderator it is called the core. The core also contains the rods, controlling the speed of the process of division and ensuring safety of the reactor.

Heterogeneous reactors are used widely at present on stationary installations for the output of electric power and for other purposes.

Heterogeneous reactors are made with a metallic shell for uranium elements. Since uranium has three modifications (rhombic, tetragonal, and cubic) with transition points at 660 and 800°C, the temperature of uranium, maximally permissible for construction of thin-walled shells, has to have a limit. In connection with this heterogeneous reactors with metallic shells of elements are useful for relatively low-temperature power plants. For production of high-temperature heterogeneous reactors new technological methods of shielding of fuel elements are required.

In a homogeneous reactor the nuclei of fissionable material are uniformly placed in the volume of the core. If in the homogeneous reactor there is a moderator, then the nuclear fuel and moderator represent an alloy, a chemical compound, a solution, or a thin uniform suspension. With a specific combination of nuclear fuel and moderator and definite temperatures the structural materials of the core of a homogeneous reactor cannot change their aggregate state; in this case heat from reactor is carried away with help of some cooling agent. Material of the core can be brought to fusion or boiling; then with the help of special pumps the liquid or vaporous

material of the core is passed through a heat exchanger, in which it gives off heat in the required amount to working substance of the power plant. A reactor with this principle is also called "boiling reactor," if in it all of the working substance or one of its components is brought to boiling. A homogeneous reactor in general has a simpler construction than heterogeneous.

For producing high temperatures substances with a low temperature of boiling or vaporization cannot be used as moderators in the core of the reactor.

A homogeneous high-temperature reactor, in which the core is a solid homogeneous body with a very high melting point, with channels for a liquid coolant can be used for light transport installations.

Due to the necessity to have a considerable amount of moderator the core in thermal-neutron reactors is large. Average quantity of heat liberated per 1 liter of core volume comprises $(1.7\text{-}6.0)\cdot 10^4$ Cal/h, which corresponds to a power of 20-70 kW. In fast-neutron reactors there is less moderator or none at all. This makes it possible to increase the quantity of liberated heat per unit of volume of core by 20 and more times in comparison with reactors on thermal neutrons. The main point here lies in the possibility of heat removal from reactor while preserving the maximum temperature of the reactor on the permissible level. For this it is required to develop surfaces of heat exchange depending on the properties and state of the coolant. It is precisely the problem of heat removal which determines the dimensions of the core for a fast-neutron reactor. Such reactors serve for research purposes or as source of fast neutrons for obtaining plutonium Pu-239 from isotope U-238 or U-233 from thorium Th-232.

There are reactors on fast neutrons with the pure isotope U-235 or Pu-239 with mercury cooling (melting point -39°C), cooling by sodium, potassium, sodium-potassium alloy, and others. The amount of liberated heat per 1 liter of core volume reaches $(10\text{-}12)\cdot 10^6$ Cal/h.

Neutron flux in reactors with fast neutrons comprises a maximum of 10^{13}-10^{15} neutrons/cm^2 s.

Multiplication factor of neutrons. The ratio of the number of newly formed neutrons to number of the previous generation of neutrons which caused the process of division is called the multiplication factor. From experience constants ν and η for fissionable materials and the connection between them are known (11.1). For each division there are η free fast neutrons with various levels of energy.

A certain number of fast neutrons leads to nuclear fission, which is considered by fast multiplication ε. For a thermal-neutron reactor and for natural uranium $\varepsilon = 1.03$; for enriched uranium $\varepsilon \approx 1.0$. For homogeneous reactors $\varepsilon \approx 1.0$ due to rapid moderation of neutrons. For a reactor with pure metallic uranium without a moderator the maximum value $\varepsilon = 1.2$. Consequently, total number of fast neutrons for 1 effective (leading to division) thermal neutron will be $\eta\varepsilon$.

Let us assume that p – share of fast neutrons, which in the process of moderation are not captured; in other words, p – probability to avoid radiative capture. Then the quantity of fast neutrons, moderated to the level of thermal neutrons, per 1 fission event will be $\eta\varepsilon p$. For reactors with pure fissionable isotopes value $p = 1$. For heterogeneous reactors with natural uranium $p = 0.85$-0.95.

After the process of moderation some (1 - f) of the thermal neutrons can be absorbed by structural elements of the reactor. If f – share of thermal free neutrons, in other words f – probability for thermal neutrons to avoid unproductive absorption, then for each 1 fission event there remains $\eta\varepsilon pf$ free thermal neutrons.

Coefficient f represents the ratio of number of thermal neutrons, absorbed in the fissionable isotope, to all the number of thermal neutrons, absorbed by the fissionable isotope, the moderator, and

structural materials. In the case of a homogeneous reactor without structural materials in the core

$$f=\frac{\Sigma_{д.м}}{\Sigma_{д.м}+\Sigma_{з}},$$

where $\Sigma_{д.м}$ – cross section of absorption for fissionable material; $\Sigma_{з}$ – the same for the moderator.

For uranium and graphite, for example:

$$\Sigma_{U}=0{,}351\ 1/см;\quad \Sigma_{C}=3{,}72\cdot10^{-4}\ 1/см;$$

therefore

$$f\approx0{,}904.$$

In examining a reactor of infinitely large dimensions and disregarding therefore leakages of neutrons from the system, we obtain a multiplication factor in an infinite medium:

$$k_{\infty}=\eta\varepsilon pf. \qquad (11.11)$$

Let us assume for example that in a heterogeneous thermal-neutron reactor $\eta = 1.34$; $\varepsilon = 1.03$; $p = 0.9$, and $f = 0.9$; for such a reactor of infinitely large dimensions

$$k_{\infty}=1{,}1,$$

i.e., a chain reaction can be developed, since $k_{\infty} > 1$ and the number of neutrons of the new generation exceeds the number of neutrons of the old generation.

Since η and ε are constants for nuclear fuel, then the value k_{∞} is determined by values of probabilities p and f, which depend on many factors (composition of medium of reactor, geometric form of lattice of core, and others).

For a reactor with pure U-235 and without a moderator – $\varepsilon = 1$, $p = 1$, $\eta = 2.08$; in addition to that $\Sigma_з = 0$ and

$$f=\frac{\Sigma_U}{\Sigma_U+\Sigma_a}=1,$$

therefore

$$k_\infty=2{,}08.$$

Transition to a reactor of finite dimensions requires an additional calculation loss of fast and thermal neutrons to the outside environment through the shell of the reactor. For decreasing these losses the reactor is furnished with material which is impervious for neutrons. A shell from such material (graphite, beryllium, and others) is called a reflector.

Full probability to avoid leakage in a finite medium

$$B=B_fB_t,$$

where B_f – probability to avoid leakage of fast neutrons; B_t – probability to avoid loss of thermal neutrons.

Values B_f and B_t depend on geometric dimensions, form, and construction of the reactor, nuclear properties of material of the reflector, and on the nature of movement of neutrons in the reactor.

In nuclear physics methods have been developed of calculation of values B_f and B_t:

$$B_f=e^{-K^2L_f^2}; \qquad (11.12)$$

$$B_t=\frac{1}{1+K^2L_t^2}. \qquad (11.13)$$

Here $L_f^2 = \tau$ – "age," or square of length of diffusion (moderation) of fast neutrons; L_t – diffusion length of thermal neutrons; K^2 – geometric parameter, considering the dimensions and form of reactor.

Knowing the probabilities of B_f and B_t and being able to calculate k_∞ by the formula (11.11), one can determine effective multiplication factor $k_{эфф}$ for a reactor of finite dimensions with known form and dimensions:

$$k_{эфф} = k_\infty B_f B_t. \qquad (11.14)$$

For the possibility of carrying out a stationary process of division in a reactor of finite dimensions it is necessary to have $k_{эфф} > 1$.

Let us give for clarity a diagram, illustrating the neutron balance in a reactor of finite dimensions, relating it to one initial neutron leading to a fission event (Fig. 11.3).

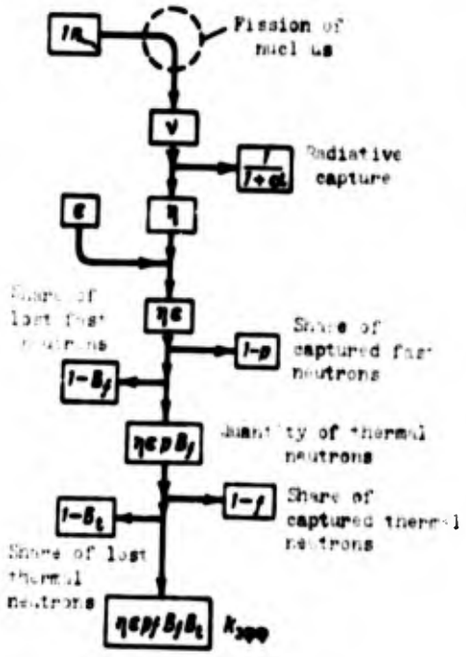

Fig. 11.3. Diagram of neutron balance.

Neutron flux in a reactor is unequal and depends on type of reactor, its form, and construction. If the source of neutrons was very small and in direct proximity to it (in the limit – in the center of the source) the neutron flux was equal to ϕ_0, then with removal from the source the neutron flux will be less.

In a reactor with a core of finite dimensions the losses of neutrons would be great, if a reflector were not set up, the mission of which would be to reflect neutrons back into the core without absorption. The ratio of number of reflected neutrons to total numoer of neutrons reaching the surface of the reflector is called reflection factor A or albedo. Value A is a function of length of diffusion and transport mean free path; furthermore, albedo depends on the material, form, and dimensions of the reflector. For a reflector of unlimited dimensions the value of albedo is given in Table 11.4.

Table 11.4. Reflectivity.

Substance	Weight density, gf/cm^3	Reflectivity (albedo)
Water	1.00	0.82
Heavy water	1.10	0.97
Beryllium	1.84	0.89
Beryllium oxide	2.80	0.93
Graphite	1.60	0.93

If thickness of reflector is limited, then the value of reflectivity will decrease comparatively with the data in Table 11.4. However, with a thickness of reflector 2-3 times greater than the length of diffusion of neutrons the relative decrease of albedo will be small. A reflector gives another advantage in that, by decreasing loss of fast and thermal neutrons from the system, it returns neutrons to the peripheral sections of the core; thanks to this the change of neutron flux in a transverse and longitudinal section of the reactor decreases, which is very important for practical purposes. In Fig. 11.4 is shown how in principle neutron flux in a bare reactor and one with a reflector is changed.

Critical mass of core of any reactor is the name given to that quantity of mass, which at given dimensions and form of core and at given relationships of different substances in it, and also with concrete dimensions and material of the reflector, ensures an effective multiplication factor $k_{эфф} = 1$.

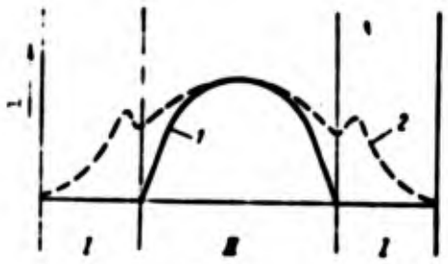

Fig. 11.4. Change of neutron flux in a reactor with a reflector and without it: I – reflector; II – cores; 1 – without reflector; 2 – with reflector.

As was already indicated, the application of reflectors ensures a condition of criticality of the reactor with smaller core dimensions by reducing or eliminating loss of neutrons; furthermore, reflectors level neutron flux inside the reactor, thus increasing the ratio of average neutron flux in the reactor on the whole to maximum neutron flux.

Relative change of neutron flux based on relative distance from the center of the core along the axis of the reactor, having the form of a sphere, cylinder, and parallelepiped, is shown in Fig. 11.5. Practically for these three different forms of reactors the law of change along the axis of reactor is identical and is expressed by the law of cosine. Setting up of a reflector, as it was shown, has the result that on the periphery of the core of the reactor $\phi > 0$.

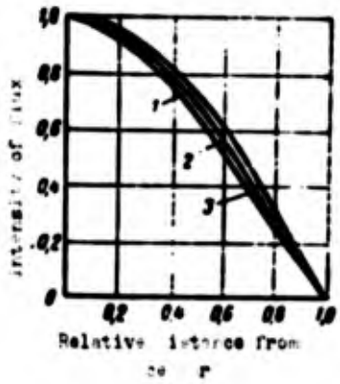

Fig. 11.5. Relative distribution of neutron flux in reactors: 1 – parallelepiped; 2 – cylinder; 3 – circle.

Irregularity of neutron flux in transverse and longitudinal sections is undesirable, especially in those cases, when it is necessary to have a uniform field of temperatures of working substance

heated in the reactor. Furthermore, decrease of neutron flux in the end section of the reactor (based on flow of heated gas) makes this section little effective. It is possible to correct this deficiency either by nonuniform distribution of fissionable material or the absorber of neutrons in the space of the core, or by a change of cross sections for the cooling agent. These solutions involve an increase of weight and dimensions of the reactor.

Critical mass is determined by many factors.

1. Dimensions and form of the reactor. Since losses of neutrons are proportional to surface F_a of the reactor core, and liberation of neutrons is proportional to its volume V_a, then other things being equal the greater the dimensions of the reactor, the less the relative losses of neutrons through the surface.

The less the ratio F_a/V_a at assigned core mass, the less the loss of neutrons. Minimum ratio F_a/V_a is attained in a spherical reactor; consequently, other things being equal a spherical reactor will have minimum critical mass.

For a cylinder or, for example, a plate there are those relationships between height and area of base, when losses of neutrons are excessively great and it is impossible to achieve critical mass. As an example in Fig. 11.6 the change of critical mass and height for a cylindrical reactor is shown. It is clear that at relatively small diameters of the base or, conversely, at relatively small heights of a cylinder critical mass attains infinity. Based on this is the storage of nuclear fuel, taking into account the proximity of other masses of fissionable material.

2. Relationship of isotopes of fissionable materials. Radiative capture, or absorption, of neutrons without division is carried out by the isotope U-238 (or thorium); consequently the dimensions of the reactor depend on the quantity of these isotopes in the core. Critical mass of the reactor decreases with enrichment of uranium with isotope U-235 and it becomes minimum for pure U-235 (or Pu-239).

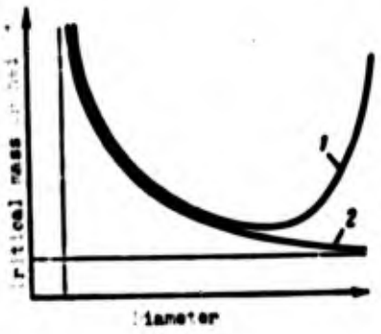

Fig. 11.6. Change of critical mass and height of cylindrical reactor depending on diameter: 1 – critical mass; 2 – height.

3. Moderator. Critical mass of a reactor also depends on the presence or absence of a moderator, on the relative quantity of it, and the type of moderator. If the reactor operates on thermal neutrons, then introduction of a moderator accelerates the process of lowering the energy level of neutrons and in known limits decreases critical mass of the reactor, and also the necessary concentration of fissionable material. The more effective the moderator, the less of it it is required to have and the smaller the dimensions of the reactor. With an assigned type of moderator there is a limit, above which an increase of concentration of moderator at first no longer exerts an influence on critical mass of the reactor, and then even increases it. An excessive quantity of moderator increases the absorption of neutrons by it. At a certain concentration of moderator the capture of neutrons by it can completely compensate for multiplication of neutrons as a result of division. In this case critical mass increases ad infinitum.

For an illustration in Fig. 11.7 is shown the change of critical mass of a spherical reactor depending on relative quantity of moderator.

4. Construction of reactor. Elements of construction, necessary for strength, cooling, regulation, and control, can absorb neutrons to a greater or lesser degree; due to this there will be a change in critical mass of the reactor. Here the concept of construction includes not only the dimensions and form of structural elements, but also materials from which they are made.

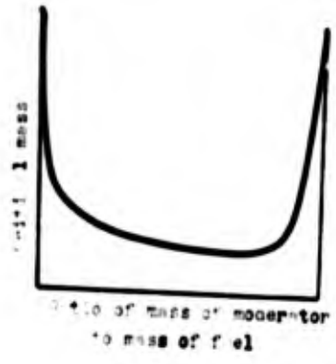

Fig. 11.7. Change of critical mass of spherical reactor depending on relative quantity of moderator.

5. Material and dimensions of reflector. They have a direct influence on neutron balance of reactor and, consequently, on its critical mass.

6. Duration of continuous operation. This influence is explained by the fact that division fragments "poison" the reactor, gradually lowering its coefficient of reactivity. The most harmful are those fragments which form in a greater quantity and are inclined to radiative capture of a neutron (for example, xenon – "xenon poisoning"). Initial coefficient of reactivity should be designated in such a manner that, taking into account duration of continuous work, especially under conditions of exploitation, when access to the reactor is excluded, toward the end of work it is $k_{эфф} \geq 1$.

Reactors which operate with frequent stops in the process should have an additional reserve of reactivity, which will be understandable from what follows.

Dimensions of the reactor also depend on energy level of neutrons, leading to division (fast, thermal, intermediate).

Coefficient of reactivity, or reactivity, of a reactor is the name given to the value

$$\rho = k_{эфф} - 1 = k_{изб} \qquad (11.15)$$

For reactor on steady-state operation $\rho = 0$; under conditions of increasing the power of the reactor $\rho > 0$, and under conditions of reducing power $\rho < 0$.

Effective multiplication factor $k_{эфф}$ and, consequently, coefficient of reactor reactivity depends on temperature, i.e., $\rho = \alpha T$, where value α – temperature coefficient of reactivity.

At $\alpha > 0$ with an increase of temperature in the core the reactor is accelerated, i.e., its power grows continuously, since there is an increase of neutron flux. At $\alpha < 0$, conversely, with an increase of temperature of the core the power of the reactor decreases due to a decrease of neutron flux. In homogeneous reactors an increase of temperature expands the substance in the core, as a result of which the concentration of fissionable material and moderator decreases, and coefficient of reactivity decreases. To ensure the stability of the process in the reactor at $\alpha > 0$ and $\alpha < 0$ it is necessary to control the reactor.

Reactors with $\alpha > 0$ in the event of disruption of the control system during operation are inclined to an increase of coefficient of reactivity with an increase of temperature. Due to this such reactors can cross border of permissible values of maximum temperatures, which as a result of self-acceleration of the fission reaction will lead to breakdown of the reactor with possible ejection of dangerous radioactive products in any phase, including gaseous.

The greater the reactor reactivity, the more rapidly the neutrons are multiplied, and the more responsible process of starting and regulation of reactor power. Value of initial reactor reactivity with selected materials and construction depends on assignment of reactor, duration of operation operating conditions, frequency, and conditions of shutdowns.

Let us assume that $\bar{\tau}$ – average lifetime of neutrons of one generation in s; then relative increase of number of neutrons in

1 s, or increase of number of neutrons in 1 s for n neutrons expended for division will be

$$\frac{dn}{d\tau}=\frac{nq}{\tau} \quad \text{or} \quad \frac{dn}{n}=\frac{q}{\tau}d\tau.$$

After integration, considering $n = n_0$ for $\tau = 0$:

$$n=n_0e^{\frac{q}{\tau}\tau}. \qquad (11.16)$$

Disregarding slowing-down time of fast neutrons as small in comparison to time of diffusion of slow neutrons (see Table 11.3), it is possible for prompt neutrons to consider lifetime equal to diffusion time of thermal neutrons and to determine this time by the formula

$$\bar{\tau}=\frac{\lambda_a}{v}=\frac{1}{v\Sigma_a},$$

where λ_a – mean free path of thermal neutron up to its absorption;
v – average speed of neutron.

If one were to calculate averaged macroscopic absorption cross section for the whole reactor taking into account leakages and absorption of neutrons by structural materials, then time $\bar{\tau}$ of life of prompt neutrons can be calculated by the formula written above. This time is close to 0.001 s. But prompt neutrons comprise around 99.25% of all neutrons of one generation, since there is still around 0.75% delayed neutrons with an average lifetime or all these neutrons of around 12.24 s. Therefore the lifetime of one generation of neutrons (prompt and delayed) will be

$$0{,}9925\cdot 0{,}001+0{,}0075\cdot 12{,}24\approx 0{,}094 \text{ s}.$$

Consequently, the presence of delayed neutrons increases the lifetime of one generation almost by one hundred times.

Reactor period T is the time, during which neutron flux or number of neutrons in reactor is increased by e times. From expression (11.16) this will be with

$$\frac{\rho}{\bar{\tau}}\tau=1,$$

from which

$$T=\tau=\frac{\bar{\tau}}{\rho}. \qquad (11.17)$$

With $\rho = 0.02$; $v = 2200$ m/s, and $\lambda_a = 40$ cm, value

$$\bar{\tau}=\frac{0,40}{2200}\approx 2\cdot 10^{-4} \text{ s}$$

and

$$n=n_0e^{100\tau}.$$

In 1 s ($\tau = 1$) neutron flux (or number of neutrons) will increase by

$$e^{100}=2,66\cdot 10^{43} \text{ times}.$$

As can be seen, already with such a reactivity neutron flux in 1 s increases very sharply. This example indicates the importance of reliable regulation and control of the reactor. Reactor period for this case will be determined from formula (11.17) and will be equal to

$$T=\frac{2\cdot 10^{-4}}{0,02}=0,01 \text{ s}.$$

Period T, determined by formula (11.17), is not an exact value. Deviation is caused by disregard of slowing-down time of fast neutrons and, especially, the influence of delayed neutrons. If one were to consider the influence of delayed neutrons and accept

$$\bar{\tau}=100\cdot 2\cdot 10^{-4}=2\cdot 10^{-2} \text{ s},$$

then the reactor period in the examined example will be no longer than 0.01 s, and

$$T = \frac{2 \cdot 10^{-2}}{0{,}02} = 1 \text{ s}.$$

Figure 11.8 contains a graph of dependence of reactor period on its reactivity and on average lifetime of neutrons taking into account the influence of delayed neutrons. It can be seen that reactor period decreases strongly with a decrease of $\bar{\tau}$, especially at $\rho > 0.01$.

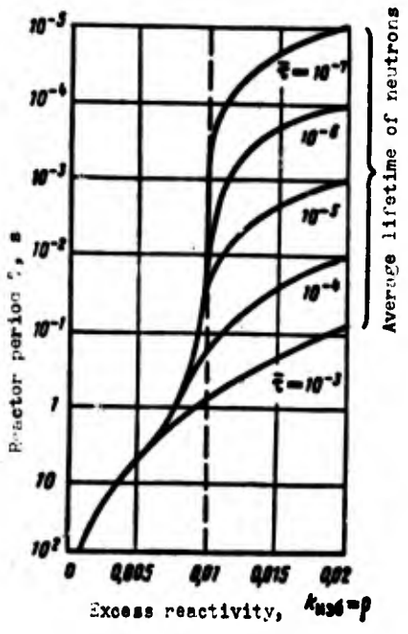

Fig. 11.8. Dependence of reactor period on reactivity and average lifetime of neutrons.

11.3. Power of Reactor. Control. Shielding. Starting.

By power of a reactor is understood the maximum quantity of heat, liberated by a reactor on steady-state operation in a unit of time (for example, in an hour). Power of a reactor relative to power plants is expressed also in kilowatts. Let us assume that $\bar{\phi}$ – average neutron flux in neutrons/cm^2 s; σ_f – microscopic fission cross section in barns; N – number of nuclei of fissionable material in 1 cm^3.

One division gives ≈195 MeV of energy; and 1 MeV = $1.6 \cdot 10^{-13}$ coulomb-volts; therefore 195 MeV ≈ $3.2 \cdot 10^{-11}$ coulomb-volts.

Since 1 W = 1 coulomb-volt in 1 s, then the number of nuclear divisions corresponding to a power of 1 W will be

$$c = \frac{1}{3{,}2 \cdot 10^{-11}} \approx 3 \cdot 10^{10}.$$

The number of divisions in 1 s in volume V_a of the core equals $\bar{\phi}\Sigma_f V_a$, where $\Sigma_f = \sigma_f N$. Therefore power of the reactor will be

$$N_p = \frac{\bar{\varphi}\Sigma_f V_a}{c} 10^{-3} \text{ kW}. \tag{11.18}$$

Thermal power of reactor per hour will be equal to

or
$$Q_p = 860\, N_p \text{ Cal} \tag{11.19}$$

$$Q_p = 2{,}86 \cdot 10^{-11} \bar{\varphi} \sum_f V_a \text{ Cal/h}. \tag{11.20}$$

If volume of the core is expressed in m^3, then

$$Q_p = 2{,}86 \cdot 10^{-5} \bar{\varphi} \sum_f V_a. \tag{11.21}$$

If Σ_f and $\bar{\phi}$ are known, one can determine V_a based on rated value Q_p or, conversely, Q_p based on known V_a.

Average neutron flux $\bar{\phi}$ is always assigned. Value $\bar{\phi} = 10^{13}$–10^{15} neutrons/cm^2 s.

Value Σ_f depends on type and relationship isotopes, and also on the presence of moderator and relative quantity of it in the reactor. Since for thermal neutrons for isotope U-235 value $\sigma_f = 582$ barns, then for it

$$\sum_f = 582 \cdot 10^{-24} N_U.$$

where N_U – number of nuclei of isotope U-235 in 1 cm^3.

If homogeneous thermal reactor is derived on the basis of UO_2 and BeO (as moderator), then with a ratio of $N_{BeO}/N_{UO_2} = 1000$ the number of UO_2 nuclei in 1 cm^3 will be

$$N_{UO_2} = \frac{N_{BeO}}{1000} = \frac{0{,}675 \cdot 10^{24}}{1000} = 6{,}75 \cdot 10^{20} \text{ nuclei/cm}^3,$$

where

$$N_{BeO} = \frac{\gamma_{BeO} N_a}{m_{BeO}} = 0{,}675 \cdot 10^{24} \text{ nuclei/cm}^3.$$

Considering the pure isotope U-235, we obtain

$$\Sigma_f = 582 \cdot 10^{-24} \cdot 6{,}75 \cdot 10^{20} = 3{,}92 \cdot 10^{-1} \text{ 1/cm};$$

with $\bar{\phi} = 10^{14}$ and $\Psi = 0.6$ (where Ψ – considers the free section for flow of reactor coolant), for $V_a = 1\ m^3$ the quantity of heat liberated in 1 hour will be

$$Q_p = 2{,}86 \cdot 10^{-8} \cdot 10^{14} \cdot 3{,}92 \cdot 10^{-1} (1 - 0{,}6) \approx 4{,}5 \cdot 10^6 \text{ Cal/m}^3 \text{ h}.$$

Power of the reactor will be equal to

$$N_p = \frac{4{,}5 \cdot 10^6}{860} \approx 525\,000 \text{ kW/m}^3.$$

Number of moles of uranium dioxide will be

$$\frac{N_{UO_2}}{N_a} = \frac{6{,}75 \cdot 10^{20}}{6{,}023 \cdot 10^{23}} 10^6 (1 - 0{,}6) = 4{,}48 \cdot 10^2 \text{ moles}$$

or ($m_{UO_2} = 267$)

$$4{,}48 \cdot 10^2 \cdot 267 \approx 11{,}8 \cdot 10^4 \text{ kgf}.$$

For 1 kgf of UO_2 the power of the reactor in this case obviously will comprise

$$\frac{526\,100}{118} \approx 4430 \text{ kW/kgf.}$$

Control of reactor power. As was shown, for a stationary process $k_{эфф} = 1$ and $\rho = 0$. It is impossible to have an uncontrolled power reactor, in which calculated effective multiplication factor would be exactly equal to a unit. In the case $k_{эфф} = 1$ it would have been impossible to ensure a stationary process in time in such an uncontrolled reactor. Actually, after starting of the reactor the temperature of its core is changed and, consequently, multiplication factor and coefficient of reactivity are changed. During a positive temperature coefficient of reactivity the reactor with an increase of T would have an increasing value of $k_{эфф}$, which would lead to a continuous increase of neutron flux, power, and temperature of the reactor up to its breakdown from overheating. After breakdown the reactor will present a danger in view of the radiation of neutrons and γ-rays, however there will be no reactor explosion, since the reactor will become subcritical from a change of neutron balance induced by leakages. With a negative temperature coefficient of reactivity a decrease of temperature against calculated makes the reactor subcritical.

It is impossible to make $k_{эфф} = 1$ in an uncontrolled reactor still because the quantity of fissionable material in reactor decreases with the flow of time and, conversely, the quantity of products of division, "posioning" the reactor, increases.

For maintaining the power of the reactor on an assigned level in time and for power control in accordance with needs it is necessary to make a reactor with $k_{эфф} > 1$. In a steady-state operation the excess quantity of neutrons should be removed from the core up to achievement of $k_{эфф} = 1$. Removal of neutrons is carried out by means of their absorption by special controlling or regulating rods made out of materials with a large cross section of capture of thermal neutrons. Such materials are boron, cadmium, and hafnium.

Boron by itself is brittel, therefore the rods are made from boron steels. Boron is preferable to cadmium, since the latter in the event of capture of a neutron is a source of γ-radiation.

If it is necessary to increase the power of the reactor, then regulating rods are set at a lesser depth; conversely, in the event of necessity to decrease the power of the reactor the rods are introduced deeper into the core, as a result of which neutron flux in the reactor decreases. There are two types of controlling or regulating rods - for rough and fine adjustment, i.e., with greater and lesser mass for absorption of neutrons. There are also rods which play the same role as control rods but are specially intended for compensating the effect of poisoning of the reactor.

Besides the channels for regulating rods, it is anticipated that the core also have channels for safety rods made from the same materials. In the event of any defects in the reactor or in the system for its regulation and control the safety rods are automatically introduced rapidly inside the reactor and make it subcritical. Safety rods remain inside the core even when the reactor shuts down; it is planned to have a blocking device, thanks to which the emergency or safety rods cannot be removed from the core until regulating rods are inserted completely.

Transition from one level of power to another, higher one should be gradual, taking into account the properties of the reactor cooling agent, otherwise overheating of the reactor is possible and its going out of commission. Change of reactor power occurs rapdily; a limiter is the inertness of the cooling system. Therefore, in order to avoid overheating and accident, special instruments which record neutron flux (neutron detectors) are mounted on power reactors.

In controlling the reactor the role of delayed neutrons is great; effective multiplication factor should be designated taking the delayed neutrons into account. In the process of increasing the power the number of prompt neutrons increases proportional to the power, but the number of delayed neutrons increases considerably more

slowly, since their formation is connected with former power level, due to the duration of the period of their emission from division fragments. Overall number of neutrons due to this increases more slowly than power of the reactor, which exerts a delaying influence on increase of reactor power.

For U-235 the share of delayed neutrons comprises 0.73%; for Pu-239 this share is equal to 0.364%, and for U-233 total of 0.242%. Thus a reactor with U-235 is more convenient from the point of view of control. In this case, if $k_{эфф}$ does not exceed 1.0073, increase of reactor power is not dangerous; for Pu this value comprises already only 1.00364, and for U-233 – a still smaller value – 1.00242.

If in the reactor the effective multiplication factor for U-235 is equal to 1.0073, for Pu-239 – 1.00364, and 1.00242 for U-233, then the reactor is in a state of "prompt criticality," i.e., a stationary reaction can be maintained on prompt neutrons alone.

Poisoning of reactor. Fission fragments, forming during operation of the reactor, and products of their radioactive decay have large cross sections of capture of thermal neutrons. Due to this with the flow of time the initial neutron balance is disturbed. At the beginning of operation of the reactor there is an increase of harmful products which absorb neutrons; on the other hand, as a result of radioactive decay of fragments and the formation of isotopes, which are transparent with respect to neutrons, there is a decrease in the quantity of harmful absorbers of neutrons. With the flow of time a certain equilibrium concentration of harmful absorbers of neutrons is established, at which the formation rate of new absorbers of neutrons and rate of their disappearances are equal. If one were to consider this factor during assignment of value of effective multiplication factor, then the reactor will work on steady-state operation and will be accessible to control as long as the result of fission of nuclear fuel and gradual poisoning of the reactor do not become subcritical.

The greatest absorption of neutrons is peculiar to isotopes of xenon Xe-135 ($\sigma_a \approx 2 \cdot 10^6$ barns) and samarium Sm-149. Xenon is formed both directly and also as a result of disintegration of a fission fragment of iodine I-135. At neutron fluxes $\phi < 10^{13}$ the accumulation of xenon increases slowly and only around 0.7% of thermal neutrons is absorbed in xenon at equilibrium concentration. If $\phi > 10^{13}$ – the quantity of xenon on equilibrium conditions of its formation and disintegration is increased; at $\phi > 10^{15}$ – xenon already absorbs up to 5% of all thermal neutrons. Xenon poisoning, depending on ϕ, limits the maximum value of neutron flux. During equilibrium concentration of xenon for steady operation of the reactor it is necessary to increase reactivity at most by 0.05 in order to eliminate the harmful influence of xenon.

Equilibrium concentration of samarium which is a product of radioactive decay of promethium Pm-149, forming directly as a fission product, in contrast to xenon practically does not depend on neutron flux. During steady operation of the reactor for removal of the harmful influence of samarium it is necessary to increase reactivity by 0.012. Poisoning of the reactor, although to a lesser degree, is a result also of other fission products (other isotopes of xenon, iodine, strontium, and others).

Poisoning of reactor is strengthened after its shutdown. This is explained by the fact that half-life for iodine I-135 is equal to 6.7 hours, but the half-life of promethium Pm-149 is equal to 47 hours; therefore after shutdown the concentration of stable products of disintegration of xenon and samarium increases, attaining a maximum after many hours after reactor shutdown. The quantity of iodine and promethium depends on conditions of shutdown of the reactor. The more slowly the reactor is turned off, the less the neutron flux before and at the time of shutdown, the less iodine and promethium and, consequently, the less will be the concentration of xenon and samarium. In Fig. 11.9 is shown the change of value, characterizing reactor poisoning, with time at various values of neutron flux. Poisoning represents the ratio of number of thermal

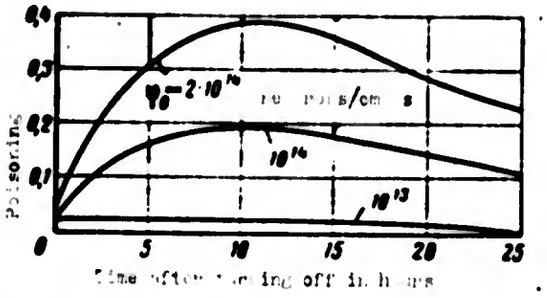

Fig. 11.9. Poisoning of reactor after shutdown in time depending on neutron flux by the moment of turning off.

neutrons, absorbed by fission products, to number of thermal neutrons, absorbed in fissionable material. At $\phi_0 = 10^{13}$ poisoning is less than 0.05; at $\phi_0 = 2 \cdot 10^{14}$ maximum of concentration of xenon is reached in 10-12 hours after turning off, and poisoning already is equal to 0.35-0.40. For repeated starting of such reactor a reactivity greater than 0.35-0.40 will be needed. At $\phi_0 = 10^{14}$ poisoning comprises 0.2 at most. Poisoning of the reactor after shutdown strongly decreases reactor reactivity.

Slow reactor shutdown essentially decreases ϕ_0 and the reactivity required for repeated starting.

General duration of possible operation of a reactor depends on conditions of continuous operation, on the number, conditions, and duration of shutdowns, and on the initial value of reactivity.

Fission fragments, enduring these or other circuits of radioactive decay, will form different stable isotopes ("ashes" or "slag").

Some of these have large cross sections of absorption (7000-50,000 barns) and are formed already soon after operation of the reactor begins. Others, although more weakly, absorb neutrons, but their quantity is relatively greater. Slags, absorbing neutrons (thermal and partly delaying), with flow of time decrease reactor reactivity and may make it subcritical, if in good time measures are not taken

for their removal. In reactors with Pu-239 absorption of neutrons by fission fragments is relatively greater than in uranium reactors.

Heat removal from reactor. In power reactors the basic goal is heating a working substance to the maximum temperature necessary for a thermodynamic cycle. Cooling can be carried out both directly by the working substance of the power plant, and also by other agents, fulfilling the role of intermediate bodies (heat-transfer agents) in system of heat exchange. Basic problems of cooling a reactor are:

1) removal of a quantity of heat, corresponding to the energy liberated in the reactor during nuclear fission on a maximum and any intermediate power level;

2) distribution of circulatory channels of cooling in such a manner that the temperature of material of the core nowhere exceeds the maximum permissible value;

3) ensuring minimum expenditures of energy for the process of cooling (drives of pumps of intermediate heat-transfer agents and others).

In case of direct preheating in reactor of working substance of the power plant which is found in a gaseous state, in certain systems the problem appears for obtaining a sufficiently uniform temperature field before the turbine or nozzle.

In this work a calculation is not made of heat transfer from reactor to the cooling agent which is circulating through the reactor. These questions are examined in books on heat transfer. Let us point out only that a peculiarity of the given case is nonuniform heat emission in the volume of the reactor from inconstancy of neutron flux in transverse and longitudinal sections of the reactor.

It is important to emphasize that calculation of surfaces, needed for heat removal from reactor at a known field of temperatures in its core and with an accepted cooling agent, is a responsible segment in designing of a reactor. In many cases, and always during

cooling by a gas, necessary surfaces for heat removal and cross section for circulation determine the construction of reactors (especially reactors of transport propulsion systems).

As liquid coolants it is possible to use:

- gases (air, nitrogen, carbon dioxide, helium);

- liquids (water, heavy water, hydrocarbons, and others);

- liquid metals (mercury, potassium, sodium, lead, bismuth, solutions of K-Na and Pb-Bi and others).

Selection of coolant depends on designation and circuit of the power plant and has an influence on construction and dimensions of the reactor and other elements of the power system. In a nuclear rocket engine the reactor issues heat directly to the working substance.

Cooling of a reactor by air can turn out to be expedient for power plants where the basic working substance is air. Use of helium can be effective on a steady-state power plant at comparatively low temperatures of cycle and with reliable fulfillment of communications of combustible gas. Helium (as also air, nitrogen, and carbon dioxide) is inert, but in the sense of heat withdrawal it possesses the best properties. Helium also possesses the least cross section of absorption.

Water and heavy water are useful for power plants with relatively low temperatures of cycle. For example, 360°C of dry saturated water vapor corresponds already to a pressure of ~190 atm (abs.).

Hydrocarbons and other substances can be examined as coolers of reactors for certain special power systems.

Liquid (melted) metals can be used in circuits, in which the working substance of the power plant is heated in a heat exchanger,

by obtaining heat from liquid metals heated in the reactor. The liquid metals circulate in the closed system reactor-heat exchanger-reactor with the help of reactor pumps. Intermediate heat-transfer metal decreases the dimensions of necessary cooling surfaces in the reactor, but requires pumps and pipelines and, furthermore, an additional heat exchanger.

It is necessary to consider that many cooling substances after reactor become radioactive (air, sodium, potassium, and others) or promote transfer of wall material from the circulation system from regions with high temperature to regions of lower temperatures (for example, pure mercury).

Potassium and sodium, passing through a reactor, will form isotopes radiating γ-rays of high energy with half-lives of 12 and 15 hours respectively. Bismuth will form an isotope which radiates α-particles. Lithium is an element which is very aggressive chemically. Hellium does not obtain any radioactivity, but its application at high temperatures and pressures requires further study.

It is necessary to consider corrosion of walls of the cooling system during application of aggressive substances. It is necessary also to consider that the use of alkali metals requires special measures for complete hermetic sealing of the system and elimination of the danger of contact of alkali metals with the air and water vapors.

Coolants are opaque for neutrons to some degree; they not only absorb neutrons, but also delay their speed by means of elastic scattering. This one should consider in designing a reactor. A change in the state of the coolant in a closed cooling system, due to dissolution of metals and other substances, changes its cross section of absorption. This circumstance also has to be considered in the selection of coolant and assignment of period for its continuous service.

Application of melted metals creates considerable operational difficulties, since their melting point is high. In Table 11.5 are given the melting points of certain metals and their solutions.

Table 11.5. Melting point of certain metals.

s[illegible]	Pb	Bi	Li	K	Na	56% Na+ +44% K
[illegible] p[illegible] [illegible] °C	327	271	179	62	98	19

Starting and turning off of installations with heat-transfer metals are a complex matter and require a great deal of exactness.

In Table 11.6 are cited the cross sections of absorption, and also average logarithmic decrement for one collision for a number of coolants. As can be seen from the table, the least cross section of absorption is possessed by atomic oxygen, and then helium, which at the same time has a relatively large ξ, but smaller than H.

Table 11.6. Nuclear properties of coolants (with slow neutrons).

Substance	H	O	Air	He	Na	K	56% Na+ +44% K	Pb	Bi	44,5% Pb+ +55,5% Bi	Li
Cross section of absorption in barns	0,33	0,0002	14	0,008	0,45	1,97	1,1	0,2	0,032	0,17	71
Cross section of scattering in barns	38	42	8,82	0,8	4,0	1,5	3,2	11,0	9,0	9,9	1,4
ξ	1,0	0,12	0,13	0,825	0,083	0,03	0,0774	0,0096	0,00958	0,0096	0,268

Requirements for a coolant can be formulated in the following way: the coolant should be stable; it should not be aggressive with respect to materials of the circulation system (neither in the sense

of corrosion nor in the sense of transfer of material); its weight density and heat capacity have to be high; it should be as opaque as possible for neutrons; circulation of it through the reactor should be combined with minimum expenditures of energy; it should allow preheating to high temperatures and should be convenient and simple in operation.

Shielding of the reactor. During nuclear fission in a reactor, as it was shown, neutrons are emitted, γ-rays are radiated, and β- and α-particles are formed.

The problem of preservation of neutrons inside the reactor is important for its process and requires the setting up of reflectors. Independent of this, in view of the biological hazard of neutrons, reactors have to have not only reflectors, but beyond their limits also a shell made from materials which absorb neutrons. Only reactors for single use, exploited without the help of man and outside of inhabited localities, can be free from the requirements for a biological neutron shielding.

α-Particles represent nuclei of hellium (two protons and two neutrons); they are emitted by radioactive heavy elements and fission fragments. Although α-particles possess high energies (speed ∿20,000 km/s), their penetrating ability is not considerable. Thus, a layer of air with a thickness of 1 cm decreases the energy of an α-particle by a value of an order of 2 MeV; a sheet of paper inhibits the majority of α-particles. Thus, α-particles in a reactor are inhibited completely thanks to the reflector.

β-Particles are electrons, emitted by radioactive fragments, and their levels of energy are diverse. Along with this there are positive β^+-particles, which is connected with the liberation of positrons by products of radioactive decay. Finally, during connection to the nucleus of an electron from the shell (K-capture) β-particles are also liberated. Although penetrating ability of β-particles is greater than that of α-particles, already aluminum

with a thickness of several mm completely restrains β-particles. Radiation of β-particles does not require special concern during shielding of a reactor.

The greatest attention, along with neutrons should be given to deeply penetrating γ-radiation, which is very dangerous for man. The properties of a medium and its thickness are judged based on the intensity of weakening of γ-rays.

If I_0 – initial energy, I – energy of γ-rays at the distance x, then the connection between I and I_0 is written in the form:

$$I = I_0 e^{-\mu x},$$

where μ – linear attenuation factor of γ-rays; it depends on the energy of γ-rays and on the medium through which they are passing.

In Fig. 11.10 a graph is given which shows the necessary thickness of different materials for lowering the intensity of γ-rays by 10 times (layer of tenfold weakening). Along the axis of ordinates the figure 1 corresponds to a thickness of ∿25 mm. In order to decrease the energy of γ-rays by 100 times two layers of tenfold weakening are needed. Thickness of shield for a reactor which is under the observation of operating personnel should be such that beyond the borders of the reactor the intensity of γ-rays is absolutely harmless.

In the case when through the reactor the working substance of the power plant flows continuously, it is especially necessary to consider leakages of neutrons and γ-radiation through entrance and exit openings in the circulation system.

Starting and control of the process of the reactor. Although in the atmosphere there are always free neutrons, which can be used for starting the reactor, in the reactor it is anticipated to have a source of neutrons to ensure control and regulation. The site of

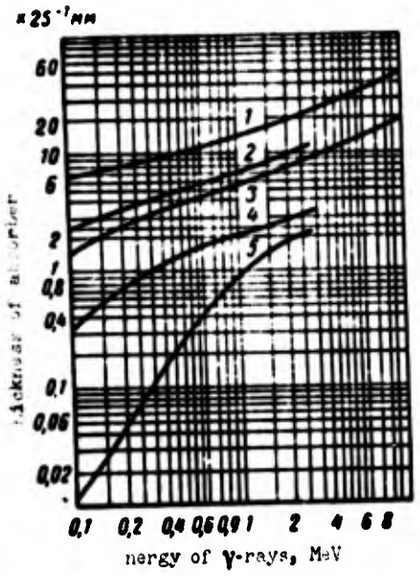

Fig. 11.10. Dependence of thickness of tenfold weakening of γ-radiation on energy for various materials: 1 – water; 2 – concrete; 3 – aluminum; 4 – iron; 5 – lead.

installation of the source of neutrons inside the core is determined by the construction of the reactor. The source of neutrons is fulfilled from polonium and beryllium or radium and beryllium and others. A neutron source from Po-Be has that positive property that it hardly gives out any γ-radiation. In the United States they use antimonic-beryllium sources (bars) made from Sb-124 in a cup made from beryllium. These sources emit neutrons with an identical level of energy. During starting the flux density comprises 10^5-10^6 neutrons/cm^2 s.

During starting and during operation of a reactor and change of its power an important role is played by counters of neutron flux. They are necessary in order to avoid the danger of excessive increase of neutron flux or excessive decrease of reactor period and increase of its power. Neutron counters have to be mounted in such a manner and in such a quantity that they guarantee reliable control of the process of starting, control, and reactor shutdown without apprehension about overheating and other malfunctions.

The reactor should be equipped with different instruments, controlling temperature, pressure, and other values in characteristic points of the reactor.

Of specific importance is the question of heat withdrawal in the period of starting, operation, and reactor shutdown, and also after it has been turned off. Processes in the reactor after turning off (disintegration of fission products) are connected with energy release and require concern about heat removal. The circuit of the power plant should allow circulation of the cooling agent through the reactor in all shown stages and control of circulation and parameters of the coolant.

Control of the reactor under all conditions from starting to turning off and subsequent servicing of it after turning off are carried out by remote control. The control system should be automatic, guaranteeing the necessary program sequence of all operations. Especially responsible are problems of control and adjustment of reactors on fast neutrons.

11.4. Systems for Nuclear Rocket Engines

In rocket engines a fully urgent problem is the use of nuclear reactors for heating suitable working substances. The working substance for this purpose should possess the following main properties: it should yield low-atomic light end products (with a high value of gas constant) and with a small value $k = c_p/c_v$; it should possess a high degree of stability of heat removal in reactor; for decreasing the dimensions of tanks (and rockets) it should, as far as possible, have a high weight density; working substance should not have restrain or absorb neutrons and should not acquire radioactivity during flow through the reactor. Simultaneous fulfillment of all these conditions is not ensured in practice.

In nuclear rocket engines [YaRD] (ЯРД), as a rule, the tanks should contain the working substance alone, with the exception of a gas phase reactor and cases when it is assumed to have combined use of nuclear energy for heating of fuel components and then the chemical energy of this fuel.

During heating of liquid working substance in a reactor it passes through the following stages: heating and vaporization; superheating of vapors and transition to a gaseous state with dissociation of molecules at high temperatures and with ionization of atoms at very high temperatures. Initial heating of working substance prior to the reactor is carried out in the engine jacket during the cooling of its walls. If the working substance possesses the ability to restrain or absorb neutrons, then these properties of it have to be considered in the designing of the reactor. Calculations for the reactor in this case are more complex than during heating of a liquid substance or gas, since on a certain length of the reactor there is a change in the aggregate state of the working substance, and then there is also the possibility of a change in the composition of products of heating due to dissociation and ionization.

In Fig. 11.11 a graph is given for the approximate dependence of theoretical specific rocket engine thrust on temperature of heating of the working substance before the exit nozzle for four substances.

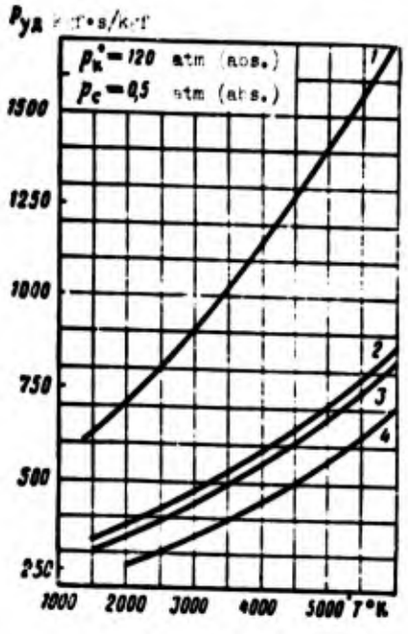

Fig. 11.11. Specific thrust of certain substances depending on temperature of heating: 1 – hydrogen; 2 – methane; 3 – ammonia; 4 – water.

Chemical fuel may be promising for obtaining maximum specific thrust of an order of 450 kgf·s/kgf. From Fig. 11.11 it can be seen that such a value of specific thrust is attained for ammonia (weight density 0.677 kgf/ℓ at -30°C) at a temperature of heating of 2500°C, and for methane (weight density in liquid phase 0.43 kgf/ℓ at -164°C) at 2300°C. The highest specific thrust is given by hydrogen – around 900 kgf·s/kgf at 3000°C and around 1400 kgf·s/kgf at 5000°C. A deficiency of hydrogen is its low weight density (∿0.07 kgf/ℓ in the liquid phase) and very low boiling point (-252.8°C), however this does not hinder its successful use. Hydrazine may give a specific thrust of an order of 500 kgf·s/kgf during heating up to 3500°C.

Heating of suitable working substances in a reactor up to temperatures of 2000-3000°C makes it possible to obtain higher specific thrusts than the specific thrusts of rocket engines on chemical energy.

As the working substance in a nuclear rocket engine it is possible to use, for example, water also. However, specific thrust obtained in this case is less than for ammonia, and is close to the specific thrusts of contemporary chemical fuels. Thus, at a temperature of heating up to 3000°C specific thrust of a YaRD on water attains a value of around 310-330 kgf·s/kgf at a comparatively high pressure drop. The advantage of water is its relatively high weight density, prevalence in nature, extremely low cost, and simplicity and safety of transformation with it; these qualities cannot be compared with any other working substance. An operational deficiency of water (under winter conditions) should be considered its high freezing point. The comparatively low value of specific thrust of a nuclear rocket engine with water as the working substance makes such an engine little suitable for large rockets.

Working substances in nuclear rocket engines in principle can be solid, gaseous, and liquid substances. However, methods of introduction of a solid into a reactor during operation of the engine

are still not developed, and the capacity for storage of the needed quantities of gaseous substances is so great even under high pressures that at present it is possible to assume the possibility of application of working substances only in the liquid phase. In this case in the liquid substance it is also possible to use solids, for example, metals in the form of suspensions.

We already mentioned liquid hydrogen, ammonia, hydrazine, methane, and water. It is possible to view as working substances hydrocarbons, alcohols, and other substances. The greatest specific thrust, other things being equal, can be obtained by using liquid hydrogen. Hydrogen up to a temperature of 2200°C remains diatomic and dissociates at higher temperatures. Upon heating hydrogen enters into a reducing reaction with carbon, hydrocarbon compounds, and with many metals. This may lead to corrosion and removal of surface layers of a solid-phase reactor, which is necessary to consider during construction.

Ammonia and hydrazine are decomposed already at a temperature of around 1400°C, forming not only diatomic, but also monatomic hydrogen and nitrogen. In this case the interaction with graphite and a number of metals will be the same as and in case of hydrogen.

Reactors for rocket engines can be of the following types:

1) reactor with core in the solid phase (solid-phase reactor);

2) reactors, in which compounds of fissionable material are in the liquid phase (liquid-phase reactor);

3) reactors with a gaseous core (gas-phase reactor);

4) combined reactors, in which the core contains the solid and liquid phases of uranium compounds or a solid and gaseous phase.

Figure 11.12 shows a diagram of a rocket engine with a solid-phase reactor.

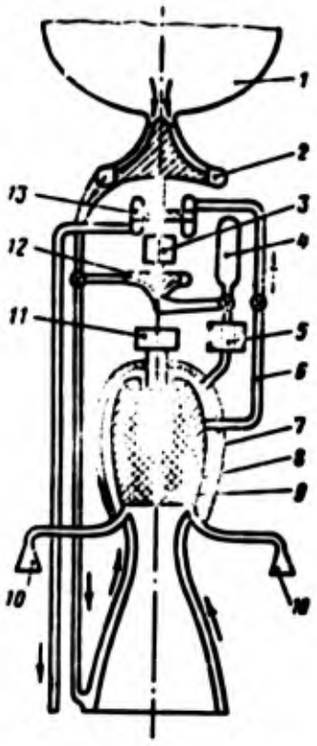

Fig. 11.12. Diagram of nuclear rocket engine with solid-phase reactor: 1 – tank for working substance; 2 – pump; 3 – aggregates; 4 – pressure accumulator; 5 – heat exchanger; 6 – tapping of gases for turbine; 7 – body of chamber with shielding; 8 – reflector; 9 – reactor; 10 – nozzles for control of flight; 11 – regulating device for reactor; 12 – pump for closed circulation; 13 – turbine.

A solid-phase reactor in principle is no different from a reactor – a heat exchanger. Inasmuch as in rockets the duration of operation of the reactor is very limited, it is possible to increase the maximum permissible temperature of core elements. The most refractory uranium compound is uranium dioxide ($t_{пл} \approx 2800°C$). Fuel elements of a reactor on the basis of uranium dioxide or uranium-tungsten compounds make it possible to raise the temperature in the core to 2750-2800°C and to ensure heating of the working substance to 2500°C. In this case as the moderator for a thermal-neutron reactor it will be necessary to use graphite, the melting point of which is 3500°C, or in an extreme case beryllium oxide, the melting point of which is equal to 2520°C. The most refractory material for control rods for a reactor is boron carbide B_4C ($t_{пл} \approx 2550°C$).

Fuel elements can be realized on the basis of ceramics from carbides of hafnium and tantalum ($t_{пл} \approx 3900°C$). It is necessary

to consider the relatively large cross sections of absorption of neutrons by tantalum and natural hafnium and tungsten.

On a graphite solid-phase reactor using liquid hydrogen as working substance it is possible in reality to calculate for a maximum specific thrust of 900 kgf·s/kgf.

In spite of the brief nature of operation of a solid-phase reactor, the development of an efficient construction is of considerable complexity. Energy release in such reactors is 2000-3500 MW per 1 m^3 of core.

Useful quantity of heat, which should be given by 1 kgf of liquid working substance in a reactor:

$$q \approx \lambda + \int_{T_{нач}}^{T_к} c_p dT \text{ Cal/kgf},$$

or, considering analogous to formula (2.8)

$$\int_{T_{нач}}^{T_к} c_p dT = \frac{A w_{вх}^2}{2g\eta_i},$$

$$q \approx \lambda + A \frac{w_{вх}^2}{2g\eta_i}$$

or

$$q \approx 4{,}186 \cdot 10^{-3} \left(\lambda + A \frac{w_{вх}^2}{2g\eta_i}\right) \text{ MW/kgf},$$

since 1 Cal/s = $4.186 \cdot 10^{-3}$ MW; here λ – heat of vaporization.

One of the serious problems of a solid-phase reactor is stability of the process in a nuclear rocket engine. Apparently, this problem for a nuclear engine will be more complex than for a rocket engine on chemical fuel.

If it is necessary to raise the temperature of working substance higher than 2800°C, when UO_2 passes into a liquid phase, it is necessary to think about liquid-phase reactors, in which uranium compounds are in a liquid state. It is possible to assume circuit for such a nuclear engine, in which liquid uranium carbide is held on the internal walls of the reactor due to rotation of a porous cylinder and the centrifugal forces which develop due to this. The working substance (for example, H_2) passes through the porous wall of cylinder into the melted mass of reactor, being heated to the required temperature and simultaneously protecting the cylinder from overheating. Being limited by a temperature of melted mass essentially lower than its boiling point, it is possible to have high temperatures of heating of working substance and specific thrusts on liquid hydrogen of an order of 1000 kgf·s/kgf.

Creation of a liquid-phase reactor presents a still more complex problem in comparison with a reactor – a heat exchanger with a solid core.

Considerably higher temperatures of working substance can be obtained in a gas-phase reactor. The simplest arrangement for a rocket engine with a gas-phase reactor is shown in Fig. 11.13. Here into the reaction chamber is introduced through one system of injectors the fissionable material which is in a liquid phase or in the form of suspension in a suitable liquid substance (for example, moderator). Through another system of injectors the working substance is introduced. Until a definite quantity of fissionable material is introduced into the chamber, the fission reaction will not take place. Only upon achievement of critical mass will the process of fission and energy release begin. Value of critical mass depends on properties of the moderator and working substance, on the nature and properties of fissionable material, on the dimensions of the chamber, and on the shielding of the engine. In addition the size of the chamber is determined by pressure in the chamber and absolute thrust of the engine. Energy which is liberated as a result of a controlled process of fission increases the temperature of the working substance to the required value.

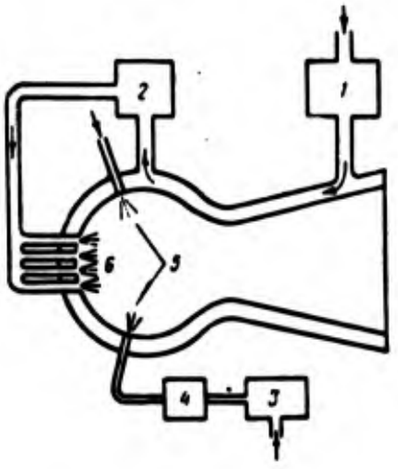

Fig. 11.13. Diagram of nuclear rocket engine with a gas-phase reactor: 1 – pump for working substance; 2 – regulating device; 3 – pump for nuclear fuel; 4 – regulating device; 5 – injector of nuclear fuel; 6 – injector of working substance.

Obviously the volume of the core of a gas-phase reactor will always be considerably larger than the volume of a solid-phase reactor under identical pressures, in spite of the fact that in the latter case it is necessary to develop sufficient surfaces for heat transfer. For decreasing the volume of a gas-phase reactor it will be necessary to use very high pressures in the chamber, which can turn out to be necessary for other considerations also.

A gas-phase reactor possesses two essential advantages: from a construction point of view it is simple since in the core there are no components, however this simplicity is made up for by complication in the problem of organization of the process; absence of structural elements in the core permits the increasing of temperature of discharge products to 10,000°C and higher, however such high temperatures require special concern for cooling of the walls of the chamber and the nozzle. This problem is more difficult than in conventional liquid propellart rocket engines since the specific heat fluxes are higher. With such high temperatures the working substance and fissionable material are ionized and are turned into plasma, which makes it possible by special procedures to exclude the contact of gases with the walls of the chamber.

The process in a gas-phase reactor is very complex. If one does not take special measures, fissionable material will be mixed with working substance, issuing fission energy to it, and it will emanate

together with it through the nozzle. Although thrust of the engine at the expense of the mass of fissionable material increases insignificantly, the loss of fissionable material is undesirable. It is necessary to reduce these losses to a minimum; at the same time it is necessary to find suitable method for transfer of energy to the working substance. At present there are still no published concrete solutions of the problem of organization of the process.

During inlet of working substance and fissionable material with the moderator it is necessary or to exclude to the utmost the possibility of their mixing, or to secure their complete separation if mixing is necessary in the initial stage. Consequently, in the chamber have to be zones, occupied only (or chiefly) by fissionable material, and zones, through which the working substance flows. Then it is necessary to develop sufficiently the surface of contact of working substance with fissionable material for the transmission of the required amount of heat; here it is necessary to remember that both substances are in a gaseous phase. Obviously it is impossible to avoid a certain exchange by masses on surfaces of heat exchange and a certain loss of fissionable material.

In foreign literature it is indicated, for example, that for retention of fissionable material in the chamber it is possible to create vortex flows, as a result of which the radial gradient of partial pressure of a heavy gas will be greater than the gradient of a light working gas and the concentration of uranium on the periphery will be increased. However, for transmission of heat to the working substance the latter should pass to the center through a peripheral cloud with a high content of uranium. Organization of such a process is subject to development and study.

For decreasing losses of fissionable material it is possible to make use of the circumstance that at high temperatures the working substance and fissionable material, as it was shown, are ionized, i.e., molecules and atoms liberate one or several electrons. The degree of ionization of fissionable material is much higher than for working substance, consequently the electrical properties of

plasma of working substance and fissionable material will be different. Due to this, with the help of an electrical current flowing through a winding around the chamber, it is possible to prevent the leakage of fissionable material.

It is necessary to point out also the difficulty of controlling a gas-phase reactor due to the possible variation of pressure in the injectors of both systems and accidental fluctuation in the value of loss of fissionable material through the nozzle. Finally, in such a reactor there is a greater probability of variations of pressure of different frequency, induced by system of supply and the process themselves in the chamber. The problem of stability in the process of a gas-phase nuclear rocket engine will apparently be one of the most important.

In a gas-phase reactor for the reliable adjustment of process it is expedient to use thermal neutrons. In the selection of a moderator it will be necessary to consider the temperature and pressure in the chamber and the moderating properties of the working substance itself. After achievement of conditions of criticality in the chamber it is necessary to maintain exactly the relationship of all components (fissionable material, working substance, and moderator).

A combined reactor can be carried out in a different way. One can imagine a section of the core filled with a solid-phase reactor, in the channels of which flows a working substance which is heated to the highest possible temperature. Through other, special channels fissionable material is fed and the supply of it, after achievement of conditions of criticality, is regulated in such a way as to compensate for loss through the nozzle. Depending on mass-ratio of fissionable material in the solid and gaseous phase there will be changes in the overall volume of the core and temperature of gases before the nozzle. The greater the share of the solid phase, the less the dimensions of the reaction chamber, but also the less the temperature of gases. For easing the problem of cooling the walls

it can turn out to be useful to cover the walls of the chamber and part of the nozzle with a solid-phase substance with a high melting point and with low thermal conductivity in which is found only the moderator or a moderator with fissionable material and which is washed by the working substance. Since the basic share of core volume is due to the moderator, the quantity of which in the reactor is greater than fissionable material, but density is less, then such a solution can lead to a noticeable decrease of overall chamber volume.

Application of gas-phase and combined reactors requires such an organization of storage of fissionable material in tanks which excludes the possibility of a spontaneous appearance of a fission reaction.

The use of reactors (especially gas-phase and combined) in rocket engines makes the discharge products radioactive; therefore nuclear rocket engines can be safely used in the second and following stages of a rocket which was launched from earth or on rockets which were launched from the orbit of an artificial satellite.

What was said above shows that in the first place one should expect implementation of a solid-phase reactor in operation. In the United States during the last few years tests were conducted on several modifications of a nuclear solid-phase reactor the "KIWI." In the beginning of 1966 successful ground tests were conducted on the nuclear rocket engine NERVA on liquid hydrogen; calculation power of the reactor was around 1000 MW; specific thrust of the engine was around 750 kgf·s/kgf. On the basis of these experiments the graphite reactor "Feb" 1 phoebus [Translator's note: This word is not verified] was developed. It was analogous to "KIWI," but made it possible to obtain greater thrust with the same value of specific thrust. A later variant of the reactor the "Feb" 2 should have considerably greater power.

In a rocket engine it is possible to use a solid-phase reactor for heating of two substances – oxidizer and combustible with a

subsequent chemical reaction between them after the reactor. In this case the temperature of combustion products will be higher than the temperature which is permissible for structural elements of the reactor. Although thermal effect of the reaction decreases with an increase of initial temperature due to increasing influence of dissociation of reaction products, it is possible to expect that in this case temperature before the nozzle will be higher than the temperature of combustion without preliminary preheating in the reactor. Heating in the reactor can be realized up to 2000°C. Selection of temperature should be connected with properties of the components in order to eliminate, in particular, deposits of undesirable products of decomposition on the walls of reactor channels. Increase of maximum temperature before the nozzle is still useful because with this the gas constant of products of combustion increases.

The use of nuclear reactors with their high energy content makes it possible to consider the application as working substances of metals, the heating and vaporization of which during chemical processes, decreases the thermal effect of reaction noticeably. Such metals can be Li, Al, Mg, Be, and others. Heat of vaporization of 1 kgf of lithium, magnesium, and aluminum is equal respectively to 4680, 1137, and 3050 Cal.

In one of the foreign works comparative approximate calculations are made of data of chemical, nuclear, and combined nuclear-chemical rocket engines with an expansion ratio of gases in the nozzle equal to 34. During the combined use of nuclear and chemical energy the temperature of heating of working substances in the reactor was accepted at 1500°C. In comparative calculations the highest specific thrust is obtained during the use of only nuclear energy for the heating of hydrogen. During chemical and nuclear-chemical processes less specific thrust is obtained, although the maximum temperatures of products of combustion reach great magnitudes. Ammonia in a chemical reaction with oxygen and fluorine should make it possible to have specific thrusts of the same order as during its heating in a reactor up to a temperature of 2230°C. Consequently it is necessary

to develop reactors which can allow preheating of working substances to higher temperatures, if the application of not just hydrogen is assumed. Available materials are still insufficient for a judgement about the comparative effectiveness of nuclear-chemical engines.

11.5. Comparison of Rockets on Chemical and Nuclear Energy

For a complete comparison of chemical and nuclear rockets it is necessary to perform detailed calculations with a determination of scales of all elements at an assigned payload and range of rocket. Here we will limit ourselves to only certain general data for an illustration of relative properties of rockets using chemical and nuclear energy.

Let us assume that on chemical energy specific rocket engine thrust is equal to $P_{уд1}$ = 300 kgf·s/kgf, and the share of fuel in the initial weight of the rocket comprises 0.85 for rockets up to 500 T in weight and 0.9 for rockets with greater initial weight. Quantities of fuel and total pulse will be determined by the initial weight of the rocket. In Table 11.7 are given the corresponding values for rockets of various initial weight.

Table 11.7.

Initial weight of rocket in T	100	250	500	1000	2000
Weight of fuel in T	85	212,5	425	900	1800
Total pulse in T·s	$25,5 \cdot 10^3$	$63,4 \cdot 10^3$	$127,5 \cdot 10^3$	$270 \cdot 10^3$	$540 \cdot 10^3$

With transition to the use of nuclear energy specific thrust depending on temperature of core and properties of working substance can have a value from 400 to 1200 kgf·s/kgf. Let us assume that

specific thrust during the use of nuclear energy has the values $P_{уд2}$, equal to 450, 600, 750, 900, and 1200 kgf·s/kgf. Thus the ratio of specific thrusts of a nuclear rocket engine comprise

$$\frac{P_{уд2}}{P_{уд1}} = 1{,}5;\ 2{,}0;\ 2{,}5;\ 3{,}0 \text{ and } 4{,}0.$$

In Table 11.8 are given the quantities $G_{р2}$ of working substances necessary so that at various ratios of specific thrust it is possible to obtain in a rocket with nuclear engine the same total pulse as in one on chemical fuel.

Table 11.8.

Initial weight of rocket in T / ratio of specific thrusts	100	250	500	1000	2000
1,5	56.7	141.6	283.2	600.0	1200.0
2,0	42.5	106.3	212.5	450.0	900.0
2,5	34.0	84.5	169.0	360.0	720.0
3,0	27.3	70.8	141.6	300.0	600.0
4,0	21.3	53.1	106.2	225.0	450.0

In Fig. 11.14 is given a graph showing by what number of tons the weight of working substance in a nuclear rocket decreases in comparison with chemical depending on initial weight of rocket and ratio of specific thrusts of nuclear and chemical rocket engines. For example, for a rocket with initial weight of 500 T the saving in weight of working substance at a ratio of specific thrusts of 2.0 comprises 42.5%, and for a rocket weighing 2000 T, at the same ratio of specific thrusts, the saving in weight of working substance comprises already 45%.

In order for a rocket with a nuclear engine to be more effective than a rocket with chemical fuel, the weight of the reactor with shielding and system for control and regulation should be less than the weight which is saved by the transition from chemical energy to

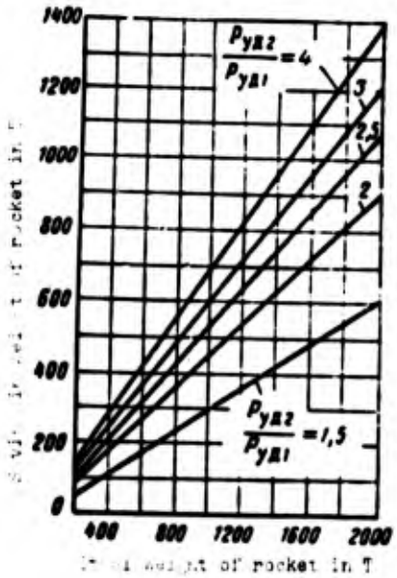

Fig. 11.14. Decrease of necessary weight of working substance in a nuclear rocket in comparison with chemical depending on initial weight of rocket and ratio of specific thrusts.

nuclear. This possibility will be greater, the greater the initial weight of the rocket and the greater the specific thrust of the nuclear engine in comparison with chemical. This is readily apparent from Fig. 11.14.

If, for example, for a rocket weighing 500 T with a thrust weight ratio of 1.5 and at a specific thrust on H_2 equal to 750 kgf·s/kgf the weight of the reactor system is taken as 100 T, then from a comparison of data in Tables 11.7 and 11.8 it is clear that with

$$\frac{P_{уд2}}{P_{уд1}}=\frac{750}{300}=2,5$$

the saving in weight of working substance comprises 425 - 169 = 256 T. Thus, transition in such a rocket to nuclear energy permits a lowering of initial weight of rocket by 156 T, i.e., by 31%, or to essentially increase the payload.

In Fig. 11.15 is given a comparative calculation chart for single-stage rockets with a nuclear engine on hydrogen and ammonia and with engines using the chemical energy of fuels. Curve A

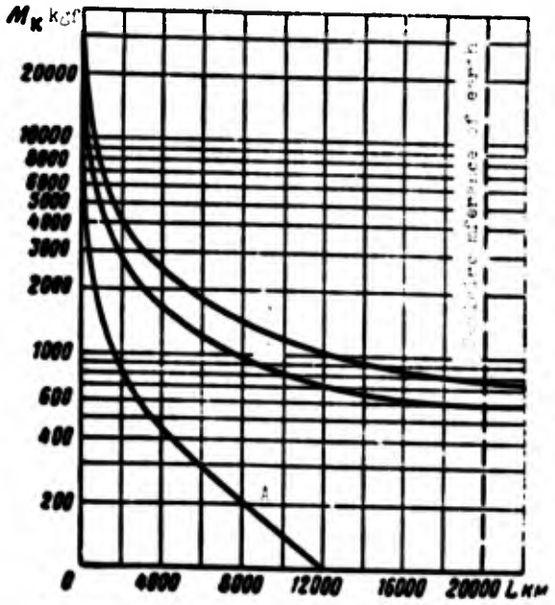

Fig. 11.15. Curves of equal effectiveness of single-stage nuclear and chemical rockets depending on flight range.

corresponds to identical effectiveness of a nuclear rocket on hydrogen and a chemical rocket on O_2-N_2H_4. In the area under curve A a chemical rocket turns out to be more effective than nuclear. Along curve B are identical degrees of effectness of a nuclear rocket on hydrogen and chemical rocket on F_2-H_2. In the area under curve B the chemical rocket is more effective than nuclear. Curve C corresponds to equal effectiveness of nuclear rocket on ammonia and a chemical rocket on O_2-N_2H_4. From the chart it is clear that with an end weight of rocket $M_к$ = 2.5 T and more and with a range L = = 6500 km and greater a nuclear single-stage rocket always turns out to be more effective than a single-stage chemical rocket. With an increase of weight of payload a greater effectiveness of nuclear rocket is attained at a lesser range. Thus, for example, with a passive weight of 4.5 T a nuclear rocket is more effective than chemical already at ranges less than 2000 km. Certainly the data in this paragraph are very approximate; they illustrate only a basic tendency of rocket construction – the use of nuclear energy in powerful rockets with great range and large payload.

The higher (almost twice) value of specific thrust of a nuclear rocket engine not only compensates for the weight of the reactor and its entire system, but gives yet an additional essential gain in weight of payload.

Part II

CONSTRUCTION, DURABILITY, AND AUTOMATIC EQUIPMENT OF ROCKET ENGINES

CHAPTER XII

CONSTRUCTION OF CHAMBERS FOR LIQUID PROPELLANT ROCKET ENGINES

At present basically cylindrical chambers find application (Fig. 12.1) and more rarely spherical or close to spherical.

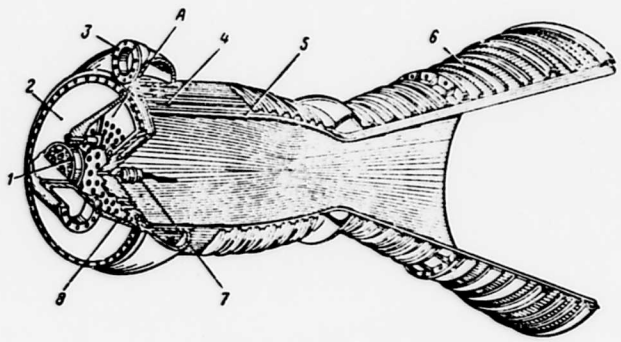

Fig. 12.1. Cylindrical chamber of a liquid propellant rocket engine: A – oxidizer cavity: 1 – inlet for oxidizer; 2 – outer wall of heat; 3 – outlet for combustible; 4 – inlet of combustible into tubes; 5 – tubes of combustion chamber; 6 – bands; 7 – igniter; 8 – injector face.

Chambers which are close in form to spherical [47] have an advantage over cylindrical chambers: with an equal working volume the surface of their walls is less, and consequently, the better the conditions for cooling, and with an equal gas load the weight of the chamber may also be less.

For engines with very large thrusts (over 500 t) a sectional multichamber construction may be rational (Fig. 12.2), where the separate chamber-sections are disposed in one or several rows around a central body. Inside the central body a turbopump assembly can be disposed. With such an arrangement it is convenient to use a nozzle with an outward flare formed by the profiled tip of the central body. Critical section of nozzle is of an annular form. A nozzle with an outward flare has good aerodynamic properties, especially on partial load conditions, for example, during turning off of separate combustion chambers for a change of value of thrust. In view of absence of an outer wall for the nozzle radial dimensions and length of the engine decrease considerably as compared to an engine of a conventional nature and the same thrust.

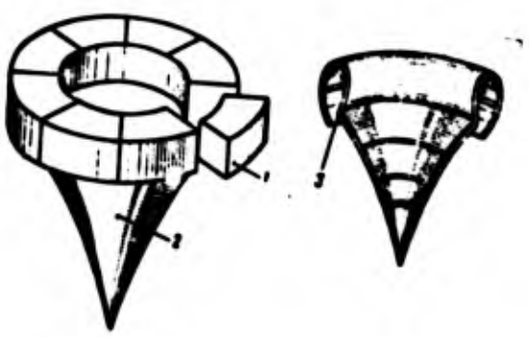

Fig. 12.2. Diagrams of sectional multichamber engine with central body: 1 – chamber-section; 2 – central body; 3 – critical section of nozzle.

Perfection in construction of a chamber is characterized by specific weight $\gamma_к = G_к/P$, where $G_к$ – weight of chamber, P – thrust of engine. Depending on fuel, pressure in the combustion chamber, special purpose assignment of the engine, and material of the chambers specific gravity lies within the limits of 0.001-0.004 kgf/kgf. Lesser values pertain to ideal chambers with pressure $p_к$ of an order of 50-100 kgf/cm^2 and thrust of 10-30 T.

12.1 Heads of Chambers

On heads are disposed devices for the inlet of fuel to the chamber. Liquid fuel is fed to the chamber by injectors, but in the case of application of circuit with afterburning of gas, proceeding from the turbopump assembly (THA), or during feeding of fuel (for

example, hydrogen peroxide) in a gaseous state – through special windows made in the head. For two-component liquid fuel the head has two cavities. In engines with thrust control by means of cutoff of groups of injectors these cavities can have additional partitions, allowing fuel to be fed separately to different groups of injectors.

Also located on the head are engine mounting lugs, valves for starting, cutoff, and thrust control of engine, and in a number of cases antivibration devices, and igniters.

The basic requirement in the construction of the head is ensuring of assigned conditions of carburetion and protection of chamber walls from excessive heating and burnout. These problems, as it was shown, are resolved by the rational distribution of injectors on the head, by the selection of productivity of separate groups of injectors and their characteristics, and also by the proper cooling of the engine. Simultaneously the construction of the head should possess sufficient rigidity in spite of the weakening of its walls due to the large number of holes under the injectors, it should ensure the possibility of feeding components with a minimum of flow friction, and it should have reliable protection from overheating by hot gases.

For the best mixing of components on the head it is desirable to place the greatest possible number of injectors. Minimum distance between injectors is determined by conditions of strength of the wall of the head, conditions of distribution of channels for feeding of components in the body of the head, if the head does not have a common component cavity, and, finally, dimensions of the injector. With swirlers the determining factor is dimension of injector, since rigidity of head can be ensured by inclusion of the body of the injector in power circuit, and the feeding of components in most cases is carried out from the general cavity. With jet injectors, having relatively small dimensions, minimum pitch is determined at a given angle of dispersion by the distance of the zone of collision of streams from the surface of the head or by conditions of feeding the component. In constructions carried out with swirlers the pitch

comprises 12-30 mm, but with jet injectors the minimum pitch can be reduced to 3-4 mm.

One or another method of distribution of injectors is selected either on the basis of available experience of miximg of components of fuel of a particular composition, or from purely construction considerations, including the feeding of fuel and rigidity of head.

Basic structural elements of the head are the injector bottom and external wall. In its turn the injector face more frequently is double-walled and less often - single-walled. With a double-walled injector face the head on the whole is three-walled. Then the wall of the injector face which is turned to the combustion chamber is called inner and the second one - middle.

The two inner cavities, formed by the walls of the three-walled head, are filled with components of fuel. Usually the pressure of the first and second components p_1 and p_2 are approximately equal, and it can be considered that $p_1 = p_2 = p_т$. Let us designate pressure in the combustion chamber $p_к$, and external pressure $p_н$. Then the outer wall of the head is found under the impact of pressure drop $\Delta p_н = p_т - p_н$, and the injector face on the whole - $\Delta p_{ф.з} = p_т - p_к$. Under calculation condition $p_т - p_к = \Delta p_ф$, where $\Delta p_ф$ — pressure drop on injectors. Since pressure drop on injectors is not great, then under calcualtion conditions the injector face is loaded comparatively little. Under conditions of pressurization, when pressure $p_н$ can be disregarded, the injector face is loaded by maximum pressure drop $\Delta p_{ф.з} = p_т$. Under operating conditions the inner wall is heated noticeably, which leads to the appearance in it of considerable temperature deformations and a lowering of strength properties of its material.

The stated factors cause bows in the injector face and outer wall. Therefore the basic requirement in the construction of the head is ensuring its sufficient rigidity, and also preservation of airtightness of its elements during possible deformations. Check of strength of the head by calculation is carried out for conditions of pressurization, when load from forces of pressure are maximum, and

under calculation conditions, when an essential influence can be exerted by heating of the inner wall.[1]

Based on the form of the wall which is turned to the combustion chamber, injector faces are subdivided into flat, hipped, and spherical. In accordance with the form of the injector face the head on the whole is frequently named.

A flat face is simple in construction and not complex in production. With a cylindrical combustion chamber a flat face gives the best homogeneity of field of speeds and composition of mixture of components on a cross section of chamber. A flat face possesses a comparatively low degree of rigidity and strength. However, it is possible with comparatively simple construction measures to ensure sufficient strength of a flat face when it has a diameter up to 1-1.5 m. These include, for example, rigid sealing of the face along the periphery at the point of connection with the combustion chamber, power coupling with the outer wall in the center of the head, and if possible in the central part with the ribs, and also reliable protection from overheating by circulation of fuel inside the face.

Flat injector faces are made both single-walled and also double-walled.

A single-walled injector face should have inside a system of channels for feeding one of the components to the injectors: the other component is fed from the cavity enclosed between the injector face and the outer wall.

There are single-walled faces with annular channels, radial channels, and radial channels with injector rings.

Annular channels A pass through a cast face (Fig. 12.3a). Thanks to massive crosspieces between the channels such a face possesses a

---

[1]Methods of calculation of injector faces for strength are expounded in works [15] and [53].

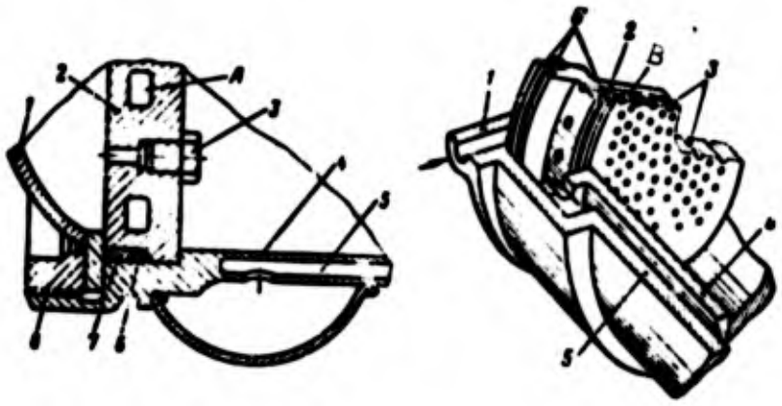

a) b)

Fig. 12.3. Heads of chambers with single-walled injector face: a) with annular channels; b) with radial channels. A) annular and B) radial channels; 1 – outer wall of head; 2 – injector face; 3 – injectors; 4 and 5 – walls of combustion chamber; 6 – liners; 7 – ring; 8 – nut.

high degree of rigidity. Deficiencies of cast faces include difficulty of ensuring identical fuel supply to groups of injectors which are fed from one channel A. Jet injectors are made in the form of drillings directly in face, and centrifugal injectors can be screwed in the face. In Fig. 12.3a, the head with the cast injector face is readily detachable, which can be convenient for engines which are reusable. Aluminum alloys are the material for cast faces. Such a type of face can find application in engines with a relatively low heat-release rate with a pressure in the combustion chamber up to 30-40 kgf/cm^2.

A single-walled injector face with radial channels is shown in Fig. 12.3b. Radial channels, usually made by drilling, are directed from the periphery of the head to the center. Angle between neighboring channels may comprise 5-10°. Axes of the injectors of that component, which is fed along the channels, usually lie on the axis of the channel. Therefore the number of injectors of this component is limited and, naturally, it is expedient to feed the combustible over the channels; in this case the injectors of oxidizer can be grouped around the injectors of the combustible. In view of

the fact that pitch along the arc of the circumference between injectors of combustible is increase toward the periphery, for a more equal distribution of mixture over the volume of the chamber additional shortened channels are made between the basic radial channels passing to the injectors of combustible which are located in the head. On heads of such a type jet injectors are used more frequently.

Additional rigidity is given to the head by a massive rim which is connected with the walls of the combustion chamber. A steel injector face is connected with the walls of the combustion chamber and the headers by welding. A face made from aluminum alloy (Fig. 12.3b) is braced to the combustion chamber on bolts. For more reliable packing grooving joints are used in which soft linings are pressed.

An advantage of disk faces with radial channels is their simplicity of construction and sufficient rigidity, obtained at the expense of their relatively great thickness. Deficiencies include a limited possibility to vary the distribution of injectors, necessity of high degree of accuracy in manufacture to ensure identical conditions of injection of fuel into the chamber from the injectors, which are fed from the injectors, which are fed from various channels, and unfavorable thermal balance of the head, connected with heat removal through the thick face.

Constructions of faces with radial channels with injector rings are free from the majority of these deficiencies (Fig. 12.4). The injector face has a massive rim and relatively thin disk, to which the injector rings, 4, are attached.

In each ring there are only injectors of one component, consequently the location of injectors is concentric. Injectors can be both jet and also centrifugal. There are great advantages in similar constructions when using jet injectors with intersecting streams. Here the form of the rings from the side turned to the combustion chamber may be selected diversely depending on the required

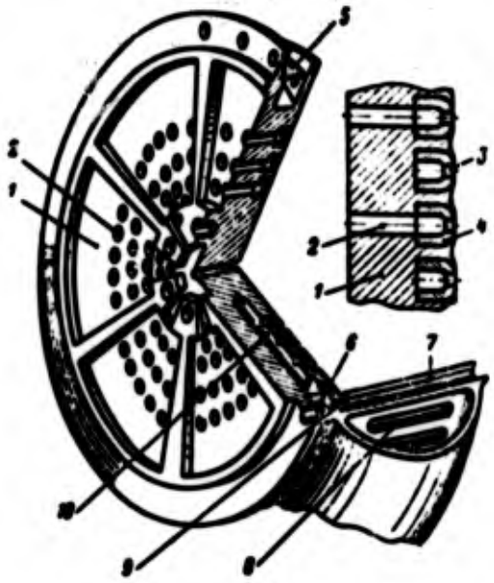

Fig. 12.4. Injector face with radial channels and injector rings: 1 – injector face; 2 – axial channels for feeding oxidizer to rings; 3 – injectors; 4 – injector rings; 5 – screen filter; 6 – injector of wall layer of combustible; 7 – tubes of chamber; 8 – entrance to tubes of combustible; 9 – exit of combustible from tubes; 10 – radial channels.

angle of impingement of streams (Fig. 12.5). It is also possible to realize a method of atomization by impingement against a barrier, for example against rib 3.

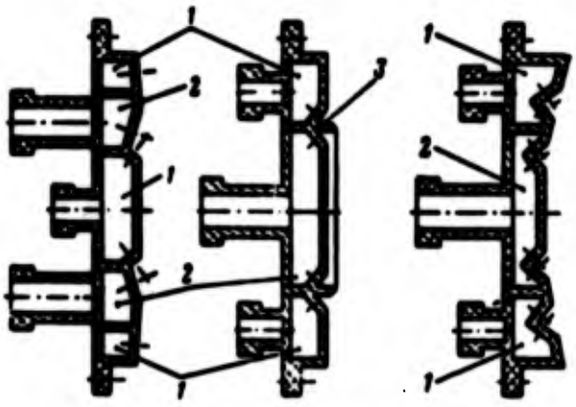

Fig. 12.5. Forms of rings and direction of streams of injectors: 1 – cavity of combustible; 2 – cavity of oxidizer; 3 – rib.

Construction of rings can be different depending on the methods of attaching them to the disk and the method of supplying the components. In Fig. 12.4 is shown one of the possible variants of construction. The component, found in cavity A of the head (see Fig. 12.1) between the outer wall and face, is fed into the rings through a series of axial channels, 2, in the disk. The second component is supplied over radial channels, which are drilled in the body of the disk, from the periphery of head from the header, into which it arrives from the cooling system. Depending on their

construction the rings can be attached to the disk and among themselves by welding or soldering, which is more technological. Preliminarily the ring can be rolled in with the material of inter-annular crosspieces of the disk.

Inasmuch as the rings are made thin-walled, conditions of protecting them from overheating are favorable. Thickness of the walls of rings when the jet injectors are obtained by direct drilling in wall is determined by the length of the injector channel. A construction with rings gives certain technological advantages during the manufacture of injectors, since conditions are improved for the treatment of inlet edges of orifices, which is difficult, for example, for injectors of combustible in a head with radial channels.

Attachment of a head with rings to combustion chamber is carried out by welding similar to the connection examined earlier. The outer wall can be welded to the bottom or braced on bolts.

The most widespread, due to simplicity of construction, are flat double-walled injector faces. For engines with relatively small diameters of the combustion chamber, the face cannot have an external power ring, and the walls of the face are welded directly to the walls of the combustion chamber or to the header, if it has one (Fig. 12.6). In those cases when great rigidity is required, the walls of the injector bottom are welded to the external power ring.

With thin walls for an injector face the basic construction problem is ensuring its sufficient rigidity. Rigidity of the face can be considerably increased by means of a power connection between its walls. Such a power connection can be achieved through point blanks or flaring and soldering of the body of injectors with the setting up of intermediate bushings. Along the sites of the blanks (Fig. 12.6a) spot selding is carried out, and then injectors of the component which is filling cavity B are set in. Injectors of the component which is found in cavity A can, if the wall is sufficiently thick, be screwed in by a thread, but more frequently they are attached with the help of flaring. In the construction shown in

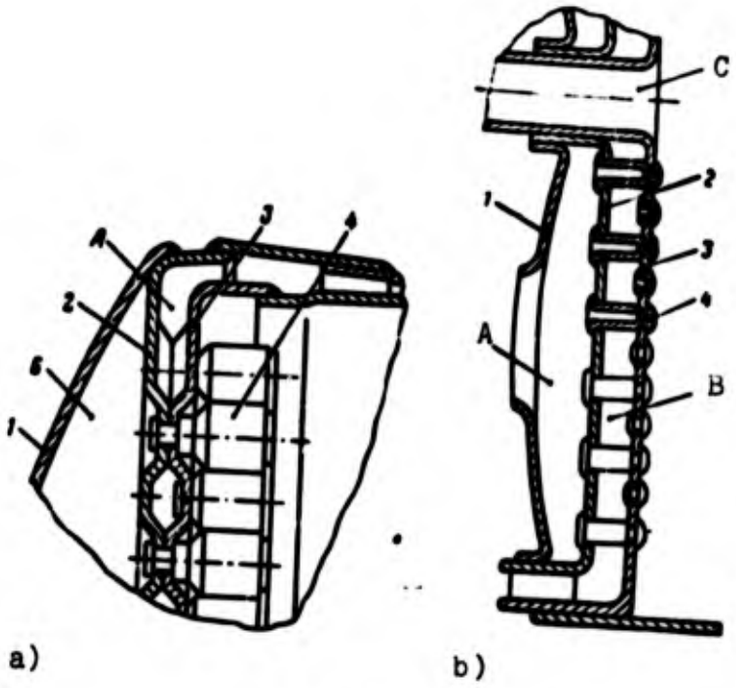

Fig. 12.6. Double-walled injector faces: a) with blanks; b) with flaring of injectors. 1 – outer wall of head; 2 – middle wall of head; 3 – inner wall of head; 4 – injectors. A. and B – cavities for components; C – opening for igniter.

Fig. 12.6b, the connection between walls is carried out through the bodies of the injectors. Identical distance between walls is ensured by a stop in the beading on the body of the injector. High requirements are presented for beading, since it is necessary to have reliable contact over the entire circumference of the flared bead. A compact joint is achieved by rolling out under a press. For preventing the deformation of the rolled connection under working conditions, which can lead to disruption of airtightness, additionally the connection is soldered with a brazing solder.

For ensuring heat withdrawal the thickness of the walls should be as little as possible (order of 2.5-5 mm). Greater magnitudes of thicknesses pertain to case of bracing swirl injectors on the wall by threading. The walls are made from heat-resistant, easily welded steels.

The advantage of faces of such a construction is the possibility

of distribution, in any desirable order, both of jet and also swirl injectors, including two-component types. It is also very simple to carry out the feeding of components. By setting inside cavities A and B additional partitions, dividing them into separate sections with separate feeding of components to each section, it is possible to regulate thrust by variation of separate groups of injectors.

Flat faces, single-walled for example, can also enter into the construction of vortex heads, which represent a special type of heads (Fig. 12.7). In center of a flat head a mushroom-shaped atomizer 1 of oxidant is mounted. The stream of oxidizer, by hitting the face plate, is injected into the combustion chamber through jet injectors, set up in the outer rim of the atomizer. Direction of movement of the streams is radial. On the periphery of the face is located a cylindrical ring with jet injectors 2, surrounded by the header 3. The injectors direct the stream of combustible on a tangent to chamber, thanks to which in the chamber a swirl flow of fuel will be formed. Such a construction is applicable on engines with low thrust.

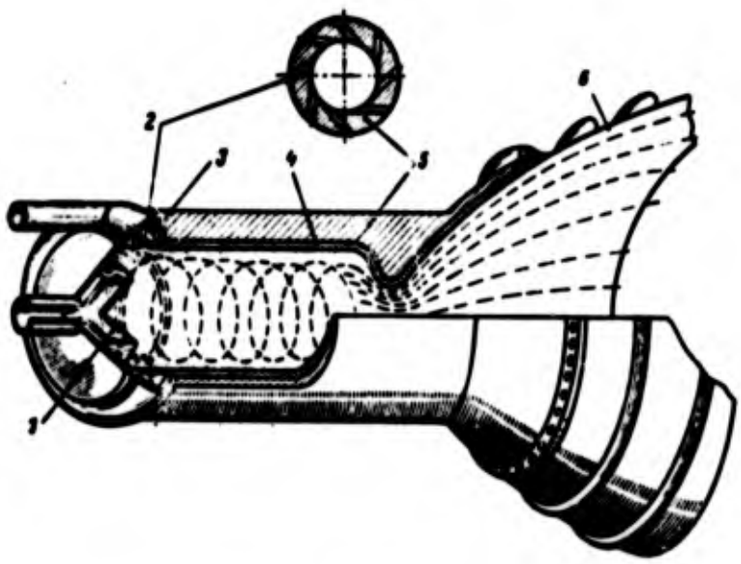

Fig. 12.7. Chamber with vortex head, erosion insert, and uncooled cap of nozzle: 1 - mushroom-like atomizer of oxidizer; 2 - injectors of fuel; 3 - head of combustible; 4 - erosion liner; 5 - wall of chamber; 6 - nozzle attachment.

Hipped and spherical heads possess a greater surface with the same diameter of combustion chamber than flat heads, and high strength properties. With the greater area of such heads it is possible to place and a greater number of injectors, thus ensuring the best atomization. In the center of the head it is simple to place the igniting device, which due to the specific nature of mixture formation is better protected from heating by hot gases. A deficiency of spherical and hipped heads, besides the complexity of their manufacture, lies in the possibility of accumulation of fuel at the axis of the chamber.

A hipped form of head can be used on engines with low thrust, for example, steering or auxiliary engines of space craft with one central fuel-supply arrangement (Fig. 12.8). The inner wall of the head is cooled by fuel. The massive outer wall of the head possesses a high degree of rigidity and is deformed little, which makes it possible to mount in it a mobile bushing, which when shifted changes the area of the injector nozzle.

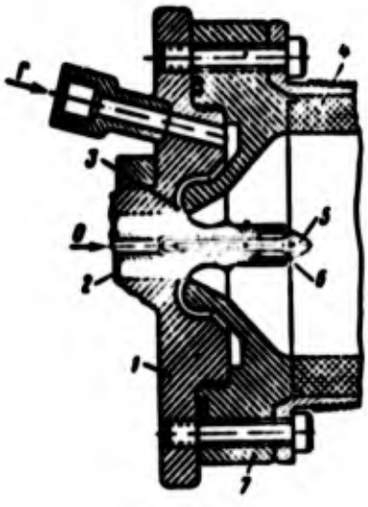

Fig. 12.8. Hipped head with two-component adjustable injector: 1 – outer wall of head; 2 – mobile bushing; 3 – slot injector of combustible; 4 – wall of combustion chamber made from fiberglass with non-directional location of fibers; 5 – mushroom valve; 6 – slot injector of oxidizer; 7 – inner wall of head. [Г = combustible; О = oxidizer]

Construction of the simplest spherical head with a double-walled injector face is shown in Fig. 12.9. The form of the wall of the face, which is turned to the combustion chamber, is selected in such a way that mixing of components of fuel occurs by three crossing jets; a central stream of combustible with lateral streams of oxidizer. Joining of the walls of the injector face is carried out by tightening

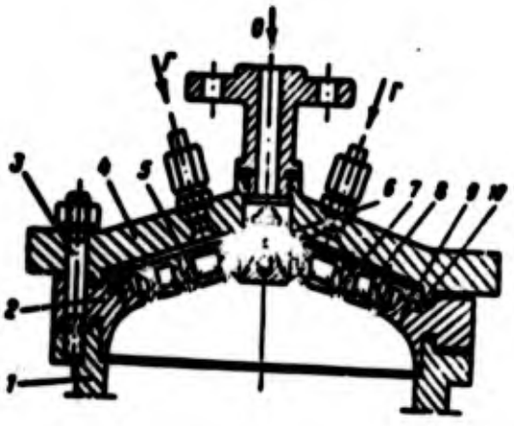

Fig. 12.9. Spherical head with double-walled injector face: 1 – wall of combustion chamber; 2 – inner wall of head; 3, 6 – pins; 4 – outer wall of head; 5, 7 – injectors of oxidizer and fuel; 8 – middle wall of head; 9 – pins; 10 – groove seals. [Г = = combustible; О = oxidizer]

the nut of pin 6 with subsequent setting up of pins 9, the axes of which are inclined to the axis of the chamber. Airtightness for the oxidizer cavity is achieved by annular groove seals 10 and the setting up of combustible injectors 7 on threads. The head is connected with the combustion by pins 3.

With a spherical head it is also possible to orgainze the prechamber displacement of components, described earlier in Chapter IV. A spherical head with prechambers has greater rigidity both due to the interconnection of its elements and also due to the relatively great thickness of the walls.

Similar to spherical heads with prechambers in a construction respect are spherical heads with flat injector bushings (Fig. 12.10), which are placed in the holes of the inner and middle walls.

Fig. 12.10. Head with flat injector bushings.

In certain constructions radial ribs are attached to the inner wall of the head from the side of the combustion chamber for preventing

the appearance of tangential fluctuations of gas. Height of ribs is determined experimentally. The ribs can be thin-walled and uncooled or with internal cooling (Fig. 12.11); in the latter case fuel is fed into central rod 1 and through apertures 2 enters the hollow ribs 8, from where along guiding partitions 3 it is conducted through apertures 4 in the injector face of the head from the ribs into the annular channels 7 of the head.

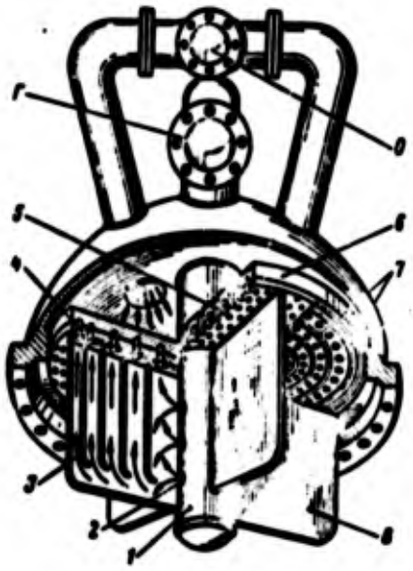

Fig. 12.11. Head with cooled ribs: Г and О – supply of combustible and oxidizer; 1 – central rod; 2 – apertures for exit of combustible from central rod into partitions; 3 – partitions; 4 – apertures for feeding combustible to annular rings of face; 5 – channels for feeding oxidizer to injectors; 6 – injector face; 7 – annular channels; 8 – ribs.

Along the uncooled ribs it is possible to mount additional injectors of combustible, forming a fuel curtain for protection of the ribs from overheating.

Certain design features have heads, intended for supplying to the combustion chambers components, one of which is in liquid, and the other in a gaseous phase, i.e., liquid-gas phase heads. These peculiarities are conditioned by the increased thermal conditions of wall which are circumvented by the hot gases, and also by requirements of special distribution of devices which are supplying the gas and liquid and the application of external and internal cooling of the head.

These problems are resolved comparatively simply when steam gas, forming during the decomposition of hydrogen peroxide and having a temperature of an order of 500°C, is admitted into the combustion chamber.

The construction of a spherical liquid-gas phase head with wing windows is shown in Fig. 12.12. Through windows steam gas is supplied from the turbopump assembly THA and from the catalyst chambers for afterburning in the combustion chamber. Liquid-gas phase heads can also be made latticed with the location of injectors of liquid component on radial and annular crosspieces of the lattice.

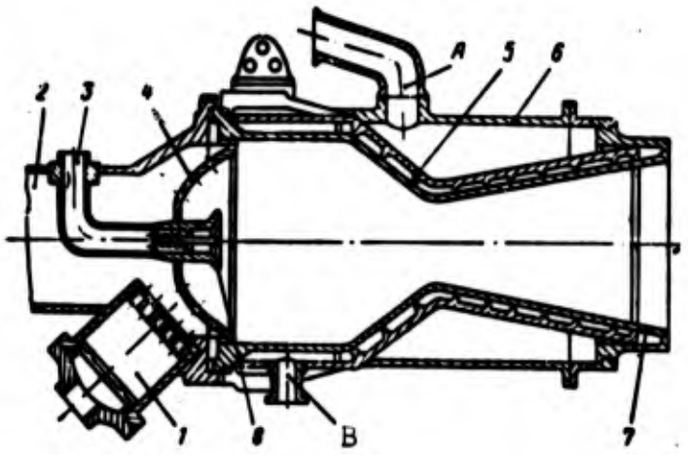

Fig. 12.12. Chamber of liquid propellant rocket engine with liquid-gas phase head with windows: A and B – coolant in and coolant out: 1 – catalyst chamber; 2 – discharge of steam gas from turbopump assemply; 3 – supply of combustible; 4 – window for supply of steam gas; 5 – outer wall of chamber; 6 – chamber housing; 7 – inner wall of chamber; 8 – gear-like injector of combustible.

12.2. Construction of Injectors

Jet injectors (Fig. 12.13a) constitute borings in the body of the head or special bushings. Diameter of injectors in constructions made, depending on productivity lies within the limits of 0.5-3.0 mm. Realization of apertures with a diameter less than 0.5 mm presents specific technological difficulties.

It is known from experience that the most advantageous relationship of geometric dimensions of jet injector is a ratio of length of injector ℓ to diameter of aperture d, lying within the limits of

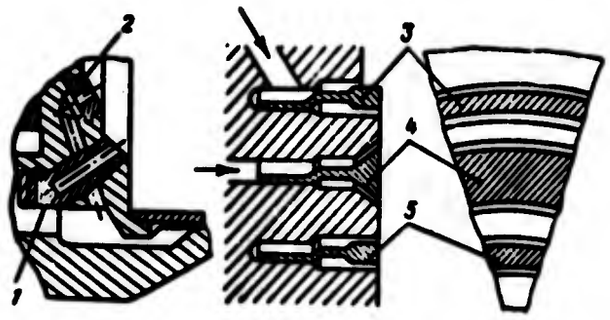

a) b)

Fig. 12.13. Injectors: a) jet; b) slot. 1 – jet injector, formed by drilling in body of head; 2 – jet injector, formed by drilling in bushing; 3, 4, 5 – inserts.

$2 < \ell/d < 4$. On the exit edge of the injector there is a fact for decreasing separation of the jet and increasing the discharge coefficient. Depth of facet is of an order of 1-2 mm angle of facet is 10-15°. The injector opening can also be conical with a ratio of diameters at the entrance to the injector and at the exit from it equal to 1.5-2.0.

The quality of atomization is influenced significantly by the purity of the surface of the injector hole. In case of application of chemically active components for fuel the material of the injector (and in a number of cases this is directly the material of the wall of the head) should possess high resistance to oxidation and corrosion, and also high strength during the action of high temperatures. Here it is necessary to ensure the absence of fusion of nozzles.

Slot injector (Fig. 12.13b), which are a variety of jet, constitute concentric slots in the head. Separate slots can be disposed with a slope to the axis of the chamber in order to ensure the impingement of jets of components. Width of the slot is made so that it is possible to obtain an area of slot injector corresponding to the expenditure of components. With a large diameter a slot injector should have such a small width that its realization becomes technologically very difficult and appears a great danger of

obstruction develops. Therefore slot injectors find application more frequently in engines with low thrust, where it is possible to install one of two-component slot injector in the center of the chamber. In this case the slot injector may have advantages over other injectors, since it is comparatively easy to regulate the area of the slot for changing fuel supply in the process of throttling the engine.

An adjustable slot injector is shown in Fig. 12.14. Fuel and oxidizer enter the chamber through two annular slots – inner and outer, forming between fixed outer cone 3, fixed inner cone 7, and mobile cone 4, connected with the piston of servomotor 8. Piston of servomotor 8 ends in the cylinder and on it on the one side acts spring 2, and on the other – force of pressure of liquid, fed from the hydraulic control system for the area of the injectors. Under the impact of the spring and the variable force of liquid pressure from the hydraulic system, piston 8 and the mobile cone 4 which is connected with it during operation of the engine occupy the corresponding positions, changing the cross sections of the slot injectors in accordance with the assigned law of thrust control

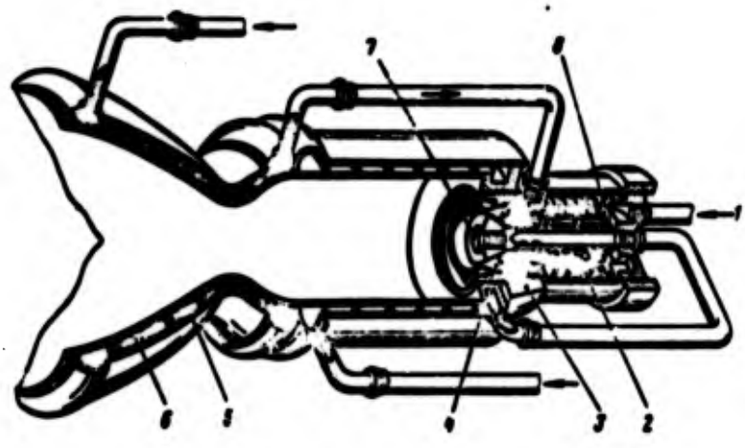

Fig. 12.14. Chamber with adjustable slot injector: 1 – supply of liquid from hydraulic control system; 2 – spring; 3 – fixed outer cone; 4 – mobile cone of injectors; 5 – outer wall of nozzle; 6 – inner wall of nozzle; 7 – fixed inner cone; 8 – piston of servomotor.

Analogous in construction is the adjustable injector shown in Fig. 12.8. In it the adjustment of areas of slot injectors of oxidizer 6 and combustible 3 is carried out during axial shifting of mobile bushing 2 and mushroom valve 5 respectively.

Swirler injectors are realized constructively as single-stage, two-stage, two-nozzle, and emulsion.

The simplest in construction and smallest in size are single-stage injectors with tangential channels (Fig. 12.15a). Selection of geometric characteristcs of an injector for an assigned expenditure can be ensured by the required flame angel (see Section 4.2). For decreasing the flame angle and increasing the flow rate without increasing pressure drop on the injector constructions are used with an additional opening 2 in the swirling chamber (Fig. 12.15b). Through a central opening 1 a portion of the fuel component is fed to the region of reduced pressure in the swirling chamber 7 and emanates from the nozzle in the form of a jet with a small cone angle. Liquid, arriving through the tangential channels, emanates from the nozzle in the form of a jet with a large flame angel. Thus can be ensured the multistage mixing of fuel.

Two-nozzle injectors at the same time are usually two-component. To each swirling chamber 3 and 4 (Fig. 12.15d) its own component is fed. Based on diametrical dimensions the two-nozzle injector is all told 20-30% larger than a single-component. Thanks primarily to the application of two-nozzle injectors it is possible to increase the flow intensity of the head.

Besides injectors with tangential channels and swirling chambers, in liquid propellant rocket engines they also use screw injectors with a multiplethread screw – a swirl vane 6 (Fig. 12.15e). Application of screw injectors is expedient, when due to conditions of arrangement a long swirling chamber is obtained. In an ordinary swirler injector this will lead to considerable losses on friction and the flame angle decreases. At the entrance to the screw injector it is possible to install a throttle washer 5, which, without considerably increasing

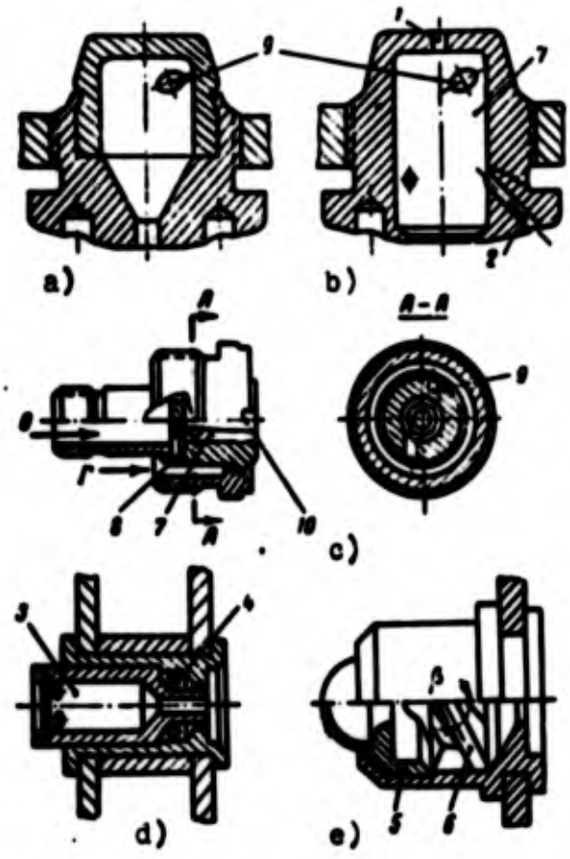

Fig. 12.15. Swirl injectors: a) single-stage; b) with central channel; c) emulsion; d) two-nozzle, integral igniter; e) auger. 1 – central opening; 2 – additional opening; 3 – inner swirling chamber; 4 – outer swirling chamber; 5 – throttle washer; 6 – screw; 7 – swirling chambers; 8, 9 – tangential channels; 10 – rod. [Г = = combustible; О = oxidizer].

the flow friction of the injector, increases its damping ability. Fluctuations of pressure of gases which develop in chamber, are smoothed out thanks to damping and do not cause an essential change of pressure of the liquid in cavities of the head. In the absence of a damping effect the development or supporting of resonance low-frequency oscillations in combustion chamber is possible. For the organization of multistage mixing it is possible to use screw injectors with a central hole in the screw, fulfilling the role of jet injector with a small flame angle and great range. Based on dimensions screw injectors are somewhat larger than injectors with tangential channels with the same productivity due to the necessity of placing the screw in the swirling chamber.

A construction of an emulsion system is shown in Fig. 12.5c, where the oxidizer and combustible are fed to the swirling chamber 7 through tangential channels 8 and 9.

In the constructions achieved the diameter of the swirling chamber $D_{к.з}$ comprises (2-4) R_c, where R_c – radius of nozzle. Size of the swirling chamber is determined to a considerable degree by the radial dimensions of the injector. Thus the outer diameter of the injector usually comprises

$$d_0 = D_{к.з} + (2+3) \text{ мм}.$$

If the body of the injector is included in the power-distribution system of the head, i.e., injector is placed in the wall on threads or is flared, then the thickness of the wall of the swirling chamber is selected from the condition of strength and rigidity of the corresponding connection. Diameter of tangential channels lies within the limits of 0.5-2.0 mm. Number of tangential channels is selected on an order of 2-6. The screw swirl vane should have a length, ensuring the curling of the liquid by no less than a 1/4 turn. With a long screw losses of pressure in the injector are increased without an essential improvement in the quality of atomization.

The cylindrical portion of the injector nozzle should be as short as possible. If the length of the nozzle is more than one gauge, then the angle of spraying is decreased. Cone angle of the swirling chamber at the entrance to the nozzle is accepted within the limits of 60-120°.

In the selection of the pitch between injectors it is necessary to originate both from the total number of injectors and also from the condition of ensuring the rigidity of the wall of the head. Here the value $d_г/t \leq 0{,}75$, where $d_г$ – dimensional diameter of injector, t – pitch between injectors.

Swirl injectors in the same set should have expenditure characteristics with an allowance of no more than 3-5%. Therefore injectors are manufactured according to the 2nd or 3rd class of accuracy. Based on productivity injectors of one component are split into groups. Injectors, included in different groups, differ in productivity and angle of flame. Productivity of peripheral

injectors of combustible for the formation of a wall layer is usually less than the productivity of injectors in the center of the head by 20-30%. Injectors of oxidizer which are set in the peripheral portion of the head, are also made with reduced productivity in order to decrease erosion of the shroud of combustible.

In the center of the head in most cases the injectors of one component have identical productivity. Sometimes, based on conditions of mixing which are determined experimentally, injectors of separate concentric rows can have productivity which differs by 25-50%.

Swirl injectors are made from low-carbon or alloy steels, and in certain cases from bronze and copper. Due to technological considerations the swirling chamber is more frequently made open. The bottom of the injector can be flared or soldered.

12.3. Construction of Combustion Chambers and Nozzles

Combustion chambers and nozzles are basically made double-walled. In separate cases single-walled and three-walled constructions find application. Combined constructions are possible when separate parts of the chamber or nozzle which is accepted on the whole as a double-walled construction can have one or three walls. All these distinctions are determined basically by the accepted system for cooling or thermal protection of the walls.

The simplest are single-walled chambers; they can be uncooled and cooled. In the event of a short duration of operation of the engine and low thermal balance sometimes single-walled chambers with capacity cooling are used.

A considerably longer duration of operation is ensured by applying on the wall heat-insulating coverings made from refractory materials or materials with low thermal conductivity. Then the wall preserves a relatively low temperature and its carrying capacity does not drop sharply toward the end of operation of the engine. Heat-insulating coverings used are ceramic and are applied directly on

the wall. Application of heat-insulating coverings in certain cases, for example, during short-term operation of an engine with a low temperature in the combustion chamber, can give saving in weight up to 25-30% as compared to a system of external cooling. Especially expedient is the application of coverings for the protection of single-walled uncooled attachments on the outlet section of the nozzle, where the wall does not carry considerable load from the forces of gas pressure. Such uncooled attachments are made from light alloys on the basis of aluminum or titanium, and also from copper. It is necessary to note that in separate cases single-walled nozzle attachments made from titanium or niobium alloy possess sufficient strength during removal of heat just by radiation and do not need a protective heat-insulating covering.

Application has also been found for constructions of combustion chambers and nozzles with the heat-insulating covering forming during the process of operation of the engine. If a single-walled chamber is made from fiberglass which is impregnated with phenol or epoxy resins, then heat-insulating coverings do not have to be applied. During heating the binding substances of fiberglass, which are burned, are carbonized, thus forming on the surface of the wall which is turned to the combustion chamber a covering which conducts heat poorly and ensures the preservation of mechanical properties of material in the nonburning layers.

In the construction shown in Fig. 12.8 the chamber is formed from fiberglass with nondirectional location of fibers. The thick-walled body of the combustion chamber is rigidly connected with a metallic flange, with the help of which the body of the chamber is attached to the head by screws. Sealing is achieved with the help of a grooving joint. The best mechanical properties under the impact of a gas load are possessed by a body of a combustion chamber which is made from narrow fiberglass tape with a directed arrangement of fibers and which in the process of winding is fitted by the rib to axis of the chamber.

The walls of the chamber can be protected from heating, as in the

construction shown in Fig. 12.7, with the help of an erosion liner 4, made from silicon tissue impregnated with phenolic resins. The liner with a clearance enters inside the aluminum body of the combustion chamber from the side of the divergent section of the nozzle. The radial clearance between liner and body is filled with insulating material. Attached to the nozzle flange of body on bolts is the uncooled nozzle attachment 6 with ribs for rigidity on the outer surface.

Cooled single-walled chambers can be with internal channels and without channels. In the first case the combustion chamber and nozzle are thick-walled with internal drilled and relatively sparsely located channels. For facilitation the chamber can be made from aluminum alloy. A deficiency of such a construction is the difficulty of making channels inside the walls on the narrowing and divergent section of the nozzle. Here is required either a greater thickness of wall for the possibility of drilling a long channel which is slanted with respect to the axis of the chamber or the manufacture of a nozzle from separate short sections.

The simplest way of cooling a single-walled combustion chamber is by locating it directly in the tank of one of the fuel components. In the construction shown in Fig. 12.16 the combustion chamber and inlet portion of the nozzle are placed in the tank for the combustible. For directed movement of the coolant the chamber is separated from the tank by a thin-walled nonpower housing 3. Such construction is applicable if the engine has comparatively low thrust and the diametrical dimensions of the aircraft make it possible to place the tank around the chamber of the liquid propellant rocket engine. The wall of the combustion chamber can be practically relieved of the action of forces of gas pressure when, as in the examined construction, cylinder feeding of fuel is used.

Double-walled constructions are used in those cases when the chambers have regenerative cooling. They differ by types of connections between the walls and forms of channels for external cooling. Double-walled chambers can be completely without power

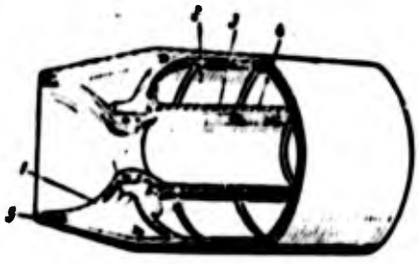

Fig. 12.16. Liquid propellant rocket engine with combustion chamber, located inside the fuel tank: 1 – wall of nozzle; 2 – fuel tank; 3 – casing; 4 – inner wall of combustion chamber; 5 – outer body of tank.

connections between the walls on the section between the head and nozzle, with sparsely located and thickly located and thickly located connections.

Double-walled chambers without intermediate connections (see Figs. 12.12 and 12.14) can be made with small diameters of combustion chamber, and also with low pressures in the chamber and a temperature of the inner wall of an order of 250-400°C. With such temperature conditions an inner wall with a thickness of 2-5 mm possesses sufficient rigidity and is able without a loss of stability to sustain the load from forces of pressure of the liquid coolant and gases. The outer wall, having still more favorable temperature conditions, is also able to take up the load from the forces of pressure of the liquid coolant.

The inner and outer walls in such a construction are connected with each other through the head and near the edge of the nozzle, and sometimes additionally at the end of the combustion chamber. Due to difference of temperatures of the inner and outer walls their lengthening during working conditions are different. For relieving the inner wall from temperature stresses, caused by difference of longitudinal temperature deformations, on the outer wall a corrugation compensator can be used or the deformation of ring headers for feeding of coolant can be used.

Under working conditions radial deformations of the walls of the chamber are also different; due to this there is the possiblity of a change of clearance between the walls and impairment of conditions of cooling. For the purpose of ensuring the minimum value of

clearance rods are welded to one of the walls, or the change in the gap is limited, as in the constructions shown in Figs. 12.12 and 12.14, by the height of the ribs.

Figure 12.17 depicts a double-walled construction of the exit section of a nozzle which is cooled by gas arriving from the turbine of the turbopump assembly. These gases create additional thrust when escaping through openings 6.

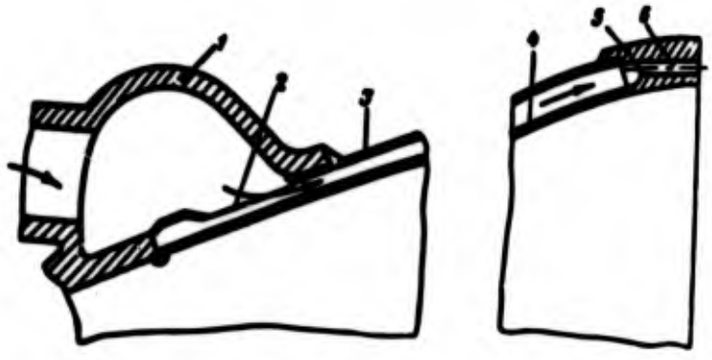

Fig. 12.17. Exit section of nozzle which is cooled by gases tapped from the turbine of the turbopump assembly: 1 - collector of gas; 2 - window; 3 - outer wall of nozzle; 4 - inner wall of nozzle; 5 - nozzle ring; 6 - opening for exit of gas from system for cooling of nozzle.

Application of a construction without a connection between the walls, which technologically is very simple, is possible for combustion chambers of engines with little thrust or for steering and auxiliary engines and at chamber pressures of 15-25 kgf/cm^2. Development of liquid propellant rocket engines accompanied by an increase of chamber diameter, combustion temperature, and pressure, made it necessary to switch to a construction at first with sparsely disposed and then with densely disposed connections.

Sparsely disposed connections are realized in the form of rigid rings, connecting the walls which promotes a decrease of deformation. Furthermore, near the rings the inner and outer walls work jointly, which increases the overall carrying capacity of the chamber. On sections between connections for relief of temperature stresses, which appear due to difference of longitudinal temperature deformations

of walls, annular compensators are placed which serve simultaneously as additional ribs for rigidity.

Such a type of construction is applicable at a wall thickness of an order of 5 mm and more, comparatively low wall temperatures, and pressures in the chamber of an order of 25-30 kgf/cm^2. In a weight ratio constructions with sparsely disposed connections are unprofitable.

The lightest and most reliable constructions are those with densely disposed connections, found so close to each other that the action of excess pressure of liquid coolant does not cause any noticeable local sags of the wall and efficiency of the chamber is determined only by the carrying capacity under the impact of forces of pressure of gases and axial force. The walls are connected with each other by welding or soldering.

With a welded joint on the outer wall point or solid blanks are realized. Point blanks can be round or oval with the large axis directed along the generating line of the chamber. Spot welding is conducted at the sites of blanks. However, in the event of very thick walls the blanks block the route of liquid coolant and do not permit connections to be situated sufficiently close.

Solid blanks under seam welding can be arranged depending on the accepted method of circulation of liquid coolant – along the generating line of the combustion chamber and nozzle or on a spiral, as in the construction shown in Fig. 12.18. With a multiplethread screw connection there is an increase in the length of contact surface of the walls as compared to longitudinal connections, which promotes an increase of rigidity of the chamber and strength of connections.

Increase of gas pressure leads to the necessity to considerably decrease the distance between connections, which is possible in soldered constructions. For soldering hard solders are used. Solders are applied preliminarily on the surface to be soldered.

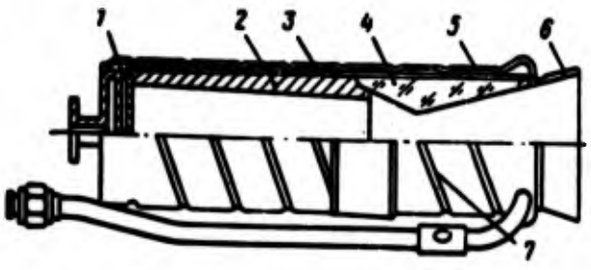

Fig. 12.18. Chamber of liquid propellant rocket engine with connection of wall by welding on helical blanks: 1 – injector face; 2 – erosion liner made from refrazila; 3 – inner wall of chamber; 4 – ceramic nozzle liner; 5 – outer wall of chamber; 6 – uncooled portion of nozzle; 7 – helical blanks.

Soldering is done in a furnace. Hard solders have a melting point up to 1500°C. With an operating temperature of 500°C at the site of the connection permissible stresses on the soldered seam comprise up to 8 kgf/mm^2, and at a temperature of 700° – around 1 kgf/mm^2.

Soldered constructions are made with ribs and of the tubular type.

The simplest construction is with the soldering of ribs which are set flush from one of the walls, for the most part from the inner (Fig. 12.19), to the other wall. Ribs on the inner wall are machined. They can have variable spacing over sections of the chamber and nozzle and are disposed along the generating line or along a spiral. For simplicity the ribs are made with a rectangular profile; their thickness should be the least permissible by technological resources. For reducing obstruction of the route for the liquid coolant and lowering the weight the ribs can be formed with thin-walled pressed profiles, which then are either soldered to both walls or are welded to one wall and soldered to the other. The difficulty of creating such soldered constructions, where the seam is inside the cooling cavity, lies in the necessity to ensure a smooth seam surface and to prevent the flowing of solder into the channels of the jacket. Free of this technological deficiency are soldered tubular constructions, for which seam is on the outside of the cooling channels.

Tubular chambers (see Fig. 12.1) are made from separate thin-walled tubes, placed along the generating line of the combustion chamber and nozzle, and sometimes along a spiral line. Tubes (Fig. 12.20) have rectangular, oval, or U-shaped section. In the

Fig. 12.19.

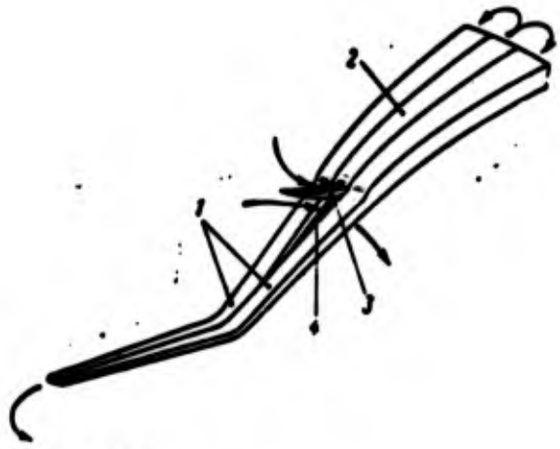

Fig. 12.20.

Fig. 12.19. Soldered connection of walls of a chamber with ribs: 1 – outer wall; 2 – inner wall with ribs.

Fig. 12.20. Tubes of combustion chamber and nozzle: 1 – tubes of combustion chamber and nozzle; 2 – shortened tubes of nozzle; 3 – feeding of component to shortened tubes; 4 – triangular window for feeding of gas from turbine of turbopump assembly to nozzle.

noncylindrical section of the combustion chamber and nozzle the area of cross section of tubes is variable. At relatively small expansion area ratios of combustion chamber and nozzle, the nozzle also can be formed from one and the same number of tubes. The number of tubes is selected so that each tube occupies an arc with a central angle of 0.75-1.25°. At large nozzle expansion area ratios with such an angular pitch on a nozzle section the tubes have to be strongly flattened, which is technologically difficult. Therefore in such cases combined constructions are used, when some of the tubes passes along all the generating line of the combustion chamber and nozzle (tube 1), and between them on the expanding section of the nozzle one or two shortened tubes 2 are placed. The tubes are soldered on lateral adjacent surfaces. The soldered seams receive a very considerable load from gas forces which are striving to disrupt the chamber along the generating line. For ensuring proper strength it is necessary to use strengthening elements. Such elements can be external housing, bands, or solid winding.

With a thick-walled metallic housing the weight of the chamber is increased considerably. Therefore more frequently separate

strengthening bands are used which are located almost next to one another on the combustion chamber and nozzle throat and with greater intervals on the expanding section of the nozzle (see Fig. 12.1). In separate constructions they use a winding on the outside of the tubular chamber with wire with a square cross section, which can be impregnated with binding epoxy resin. Instead of wire they also use a covering of fibreglass with a directed arrangement of fiber.

Specific conditions of cooling can also lead to the use of a three-walled tubular chamber (Fig. 12.21). In it through the inner series of tubes 2 the liquid coolant flows from the head to the nozzle section, and through the outer series 1 – in the opposite direction. Sometimes, for example in the construction shown in Fig. 12.1, a system of cooling is used in which through one of two neighboring tubes the liquid coolant flows from the head to the nozzle, and through the other – in the opposite direction.

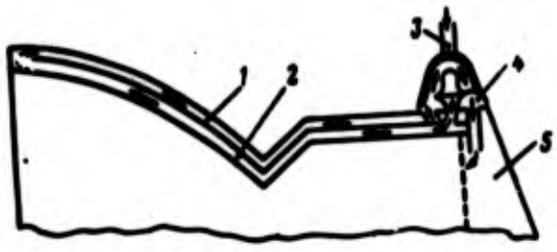

Fig. 12.21. Three-walled chamber: 1 – tubes of outer series; 2 – tubes of inner series; 3 – entry of fuel; 4 – main fuel valve; 5 – head of engine.

With a tubular construction it is comparatively simple to realize admission into the chamber of exhaust gas from the turbine of the turbopump assembly for the creation of additional thrust (Fig. 12.22). Windows for admission of gas have a triangular form and are formed in that section of the nozzle, where between the main long tubes 1 the shortened tubes 2 (see Fig. 12.20) are inserted.

A chamber with regenerative cooling can have heat-insulating covering in those cases, when heat capacity of the coolant is insufficient and there is no internal cooling, and also if fuel with a very high combustion temperature is used.

Walls of the chambers for the most part are made composite and are connected by longitudinal and transverse seams; less often

Fig. 12.22. Chamber of liquid propellant rocket engine with admission of gases from turbopump assembly into the nozzle: 1 - head of chamber; 2 - feeding of gases from turbine of the turbopump assembly; 3 - feeding of combustible (liquid hydrogen); 4 - annular collector for joining one inlet and two return tubes.

seamless chambers are used. Walls of cylindrical combustion chambers are welded from sheet material. Entrance section of the nozzle up to the critical section is usually stamped, just as a profiled nozzle. It is convenient to locate the welded seam of the entrance and exit sections of the nozzle in the critical section. For greater strength such a seam, and also longitudinal and transverse seams of the inner wall, are forged, and their surface which is turned to the gas flow is ground.

Thickness of the inner wall of the chamber is determined by conditions of cooling. In engines with high thermal intensity the thickness of the inner wall comprises approximately 0.8-2 mm. Thickness of the outer wall, due to conditions of required carrying capacity and depending on operational load, temperature, material, and permissible radial deformations, has greater dimensions.

Inner walls are made from heat-resistant steels or alloys or from materials with high thermal conductivity, for example, from copper, bronze, or aluminum. Outer walls in the case of small relative loads can be made from low-carbon or heat-resistant steel, and with large loads - from highly durable materials.

Thicknesses for the walls of tubes are of the order of 0.2-0.4 mm; materials for tubes are steel and nickel, and aluminum alloys.

12.4. Systems for Cooling the Chambers of a Liquid Propellant Rocket Engine

Elements of the cooling systems include collectors, bringing in and taking out the coolant, and devices for the directed movement of coolant through the clearance between the walls and for internal cooling of the chamber.

Collectors are welded to the outer wall of the chamber. In the collector the field of speeds of liquid coolant is levelled along the circumference before entrance into the clearance between the walls. The coolant is usually fed to the collector through several pipelines. At the site of location of the collector which supplies coolant to the end of the nozzle the outer wall can be absent (see Fig. 12.14), it can have a window (Fig. 12.23a), or it can form a deflector, directing the coolant to the nozzle exit section (Fig. 12.23b). If in the cooling system the liquid moves over some of the channels in the direction of the nozzle, and on the remaining channels – in the opposite direction, then the feeding collector should be located in the front section of the chamber, and at the end of the nozzle – the return collector. On the chamber there can be several collectors, if, for example, the liquid coolant is supplied at the nozzle, and is removed from the coolant passage not directly into the corresponding cavity of the head, but through valves or units of the control system, when separate elements of combustion chamber and nozzle are cooled by different components.

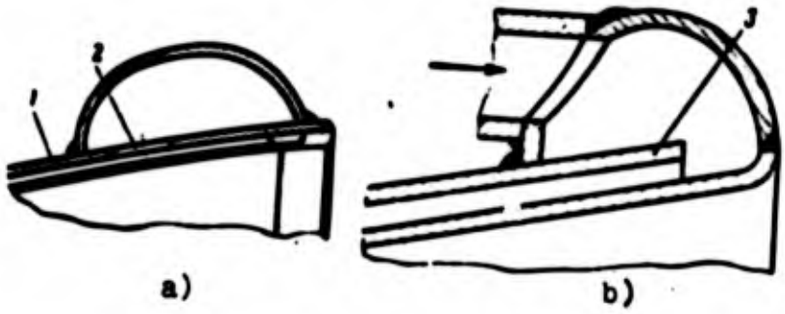

Fig. 12.23. Diagram of collectors, located at the end of the nozzle: a) with window in outer wall; b) with deflector; 1 – outer wall; 2 – window; 3 – deflector.

Different methods of removing liquid from the cooling system into the head are shown in Figs. 12.1, 12.4, 12.12, and 12.14.

Increasing the area of cooled surface and organization of movement of coolant in the clearance between the walls is furthered by channels which are formed by ribs on the inner or outer wall, tubes, rods, or spirals. Rods and spirals most frequently do not enter the power system of the chamber.

In the majority of constructions the channels are directed along the generating line. Spiral movement of the liquid is used in those cases when it is necessary to extend the path of the cooler over the clearance. During movement along a spiral channel, due to the action of centrifugal forces there is a separation of coolant: liquid particles are rejected to the periphery, and the vapors formed accumulate at the hot inner wall, which worsens heat withdrawal from it and can lead to burnout.

The size of the clearance between walls (area of channels) is determined by the speed of the coolant during calculation of the cooling system. In engines which have been realized, at the nozzle throat speed of the coolant reaches 25-30 m/s, and near the exit of the nozzle 8-10 m/s. When liquid oxygen is used as a coolant speed at the nozzle throat can reach 200 m/s and more. Clearances of less than 2 mm are difficult to achieve during normal construction of a chamber. When liquified gases are used for cooling the clearance can be increased.

If the coolant is chemically active in respect to the material of the channels, then protective coverings are applied to surfaces over which it flows, for example, parkerizing is carried out. Coverings are especially necessary in engines which are reusable.

12.5. Starting Devices

For starting engines on nonhypergolic components chemical, pyrotechnic, and electrospark ignition are used.

During chemical ignition of nonhypergolic components the basic fuel feeding devices are used. During the period of starting pipelines from priming fuel system, which is filled with hypergolic components, are connected to these devices. After formation of a powerful burning flame in the chamber the starting system is disconnected. During chemical ignition the chamber does not have any design peculiarities.

Pyrotechnic ignition is carried out with the help of explosive cartridges. The cartridges can be mounted in the head of the chamber, being one of its structural elements, but more frequently they are located on a special holder which is introduced inside the chamber from the side of the nozzle. In this case no limitations are placed on dimensions and construction of igniters. After ignition of basic components the igniting device is ejected with the flow of gases from chamber or remains on the lauching pad.

Certain peculiarities in the construction of the head area introduced by electrical starting devices which are usually placed in the middle of the head. Such devices are spark plugs, plug-igniters, or two-stage igniters.

For creating a spark of high power semiconductor spark plugs are used which consist of two concentric electrodes, the insulator between which is covered by a layer of semiconductor. Following the supply of voltage on the electrodes a current emerges in the semiconductor and heating of the semiconductor occurs. At a sufficiently high temperature of the semiconductor conditions are created for the ionization of the fuel mixture near electrodes, and between them a strong spark discharge develops. Periodicity of the discharge is of the order of 1 microsecond.

In a spark plug-injector an easily ignitable fuel, for example, gasoline or a mixture of combustible with oxygen, is blown through the discharge between the annular electrodes.

For protecting the igniter grom hot gases shielding is required by means of creating a fuel curtain when the starter is disconnected. For organization of a stable flame source during the entire time of

operation of the engine and easing the conditions of cooling, nondisengaging igniters are used.

The nondisengaging igniter (Fig. 12.24), placed in the center of the head of the engine, consists of two chambers located in series: a small one 5 (1st stage) and a large one 9 (2nd stage). In the small chamber there are spark plugs 4, injector of combustible 6, and injector of oxidizer 2. Oxidizer is supplied in a gaseous state. Products of combustion pass into the second chamber and ignite the fuel, supplied after firing up of the first chamber. The chamber of the 2nd stage, which is of three-walled construction, is cooled by fuel which is injected into the chamber through jet injectors located both on the head and also in several belts on the inner wall of the chamber. Oxidizer enters the second chamber through slot injector 11. For preservation of the ratio of components in the starting device regulators of supply are placed in the main lines. After cutoff of the engine the igniter is used for blowing out the chamber.

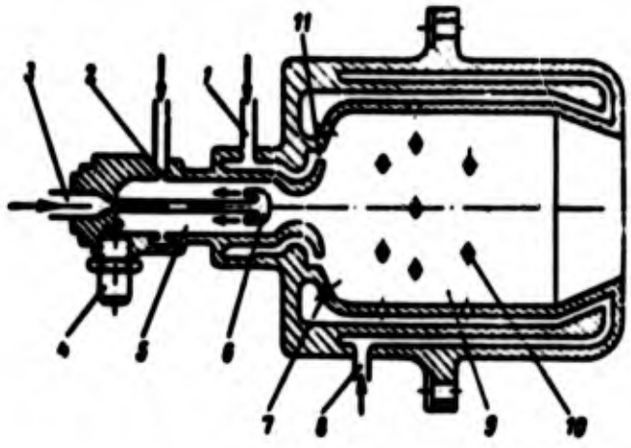

Fig. 12.24. Nondisengaging two-stage igniter: 1 - supply oxidizer (liquid oxygen) to chamber of 2nd stage; 2 - injector of gaseous oxidizer of 1st stage; 3 - supply of combustible (liquid ammonia) to 1st stage; 4 - spark plug; 5 - chamber of 1st stage of igniter; 6 - injector of combustible of 1st stage; 7 - injector of combustible in head of 2nd stage; 8 - supply of combustible to 2nd stage; 9 - chamber of 2nd stage; 10 - jet injectors of combustible; 11 - slot injector of oxidizer of 2nd stage.

Especially important in the process of starting is the order of entry of components into the combustion chamber, which is determined by the properties of components used and the construction of the chamber. Fuel during starting should be fed into the combustion chamber in a quantity which would avoid explosive accumulation of components. No less important also is fuel flow control during stopping of the engine. Program of supply during starting and stopping (Fig. 12.25) will be selected experimentally and is ensured by regulating devices, including main and auxiliary valves of components which are mounted in the main lines before the chamber.

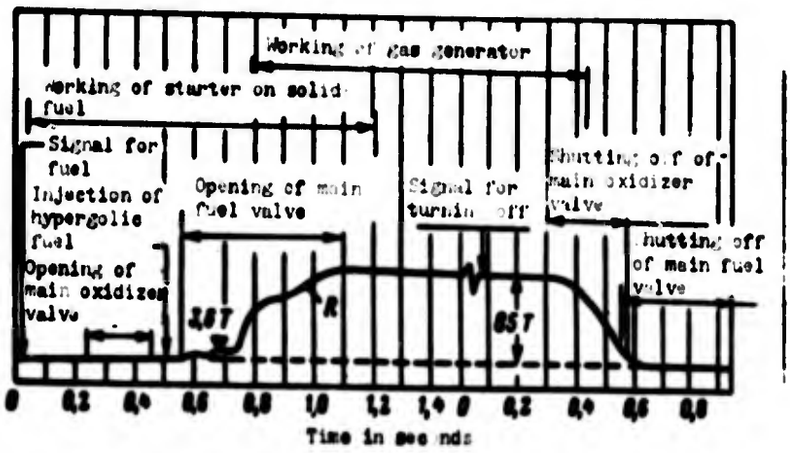

Fig. 12.25. Diagram of sequence of operations during starting and stopping engine H-1 (United States).

C H A P T E R XIII

STRENGTH OF CHAMBERS OF LIQUID PROPELLANT ROCKET ENGINE AND VIBRATION OF WALLS

13.1. Load Conditions of Chamber Walls and Calculation Scheme

Load conditions of the walls of combustion chambers and nozzles are determined by operating conditions of the engine and power circuit of the chamber. In general the most characteristic conditions are pressurization, starting, and a steady state of nominal thrust.

Conditions of pressurization correspond to control tests, conducted in the cold, of the airtightness of a double-walled chamber with external cooling. In this case in the interwall space the liquid coolant is fed under pressure p_{on} which is established for control. Element of a double-walled chamber with densely located connections will be loaded from within by forces of pressure p_{on}, and on the outside – by pressure $p_н$ of the environment (Fig. 13.1). These forces of pressure cause sags of chamber walls $y_н$ and $y_в$. Thickness of the walls should be selected so that no permanent deformation appear as a result of sag. As a rule calculation of thickness of walls from these conditions is not determining. Connections between the walls under conditions of pressurization are also loaded. The welded or soldered seam of the connections is calculated for break under the impact of the load per unit of length of the seam. By this calculation the strength of wall connections is checked.

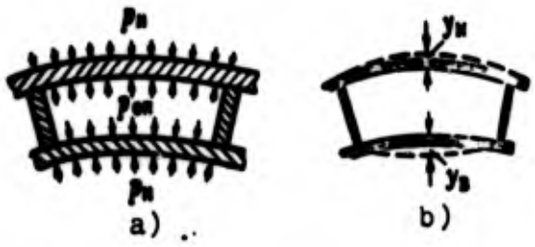

Fig. 13.1. Diagrams of load a and deformation b of an element of a double-walled chamber during pressurization.

Conditions of starting are irregular, namely: in process of starting there are changes in the pressure of gases in the combustion chamber, pressure of the coolant, temperature of gases in the combustion chamber, temperature of walls, and loads on elements of the chamber. It is possible to accept [53] that in process of starting, which lasts for 0.1-0.2 s, the pressure of gases $p_г$ changes in time by an exponential law (Fig. 13.2). One may assure also that the pressure of liquid in the system of external cooling, which is greater than pressure $p_г$, also follows this law. Temperature of the wall in the examined section is changed in process of starting by laws of non-stationary thermal conductivity, since there is heating of the walls of the chamber and liquid coolant enclosed between the walls. Due to thermal inertia the walls are heated more slowly than the increase of temperature of gases takes place in the combustion chamber and attain a stabilized temperature in an average of 2-4 s.

As can be seen from Fig. 13.2, only toward the end of starting the pressure of gases, and consequently also the load on the walls from gas forces, attain maximum value. But by this moment the temperature of the walls still has not reached maximum value and the strength of the material is sufficiently great. Therefore the conditions of starting do not present a danger from the point of view of strength of the chamber. This pertains also to that case, when in process of starting there is the possibility of a surge of pressure $p_г$ higher than the value corresponding to normal rating.

After termination of heating of the walls when the chamber is already brought to conditions of nominal thrust, temperature

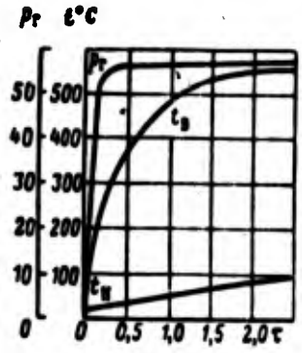

Fig. 13.2. Change of pressure of gases $p_г$ and average temperatures of outer $t_н$ and inner $t_в$ walls in the process of starting and heating.

loads also attain their maximum value. Therefore determining for the strength of the chamber are conditions of nominal thrust after termination of heating of the walls when their average temperatures obtain maximum value.

During calculation for strength the following basic assumptions and calculation scheme.

The walls of the chamber are viewed as an axisymmetrical shell of relatively little thickness, therefore stresses based on thickness of wall can be considered constant. Gas load is accepted as axisymmetrical and constant in time. The temperature field of the shell is also axisymmetrical. Strength properties of the material of the walls are taken as corresponding to their average temperature. In a number of cases high heating, accompanied by a change of properties of the material, leads to the appearance of plastic deformations.

It is assumed that from moment of starting active deformation in the walls of the combustion chamber takes place. During repeated startings there is an accumulation of plastic deformations. Calculation of this phenomenon can be performed by methods expounded in [53].

The walls of the chamber are loaded in circumferential and axial directions, which corresponds to their plane stress.

The calculation scheme for a two-walled cylindrical chamber of a liquid propellant rocket engine is shown in Fig. 13.3. Lengths of edges of the element with a central angle d_ϕ are accepted as equal to a unit. Acting on the edges of the element in an axial direction are loads P_x, in this case being specific loads. In a circumferential direction specific loads are designated by P_y.

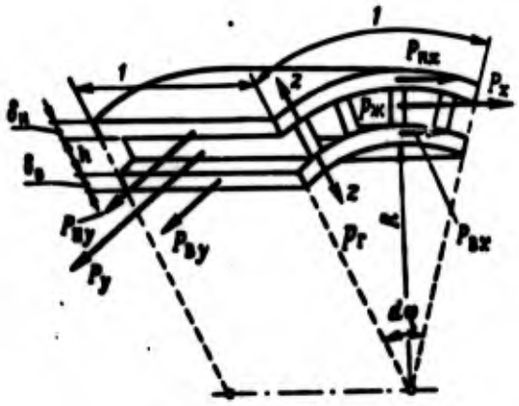

Fig. 13.3. Diagram of load of an element of a double-walled chamber.

In a calculated section of the chamber axial force X is acting. Value of X is determined by the curve of distribution of axial forces along the length of the chamber (Fig. 13.4).

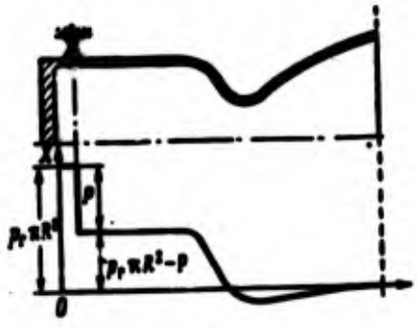

Fig. 13.4. Curve of axial forces of a liquid propellant rocket engine.

Acting on the element from within is a load, which is numerically equal to the pressure of gas in the given section of chamber $p_г$ and which is directed normally to the surface of the element. In the clearance between the walls with a height h there is a liquid coolant with pressure $p_ж$. Load on the wall from forces of pressure

of the liquid is numerically equal to $p_ж$ and is also directed normally to the surface of the wall.

The connections between the walls we do not consider loaded either with circumferential or axial loads. This assumption goes into the safety factor.

Subsequently all values of forces, deformations, and stresses relative to the outer wall we will designate by the supplementary index "н", and for the inner wall we will take the index "в".

By planning all the forces acting on the element in the direction of normal, conducted through its middle, we obtain

$$p_r R\,d\varphi\cdot 1+2p_ж h\cdot 1\cdot\sin\frac{d\varphi}{2}=2P_{в\varphi}\sin\frac{d\varphi}{2}\cdot 1+2P_{н\varphi}\sin\frac{d\varphi}{2}\cdot 1.$$

In view of the smallness of angle d_ϕ we take $\sin(d\varphi/2)\approx d\varphi/2$. Then we obtain the first condition of equilibrium of the element

$$P_{в\varphi}+P_{н\varphi}=p_r R+p_ж h.$$

Designating stresses on the edges of walls of the element $\sigma_{Ну}$, $\sigma_{Ву}$, $\sigma_{Нх}$, $\sigma_{Вх}$ and disregarding, in view of smallness of clearance $h \ll R$, the value $p_ж h$, we obtain

$$\sigma_{в\varphi}\delta_в+\sigma_{н\varphi}\delta_н=p_r R. \qquad (13.1)$$

During action in the calculation section of the chamber of axial force X the specific load per unit of length of cross section comprises $\bar{X} = X/2\pi R$. Then the second condition of equilibrium has the form

$$\bar{X}=P_{вx}+P_{нx}-p_ж h.$$

Hence, just as earlier, by disregarding the value $p_ж h$ and expressing force through stresses, we obtain

$$\sigma_{вx}\delta_в+\sigma_{нx}\delta_н=\bar{X}. \qquad (13.2)$$

We will designate $k = \bar{X}/p_r R$.

Value k characterizes the ratio of axial load per unit of length of section of chamber to circumferential specific load. Then expression (13.2) gives

$$\sigma_{нx}\delta_н + \sigma_{вx}\delta_в = k p_r R. \qquad (13.3)$$

Equations of equilibrium (13.1) and (13.3) are conveniently presented in the following form:

$$\frac{\delta_н}{\delta_в} = \frac{\sigma_{вx} - k\sigma_{вy}}{k\sigma_{нy} - \sigma_{нx}}; \qquad (13.4)$$

$$\frac{p_r R}{\delta_в} = \frac{\delta_н}{\delta_в}\sigma_{нy} + \sigma_{вy}. \qquad (13.5)$$

Value $p_r(R/\delta_в)$ is called the parameter of circumferential gas load.

13.2. Relationships Between Stresses and Deformations of a Double-Walled, Working in an Elastic Plastic Region

In the presence of rigid connections between the walls of the chamber it is possible to consider that full relative deformations of both walls in each of the directions – axial and circumferential – are identical [53]. Consequently, the following equality take place

$$\left.\begin{aligned} \varepsilon^{n}_{нy} &= \varepsilon^{n}_{вy} = \varepsilon^{n}_{y}; \\ \varepsilon^{n}_{нx} &= \varepsilon^{n}_{вx} = \varepsilon^{n}_{x}. \end{aligned}\right\} \qquad (13.6)$$

where index "n" designates full relative deformations.

Full deformation of a wall of the element is composed of relative deformations from corresponding stresses ($\sigma_{нy}$ and $\sigma_{нx}$ or $\sigma_{вy}$ and $\sigma_{вx}$) – force deformations, and temperature deformations. Let us designate deformations from stresses $\sigma_{нx}$, $\sigma_{нy}$, $\sigma_{вx}$ and $\sigma_{вy}$

respectively by $\varepsilon_{нx}$, $\varepsilon_{нy}$, $\varepsilon_{вx}$, and $\varepsilon_{вy}$. Temperature deformations of the walls we will designate by $\varepsilon_{нt}$ and $\varepsilon_{вt}$. Temperature deformations are determined by the dependences:

$$\left.\begin{aligned}\varepsilon_{нt}&=\beta_н t_н;\\ \varepsilon_{вt}&=\beta_в t_в.\end{aligned}\right\} \qquad (13.7)$$

where $\beta_н$, $\beta_в$ – coefficients of linear expansion of wall material at their assigned temperature; $t_н$, $t_в$ – average temperatures of walls. Consequently:

$$\begin{aligned}\varepsilon_y^в&=\varepsilon_{вy}^c+\varepsilon_{вt}=\varepsilon_{нy}^c+\varepsilon_{нt};\\ \varepsilon_x^в&=\varepsilon_{вx}^c+\varepsilon_{вt}=\varepsilon_{нx}^c+\varepsilon_{нt}.\end{aligned}$$

where $\varepsilon_{нy}^c$, $\varepsilon_{нx}^c$, $\varepsilon_{вy}^c$, $\varepsilon_{вx}^c$ – force deformations in walls.

According to the designations accepted earlier

$$\begin{aligned}\varepsilon_{нy}^c&=\varepsilon_{нy}-m\varepsilon_{нx};\\ \varepsilon_{нx}^c&=\varepsilon_{нx}-m\varepsilon_{нy};\\ \varepsilon_{вy}^c&=\varepsilon_{вy}-m\varepsilon_{вx};\\ \varepsilon_{вx}^c&=\varepsilon_{вx}-m\varepsilon_{вy}.\end{aligned}$$

where m – Poisson's ratio, depending on nature of deformation of wall. During plastic deformations m = 0.5.

As a result we have

$$\left.\begin{aligned}\varepsilon_y^в&=\varepsilon_{вy}-m\varepsilon_{вx}+\varepsilon_{вt}=\varepsilon_{нy}-m\varepsilon_{нx}+\varepsilon_{нt};\\ \varepsilon_x^в&=\varepsilon_{вx}-m\varepsilon_{вy}+\varepsilon_{вt}=\varepsilon_{нx}-m\varepsilon_{нy}+\varepsilon_{нt}.\end{aligned}\right\} \qquad (13.8)$$

From here it is possible to obtain the connection between force and temperature deformations of the walls.

$$\varepsilon_{вy}-\varepsilon_{нy}=\varepsilon_{вx}-\varepsilon_{нx}=\frac{\varepsilon_{вt}-\varepsilon_{нt}}{1-m}. \qquad (13.9)$$

A plane stress is characterized by intensity of stresses σ_i, connected with stresses σ_x and σ_y by the relationship

$$\sigma_i = \sqrt{\sigma_x^2 + \sigma_y^2 - \sigma_x \sigma_y}. \qquad (13.10)$$

Here the relative deformation of the element is characterized by intensity of deformations

$$\varepsilon_i = \sqrt{\varepsilon_x^2 + \varepsilon_y^2 - \varepsilon_x \varepsilon_y}. \qquad (13.11)$$

During tests of material in a uniaxial state of strain at its assigned temperature a diagram of deformation is obtained (Fig. 13.5). For a case of plane stress the same diagram of deformation is taken, but plotting on its axes not σ and ε, but σ_i and ε_i.

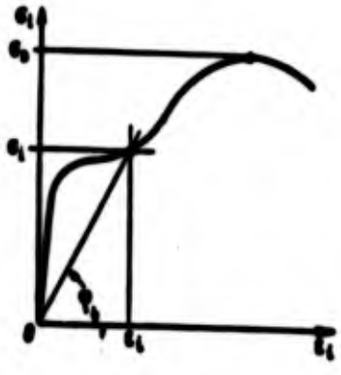

Fig. 13.5. Diagram of deformation of material.

In the plastic region the connection between stresses and deformations by analogy with the elastic region is expressed through the intersecting elastic modulus E':

$$\sigma_i = E' \varepsilon_i,$$

and

$$E' = \operatorname{tg} \gamma.$$

In reference to a double-walled shell we have

$$\left.\begin{aligned} \sigma_{0i} &= \sqrt{\sigma_{0x}^2 + \sigma_{0y}^2 - \sigma_{0x}\sigma_{0y}}; \\ \varepsilon_{0i} &= \sqrt{\varepsilon_{0x}^2 + \varepsilon_{0y}^2 - \varepsilon_{0x}\varepsilon_{0y}}. \end{aligned}\right\} \qquad (13.12)$$

where ε_{Hi}, ε_{Bi}, – intensity of deformations of outer and inner walls.

These values of intensities of deformations make it possible on the curves of deformation to determine the intersecting moduli of materials of the outer and inner walls E'_H and E'_B, and further by the formulas

$$\left.\begin{aligned} \sigma_{z,H} &= E'_H \varepsilon_{z,H}; & \sigma_{z,B} &= E'_B \varepsilon_{z,B}; \\ \sigma_{\theta,H} &= E'_H \varepsilon_{\theta,H}; & \sigma_{\theta,B} &= E'_B \varepsilon_{\theta,B} \end{aligned}\right\} \qquad (13.13)$$

to determine also the mean values of stresses in the walls of the chamber.

13.3. Calculation for Strength of Double-Walled Chambers

Strength calculation of a double-walled chamber is preceded by its thermodynamic and gas-dynamic calculations, selection of wall material, and calculation of cooling system. As a result of these calculations the geometric dimensions of the chamber in a calculation section, distribution of axial and circumferential loads, height of the interwall channel h, pressure of liquid coolant, average temperatures of outer and inner walls, and thickness of inner wall are known.

During a calculation on strength of combustion chamber stresses and deformations in the walls are determined, and also the forces having an effect on the connection.

Calculation is made conveniently by the graphoanalytical method with the use of a generalized graph of state of stress for walls of a chamber (Fig. 13.6). The graph constitutes a grid of dependences $\frac{\delta_2}{\delta_0} = \frac{\delta_2}{\delta_0}\left(\rho_r \frac{R}{\delta_0}\right)$ and $\varepsilon_{\theta,B} = \varepsilon_{\theta,B}\left(\rho_r \frac{R}{\delta_0}\right)$, constructed for several (in Fig. 13.6 – for nine) fixed values of full circumferential deformation ε_y^n.

Community of this graph emanates from the following. During its construction only the materials of the outer and inner walls, their

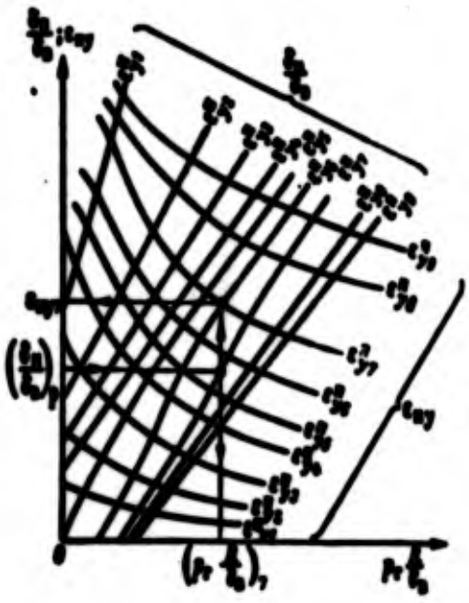

Fig. 13.6. Generalized graph of state of stress for the walls of a chamber.

average temperatures $t_н$ and $t_в$, and coefficients k are assigned (13.3). One should also know the diagrams of deformation of the given materials at assigned temperatures, and also coefficients of linear expansion $\beta_н$ and $\beta_в$.

Thus, it is possible to use this graph for calculation of strength of chamber walls for a liquid propellant rocket engine with various pressures of gases $p_г$, thicknesses of walls, and absolute radial dimensions during conditions stipulated above.

Order of construction of the generalized graph is the following.

Based on known $t_н$, $t_в$, $\beta_н$, $\beta_в$ temperature deformations of the outer and inner walls are determined.

Further several, for example m, values of full relative circumferential deformation $\varepsilon^п_{yj}$ are assigned where j takes values 1, 2. . . m. It is possible to recommend that $\varepsilon^п_{yj}$ be selected lying within the limits $\varepsilon_{в.т} \leqslant \varepsilon^п_{yj} \leqslant \varepsilon^п_{ут}$, where $\varepsilon^п_{ут} = \varepsilon_{в.т} + m(\varepsilon_{в.т} - \varepsilon_{в.т}) + 0{,}003$.

We assign n values of relative deformation of the outer wall

$\varepsilon_{нyk}$, where k = 1, 2. . . n.

Calculation is conducted for each pair of values (ε^{n}_{yj}, $\varepsilon_{нyk}$) in the following order.

From first equation of system (13.8) based on known ε^{n}_{yj}, $\varepsilon_{нyk}$ and $\varepsilon_{нt}$ we find $\varepsilon_{нx}$. From equation (13.9) based on known $\varepsilon_{нy}$, $\varepsilon_{нx}$, $\varepsilon_{вt}$, $\varepsilon_{нt}$, we determine $\varepsilon_{вy}$ and $\varepsilon_{вx}$. Further based on formula (13.12) $\varepsilon_{нi}$ and $\varepsilon_{вi}$ are determined, and based on diagrams deformation – intersecting moduli of materials of outer and inner walls $E'_{н}$ and $E'_{в}$. According to expression (13.13) effective stresses $\sigma_{нx}$, $\sigma_{нy}$, $\sigma_{вx}$, and $\sigma_{вy}$ are determined. Putting these stresses and value k in equations (13.4) and (13.5), we find $p_г(R/\delta_в)$ and $\delta_н/\delta_в$, corresponding to assigned ε^{n}_{yj} and $\varepsilon_{нyk}$. By carrying out the consecutive calculation for all pairs (ε_{yf}, $\varepsilon_{нyk}$), it is possible to construct a generalized graph of chamber stress.

With the help of the generalized graph of stress for chamber walls it is possible with a known gas load $p_г$, radius of chamber R and thickness of inner wall $\delta_в$ (it should be assigned during calculation of cooling of the chamber), to determine the thickness of the outer wall $\delta_н$, stresses and deformations effective in the wall, and reserve of carrying capacity of the chamber. Significance of the last value will be explained below.

Let us assume that from constructive considerations or on the basis of design experience with a known $p_г$ and $\delta_в$ the thickness of outer wall $\delta_н$ is selected. Then the rated value $(\delta_н/\delta_в)_p$ is known.

By drawing in Fig. 13.6 a horizontal with the ordinate $(\delta_н/\delta_в)_p$ on the points of its intersection with curves $p_в\frac{R}{\delta_в}=p_г\frac{R}{\delta_в}(\varepsilon^{n}_{y})$, data are determined for construction of curve of deformation $\varepsilon_в/\varepsilon_в=\varepsilon_в/\varepsilon_в\left(p_г\frac{R}{\delta_в}\right)$, shown in Fig. 13.7. Simultaneously in Fig. 13.6 are found the pairs of values $\delta_{нy}$ and ε^{n}_{y} for construction of dependence $\varepsilon_{нy}=\varepsilon_{нy}(\varepsilon^{n}_{y})$, also shown in Fig. 13.7. In Fig. 13.6 a method is shown for determination of a pair of particular values ε^{n}_{y7} and $\varepsilon_{нy7}$, and also the value $\left(p_г\frac{R}{\delta_в}\right)_7$.

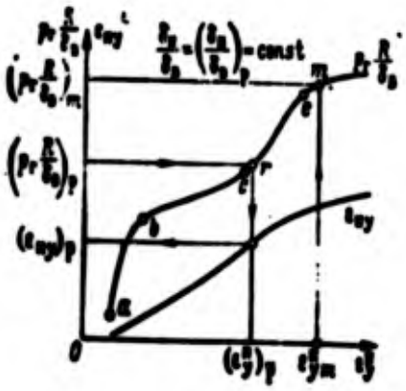

Fig. 13.7. Curves of deformation of chamber.

On the curve of deformation characteristic sections are separated by points a, b, c, e, and m. At the assigned value of parameter of gas load $\left(p_r \frac{R}{\delta_0}\right)_p$ the determinate is the position of calculation point r on the curve of deformation.

The position of the operating point on a specific section of the diagram makes it possible, first of all, to judge the value of possible error in determination of full circumferential deformation under calculation conditions with a known value of probable deviation of pressure in the chamber from calculated, and, secondly, about reserve of carrying capacity of the chamber.

It is possible to consider that values of ε_y^n, corresponding to the position of the operating point r on sections ab and ce of the diagram, are more reliable than values which correspond to positions of the operating point on sections bc and em. In cases of location of the operating point on sections bc and em small deviations of pressure of gases in the chamber cause large changes of full circumferential deformation. Therefore during designing one should avoid location of the operating point on these sections. As a rule, the operating point strives to combine with that section of its diagram where the parameter of gas load is greater than on section ab.

The reserve of general carrying capacity of a double-walled shell of a chamber in a liquid propellant rocket engine is what we will agree to call, following from work [57], the ratio of a certain

limiting value of parameter of circumferential gas load to its calculation value:

$$n=\frac{\left(p_r\frac{R}{t_в}\right)_m}{\left(p_r\frac{R}{t_в}\right)_p}.$$

Limiting value of the parameter of circumferential gas load can be selected in accordance with recommendations contained in work [53]. The reserve of carrying capacity of the chamber, depending on temperature regimen of the walls and pressure of gases in the chamber, can be within the limits n = 1.5-2.5.

If the reserve of carrying capacity at the given thickness of the outer wall is less than the shown values, it is necessary to assign a larger value of $(\delta_н/\delta_в)_p$ and to construct a new deformation diagram for the chamber. With a position of calculation point, satisfying the necessary reserve of carrying capacity n, the pair of values $(\varepsilon_{нy})_p$ and $(\varepsilon_y^n)_p$ is determined by the method shown in Fig. 13.7. Based on these values in the order described above components of deformations and stresses in the walls of the chamber are determined.

This calculation of the strength of double-walled chambers gives values of deformations of walls without considering the influence of forces of pressure of liquid enclosed in the clearance between them. During derivation of basic calculation relationships it was assumed that forces of pressure of the liquid coolant are internal and do not exert an influence on deformation. In reality, with a dense distribution of longitudinal connections in a double-walled chamber sags will be formed in the walls between the connections. The presence of connections exerts an influence on the form of wall in the case when connections are loaded.

The extent of local sags in the walls of a chamber is determined, for example, by the method expounded in work [53].

For determination of load which has an effect on the connection,

let us examine the equilibrium of an element of the outer wall with discarded connections (see Fig. 13.3) and substituted linear loads z. The action of n connections can be replaced by conditional pressure $p_{св}$:

$$p_{св} = -\frac{nz}{2\pi R},$$

where

$$z = \frac{2\pi}{n}(p_{ж}R - P_{в.у}).$$

If the connection between walls is realized with the help of spot welding [53], then the force on each point

$$P = p_{св}F_{т},$$

where $F_т$ – surface area of shell relative to one welded point.

If points are uniformly distributed over the surface of shell S and their number is equal to i, then

$$F_{т} = \frac{S}{i}.$$

With linear connections of the welded seam type or soldering on the ribs one can determine the force $q_ш$ which is exerted on a unit of length of seam:

$$q_{ш} = p_{св}\frac{S}{L},$$

where L – total length of seams on surface S.

The forces found on a connection are compared with destroying. The comparison should be conducted only in those cases, when the value of $p_{св}$ is positive. If $p_{св}$ is negative, then this means that under given operating conditions of a chamber its walls are not detached from each other, but are pressed together. This can occur due to the fact that at comparatively small forces of pressure of gases a considerable expansion of the inner wall from heating takes place.

Hence, in particular, it can be concluded that one of the most dangerous conditions for the strength of connections is pressurization of the engine.

13.4. Vibrations of Chambers of Liquid Propellant Rocket Engines

As it was shown in Chapter VI, in chambers of liquid propellant rocket engines low-frequency and high-frequency vibrations of gas can develop. These vibrations in a number of cases can lead to the onset of vibrations of chambers of liquid propellant rocket engines, and in the end – to breakdown of the chamber. For an analysis of causes of vibration destruction of chambers and development of measures for their elimination it is necessary to have knowledge of spectrum of frequencies of natural vibrations of a chamber and amplitude of variable forces which stimulate vibrations. In individual cases vibration of chambers can support intrachamber instability.

Two forms of basic natural vibrations are distinguished: axisymmetrical and flexural.

During axisymmetrical vibrations the shell is subjected to variable compression and expansion while preserving a correct annular form of its cross sections, i.e., with preservation of the symmetry relative to longitudinal axis (Fig. 13.8). Here along the length of the chamber, if one were to consider the shell rigidly sealed along the edges, the average surface of the wall is bent in such a way that between stops n half-waves are disposed, where n – an integar. Points which remained fixed in the process of vibrations are disposed over angular circumferences A. Forms of axisymmetrical vibrations are named according to number of half-waves respectively: with one half-wave along the length – first axisymmetrical form, with two – second, etc. Practically dangerous can be the resonance vibrations of chambers based on the first three forms of axisymmetrical vibrations.

For determination of frequencies of axisymmetrical natural

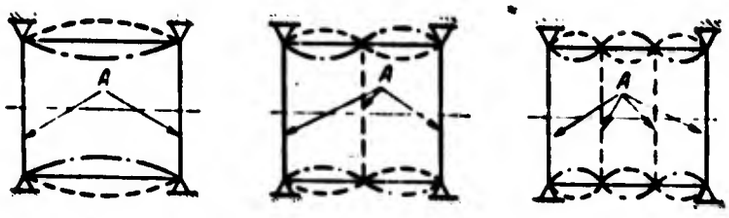

a) b) c)

Fig. 13.8. Forms of axisymmetrical vibrations of the wall of a cylindrical chamber of a liquid propellant rocket engine: a) first; b) second; c) third. A – angular circumferences.

vibrations with n half-waves of thin-walled cylindrical shells with length L, radius R, and thickness of wall δ, it is possible to use [9] the formula:

$$f_{ос}^2 = \frac{E\delta}{\mu R^2 (1-m^2)}(1+k\lambda^4), \qquad (13.14)$$

where

$$k = \frac{1}{12}\left(\frac{\delta}{R}\right)^2; \qquad (13.15)$$

$$\lambda = \frac{\pi R n}{L}; \qquad (13.16)$$

$$\mu = \frac{\gamma}{g}\delta. \qquad (13.17)$$

With sufficient accuracy for practical purposes the frequencies of axisymmetrical vibrations of a double-walled cylindrical chamber of a liquid propellant rocket engine with densely distributed connections can be calculated taking into account the mass of liquid coolant, enclosed in the clearance between the walls by the formulas (13.14)-(13.17) under the condition of replacement of values Eδ, δ, and μ, included in them by the corresponding given values

$$\delta_{пр} = \delta_в + \delta_н;$$

$$(E\delta)_{пр} = E_в\delta_в + E_н\delta_н;$$

$$\mu_{пр} = \frac{1}{g}(\gamma_в\delta_в + \gamma_н\delta_н + \gamma_{св}\delta_{св} + \gamma_ж h),$$

where $\delta_{св}$ – thickness of material of connections which is obtained with their uniform "smearing" over one of the walls of the chamber; h – height of interwall channel for liquid coolant taking into account its obstruction by connections; $E_в$, $E_н$ – elastic moduli of material of inner and outer walls with their corresponding average temperatures; $\gamma_в$, $\gamma_н$, $\gamma_{св}$, $\gamma_ж$ – densities of material of walls, connections, and liquid coolant.

As can be seen from expression (13.14), the frequency of inherent axisymmetrical vibrations does not depend on the value of excess pressure acting on the wall.

During flexural vibrations the wall loses its annular form in a cross section. It is bent and fluctuates near a position of equilibrium of the middle surface, having several (but no less than two) pairs of fixed nodes of vibrations (Fig. 13.9). Points which remain fixed in the process of vibration will form nodal lines disposed along the generating lines of the chamber. The form of flexural vibrations is characterized by the number of waves q, packed along a length of circumferences of cross section. The least number of waves is $q_{min} = 2$. During flexural vibrations on a length of chamber several half-waves can be fixed. In a practically important frequency range of flexural vibrations on a length of shell one half-wave is established, i.e., $n = 1$.

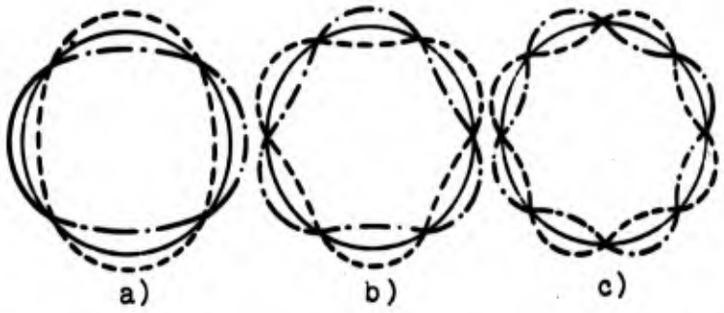

Fig. 13.9. Forms of flexural vibrations of the wall of a chamber for a liquid propellant rocket engine: a) with two waves; b) with three waves; c) with four waves.

Frequency of flexural vibrations depends on excess pressure $p_{изб}$. Taking into account excess pressure the frequency of inherent flexural vibrations of any of the walls of the chamber in the absence of connections between the walls can be determined [9] by the formula

$$f^2_{изг} = \frac{E\delta}{\mu R^2(1-m^2)} \frac{(1-m^2)\lambda^4 + k(\lambda^2-q^2) + \gamma(\lambda^2+q^2)^2(q^2-1)}{\lambda^2 + q^2(1+2\lambda^2)+q^4}, \qquad (13.18)$$

where

$$\gamma = \frac{p_{изб}R(1-m^2)}{E\delta}. \qquad (13.19)$$

Values k and λ are calculated respectively by the formulas (13.15) and (13.16).

Frequency of flexural vibrations at a given excess pressure depends on number of waves q. For every chamber depending on its geometric dimensions at a given excess pressure there exists that number of waves q, at which the frequency of inherent vibrations turns out to be minimum (Fig. 13.10). The general nature of dependence of frequencies of inherent flexural vibrations on number of waves is such that with an increase of q the frequency at first decreases, and then is increased.

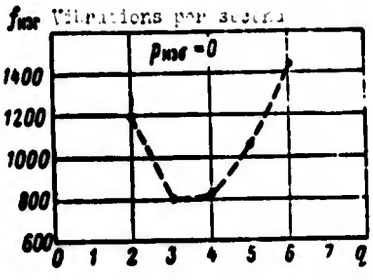

Fig. 13.10. Dependence of frequency of inherent flexural vibrations of chamber wall on the form of vibrations.

In formula (13.19) internal excess pressure is taken as positive, and external – negative. During calculation of the outer wall the internal excess pressure is taken as equal to the pressure of the liquid in the clearance between the walls. During calculation of the inner wall $p_{изб} = p_{жс} - p_г$ and is negative.

Increase of internal excess pressure leads to an increase of frequencies of inherent flexural vibrations. Conversely, an increase

of excess external pressure causes their decrease. Dependence of frequencies of inherent flexural vibrations on internal excess pressure at a various number of waves q is shown in Fig. 13.11.

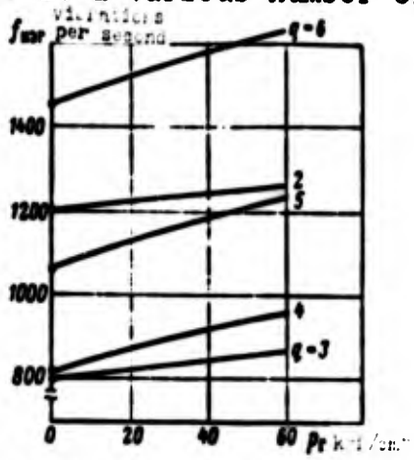

Fig. 13.11. Dependence of frequency of inherent flexural vibrations of chamber wall on the value of excess pressures for various forms of vibrations.

At a certain excess pressure $p_{изб.кр}$ the frequency of inherent flexural vibrations of a given form may become equal to zero. This means that at a given pressure the shell loses stability with the formation of the corresponding number of waves. Usually the minimum value of $p_{изб.кр}$ corresponds to that number of waves q, at which the frequency of inherent vibrations is minimum.

Frequency of inherent flexural vibrations of a double-walled chamber with density distributed connections between the walls is determined [9] by the formula:

$$f^2_{изг} = \frac{E_в\delta_в + E_н\delta_н}{\mu R^2}\,\frac{\lambda^4 + k_1(\lambda^2+q^2)^4 + \varphi_1(\lambda^2+q^2)^2(q^2-1) + \varphi_2\lambda^2(\lambda^2+q^2)^2}{q^2+(\lambda^2+q^2)^2}, \qquad (13.20)$$

where

$$\mu = \frac{1}{g}(\gamma_в\delta_в + \gamma_н\delta_н + \gamma_{св}\delta_{св} + \gamma_м h);$$

$$k_1 = \frac{E_в J_в + E_н J_н}{(E_в\delta_в + E_н\delta_н)R^2};$$

$$\varphi_1 = \frac{P_{вy} + P_{нy}}{E_в\delta_в + E_н\delta_н}; \quad \varphi_2 = \frac{P_{вx} + P_{нx}}{E_в\delta_в^2 + E_н\delta_н},$$

$J_в$, $J_н$ – moments of inertia of inner and outer walls with their unit length relative to the axis passing through the center of gravity of the calculation section parallel to the axis of the chamber;

$p_{вy}$, $p_{вx}$, $p_{нy}$, $p_{нx}$ – circumferential and axial loads of inner and

outer walls under calculation conditions.

As can be seen, frequencies of inherent flexural vibrations depend to a certain degree on value of axial force. With an increase of stresses of expansion the frequencies of natural vibrations are increased.

The column of gas in the chamber of a liquid propellant rocket engine constitutes an elastic system and has an infinite number of frequencies and forms of inherent acoustic vibrations – waves of pressure. As was shown in Chapter VI, the basic types of acoustic oscillations are longitudinal and transverse. The latter in turn are subdivided into radial and tangential.

During acoustic oscillations of gas based on any form of natural vibrations in the combustion chamber nodal surfaces will be formed on which the pressure of the gas constant, and surfaces of antinodes on which amplitudes of variable pressure reach to the maximum. As example in Fig. 13.12 are shown diagrams of pressure at longitudinal vibrations of gas in a combustion chamber with a nozzle, which can be reduced to a certain equivalent tube: Length of equivalent tube $L_э$ is taken equal to the distance from head to a section, the area of which is equal to three throat areas. During low forms of vibrations – first and second – antinodes of pressure appear at the head of the chamber and the nozzle.

During the action of a variable pressure of gases with an amplitude of vibrations Δp_r in the walls of the chamber forced vibrations emerge. They will be axisymmetrical, if the variable pressure is uniformly distributed over the circumference of cross sections of the chamber. Such conditions are created during low-frequency vibrations of pressure and during longitudinal or radical forms of high-frequency vibrations. With an equality of frequency of disturbing variable pressure of one of the frequencies of natural vibrations of the chamber resonance vibrations of the walls develops. It is obvious that the best conditions for excitation of forced

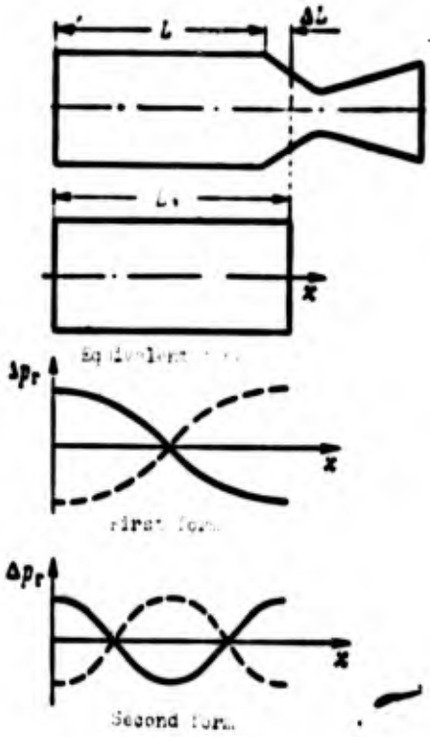

Fig. 13.12. Equivalent circuit of combustion chamber of a liquid propellant rocket engine and forms of longitudinal acoustic oscillations of gases.

vibrations are created when the greatest share of work accomplished by variable pressure will go to rocking of the walls. For this during forced axisymmetrical vibrations the diagram of pressure for chamber length should repeat the form of natural vibrations, i.e., be similar to it.

The first form of axisymmetrical vibrations can be excited during a simultaneous change of pressure over the entire volume of the chamber. However, here the frequency of change of pressure is low (order of tens of cycles per second), and natural frequency is very high (thousands of cycles per second). Therefore forced vibrations of this form occur far from resonance.

Frequency of the first form of natural vibrations can coincide, for example, with the frequency of high-frequency longitudinal vibrations of gas based on the second form. As can be seen from Fig. 13.13, in the central part of the chamber the amplitudes of pressure and shift are in one phase, and on the ends of the chamber – in a reversed phase. Consequently, on the ends of the

chamber the vibrations of pressure counteract the vibrations of the walls. Thus, it may be concluded, that for the appearance of resonance vibrations of chamber walls, when amplitudes will increase so that they are made dangerous for the strength of the walls, besides the basic condition of resonance – coincidence of frequencies of natural and forced vibrations, no less important is the similarity or proximity in the form of diagram of variable pressure to the diagram of sags in the wall during its natural vibrations by the given form. These conditions during longitudinal vibrations of gas, as was shown above, usually are rarely realizable.

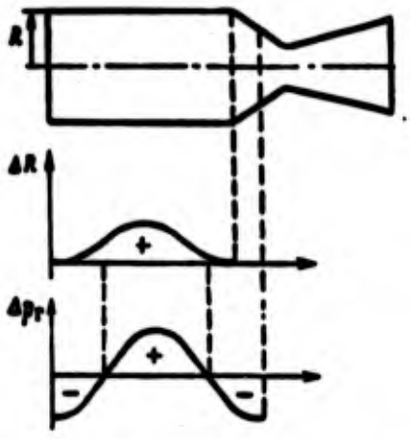

Fig. 13.13. Diagrams of radial deformation of chamber wall and pressure of gases along the length of the chamber.

More favorable are conditions of resonance during forced flexural vibrations of walls developing from high-frequency transverse and tangential forms of vibrations of pressure of gases in the combustion chamber, and also during parametric and flexural vibrations. Parametric vibrations are characterized by the fact that external variable force accomplishes work not on the basic shifts of mass, but on its secondary shifts, i.e., when the influence of external force is reduced to a periodic change of elastic parameters of the system.

The simplest model of parametric vibrations can be a vibration system in the form of vertical strained filament with a mass on

middle (Fig. 13.14). If on the filament variable force $T = T_0 + \Delta T \sin \Omega t$ is acting and the filament is in an equilibrium vertical position, a change of tension of filament does not cause lateral vibrations of the mass. If, however, the mass is removed from equilibrium by a transverse force, then a change of tension of the filament will lead the mass to a position of equilibrium, and then, by inertia, to transition through the position of equilibrium, i.e., to the onset of vibrations. If tension of the filament is increased during movement of the mass to a position of equilibrium and decreased during removal from the position of equilibrium, then amplitudes of vibrations will be increased. Resonance, which is called parametric, can set in.

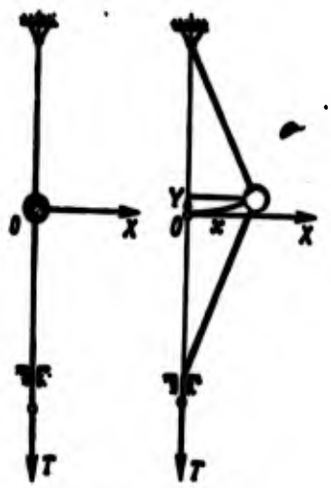

Fig. 13.14. Diagram of parametric vibrations of a mass on a vertical stretched filament.

Parametric vibrations also take place in combustion chambers of liquid propellant rocket engines. Let us assume that in a certain instant the annular form of cross section of a chamber under the impact of any disturbance was turned into one similar to elliptic a (Fig. 13.15). If at the time of distortion internal pressure reached a maximum, the ring starts to be straightened out and, passing by inertia a neutral position corresponding to the form of the circumference, again takes the distorted form b. If by this moment the internal pressure again reaches a maximum, the phenomenon will be repeated. According to set conditions the pressure for the entire period of vibrations of the ring reached a maximum twice. This

corresponds to maximum transfer of energy of pressure to a vibration system. As also in the case of parametric vibrations of a filament, variable force – the pressure of gases, accomplishes work on the secondary shift of the system, since the bending moment from forces of pressure appears only when the cross section of the chamber differs from a circular form. Therefore such a vibration mode can be related to parametric, and resonance, in the event of its appearance, is parametric resonance.

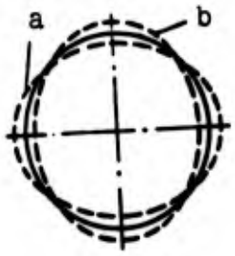

Fig. 13.15. For an explanation of appearance of parametric vibrations of a shell.

Investigations of parametric resonance of different elastic systems, which by analogy can include the shell of combustion chamber, show that not just separate resonance states exist, but a whole region of parametric resonance [53]. If one were to designate ω and Ω the frequencies of natural vibrations and vibrations of pressure, and $\Delta p_г$ the amplitude of vibrations of pressure of gas, then it is possible to construct a diagram of parametric resonance similar to that shown in Fig. 13.16. On diagram the three zones of parametric vibrations are shaded. The most dangerous is the zone where $\Omega \approx 2\omega$. In the other two zones the amplitudes of vibrations in the presence of damping are small and do not present a practical danger. The diagram shows that in shells of a chamber of a liquid propellant rocket engine parametric resonance appears if the point with coordinates Ω/ω and $\Delta p_г/p_г$ falls in one of the shaded regions. In view of the presence of regions of resonance the probability of its appearance is increased. An additional condition for the appearance of parametric resonance is, as was indicated above, the presence of vibrations of pressure of gases in the combustion chamber of type of radial or tangential acoustic oscillations, which are one of the most characteristic forms.

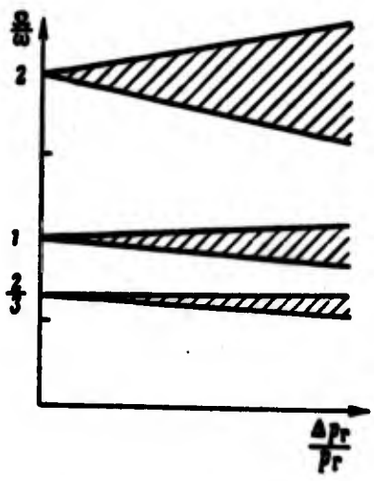

Fig. 13.16. Areas of parametric resonance of the chamber wall of a liquid propellant rocket engine.

Combatting dangerous resonance vibrations of shells of combustion chambers is usually conducted by constructional means. They can be reduced to measures, directed towards either a change of frequencies of natural vibrations of chambers or of frequencies of acoustic oscillations. Frequencies of acoustic oscillations can be modified with a change of geometric dimensions of the chamber or by carrying out special measures for decreasing the pulsations of gas.

Frequencies of natural vibrations of shells depend on the dimensions of the chamber, thickness of walls and properties of the material. The most probable path of changing frequencies of natural vibrations is changing the thickness of the outer wall, inasmuch as this is not connected with a change of conditions of cooling a chamber with densely distributed connections. In chambers with sparsely distributed connections a frequency shift of vibrations can be basically achieved by means of changing the rigidity and sites of location of reinforcing elements.

Forced vibrations or parametric flexural vibrations can also occur in walls of conical or profiled nozzles. Usually the narrow part of the nozzle possesses great rigidity and is hardly deformed. Therefore one may assume that in the critical section the nozzle is fastened or supported by a hinge on an annular contour. Nozzles have the greatest amplitudes at the free end. Nodal lines during

flexural vibrations appear along the generating line of the cone (Fig. 13.17). In a conical nozzle parametric vibrations can appear also.

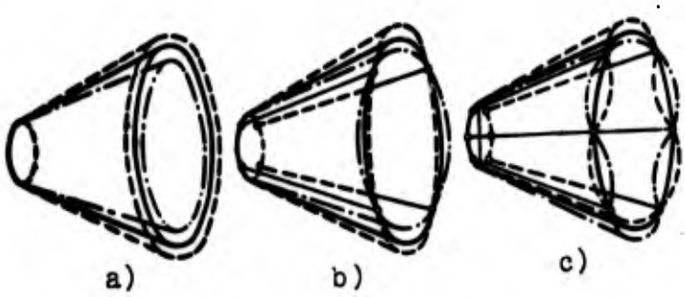

Fig. 13.17. Forms of natural vibrations of conical nozzle walls of a liquid propellant rocket engine: a) first form of axisymmetrical vibrations; b) first (four-nodal); c) second (six-nodal) forms of flexural vibrations.

C H A P T E R XIV

TURBOPUMP ASSEMBLIES OF LIQUID PROPELLANT ROCKET ENGINES

In a pump feed system a turbopump assembly (TNA) is used as the basic unit for creation of pressure. To ensure operation of the centrifugal pumps without cavitation a preliminary increase of inlet pressure in the pump is required. Increased pressure can be created by pressurizing the tanks, i.e., essentially by creating pressure feed system of fuel to the TNA or by booster jet pumps. Jet pumps can be used as the basic units of the pump feed system. In this case the necessity of having a pressure feed system of fuel to the basic pumps is not eliminated.

In the turbopump assemblies of a liquid propellant rocket engine basically there are found axial impulse-type turbines and centrifugal pumps. The design of a turbopump assembly of an engine with a bi-propellant is shown in Fig. 14.1. The main units of a turbopump assembly are turbine A, fuel pump B, and oxidizer pump C. The turbine has housing consisting of two halves 2 and 17, a rotor wheel 4, nozzle boxes 15 and 16, an inlet header 3, and a gas header 1. Subassemblies of the pumps consist of housings 6 and 10, in which are carried out the inlet nozzles and diffusers with collection chambers and impellers 7 and 11. The shaft of the rotor of the turbopump assembly rests on supports 5. For insulation of the cavities of the turbine and pumps packing 8, 9, 13 and 14 are placed on the shaft.

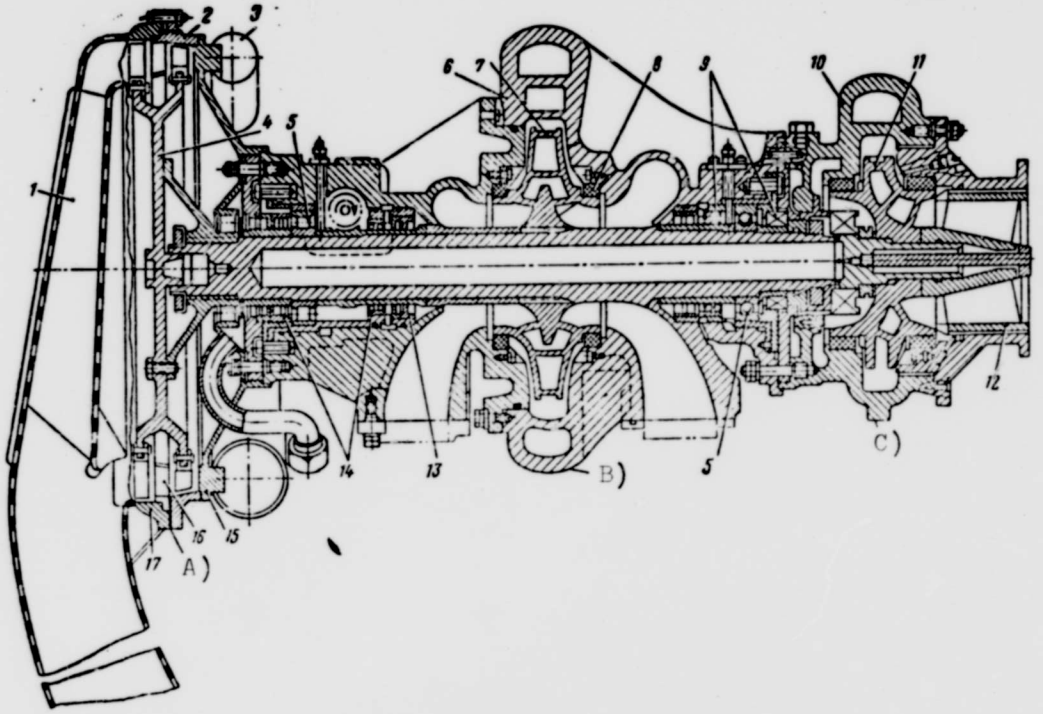

Fig. 14.1. Turbopump assembly of a liquid propellant rocket engine: A) turbine, B) fuel pump, C) oxidizer pump. 1 – housing of gas header of the turbine; 2, 17 – half a turbine housing; 3 – inlet header of the turbine; 4 – turbine rotor wheel; 5 – bearings; 6, 10 – housings of pumps; 7, 11 – pump impellers; 8, 9, 13, 11 – packing; 12 – axial stage of the pump; 15, 16 – nozzle boxes.

The turbopump assembly in addition has a reduction gear, if the number of revolutions of pumps and turbine are not the same. The number of pumps in a turbopump assembly may be more than two, if the basic fuel components are not used for feeding the turbine or if there are required two or more pumps for the supply of each component for production of assigned flow rate or pressure. As additional devices, a turbopump assembly may have an oil pump for systems for lubricating the bearings and reduction gear, a pump for supply of the actuating medium to the control system or for controlling the aircraft, a powder or electrical starter for starting, a speed control regulator for the turbopump assembly, etc. The structural perfection of a turbopump assembly and its arrangement, and also the rational use of strength properties of the material have an essential effect on the perfection of the propulsion system as a whole.

14.1. Assembly Diagrams of a Turbopump Assembly

The assembly diagram of a turbopump assembly is basically determined by the diagram of its rotor, to which all the revolving elements of a TNA pertain: rotor wheels of the turbines, pump impellers, shafts and their connecting subassemblies, drives of the assembly. Turbopump assemblies are more frequently single-rotor and more rarely two-rotor. The number of rotors is determined by the corresponding number of turbine rotor wheels having different numbers of revolutions.

Each rotor may have one or several shafts. In the latter case, the shafts are connected through a reduction gear (in the reduction gear of the turbopump assembly) or connector sleeves.

The simplest in construction and easiest to assemble are single-rotor turbopump assemblies without reduction gears. They occur more frequently with two- and four-supports; they rarely have three supports.

Dual-support rotors are used with relatively rigid shafts, when the mass of the rotor turbine wheel and pumps is comparatively small, and consequently there is little shaft sag. Dual-support rotors are distinguished by location of the turbine and pump inlets. With two pumps the turbine can be located between them or on the end of the rotor.

A turbopump assembly with overhung arrangement with respect to the turbine supports and one of the component pumps is shown in Fig. 14.1. With such an arrangement feed is facilitated and, especially the elimination of hot gases from the turbopump assembly. Such a diagram is especially expedient when one of pumps has a bilateral inlet. If both pumps have a one-sided inlet, they can be disposed either with inlets inside as on the diagram represented in Fig. 14.2a or a pump located on end of the shaft is made with an axial inlet (Fig. 14.2b). In the first case, axial forces having an effect on the rotor are easier to balance, and in the second — it is convenient to use a pump with a preliminary stage at the inlet.

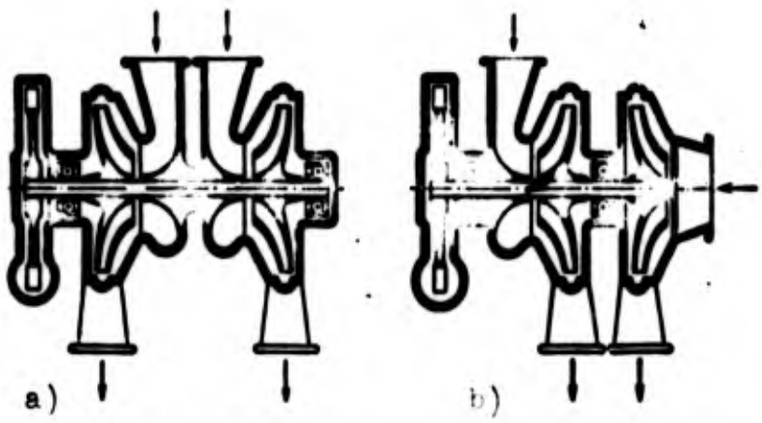

Fig. 14.2. Diagrams of turbopump assemblies with an overhung turbine: a) pumps have inlets inside, b) one pump has an axial inlet.

With the turbine located in the middle of the rotor, in most cases, both pumps are placed with inlets inside (Fig. 14.3a) or inlets outside (Fig. 143b). With pump inlets outside the length of the shaft is reduced and the conditions for feed of component to the pump and disposal of preliminary stages on inlet are improved.

The rotor may have only two supports. A disadvantage in this arrangement is the necessity of locating the bearings on the rear side of the pump impellers, where usually the components have increased pressure. If in so doing, the bearings are lubricated not by fuel components but by lubrication passed from the oil system, or by packed grease lubricant, then it is difficult to organize reliable packing. In a rotor made as in the diagram shown in Fig. 14.3a, one of bearings is located on the low pressure side.

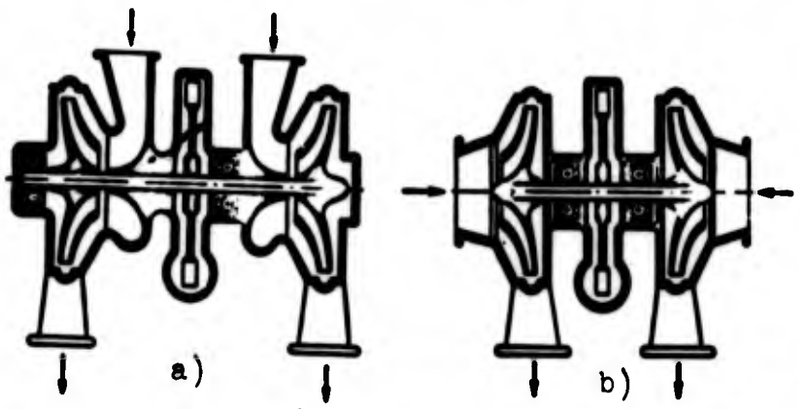

Fig. 14.3. Diagrams of TNA with turbine in the middle of the rotor: a) pumps have inlets inside; b) pumps have inlets outside.

When the turbine is located between the pumps, the component cavities are separated more safely and torque is distributed more rationally along the shafts of the unit.

An example of the arrangement of a single-rotor three-support turbopump assembly with a radial turbine located on the end of the shaft is shown in Fig. 14.4. With such a diagram conditions are facilitated for elimination of gases from the turbine, in particular, for afterburning in the combustion chamber.

The construction of a four-support single-rotor turbopump assembly is represented in Fig. 14.5. The turbine of the turbopump assembly is located cantilever fashion on the shaft of the fuel pump, resting on two antifriction bearings. The shaft of the pump

for the oxidizer, liquid oxygen, also with dual supports, has plain bearings. Each of pumps has its own separate housing connected with the housing of the turbine in such a way as to eliminate the mutual effect of temperature deformations. With a four-support rotor, in the design there is included a coupling to ensure transmission of torque, taking into account possible noncoaxiality of the pump shafts.

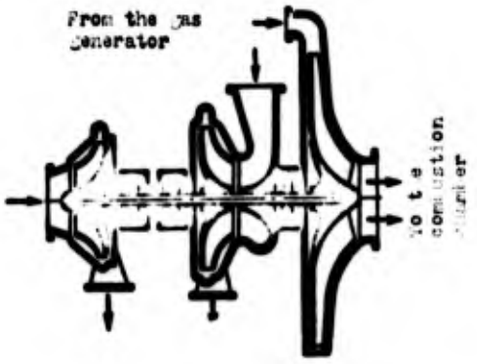

Fig. 14.4. Diagram of a turbopump assembly with radial turbine.

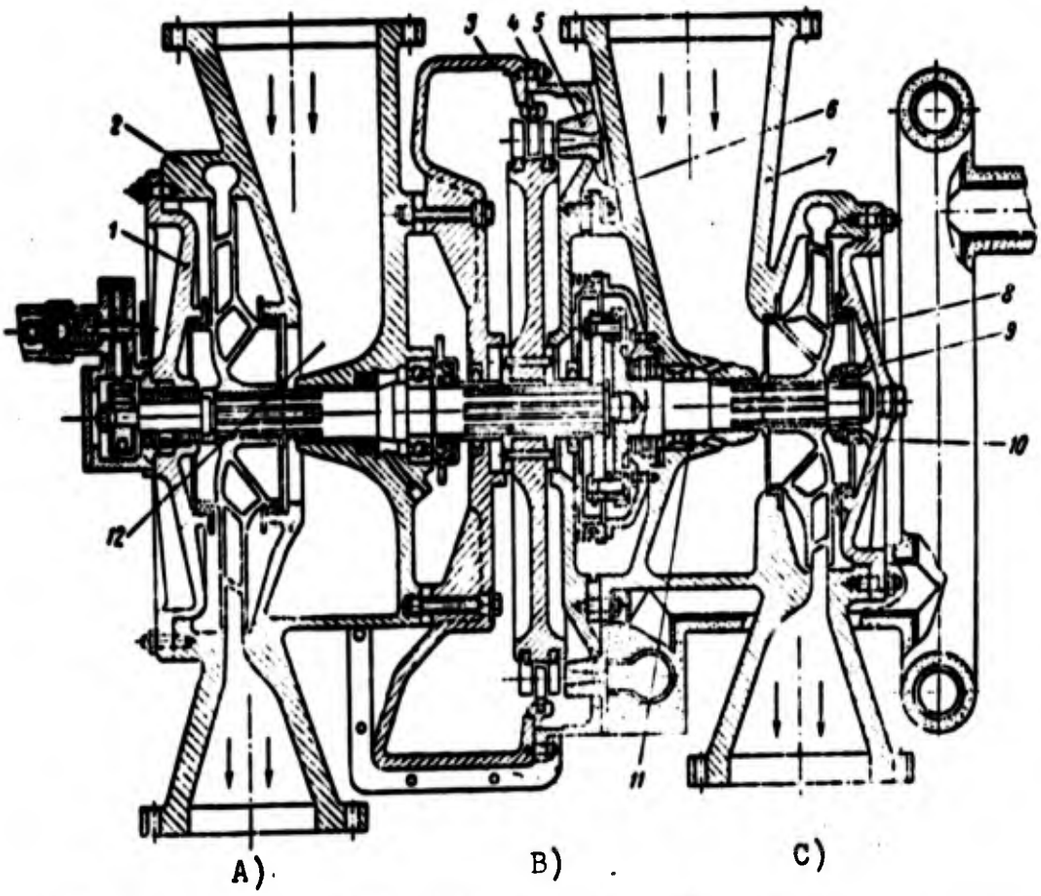

Fig. 14.5. Turbopump assembly with four-support rotor: A) fuel pump; B) turbine; C) oxidizer pump; 1, 8 – covers of pump housings; 2, 7 – pump housings; 3, 4 – turbine housings; 5 – nozzle; 6 – blocks; 9 – thrust bearing bushing with radial ducts; 10, 11 – plain bearings; 12 – duct baffle.

A diagram of a turbopump assembly with two pumps driven from a reduction gear is shown in Fig. 14.6a. The general disadvantages of a reduction gear turbopump assembly are complexity of construction and the necessity of organization of lubrication and cooling of the reduction gear.

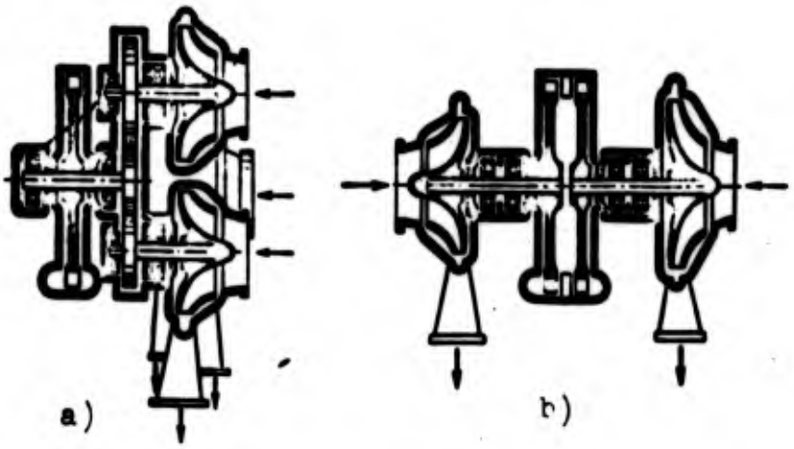

Fig. 14.6. Diagrams of a turbopump assembly:
a) driving two pumps through a reduction gear,
b) dual-shaft.

A two-rotor turbopump assembly may have several variants in relative distribution of pumps and supports. They have an advantage in simplicity of construction over a reduction gear turbopump assembly, but yield to all types of turbopump assembly in simplicity of fuel flow control. The absence of a rigid connection between the rotors requires the installation of two speed regulators of the turbopump assembly instead of a single regulating unit providing a specific number of revolutions of the turbine of a single-shaft and reduction gear turbopump assembly. One variant of such an arrangement is shown in Fig. 14.6b.

Selection of a single-rotor, without reduction gear or with reduction gear, or two-rotor diagram of a turbopump assembly is made based on the possibility of coordinating the characteristics of the pumps and turbines.

A turbopump assembly may have least dimensions and weight, and also efficiency of pumps and turbines with the greatest permissible conditions of strength and number of r/min of its elements. However, for the pumps, in a number of cases, depending upon the fuel properties, the arrangement of the feed system and the construction, the maximum permissible number of r/min is determined by conditions of absence of cavitation at the inlet. This number of revolutions can be determined [47] by the formula

$$n_{max}=\left(\frac{p_{вх}-p_s}{10\gamma}\right)^{3.4}\frac{c_{кр}}{\sqrt{Q}},$$

where $p_{вх}$ – pressure of the component on inlet into the pump; p_s – pressure of saturated vapors of a given fuel component; γ – density of fuel component; Q – pump capacity; $c_{кр}$ – critical coefficient of cavitation, characterizing the design of the pump.

For pumps without special anticavitation devices, $c_{кр}$ = 800-900. In the presence of the anticavitation devices described below, $c_{кр}$ can be brought to 2000-2200, and in a case of installation in front of the entrance to the impeller of axial pump – 3000-4000 and higher.

It is obvious that value n_{max} of the component pumps in general are different. If they differ by less than 20-30%, then it is preferable to use the simplest single-rotor without reduction gear diagram with an identical number of revolutions of pumps and turbine equal to the minimum values of n_{max} obtained for individual pumps.

Selection of a diagram is checked against the gas-dynamic calculation of the turbine. Diagram is acceptable with sufficiently high efficiency, close to minimum expenditures of working substance, and optimum ratio of radial dimensions of turbine and pumps. The most compact and lightest is a design of a turbopump assembly with a ratio of $R_{ср}/R_{max\,н}$ = 1.2-1.5, where $R_{ср}$ – average radius of turbine, $R_{max\,н}$ – maximum radius of the largest pump (usually the fuel pump).

If the results of calculation of the turbine do not confirm the expediency of using a single-rotor without reduction gear diagram, a check is made of the reduction gear diagram with the drive of one or all pumps from the reduction gear, a two-rotor diagram and, finally, a diagram with a separate turbopump assembly for supply of each component. Criteria of advantage of one or another solution are simplicity of construction, minimum weight of the turbopump assembly, and minimum flow rate of working substance.

14.2. Design of Centrifugal Pumps

The basic elements of a centrifugal pump are the impeller and the housing. In individual cases, ahead of the impeller there is set the preliminary stage in the form of worm or axial prepump. In the design of the pump there is also included the packing of the impeller.

The pump impellers are made closed type and open. Closed impellers have vane channels closed at the ends; for open – vane channels have open ends. Blades of closed impellers, as a rule, are bent opposite to rotation [47]; for open impellers, the blades are radially disposed.

Impellers of the open type with radial blades (Fig. 14.7) are very simple in construction, but their efficiency is below that of impellers of the closed type. They are usually made of steel, since fin of the blade, not braced at the end by a disk, is subject to considerable centrifugal force.

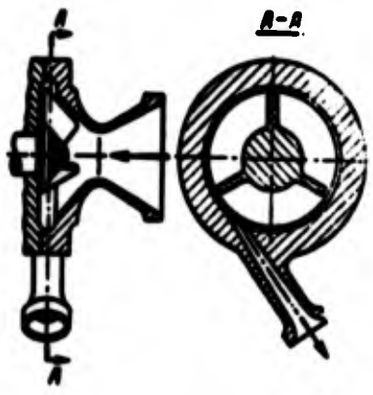

Fig. 14.7. Pump with open-type impeller.

Closed impellers can be cast (see Figs. 14.1 and 14.5) or assembled (Fig. 14.8). Cast impellers, made from cast alluminum alloys, are usually massive. Due to conditions of the technology of manufacture, the strength thickness of the walls is on the order of 4-5 mm. The basic quality of cast impellers – simplicity in manufacture.

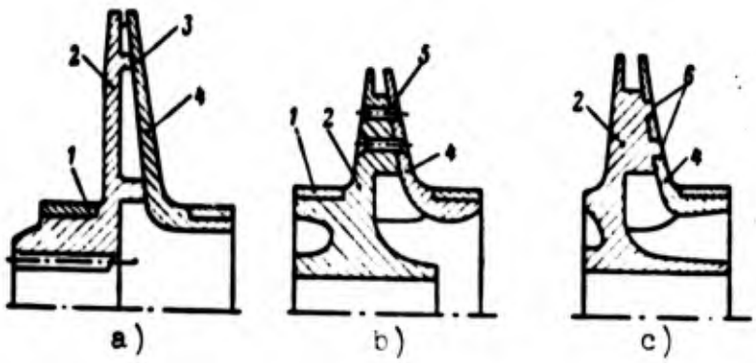

Fig. 14.8. Assembled impellers of pumps of turbopump assembly: a) with brazed cover; b) with riveted joint of the cover; c) with cover joined by calking in of flanges on blades of the impeller; 1 – slit gasket ring; 2 – impeller with blades; 3 – place of soldering; 4 – cover; 5 – rivet; 6 – calked flanges.

Assembled closed impellers usually consist of a disk with blades 2 and separate cover 4. The impeller and cover are made from aluminum alloy or steel. The cover can be stamped, while the disk with the blades usually requires machining. Thicknesses of the walls of assembled impellers may be considerably thinner than for cast impellers, and in individual designs equal 2.5-3 mm. The thickness of the wall of the disk is determined by calculation based on the strength of the pump.

The fastening of the cover to the blades is produced by brazing (Fig. 14.8a) or by riveting (Fig. 14.8b), or by calking in of flanges, carried out on the blades of the impeller and entering breachings of the cover (Fig. 14.8c). Brazed constructions are stronger than riveted. Brazing is produced over the entire surface of the edges of the blades turned to the cover by solid solders.

A riveted connection can be used with sufficient blade thickness. With thin blades calking can be used. Calking is technologically more complicated, since it requires exact filling of the breachings on the cover.

In the turbopump assembly shown in Fig. 14.9, assembled construction of impellers is used: the peripheral part of the impeller cover is carried out as a unit with the blades and disk, but rings 2 and 5 are removable.

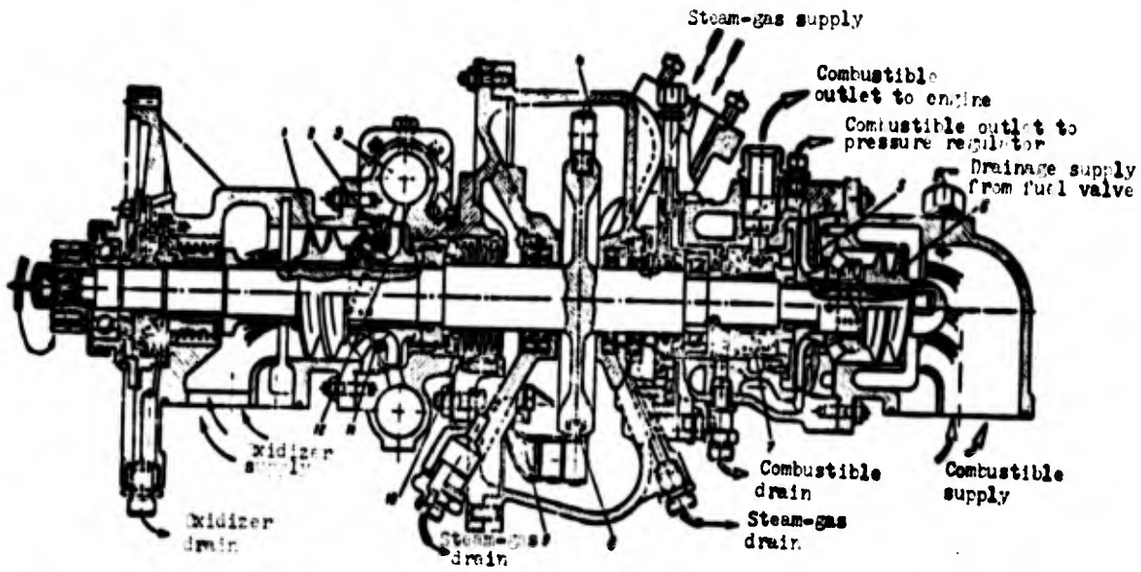

Fig. 14.9. Diagram of a turbopump assembly with assembled impellers: 1, 6 – worm screws; 2, 5 – removable rings of covers of closed pump impellers; 3 – spiral oxidizer header; 4 – banding of turbine blades; 7, 10 – face seal; 8 – turbine blade; 9 – gas header of the turbine; 11 – slit gasket; 12 – key.

It is possible to ensure favorable conditions for flow of liquid in the duct, as practice has shown, using an impeller with widening at the inlet, which is achieved either by profiling the inlet as in Fig. 14.10a, or by distortion of the rear wall, as in Fig. 14.10b. In these cases, inlet pressure in the impeller is increased, which prevents cavitation.

To improve the cavitational properties of pump by means of increasing the inlet pressure before the centrifugal pumps there are placed worm screws (see Fig. 14.9) or axial pumps (see Fig. 14.1).

The worm screws are most frequently made double-screws with two-four turns, having angle of pitch of 3-7°. External diameter of the worm screw is determined by the diameter of the inlet to the impeller, while the internal – by design considerations. The smaller the internal diameter of the worm screw, the higher the anticavitation properties of the pump. An axial pump has 4-6 blades. If conditions require strength, the blades of an axial pump are shrouded. Efficiency of an axial stage is usually 1.5-3 times greater than the required efficiency of the impeller of a centrifugal pump.

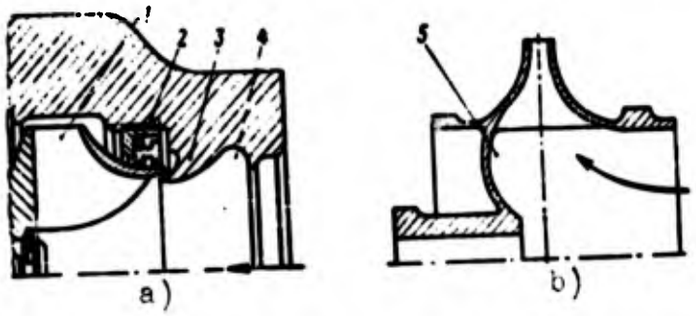

Fig. 14.10. Pump impellers of a turbopump assembly with widening of the inlet duct: a) profiling of the inlet channel; b) distortion of the rear wall; 1 – pump impeller; 2 – floating ring of labyrinth seal; 3 – deflector; 4 – profiled expansion at inlet; 5 – rear wall.

Liquid pressure forces get a closed impeller including the clearance between the impeller and the housing. In order to decrease the axial force appearing as a result of difference in liquid pressures, and to decrease the flow of fuel from the delivery side in the direction of the inlet, a seal is placed on the closed impellers. If the seal from the front and rear side of the impeller is set on an identical radius, and the cavity on rear side of impeller connects with the cavity on inlet to the pump, then the axial force having effect on the impeller will be practically equal to zero.

Seals may be contact (see Fig. 14.1) or contactless – slot and labyrinth (Fig. 14.11). Contactless seals consist of narrow annular slots between cylindrical belts on the disk and cover of

the impeller and sealing rings rigidly fastened to the pump housing (see Fig. 14.5). A combination of contactless and labyrinth seal are free-floating rings (see Fig. 14.10). The ring is pressed by liquid pressure endwise against the housing, and leakage through the annular slot diminishes because of labyrinth grooves of simplified, rectangular profile. Contact seals are made from soft materials possessing good antifriction properties, for example, from teflon. With contact seals the leakage of fuel from the cavity with raised pressure is minimum. Disadvantages of contact seals include difficulty in selection of appropriate material for sealing rings when using aggressive fuel components, and their short life. To ease the operating conditions of the seals on the rear side of the impeller sometimes there are made low radial blades, preventing motion of the liquid in clearance from the pressure side to the seal.

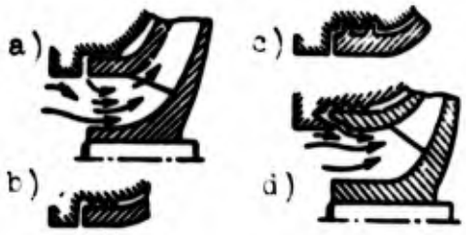

Fig. 14.11. Types of sealing for impellers: a) slot; b) labyrinth with lugs; c) labyrinth with rectangular teeth; d) labyrinth with a baffle.

Torque from the shaft on the impellers of centrifugal pumps or preliminary stages is transmitted through keys or slits. Key joints, (see Fig. 14.9) are used with relatively low torques. With a key joint the impeller is centered on the shaft. In powerful turbopump assemblies slot joints with rectangular or evolvent slits are used (see Figs. 14.1 and 14.5). To ensure reliable centering push fit of the impeller on the centering belt of the shaft can be used (see in Fig. 14.1 centering of a bilateral impeller). In individual cases, when the impellers are steel and when this is permitted by assembly conditions, the impeller can be welded to the shaft or are made as a unit with it.

Construction of the housings of pumps depends on the material and the method of manufacture. Housings can be divided into cast, welded, and made by machining from a one-piece billet. When this is permitted by strength conditions, the housings are made by casting from aluminum alloys. In similar cases, the pump housing consists usually of two parts: the header housing (collection chamber), made as a unit with one of the walls, and a removable cover, which in the case of a one-sided impeller is located on the inlet side in the pump, if the inlet is external (see Fig. 14.1, pump B, and Fig. 14.9), and on the side of the rear wall of the impeller if the inlet is located inside (see Fig. 14.5).

The cover and housing of the collector are joined by pins or screws. To ensure a reliable seal linings are placed in the joint.

With high fuel pressures and considerable radial dimensions of impellers steel housings are used which are made from castings or stampings. Strong axial forces, having an effect on the removable cover, in a number of cases require the installation of a large number of bolts and considerable thickening of the walls in the places where they are set. A welded joint permits decreasing the thickness of the wall of the flanges. Welding is produced in the joint or by flanging (Fig. 14.12). A disadvantage of welded housings is the complexity of working in finishing or repairing the unit.

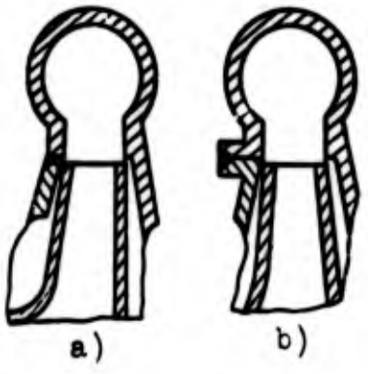

Fig. 14.12. Housings of pumps: a) with welding of the joint; b) with welding by flanging.

The shape of the inlet part of the pump housing depends basically on the selected diagram for the arrangement of the turbopump assembly, i.e., on the location of inlets inside or outside (see, for example, Fig. 14.3a and c). In the first case, housings are

used with a radially located inlet duct, in the second – with axial or axial with a knee usually at an angle of 90°.

With radial location of the nozzle, in the design of the housing there should be ensured uniform filling of the inlet to the impeller. For this purpose in the inlet radial nozzle (see Fig. 14.5) there is placed partition 12, lying in the plane of symmetry of the nozzle, which divides the flow in two, and the nozzle passes into the annular chamber where the flow is levelled by the circumference. The inlet in a bilateral impeller is made in a similar manner.

To prevent intersecting the flow approaching the impeller of the liquid proceeding into the suction pipe from the seal, on the housing is an annular deflector 3 is made (see Fig. 14.10a) which directs directly onto the impeller.

If, according to the conditions of arrangement, at the inlet to the impeller located on the end of the shaft there are set nozzles with a knee (see Fig. 14.9), then for uniform filling of the inlet section of the impeller in the nozzle there can be set guide vanes.

In the housing of the pumps there are also made sockets for seating bearings and placement of the shaft seal, as shown in Figs. 14.1, 14.5 and 14.9.

14.3. Design of Turbines of Turbopump Assemblies

A turbine, in general, consists of rotor wheels, nozzle boxes, housing and exhaust duct for removal of waste working substance.

In a turbopump assembly basically there are employed gas action turbines, in which gas expands only in the nozzle box and the pressure ahead of the rotor wheel and behind it are identical. The use of impulse-type turbines is explained besides by considerations of simplicity in construction by the following. By conditions of

strength and arrangement of the turbopump assembly the values of peripheral velocities U of the blades of the turbines are limited to 250-300 m/s. Exit velocity of the working substance from the nozzle boxes c_1 of modern turbines is on the order of 1000 m/s and more. The totality of values U and c_1 determines such values of parameter U/c_1, with which maximum efficiency can be obtained exactly in impulse-type turbines [47]. Furthermore, turbines, as a rule, are made fractional, i.e., with incomplete feed of gas over the whole circumference of the blade rim, since with relatively low flow rates of working substance the necessary area of nozzle box at the outlet is considerably less than the blade annulus area of the rotor wheel. With fractional feed impulse-type turbines are profitable, inasmuch as losses in overflowing of gas in unstreamlined flow channels are small with identical pressures on both sides.

Turbines are made mono- and two-stage, i.e., with one or two rows of rotor blades. In a two-stage turbine, between the first and second row of rotor blades there may be set a nozzle box (expansion type) or a stator (velocity stage turbine). In the two-rotor diagram with stages of velocity during rotation of rotors in opposite directions, a rectifier is not installed.

The rotor wheel consists of a disk with one or two rows of rotor blades. In turn, the disk has profiled part and a thickened rim to which the blades are attached. With two rows of rotor blades, i.e., with two-rim construction (see Fig. 14.1 and 14.5) the rim is made wide. With great peripheral velocity, according to strength conditions such a construction may be impracticable. In similar cases they are changed to two-disk designs.

When disk has central opening for the shaft, then at the opening there is placed a thickened nave, smoothly changing into the profiled part (see Fig. 14.5). In the central part of the disk there may be placed collars for bracing the shaft or for centering on the shaft, as in the construction shown in Fig. 14.1.

The turbine blades are made individually or as a unit with the disk. In the latter case, they are milled with subsequent electro-spark machining of the vane ducts. By milling it is impossible to obtain optimum profiles both of the blades proper, and also the vane channels which leads to additional losses in the turbine; due to this, as a rule, blades are made separately.

The blade consists of a profiled part – the foil, and the root (Fig. 14.13). The root serves for attaching the blade to the rim of the disk. In those cases when lock fastening to the disk is used, on the root there is a lock. Sometimes blades are made as a unit with a shroud 3, forming a band.

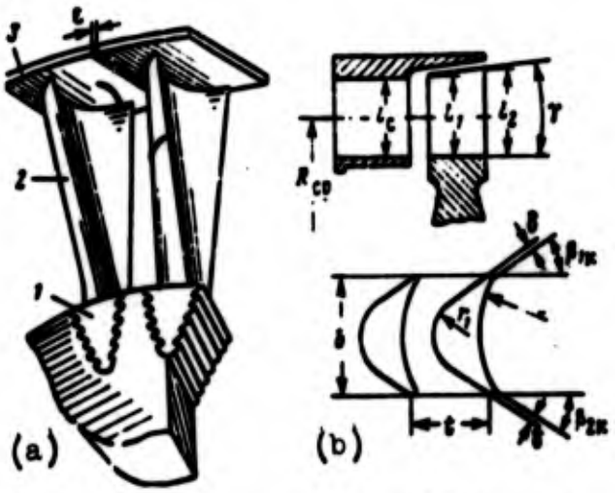

Fig. 14.13. Turbine blades of a turbopump assembly (a) and diagram for determination of blade dimensions (b): 1 - root; 2 – foil; 3 – shroud.

The turbine blades of a turbopump assembly, for the purpose of simplification in manufacture, have constant profile in height. The foil of the blade has trough and back. The trough is cylindrical with a certain radius r_2 (Fig. 14.13b). With symmetric profile, which is used in most cases, the back in the central part of the profile is also cylindrical with radius r_1, joined with two rectilinear sections leading to the front and trailing edges. The angles between rectilinear sections and face planes of the blade rim $\beta_{1л}$ and $\beta_{2л}$ are identical.

Blade width b is selected based on strength considerations. In the designs carried out it lies within limits of 15-20 mm and more. Thickness of blade edges δ = 1.0-2.0 mm. Lengths of the rotor blade on front and trailing edges l_1 and l_1 may be identical, but more frequently they differ. In that case, the cone angle γ equals 6-10°. If the blade has constant height, then a length of leading edge is selected greater than the height of the nozzle l_c. Here one should consider that if the height of the rotor blades is considerably more than that of the nozzles, it may lead to formation of stagnant zones in the channels, sucking gas into them, and to eddy formation, and, consequently, increased losses. A great difference in heights on front and trailing edges can lead to separation of flow and is undesirable. Usually the ratio l_2/l_1 is within limits of 1.2-1.5.

Blades are set on the disk with pitch t, selected from the condition t/b = 0.5-0.7.

The blades are attached to the disk with or without a locked joint. A joint without lock is produced by means of welding or soldering (Fig. 14.14a). The welded or soldered joint is constructively the simplest. Very high requirements are imposed on seam quality. The seam is controlled by X-ray radioscopy; the external surface of the seam is ground.

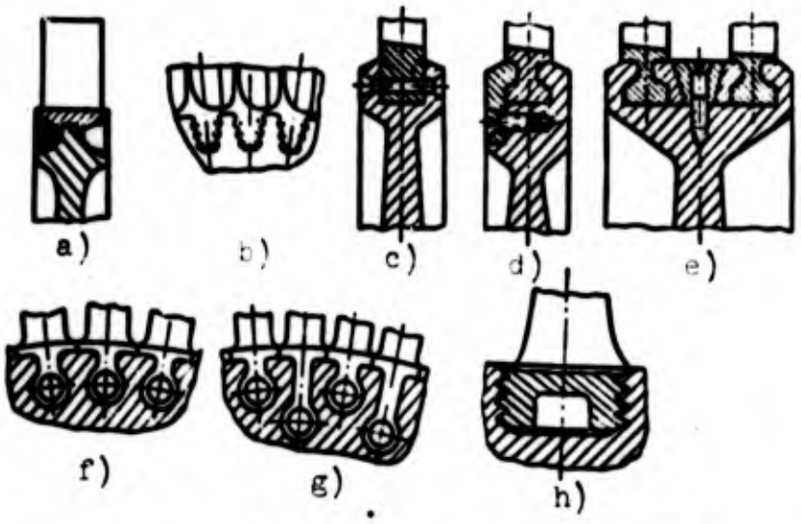

Fig. 14.14. Types of joints of blades with turbine disks: a) a welded joint without lock; b) fir-tree lock; c, d, e) T-shaped locks; f), g) cylindrical locks; h) lock with triangular flanges.

A locked joint ensures transmission of torque and fixes the blade under the action on it of axial forces, centrifugal forces, and bending moments. Locks are made like a fir tree, or dowels, T-shaped, cylindrical, and with triangular flanges on the root.

Fir tree locks (Fig. 14.14b) constructively and technologically are the most complicated and can be used only in a turbopump assembly of an engine of great thrust. They work reliably under conditions of appearance of plastic deformations in the teeth.

The most widely used fastenings are T-shaped locks set in annular grooves in the rim of the disk. The blades are consecutively introduced into the groove through a slot designed for this. The last blade is made without a T-shaped lock and is riveted (Fig. 14.14c), and in case of identical locking with the remaining blades can be fastened with a lateral insert, closing the slot (Fig. 14.14d), or to be fitted by a wedge-shaped block (Fig. 14.14e). Joints with T-shaped lock are simple and are technological, but strength of the lock part of the blade and the lateral part of the rim of the disk is insufficient.

Pin locks (see Fig. 14.1) make it possible to considerably reduce the weight of the turbine rim. The pins are inserted in holes jointly drilled and turned in the root of the blade and rim of the disk, and then spread. For a decrease in weight, the pins can be made hollow.

Cylindrical locks in turbines of a liquid propellant rocket engine (Fig. 14.14f) according to conditions of location are more frequently made with checkerboard location of grooves (Fig. 14.14g). A disadvantage in cylindrical locks – low strength of the crosspiece between grooves in the rim of the disk.

Locks with triangular flanges, assembled in annular grooves of rim (Fig. 14.14h), differ little in respect to conditions of installation and work from T-shaped locks, and although they possess greater strength are rarely used.

Shrouded blades (see Fig. 14.13a) are made singly or in sections, sometimes including up to 20 blades. The circumferential clearance ε between ends of shrouds of separate sections equals 0.5-1 mm. With individual shrouded blades, the clearance is taken on the order of 0.1-0.2 mm. Removable shrouds are made in the form of rings or belts, slipped onto the blade rim (see Fig. 14.9); cuts are made for compensation of temperature deformations on such a shroud.

Blades are made by milling or casting. Cast blades sometimes can be in pairs and threes (Fig. 14.15), where a group of blades has one stem with a lock. For simplicity cast blades are made hollow.

Fig. 14.15. Cast blades.

Blades and disks of a turbine operating at a gas temperature of 350-450°C are made of aluminum alloy. When operating at a higher gas temperature, steels are used, and with an aggressive working substance – stainless steels.

The steel disks of turbines in certain cases can be made as a unit with the shaft (see Fig. 14.9) or be welded to the shaft. In most cases, the fastening of the disk to the shaft split is by slots, bolts, or on radial pins. With a disk made of aluminum alloy, in order to increase the strength of the spline fitting, the disk is fitted on intermediate steel bushings with slots (see Fig. 14.7). Bushings and disk are joined by rivets. With a steel disk it is possible to directly spline fit disk with the shaft. The simplest and cheapest is a bolt connection of the disk with the flange of the shaft either with an intermediate cone-shaped disk, which in turn is united with shaft by slots (see Fig. 14.1). The use of a

bolt connection renders the construction somewhat heavier as compared to a joint on slots. One of the lightest and most simple connections is fastening the disk to the shaft by means of radial pins both with a solid shaft (Fig. 14.16a), and also with a slotted one. Types of joints on flanges and on face slots are shown in Fig. 14.16b and c.

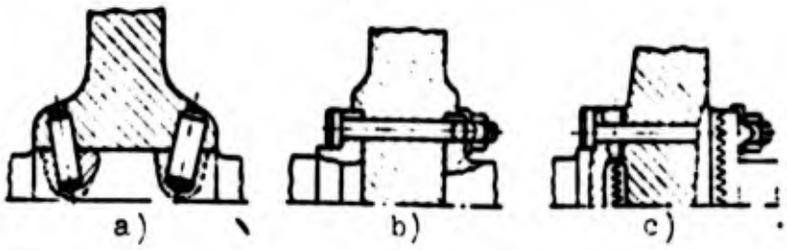

Fig. 14.16. Types of joints of turbine disks with shafts: a) pin; b) flanged; c) on face slots.

Nozzle boxes most frequently are made with conical channels (Fig. 14.17a) completely axisymmetrical or with deformed outlet section. Axisymmetrical nozzles are the simplest to manufacture, but with them it is difficult to coordinate the dimensions of the outlet section with the dimensions of the rotor blades. In order to eliminate this deficiency nozzles are used in which from the round form of the critical section the outlet part changes to an oval or close to round sector.

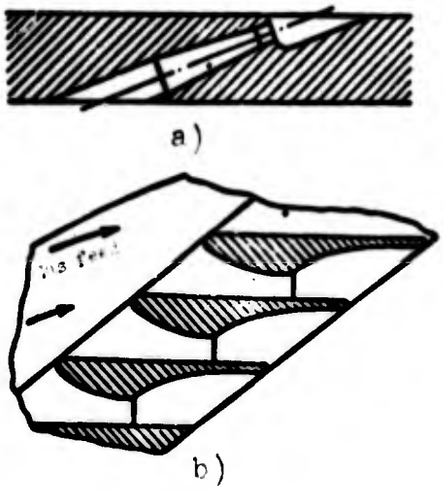

Fig. 14.17. Profiles of nozzles of nozzle boxes: a) with conical nozzle; b) nozzle cascade.

Structurally conical nozzles can be made in the form of separate nozzle blocks (see Fig. 14.5) or directly in the turbine housing. With separate nozzle blocks construction of the turbine housing is simpler. Blocks of nozzle boxes are set in windows of the housing and can be attached to it by welding or with bolts. When the turbine is operating on steam gas, in order to reduce thermal losses, nozzle blocks can consist of housings filled with glass wool (see Fig. 14.5). Nozzles can be made both directly in the nozzle block and also separate from it; in the latter case, the nozzle can be pressed in. Nozzles and nozzle blocks, depending upon the service life of the turbopump assembly and the temperature of the working substance can be made from carbon, heat-resistant, or stainless steel or from cast iron.

In turbines with great admission, the most expedient design for the nozzle box is a nozzle cascade composed of blades which form channels of prescribed configuration (Fig. 14.17b). Blades for similar cascades can be made casting or milling, and can also be united in blocks. For simplicity of manufacture, one of the walls of the blade is made flat.

In a fractional turbine, the location of nozzles renders a considerable effect on losses. The least losses are in turbines whose nozzles are grouped in one place. If the nozzle or group of nozzles is located around the circumference in two diametric sectors, then the efficiency of the turbine drops 4-6%. If the nozzles are placed in three sectors evenly spaced around the circumference, then the efficiency may drop 7-9%, and if in four places, then 10-12%, etc. Because of these considerations, it is expedient to group the nozzles in one sector, however in so doing there will be an increase, as will be shown below, in vibrational stress in the blades. In order to reduce the level of vibrational stresses, recourse is had to an increase of the axial clearance between nozzle box and cascade of rotor blades, which is accompanied by an insignificant reduction of turbine efficiency. In turbopump assemblies carried out the axial clearance composes 1.5-4.0 mm and more. Finally, the number of nozzle box sectors and their

location are selected as a compromise solution, considering the hydraulic perfection of the turbine and the fatigue strength of the blades. Turbines are also used with equidistant spacing of nozzles around the circumference.

In two-stage impulse-type turbines, the intermediate nozzle box consists of a cascade composed of blades having a profile similar to the profile of the rotor blades. With partial feed of the working substance, an intermediate apparatus is placed after the cascade of rotor blades of the turbine first stage opposite the nozzle outlets (Fig. 14.18a). In such cases, the nozzle blades can be made in groups and be fastened to segment ring by locks, basically T-shaped. In order to reduce losses, blades with an internal shroud are used. Segment rings are attached to the turbine housing by bolts or by welding.

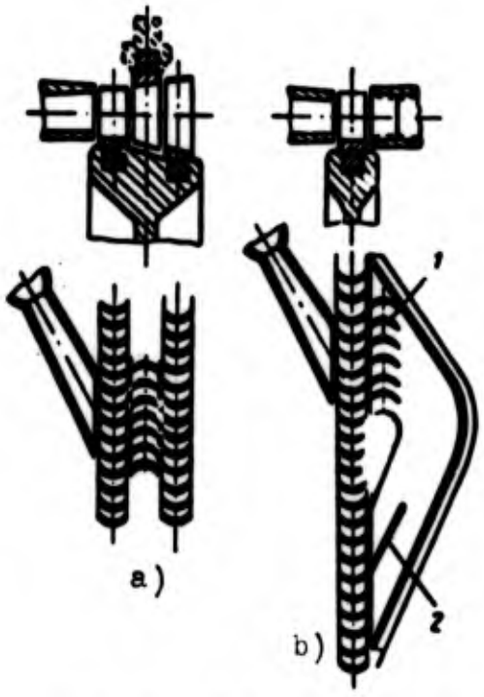

Fig. 14.18. Intermediate nozzle boxes: a) partial with attachment to a segment ring; b) rotating gas header; 1 – stator blade; 2 – baffle.

In special case, a two-stage turbine may have one blade rim. Then the bend of the current is produced by turning the gas header, a diagram of which is shown in Fig. 14.18b, by means of stator blades 1 and longitudinal baffle 2.

Turbine housings are cast, welded, and made by means of machining from a one-piece billet. Housings of turbines working on steam gas, frequently are cast from aluminum alloy, while those working on gases with high initial temperature, – from stainless or carbon steel with subsequent chromium calorizing or zinc coating. Welded housings are simple to manufacture, cheap, and light (see Fig. 14.1). The lightest are constructions in which sheet material is used with appropriate strengthening of the walls by reinforcing ribs.

In the turbopump assembly shown in Fig. 14.5, is used a movable joint between the turbine housings and pumps is used, carried out by means of blocks. This type of joint allows mutual displacement of the housings in a radial direction because of temperature deformations while preserving coaxiality of turbine and pumps. In the design under discussion this is caused by the fact that as a fuel component liquid oxygen is used and there is a great difference in the temperatures of housings of the pump and the turbine.

In those cases, when possible, it is more preferable to have the housings joined by bolts or by welding. A welded joint is cheaper and the turbopump assembly is lighter, but in so doing disassembly of the unit in process of final adjustment is complicated.

At relatively low temperatures of working substance (on the order of 500-600°C) the gas can proceed directly to the cavity of the turbine housing and then be removed by the exhaust duct (see Fig. 14.9). In the design shown in Fig. 14.5, for collection of waste steam gas a cast collector is used which enters the power circuit of the turbopump assembly. At high temperatures of gases it is desirable to use a special gas collector which does not enter the power circuit of the turbopump assembly (see Fig. 14.1). In such cases, the gas collector, passing directly into the exhaust duct, can be made of sheet material with thermal insulation against overheating of the manifold and fittings located in direct proximity to it.

14.4 Bearings and Lubrication of Turbopump Assemblies

In the turbopump assembly of a liquid propellant rocket engine usually there are used antifriction bearings, most frequently ball bearings. A thrust bearing is used under the most favorable conditions: where there is less load from radial forces or less heating from the turbine. Bearings are assembled on the shaft in case hardened or nitrided belts.

Antifriction bearings can be lubricated by pumped fuel component, grease lubricant or liquid oil passed from a special pump driven from the turbopump assembly; in an aircraft liquid propellant rocket engine the drive can be nonautonomous (from a turbojet engine (TRD) in a composite propulsion system).

The simplest is a system of lubrication by pumped component. Its advantage lies in the fact that it is comparatively easy to ensure cooling of the bearing, there is no necessity for special lubrication and there is a somewhat simplified system of sealing the turbopump assembly. Such a system is used in those cases when the fuel components possess sufficient viscosity and are nonaggressive with respect to the material of the bearing. Among such components, in particular, belong the combustibles. Bearings can be lubricated with nitric acid; in so doing the lubrication system is made in such a manner that the acid proceeds directly to the bearings before starting the engine. In restartable engines it may be necessary to wash the bearings which are lubricated by nitric acid, after each stop. Alcohol, having low viscosity is not used for lubrication and direct cooling of bearings.

A system of lubrication by pumped fuel component usually is carried out according to the following diagram. The fuel component from the high pressure cavity passes through the sealing of impeller, usually from its rear side, and proceeds to the bearing, and then to the side of suction of pump via the external main line by the channel in the housing of the pump or, which is the most simple,

through the hollow pump spindle. In the latter case, the circulation of lubrication is somewhat impaired due to the necessity of overcoming centrifugal forces preventing motion of the liquid inside the shaft. For improving the lubricating ability of certain types of fuels, additives are used. Such an additive, for example, can be dithiophosphate of zinc dialdehyde, introduced into the combustible directly before it enters the bearing which is being lubricated.

Grease lubricant is inserted in the bearings during assembly or packed before starting. In case of prolonged storage of a turbopump assembly periodic lining of the lubrication is required. A similar system of lubrication is rather simple but requires reliable packing of bearing from the side of the pump. Bearings which are subject during operation to intense heating are lubricated by high-melting lubrication. For bearings located in direct proximity to pumps with cryogenic components cold-resistant lubrication is used. Combined systems of lubrication find application: bearings during assembly are covered with solid lubrication, but during operation are cooled by the pumped component, in such cases more frequently – by the oxidizer. Grease lubricant is usually used in a relatively small turbopump assembly which is nonrestartable.

Lubrication and cooling by liquid oil under pressure is used usually in a turbopump assembly with strongly loaded bearings, with long duration of operation and, especially, in the presence of a reduction gear. It must be noted that in the construction of the reduction gear there may be bearings, the lubrication of which is difficult under pressure; such bearings are lubricated by grease lubricant.

The presence in one unit of different systems of lubrication is a cause of operational inconveniences. In those cases when a reduction gear turbopump assembly enters into a combined propulsion system with a turbojet engine, the reduction gear is lubricated from the pump driven from the turbojet engine. But there are possible such arrangements, when due to the length and great weight of oil main lines it is more expedient to drive oil pump directly from the

turbopump assembly. A deficiency in systems with liquid lubrication is the possibility of thickening of oil in the bearings located near pumps with cryogenic components. Then in the design of the turbopump assembly the possibility of preheating of bearing before starting is provided for.

In individual cases, the use of cryogenic liquids as fuel components forces the use of plain bearings working reliably under conditions of lubrication by liquid oxygen, if the peripheral velocities of the journal do not exceed 20-30 m/s. Such bearings are used, for example, in the turbopump assembly represented in Fig. 14.5; in the same place reliable lubrication of the support-thrust bearing by liquid oxygen is ensured with help of bushings with radial channels, playing the role of a centrifugal pump [47].

In a low-inverse turbopump assembly antifriction bearings can be lubricated by liquid oxygen; in so doing the flow of oxygen through the bearing should be intense and uniform. It is impermissible to have formation of vapor locks, which cause local cessation of heat removal, overheating of separate sections of the bearing and cause it to go out of commission due to great thermal stresses.

14.5. Seals of Turbopump Assembly Shafts

A very important role in the design of a turbopump assembly is played by the shaft seals. This emanates from the fact that in a turbopump assembly in direct proximity to each other there are fuel components which besides aggressivenesses are able during mixing among themselves or with the lubricating materials to enter into reaction. Besides the above-described seals dividing the cavity of high and low pressure of the pumps, in a turbopump assembly there are placed seals separating the working cavity of turbine or pumps from the bearings and other cavities. These seals are made contactless, contact, and hydrocentrifugal.

Contactless seals for the above-indicated purposes are used comparatively rarely. An example of the use of a contactless double labyrinth seal as the preliminary stage in sealing of a turbine cavity is shown in Fig. 14.19. In carried out constructions, the radial clearance between lugs and bushing composes 0.1-0.2 mm. Such sealing works on the principle of throttling gas in the interlug cavities – the chambers of the labyrinth. A labyrinth seal is not insulating. Gases passing through the labyrinth seal must necessarily be removed through the drain system. A labyrinth seal is very sensitive to change in the radial clearance between the rotating bushing and the stationary lugs. In the selection of initial clearance, there must of necessity be considered possible temperature deformations under operating conditions. For the purpose of reducing the area of the slot in a labyrinth seal is disposed as far as possible on the shortest radius possible.

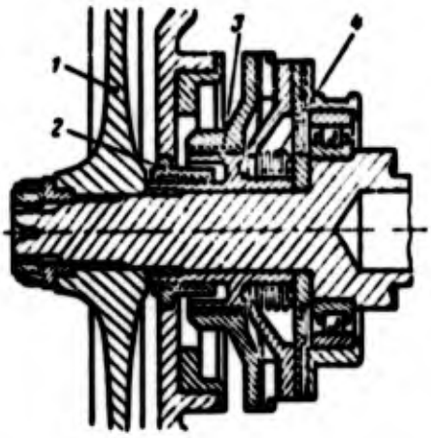

Fig. 14.19. Contactless labyrinth and bellows seal: 1 – impeller disk; 2, 3 – labyrinth bushings; 4 – bellows sealing.

Most frequently in a turbopump assembly contact seals are used: stuffing box, with elastic rings, with annular sectors, and face.

The simplest are stuffing-box seals. They are used for the insulation of cavities with relatively small drop in pressure, for example, the cavity of a bearing with packed lubrication or with lubrication under pressure, from the cavity connected with the draining system. Annular stuffing boxes inserted in grooves of the stuffing box covers, are made from ordinary, and also from cape blue or graphitized asbestos. Such seals are unstable in an acid medium or in low-viscosity liquid, since an asbestos filling is quickly

moistened and washed out. Examples of application of annular stuffing-box seals are shown in Figs. 14.9 and 14.5. Stabler and more hermetic are collar seals pressed to the shaft either by spring rings, or only by the pressure of the liquid found in the packed cavity. Collars are made from special rubbers, leather, or plastics resistant to those liquids, the leakage of which they must prevent. For example, for work in a cavity where there is acid, teflon collars are used. In the sealing shown in Fig. 14.20, teflon collars 1 work in combination with teflon labyrinth bushing 2.

Fig. 14.20. Collar sealing:
1 – collar made of teflon;
2 – bushing made of teflon.

Contact multiple seals with elastic rings (Fig. 14.21) can be used for the separation of cavities with considerable drop in pressure. Rings 1, set in grooves of the bushing-ringholder, work on the cemented or nitrided surface of the bushing fastened to the housing of the turbopump assembly. The rings are made of bronze or antifriction cast iron. Sealing is achieved by means of tight pressing of the rings to the bushing and on ends to the surface of the grooves of the ringholder by means of the pressure in the sealed cavity. Annular seals work reliably with peripheral velocity of the bushing-ringholder up to 50-70 m/s. To decrease abrasion, the surface of the rings is covered with porous chromium.

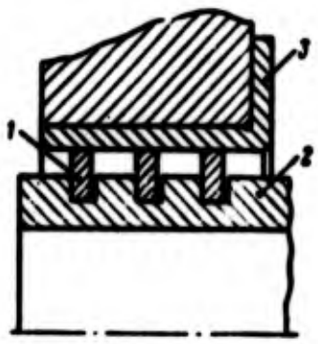

Fig. 14.21. Sealing with elastic rings: 1 – elastic ring; 2 – bushing-ringholder; 3 – fixed bushing.

Contact seals with annular segments are used most frequently for insulation of the gas cavity of the turbine (fig. 14.22). They consist of several rows of rings, each of which is formed by three-four segments. Between segments in the nonworking state there is a small clearance. Segments are packed in the grooves of the fixed bushings so that side play between them and grooves composes not more than 0.05 mm. Segments are pressed to shaft by spiral annular spring 2, lying in the groove on their external cylindrical surface. With turning the segments are held by pins 3. The segments are ground to the shaft and in working state under pressure from packed cavity they are pressed by their lateral surfaces to the walls of the grooves of the bushings so that simultaneously they seal cylindrical and face surfaces. As the segments wear, contact on the surface of the shaft is maintained by means of the decrease in the clearance between the segments. Such seals ensure better airtightness than elastic rings because of the greater contact area, but they are more complex, are easily damaged, and are used with a peripheral velocity of not more than 30-40 m/s. Segments are made of graphite or antifriction cast iron.

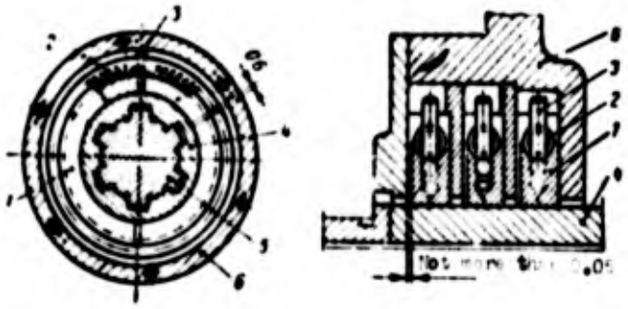

Fig. 14.22. Contact sealing with annular segments: 1 – annular segments; 2 – spring; 3 – pin; 4 – shaft bushing; 5 – shaft; 6 – bushing-ringholder.

Contact face sealing is usually used in combination with slot, diaphragm, or bellows seal. Strictly face sealing consists of two rings, touching along their face surfaces. One of the

rings 3 (Fig. 14.23a) revolves together with the shaft, while the second ring 4 is fixed but is capable of a certain axial shift. This shift is necessary to ensure tight pressing of the ring faces against one another under pressure of the liquid in the sealed cavity and the spring. In the examined packing ring 4 pressed to bushing 5, which in turn is pressed by spring 2 to a tight contact of facets of rings 4 and 3. The spring is necessary for preliminary sealing with a pressure on the order of 1.5-5 kgf/cm^2. In working state, tight contact is usually created by liquid pressure. It is obvious that, besides sealing on the end, it is necessary to ensure further sealing between the forward moving part of the seal and the housing. In the design represented in Fig. 14.23a, for this purpose a slotted seal is used between bushing 5 and hollow in bushing 12. A deficiency of a slotted seal, besides its lack of airtightness, is sensitivity to misalignment which can appear due to irregularity of wear of the facets of the rings, which can lead to jamming or to increase of leakages. A seal which is free from this deficiency is one in which in combination with face sealing there is used a diaphragm or bellows seal.

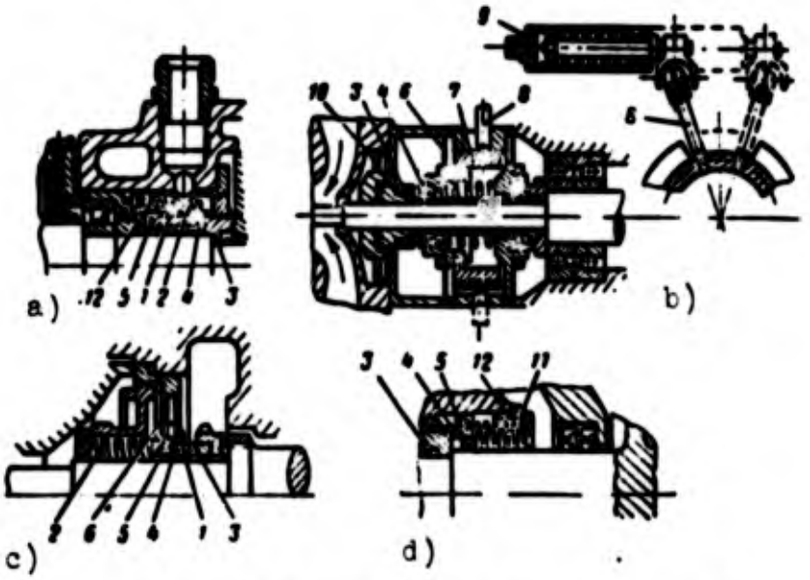

Fig. 14.23. Face sealings: a) in combination with slot; b) with diaphragm; c) closed; d) with bellows; 1 – stop; 2 – spring; 3 – rotating ring; 4 – nonrotating ring; 5 – bushing; 6 – diaphragm; 7 – threaded bushing; 8 – guide; 9 – servomotor; 10 – hydrolock; 11 – bellows; 12 – bushing.

In diaphragm sealing (Fig. 14.23b) forward sealing bushing with ring 4 is suspended on diaphragm 6, fastened to the housing. The revolving part of the seal consists of a bushing screwed on the shaft with ring 3. In a nonworking state, rings 3 and 4 are pressed by spring 2. The disadvantages of diaphragm seals include the possibility of only comparatively slight axial shift of bushing 5, on the order of 0.8-1.2 mm. Total wear of facets, depending upon the material of the rings attains 0.1-0.8 mm/h. Closing face seals extend the life of face seals with a diaphragm. They must work in combination with other seals, for example, with a hydrolock (Fig. 14.23c). Contact sealing between rings 3 and 4 works from the beginning of starting the turbopump assembly until achievement of a specified pressure of fuel behind the pump. With an increase in fuel pressure passed into servomotor 9, its piston, surmounting the force of the spring, shifts guide 8, which in turn turns threaded bushing 7. In so doing, ring 4 is separated from ring 3, the face seal will be closed and the hydraulic seal begins to work.

In a bellows seal (Fig. 14.23d) bushing 5, carrying the nonrotating ring 4 of the face seal, is united with bushing of the housing 12 by bellows 11. As compared to the diaphragm type, the bellows permits greater axial shift (up to 4-6 mm) which increases period of service of the seal and its reliability. This also promotes smaller forces in the contact seal due to the action of the forces of fuel pressure, since the effective area can be made smaller than for the diaphragm. Face sealing in combination with a bellows is the most reliable of contact seals. Its disadvantages are comparatively large axial dimensions and complexity.

The material of the face rings is selected depending upon the purpose of the sealing, speed of slip at the ends, and the properties of the liquid, in which the rings work. In carried out constructions, speed of slip at the ends is allowed within limits of 20-50 m/s. Rings in pairs are usually made from different materials. For sealing the oil cavity a rotating ring of steel can be used steel, and the nonrevolving – in the form of packing made of cape blue asbestos.

Oil, moistening asbestos, protects it from wear. Cavities where there are acids are usually sealed with steel rings. High requirements are imposed on accuracy in the manufacture of rings and the smoothness of the friction surfaces.

For sealing cavities in which there are hydrogen peroxide, kerosene or tonka, one of the rings (more frequently the revolving one) is made stainless steel, and the other from graphite. When wetting is by kerosene there can be used a pair – steel + ceramic metal (copper-graphite-lead mixture). Use is also made of a pair – steel + teflon. To increase wear resistance, sometimes stellite is fused on steel rings. In short-life engines there can be used a fixed ring made of solid rubber, however the reliability of such a seal is low.

Bellows most frequently are made from tombac type alloys. Bellows working in hydrogen peroxide are chrome-plated over a nickel coating. Bellows, placed at the side of turbines whose working substance is gas produced by the combustion of basic components are made of stainless steel.

Hydrocentrifugal sealing, or hydrolock, works according to the following principle (Fig. 14.24). The blades of the impeller are turned in the direction of cavity a, into which liquid must not be admitted, so that during rotation of the impeller, the fuel getting from the side of cavity b to the blade is repelled by centrifugal forces. A disadvantage in hydrocentrifugal sealing is the necessity of having, besides it, still other sealing, working up to the moment when the pressure created by the hydraulic lock resists the pressure of the sealing liquid. In the example shown at low rotation rate of the shaft, sealing is carried out the pressure of leather collar 1 against the disk of the impeller by fuel pressure on the side of cavity b. With a certain number of turns of the blade pressure is created balancing the pressure on the side of cavity b, and the hydraulic seal begins to work. The collar, under the impact of forces of elasticity moves away from the

surface of the impeller and the contact sealing is broken. Another method of breaking the contact sealing is used in the design represented in Fig. 14.23c.

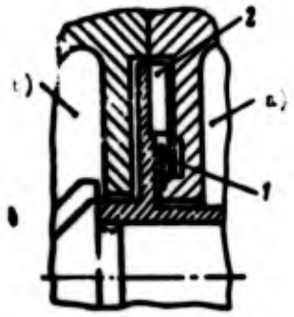

Fig. 14.24. Hydrocentrifugal sealing: a, b) cavities; 1 – collar; 2 – impeller hydrolock.

A combination of hydrolock with closing face packing is the most reliable and long-lasting sealing.

In all cases where there are located two or more sealing elements in a row the cavity between them of necessity is drained.

14.6 Strength of Turbine Blades and Axial Pumps of a Turbopump Assembly

Blades of the turbines of a turbopump assembly are loaded by centrifugal and gas forces depending on operating conditions. At the time of starting the turbopump assembly, on basically a gas force the turbine blades acts, causing them to bend. Maximum bending stresses take place in the root section of blade at the place of transition between the profiled part and the root. During starting there also occurs comparatively rapid heating of the blades. Heating begins at the sharp front and trailing edges and surface layers of the blade. Because of nonuniform heating temperature stresses appear in the blades. During rotation of the turbopump assembly centrifugal forces to the gas forces are added, causing tension of the blades. Maximum tensile stress will be at the maximum number of revolutions of the rotor. Full heating of the turbine blades is usually completed after the turbopump assembly achieves its rated number of revolutions. Therefore, considerable temperature stresses can act at the maximum number of revolutions.

If the turbine is partial, then bending of blades by gas forces occurs only at those moments when the blade is opposite the nozzles. When the blade during rotation of the rotor is in intervals between the nozzles, it is loaded only by centrifugal forces. Consequently, blades of partial turbines are subject to cyclical action of gas forces.

Blades of axial pumps are loaded by centrifugal forces and hydraulic loading. The strength of blades of axial pumps is basically determined by hydraulic load, which is usually very great.

The blades of nozzle boxes of turbines are loaded only by gas forces, but on them there can additionally act considerable stresses due to nonuniform heating.

Blades of turbines and axial pumps during strength calculations are considered as cantilever beams, rigidly sealed in the rim of a disk and free at the end. The effect that fastening shrouds on the free end of the blades has on bending stresses will usually be disregarded.

Tensile stresses from centrifugal forces σ_p are calculated on conditions of maximum number of revolutions of the rotor. Distribution of stresses σ_p over the cross section of blade is taken as uniform. For any section of blade located on radius R (Fig. 14.25),

$$\sigma_p = \varrho \frac{\omega^2}{F} \int_R^{R_2} rf\,dr + \varrho \frac{\omega^2}{F_0} F_\text{ш} h_\text{ш} R_\text{ш}, \qquad (14.1)$$

where ϱ – mass density of the material of the blade; ω – angular velocity of the turbopump assembly rotor; F, f, F_0 – areas of blade cross sections on radii R, r and R_2 respectively; $F_\text{ш}$ – area of cross section of shroud; $h_\text{ш}$ – height of shroud; R_2 – radius of end section of blade; $R_\text{ш}$ – radius of center of gravity of shroud, which usually in view of the smallness of height of the shroud is taken as equal to R_2.

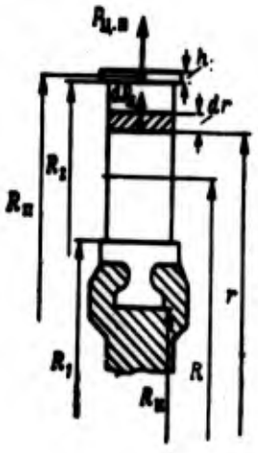

Fig. 14.25. Calculation of blade under tension from centrifugal forces.

By formula (14.1) stresses are determined in sections of blade with variable area of cross section lengthwise. Usually, blades of reactive gas turbines are made with constant section lengthwise. Then formula (14.1) is simplified and takes the form:

$$\sigma_p = \frac{1}{2}\rho\omega^2(R_2^2 - R^2) + \rho\omega^2 F_в \bar{h}_в R_2^2, \qquad (14.2)$$

where

$$F_в = \frac{F_в}{F}; \quad \bar{h}_в = \frac{h_в}{R_2}.$$

Diagram of stresses σ_p, calculated for a blade of sonstant section, is shown in Fig. 14.26 by line 1. The greatest values of tensile stress $\sigma_{p.к}$ are attained in the root section of the blade, where $R = R_1$. Then

$$\sigma_{p.к} = \frac{1}{2}\rho u_2^2(\zeta_в - \nu^2), \qquad (14.3)$$

where

$$\zeta_в = 1 + 2F_в\bar{h}_в; \quad \nu = \frac{R_1}{R_2};$$

$\sigma_{p.к}$ – tensile stress in root section of a blade of constant section;
u_2 – peripheral velocity of the blade end.

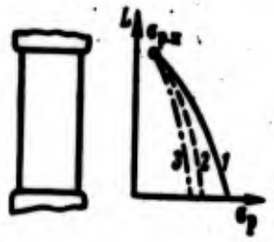

Fig. 14.26. Diagrams of tensile stresses in blades; 1 – of constant section; 2, 3 – wedge-shaped.

If the blade does not have a shroud, then $\zeta_{\text{ш}}=1$ and

$$\sigma_{p.\text{ш}}=\frac{1}{2}\rho\omega_{\text{ср}}^2(1-\nu^2). \qquad (14.4)$$

From equation (14.4) it follows that tensil stresses in the root section due to centrifugal forces do not depend on area of cross section of the foil if it is constant in length. An increase in area of cross section, as follows from expression (14.3), leads only to a decrease of stresses due to centrifugal forces of the blade shroud. To decrease $\sigma_{p.\text{ш}}$ blades are made with an area of section of fin decreasing from the root to the end. Blades of such form are called by wedge-shaped. The value $\sigma_{p.\text{ш}}$ characterizes tensile stress due to centrifugal forces of the shroud. In the absence of a shroud on the end of the blade, stresses are equal to zero. The effect of a shroud on the value of stresses in the blade is the greater the more massive the shroud and the shorter the blade.

In completed constructions of turbopump assemblies the tensile stresses due to centrifugal forces lie within limits:

$\sigma_{p.\text{ш}}$ = 600-1800 kgf/cm^2 for blades of turbines;

$\sigma_{p.\text{ш}}$ = 200-400 kgf/cm^2 for blades of axial pumps.

Blades are calculated for bending on conditions of maximum flow rate of working substance. The action of forces of gas pressure, or hydraulic load can be considered in the example of a turbine blade (Fig. 14.27). Conditionally one may assume that on the average radius of blade on it from the side of gas flow there act concentrated components of full gas force P_a and P_u, corresponding to axial, parallel to axis Oy, and circumferential parallel to axis Ox.

These forces create moments M_x – in plane yOr and M_y – in plane xOr. Forces P_a and P_u can be defined by known intensities of load (linear loads) p_a and p_u in corresponding planes:

$$P_a = \int_{R_1}^{R_2} p_a dr;$$

$$P_u = \int_{R_1}^{R_2} p_u dr.$$

Fig. 14.27. Diagram of the action of gas forces.

Intensity of loads on radius r are determined [15] by the formulas

$$p_a = (p_1 - p_2)\frac{2\pi r}{z} - \frac{2\pi r}{z} Q_1 c_{1a}(c_{2a} - c_{1a}); \qquad (14.5)$$

$$p_u = -\frac{2\pi r}{z} Q_1 c_{1a}(c_{2u} - c_{1u}), \qquad (14.6)$$

where z – number of blades; u – peripheral velocity; c_{1u}, c_{1a} – circumferential and axial components of speed on entrance to the blade; c_{2u}, c_{2a} – circumferential and axial components of speed on exit from the blade; Q_1 – mass density of working substance on entrance to the blade; p_1, p_2 – pressures of working substance on entrance to and exit from the blade.

By formulas (14.5) and 14.6) it is possible to calculate the intensity of loads with any method of profiling of blades. In the calculation of blades of reactive gas turbines it is possible to consider $p_1 - p_2 = 0$. With partial turbines instead of the total number of blades, one should put in these formulas number of blades z', actually being subjected in each moment to the action of gas forces.

In view of considerably greater rigidity of blade against bending in plane yOr, than in plane xOr, during calculation of blades for bending it is possible without essential error to disregard the action of moment M_x, and to determine only stresses due to the action of moment M_y.

With relatively short blades, as in the turbines of the turbopump assembly, intensity of load p_u can be considered constant over the length of the blade, i.e., to consider $P_u = p_u L$, where L – length of blade. Here, for calculation of p_u, instead of formula (14.5), it is possible to use, emanating from the equation

$$M_{кр} = P_u R_{ср} z$$

dependence

$$p_u = \frac{2 \cdot 71620 N}{nL(R_2 + R_1)z}, \qquad (14.7)$$

where N – power of the turbine; n – number of r/min of turbopump assembly rotor.

This dependence can be used in the calculation of intensity of load p_u on blades of an axial pump.

In an arbitrary section of blade on radius R, the bending moment due to gas force, as follows from Fig. 14.28, equals

$$M_{изг}^{r} = p_u \frac{(R_2 - R)^2}{2}.$$

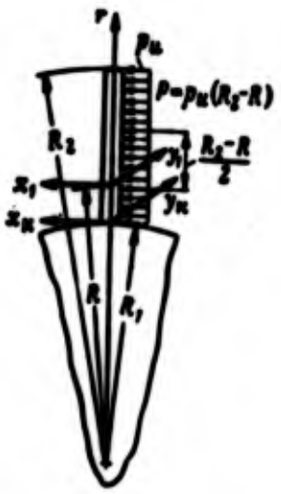

Fig. 14.28. Determination of bending moment from force P_u.

Bending moment attains maximum value in the root section:

$$M^r_{y_u} = p_u \frac{R_2^2}{2}(1-\nu)^2 = P_u \frac{L}{2}. \qquad (14.8)$$

Bending stress in an arbitrary point of cross section of blade (Fig. 14.29) in a system of coordinates x_1Oy_1, where point O coincides with center of gravity of section, is determined by the formula

$$\sigma_u = -\frac{M^r_{y1}}{W_{y1}} = -\frac{M^r_{y_1}}{J_{y1}} x_1, \qquad (14.9)$$

where W_{y1} – section modulus of profile of blade for a given point; J_{y1} – minimum moment of inertia of profile of blade relative to corresponding principal axis, which can be considered as coinciding with axis Oy_1; x_1 – distance of the point from axis Oy_1 in which stress is determined.

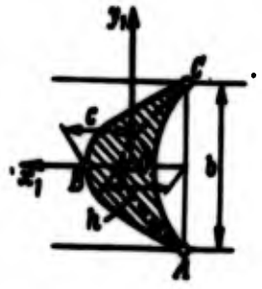

Fig. 14.29. Profile of cross section of blade of an impulse-type turbine.

With a symmetric profile of blade of an impulse-type turbine (Fig. 14.29), the area of cross section and moment of inertia can be defined by the following approximate dependences:

$$F = 0{,}67\,bc;$$
$$J_{y1} = 0{,}038\,bc\,(c^2 + 0{,}8h^2),$$

where b – profile chord; c – maximum thickness of profile; h – maximum rise (curvature) of center line of profile.

Bending stresses are usually determined for three characteristic points of profile A, B, and C, most remote from axis O_{y1}. In turbine blades, maximum bending stresses appear on the ends of sharp edges of profile, i.e., at points A and C. Section modulus of profile for points A and C is determined by the formula

$$W_A = W_C = 0{,}038\,\frac{bc}{h}\,(c^2 + 0{,}8h^2).$$

With constant section of blade, bending stresses have their maximum in the root section and change along the length of the blade as shown by curve 1 in Fig. 14.30. For wedge-shaped blades, bending stresses can change along the length of blade in conformity with curves 2 and 3.[1] In carried out constrictions of turbopump assemblies, bending stresses from the action of gas forces in the root section of blades lie within limits of:

σ_u^g = 100-400 kgf/cm^2 for blades of turbines;
σ_u^g = 1500-4000 kgf/cm^2 for blades of axial pumps.

Fig. 14.30. Diagrams of bending stresses due to gas forces for blades: 1 – of constant section; 2, 3 – of wedge-shaped.

Usually, blades of impulse-type turbines are made linear extension of centers of gravity of section in plane xOr in the direction of rotation of the disk, as shown in Fig. 14.31. Generators of the profiled part are disposed parallel to base line OA. In so doing, in each section of blade moment M^{u}_{y1} appears due to centrifugal force of the part of the blade lying higher than the examined section. This moment bends the blade, opposite to direction of rotation, and compensates to this or that degree the action of bending forces due to gas forces.

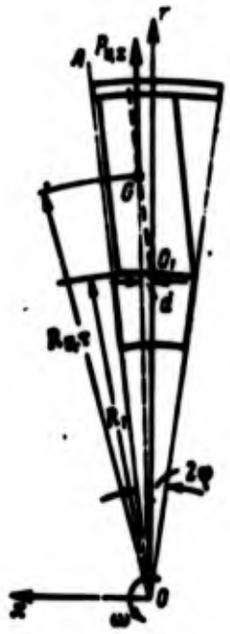

Fig. 14.31. Diagram of extension of centers of gravity of blade section.

Maximum value of bending moment M^{u}_{y1} is attained in the root section of the blade. If one were to consider the centrifugal force of the foil and shroud of the blade $P_{л}$ applied at the center of gravity of the blade G, then with respect to center of gravity of root section O_1 it gives a bending moment:

$$M^{u}_{y1} = P_{л} d,$$

where d – arm of force $P_{л}$ with respect to the center of gravity of the root section.

Arm d is determined by the dependence

$$d=\operatorname{tg}\varphi(R_{a.r}-R_1),$$

where $\varphi=\pi/z$.

Bending stresses due to the action of centrifugal forces are calculated by formula (14.8), where, instead of M^{c}_{g1}, there is substituted $M^{c}_{g.r}$. In carried out constructions, bending stresses due to the action of centrifugal forces in the root section of the blades of a turbopump assembly equal:

σ^{c}_{u} = 300-600 kgf/cm^2 for blades of turbines,
σ^{c}_{u} = 3000-7000 kgf/cm^2 for blades of axial pumps.

Total bending stresses due to gas and centrifugal forces

$$\sigma_{u}=\sigma^{g}_{u}+\sigma^{c}_{u}. \qquad (14.10)$$

In formula (14.10) the stresses are substituted with their signs; positive are considered tensile stresses. Total bending stresses in the root section of blades of a turbopump assembly equal σ_{u} = 200-400 kgf/cm^2 for the blades of the turbines and σ_{u} = = 1000-3500 kgf/cm^2 for the blades of the axial pumps.

With a nonstationary thermal rate, the blades of the turbines of a turbopump assembly are heated unequally at all points of cross section. The relatively thin front and trailing edges are heated more, and the massive central part of blade is heated more slowly. The approximate character of change in temperature along the length of the center line of the blade profile is shown in Fig. 14.32a. In Fig. 14.32b there is shown the character of change of stresses along the center line of the profile corresponding to the given character of change in temperature. As can be seen, along edges of the blade compression stresses appear because of the fact that expansion of the more heated fibers of the blade is prevented by the less heated. Conversely, in the central part of

the blade, the less heated fibers are stretched because of the effect of the more heated.

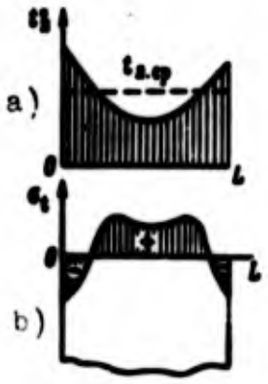

Fig. 14.32. Distribution along the center line of the blade profile of temperatures a) and temperature stresses b).

Methods of calculating the temperature stresses σ_t are complicated. Therefore in practice they are limited to calculation of possible temperature stresses on the basis of statistics. In carried out turbopump assemblies the maximum values of temperature stresses attain 1500 kgf/cm^2.

Estimation of the strength reserve of blades is produced according to maximum value of total stresses. In general, total stress in a given section equals

$$\sigma_\Sigma = \sigma_p + \sigma_{u.s} + \sigma_t.$$

As an example, in Fig. 14.33 there is shown the character of distribution of stresses along the length of a blade at point A of the profile (see Fig. 14.29) directly after starting and after full heating.

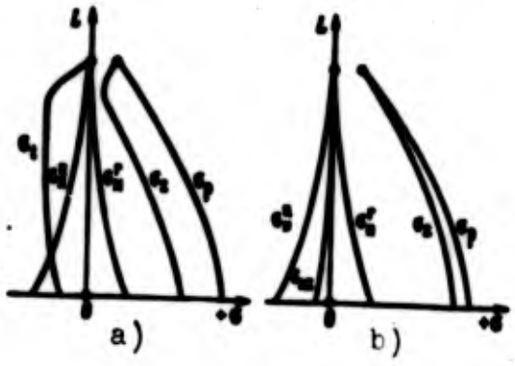

Fig. 14.33. Diagrams of stress at point A of a blade: a) immediately after starting the turbopump assembly; b) after full heating of the blade.

The safety factor in a given moment of work is determined by the formula

$$k_0 = \frac{\sigma_0}{\sigma_{1\max}},$$

where σ_0 – ultimate tensile strength of the material of the blade at a given temperature in a calculated point at a given instant. Value of the safety factor should be not less than 1.2-1.5. Under maximum total stresses $\sigma_{1\max}$ = 800-1200 kgf/cm^2 in the blades of the turbines and $\sigma_{1\max}$ = 1500-4000 kgf/cm^2 in the blades of the axial pumps, safety factors equal 3-8 and 1.2-4 respectively.

Blades of partial turbines, as noted above, are subjected to the cyclical action of stresses. Total stresses for such blades change from maximum value $\sigma_{1\max} = \sigma_p + \sigma_{u1} + \sigma_{i1}$ when the blades pass before the nozzles, to minimum $\sigma_{1\min} = \sigma_p + \sigma_{u2} + \sigma_{i1}$ when the blades pass through the section between the nozzles. The cyclical action of bending stresses can lead to blade breakdowns due to fatigue of the material.

The blade of a partial turbine should be checked for fatigue in accordance with a fatigue safety factor

$$k_\sigma = \frac{\sigma_r}{\sigma_{1\max}},$$

where σ_r – fatigue limit with a given coefficient of asymmetry of cycle of effective stresses.

In carried out constructions of blades of partial turbines of turbopump assemblies, the fatigue safety factor k lies within limits of 2-3.

Forces having an effect on the blade are transmitted through the joint elements to the disk. The locking part of the blade is loaded by tension due to centrifugal forces and bending due to centrifugal and gas forces. Using the formulas (14.1) and (14.9)

there can be found bending and tensile stresses for it in any section. In carried out constructions, total tensions do not exceed 1000-2500 kgf/cm^2, which corresponds to a safety factor $k_в$ = 2.0-3.0.

In locks of fir tree and T-shape types and with triangular teeth, the teeth also are subjected to strength calculation. The teeth are calculated for strength against the action of centrifugal forces at maximum number of revolutions of the rotor of the turbopump assembly. It is assumed that the centrifugal force is distributed among the teeth in proportion to the value of their contacting surface, i.e., bearing stresses are identical on all teeth. The contacting surface is checked for crumpling, and the base of the tooth – for bending and shear (Fig. 14.34a). If the contacting surfaces of all teeth are taken as identical, then one may assume approximately that on each tooth a force $P_1 = P_{лс}/i$, where $P_{лс}$ – total centrifugal force of blade with locks; i – number of teeth. Then the normal bearing stresses $\sigma_{см}$, bending $\sigma_и$ and tangential shear stress $\tau_{ср}$ are determined by the formulas

$$\sigma_{см} = \frac{P_1}{F_{см}}; \quad \sigma_и = \frac{P_1 l}{W_и}; \quad \tau_{ср} = \frac{P_1}{F_{ср}},$$

where $F_{см}$ – area of contacting surface of a tooth; $F_{ср}$ – area of sheared section of a tooth; $W_и$ – moment of resistance to bend of the area of the calculated section of tooth at its base.

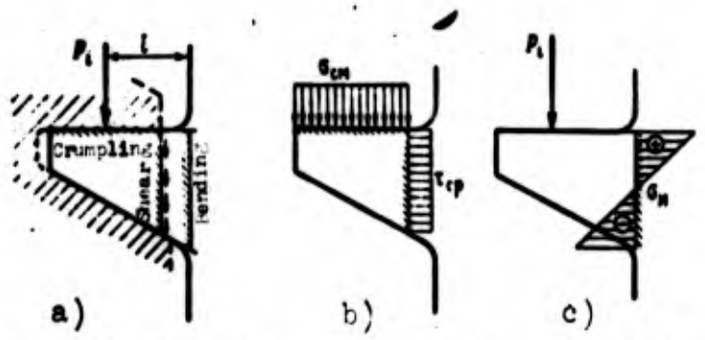

Fig. 14.34. Calculation of a tooth of a lock for strength. a) calculation diagram; b, c) diagrams of bearing stresses bending and shearing stresses of a tooth of a blade lock.

Diagrams of stresses $\sigma_{см}$, $\sigma_и$ and $\tau_{ср}$ for a tooth of a fir-tree lock are shown in Fig. 14.34b, c. On the average $\sigma_{см}$ = 1000-1600 kgf/cm^2, $\sigma_и$ = 400-1000 kgf/cm^2, $\tau_{ср}$ = 800-1200 kgf/cm^2.

In the case of a pin lock (Fig. 14.35) a check is made on the stretching of section I-I due to the action of centrifugal forces of the foil of the blade and the part of the root lying higher than the datum section, and also on bearing stress and shear of the pin:

$$\sigma_{см}=\frac{P_{л.з}}{da};\quad \tau_{ср}=\frac{P_{л.з}}{\frac{1}{2}\pi d^2},$$

where $P_{л.з}$ – total centrifugal force of a blade with a lock; d – diameter of pin; a – width of blade root.

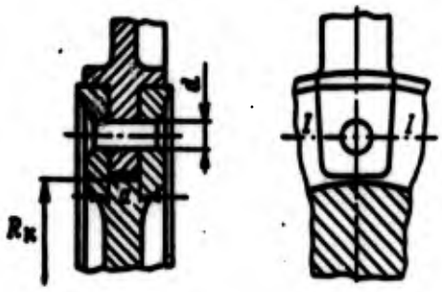

Fig. 14.35. Calculation of a pin lock.

On the average $\sigma_{см}$ = 1200-1500 kgf/cm^2, $\tau_{ср}$ = 1300-1500 kgf/cm^2.

In joining the blade to the disk by welding or brazing (Fig. 14.36) tensile stresses on the seam are determined as

$$\sigma_р=\frac{P_{л.з}}{\psi F_ш},$$

where $F_ш=2\pi R_{об}c$ – area of cylindrical section of seam; ψ – coefficient of seam strength, taken as equal to 0.8-0.95.

Tensile stress in the welded seam $\sigma_р$ = 1000-2000 kgf/cm^2, and safety factor $k_р=\frac{\sigma_{р.ш}}{\sigma_р}$=3–6, where $\sigma_{р.ш}$ – tensile strength of the material of the seam.

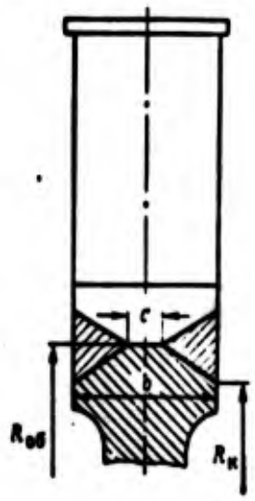

Fig. 14.36. Calculation of a welded seam.

14.7. Blade Vibrations

Irregularity of gas flow around the circumference of the flow-through part of a turbine causes periodic change in forces acting on the blades which can lead to the appearance of forced vibrations of the blades, and during resonance due to fatigue of the material of the blades their breakdown is possible. Resonance vibrations more frequently appear in blades of partial turbines. During investigation of blade vibrations there is produced a determination of the frequencies of natural and forced oscillations, resonance numbers of rotor revolutions of the turbopump assembly and vibration stresses in the blades.

The basic forms of natural vibrations of blades are flexural, torsional, and flexural-torsional. Depending upon the number of nodel lines of vibration they are subdivided into uninodel, or vibration of the first form; binodal, or vibration of the second form; trinodal, etc.

Forms of flexural and torsional vibrations of blades are shown in Fig. 14.37. Besides similar pure flexural and torsional vibrations, a blade can have complex, flexural-torsional vibrations. However, the frequencies of these oscillations are such that possible resonances are not dangerous.

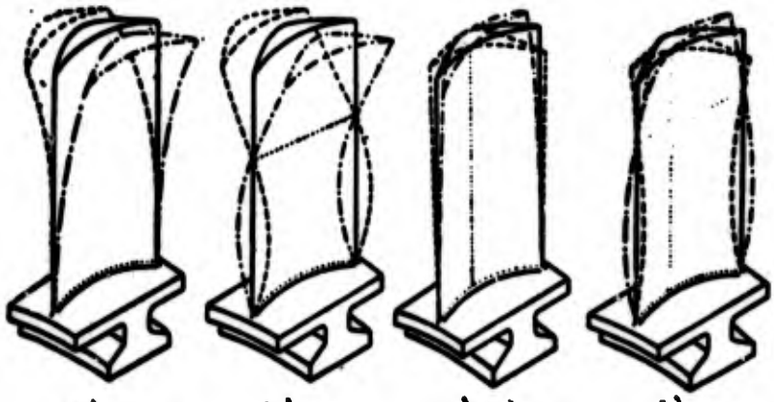

Fig. 14.37. Forms of vibrations blades: a and b) first and second flexural; c, d) first and second torsional. Nodal lines are shown by dots.

For a blade of constant section without shroud, the frequency of natural flexural oscillations of i-th form is determined by the formula

$$f_{i\,изг}=\frac{a_i}{2\pi L^2}\sqrt{\frac{EJ}{\varrho F}},$$

where L – length of blade; J, F – moment of inertia and area of cross section; E, ϱ – elastic modulus and mass density of the blade material; i – number of form of vibration; a_i – form factor of vibrations. The greater the flexural rigidity of blade, the higher the frequency of its flexural vibrations.

In view of the great rigidity of turbine blades, in practice usually determination is made only of the frequency of first (low-frequency) form of flexural vibrations, at which the appearance of dangerous resonances is most possible. Taking into account an analytic dependencies given above which connect the geometric characteristics of the profile, area, and moment of inertia of a section, for the frequency of flexural vibrations of the first form there is obtained the dependence:

$$f_{изг}=0{,}243\frac{a_1 c}{2\pi L^2}\sqrt{\frac{E}{\varrho}\left(1+\frac{h^2}{c^2}\right)}, \qquad (14.11)$$

where $a_1=3{,}52$.[2]

If the blade has a shroud, then the frequency of its flexural vibrations is also calculated by formula (14.11) with substitution instead of form factor α_1 coefficient $\bar{\alpha}_1$, the value of which depends on the ratio $\bar{m}=m_ш/m_л$, where $m_л$ – mass of the foil of the blade; $m_ш$ – mass of the shroud, as shown in Fig. 14.38.

The frequency of natural flexural vibrations of blades obtained experimentally is somewhat less enumerable by formula (14.11); this is explained by the elasticity fitting of the blade into the disk, whereas during calculation the fitting of the blade was assumed to be rigid.

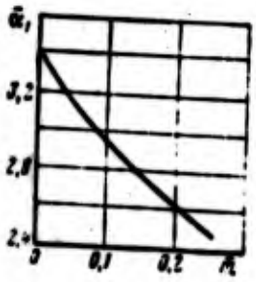

Fig. 14.38. Dependence of coefficient of the first form of flexural vibrations $\bar{\alpha}_1$ on the ratio of mass of shroud to mass of foil of the blade $\bar{m}$.

The frequency of natural flexural vibrations of a blade revolving together with a disk is increased according to the increase in the number of revolutions. This occurs due to the fact that during deflections of the vibrating blade from equilibrium position during rotation not only the force of elasticity, but also centrifugal forces strive to return it to a position of equilibrium. The action of centrifugal forces is equivalent to an increase of flexural rigidity of the blade. The frequency of natural vibrations of a revolving blade f_d is called dynamic frequency. It is determined by the formula

$$f_д=\sqrt{f_{нат}^2+Bn_c^2},$$

where n_c – number of revolutions of the rotor per second;
B – a coefficient, the value of which depends on the form of vibrations and the ratio $R_1/R_2 = \nu$; where ν = 0.4-0.6, the value of B accordingly equals 4-6.

As can be seen from formula (14.11), the frequency of natural flexural vibrations of a blade does not depend on the material of the blade (inasmuch as for the majority of materials, the ratio E/ϱ is identical), but depends on temperature, since with an increase in temperature, the elastic modulus of the material decreases. Therefore, as the blades become heated in the process of exit from the turbopump assembly to the mode, the frequency of natural flexural vibrations is increased due to the restoring action of centrifugal forces and decreases due to the temperature rise. The combined effect of these factors leads to a change in frequencies of flexural vibrations f_d according to the number of revolutions of the turbopump assembly rotor.

For a blade of constant section, the frequency of natural torsional vibrations of the i-th form is determined by the formula

$$f_{i\,\text{кр}} = \frac{2i-1}{4L}\sqrt{\frac{GT}{\rho J_p}},$$

where G – elastic modulus of the second type; T – geometric rigidity of the blade against torsion with respect to center of gravity; J_p – polar moment of inertia of the section.

The frequency of natural torsional vibrations of a blade of constant section depends on its material and geometric characteristics of profile.

A characteristic of torsional vibrations of blades with shrouds (shrouded), besides the dependence of frequency of vibrations on shroud mass, is the possibility of damping. If the clearance between the shrouds of neighboring blades is so great that the shroud during vibrations do not touch, then the forms of vibrations of the blades do not differ from the form of vibrations of isolated blades. If the adjusting clearance is small, during heating there is possible such a decrease in the clearance that the neighboring shrouds during counter vibrations can collide. This leads to a

considerable decrease in amplitudes of vibrations, i.e., to damped vibrations. In the absence of a clearance, the shrouds will form a solid shroud. Then there are possible only those vibrations of blades according to the first form, when all of them simultaneously are deflected to one side (Fig. 14.39a). Inasmuch as individual blades have somewhat different frequencies of first form of flexural vibrations, the described vibrations of shrouded blades are poorly excited and usually are not dangerous. A possible mutual arrangement of shrouded blades during vibrations according to the second flexural form is shown in Fig. 14.39b. The frequency of natural vibrations of such form is determined by experimental means.

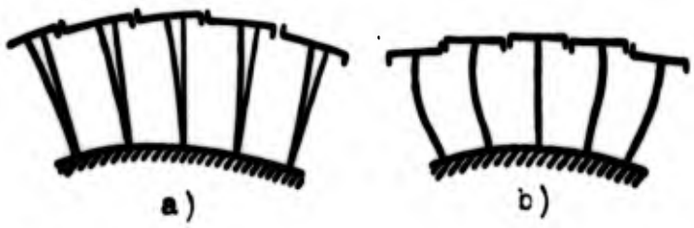

Fig. 14.39. Oscillations of shrouded blades: a) uninodal; b) binodal.

Forced oscillations of revolving blades cause periodic forces acting from the side of the gas flow. These forces are changed along the circumference of the flow-through part of the turbine according to the law of change of field of pressure and velocity of a gas, described by a certain periodic function. This periodic function can be subjected to harmonic analysis, i.e., to be represented by the sum of harmonic components 1, 2, 3, and subsequent orders. In general, the order of the k-th harmonic (where k = = 1, 2, 3, ...) is equal to the number of full cycles of change of exciting force for one revolution. Frequency of the k-th harmonic of exciting force is equal to the product of the number of revolutions of the rotor per second times the index number of harmonic k:

$$f_{возб} = kn = \frac{kn}{60},$$

where n – number of revolutions of the rotor per minute.

The frequency of forced vibrations $f_{вын}$ is equal to the frequency of exciting force: $f_{вын}=f_{возб}$. As the number of revolutions increase forced vibrations are increased. At a certain number of revolutions, the forced vibrations may become equal to one of the frequencies of natural vibrations of the blade. Here resonance vibrations appear, accompanied by growth of amplitudes and, consequently, vibration stresses which can lead to breakdown of the blade.

The number of revolutions of the rotor per minute, at which resonance begins, is called resonance $n_{рез}$ and is determined from the condition of equality of frequency of the i-th form of natural vibrations (flexural or torsional) f_i with frequency of the k-th harmonic of the exciting force:

$$f_i=f_{возб\,k}=\frac{kn_{рез}}{60}.$$

Hence resonance number of revolutions

$$n_{рез}=\frac{60f_i}{k}. \qquad (14.12)$$

In formula (14.12) there is substituted the frequency of the i-th form of natural vibrations at a corresponding number of revolutions and temperature of blade. Therefore, analytic determination of the resonance number of revolutions is difficult. For determination of resonance numbers of revolutions usually use is made of the frequency diagram (Fig. 14.40), on which is constructed the dependence of frequency of the i-th form of natural vibrations (for example, first flexural, as in Fig. 14.40) on the number of revolutions $f_i=f_i(n)$ and rays $f_{возб\,k}=f_{возб\,k}(n)$, corresponding to k-th harmonics of the exciting forces. Points of intersection of rays with curves of frequencies of natural vibrations give the resonance numbers of revolutions. In Fig. 14.40 the region of frequencies of natural vibrations obtained by virtue of the following is shaded.

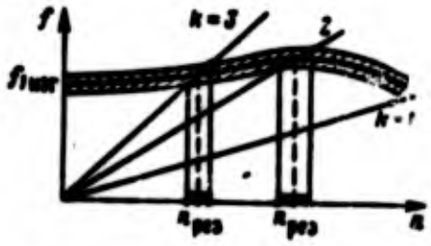

Fig. 14.40. Frequency diagram of blade vibrations.

The blades, because of technological tolerances, have certain differences in dimensions, which leads, naturally, to scattering of their frequencies of natural vibrations (up to 15-20%). From each vibrating blade on the disk, waves of elastic deformations are transmitted through the disk to other blades, exciting vibrations in coupled circuit in a group of blades. All the blades of the group vibrate in one phase and to each group there corresponds its frequency of natural vibrations of a given form. Therefore, there is characteristic not any one frequency of natural vibrations of all blades, but a frequency band. Therefore resonance vibrations occur not at a certain fixed value of number of revolutions, but occupy specified regions of working range of number of revolutions, called resonance conditions. An example of determination of resonance conditions where k = 2 and k = 3 is shown in Fig. 14.40.

Amplitudes of resonance vibrations depend on the value of the forces of exciting vibrations and of the suppressing forces (damping). Even with very great exciting forces, the amplitudes of vibrations can be insignificant, if there are great suppressing forces. The basic suppressing forces are the frictional forces in the lock and aerodynamic forces, and also hysteresis of the material of the blade and lock. Those resonance conditions under which the amplitudes of vibrations are dangerous to the strength of the blades are called critical. Critical resonance conditions must not occur in the zone of operating numbers of revolutions of the turbopump assembly.

The amount of permissible vibration stresses in blades depends on the duration of operation of the turbopump assembly under resonance conditions, and also on the level of tensile and bending

stresses acting on the blade. Usually, the value of vibration stresses in blades does not exceed 400-800 kgf/cm^2. Vibration stresses in blades are determined usually by experiment, using a tensometer.

In breakdowns of blades due to vibration under specified resonance conditions there is known the form of vibrations corresponding to the given resonance. It is possible to remove critical resonance by changing in the first place, the frequency of natural vibrations, which is attained, for example, by changing form of the blade profile or the setting of the shroud. It is more complicated constructively to change the frequency of the disturbing forces; it is possible to do this, for example, by changing the number of nozzles and their relative position. To decrease the amplitude of the disturbing forces they sometimes have recourse to increasing axial clearance between the nozzles and blades of the turbine.

14.8. Strength of Turbine Disks and Centrifugal Pumps

The disks of gas turbines are loaded by centrifugal forces from their own masses and the masses of blades set on them, and due to nonuniform radial heating – are subject to the action of considerable temperature stresses. The level of stresses due to centrifugal forces and temperature stresses frequently exceeds the elastic limit, and plastic deformations appear in the disk. If plastic deformations in the disk exceed the yield point, breakdown of the disk is possible.

Calculating the strength of a disk consists in determining the circumferential and radial stresses due to centrifugal forces and nonuniform heating. Usually they are limited in designing the disk to assumption of elastic deformations, and an estimate of strength is produced by comparison of calculated stresses with stresses in analogously carried out constructions of disks of the turbines of a turbopump assembly.

Determination of the distribution of temperatures radially for a disk under conditions of nonstationary heating constitutes an independent problem, which is decided, for example, by the method of

elementary balances. In approximate calculation of disk strength it is possible to pursue a certain law of distribution of temperature by radius, proceeding from available experimental or calculation data for analogous constructions and operating conditions.

Usually, the maximum difference in temperatures of the peripheral part and the center of a disk equals $\Delta t = (0{,}5—0{,}7)t_r$, where t_r — temperature of working sobstance under established conditions of a turbopump assembly in °C. In so doing, the temperature of the rim of the disk, not having special cooling or heat shielding is established on the order of (0.85-0.75) t_r. In the central part of the disk there is established a temperature of (0.15-0.25) t_r. In calculating strength is is assumed that the temperature of the disk throughout the thickness is constant.

Dependences of tensions in disk on its dimensions, material, loads due to centrifugal forces, and irregularity of heating are written as equations of stress conditions. In derivation of the equations it is taken that the disk is symmetrical relative to the middle of the plane. it is in plane stress condition and the stresses on any radius of disk do not change throughout its thickness. Equations of stress condition are derived from conditions of equilibrium and deformation of elementary section separated from the disk on radius r, the diagram of load and deformation of which is shown in Fig. 14.41.

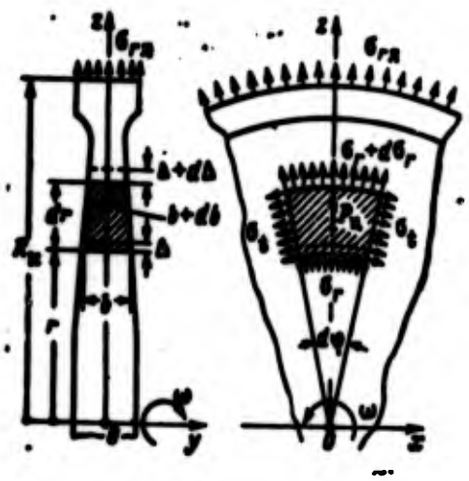

Fig. 14.41. Derivation of fundamental equations of stress condition of a disk.

Along the edges of the separated element there act radial σ_r and circumferential σ_t normal stresses. The element is loaded by centrifugal force of its own mass $P_э$. Along the periphery on radius $R_к$, the disk is loaded with radial stresses $\sigma_{r.к}$. Radius $R_к$ is conducted to the edge of the slotted part of the rim, i.e., that part of the rim, where the locks of the blades are located. Examples of determination of radius $R_к$ for several types of blade locks are shown in Fig. 14.25, 14.35, and 14.36. Consequently, stresses $\sigma_{r.к}$ appear from the action of centrifugal forces of the masses of the blades and the mass of the part of the rim lying higher than radius $R_к$, including the mass of the blade locks:

$$\sigma_{r.к} = \frac{P_{л.л} z + P_{л.об}}{2\pi R_к b_к},$$

where $P_{л.л}$ – centrifugal force of the blade foil; $P_{л.об}$ – centrifugal force of the mass of the blade locks and the part of the rim lying higher than the section conducted on radius $R_к$; $b_к$ – width of rim on radius $R_к$.

Stresses σ_r and σ_t are variable by radius.

Due to the action of centrifugal forces and heating, the element in working state is deformed so that its radial deformation on radius r becomes Δ, and on radius $r + dr$ – $\Delta + d\Delta$ accordingly.

In the accepted designations from the conditions shown there can be obtained differential equations of stressed condition of a disk [15]:

$$d\sigma_r = -\sigma_r\left(\frac{db}{b}+\frac{dr}{r}\right)+\sigma_t\frac{dr}{r}-\rho\omega^2 r^2\frac{dr}{r}; \qquad (14.13)$$

$$d\sigma_t = \sigma_t\left(-\frac{dr}{r}+\frac{dE}{E}\right)+\sigma_r\left(\frac{dr}{r}-m\frac{db}{b}-m\frac{dE}{E}\right)-$$

$$-m\rho r^2\omega^2\frac{dr}{r}-Ed(\beta t). \qquad (14.14)$$

where ϱ — mass density of material; m — Poisson's ratio; E — elastic modulus of the material of the disk at given temperature t on radius r; β — coefficient of linear expansion of the material of the disk at temperature t; ω — angular velocity of rotation of the disk.

The system of equations (14.13) and (14.14) usually is expanded by the method of finite differences. The method of such calculation of the distribution of stresses by radius of the disk is given in [15].

A character diagram of stress with corresponding laws of distribution of temperatures by radius of disk for single-stage turbines with a solid disk and a disk with a central hole is shown in Fig. 14.42a, b.

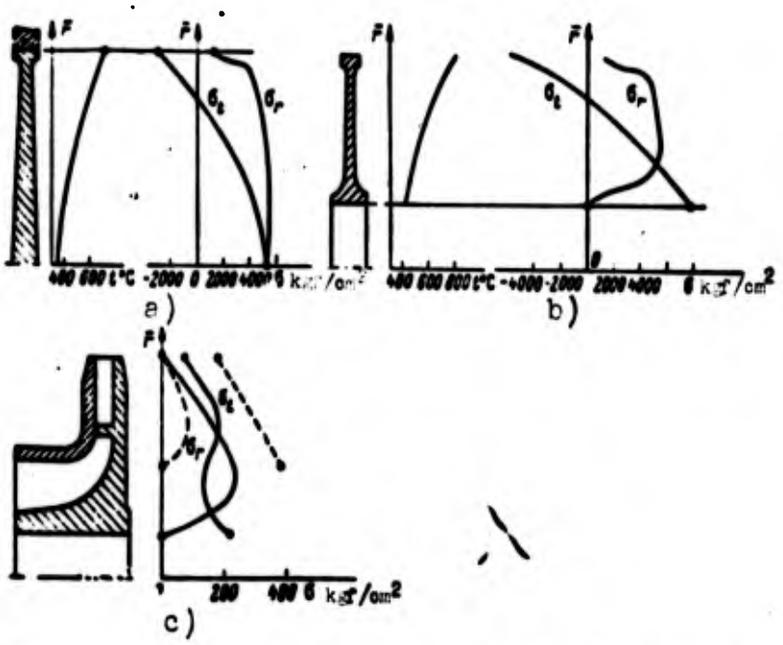

Fig. 14.42. Distribution of temperatures and stresses by radius: a) turbine disk without central hole; b) turbine disk with central hole; c) impeller disk (solid lines) and removable cover (dotted lines).

In carried out constructions of turbines with peripheral velocities on the external radius of the disk on the order of 180-240 m/s, and a temperature gradient of 200-400°C, the stresses from the blade rim usually do not exceed $\sigma_{r.l}$ = 500-1500 kgf/cm^2;

stresses in the center of a solid disk $\sigma_r = \sigma_t$ on the order of 3500-5500 kgf/cm^2; in a disk with hole, on the border of the hole σ_t = 6000-8000 kgf/cm^2 (neglecting plastic deformations), and $\sigma_r = 0$, if not pressed on the shaft, and $\sigma_r = \sigma_{пр}$, where $\sigma_{пр}$ – fitting stresses, if the disk is pressed onto the shaft.

On the periphery of the disk with the indicated gradient of temperatures, due to constraint of deformation of the more heated rim on the side of the central part of disk, on the rim there may appear, as shown in Fig. 14.42a, b, compression stresses σ_t, attaining 2000-4000 kgf/cm^2.

Characteristics of the calculation for strength of impellers of centrifugal pumps consist of the following. The blades of centrifugal pumps additionally load the disk with centrifugal forces in the places of their attachment. In calculating the strength of a blade conditionally they are replaced by a certain mass, which is equally distributed on the surface of the disk. In so doing, the intrinsic carrying capacity of the blades is not considered and goes as a safety factor of the disk. Calculation is produced by the above-indicated method, but instead of mass density of the material of the disk, in corresponding formulas the given density is substituted. On a given radius the given density is determined by the formula

$$\gamma_{пр} = \left(1 + \frac{f_л z}{2\pi r b}\right)\gamma,$$

where $f_л$ – area of cross section of blade on radius r; z – number of impeller blades; b – width of impeller disk on radius r.

With peripheral velocities of impellers of centrifugal pumps on the order of u_2 = 100-180 m/s, the maximum value of circumferential stresses on the radius of the hole is obtained as equal to 100-400 kgf/cm^2 for impellers made out of aluminum alloys, and 2000-4000 kgf/cm^2 for impellers of steel. Removable disks of closed impellers are calculated for strength separately. The level of stresses in removable disks is usually the same as in the impeller disks.

In Fig. 14.42c there are diagrams showing stresses in a one-sided impeller and a removable disk.

14.9. Vibrations of Disks

Variable gas forces, having an effect on the blades, are transmitted to the disks and cause their forced vibrations. Vibrations of disks can be caused by flexural vibrations of the rotor. The frequency of forced vibrations of disks is equal to or is a multiple number of the revolutions of the rotor. With coincidence of frequencies of forced and natural vibrations of the disk there appear resonance vibrations which can serve as the cause of fatigue breakdown of the disks.

Most characteristic are the following forms of vibrations of the disk: vibrations with one or several nodal diameters (Fig. 14.43a, b), vibrations with one or several nodal circumferences (Fig. 14.43c, d) and combined vibrations with nodal diameters and nodal circumferences (Fig. 14.44). The most frequently observed are vibrations with nodal diameters and combined vibrations.

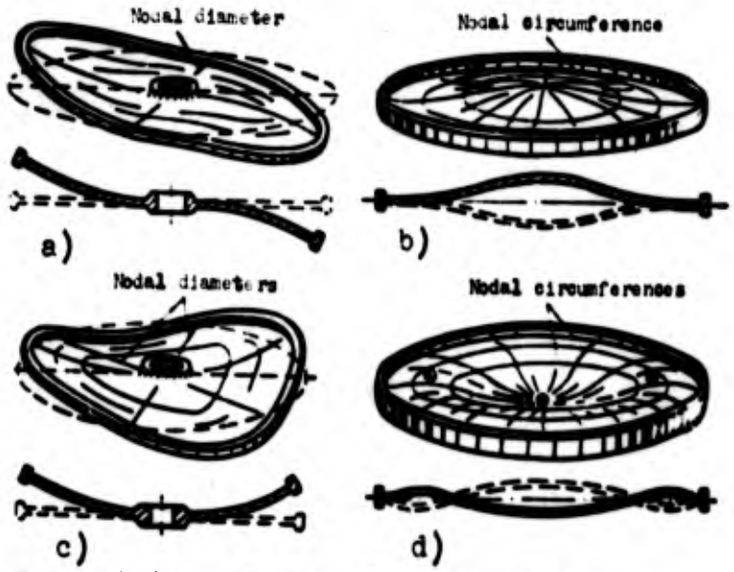

Fig. 14.43. Forms of disk vibrations: a) with one nodal diameter; b) with two nodal diameters; c) with one nodal circumference; d) with two nodal circumferences.

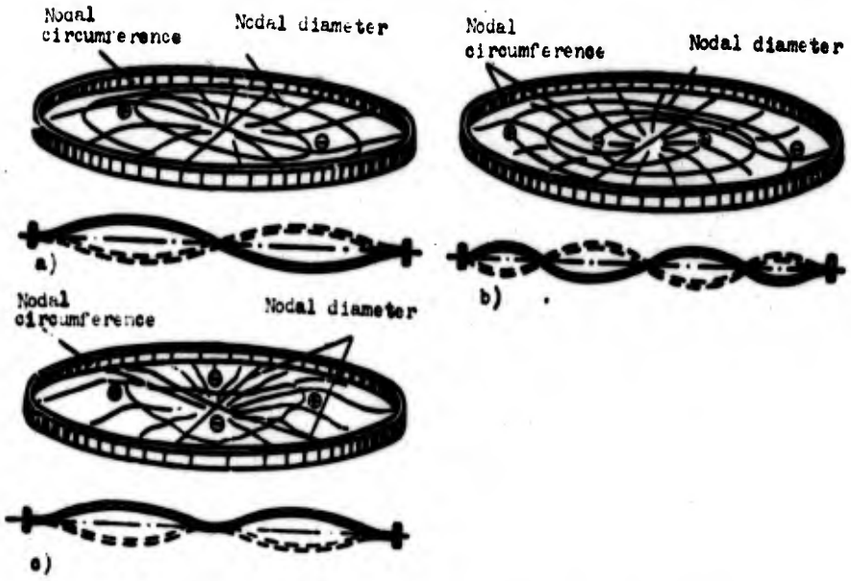

Fig. 14.44. Combined forms of disk vibrations: a) with one nodal circumference and one nodal diameter; b) with one circumference and two diameters; c) with two circumferences and one diameter.

Frequency of natural oscillations of a disk, neglecting irregularity of heating is determined by the formula

$$f_{qs} = \frac{a_{qs}}{2\pi R_2^2}\sqrt{\frac{E}{10.9\varrho}},$$

where R_2 – external diameter of the disk; h – average thickness of the disk; a_{qs} – form factor of vibrations, depending on the number of nodal diameters and circumferences; q, s – number of nodal diameters and nodal circumferences.

For a disk close to flat, it is possible to take $a_{01} = 10.24$; $a_{11} = 21.25$; $a_{22} = 39.8$; $a_{12} = 60.8$.

During vibrations of a revolving disk the nodal diameters do not remain fixed with respect to the disk, but revolve to this side or that. A similar shift in the deformation wave over the disk is called a traveling wave. Fixed fields of pressures and velocities of gas flow cause vibrations with nodal diameters fixed

in space (with respect to the disk the diameters revolve with its number of revolutions). With coincidence of frequencies of natural and forced oscillations in this case the most dangerous resonances appear, since they are excited by constantly acting disturbances (for example, from partial feed of gas).

Resonance numbers of revolutions are determined by the formula

$$n_{рез} = \frac{60 f_{св}}{k}.$$

For combatting dangerous resonances a number of constructive measures are used: change in the configuration and dimensions of the disks, which leads to change of $f_{св}$, change in the configuration and dimensions of the disks, which leads to change of $f_{возб}$, increase in the axial clearance between nozzle box and disk, leading to a decrease in the amplitude of the exciting forces.

Footnotes

[1]Calculation for blades of variable section by length is provided in [15].

[2]Methods of calculating the frequencies of natural vibrations of blades of arbitrary profile are given in [15].

C H A P T E R XV

ELEMENTS OF FUEL SUPPLY SYSTEMS

15.1. High-Pressure Gas Containers and High-Pressure Containers with Liquified Gases

A high-pressure gas container consists of a cylinder filled with compressed gas. In most cases the cylinder has a spherical shape. If, during calculation of the required volume of a spherical cylinder its diameter turns out to be larger than the midsection of the aircraft or engine compartment, no cylinder can be made with elliptical section or in the form of a cylinder with spherical bottoms of the same volume.

The cylinder is supplied with fittings: servicing devices, safety and scouring valves and subassemblies for fastening. The weight of this equipment can amount to from 20 to 50% of the cylinder's own weight.

The cylinders are usually steel welded. Calculated safety factor $k_в$ according to ultimate tensile strength of material $\sigma_в$ is taken as equal to 2-3.

Thickness of the wall of a spherical cylinder with known design pressure $p_б$ and internal diameter D is determined by the formula

$$\delta = \frac{k_в p_б D}{4\sigma_в}.$$

By this formula there is also determined the required thickness of walls of the spherical bottoms of the cylinders. Thickness of walls of a cylindrical container is determined by the formula

$$\delta = \frac{k_3 p_3 D}{2\sigma_0}.$$

Dry weight of a spherical high-pressure container without fittings

$$G_A = (1{,}2 - 1{,}5)\pi D^2 \delta \gamma_6,$$

where γ_6 – weight density of the material of the cylinder.

It must be noted that under assigned pressure in the fuel tanks and their volume, the weight of the cylinders practically does not depend on the value of initial pressure, since with an increase of it the calculated volume of the cylinder simultaneously decreases almost in the same degree. For the purpose of decreasing the dimensions of the cylinder it is desirable to increase initial pressure in it, which is limited in basic possibilities of means of charging, which most frequently develop pressure up to 250-300 kgf/cm^2.

Dry weight of a cylindrical pressure container with the same pressure and volume as a spherical one, is almost twice as large.

The volume of cylinders of pressurized systems of fuel supply can amount to 30% of the volume of the fuel tanks.

In pressurized fuel supply systems, and also for pressurizing the tanks with a pump supply system, containers are also used with liquified gases. Such containers are lighter in weight than gas ones, since the volume of the container with liquified gas in view of the greater density of the working substance is less, and the pressure in the container is also less. The supply system is considerably simplified if the same liquified gas is used for pressurizing

and as one of the fuel components. A diagram of such a system is shown in Fig. 15.1. Liquid oxygen from pump 6 reaches the coil of heat exchanger 5 through control valve 3 and check valve 4. In the heat exchanger the liquid oxygen is heated by waste steam gas coming out of turbine 2. With the vaporized liquid oxygen under a pressure on the order of 2-3 kgf/cm^2 the liquid oxygen tank 1 is pressurized. Under these conditions the consumption of liquid oxygen for pressurizing composes 0.5-0.6% of the consumption of oxygen for the chamber of the liquid propellant rocket engine.

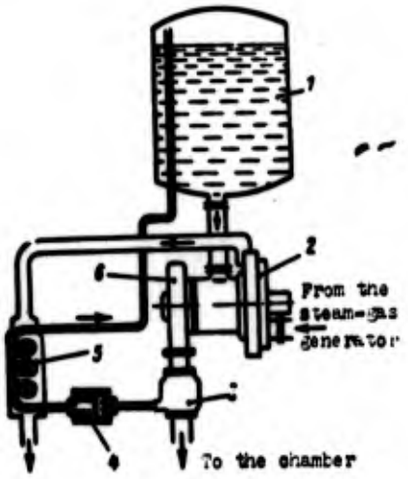

Fig. 15.1. Diagram of a system of tank pressurization with a pressure container working on liquified gas: 1 – tank; 2 – turbine of the turbopump assembly; 3 – distributing valve; 4 – check valve; 5 – heat exchanger coil; 6 – liquid oxygen pump.

15.2. Solid Propellant Generators and Starters of a Turbopump Assembly

A solid propellant generator (PAD) consists of a combustion chamber (Fig. 15.2) in which is contained charge 3 made of powder or other solid fuel, a front bottom with igniter 1 placed on it and a rear bottom. According to their principle of operation PAD's are subdivided into supercritical and subcritical [47]. In a supercritical PAD the ratio of feed pressure $p_н$ to pressure in the chamber $p_к$ is less than critical or equal to it. In a subcritical PAD, this ratio is greater than critical, but pressure difference $p_н - p_к$ is small and is determined by losses in the feeder tubing. In a supercritical PAD in the rear wall a throttling nozzle 4 is set (Fig. 15.2a); in a subcritical PAD (Fig. 15.2b) the throttling nozzle is absent.

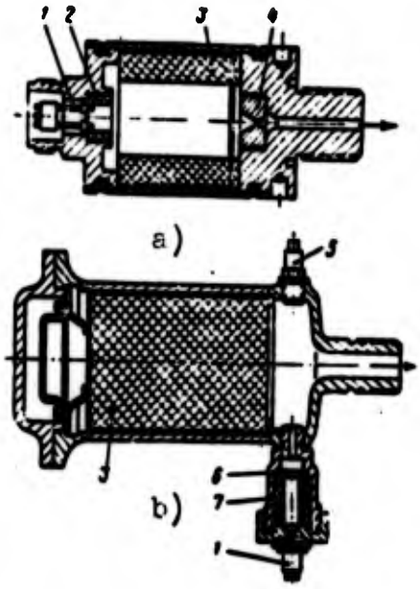

Fig. 15.2. Diagrams of solid propellant generators:
a) supercritical; b) subcritical;
1 – igniter; 2 – igniting charge;
3 – charge; 4 – nozzle; 5 – safety valve, 6 – diaphragm;
7 – auxiliary charge.

A PAD should ensure separation of constant quantity of gas in a unit of time. Therefore, charges are used which have constant burning surface; face charge (Fig. 15.2b) or tubular grain, burning from external and internal surface. Those surfaces of the charge, on which burning should not occur, are armored with a special composition which does not support combustion. Between the charge and the walls of the combustion chamber, when they are open for action of hot gases, there is placed a heat-insulating covering. The simplest covering is asbestos.

Charges intended for prolonged combustion are made from fuels with low combustion rates. In the operation of a PAD in a pressure feed fuel system, slowly burning fuel cannot ensure rapid achievement of rated conditions of the engine, since the gases formed in the first period of operation of the PAD have to at first fill the main line and free volume of the tanks and to ensure heating of the elements of the fuel supply system. For the purpose of accelerating achievement of rated conditions, the PAD is supplied with an auxiliary charge 7 (Fig. 15.2b), fulfilling the role of starting charge and igniter. This charge is made from quick-burning solid fuel. Dimensions of this auxiliary charge are selected from calculation of the required gas generation for preliminary creation of pressure in the systems.

A supercritical PAD, which characteristically have high gas pressure in the combustion chamber (on the order of up to 200-250 kgf/cm^2) possesses sufficient stability and is capable of operating without additional regulating devices [47].

A subcritical PAD works with pressures in the combustion chamber insignificantly exceeding that necessary for feed pressure. With pressure greater than the calculated, the quantity of forming gases becomes larger than quantity of outflowing gases, and thus because of the difference in these quantities, pressure in the chamber must continue to increase [47].

In the combustion chamber of a subcritical PAD a safety valve 5 is set (Fig. 15.2b), which opens at a specified pressure p_r to release into the atmosphere the excess quantity of gases. In the presence of such conditions, a subcritical PAD works with continual discharge of excess gases and its operating conditions become stable.

In spite of the great simplicity of construction and operational reliability of a supercritical PAD in the fuel supply systems of liquid propellant rocket engines, basically the subcritical PAD are used since they are considerably lighter, thanks to smaller design pressure. The supercritical PAD's are found useful as starters in liquid gas generators of a turbopump assembly. They have a charge calculated for a working time of 0.05-0.2 seconds. During this time, gases fill the corresponding main lines and the gas generator and ensure ignition of fuel components supplied to the gas generator.

For ignition of the charge of a PAD an igniter is used, including a weighed portion of rapid acting, course grained powder and an electric detonator.

In individual cases, when the gas generator of a turbopump assembly works on the basis spontaneously combustible components and when during starting it is not required to be filled with gases from the PAD, the solid propellant generator is used as a starter supplying gas to the turbine of the turbopump assembly for its overspeeding.

An example of the construction of cartridge starter is shown in Fig. 15.3. The starter has a cylindrical chamber 5 with a head in which there are set two igniter charges 11, igniter 10 and a pressure capsule 12. The igniters and the pressure capsule are enclosed by breakthrough membranes 3. To the combustion chamber by bolts 14 through lining 4 there is fastened rear bottom 1 with nozzle 2, also enclosed by the breaking membrane. In the chamber there is a telescopic charge consisting of three tubular charges 6, 7 and 8. At the ends, the charges are covered by armoring 9.

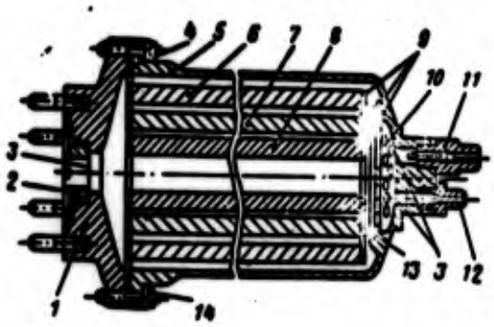

Fig. 15.3. Cartridge starter
1 – rear bottom; 2 – nozzle;
3 – breakthrough membranes;
4 – lining; 5 – chamber;
6, 7, 8 – tubular charges;
9 – armoring; 10 – igniter;
11 – igniter charges;
12 – pressure capsule;
13 – elastic ring; 14 – bolt.

The PAD housings are made of heat-resistant steels. The bottoms of the PAD are usually made removable to simplify the installation of the igniter and the main charge. Thicknesses of walls of the PAD are determined according to formulas given in § 15.1 with values of $\sigma_в$ corresponding to the design temperature of the wall. It is taken as equal to maximum temperature of the wall at the end of operation. In calculating the temperature of the wall there is considered the effect of the heat-protective covering (if any) or the fuel dome in case of fastening of charge to the housing.

15.3. Gas Generators

Gas generators are made mono, bi-, and tri-component.

Monocomponent gas generators work on monopropellants, for example, hydrogen peroxide, hydrazine (parameters of its decomposition: $T = 365^{\circ}K$; $k = 1.37$; $R = 67 \cdot 10^3$), isopropyl nitrate, and others.

The most widely used are monocomponent gas generators working on hydrogen peroxides, usually called steam-gas generators (PGG). The parameters of decomposition products of hydrogen peroxide depend on its concentration (Fig. 15.4).

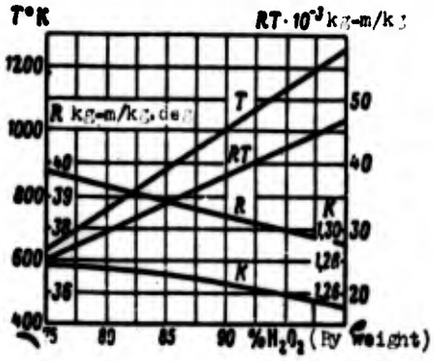

Fig. 15.4. Parameters of decomposition products of hydrogen peroxide.

The basic element of a PGG is the reactor, in which in presence of catalyst decomposition of hydrogen peroxide occurs. An advantage of the PGG is the simplicity of the feed control of steam gas. At a constant temperature and constant concentration of hydrogen peroxide, the temperature of the steam gas is constant, and the quantity of steam gas evolved depends only on the quantity of peroxide passed into the reactor. Thus, for example, for maintaining the assigned operating conditions of a turbopump assembly, the turbine of which works on steam gas, it is necessary to have before the reactor only a regulator for constancy of supply of hydrogen peroxide. The temperature of the steam gas rises with an increase in concentration of hydrogen peroxide, which makes the use of concentrated solutions more beneficial.

Solutions of hydrogen peroxide of high concentration are unstable and have a high freezing point, which creates operational inconveniences, therefore in practice, solutions with concentration of more than 90-95% are rarely used. Maximum temperature of steam gas with such a concentration reaches near 700-800°C. Higher temperature of steam gas can be obtained by introducing into solution hydrogen peroxide additives which burn in gaseous oxygen: phenol, methanol, glycerine. These solutions did not find wide use in view of the insufficient mastery of their operational properties.

The design of the reactor basically is determined by type of catalyst used. There are PGG's with solid and with liquid catalyst [47].

The expenditure of liquid catalyst does not exceed 7-10% of the expenditure of hydrogen peroxide. An advantage of such a reactor is the possibility of prolonged operation, a disadvantage – the necessity of having a control system for the supply of liquid catalyst; furthermore, addition of a liquid catalyst lowers the hydrogen peroxide concentration.

These deficiencies do not apply to PGG with a solid catalyst, consisting of grains of solid porous base-carriers (gypsum, cement, fire clay, etc.), impregnated by catalytically active salts, for example, permanganates, chromates, and others.

A disadvantage in a PGG with solid catalyst in the form of grains is the possible removal of particles of the catalyst with steam gas. Besides decreasing the activity of the catalyst this leads to wear of the turbine blades, since, for example, potassium permanganate is decomposed with separation of solid particles of manganese peroxide. In order to decrease the carrying out of solid particles from the reactor, in the examined design there is a filter, and outlet pipe 5 is located on the side of the reactor and has a baffle.

More nearly ideal is the design of a reactor with catalyst in the form of a metallic grid (Fig. 15.5). The hydrogen peroxide, through plate 1 with holes, passes into the chamber of the reactor, in which are located two packs of metallic grids. Pack 2 consists of grids covered with the catalyst, while lower pack 4 – of grids without coating. The grids of pack 2 are made of silver and are coated with samarium oxide. Grids made of brass with silver plating are also used. Silver or silvered grids are a very active catalysts, but their cost is high. Pack 4 has nickel or Monel-Metal grids. These materials are considerably cheaper but less active. A second

pack is intended for decomposition of that part of the hydrogen peroxide which remained undecomposed after flowing through the first pack, and also for retaining those particles of silver removed by the steam gas. To avoid a flow of hydrogen peroxide in the clearance between the packs and the housing there are press fitted rings 3.

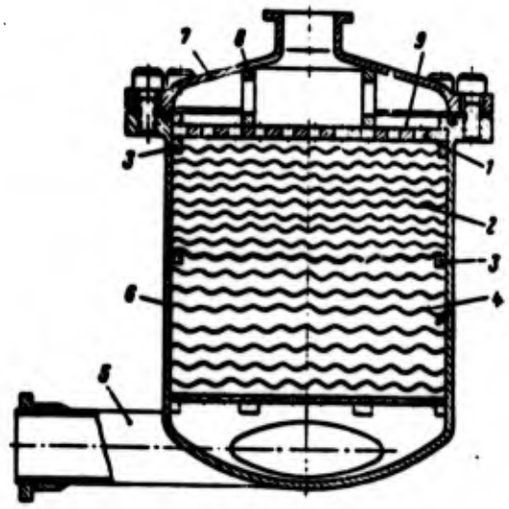

Fig. 15.5. PGG with catalyst in the form of grid: 1 – plate; 2, 4 – packs of metallic grids; 3 – rings; 5 – outlet pipe; 6 – reactor housing; 7 – housing cover; 8 – scattering device; 9 – cavity above the plate.

The grids of the catalyst are pressed under high pressure and have 100-400 holes for 1 cm^2. The holes in plate 1 are located in such a way that they ensure uniform expenditure of the hydrogen peroxide over all the area of cross section of the packs. The area of the holes amounts to 20-25% of the plate area; their diameters are 0.8-3.2 mm. The total area of peripheral holes is considerably larger than the area of the holes in the central zone of the plate.

The volume of cavity 9 above the packs of catalyst will be selected by experiment. It should be as small as possible for quick starting of the PGG, but at the same time sufficient for equal distribution of hydrogen peroxide over the surface of the plate.

In individual constructions use is made of packs carried out from alternate silver covered steel grids and grids made of stainless steel. The total number of grids may exceed 70. The diameter of the reactor chamber depends on the expenditure of steam gas. In a number of constructions, reactors of spherical form are used.

Calculation of the strength of reactors is produced by the same method as calculation of PAD chambers and gas pressure generators. The chambers of the reactors are made of stainless steel.

In a bi-component gas generator the working substance usually is obtained by means of combustion of an oxidizer and combustible, utilized in the basic chamber of the engine. Such gas generators are frequently called liquid-gas generators (ZhGG). They consist of a special combustion chamber, the process in which has its own characteristics.

In particular, the turbine operating conditions require that temperature of gases ahead of it should be not higher than 1200-1500°K. Such a low temperature can be obtained only with a considerable surplus of one of the components.

In this case, besides the products of oxidation, there may be obtained a vapor of one of components. If the excess component has a complex structure, then, furthermore, products of its decomposition are obtained. Thus, in using petroleum and certain other combustibles; in case of surplus combustible, there enter into the composition of the products of reaction hydrocarbons, for example, CH_4, C_2H_6, and free solid carbon. With small values of excess oxidant ratio formation of coke and soot is observed, which during prolonged and repeated operation can lead to considerable contamination of the working substance duct.

Various circumstances have an effect on selection of excess component. Thus, it is undesirable to have the oxidizing medium ($\alpha > 1$) when the gas washes parts which are made of materials subject to oxidation. It is necessary also to consider parameters R and k of the working substance, so that at a given temperature it is possible to obtain the greatest possible operation of the turbine.

In Fig. 15.6 there are calculated dependences of parameters of products of combustion on excess oxidant ratio for two fuels. From the graph it is clear that a temperature of less than 1500°K can be obtained with $\alpha < 0.25$-0.35 and with $\alpha > 4$-5.

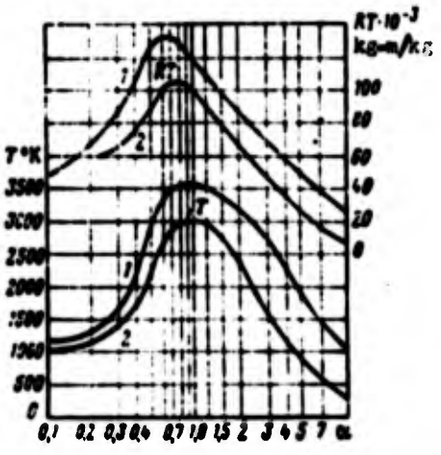

Fig. 15.6. Design temperature of combustion of two fuels depending upon α: 1 – oxygen-kerosene; 2 – nitric acid-kerosene.

It is necessary, however, to consider that with very rich mixtures, the calculated values of temperature, in a number of cases, turn out to be 100-200°C higher than the experimental. This is explained by the complex chemical composition of products of reaction for certain fuels, which cannot always be considered in calculation, and also by the fact that due to slow reaction speeds thermodynamic equilibrium does not succeed in being established, whereas in calculation there are determined equilibrium composition and temperature of the combustion products. For exact calculations, one should be oriented on experimental data recording the composition and temperature of the working substance of the turbine.

There are different possible diagrams for the organization of the process in a bicomponent ZhGG: with fuel supply only from the side of head, and with two-stage mixing. Since for bicomponent gas generators it is characteristic to have fuel combustion with very small or great excess oxidant ratios, and consequently, at low gas temperatures, then the use of such a diagram is feasible for readily evaporating or readily inflammable fuels. With two-stage mixing the fuel components move from the side of head with a relatively high excess oxidant ratio (α = 0.5-0.7).

The remaining part of the excess component (in this case the combustible) moves a certain distance from the head. In this case, combustion of the main part of fuel occurs at high temperatures (2000-3500°K), and therefore the process differs in high speed and stability. The excess component, proceeding a certain distance from the head, is subjected to the action of hot gases and, evaporating, cools them to the required temperature. Such a diagram of a gas generator is expedient for low-activity high-boiling substances.

Liquid-gas generators, working on bicomponent or tricomponent fuel, usually consist of the same elements as the chamber of a liquid propellant rocket engine and is similar to it in constructive shaping — they have a combustion chamber, head, and outlet duct.

Combustion chambers, in most cases, are cylindrical, double-walled, with regenerative cooling. Fuel is used more frequently as a cooler since ZhGG with an excess oxidant ratio of $\alpha = 0.1\text{-}0.5$. Since gas loads on the wall of a ZhGG combustion chamber are relatively small and their thermal balance favorable, it is possible to use a construction with widely-spaced joints between the walls or with unconnected walls. As widely-spaced joints, for example, point stampings can be used.

With the composition of a mixed fuel, differing sharply from stoichiometrical, it is possible to have considerable irregularity in the field of temperatures of the gas, which is impermissible for the turbine blades. For the purpose of creating more favorable conditions for leveling off of field of outlet temperatures from the ZhGG, the combustion chambers are made with greater volume-to-throat area than is used with those same components for the basic chambers of a liquid-propellant rocket engine. Relatively greater volume-to-throat areas are found in ZhGG chambers with two-zonal feed of components.

With cylindrical combustion chambers and pressure jet atomizers the chamber heads are made flat with three walls. The external wall, as also in the basic chambers of a liquid propellant rocket engine, has a form close to spherical. The attachment of the pressure

jet atomizers is analogous to that used in the basic chambers. To decrease carbon, it is more profitable to use a honeycomb location of injectors, ensuring more uniform mixture of components. In view of the relatively low temperature of gas in the chamber internal cooling by creation of a boundary layer of liquid is not used. A higher pressure drop at the injectors is selected than in the basic chambers (12-16 kgf/cm^2).

With two-stage mixing of components, the injector of the second belt can be made as a jet, in the form of openings in the internal combustion chamber. More complex is the design with injectors passing the component toward the current of gases or in the same direction. Such injectors can be set on special grid located in the combustion chamber, or on bracket, the role of which can be fulfilled by the combustible supply line; in the latter case, the reliability of operation of the ZhGG is impaired due to possible overheating.

In a tricomponent ZhGG, lowering of the temperature of products of combustion is attained by supplying the oxidizer and combustible with high α (0.5-0.8) with the addition of a third inert component (for these purposes it is possible to use water).

A diagram of a tricomponent generator with spherical head and cooling of the walls of the combustion chamber with water is shown in Fig. 15.7. In the center of the head an igniter device 2 is placed. The combustible and oxidizer are supplied respectively by injectors 1 and 3, water is supplied to the jacket by connecting pipe 4, and proceeds into the combustion chamber through injectors 5. The outlet duct of the gas generator is not cooled.

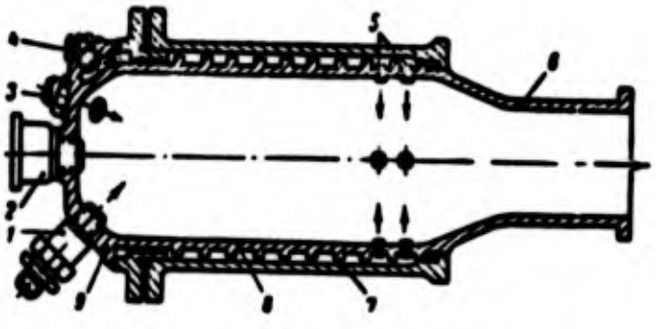

Fig. 15.7. Tricomponent ZhGG: 1 – combustible injector; 2 – igniting device; 3 – oxidizer injector; 4 – pipe connection for supply of water; 5 – water injectors; 6 – outlet duct; 7 – external wall of chamber; 8 – internal wall of chamber; 9 – head.

The diagram of a gas generator with lateral extraction of gases, shown in Fig. 15.8 promotes good mixing of the products of combustion and a certain decrease in soot falling into the turbine. On the spherical uncooled injector head 5, along the periphery, the combustible injectors 6 are located in concentric rows, and in the center – atomizer 7 injectors injecting the oxidizer in a radial direction. Two cartridge igniters 4 are placed for ignition of the fuel. Gases from the head are fed into an internal cylindrical monowall chamber 3. In center of this chamber at a certain distance from the head, there is set vortex combustible injector 8. Through it to the chamber nearly 8-10% of the fuel is fed. Bleeding of gases from the cylindrical chamber is produced by holes 2, and the gas proceeds to the turbine through the duct on the spherical uncooled housing of gas generator 9. The gas generator has removable heads 5 and 1. For sealing, soft linings are inserted in the joints. The weight of a similar ZhGG, due to the use of an uncooled chamber and cylindrical chamber 3, decreasing the heat withdrawal in the wall can be decreased as compared to the usual direct-flow chambers.

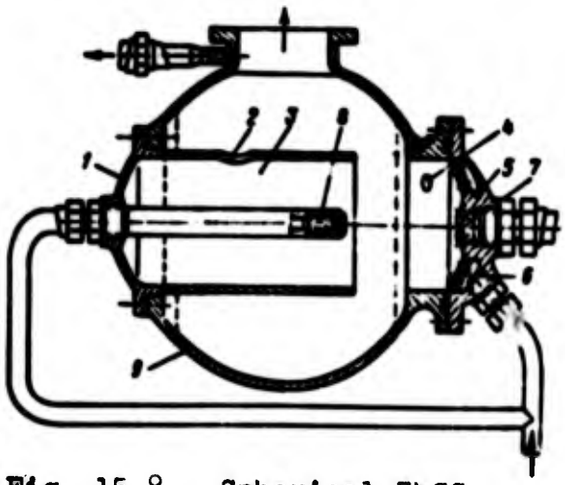

Fig. 15.8. Spherical ZhGG:
1 – head of cylindrical chamber;
2 – window; 3 – cylindrical chamber;
4 – igniters; 5 – injector head of the chamber; 6 – combustible injector;
7 – oxidizer atomizer; 8 – swirl combustible injector; 9 – spherical housing of the ZhGG.

Strength calculation of the ZhGG are produced according to the above-stated methods, taking into account the temperature of the walls. In restartable engines, due to the relatively low thermal stress, the life of the ZhGG can be greater than the life of the basic combustion chamber.

15.4. Valves of Fuel Supply Systems

Control of fluid flow in fuel supply systems of a liquid propellant rocket engine is effected by valves. According to the method of actuation, valves are subdivided into uncontrolled and controlled. Uncontrolled valves do not have a servomotor for opening or shutting the valve. An uncontrolled valve is opened by the difference in forces of liquid or gas pressure on the valve. Controlled valves have servomotors, actuated by gas or liquid pressure and also by electromagnets.

Valves are normally closed or normally open; the former under a supply of pressure or electrical current are opened, the second — are closed. The main parts of each valve are the valve itself (disk) (Fig. 15.9 and 15.10) and the valve seat against which the valve is pressed. In the valve seat or in the actual plate is a sealing insert. The insert, depending upon the properties of the liquid and amount of pressure is made of rubber, plastic, or soft metal or material. In those cases, when the aggressiveness of the liquid or gas does not permit using nonmetallic materials, the valve and valve seat are made of stainless steel. Such a valve is ground to the valve seat and is reset.

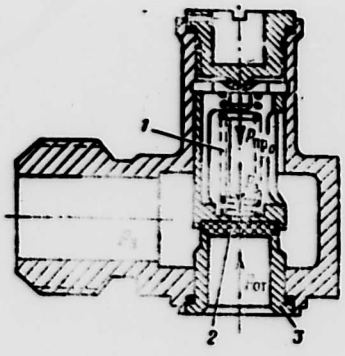

Fig. 15.9. Diagram of an uncontrolled valve: 1 — spring; 2 — valve (disks); 3 — valve seat.

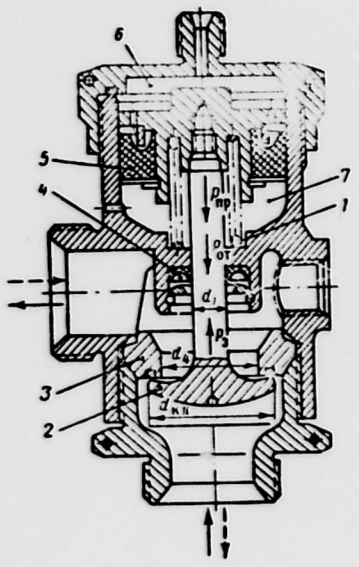

Fig. 15.10. Valve with a servomotor: 1 — spring; 2 — valve; 3 — valve seat; 4 — packing; 5 — packing of the servopiston; 6, 7 — servomotor cavities.

A valve must satisfy two basic requirements: ensure airtightness in the closed state and to pass the prescribed amount of flow with a specific pressure drop in open states.

Airtightness of a valve depends on pressure drop on the valve, the properties of the material in the place of contact, and the contact area of valve with the valve seat. It is considered that the area of contact has no gaps in its circumference. The effort which is necessary to apply to the valve in closed state to ensure airtightness is found by the formula

$$P_r = k_r p_r F_c, \qquad (15.1)$$

where k_r — margin of airtightness; p_r — minimum required pressure of airtightness; F_c — area of contact between valve and valve seat.

Usually $k_r > 2$ is used. The minimum required pressure of airtightness p_r is determined by the properties of the materials used for sealing, and the difference in inlet and outlet pressure of the valve. For flat disks, the value p_r is determined by embirical dependences:

for hard materials

$$p_т = a(p_{вх} - p_{вых})^b;$$

for soft materials

$$p_т = a(p_{вх} - p_{вых}) + c,$$

where $p_{вх}$ – inlet pressure; $p_{вых}$ – outlet pressure; a, b, c – constant coefficients, the values of which for the most widely used materials for sealing are given in Table 15.1.

Table 15.1. Characteristics of packing materials.

Material	a	b	c
Ebonite	100	0,121	
Hard fiber	100–135	0,167	
Lead	2700	0,057	
Annealed red copper	1000	0,16	
Aluminum	8000	0,54	
Rubberized asbestos	0,78		30
Rubber of varying hardness	0,20–0,85		40–55
Soft fiber	0,45		45
Leather	0,9		25
Asbestos	0,7		33

Calculation of an uncontrolled valve is reduced to determination of the characteristics of the spring to ensure the required force of pressure of valve to valve seat for airtightness in the closed state with a prescribed pressure drop on the valve, and also the maximum valve lift for obtaining the calculated amount of flow.

Three forces act on a valve in open and closed state: force of the spring $P_{пр}$, force of liquid pressure $P_ж$ directed in the direction of closing the valve, and force of pressure $P_{от}$, directed in the direction of opening of valve. With the valve closed there should be ensured a condition of airtightness (see Fig. 15.9)

$$P_т = P_{пр.0} + P_ж - P_{от}. \qquad (15.2)$$

where

$$P_{пр0}=k_{пр}h_0;\quad P_з=p_зF_з;\quad P_{от}=p_{от}F_{от}.$$

Here $k_{пр}$ – coefficient of elasticity of the spring; h_0 – preliminary compression of the spring; $p_{от}$, $p_з$ – pressures, acting to open and close the valve, respectively; $F_{от}$, $F_з$ – areas of the valve in the direction of pressures $p_{от}$ and $p_з$.

In open state, when the valve is lifted from the valve seat by value h, flow G through it is determined by the equation

$$G=Ad_{кл}h,$$

where

$$A=\pi\mu\sqrt{2g\gamma(p_{вх}-p_{вых})},$$

$d_{кл}$ – diameter of the valve; $p_{вх}$, $p_{вых}$ – pressures of liquid on inlet and outlet; μ – discharge coefficient of the valve, usually taken as equal to 0.65-0.75.

By the equation of expenditure there is determined the required value of valve lift h. In the open position, the valve is in equilibrium with the condition

$$P_{пр}+P'_з-P'_{от}=0, \qquad (15.3)$$

where

$$P_{пр}=k_{пр}(h_0+h);\quad P'_з=p_{вых}F_з;\quad P'_{от}=p_{вх}F_{от}.$$

Solving equations (15.2) and (15.3), one can determine the rigidity of the spring $k_{пр}$ and amount of deformation of the spring during preliminary compression h_0:

$$k_{пр}=\frac{1}{h}[(p_{вх}-p_{от})F_{от}-(p_{вх}-p_з)F_з-P_т];$$

$$h_0=\frac{1}{k_{пр}}(P_т-P_з-P_{от}).$$

They are also used as controlling elements in pneumatic systems, passing the working substance to the valves with pneumatic servomotors. A diagram of a similar valve – an electropneumatic valve – is shown in Fig. 15.11.

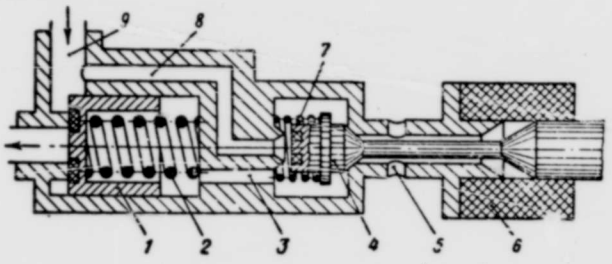

Fig. 15.11. Diagram of an electropneumatic valve: 1 – piston-valve; 2 – valve spring; 3, 8 – channels; 4 – control valve; 5 – connecting openings; 6 – electromagnet; 7 – control valve spring; 9 – supply duct.

The core of electromagnet 6, through a rod is connected with control valve 4. When switched on, electromagnet valve 4, overcoming the force of spring 7, is seated in the valve seat, closing channel 8. Gas under high pressure arrives via channel 9 and, compressing spring 2, opens valve 1. During de-energizing of the electromagnet, spring 7 opens the valve and air from channel 8 through channel 3 gets into the cavity under piston 1. Since the air pressure on both sides of the valve is equal, spring 2 puts the valve in the valve seat. With the valve closed, the cavity above piston 1 through channel 3 and opening 5 is connected with the environment.

For control of the valves explosive cartridges can be used. The merit of the explosive cartridges lies in the fact that they ensure high speed operation of the valves, are light, and do not require long piping. They are used in fuel supply systems of nonrestartable liquid propellant rocket engines.

The design of a normally open valve with electromagnetic drive is shown in Fig. 15.12. With the electromagnet 3 de-energized valve 2 is opened by spring 1. When the electromagnet is switched on, core 4 moves downwards and closes the valve.

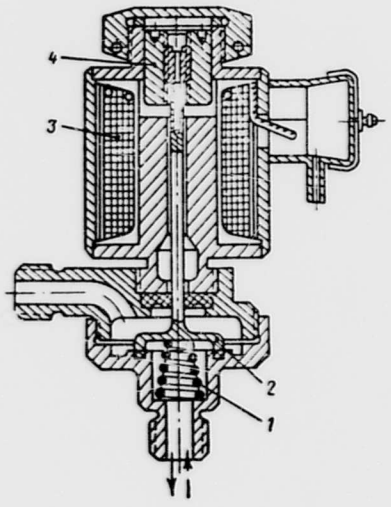

Fig. 15.12. Electromagnetic valve· 1 — spring; 2 — valve; 3 — electromagnet; 4 — core.

In the calculation of controlled valves the forces required for creation of airtightness and lift and retention of valve in the assigned open state are determined.

A normally closed valve (see Fig. 15.10) is under the impact of spring force $P_{пр0}$, force $P_{от}$, acting in the direction of opening, and force $P_э$, acting in the direction of closing. The condition of airtightness of the valve is recorded by formula (15.2).

For example, if the valve is opened in the direction of entrance of liquid, the movement of which is shown in Fig. 15.10 by solid arrows, then taking into account entered dimensions and conditions $p_э = p_{вх}$, $p_{от} = p_{вых}$ we have

$$P_{от} = p_{вых} \frac{\pi}{4} (d_4^2 - d_1^2); \quad P_э = p_{вх} \frac{\pi}{4} d_{кл}^2.$$

A controlled value is equipped with a servomotor, which develops the required force for opening or closing the valve and for retaining it in open state.

A valve with a pneumatic or hydraulic servomotor is shown in Fig. 15.10. Valve 2 is connected by a rod with the piston of the servomotor which has a sealing collar 5. The servomotor moves the working substance into cavity 6. In cavity 7, connected with the atmosphere, is spring 1. For sealing the movable parts of the valve leather or rubber collars 4 are used. The valve can be normally closed or open. In normally closed state the working substance is not moved to the servomotor and the valve is pressed against the valve seat by the force of the spring. To open the valve it is necessary to create pressure in cavity 6 of the servomotor, which should overcome the force of the spring and in working state hold the valve in a position to ensure the prescribed amount of flow. A normally open valve has servomotor which is under the impact of the pressure of the working substance. In order to close the valve, it is necessary to remove pressure from cavity 6. Structurally, the valve can be carried out so that the working substance moves into cavity 7 of the servomotor while the spring is located in cavity 6. Then, in normally closed state, the valve is subject to pressure, but in normally open state – to the spring.

If valve must be opened after starting the engine, then the latter variant is more feasible from the point of view of reliability in operation: during the pre-start check, presence of pressure in cavity 7 of the servomotor testifies to the good condition of the system and its readiness for starting. Such a state is easily controlled. To bring the valve to operating state it is necessary only to remove pressure from the servomotor and not to supply pressure to the servomotor, as with the design shown in Fig. 15.10.

Valves with a pneumatic and hydraulic servomotor are usually used when great shifting forces are required – in the main lines with great volume of flow and under high pressures. In pipelines with small volume of flow valves with an electromagnet can be used.

With movement of the liquid in the direction shown in Fig. 15.10 by dotted arrows, $p_{от}=p_{вх}$ and $p_з=p_{вых}$;
then

$$P_{от}=p_{вх}\frac{\pi}{4}(d_4^2-d_1^2);\ P_з=p_{вых}\frac{\pi}{4}d_{кл}^2.$$

From equation (15.2) there can be obtained the force of preliminary compression of the spring required to ensure airtightness of valve, taking into account values corresponding to direction of movement of liquid $P_з$ and $P_{от}$:

$$P_{пр0}=P_т-P_з+P_{от}.$$

For opening a normally closed valve the force of a servomotor is required

$$P_с=P_{пр0}+P_з+P_{от}+\sum_{i=1}^{i=n}P_{тр\,i},$$

where $\sum_{i=1}^{i=n}P_{тр\,i}$ – sum of all the forces of friction acting on n friction surfaces of the sealing or collar of the piston.

Frictional force is determined by the formula

$$P_{тр\,i}=f_{тр\,i}p\pi d_{тр}h_{тр},$$

where $f_{тр\,i}$ – coefficient of friction of i-th pairs; p – pressure in cavity of collars or sealing; $d_{тр}$, $h_{тр}$ – diameter and height of cylindrical friction surface of collars and sealing.

The coefficient of friction depends on the sealing material. For soft leather working in a low-viscosity liquid, $f_{тр}$ = 0.03-0.07: for hard leather $f_{тр}$ = 0.10-0.13; for leather working without lubrication, $f_{тр}$ = 0.2. The force of rest static friction can be 3-4 times greater than the frictional force of friction of motion. For exclusion of frictional force, the sealing can be carried out by means of bellows.

For retention of valve in open state, with known value of valve lift h, the force of the servomotor is determined by the formula

$$P_c' = P_{пр} + P_з - P_{от},$$

where

$$P_{пр} = k_{пр}(h_0 + h).$$

The servomotor is calculated on that force P_c or P_c' (taking into account the margin of force k_c), whichever is the greater

$$P_{с.р} = k_c P_c$$

or

$$P_{с.р} = k_c P_c',$$

where $P_{с.р}$ – calculated force of the servomotor.

The margin of force k_c is taken, depending upon type of sealing, within limits of 1.2-2.

With a normally open valve, the force of the servomotor holding the valve in closed state (see Fig. 15.12) is determined by the formula

$$P_c = P_г + P_{пр} - P_з + P_{от},$$

where

$$P_{пр} = k_{пр} h_0$$

h_0 – deformation of spring with the valve closed.

Values of forces $P_з$ and $P_{от}$ are determined taking into account the direction of movement of the liquid.

According to known force $P_в$, in the case of a hydraulic or pneumatic servomotor there can be determined the required pressure in the cavity of the servomotor or with known pressure of the working substance – area of the piston. With large values of shifting force, in order to avoid increasing the dimensions of piston or in order not to excessively increase the pressure in the control system, hydraulic servomotors can operate from boosters (Fig. 15.13). With a supply of pressure to cavity 9 differential piston 4, 8 shifts in the direction of cavity 6, compressing liquid into channel 7. The pressure in channel 7 will be as many times greater than the pressure in channel 2, as many times the area of piston 8 is greater than the area of piston 4.

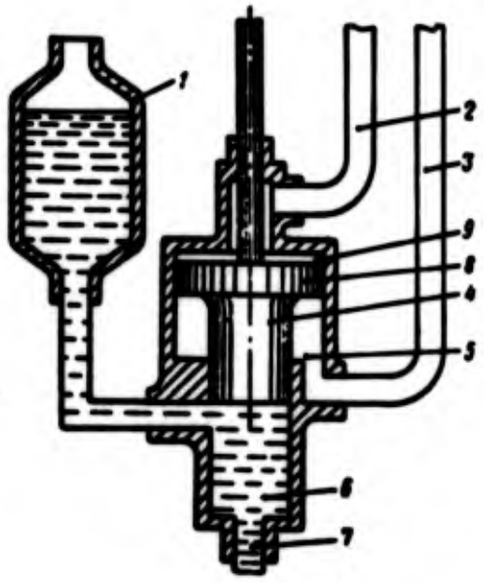

Fig. 15.13. Diagram of a booster: 1 – tank; 2, 3, 7 – ducts; 4, 8 – differential piston; 5, 9 – air cavities; 6 – liquid cavity.

15.5. Pressure Reduction Valves

Pressure reduction valves are intended for lowering and maintaining at a prescribed level the pressure of gas or liquid on exit from the reduction valve. Thus, the reduction valve constitutes the simplest automatic pressure regulator. In view of absence

of a servomotor, it can be referred to as a direct action regulator. Adjustment of a reduction gear for the most part, remains constant and is not changed during operation of the engine. Use is also made of adjustable reduction gears, in which a given value of pressure, depending upon external conditions can, before starting, be changed in accordance with technical conditions. If, for adjustment of the engine it is required to change the pressure after the reduction gear in process of operation, it is made with variable adjustment.

Diagrams of reduction valves with constant adjustment are shown in Fig. 15.14. The reduction valve consists of a regulating element — valve 7 and sensing device — diaphragm 4. The amount of valve lift from valve seat determines the area of cross section of the valve, and consequently also its throttling action. Diaphragm 4, together with springs 2 and 8, serves for creation of the force necessary to lift valve 7, with which it is connected by rod 6. The adjusting element of the reduction valve is screw 3, by which it is possible to change the tension of spring 2. The working substance enters the reduction valve via duct 1 with a pressure $p_{вх}$ and, passing the valve, reaches cavity 5, where the prescribed pressure $p_{вых}$ is set. In the reduction valve shown in Fig. 15.14a, high pressure promotes opening of the valve. Such reduction valves are called direct acting; in a reduction valve of reverse action (Fig. 15.14b), high pressure promotes pressing the valve to the valve seat. A bellows or piston can be used as a sensing device instead of a diaphragm.

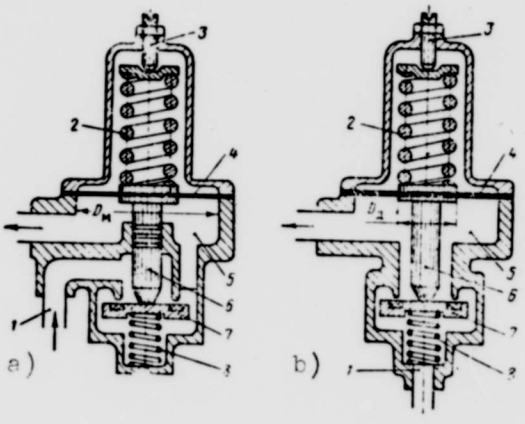

Fig. 15.14. Diagrams of reduction gears: a) direct action; b) reverse action; 1 — inlet channel; 2 — spring; 3 — regulating screw; 4 — diaphragm; 5 — outlet cavity of the reduction gear; 6 — valve rod; 7 — valve; 8 — locking spring.

The operating principle of a reduction valve is reduced to the following. Spring 2 strives to open valve 7. From channel 1 through the valve into cavity 5 the working substance proceeds, but on diaphragm 4 there appears a force striving to close the valve. As a result, equilibrium of forces is established, with which the valve will be lifted a certain height corresponding to a given pressure in cavity 5.

In the fuel supply systems of a liquid propellant rocket engine basically reverse action reduction valves are used. Their advantage over direct action reduction valves lies in the fact that in case of a breakdown of locking spring 8 there is no danger of a sharp increase in outlet pressure from the reduction valve. In a direct action reduction valve for removal of this deficiency in lieu of a locking spring, there is used a method of connecting the valve rigidly with a rod, or placing under the valve a piston on which the gas pressure acts.

Examples of design of reduction valves with sensing devices, carried out in the form of a diaphragm, a bellows and a piston, are shown in Figs. 15.15-15.17.

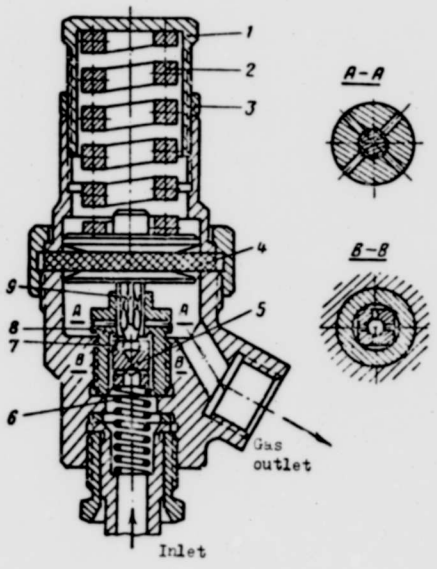

Fig. 15.15. Reverse action reduction valve with membrane: 1 – nut; 2 – spring; 3 – lock nut; 4 – diaphragm; 5 – valve; 6 – locking spring; 7 – lining; 8 – valve seat; 9 – valve rod.

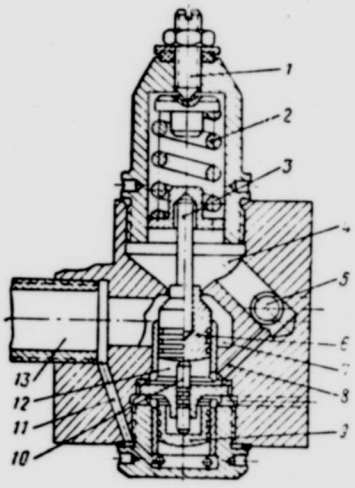

Fig. 15.16. Direct action reduction valve with a piston sensing device: 1 – regulating screw; 2 – spring; 3 – valve rod; 4 – inlet cavity; 5 – inlet duct; 6 – piston-valve; 7 – outlet cavity; 8 – duct; 9 – sensing device piston; 10 – rod; 11 – duct; 12 – unloading cavity: 13 – outlet duct.

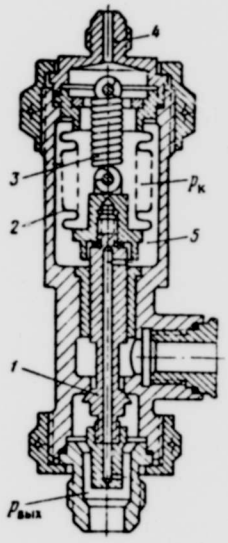

Fig. 15.17. Reduction valve with variable adjustment and bellows sensing device: 1 – valve; 2 – bellows; 3 – spring; 4 – pipe connection for supply of command pressure; 5 – bellow chamber.

The effective area of diaphragm in designs with disks (see Fig. 15.14) equals

$$F_м = a \frac{\pi}{4} D_м^2, \qquad (15.4)$$

where $D_м$ – diameter of diaphragm; ε – correction factor, considering the effect of the disks.

The correction factor a can be calculated by the formula

$$\varepsilon=0{,}33\left[1+\frac{D_д}{D_м}+\left(\frac{D_д}{D_м}\right)^2\right],$$

where $D_д$ – diameter of disk.

The diaphragm sensing device ensures a relatively small shift of the center of the diaphragm, and consequently also the movement of the valve. In those cases when large movement of the valve is required, it is more expedient to use bellows or piston sensing devices.

In calculating the force having an effect on the bellows, the effective area of the bellows can be taken as equal to

$$F_с=\frac{\pi}{4}D_{ср}^2,$$

where $D_{ср}$ – average diameter of bellows corrugations.

A reduction valve with piston sensing device (see Fig. 15.16) – direct action. Gas is supplied to the reduction valve through inlet duct 5 and enters cavity 4, promoting the opening of valve 6. Piston 9 of the sensing device is under the impact of the pressure of exhaust gas supplied by channel 11. Spring 2 of the sensing device is linked with piston 9 by rod 3 and through valve 6 by rod 10. For unloading the valve from forces of gas pressure on inlet there is a device in the form of a piston made as a single unit with valve 6. Under piston-valve 6 via duct 8 gas pressure moves to the inlet in the reduction valve. In view of the greater effective area of the piston-valve on the side of cavity 12 force of pressure of inlet gas will act in the direction of closing the valve, as in a reverse action reduction valve.

Besides the reduction valves with constant adjustment considered above, in control systems use is made of reduction valves with variable adjustment, playing the role of flow-rate regulators. A schematic diagram of such a reduction valve is shown in Fig. 15.18. In it, instead of a spring having constant adjustment, on the side of cavity 6 on membrane acts the force of air pressure acts on the diaphragm. This pressure $p_к$ is called command pressure. With variable command pressure there can be obtained the pressure or expenditure of working substance needed for the engine process on outlet from the reduction valve. The merits of a reduction valve with command pressure are flexibility of control system by outlet pressure and reduction of the residual inequality of adjustment. The engine control system is simplified, since one command pressure reduction valve can control work of several reduction valves regulating the expenditure of components. In the presence of command pressure, additionally for lowering the maximum amount of command gas pressure, in the chamber above the diaphragm there is set a constant adjustment reduction valve spring.

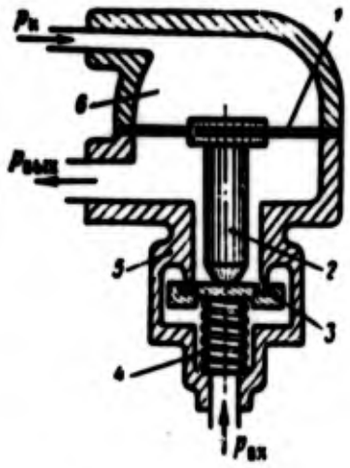

Fig. 15.18. Diagram of a reduction valve with variable adjustment: 1 — diaphragm; 2 — rod; 3 — valve; 4 — locking spring; 5 — valve seat; 6 — reduction valve chamber.

A diagram of a reduction valve with a bellows sensing device and reduction valve spring with supply of command pressure inside bellows is shown in Fig. 15.17. Into the chamber of bellows 5 via a drilling in the rod of valve 1 pressure $p_{вых}$ is fed. Command pressure $p_к$ moves via pipe connection 4. Spring 3 works on extension and fulfills role of a locking spring, ensuring the airtightness of the valve.

The equation of equilibrium of forces having effect on the valve, taking into account unloading it from the action of inlet pressure will be as follows:

$$p_{вых}(F_с+f_{кл})+k_{пр.с}(h+h_0)-p_вF_с=0, \qquad (15.5)$$

where $F_с$ – effective area of bellows; $k_{пр.с}$ – rigidity coefficient of spring together with the the bellows; h_0 – deformation of spring during preliminary compression.

From equation (15.5) we find

$$p_{вых}=p_в\frac{F_с}{F_с+f_{кл}}-k_{пр.с}\frac{h+h_0}{F_с+f_{кл}}. \qquad (15.6)$$

As can be seen from formula (15.6), outlet pressure depends not only on command pressure, but also on the height of valve lift, i.e., on expenditure of component. Thus, this regulator possesses statism, which is increased with growth of the spring force of the spring.

The reduction valve housings are made of aluminum alloys or steel. The diaphragms and bellows are made from materials, used for analogous components in other elements of the fuel supply system. The valves, in the majority of cases, are made of steel, especially, if they do not have special sealing linings and are set on their comical tips in the valve seat. With soft material for the valve, in such cases cold hardening and disturbance of airtightness is possible. The method of calculating the characteristics of reduction valves and recommendations in respect to selection of dimensions of their elements are expounded in detail in [47].

15.6. Fuel Lines. Auxiliary Units of Fuel Supply Systems of Liquid Propellant Rocket Engines

In fuel supply systems of liquid propellant rocket engines flexible and rigid fuel lines are used. Flexible lines are insensitive to misalignments, are vibration proof, and are convenient

to install. However, they are used less frequently than rigid lines made from stainless steel or aluminum alloys, in view of lower cost and light weight of the latter.

Fuel lines must have the smallest possible diameter, especially with high component pressures, which are limited by permissible velocity of the liquid. In fuel lines supplying a fuel component to the pumps, the rate of liquid, to avoid cavitation, should not exceed 5-12 m/s. Feeder fuel lines, if there are no special reasons, are made short and avoid, as far as possible, sharp turns and changes in areas of section. In pressurized fuel lines rates of liquid up to 15-18 m/s are allowed.

Flexible fuel lines are made from rubber. They are also made of plastic reinforced with stainless steel wire or mesh.

To ensure operational reliability of fuel supply systems high requirements are imposed for airtightness and strength of flanged, nipple, and bellows couplings of fuel lines.

Nipple connection with expansion of the lines or soldering of nipple are used in joining fuel lines with diameters up to 25-40 mm. With greater diameters of fuel lines along with nipple connections flanged joints are used (Fig. 15.19a). A flanged joint can, if necessary, include throttle washer or burster disk 1, pressed between the flanges. Sealing with nipple and flanged joints is achieved by installing washers 2 or rings made of soft metals, rubber, or plastic. A bellows coupling (Fig. 15.19b) makes it possible, with high airtightness to easily compensate for inaccuracy in manufacture or installation, and also for temperature deformations of fuel lines and other subassemblies of the propulsion system. A bellows coupling can be made with internal bushing, which significantly decreases pressure loss and the possibility of formation of eddies of the liquid, which is especially impermissible before entrance into the pumps.

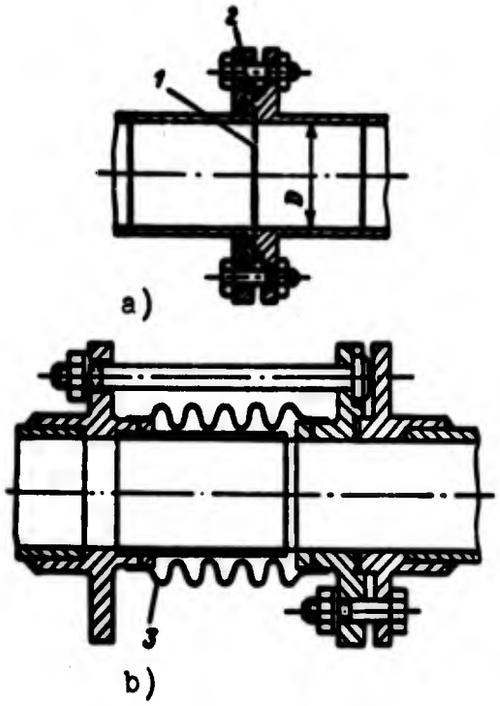

Fig. 15.19. Joints of fuel lines: a) flanged; b) bellows. 1 – burster disk; 2 – sealing; 3 – bellows.

As shut-off attachments in fuel supply systems, besides valves, burster disks can be used, but only in a nonrestartable engine. According to the method of bursting the disk they are subdivided into those bursting directly by pressure of liquid or gas and those bursting by a servomotor. Disks burst by servomotor are used when a strictly fixed instant of burst is required. In construction, shut-off attachments are complicated, and in respect to cost, size and weight are equivalent to valves.

Disks which burst under flow pressure are used chiefly in a pressure feed system. They are usually made of aluminum. In order to facilitate bursting of the disk, in a specified spot on it there is a weakening in the form of annular or cross-shaped incisions (Fig. 15.20). Thickness of a disk is usually selected by experimental means. Without calculating the incision, thickness of the disk $\delta_д$ can be determined preliminarily by the formula

$$\delta_д = k_p \frac{p_p D}{4\tau_д},$$

where D – inside diameter of the disk; p_p – pressure at which disk should burst; τ_s – rupture stress of the cut of the material; k_p – guarantee reserve, selected within limits of 1.1-1.2.

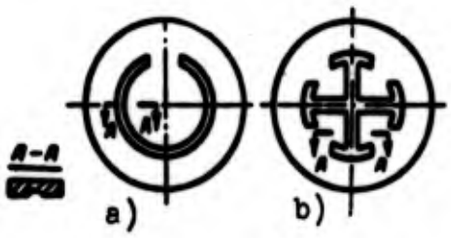

Fig. 15.20. Burster disks:
a) with annular incision;
b) with cross-shaped incision.

For annealed aluminum τ_s = 600 kgf/cm^2, and for cold worked τ_s = 900-950 kgf/cm^2.

CHAPTER XVI

BASIC INFORMATION ON SYSTEMS OF AUTOMATIC CONTROL AND ADJUSTMENT OF LIQUID PROPELLANT ROCKET ENGINES

16.1. Requirements for Automatic Control and Adjustment of Liquid Propellant Rocket Engines

A system of automatic control and adjustment of liquid propellant rocket engines is an element in the general control system of a rocket, from which it obtains controlling signals for the purpose of guaranteeing specified flight conditions of the rocket. Control system by rocket in this work is not examined.

Control of a liquid propellant rocket engine has as a basic purpose, starting the engine, bringing it to assigned conditions, changing the operating conditions, and consequently, thrust in flight and shut-down of the engine. Depending upon the mission of the flight vehicle it either pursues a defined program of change of thrust in time, or control of thrust is carried out from the flight control system of the flight vehicle. The simplest program is maintaining the constancy of any parameter which well characterizes thrust.

In conformity with its mission, a system of automatic control of a liquid propellant rocket engine includes a device for starting and thrust buildup, a device for maintaining operating conditions

of the engine and a device to shut down the engine. Since control of a liquid propellant rocket engine is carried out by means of changing the supply of fuel components to the basic chamber and to the gas generator, then an automatic control and adjustment system of a liquid propellant rocket engine in a constructive respect is closely linked with the fuel supply system.

A schematic diagram of a control and adjustment system, in considerable measure, depends on the diagram and design features of the fuel supply system of the engine and is determined by the type and mission of the flight vehicle.

As the liquid propellant rocket engine develops and the effectiveness of the flight vehicles which are supplied with these engines improve, there takes place a certain complication of the fuel supply systems, the requirements are increased for accuracy in maintaining adjustable values and for stability of engine operation there is an increase in the quantity of adjustable values for the entire propulsion system on the whole, and there is an expanded range of operating conditions of the engine. All these circumstances impose an essential imprint on the structure of the system of automatic adjustment and control and on the construction of elements of these systems. It is possible to formulate only the most general requirements which are characteristic for a majority of systems:

1) the system should ensure, in accordance with the accepted program, control of the engine by maintaining constancy of any parameter which well characterizes thrust with the required degree of accuracy or change of thrust according to a given law;

2) the ratio between consumption of combustible and oxidizer must be kept constant or must be changed according to a specific law;

3) the schematic diagram of the automatic control system and the parameters of the system must ensure stability of system and necessary quality of transition processes;

4) the starting of the engine and control of the engine on pilotless flight vehicles must be fully automated; on piloted vehicles the engine control must be carried out by means of one control lever;

5) on ballistic missiles, the automatic devices for switching on the engine during achievement by rocket of a predetermined speed, must possess high speed of operation and must ensure minimum amount and high stability of "after-effect impulse."

6) the construction of the elements of the automatic control system should guarantee a high degree of reliability; units and subassemblies with relatively low reliability should, as far as possible, be duplicated.

On the automatic control systems of a liquid propellant rocket engine there are imposed very stringent requirements with respect to accuracy.

For surface-to-air guided missiles, maximum permissible errors tentatively compose for thrust not more than ±2%, for mixture ratio in the basic chamber ±2.5-3.0%, in the gas generator ±3.0%, and in tank pressurizing not more than ±3.5-4.0%. For ballistic missiles, these requirements are more rigid. Maximum permissible errors tentatively compose, for thrust ±2%, for mixture ratio in the basic chamber ±1.5%, and in gas generator ±2.0%, and in tank pressurizing ±3.0% [58].

On flight vehicles and accordingly on the fuel supply system and the automatic adjustment of the engine in flight considerable overloads act. Especially great are the overloads for surface-to-air guided missiles, which accomplish maneuvers in the process of approach to the target.

Axial overload of the flight vehicle is the basic external disturbing effect of a liquid propellant rocket engine. On the axial overload depend pressure on inlets to the combustible and oxidizer pumps, and pressure behind the pumps and flow rates of

the components. The automatic control system of the engine during considerable changes of overloading of the flight vehicle should quickly restore the assigned operating conditions of the liquid propellant rocket engine.

As adjustable values for a liquid propellant rocket engine there is taken any parameter well characterizing engine thrust, for example, fuel component ratio for the basic chamber and the fuel component ratio for the gas generator in the case of a bicomponent gas generator.

Action controls are flow rates of the fuel components passing into the basic chamber and the gas generator.

Direct measurement of engine thrust in flight is impossible, therefore the sensing element of the thrust regulator usually carries out measurement of any parameter of conditions which sufficiently well characterize thrust. Such a parameter can be the gas pressure $p_к$ in the basic chamber of the engine.

Sensing elements of ratio controllers of fuel components are flowmeters or levelmeters, measuring actual consumption of components. As values characterizing the flow rates of fuel components, there can also be used the pressures of fuel components before the injectors.

In the simplest liquid propellant rocket engine control systems having one adjustable value, it is usually some parameter which well characterizes engine thrust.

The mixture ratio in the basic chamber renders an effect on the effectiveness of the engine and the flight vehicle. Maximum value of specific impulse corresponds to a defined optimum ratio of components. Adjustment of the mixture ratio is necessary also to ensure uniform output of components from the tanks. A considerable

surplus of a fuel component remaining in one of the tanks toward the end of the flight, as was shown earlier, impairs the effectiveness of the flight vehicle.

In the case of a bicomponent gas generator, it is expedient to regulate the mixture ratio proceeding into the gas generator, so that the temperature of the gas ahead of the turbine is within permissible limits. This circumstance especially must be taken into account for an engines having a comparatively long life.

As was shown above, the structural diagram of the engine and type of flight vehicle for which the engine is intended have considerable effect on the automatic control system of a liquid propellant rocket engine.

In Figs. 1.3-1.7 different schematic diagrams were given for systems of fuel supply and adjustment of liquid propellant rocket engines with pressure feed of fuel components to the basic chamber.

In the diagram in Fig. 1.3, pressure $p_к$ determining the flow rate of components and thrust of the engine, is supplied by means of adjusting regulator 2. Control signal h, passed to the regulator, and the longitudinal overload of flight vehicle n_x determine engine thrust.

Mixture ratio in diagram mentioned is not regulated. For this, a special regulator with regulating element on one of the main lines is necessary, feeding basic chamber with fuel components.

In those constructions where fuel components are displaced from the tank not by compressed gas from containers, but by gas proceeding from the gas generator, the engine thrust depends on burning rate of the charge in the gas generator. In the case of a liquid gas generator, engine thrust depends on quantity and mixture ratio, proceeding into the gas generator.

The schematic diagram of the system of fuel supply and automatic admustment of a liquid propellant rocket engine with a turbopump feed of fuel components and a monocomponent gas generator (see Fig. 1.4) has one variable value – engine thrust. In similar systems hydrogen peroxide is usually used as fuel for the gas generator.

The gas pressure displacing hydrogen peroxide in the gas generator, is designated $p_в$; gas pressure in the gas generator is designated $p_г$. Gas pressure $p_в$ is supplied by adjusting regulator 2. The adjusting signal of the regulator is designated h. On the value of pressure $p_в$ depends the flow rate of hydrogen peroxide $G_{в.п.}$ gas pressure $p_г$, and the number of revolutions of the rotor of the turbopump assembly. Operating conditions of the turbopump assembly determines the flow rates of fuel components into the basic chamber and the thrust of the engine.

Thus the adjustment signal of the regulator h is a controlling signal for engine thrust. External disturbance for thrust is longitudinal overload n_x.

The mixture ratio in this diagram is not regulated, and is set for normal rating by selection of flow frictions of the main lines.

A schematic diagram of an automatic control system of a liquid propellant rocket engine with turbopump feeding of fuel components and a bicomponent gas generator (see Fig. 1.5) includes one engine thrust regulator.

Flow rates of combustible and oxidizer to the gas generator are designated $G_{г.г}$ and $G_{о.г}$ respectively.

Control of engine thrust is effected by means of shift regulating element 2, apportioning the admission of combustible to the gas generator. With a change in the position of the control element gas pressure in the gas generator changes, and also the number of revolutions of the rotor of the turbopump assembly and

the flow rates of fuel components into the basic chamber and the thrust of the engine. Regulating element 2 is brought into action from the thrust regulator. Sensing device of the thrust regulator measures gas pressure in the basic chamber $p_к$. With deviation of pressure $p_к$ from rated value, the regulating element receives a shift, directed towards removal of the pressure deviation being caused in the system. Value of pressure $p_к$, and accordingly, engine thrust under defined conditions is supplied by means of adjusting the thrust regulator. Thrust developed by the engine depends on the controlling adjustment signal h and external disturbance $n_в$.

Analogously to diagrams given earlier, the mixture ratio in this system is not regulated.

It is possible to regulate the mixture ratio entering the basic chamber by means of a component ratio regulator set in one of the main lines feeding the chamber.

A schematic diagram of an automatic control system of fuel supply, thrust, and mixture ratio for the basic chamber is shown in Fig. 1.6.

The signal for adjusting the thrust regulator is designated $h_р$, the signal for adjusting the mixture ratio regulator – $h_м$.

Engine thrust adjustment and control of thrust are carried out in the examined system just as in the preceding system (see Fig. 1.5).

The mixture ratio regulator compares their actual ratio with rated value. With deviation the regulator restores the assigned ratio of components by shifting regulating element 7 (see Fig. 1.6) located on the fuel supply line of the chamber of the engine.

The adjustment signal of the mixture ratio regulator $h_м$ makes it possible to change as necessary the ratio of components. In case of constant mixture ratio assigned for all conditions there will not be a change of adjustment signal $h_м$.

The engine being considered has two controlling actions: shift of thrust regulating controls 2 and mixture ratio control 7. The mixture ratio entering into a bicomponent gas generator in this system is not regulated.

In Fig. 1.7 there is a simplified schematic diagram of system of fuel supply and automatic control of a liquid propellant rocket engine with a bicomponent gas generator for a case of three adjustable values: engine thrust, mixture ratio for the basic chamber, and mixture ratio for the gas generator.

Thrust control of the engine and control of the mixture ratio entering the basic chamber are carried out just as in the system, the diagram of which is in Fig. 1.6.

The regulator of the mixture ratio for the gas generator compares the actual ratio of components with rated value and with the appearance of deviation restores the ratio of components by shifting control element 7.

The engine, as the object of control, has three controlling actions – shift of thrust regulating controls 2, the control of ratio of fuel components for the basic chamber 11 and control of the mixture ratio for the gas generator 7.

Likewise there can be constructed a schematic diagram of automatic control for engines with generator gas afterburning.

16.2. A Liquid Propellant Rocket Engine as an Object of Automatic Control

Formulation of the Problem

A study of the static and dynamic properties of a liquid propellant rocket engine as an object of automatic adjustment and control is a necessary prerequisite to the creation of automatic control systems.

First of all, it is necessary to establish, how the variable values determining the operating conditions of the engine will be changed, with change of controlling actions and external disturbances applied to the engine. Static properties of the object of control are reflected by dependence of values characterizing the smooth performance of the engine on control actions on those established conditions. Dynamic properties of the engine are sufficiently well described by transfer functions and frequency-response curve of the object.

For a liquid propellant rocket engine a great number of dynamic sections connected to each other by numerous cross connections is a characteristic. These include the chamber of the engine, the liquid gas generator, the turbopump assembly, fuel manifolds, regulating elements, and others. The number of these sections and their interconnection are determined by the schematic diagram of the engine.

One of the first problems in the investigation of an object of control is a rational separation of it into dynamic sections and discovery of the connection between them.

Each section of the object is described according to its differential or algebraic equation connecting outlet and inlet coordinates of the link and reflecting the basic features of the physical processes occurring in the section. Outlet and inlet coordinates of a section are values characterizing processes in the engine.

In the composition of equations of sections of a liquid propellant rocket engine an assumption is made on smallness of deviations of coordinates from their absolute values. This assumption enables linearization of equations of the sections. After composing such a system of equations it is necessary to compose the transfer functions and to calculate the frequency-response curves of the object of control.

In view of the large number of sections and multiplicity of connections between them, to record the transfer functions of object of control in visual form is very difficult, tedious and inexpedient.

For appraisal of dynamic properties of a complex object of control, the best of all is to use frequency responses, which without special difficulties can be calculated with help of electronic digital or analog computers, and then estimated from the point of view of requirements imposed on the automatic control systems of a liquid propellant rocket engine.

It is necessary to estimate also the influence of separate sections and characteristic dynamic parameters on the frequency-response curves of the object of control as a whole. For appraisal of the dynamic properties of the control system at lowered conditions it is desirable to show the effect of throttling the engine on its dynamic properties.

Controllers of thrust and mixture ratios are connected to each other through the object of control. It is necessary to investigate the mutual influence of the control channels. The connection between them is estimated with help of frequency-response curves of the object for pressure in the basic chamber according to shift of the control elements and for ratio of components – according to shift of the thrust control element.

It is very important to compare the dynamic properties of engines of different thrust, but close in their diagram and structural fulfillment to the one being investigated, which can make it possible to essentially reduce the work on investigation of the object of control.

For appraisal of accuracy of automatic control systems it is desirable to reveal the scattering of static and frequency-response curves of engines for different specimens of the same model.

Block Diagrams of Liquid Propellant Rocket Engines

On schematic diagrams of engines (see Figs. 1.3-1.9) there are shown the structural elements in which there take place defined physical processes, and the communication of liquids and gases.

The block diagram of an engine is determined by the schematic diagram and reflects the connection between its elementary dynamic units, the number of which, however, is equal to the number of elements of the schematic diagram.

The basic chamber of the engine is a structural element and constitutes one link in the block diagram of the object of control. The outlet coordinate of the basic chamber – gas pressure in the chamber $p_к$; two inlet coordinates are flow rate of the combustible $G_{г.к}$ reaching the chamber through the injectors, and flow rate of the oxidizer $G_{о.к}$.

In this way in a block diagram a bicomponent liquid gas generator is represented.

The turbopump assembly, consisting of a turbine and two pumps, can be expediently represented on a block diagram of the object of control in the form of a totality of three sections: the turbine rotor, combustible pump, and oxidizer pump. For the

rotor the outlet coordinate is the number of revolutions per minute n, the inlet coordinates – total consumption of combustible $G_{т.}$, total expenditure of oxidizer $G_{о.}$, and the gas pressure before the nozzle box of the turbine $p_{тг}$. Each of the pumps has as outlet coordinate the pressure of the fuel component after the pump. Inlet coordinates of the pump are the pressure of the fuel component on inlet to the pump, the number of revolutions of the impeller and the flow rate of the component through the pump.

The block diagram of the control system of the engine, the schematic diagram of which is given in Fig. 1.3, is shown in Fig. 16.1.

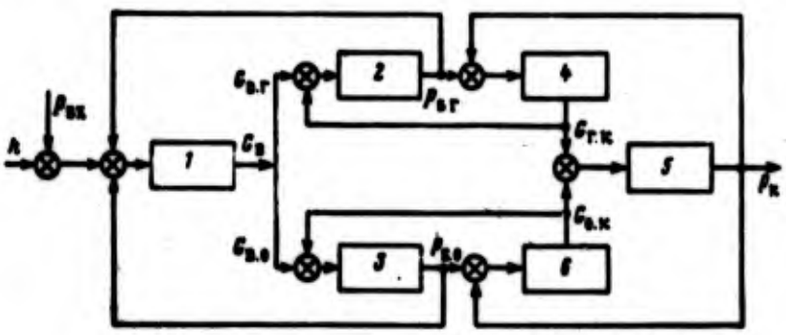

Fig. 16.1. Block diagram of the automatic control system of a liquid propellant rocket engine with pressure feed of fuel components: 1 – gas pressure regulator; 2, 3 – fuel and oxidizer tanks; 4, 6 – main lines for supply of combustible and oxidizer to the engine chamber; 5 – engine chamber.

The flow rate of the combustible $G_{г.к}$ depends on inlet coordinates of main combustible line: pressure in the combustible tank $p_{б.г}$ and pressure in the basic chamber $p_к$. Analogously, flow rate of oxidizer depends on the pressure in the oxidizer tank $p_{б.о}$ and pressure $p_к$. Pressure in each of the tanks is determined by pressure of pressurized gas $p_г$ and flow rate of the respective fuel component from the tank.

The basic chamber of the engine, the main lines and the tanks compose, in this case, the object of control. The system of

automatic control consists of the object of control and the pressure regulator of the pressurized gas. For the object of control the inlet coordinate is the pressure of pressurized gas $p_в$, and the outlet coordinate – pressure in the basic chamber of engine $p_к$.

In accordance with the block diagram a system of differential equations is composed, describing the dynamics of the object of automatic control.

A block diagram of a control system of a liquid propellant rocket engine with monocomponent gas generator, working on hydrogen peroxide, and turbopump feeding of hydrogen peroxide to the gas generator reactor (see Fig. 1.4) is shown in Fig. 16.2.

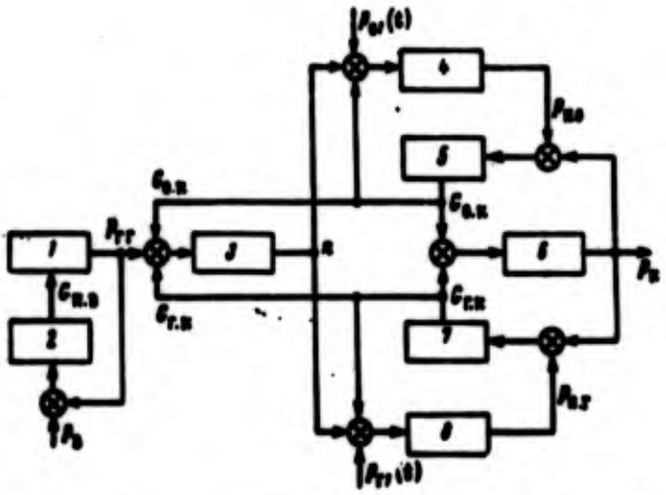

Fig. 16.2. Block diagram of a liquid propellant rocket engine with turbopump assembly and monocomponent gas generator: 1 – reactor of the gas generator; 2 – main line and injector for supply of hydrogen peroxide to the reactor; 3 – turbopump assembly; 4, 8 – pumps of oxidizer and combustible; 5, 7 – main line for supply of of oxidizer and combustible to the engine chamber; 6 – engine chamber.

The basic values characterizing the performance of an engine and representing inlet and outlet coordinates of sections are designated just as in Fig. 1.4 and in addition there is taken: inlet pressure to the combustible pump – $p_{н1}$; inlet pressure

to the oxidizer pump – p_{o1}; the number of revolutions of the rotor of the turbopump assembly – n, pressure after the combustible pump $p_{n.r}$, pressure after the oxidizer pump – $p_{n.o}$. For the object of control as a whole, the inlet controlling action is gas pressure p_b, displacing hydrogen peroxide from the tank.

Transfer functions of the object of control are composed for different values characterizing the operating conditions of the engine. Of greatest interest is the transfer function for variable value – for the gas pressure in the chamber of the engine.

Consideration of the block diagram shows that along with the direct connections between elementary sections in system there are a number of internal feedbacks. Between each main line and corresponding pump there is feedback from expenditure of fuel component. If the characteristics of the pump expressing dependence of pressure on flow rate with a constant number of revolutions has a maximum, then during operation on the left branch, the characteristic feedback will be positive, and during operation on the right branch – negative.

The chain of sections, consisting of the turbopump assembly rotor, the combustible pump and main combustible line is enveloped by negative feedback from the expended fuel. The idea of feedback consists in the fact that with a constant pressure of gas in the reactor of the gas generator, an increase in combustible flow rate leads to growth of torque of the pump and reduction in the number of revolutions of the turbine rotor. The oxidizer flow rate is analagous.

Internal negative feedbacks play a stabilizing role. They increase the stability of the object of control.

A block diagram of the control system of a liquid propellant rocket engine with bicomponent gas generator working on basic fuel components (see Fig. 1.6), in the presence of two controlling actions for the engine is shown in Fig. 16.3.

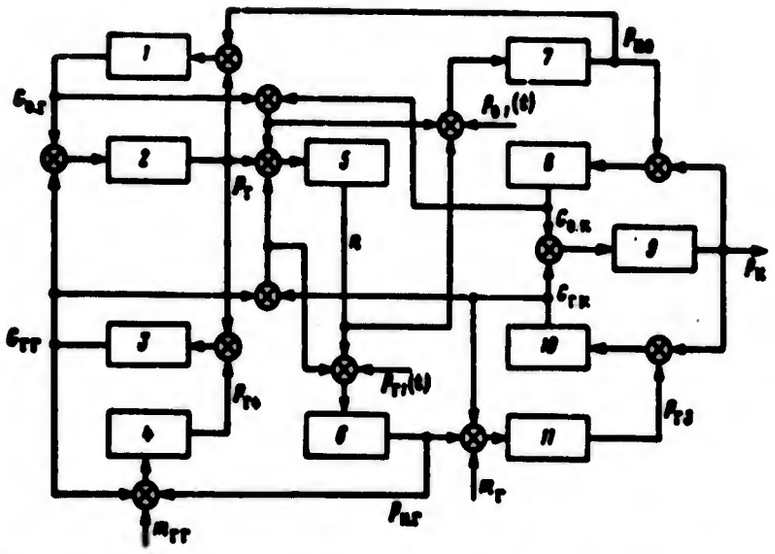

Fig. 16.3. Block diagram of a liquid propellant rocket engine with bicomponent gas generator and two controlling actions: 1, 3 – main line and injector for supply of oxidizer and combustible to the gas generator; 2 – gas generator reactor; 4 – regulating element on main line 3; 5 – turbopump assembly; 6, 7 – combustible and oxidizer pumps; 8, 10 – main lines for supply of oxidizer and combustible to the engine chamber; 9 – engine chamber; 11 – regulating element on main line 10.

For additional coordinates as compared to Fig. 16.2 there are taken the following designations: p_{m6} – pressure after the regulating element on line for supply of fuel to the basic chamber; p_{m4} – pressure after the regulating element on the gas generator fuel feed line; $G_{г.г}$ – combustible flow rate through the gas generator injectors; $G_{о.г}$ – oxidizer flow rate through the injector of the gas generator; $m_т$ – shift of regulating element 11, $m_{г.г}$ – shift of control element 4.

In the system there exist internal negative feedbacks between sections, analogous to the connections noted on the diagram in Fig. 16.2. Besides them, the object includes two internal positive feedbacks: one involves combustible pump 6, the fuel supply line of gas generator 3, gas generator chamber 2 and the rotor of the

turbopump assembly; the second – oxidizer pump 7, oxidizer feed line of gas generator 1, gas generator chamber 2 and the rotor of the turbopump assembly. These positive feedbacks are destabilizing, since they impair the stability of the object of control.

A block diagram of the control system of a liquid propellant rocket engine with a bicomponent gas generator (Fig. 1.7) in the presence of three controlling actions for the engine is shown in Fig. 16.4.

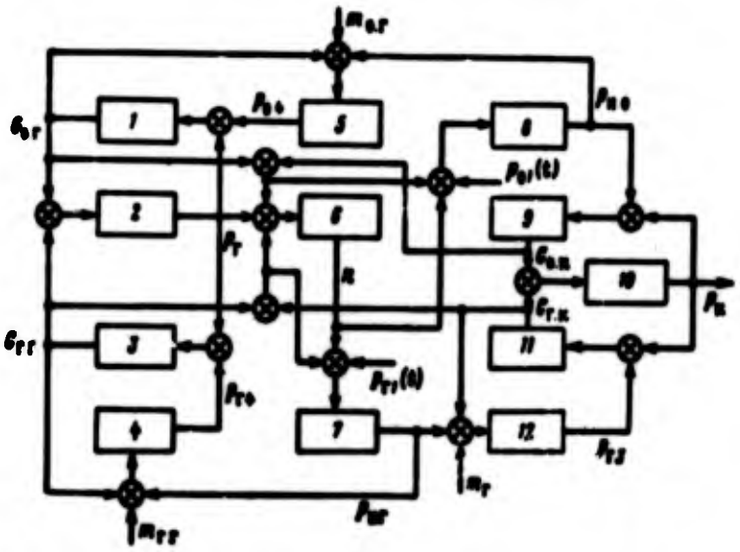

Fig. 16.4. Block diagram of a liquid propellant rocket engine with bicomponent gas generator and three controlling actions: 1, 3 – main line and injectors for supply of oxidizer and combustible to the gas generator; 2 – reactor of the gas generator; 4, 5 – regulating elements on main lines 3 and 1; 6 – turbopump assembly; 7, 8 – combustible and oxidizer pumps; 9, 11 – main lines for supply of oxidizer and combustible to the engine chamber; 10 – engine chamber; 12 – regulating element on main line 11.

To the block diagram of Fig. 16.4 as compared to the diagram of Fig. 16.3 there is added one section – regulating element 5 for feeding oxidizer to the gas generator. The shift of this regulating element is designated – $m_{o.r}$. Accordingly, on the diagram there is shown one additional coordinate – pressure of the oxidizer after regulating element p_{o4}.

Internal positive and negative feedback for the object represented in the diagram of Fig. 16.4 are the same as for the object of control according to the diagram in Fig. 16.3.

Dynamic Properties of the Basic Chamber of the Engine and Gas Generator

Dynamic properties of the chamber, in considerable measure, are determined by two capacities — working substance and thermal. To the variable operating conditions of an engine in the chamber there can be added working substance and heat. On the dynamics of the chamber, furthermore, an essential effect is rendered by the character of the conversion process the liquid fuel components into gaseous products of combustion entering the chamber.

In general, during deviation from steady state there can be changed both the quantity of entering fuel components, and also the pressure and temperature in the chamber. Examining the dynamics in this case, it is necessary to take into account both capacities of the chamber. If however, only the quantity of fuel admitted to the chamber is changed and the ratio of components remains constant, then for small deviations, the temperature in the chamber can be considered as constant; only the pressure in the chamber is changed. In so doing it is possible not to take into account the thermal capacity of the chamber, and to consider the chamber as a single capacity link.

At present in solution of the many problems of the dynamics of liquid propellant rocket engines the process of conversion of liquid fuel components into gaseous products of combustion are treated as instantly taking place with a certain constant time of delay with respect to the moment of introduction of the fuel components into the chamber [27], [58]. In examining the processes taking place in an automatic control and adjustment system of an engine, such an assumption appears to be fully founded, since time constants of many sections of the system exceed by tens of times the time of conversion of liquid components to gaseous products of combustion.

Everything that has been said about the basic chamber of the engine equally applies to the bicomponent liquid gas generator.

Let us consider the dynamics of an engine chamber with a constant mixture ratio.

The equation for the flow rate of gas from the chamber was written in form of (2.48).

During deviation from steady state the stabilized balance of working substance in the chamber is disturbed. The process of accumulation of gaseous products in the chamber can be described by a differential equation

$$V_к \frac{d\gamma_к}{dt} = \Delta G_{т(t-\tau_1)} - \Delta G, \tag{16.1}$$

where $V_к$ – volume of the chamber; $\gamma_к$ – average weight density of gaseous products in the chamber; $\Delta G_т$ – deviation of total flow rate per second of fuel components; ΔG – deviation of flow rate per second of gas from the chamber; τ_1 – time of conversion of liquid fuel components into gaseous products of combustion.

Index $(t-\tau_1)$ characterizes the circumstance where the liquid components are turned into gaseous products of combustion after time τ_1 after entering the chamber.

From equation (2.48) it follows that with constant fuel mixture ratio, deviation of the gas flow rate depends only on deviation of pressure in the chamber:

$$\Delta G = \left(\frac{\partial G}{\partial p_к}\right)_0 \Delta p_к = \left(\frac{G_т}{p_к}\right)_0 \Delta p_к. \tag{16.2}$$

The sign of deceleration « * » with pressure and temperature we will subsequently omit in order to reduce the recording.

Value of partial derivative in formula (16.2) is taken with pressure and flow rate of a steady state, which is noted by the index "0".

From the equation of state, the derivative of weight density of products of combustion according to time with constant fuel mixture ratio is equal to

$$\frac{d\gamma_{\text{п}}}{dt}=\frac{1}{RT_{\text{г}}}\frac{dp_{\text{г}}}{dt}. \tag{16.3}$$

Let us substitute expressions (16.3) and (16.2) in the fundamental equation (16.1); after conversion and transition to dimensionless relative deviations we will obtain an equation of the dynamics of the basic chamber of the engine:

$$T_1\frac{d\bar{p}_{\text{г}}}{dt}+\bar{p}_{\text{г}}=K_1\bar{G}_{2(t-\tau_1)}, \tag{16.4}$$

where

$$T_1=\frac{V_{\text{г}}p_{\text{г}}}{RT_{\text{г}}G_{\text{г}}} \tag{16.5}$$

– time constant of the basic chamber;

$$K_1=\frac{G_{\text{г0}}}{p_{\text{г0}}}\frac{p_{\text{г}}}{G_{\text{г}}} \tag{16.6}$$

– amplification factor of the chamber according to total expenditure of fuel components;

$$\bar{p}_{\text{г}}=\frac{\Delta p_{\text{г}}}{p_{\text{г0}}},\quad \bar{G}_{\text{г}}=\frac{\Delta G_{\text{г}}}{G_{\text{г0}}}$$

– relative deviations of pressure and flow rate; $p_{\text{г0}}$ and $G_{\text{г0}}$ – base values of pressure and flow rate in steady state.

Deviation of total consumption of fuel components is composed of deviations of consumption of oxidizer and combustible

$$\Delta G_{\text{г}}=\Delta G_{\text{о.г}}+\Delta G_{\text{г.г}}. \tag{16.7}$$

Taking into account two inlet effects (16.7), the equation of dynamics of the chamber takes the following form:

$$T_1\frac{d\bar{p}_к}{dt}+\bar{p}_к=K_{1г}\bar{G}_{г.вх(t-\tau_1)}+K_{1т}\bar{G}_{т.вх(t-\tau_1)}, \qquad (16.8)$$

where $K_{1г}$ – amplification factor of the chamber according to expenditure of oxidizer; $K_{1т}$ – amplification factor of chamber according to expenditure of combustible.

With identical base values of flow rates of combustible and oxidizer

$$K_{1г}=K_{1т}=\frac{G_{вх0}}{p_{к0}}\frac{p_к}{G_в}=K_в. \qquad (16.9)$$

The value of pressure, flow rate of components and temperature in formulas (16.5), (16.6), and (16.9) are taken for an initial steady state.

Time constant of the chamber T_1 coincides with parameter $\tau_к$, called the average time of stay of gas in the chamber (see formula 4.10).

Since

$$\frac{p_к F_{кр}}{G_в}=\beta,$$

where β – pressure pulse in the chamber, and the ratio

$$\frac{V_к}{F_{кр}}=L^*,$$

that time constant (16.5) is expressed through pressure pulse in the chamber and characteristic length:

$$T_1=\frac{\beta}{RT_к}L_*. \qquad (16.10)$$

For engines with identical fuel components and identical pressures in the chamber the complex of parameters

$$\frac{\beta}{RT_к} = \text{const.}$$

The time constant of the chamber (16.10) in this case is proportional to the characteristic length of the chamber.

An increase in pressure in the chamber with those same fuel components is accompanied by a rise in temperature of the gas in the chamber and, consequently, leads to certain lowering of the time constant.

The effect of the mixture ratio on the time constant of the chamber for a fuel consisting of kerosene and nitric acid is shown in Fig. 16.5. The complex of parameters $\beta/RT_к$ and consequently also the time constant (where $L_к$ = const) have a minimum with an excess oxidant ratio $\alpha \approx 0.7$-0.8. With deviation from the mentioned ratio the time constant of the chamber increases. A more intensive growth of the time constant of the chamber takes place with enrichment of mixture with the combustible.

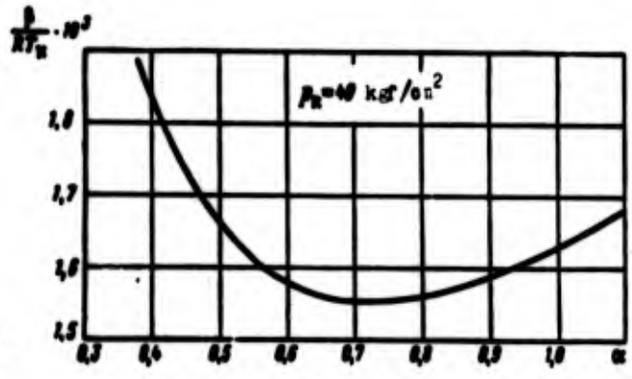

Fig. 16.5. Dependence of complex of parameters $\beta/RT_к$ on excess oxidant ratio.

A change of mixture ratio during the transition process leads to a change in temperature of the gas in the chamber, which, in turn, affects the value of pressure in the chamber and the flow rate per second of gas from the chamber.

The process of accumulation of gas in the chamber with deviation from steady state in case of a variable mixture ratio is described by the same differential equation (16.1), however in the equation for flow rate per second of gas as variables it is necessary to examine not only pressure $p_к$, but also temperature $T_к$, gas constant R and value of χ.

Gas constant R and value of χ depend on the mixture ratio.

Deviation of flow rate per second of the gas with variables $p_к$ and $T_к$ in the chamber will be obtained from the equation

$$\Delta G=\left(\frac{\partial G}{\partial p_к}\right)_0\Delta p_к+\left(\frac{\partial G}{\partial R}\right)_0\Delta R+\left(\frac{\partial G}{\partial T_к}\right)_0\Delta T_к+\left(\frac{\partial G}{\partial \chi}\right)_0\Delta\chi. \qquad (16.11)$$

Mixture ratio is characterized by the coefficient

$$x=\frac{G_{о.к}}{G_{г.к}},$$

the deviation of which is equal to

$$\Delta x=\frac{1}{G_{г.к}}\Delta G_{о.к}-\frac{G_{о.к}}{G^2_{г.к}}\Delta G_{г.к}. \qquad (16.12)$$

Deviation of the gas constant and value of χ depend on deviation x:

$$\Delta R=\left(\frac{\partial R}{\partial x}\right)_0\Delta x; \qquad (16.13)$$

$$\Delta\chi=\left(\frac{\partial\chi}{\partial x}\right)_0\Delta x. \qquad (16.14)$$

With differentiation of the equation of state it is necessary to take into account change of gas constant and temperature of products of combustion

$$\frac{d\gamma_к}{dt}=\frac{1}{RT_к}\frac{dp_к}{dt}-\frac{p_к}{R^2T_к}\frac{dR}{dt}-\frac{p_к}{RT^2_к}\frac{dT_к}{dt}. \qquad (16.15)$$

In equation (16.1), the increase of flow rate of gas and derivative of weight density are substituted according to expressions (16.11) and (16.15) taking into account relationships (16.12-16.14).

After transition to dimensionless values, the equation of the dynamics of the basic chamber in respect to pressure for a case of variable mixture ratio will be obtained in the following form:

$$T_1\frac{d\bar{p}_к}{dt}+\bar{p}_к=K_{12}\bar{G}_{0.к(t-\tau_1)}+K_{13}\bar{G}_{г.к(t-\tau_1)}+$$

$$+K'_{12}\frac{d\bar{G}_{0.к(t-\tau_1)}}{dt}+K'_{13}\frac{d\bar{G}_{г.к(t-\tau_1)}}{dt}+K_{11}\bar{T}_к+K'_{11}\frac{d\bar{T}_к}{dt}. \qquad (16.16)$$

In equation (16.16), the time constant of the chamber T_1 has the same value as for a case of constant mixture ratio (16.5); amplification factors respectively are equal to

$$K_{12}=\frac{G_{0к3}}{p_{0к3}}\left[\frac{p_к}{G_3}+p_к\left(\frac{1}{2R}\frac{\partial R}{\partial к}-\frac{1}{\chi}\frac{\partial\chi}{\partial к}\right)_0\frac{1}{G_{г.к}}\right]; \qquad (16.17)$$

$$K_{13}=\frac{G_{0к0}}{p_{0к3}}\left[\frac{p_к}{G_3}-p_к\left(\frac{1}{2R}\frac{\partial R}{\partial к}-\frac{1}{\chi}\frac{\partial\chi}{\partial к}\right)_0\frac{G_{0.к}}{G^2_{г.к}}\right]; \qquad (16.18)$$

$$K'_{12}=\frac{G_{0к3}}{p_{0к3}}\frac{V_к p^2_к}{G_3R^2T_к}\left(\frac{\partial R}{\partial к}\right)_0\frac{1}{G_{г.к}}; \qquad (16.19)$$

$$K'_{13}=-\frac{G_{0к3}}{p_{0к3}}\frac{V_к p^2_к}{G_3R^2T_к}\left(\frac{\partial R}{\partial к}\right)_0\frac{G_{0.к}}{G^2_{г.к}}, \qquad (16.20)$$

$$K_{11}=\frac{T_{0к3}}{p_{0к3}}\frac{p_к}{2T_к}, \qquad (16.21)$$

$$K'_{11}=\frac{T_{0к3}}{p_{0к3}}\frac{V_к p^2_к}{G_3RT^2_к}. \qquad (16.22)$$

The process of accumulation of energy in the chamber of a liquid propellent rocket engine during small deviations from steady state is described by a linear differential equation

$$V_к\frac{d}{dt}(\gamma_к c_p T_к)=G_3\Delta Q_1+Q_1\Delta G_{3(t-\tau_1)}-$$

$$-c_p T_к\Delta G-c_p G\Delta T_к-GT_к\Delta c_p, \qquad (16.23)$$

where $c_к$ and c_p – head capacity of products of combustion in the chamber; Q_1 – quantity of heat, given off during combustion of 1 kg of fuel:

$$Q_2 = c_p T_к G \qquad (16.24)$$

– enthalpy of products of combustion coming out of the chamber through the nozzle in a unit of time.

The quantity of heat given off during combustion 1 kg of fuel equal to working calorific value h_u with a given $\varkappa$:

$$Q_1 = h_u.$$

At steady states

$$Q_1 = h_u \approx c_p T_к.$$

Deviation of the evolved heat depends on change of fuel mixture ratio

$$\Delta Q_1 = \Delta h_u = \left(\frac{\partial h_u}{\partial \varkappa}\right)_0 \Delta \varkappa. \qquad (16.25)$$

We will substitute in equation (16.23) the deviation of flow rate of gas (16.11) and deviation of evolved heat (16.25); after conversion and transition to dimensionless values we will obtain an equation of dynamics of the chamber according to temperature of products of combustion for a case of variable mixture ratio:

$$\bar{T}_к = K_{f1}\bar{p}_к + K'_{f1}\frac{d\bar{p}_к}{dt} + K_{f2}\bar{G}_{в.к(t-\tau_1)} + K_{f3}\bar{G}_{г.к(t-\tau_1)} +$$
$$+ K'_{f2}\frac{d\bar{G}_{в.к(t-\tau_1)}}{dt} + K'_{f3}\frac{d\bar{G}_{г.к(t-\tau_1)}}{dt}. \qquad (16.26)$$

In deriving equation (16.26) we use the substitution

$$\gamma_к c_p T_к = \frac{c_p p_к}{R}.$$

Amplification factors in equation (16.26) are determined according to the following calculation formulas:

$$K_{11} = -\frac{p_{ga2}}{T_{ga2}} \frac{2T_x}{p_x}; \qquad (16.27)$$

$$K'_{11} = -\frac{p_{ga2}}{T_{ga2}} \frac{2V_x}{kRG_x}. \qquad (16.28)$$

where $k = c_p/c_v$:

$$K_{12} = \frac{G_{ga2}}{T_{ga2}} 2\left[\frac{T_x}{G_x} + \left(\frac{1}{c_p}\frac{\partial h_x}{\partial x} + \frac{T_x}{2R}\frac{\partial R}{\partial x} - \frac{T_x}{k}\frac{\partial k}{\partial x} - \frac{T_x}{c_p}\frac{\partial c_p}{\partial x}\right)_0 \frac{1}{G_r}\right]; \qquad (16.29)$$

$$K_{13} = \frac{G_{ga2}}{T_{ga2}} 2\left[\frac{T_x}{G_x} - \left(\frac{1}{c_p}\frac{\partial h_x}{\partial x} + \frac{T_x}{2R}\frac{\partial R}{\partial x} - \frac{T_x}{k}\frac{\partial k}{\partial x} - \frac{T_x}{c_p}\frac{\partial c_p}{\partial x}\right)_0 \frac{G_{0.x}}{G^2_{r.x}}\right]; \qquad (16.30)$$

$$K'_{12} = \frac{G_{ga2}}{T_{ga2}} \frac{2V_x p_x}{RG_x}\left(\frac{1}{kR}\frac{\partial R}{\partial x} - \frac{1}{c_p}\frac{\partial c_p}{\partial x}\right)_0 \frac{1}{G_{r.x}}; \qquad (16.31)$$

$$K'_{13} = -\frac{G_{ga2}}{T_{ga2}} \frac{2V_x p_x}{RG_x}\left(\frac{1}{kR}\frac{\partial R}{\partial x} - \frac{1}{c_p}\frac{\partial c_p}{\partial x}\right)_0 \frac{G_{0.x}}{G^2_{r.x}}. \qquad (16.32')$$

Dynamic properties of the basic chamber in case of a variable mixture ratio are described by a system consisting of two equations (16.16) and (16.26).

The equation of dynamics of the chamber according to pressure can be obtained, excluding deviation of temperature from these equations, and the equation of dynamics according to temperature – by excluding deviation of pressure.

Calculations show that for a liquid propellant rocket engine of open diagram without afterburning of gas after the turbine, the effect of variable mixture ratio on the dynamics of the basic chamber and gas generator is comparatively slight.

Dynamic Properties of a Turbopump Assembly

As was shown above, in considering the dynamics of a liquid rocket engine, it is expedient to separate the turbopump assembly into three dynamic sections, which are the pumps and the rotor of the turbopump assembly.

The characteristic curve of a centrifugal pump shows the dependence of head, or pressure after the pump, on the number of revolutions of the impeller and flow rate of liquid through the

pump with a specific suction pressure. That is:

$$p_н = p_н(p_1, G_н, n),$$

where $p_н$ – pressure after the pump; p_1 – suction pressure; $G_н$ – flow rate of fuel component through the pump; n – number of revolutions of the impeller.

In Fig. 16.6 the pressure characteristics of centrifugal pump is shown schematically. On characteristic curve there are frequently plotted lines of constant value of efficiency.

The mass of liquid, found inside the pump is small compared to the mass of liquid inside the lines. Calculation of the inertness of the column of liquid inside the pump shows that the time constant of the pump is 2-3 orders lower than the time constants of the lines and the basic chamber of the engine. This makes it possible to consider the centrifugal pump as an inertialess link.

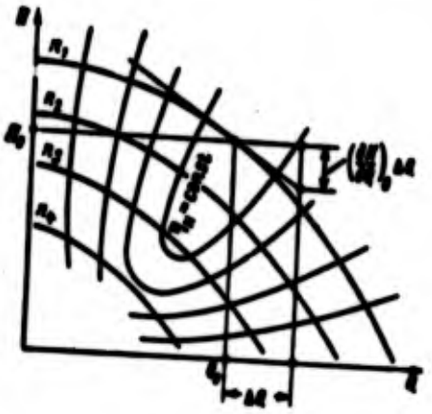

Fig. 16.6. Characteristic curve of a centrifugal fuel pump.

For small deviations from steady state in linear approximation we will obtain an increase of pressure after pump

$$\Delta p_н = \Delta p_1 + \left(\frac{\partial p_н}{\partial n}\right)_0 \Delta n + \left(\frac{\partial p_н}{\partial G_н}\right)_0 \Delta G_н.$$

The values of partial derivatives, entering as coefficients into this equation, can be obtained by graphic means according to the characteristics of the pump (see Fig. 16.6) or by differentiation of analytic dependences, if any.

After conversion to relative dimensionless deviations we will obtain an equation of the pump in the following form:

$$\bar{p}_н = \bar{p}_1 + K_{нn}\bar{n} + K_{нG}\bar{G}_н. \qquad (16.32)$$

where $K_{нn}$ – amplification factor of the pump according to number of revolutions of the rotor; $K_{нG}$ – amplification factor of the pump according to expenditure of fuel component;

$$\bar{p}_н = \frac{\Delta p_н}{p_{нк}}; \quad \bar{p}_1 = \frac{\Delta p_1}{p_{нк}}; \quad \bar{n} = \frac{\Delta n}{n_{нк}}; \quad \bar{G}_н = \frac{\Delta G_н}{G_{нк}}.$$

Amplification factors of pump equal

$$K_{нn} = \frac{n_{нк}}{p_{нк}}\left(\frac{\partial p_н}{\partial n}\right)_0;$$
$$K_{нG} = \frac{G_{нк}}{p_{нк}}\left(\frac{\partial p_н}{\partial G_н}\right)_0.$$

In the case when the characteristic curve of the pump is unknown beforehand, it is possible to construct a section of characteristic curve in proximity to the operating point by following one of the theoretical methods expounded in handbooks on centrifugal pumps [28], [37], and further to determine the values of partial derivatives of pressure according to the number of revolutions and expenditure.

The rotor of the turbopump assembly consists of a capacity of kinetic energy, the accumulation or expenditure of which takes place under unsteady operating conditions.

On steady state, torque $M_т$ developed by the turbine, is equal to the sum of the moments of the oxidizer pump $M_{н.о}$ and combustible pump $M_{н.г}$:

$$M_т = M_{н.о} + M_{н.г}.$$

On unsteady conditions, the dynamics of the rotor of the turbopump assembly is described by the following differential equation:

$$\frac{\pi}{30} J \frac{dn}{dt} = \Delta M_т - \Delta M_{н.о} - \Delta M_{н.р}, \tag{16.33}$$

where J – mass moment of inertia of the rotor with respect to the axis of rotation.

For an engine with supercritical pressure drop on turbine and with constant mixture ratio in the gas generator, the torque developed by the turbine depends only on the pressure of gas before the nozzle box and on the number of revolutions of the rotor:

$$M_т = M_т(n, p_т).$$

Torque on the pump shaft depends on the number of revolutions of the impeller, the flow rate of component through the pump, and pressure after the pump. Pressure after pump, in turn, depends on flow rate and number of revolutions. Thus takes place the dependence

$$M_н = M_н(n, G_н).$$

Deviations in linear approximation are equal to

$$\Delta M_т = \left(\frac{\partial M_т}{\partial n}\right)_0 \Delta n + \left(\frac{\partial M_т}{\partial p_т}\right)_0 \Delta p_т; \tag{16.34}$$

$$\Delta M_н = \left(\frac{\partial M_н}{\partial n}\right)_0 \Delta n + \left(\frac{\partial M_н}{\partial G_н}\right)_0 \Delta G_н. \tag{16.35}$$

Substituting expressions (16.34) and (16.35) in equation (16.33) and going over to relative deviations, we obtain an equation of dynamics of the rotor of a turbopump assembly:

$$T_р \frac{d\bar{n}}{dt} + \bar{n} = K_{нр}\bar{p}_т - K_{нн}\bar{G}_р - K_{нт}\bar{G}_т, \tag{16.36}$$

where $T_р$ – time constant of the rotor; $K_{нр}$ – amplification factor according to pressure of gas before the nozzle box; $K_{нн}$ – amplification

factor according to expenditure of oxidizer; $K_{ог}$ – amplification factor according to expenditure of combustible:

$$\bar{p}_т = \frac{\Delta p_т}{p_{т0}}; \quad \bar{G}_о = \frac{\Delta G_о}{G_{во}}; \quad \bar{G}_г = \frac{\Delta G_г}{G_{во}}.$$

Time constant of rotor and amplification factors equal

$$T_р = \frac{\pi J}{30\left(\frac{\partial M_{в.о}}{\partial n} + \frac{\partial M_{в.г}}{\partial n} - \frac{\partial M_т}{\partial n}\right)_0}, \tag{16.37}$$

$$K_{ор} = \frac{p_{т0}}{n_{во}} \frac{\left(\frac{\partial M_т}{\partial p_т}\right)_0}{\left(\frac{\partial M_{в.о}}{\partial n} + \frac{\partial M_{в.г}}{\partial n} - \frac{\partial M_т}{\partial n}\right)_0}; \tag{16.38}$$

$$K_{оо} = \frac{G_{во}}{n_{во}} \frac{\left(\frac{\partial M_{в.о}}{\partial G_о}\right)_0}{\left(\frac{\partial M_{в.о}}{\partial n} + \frac{\partial M_{в.г}}{\partial n} - \frac{\partial M_т}{\partial n}\right)_0}; \tag{16.39}$$

$$K_{ог} = \frac{G_{во}}{n_{во}} \frac{\left(\frac{\partial M_{в.г}}{\partial G_г}\right)_0}{\left(\frac{\partial M_{в.о}}{\partial n} + \frac{\partial M_{в.г}}{\partial n} - \frac{\partial M_т}{\partial n}\right)_0}. \tag{16.40}$$

Calculation formulas for determination of values of partial derivatives of torques we obtain, differentiating equations of torque.

Torque on the pump shaft

$$M_н = \frac{30HG_н}{\pi n \eta_н n}, \tag{16.41}$$

where $G_н$ – flow rate of component through the pump; H – total head developed by the pump; n – number of revolutions of the impeller; $\eta_н$ – efficiency of the pump.

Let us differentiate the ratio (16.41) according to number of revolutions and expenditure of component, taking into account the dependence of pressure and efficiency on the number of revolutions and expenditure:

$$\left(\frac{\partial M_к}{\partial n}\right)_0 = -M_к\left[\frac{1}{\gamma H}\frac{\partial p_к}{\partial n} - \frac{1}{n} - \frac{1}{\eta_м}\frac{\partial \eta_м}{\partial n}\right]_0;$$

$$\left(\frac{\partial M_к}{\partial G_т}\right)_0 = -M_к\left[\frac{1}{\gamma H}\frac{\partial p_к}{\partial n} + \frac{1}{G_т} - \frac{1}{\eta_м}\frac{\partial \eta_м}{\partial G_т}\right]_0.$$

Torque developed by the turbine is expressed through effective work of 1 kg of gas, flow rate of gas $G_т$ and angular velocity of the rotor ω.

$$M_т = \frac{L_{эф} G_т}{\omega}. \qquad (16.42)$$

Effective work is connected with work on circumference of a wheel L_u.

$$L_{эф} = \frac{L_u}{\eta_{тр}}$$

where $\eta_{тр}$ – efficiency, considering friction loss in bearings and friction loss of the wheel against the gas.

Work of 1 kg of gas on the circumference of a wheel of an active single-stage turbine [21] is equal to

$$L_u = \frac{u}{g}(1+\psi)(c_1 \cos\alpha_1 - u), \qquad (16.43)$$

where u – peripheral velocity on average radius of the turbine; c_1 – velocity of gas on exit from the nozzle box of the turbine; α_1 – exit angle of gas from the nozzle box; ψ – coefficient, considering loss of relative velocity during motion of the gas between rotor blades of the turbine.

Substituting expression (16.43) in formula (16.42) and expressing peripheral velocity through average radius of the blade rim of turbine $R_{ср}$ and number of revolutions of the rotor, we obtain:

$$M_т = \frac{R_{ср}(1+\psi) G_т}{g\eta_{тр}}\left(c_1 \cos\alpha_1 - \frac{\pi R_{ср}}{30} n\right). \qquad (16.44)$$

By means of direct differentiation of dependence (16.44) we obtain partial derivative of torque of the turbine according to number of revolutions:

$$\frac{\partial M_т}{\partial n} = -\frac{\pi R_{ср}^2 (1+\psi) G_г}{30 g n_р}.$$

Since the torque of the turbine linearly depends on flow rate of gas through the turbine, and the flow rate of gas, in turn, linearly depends on the pressure of the gas before the nozzle box, which

$$\left(\frac{\partial M_т}{\partial p_г}\right)_0 = \left(\frac{M_т}{p_г}\right)_0.$$

Calculation formulas are used in the calculation of the time constant and amplification factors of the rotor of the turbopump assembly.

A variable fuel mixture ratio in the gas generator means that in the chamber of the gas generator the temperature of gas $T_г$, gas constant $R_г$, and adiabatic index of products of combustion $k_г$ do not remain constant.

In this case, the change in flow rate of gas through the turbine will depend on the change of pressure in gas generator, temperature $T_г$, and gas constant and k.

Exit velocity of the gas from the nozzle box of the turbine here is also a variable value

$$c_1 = c_1(T_г, R_г, k_г).$$

Temperature $T_г$ must be included as an additional inlet coordinate for the rotor of a turbopump assembly. In so doing it is required to construct a differential equation of heat accumulation in the chamber of the gas generator analogous to equation (16.23) for the basic chamber.

Deviations of gas constant $R_г$ and value k depend on the coefficient of fuel mixture ratio in the chamber of the gas generator

$$z_г = \frac{G_{ок.г}}{G_{т.г}}.$$

This means that flow rates of fuel components through the injector of the gas generator must also be considered as additional inlet coordinates for the rotor of the turbopump assembly.

In the presence of a subcritical drop on the nozzle box of the turbine, the additional inlet coordinate for the rotor of the turbopump assembly will be the pressure of gas in the gas duct after the turbine, since torque on the turbine depends on pressure drop.

Dynamic Properties of Main Lines and Regulating Elements

Change in pressure after the pump or after the regulating element on the feed line of the chamber of the engine by a fuel component leads to a change in the supply of the component to the chamber. The characteristic of the main line expresses the dependence of flow rate on pressure drop:

$$G_м = G_м(p_м - p_к).$$

where $G_м$ – flow rate of fuel component; $p_м$ – pressure on the pump or after the regulating element; $p_к$ – pressure of gas in the chamber.

The characteristic of the main line is determined by flow friction of lines and injectors, and in the case of cooling the basic chamber by the oxidizer – again by the flow friction of the cooling cavity.

With small deviations from steady state in linear approximation we obtain:

$$\Delta G_м = \left[\frac{\partial G_м}{\partial (p_м - p_к)}\right]_0 (\Delta p_м - \Delta p_к). \qquad (16.45)$$

Dependence (16.45) is valid for static deviations. During transition processes, a change in flow rate does not follow instantly after a change in pressure drop in view of inertness of the column of liquid. Part of the pressure drop is expended on surmounting the forces of inertia of the column of liquid. Let us designate this part of drop as Δp_j and for a cylindrical column of liquid we obtain

$$f\Delta p_j = fl\frac{\gamma}{g}\frac{dv}{dt},$$

where f – area of cross section of the line; l – length of the line; γ – weight density of the liquid; v – velocity of the liquid.

Let us replace the velocity by the mass flow rate of the liquid:

$$\Delta p_j = \frac{1}{g}\frac{l}{f}\frac{dG_{\text{ж}}}{dt}.$$

In the case of a line consisting of a n cylindrical sections it is necessary to produce summation. Then

$$\Delta p_j = \frac{1}{g}\frac{dG_{\text{ж}}}{dt}\sum_{i=1}^{n}\frac{l_i}{f_i}. \qquad (16.46)$$

Taking into account expressions (16.45) and (16.46) after transition to dimensionless values, the equation of the main line will be recorded in the following way:

$$T_{\text{м}}\frac{d\bar{G}_{\text{ж}}}{dt} + \bar{G}_{\text{ж}} = K_{\text{м}}(\bar{p}_{\text{н}} - \bar{p}_{\text{к}}), \qquad (16.47)$$

where

$$T_{\text{м}} = \frac{1}{g}\left[\frac{\partial G_{\text{ж}}}{\partial(p_{\text{н}} - p_{\text{к}})}\right]_0 \sum_{i=1}^{n}\frac{l_i}{f_i} \qquad (16.48)$$

– time constant of the main line;

$$K_{\text{м}} = \frac{p_{\text{вых}}}{G_{\text{вых}}}\left[\frac{\partial G_{\text{ж}}}{\partial(p_{\text{н}} - p_{\text{к}})}\right]_0 \qquad (16.49)$$

– amplification factor of the main line.

In formula (16.48) summation extends to sections of the main line from the tank to the basic chamber, including cavity cooling the chamber by fuel component.

In long fuel main lines under unsteady conditions wave processes take place. The interaction of wave processes in the main lines with the process of gas formation in the chamber can lead to self-oscillation conditions [47].

Frequency of natural oscillations are rather great and lie usually beyond the borders of the passband of the automatic control system.

The flow rate of fuel component through the regulating element located on feed line of the basic chamber or gas generator depends on pressure drop on the regulating element and position of the regulating element:

$$G_к = G_к[(p_н - p_з), m],$$

where $p_н$ – pressure after the pump; $p_з$ – pressure after the regulating element; m – shift of the regulating element.

With small deviations from steady state deviations in flow rate equal

$$\Delta G_к = \left[\frac{\partial G_к}{\partial (p_н - p_з)}\right]_0 (\Delta p_н - \Delta p_з) + \left(\frac{\partial G_к}{\partial m}\right)_0 \Delta m. \qquad (16.50)$$

Values of partial derivatives $\left[\frac{\partial G_к}{\partial (p_н - p_з)}\right]_0$ and $\left(\frac{\partial G_к}{\partial m}\right)_0$ are determined for given conditions according to flow characteristic of the regulating element.

The force of inertia having effect on the column of liquid in cavity of the regulating element, in view of its weakness compared with the force of inertia of the column of liquid in the main line we will disregard.

After conversion of equation (16.50) and transition to dimensionless parameters, we obtain the equation of the regulating element in the following form:

$$\bar{p}_3 = \bar{p}_2 - K_Q \bar{G}_2 + K_m \bar{m}. \qquad (16.51)$$

The amplification factors entering into equation (16.51) respectively are equal to

$$K_Q = \frac{G_{2\,0}}{p_{2\,0}} \frac{1}{\left[\frac{\partial G_2}{\partial (p_2 - p_3)}\right]_0};$$

$$K_m = \frac{m_{2\,0}}{p_{2\,0}} \cdot \frac{\left(\frac{\partial G_2}{\partial m}\right)_0}{\left[\frac{\partial G_2}{\partial (p_2 - p_3)}\right]_0}.$$

Values of amplification factors K_Q and K_m depend on pressure drop on the regulating element and on the profiling of the regulating element.

Dynamic Properties of a Liquid Propellant Rocket Engine as an Object of Automatic Control

It was indicated above that for appraisal of dynamic properties of a liquid propellant rocket engine as an object of automatic control it is convenient to use frequency responses, which can easily be calculated with help of digital or analog electronic computers.

For each link in the object of automatic control there is a corresponding differential or algebraic equation. Derivation of the equations of separate sections was given above. In Laplace transformations the system of equations of dynamic sections of the object will be recorded in general form in the following way:

$$\left.\begin{aligned}
(T_1 p+1)e^{p\tau_1}x_1 &= K_{12}x_2+\ldots+K_{1n}x_n+\\
&+l_{11}m_1+l_{12}m_2+l_{13}m_3+l_{1f}n_x;\\
&\cdots\cdots\cdots\cdots\cdots\cdots\\
(T_n p+1)e^{p\tau_n}x_n &= K_{11}x_1+\ldots+K_{1(n-1)}x_{n-1}+\\
&+l_{n1}m_1+l_{n2}m_2+l_{n3}m_3+l_{nf}n_x.
\end{aligned}\right\} \qquad (16.52)$$

In equations (16.52), the coordinate of sections are designated as x_i, time constants T_i, amplification factors K_{ij}, time lag τ_i, amplification factors for controlling actions l_{ij}, amplification factors for external disturbance l_{if}, and Laplace transformations for controlling actions m_i.

The object of control has n dynamic sections and a corresponding number of coordinates. The number of controlling actions equals three. External disturbance for all sections is the same. Inertialess sections have time constants equal to zero. Sections without lag have by parameters τ_i equal to zero. Coefficients l_{if} are not equal to zero only in equations of regulating elements. External disturbance n_x is an inlet coordinate only in the equations of fuel pumps. Recording the systems of equations in most general form (16.52), is necessary for development of a general algorithm by calculation of frequency-response curves of the object of control.

The system of equation (16.52) can be recorded [32] in matrix form

$$A(p)x = Lm + L_f n_x. \qquad (16.53)$$

where $A(p)$ – characteristic matrix of the object of control; L – matrix of amplification factors during controlling actions; L_f – column of amplification factors during disturbance; x – column of coordinates of the object; m – column of controlling actions.

Matrices entering into equation (16.53) respectively equal

$$A(p)=\begin{bmatrix}(T_1p+1)e^{p\tau_{11}} & K_{12}\ldots & K_{1n}\\ K_{21}(T_2p+1)e^{p\tau_{21}} & \ldots & K_{2n}\\ \ldots\ldots\ldots\ldots & & \\ K_{n1} & K_{n2}\ldots & (T_np+1)e^{p\tau_{nn}}\end{bmatrix},$$

$$L=\begin{bmatrix}l_{11} & l_{12} & l_{13}\\ \ldots\ldots & & \\ l_{n1} & l_{n2} & l_{n3}\end{bmatrix};\quad x=\begin{bmatrix}x_1\\ \ldots\\ x_n\end{bmatrix};\quad m=\begin{bmatrix}m_1\\ m_2\\ m_3\end{bmatrix}.$$

From the matrix of the equation of dynamics of the object of control (16.53) we obtain the equation for transfer functions of object of control for controlling actions –

$$A(p)W(p)=L \tag{16.54}$$

and the equation for transfer functions of object of control for external disturbance –

$$A(p)W_f(p)=L_f, \tag{16.55}$$

where $W(p)$ – matrix of transfer functions of the object of control for controlling actions, having n rows and three columns; $W_f(p)$ – column of transfer functions of the object of control for external disturbance, having n elements.

Matrix $W(p)$ is obtained with solution of equation (16.54):

$$W(p)=A^{-1}(p)L, \tag{16.56}$$

and column $W_f(p)$ – with solution of equation (16.55):

$$W_f(p)=A^{-1}(p)L_f,$$

where $A^{-1}(p)$ – matrix, reverse to characteristic matrix of the object of control.

Analysis of the stability of the object of control by the usual methods used in the theory of automatic control is produced by examining the characteristic equation of the object, which we obtain, equating with zero to determine the characteristic matrix of the object $|A(p)| = 0$.

In the case of the accepted form of recording the characteristic equation, a very effective method of analysis of stability is the D-partition method [2], [36].

The matrices of transfer functions (16.56) and (16.57) correspond to matrices of frequency-response curves of the object of control:

$$W(j\omega) = A^{-1}(j\omega)L;$$
$$W_f(j\omega) = A^{-1}(j\omega)L_f.$$

The matrix of frequency-response curves of the object for controlling actions is obtained as the product of the reverse frequency characteristic matrix $A^{-1}(j\omega)$ and the matrix of amplification factors of sections for controlling actions L.

The column of frequency-response curves of the object for external disturbance consists of the product of matrix $A^{-1}(j\omega)$ and column L_f.

Inversion of the frequency characteristic matrix can easily be carried out with the help of an electronic digital computer. Direct matrix inversion, consisting of complex elements, cannot be carried out on a digital computer. It is necessary to change to matrices composed of real elements.

Matrix $A(j\omega)$ can be represented in the form of the sum of real and imaginary matrices:

$$A(j\omega) = P_A(\omega) + jQ_A(\omega).$$

Analogously the inverse matrix can be represented

$$A^{-1}(j\omega)=C(j\omega)=P_C(\omega)+jQ_C(\omega).$$

The product of direct and inverse matrices is equal to a unit matrix on the order of n:

$$A(j\omega)C(j\omega)=E_n. \qquad (16.58)$$

Performing multiplication of matrices and separating in equality (16.58) the real and imaginary part, we obtain:

$$P_A(\omega)P_C(\omega)-Q_A(\omega)Q_C(\omega)=E_n; \qquad (16.59)$$
$$Q_A(\omega)P_C(\omega)+P_A(\omega)Q_C(\omega)=0. \qquad (16.60)$$

A system from two matrix equations (16.59) and (16.60) can be recorded in the form of one matrix equation

$$F(\omega)R(\omega)=S, \qquad (16.61)$$

where for matrices composed of cells, the following designations are accepted:

$$F(\omega)=\left[\begin{array}{c|c} P_A(\omega) & -Q_A(\omega) \\ \hline Q_A(\omega) & P_A(\omega) \end{array}\right];$$

$$R(\omega)=\left[\begin{array}{c} P_C(\omega) \\ \hline Q_C(\omega) \end{array}\right]; \quad S=\left[\begin{array}{c} E_n \\ \hline 0 \end{array}\right].$$

Solution of equation (16.61) gives matrix $R(\omega)$, composed of real and imaginary frequency-response curves of the object of control:

$$R(\omega)=F^{-1}(\omega)S.$$

Thus, for obtaining real and imaginary frequency-response curves $P_C(\omega)$ and $Q_C(\omega)$ it is necessary that several values of frequency ω fulfill matrix inversion $F(\omega)$, composed of real elements,

and produce multiplication of matrices $F^{-1}(\omega)$ and S. These operations are easily performed with help of a digital computer.

The full characteristic of dynamic properties of an engine as an object of automatic control is given by the totality of frequency response curves for all outlet coordinates of sections according to shifts of each of the regulating elements and according to external disturbance.

For the engine, the block diagram of which is represented in Fig. 16.3, the frequency matrix of the object of control has eleven rows and two columns:

$$W(j\omega)=\begin{bmatrix} W_{11}(j\omega) & W_{12}(j\omega) \\ \cdots & \cdots \\ W_{111}(j\omega) & W_{112}(j\omega) \end{bmatrix}. \qquad (16.62)$$

The frequency matrix of this same engine according to external disturbance constitutes a column consisting of eleven elements:

$$W_f(j\omega)=\begin{bmatrix} W_{1f}(j\omega) \\ \cdots \\ W_{11f}(j\omega) \end{bmatrix}.$$

An engine with three controlling actions, the block diagram of which is represented in Fig. 16.4, has a frequency matrix according to shifts of regulating elements including twelve rows and three columns:

$$W(j\omega)=\begin{bmatrix} W_{11}(j\omega) & W_{12}(j\omega) & W_{13}(j\omega) \\ \cdots & \cdots & \cdots \\ W_{121}(j\omega) & W_{122}(j\omega) & W_{123}(j\omega) \end{bmatrix}. \qquad (16.63)$$

The column of frequency-response curves according to external disturbance for this engine numbers twelve elements.

In many cases there is no necessity to compose a full matrix of frequency-response curves of the object of control. It is expedient to include in the matrix the frequency-response curves only for those coordinates, the change of which during the transition process essentially characterizes the operating conditions of the engine. Such coordinates include pressure in the basic camera and gas generator, the number of revolutions of the rotor of the turbopump assembly and flow rates fuel components in a unit of time.

Investigation of the dynamics of closed automatic control systems requires the composition of a matrix of frequency-response curves of the object of control for variable values. Such a matrix is square, since the number of variable values. Such a matrix is square, since the number of variable values of the object equals the number of controlling actions.

In reference to the engine with two controlling actions, the block diagram of which is represented in Fig. 16.3, the matrix of frequency-response curves of the object of control has the form

$$W(j\omega)=\begin{vmatrix} W_{11}(j\omega) & W_{12}(j\omega) \\ W_{21}(j\omega) & W_{22}(j\omega) \end{vmatrix}, \qquad (16.64)$$

where $W_{11}(j\omega)$ – frequency-response curve for pressure in the basic chamber according to shift of the regulating element controlling thrust; $W_{12}(j\omega)$ – frequency-response curve for pressure in the basic chamber according to shift of the regulating element, controlling fuel mixture ratio; $W_{21}(j\omega)$ – frequency-response curve for the fuel mixture ratio according to shift of the regulating element controlling thrust; $W_{22}(j\omega)$ – frequency-response curve for the fuel mixture ratio according to shift of the regulating element controlling the ratio of components.

The matrix of frequency-response curves of the object for variable values according to external disturbance in the given case constitutes a column consisting of two elements.

An engine with three variable values, the block diagram of which is shown in Fig. 16.4, has a matrix of frequency-response curves of the object for variable values, including three rows, and three columns:

$$W(j\omega)=\begin{bmatrix} W_{11}(j\omega) & W_{12}(j\omega) & W_{13}(j\omega) \\ W_{21}(j\omega) & W_{22}(j\omega) & W_{23}(j\omega) \\ W_{31}(j\omega) & W_{32}(j\omega) & W_{33}(j\omega) \end{bmatrix}. \qquad (16.65)$$

The object of control, as was shown above, has internal cross coupling. These connections are reflected in the matrix of frequency-response curves of the object.

On main diagonals of the matrices (16.64) and (16.65) there are located the frequency-response curves of the basic channels of control of the object. Nondiagonal elements of these matrices characterize mutual cross coupling between control channels in the object.

The equation of dynamics of the object of control in Laplace transformations in matrix form is recorded in the following way:

$$x=W(p)m+W_f(p)n_x, \qquad (16.66)$$

where x – column of variable values; m – column of shifts of control elements; n_x – scalar quantity of external disturbing actions; $W(p)$ – square transfer matrix of the object for adjustable values; $W_f(p)$ – column of transfer functions of the object according to external disturbance.

This equation of the object (16.66) is examined jointly with equations of the regulators during investigation of the dynamics of an automatic control system.

For specific engines, in the beginning there are calculated dynamic parameters of sections, comprising the object of control, and after that there are calculated frequency-response curves of the object of control entering into the matrices (16.64) or (16.65).

With the necessity to investigate in the dynamics, the change of values which are not directly variable, it is necessary to calculate frequency-response curves entering into matrices (16.64) or (16.63).

CHAPTER XVII

AUTOMATIC CONTROL SYSTEMS OF LIQUID PROPELLANT ROCKET ENGINES

17.1. Automatic Control Liquid Propellant Rocket Engines with Pressure System of Component Feed

A block diagram of control system being considered was shown in Fig. 16.1. The pressure regulator of the pressurized gas consists of a pressure reducing valve with variable adjustment and usually possesses very high speed operation.

Let us consider in the beginning the dynamic properties of the object of control on the assumption that pressure regulator of the pressurized gas is ideal, that is, it maintains during each adjustment value h a strictly constant pressure of the pressurized gas in the tanks, equal to pressure after the regulator $p_{вх}$, which here represents an inlet coordinate for the object of control.

The dynamic properties of the object of control are described in Laplace transformations by a system consisting of three differential equations, into which enter the equation of the basic chamber

$$(T_1 p + 1) e^{\tau_1 p} \bar{p}_к = K_{12} \bar{G}_{ок} + K_{13} \bar{G}_{гк}; \qquad (17.1)$$

the equation of the main line and oxidizer injectors

$$(T_2 p + 1) \bar{G}_{ок} = K_{24} (\bar{p}_н - \bar{p}_к) + K_{25} \bar{n}_x, \qquad (17.2)$$

and the equation of the main line and combustible injectors

$$(T_3p+1)\bar{G}_{r.x}=K_{34}(\bar{p}_0-\bar{p}_x)+K_{f3}\bar{n}_x. \qquad (17.3)$$

This system of equations is generalized by matrix equation (16.53), where the characteristic matrix of the object and the matrix of amplification factors of sections respectively equal

$$A(p)=\begin{bmatrix}(T_1p+1)e^{p\tau_1} & -K_{12} & -K_{13}\\ K_{24} & (T_2p+1) & 0\\ K_{34} & 0 & (T_3p+1)\end{bmatrix}; \qquad (17.4)$$

$$L=\begin{bmatrix}0\\ K_{24}\\ K_{34}\end{bmatrix}; \qquad (17.5)$$

$$L_f=\begin{bmatrix}0\\ K_{f2}\\ K_{f3}\end{bmatrix}. \qquad (17.6)$$

Amplification factors of the main lines in respect to longitudinal overload of the flight vehicle K_{f2} and K_{f3} depend on the heights of the columns of liquids in tanks and main lines and on the configuration of the main lines.

The characteristic polynomial of the object of control, equal to the determinant of the characteristic matrix (17.4), is recorded in the following way:

$$D(p)=|A(p)|=(T_1p+1)(T_2p+1)(T_3p+1)e^{p\tau_1}+ \\ +K_{12}K_{24}(T_3p+1)+K_{13}K_{34}(T_2p+1). \qquad (17.7)$$

For estimating the stability of the object of control there is used the characteristic equation

$$D(p)=0. \qquad (17.8)$$

Consideration of characteristic equation (17.8) shows that the object of control, neglecting lag in the basic chamber τ_1 is structurally stable, i.e., it is stable with any value of time constants and amplification factors of sections.

With sufficiently great lag τ_1, the object of control can become unstable. Critical value of delay $\tau_{1кр}$, with which the object of control loses stability can be determined by a D-partition equation [2].

The comparatively low order of the system of equations permits obtaining in evident form the transfer functions of the object of control:

$$W_{11}(p)=\frac{(K_{12}K_{24}T_3+K_{13}K_{34}T_2)p+(K_{12}K_{24}+K_{13}K_{34})}{D(p)} \qquad (17.9)$$

– transfer function for pressure of gas in the basic chamber according to displacement pressure;

$$W_{21}(p)=\frac{K_{24}(T_1p+1)(T_3p+1)e^{p\tau_1}}{D(p)} \qquad (17.10)$$

– transfer function for flow rate of oxidizer according to displacement pressure;

$$W_{31}(p)=\frac{K_{34}(T_1p+1)(T_2p+1)e^{p\tau_1}}{D(p)} \qquad (17.11)$$

– transfer function for flow rate of combustible according to displacement pressure;

$$W_{f1}(p)=\frac{(K_{f2}K_{12}T_3+K_{f3}K_{13}T_2)p+(K_{f2}K_{12}+K_{f3}K_{13})}{D(p)} \qquad (17.12)$$

– transfer function for pressure of gas in the basic chamber according to external disturbance.

These formulas can be used for calculation of frequency-response curves of the object of control and for calculation of transition processes with specific controlling signals and external disturbances.

In that case when the elapsed time of the transition process in the system "regulator of pressure of displaced gas – fuel tanks" is commensurable with the elapsed time of transition processes in the main lines and basic chamber, the gas pressure regulator cannot be considered as ideal. Pressures of the displaced gas in the tanks, in contrast to the case examined earlier, will lag behind controlling signal passed to adjust the regulator.

It is necessary to consider the inertness of the fuel tanks and to examine the dynamics of the tank in respect to pressure of the displaced air.

Under unsteady conditions, the process of accumulation of gas in the gas ullage of the tank is described by a differential equation

$$V_{\text{г.г}} \frac{d\gamma_{\text{г.г}}}{dt} = \Delta G_{\text{в.г}} - \Delta G_{\text{г.г}} \qquad (17.13)$$

$V_{\text{г.г}}$ – volume of ullage at the instant under consideration; $\gamma_{\text{г.г}}$ – weight density of gas in the tank; $G_{\text{в.г}}$ – flow rate of displaced gas into the tank: $G_{\text{г.г}}$ – quantity of gas passing in the volume liberated from the fuel component.

The quantity of gas $G_{\text{в.г}}$ can be expressed as the flow rate of fuel component $G_{\text{г.т}}$ and density ratio of gas and fuel component $\gamma_{\text{г}}$

$$G_{\text{в.г}} = \frac{\gamma_{\text{в.г}}}{\gamma_{\text{г}}} G_{\text{г.т}}. \qquad (17.14)$$

Deviation in flow rate equals

$$\Delta G_{\text{в.г}} = \frac{1}{\gamma_{\text{г}}} (\gamma_{\text{в.г}} \Delta G_{\text{г.т}} + G_{\text{г.т}} \Delta \gamma_{\text{в.г}}). \qquad (17.15)$$

The process in the tank takes place rather rapidly. Disregarding heat exchange of the gas with the fuel and walls of the tank, the process in the tank can be considered as adiabatic:

$$\frac{p_{\text{г.г}}}{\gamma_{\text{в.г}}} = \text{const}. \qquad (17.16)$$

Taking into account expression (17.16), deviation of weight density $\Delta\gamma_{\text{г.р}}$ is expressed as a deviation of pressure:

$$\Delta\gamma_{\text{г.р}}=\left(\frac{\gamma_{\text{г.р}}}{\Delta p_{\text{г.р}}}\right)_0\Delta p_{\text{г.р}}. \tag{17.17}$$

Substituting equations (17.15) and (17.17) in initial equation (17.13), after conversion and transition to dimensionless values, we obtain the equation of dynamics of fuel tank according to gas pressure:

$$T_{\text{г}}\frac{d\bar{p}_{\text{г.г}}}{dt}+\bar{p}_{\text{г.р}}=K_{\text{г.в}}\bar{G}_{\text{в.р}}-K_{\text{г.р}}\bar{G}_{\text{р.м}}. \tag{17.18}$$

The time constant and amplification factors entering into equation (17.18) respectively are equal to

$$T_{\text{г}}=\frac{\gamma_{\text{г}}V_{\text{г.г}}}{G_{\text{р.м}}}; \tag{17.19}$$

$$K_{\text{г.в}}=\frac{G_{\text{в.в}}}{p_{\text{г.в}}}\frac{\Delta p_{\text{г.г}}\gamma_{\text{г}}}{G_{\text{р.м}}\gamma_{\text{г.р}}}; \tag{17.20}$$

$$K_{\text{г.р}}=\frac{G_{\text{в.в}}}{p_{\text{г.в}}}\frac{\Delta p_{\text{г.г}}}{G_{\text{р.м}}}. \tag{17.21}$$

The flow rate of gas through throttling value of the regulator depends on pressure of gas on inlet to the regulator $p_{\text{вх}}$, counter-pressure in the tank $p_{\text{г.р}}$ and value lift m:

$$G_{\text{в}}=G_{\text{в}}(p_{\text{вх}}, p_{\text{г.р}}, m). \tag{17.22}$$

Linearization of the equation of flow rate (17.22) for small deviations gives

$$\bar{G}_{\text{в}}=K_{m}\bar{p}_{\text{вх}}+K_{p.\text{г}}\bar{p}_{\text{г.р}}+K_{m}\bar{m}. \tag{17.23}$$

Amplification factors are determined according to the following formulas:

$$K_{m}=\frac{p_{\text{в.в}}}{G_{\text{в.в}}}\left(\frac{\partial G_{\text{в}}}{\partial p_{\text{вх}}}\right)_0; \tag{17.24}$$

$$K_{p.\text{г}}=\frac{p_{\text{в.в}}}{G_{\text{в.в}}}\left(\frac{\partial G_{\text{в}}}{\partial p_{\text{г.р}}}\right)_0; \tag{17.25}$$

$$K_{m}=\frac{a_{\text{в.в}}}{G_{\text{в.в}}}\left(\frac{\partial G_{\text{в}}}{\partial m}\right)_0. \tag{17.26}$$

The lift of the throttling valve of the regulator depends on pressure of gas in the tank and compression force of the spring, which is determined by the position of the regulator adjusting screw h:

$$m = m(p_{б.г}, h). \tag{17.27}$$

After linearization of equation (17.27) we obtain

$$\bar{m} = -K_p \bar{p}_{б.г} + K_h \bar{h}, \tag{17.28}$$

where amplification factors respectively are equal to

$$K_p = \frac{p_{бг0}}{m_{г0}} \left(\frac{\partial m}{\partial p_{б.г}}\right)_0; \tag{17.29}$$

$$K_h = \frac{h_{г0}}{m_{г0}} \left(\frac{\partial m}{\partial h}\right)_0. \tag{17.30}$$

Values of partial derivatives entering into the formulas for amplification factors in flow rate equation (17.23) and in the regulator equation (17.28) are determined according to the static characteristics of the regulator (17.22) and (17.27).

In examining the control system as a whole, it is necessary to consider that the flow of gas passing through the regulator branches for pressurization of the combustible tank and the oxidizer tank

$$\bar{G}_г = \bar{G}_{г.г} + \bar{G}_{г.о}. \tag{17.31}$$

For investigation of the control system, taking into account the inertness of the fuel tanks, it is necessary along with equations of the basic chamber and fuel main lines (17.1), (17.2), (17.3) to construct an equation of dynamics of the fuel and oxidizer tanks, an equation of flow rate of displaced gas (17.23), equation of the regulator (17.28) and equation of branching of the gas flow (17.31).

Transfer functions and formulas for frequency-response curves of the system can be obtained in explicit form, but it is more convenient to accomplish the calculation of frequency-response

curves and transition processes, and also analysis of stability of the automatic control system with help of electronic computers.

17.2. Automatic Control of Liquid Propellant Rocket Engines with Turbopump Feeding of Fuel Components and a Monocomponent Gas Generator

A block diagram of an engine as an object of automatic control is provided in Fig. 16.2. Besides the elements shown in the block diagram of an object of control, the control system includes a container with high pressure gas, a tank with hydrogen peroxide, and a pressure regulator for the displaced gas.

The dynamics of the automatic control system is described by eleven equations: basic chamber (16.8), main lines of oxidizer and fuel (16.47), pumps of oxidizer and fuel (16.32), rotor of the turbopump assembly (16.36), gas generator, main line of the hydrogen peroxide, tank of hydrogen peroxide (17.18), flow rate of the regulator (17.23) and the equation of pressure regulator for the displaced gas (17.28).

The equation of dynamics of the gas generator is analogous in form to the equation of the basic chamber according to pressure:

$$T_{g.r}\frac{d\bar{p}_r}{dt}+\bar{p}_r=K_{g.r}\bar{G}_{n.g}(t-\tau_3), \qquad (17.32)$$

where $T_{g.r}$ – time constant; $K_{g.r}$ – amplification factor of the gas generator; τ_3 – time of conversion hydrogen peroxide into steam gas.

Calculation formulas for $T_{g.r}$ and $K_{g.r}$ are the same as in the case of the basic chamber of the engine.

Frequency-response curves of the automatic control system and transition processes in the system are calculated with help of electronic digital or analog computers.

An automatic control system can be divided into two successively connected circuits. The first circuit is made up of the pressure regulator of the displaced gas, the hydrogen peroxide tank, the main hydrogen peroxide line and the gas generator. The second circuit includes the turbopump assembly rotor, the pumps and main feed line of the basic chamber and the basic chamber of the engine. Between the first and second circuit there are no feedbacks, therefore the transfer functions and frequency-response curves of each of the circuits can be obtained independently of the other. The transfer function and frequency-response curve of the whole control system according to the controlling action which is the adjustment signal of regulator are obtained as the product of transfer functions or frequency-response curves of the first and second circuits. This simplifies and accelerates calculations on dynamics of the automatic control system under examination.

The time constant of the turbopump assembly rotor essentially exceeds in value the time constants and time lags of the other sections. This makes it possible for an approximate analysis of dynamics of a system to consider all links, besides the turbopump assembly, as inertialess.

17.3. Automatic Control of Thrust of an Engine with a Bicomponent Gas Generator

The block diagram was shown in Fig. 16.3. The method of calculation of frequency-response curves of an object of control is expounded in § 2.16.

In Fig. 17.1 there is shown one of possible schematic diagrams of a thrust regulator with hydraulic static servomotor. For feeding the servomotor pressure is supplied with a pressure p_c.

Shift y of the controlling element of servomotor 5, connected with the diaphragm of sensing device 3, depends on pressure in chamber p_x and signal of adjusting regulator h:

$$y = y(p_x, h). \tag{17.33}$$

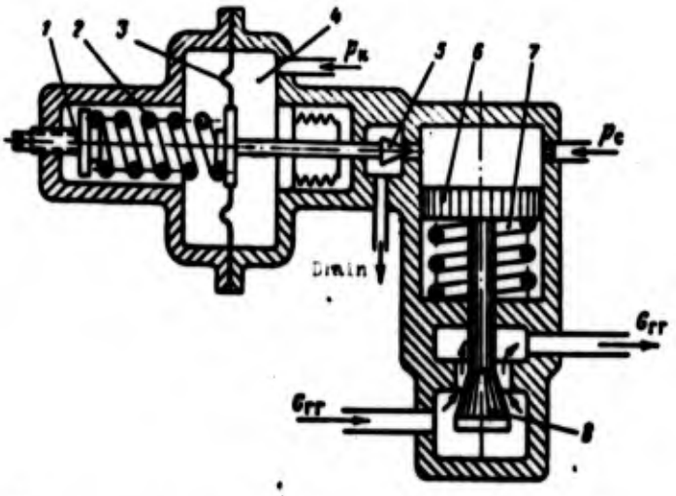

Fig. 17.1. Schematic diagram of a thrust regulator with hydraulic static servomotor: 1 – regulator adjusting screw; 2 – sensing device spring; 3 – sensing device diaphragm; 4 – gas feed cavity with pressure $p_к$; 5 – servomotor controlling element; 6 – servomotor piston; 7 – servomotor spring; 8 – regulating element.

Linearizing equation (17.33) for small deviations from steady state and going over to relative deviations, we obtain:

$$\bar{y} = -K_1 \bar{p}_к + K_h \bar{h}, \tag{17.34}$$

where

$$K_1 = \frac{p_{к0}}{p_{c0}} \left(\frac{\partial y}{\partial p_к}\right)_0 \tag{17.35}$$

– amplification factor of the sensing device according to gas pressure;

$$K_h = \frac{h_{c0}}{p_{c0}} \left(\frac{\partial p}{\partial h}\right)_0 \tag{17.36}$$

– amplification factor of the sensing device according to controlling adjustment signal.

Shift of the regulating element 8 connected with the piston of servomotor 6 depends on the shift of the servomotor controlling:

$$m=m(y). \qquad (17.37)$$

Linearization of equation (17.37) for unsteady conditions in case of a static hydraulic servomotor gives the equation of dynamics of this servomotor in the following form [24]:

$$T_c\frac{d\bar{m}}{dt}+\bar{m}=K_c\bar{y}, \qquad (17.38)$$

where T_c and K_c – time constant and amplification factor of the servomotor.

Designating the amplification factor of regulator as

$$K_p=K_rK_c, \qquad (17.39)$$

we record the transfer function of regulator as

$$N(p)=\frac{K_p}{T_cp+1}. \qquad (17.40)$$

The equation of the dynamics of the regulator has the following form in Laplace transformations:

$$\bar{m}=N(p)(K_1\bar{h}-\bar{p}_c); \qquad (17.41)$$

with $K_1=K_n/K_r$ designating the coefficient during the controlling signal.

The equation of dynamics of the object of control in Laplace transformations will be recorded in the following way:

$$\bar{p}_c=W_{11}(p)\bar{m}+W_{1f}(p)\bar{n}_x; \qquad (17.42)$$

Here $W_{11}(p)$ – transfer function of the object of control for pressure in the basic chamber for shift of the regulating element; $W_{12}(p)$ – transfer function of the object of control for pressure in the basic chamber for external disturbance.

Excluding from equations (17.41) and (17.42) the shift of the regulating element, we obtain the equation of the dynamics of a closed automatic control system:

$$[1+W_{11}(p)N(p)]\bar{p}_{\text{в}} = -K_1 W_{11}(p)N(p)h + W_{12}(p)\bar{n}_{\text{в}}. \tag{17.43}$$

The characteristic equation of a closed system we obtain, equating the characteristic polynomial to zero:

$$1+W_{11}(p)N(p)=0. \tag{17.44}$$

This equation is used in analyzing the stability of the system. With help of D-partition it is possible, with a known frequency-response curve of the object of control, to investigate the effect of the dynamic parameters of the regulator on the stability of the system.

Solution of equation (17.43) in respect to variable value $\bar{p}_{\text{в}}$ gives:

$$\bar{p}_{\text{в}} = \Phi_{1h}(p)\bar{h} + \Phi_{12}(p)\bar{n}_{\text{в}}, \tag{17.45}$$

where

$$\Phi_{1h}(p) = \frac{K_1 W_{11}(p)N(p)}{1+W_{11}(p)N(p)} \tag{17.46}$$

– transfer function of a closed loop control system for $\bar{p}_{\text{в}}$ according to controlling signal h;

$$\Phi_{12}(p) = \frac{W_{12}(p)}{1+W_{11}(p)N(p)} \tag{17.47}$$

– transfer function of closed loop control system for $f_н$ according to external disturbance.

Transfer functions (17.46) and (17.47) correspond to frequency-response curves

$$\Phi_{1h}(j\omega)=\frac{K_1 W_{11}(j\omega) N(j\omega)}{1+W_{11}(j\omega) N(j\omega)}; \qquad (17.48)$$

$$\Phi_{1f}(j\omega)=\frac{W_{1f}(j\omega)}{1+W_{11}(j\omega) N(j\omega)}. \qquad (17.49)$$

The real part of frequency-response curve (17.48) is used in construction of the transfer process in a closed automatic control system, appearing in case of supply to the adjustment of the regulator for controlling signal h, and in analyzing the effect of dynamic parameters of the regulators on the character of the transition process.

Frequency-response curve (17.49) is used in investigating the effect of external disturbance on the control. In the case of defined external disturbing effect with help of frequency-response curve (17.49) there is constructed a transition process in a closed system, and during accidental external perturbing influence, frequency-response curve (17.49) serves for determination of dispersion and correlation functior of the variable value [42]. Probabilistic characteristics of the external accidental disturbing effect here must be known.

17.4. Control Systems of Thrust and Mixture Ratio for a Liquid Propellant Rocket Engine

The block diagram of a liquid propellant rocket engine with thrust and mixture ratio control for the basic chamber was shown in Fig. 16.3. In Fig. 16.4 there was provided a block diagram of a liquid propellant rocket engine with thrust and mixture ratio control both for the basic chamber and also for the gas generator. One possible schematic diagram of a thrust regulator was shown in Fig. 17.1.

A possible diagram of a mixture ratio regulator is shown in Fig. 17.2. The regulator consists of a diaphragm sensing device and a static hydraulic servomotor.

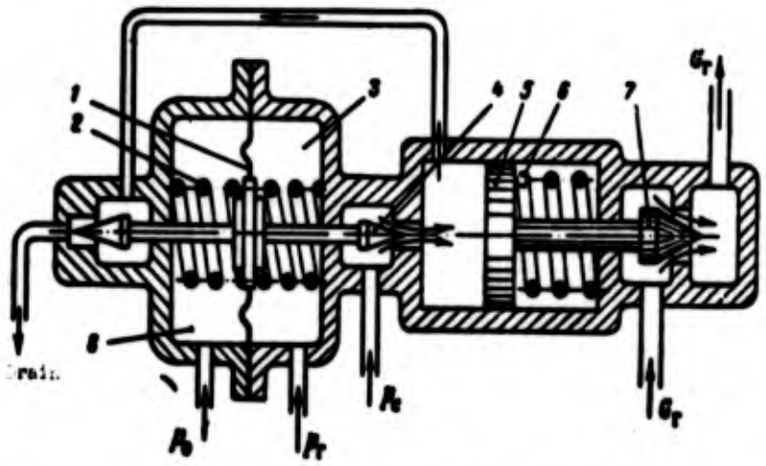

Fig. 17.2. Schematic diagram of a mixture ratio regulator: 1 – diaphragm of the sensing device; 2 – springs of the sensing element; 3 – fuel feed cavity; 4 – controlling elements of the hydraulic servomotor; 5 – servomotor piston; 6 – servomotor spring; 7 – regulating element; 8 – oxidizer feed cavity.

As values, characterizing the flow rates of fuel components there are used pressure of the combustible after the regulating element and the pressure of the oxidizer after the pump. On diaphragm 1 of the sensing device these pressures are compared. If the mixture ratio corresponds to rated value, then the diaphragm of the sensing device is in equilibrium position. With deviation the diaphragm is deflected, the hydraulic servomotor is set in action and regulating element 7 changes the flow rate of the combustible in the direction of restoring the assigned mixture ratio.

The value characterizing the deviation of the mixture ratio from rated value is the difference in pressures of combustible and oxidizer acting on the diaphragm of the sensing element:

$$p_* = p_T - p_0. \qquad (17.50)$$

The deflection for the diaphragm of the sensing device and the shaft of the servomotor controlling elements firmly attached to it are equal and depend on the difference of pressure p_*:

$$y=y(p_*). \tag{17.51}$$

After linearization of equation (17.51) and transition to relative deviations we obtain the equation of the sensing element:

$$\bar{y}=-K_*\bar{p}_*, \tag{17.52}$$

where

$$K_*=\frac{p_{*0}}{y_{*0}}\left(\frac{\partial y}{\partial p_*}\right)_0 \tag{17.53}$$

– amplification factor of sensing device of the mixture ratio regulator.

We obtain the equation of the hydraulic servomotor analogously to equation (17.38).

The transfer function of the regulator in the special case examined has the same form (17.40) as for the thrust regulator. The amplification factor of the regulator consists of the product of the amplification factors of the sensing device and the servomotor (17.39).

For the regulator schematically represented in Fig. 17.2, adjustment is constant under all conditions. Consequently, controlling signal h is absent, and equation of dynamics of regulator in the Laplace transformations will be recorded in the following way:

$$\bar{m}=-N(p)\bar{p}_*. \tag{17.54}$$

Block diagrams of the automatic control systems show the interconnection of the object of control and the regulators.

A block diagram of the control system of a liquid propellant rocket engine with two variable values is shown in Fig. 17.3, and a block diagram with three variable values in Fig. 17.4.

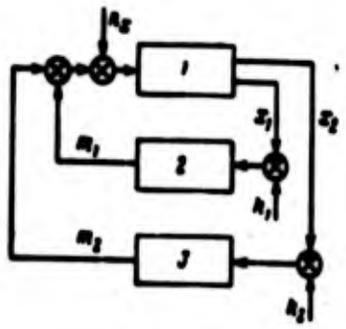

Fig. 17.3. Block diagram of an automatic control system of a liquid propellant rocket engine with two variable values: 1 – liquid propellant rocket engine; 2 – thrust regulator; 3 – regulator of fuel mixture ratio for chamber of the engine.

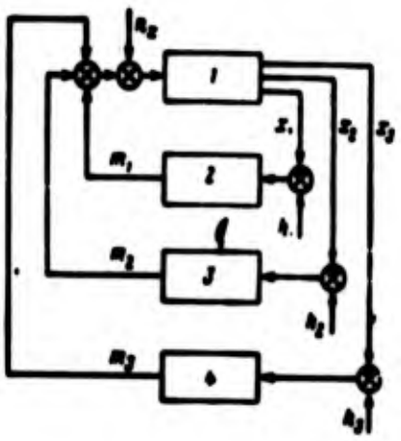

Fig. 17.4. Block diagram of an automatic control system of a liquid propellant rocket engine with three variable values: 1 – liquid propellant rocket engine; 2 – thrust regulator; 3, 4 – regulators of fuel mixture ratio for chamber of the engine and the gas generator.

Variable values characterizing thrust and ratio of fuel components in the basic chamber and gas generator are designated as x_1, x_2 and x_3 respectively. Shifts of regulating elements controlling thrust and ratios of fuel components are designated as m_1, m_2 and m_3 respectively. The controlling signal, giving the necessary value of engine thrust, constitutes a change of adjustment of the thrust regulator and is designated as h_1. Controlling signals of the ratio of fuel components – h_2 and h_3. In the case of maintaining constant mixture ratios under all operating conditions of the engine, controlling signals h_2 and h_3 are absent.

External disturbances for all variable values are the same: longitudinal overloads of the flight vehicle n_x.

Knowing the dynamic properties of the object of automatic control and of the regulators, it is necessary to find transfer functions and frequency-response curves of closed systems of automatic control, which are necessary for estimating the dynamic properties of systems and solution of problems of synthesis of regulators and analysis of the accuracy of systems.

As was shown above, in view of the complexity of the object of control, the transfer functions are expediently recorded only in general form and from general expressions of transfer functions we pass to calculation of frequency-response curves.

Systems with two and three variable values are multidimensional systems. Essential simplification of conversion with finding of transfer functions and frequency-response curves in the case of multidimensional systems is attained by means of application of a matrix form of recording the equations [24], [56], which also facilitates preparation of problems for solution with help of electronic digital computers.

Let us consider transfer function in the most general case – for the control system of a liquid propellant rocket engine with three variable values.

The equation of dynamics of the object of control in matrix form was recorded as follows:

$$x = W(p)m + W_f(p)n_x.$$

The equations of dynamics of the three regulators in the absence of cross coupling between regulators and without joint control of the regulators will be recorded in the following way:

$$\left.\begin{aligned} \bar{m}_1 &= N_{11}(p)[K_{x11}\bar{h}_1 - x_1]; \\ \bar{m}_2 &= N_{22}(p)[K_{x22}\bar{h}_2 - x_2]; \\ \bar{m}_3 &= N_{33}(p)[K_{x33}\bar{h}_3 - x_3]. \end{aligned}\right\} \qquad (17.55)$$

where $N_{11}(p)$, $N_{22}(p)$, $N_{33}(p)$ – transfer functions of the regulators; $K_{\text{ш}1}$, $K_{\text{ш}2}$, $K_{\text{ш}3}$ – amplification factors during controlling actions.

The three equations (17.55) are generalized by one matrix equation

$$m=N(p)[K_{\text{ш}}h-x], \tag{17.56}$$

where x – column of variable values; m – column of shifts of regulating elements;

$$h=\begin{bmatrix}\bar{h}_1\\ \bar{h}_2\\ \bar{h}_3\end{bmatrix}$$

– column of controlling signals;

$$N(p)=\begin{bmatrix}N_{11}(p) & 0 & 0\\ 0 & N_{22}(p) & 0\\ 0 & 0 & N_{33}(p)\end{bmatrix} \tag{17.57}$$

– matrix of transfer functions of regulators without cross coupling;

$$K_{\text{ш}}=\begin{bmatrix}K_{\text{ш}1} & 0 & 0\\ 0 & K_{\text{ш}2} & 0\\ 0 & 0 & K_{\text{ш}3}\end{bmatrix} \tag{17.58}$$

– matrix of amplification factors during controlling actions in the case of absence of joint control of the regulators.

In the presence of joint control of the regulators, the matrix (17.58) contains along with diagonal elements also nondiagonal.

If the regulators of ratio of fuel components for the basic chamber and for the gas generator have constant adjustment, and only the thrust regulator has variable adjustment, then the matrix (17.58) contains only one nonzero element $K_{\text{ш}1}$; all other elements – zero.

Excluding from equations (16.66) and (17.56) the column of shifts of regulating elements m, we obtain an equation of dynamics of a closed loop control system:

$$[E_3+W(p)N(p)]x=$$
$$=W(p)N(p)K_1h+W_f(p)n_z, \qquad (17.59)$$

where E_3 – unit matrix of the third order.

Matrix $H(p)$ constitutes a characteristic matrix of the system

$$H(p)=E_3+W(p)N(p), \qquad (17.60)$$

which in the case being examined has the following form:

$$H(p)=\begin{bmatrix} 1+W_{11}(p)N_{11}(p) & W_{12}(p)N_{22}(p) & W_{13}(p)N_{33}(p) \\ W_{21}(p)N_{11}(p) & 1+W_{22}(p)N_{22}(p) & W_{23}(p)N_{33}(p) \\ W_{31}(p)N_{11}(p) & W_{32}(p)N_{22}(p) & 1+W_{33}(p)N_{33}(p) \end{bmatrix}. \qquad (17.61)$$

The determinant of a characteristic matrix is a characteristic polynomial of closed loop control system

$$D(p)=|E_3+W(p)N(p)|. \qquad (17.62)$$

Equating the characteristic polynomial to zero, we obtain the characteristic equation of the control system:

$$D(p)=0, \qquad (17.63)$$

which is used in the analysis of the stability of the system.

Solution of equation (17.59) with respect to the column of variable values x with a nonsingular characteristic matrix gives

$$x=H^{-1}(p)[W(p)N(p)K_1h+W_f(p)n_z] \qquad (17.64)$$

or

$$x = \Phi_h(p)h + \Phi_f(p)n_x, \tag{17.65}$$

where $H^{-1}(p)$ – matrix, reverse to the characteristic matrix of the system;

$$\Phi_h(p) = H^{-1}(p)W(p)N(p)K_h \tag{17.66}$$

– transfer matrix according to controlling actions for a closed automatic control system;

$$\Phi_f(p) = H^{-1}(p)W_f(p) \tag{17.67}$$

– transfer matrix according to external perturbing effects for a closed loop control system.

The transfer matrix according to controlling actions generally consists of a square matrix, composed of transfer functions according to controlling actions:

$$\Phi_h(p) = \begin{bmatrix} \Phi_{1h}(p) & \Phi_{12h}(p) & \Phi_{13h}(p) \\ \Phi_{21h}(p) & \Phi_{22h}(p) & \Phi_{23h}(p) \\ \Phi_{31h}(p) & \Phi_{32h}(p) & \Phi_{33h}(p) \end{bmatrix}. \tag{17.68}$$

where $\Phi_{11h}(p)$ – transfer function for the first variable value according to the first controlling signal; $\Phi_{22h}(p)$ – transfer function for the second variable value according to the second controlling signal, etc.

In the presence of one controlling signal h_1, the transfer matrix (17.68) degenerates into a column

$$\Phi_h(p) = \begin{bmatrix} \Phi_{1h}(p) \\ \Phi_{2h}(p) \\ \Phi_{3h}(p) \end{bmatrix}. \tag{17.69}$$

The transfer matrix according to external disturbance is identical for all variable values, constitutes the column

$$\Phi_f(p)=\begin{bmatrix}\Phi_{1f}(p)\\ \Phi_{2f}(p)\\ \Phi_{3f}(p)\end{bmatrix}. \qquad (17.70)$$

where $\Phi_{1f}(p)$, $\Phi_{2f}(p)$ and $\Phi_{3f}(p)$ – transfer functions for first, second, and third variable values according to external disturbance.

To the transfer functions entering into matrices (17.68) and (17.70) there correspond frequency-response curves, which can most expediently be calculated with help of digital electronic computers. The program of these calculations corresponds to the sequence matrix operations recorded in formulas (17.66) and (17.67). The program of calculating the coefficients of the characteristic polynomial is composed according to formula (17.62).

The basic computing operations during calculation of frequency-response curves are inversion of matrices and multiplication of matrices. On many machines, there are standard programs for the production of these operations.

17.5. Partial Derivatives of Transfer Functions and Frequency-Response Curves of a Control System According to Dynamic Parameters of the Regulators

During the analysis and synthesis of automatic control systems it is necessary to qualitatively and quantitatively estimate the effect of change of dynamic parameters of the regulators on the transmission of controlling signals through the system and on filtration of external disturbances by the system [42].

For such an estimate there can be used partial derivatives of transfer functions and frequency-response curves of the control system according to dynamic parameters of the regulators which characterize the sensitivity of the control system to change of

dynamic parameters. These partial derivatives may also be used very effectively in the selection of optimum values of dynamic parameters of regulators.

Let us consider finding partial derivatives of transfer functions and frequency-response curves of a closed automatic control system according to dynamic parameters of the regulators with known transfer functions or frequency-response curves of the object of control and the regulators.

Direct differentiation with respect to dynamic parameters of matrix ratios (17.66) and (17.67) is practically inexpedient, since differentiation of an inverse matrix is connected with very cumbersome conversions.

In order to avoid differentiation of an inverse matrix, we will copy ratios (17.66) and (17.67) in the following form:

$$[E_s+W(p)N(p)]\Phi_h(p)=W(p)N(p)K_h; \qquad (17.71)$$

$$[E_s+W(p)N(p)]\Phi_f(p)=W_f(p). \qquad (17.72)$$

Differentiating ratio (17.71) according to the dynamic parameter of one of regulators K_i, considering that the transfer matrix of the object of control $W(p)$ and the matrix of coefficients during controlling actions K_h do not depend on parameter K_i; in this case

$$[E_s+W(p)N(p)]\frac{\partial\Phi_h(p)}{\partial K_i}+W(p)\frac{\partial N(p)}{\partial K_i}\Phi_h(p)=-W(p)\frac{\partial N(p)}{\partial K_i}K_h. \qquad (17.73)$$

Solving equation (17.73) with respect to the matrix of partial derivatives of transfer functions according to the dynamic parameter, we obtain

$$\frac{\partial\Phi_h(p)}{\partial K_i}=-[E_s+W(p)N(p)]^{-1}W(p)\frac{\partial N(p)}{\partial K_i}[K_h-\Phi_h(p)]. \qquad (17.74)$$

Formula (17.74) shows in general form the sequence of matrix operations which it is necessary to perform for production of matrix $\partial\Phi_h(p)/\partial K_i$.

Let us differentiate according to dynamic parameter K_i equation (17.72) –

$$[E_3+W(p)N(p)]\frac{\partial\Phi_f(p)}{\partial K_i}+W(p)\frac{\partial N(p)}{\partial K_i}\Phi_f(p)=0. \qquad (17.75)$$

The expression for the matrix of partial derivatives of transfer functions $\partial\Phi_f(p)/\partial K_i$ we obtain in general form, solving equation (17.75):

$$\frac{\partial\Phi_f(p)}{\partial K_i}=-[E_3+W(p)N(p)]^{-1}W(p)\frac{\partial N(p)}{\partial K_i}\Phi_f(p). \qquad (17.76)$$

In the differentiation of equations (17.71) and (17.72) as a necessary condition it is taken that transfer function $\Phi_h(p)$ and $\Phi_f(p)$ and frequence-response curves corresponding to them are continuous functions of parameter K_i in the proximity of its nominal value.

To matrices (17.74) and (17.76) correspond the matrices of derivatives of frequency-response curves of the system according to dynamic parameters of the regulators

$$\frac{\partial\Phi_h(j\omega)}{\partial K_i}=[E_3+W(j\omega)N(j\omega)]^{-1}W(j\omega)\frac{\partial N(j\omega)}{\partial K_i}[K_h-\Phi_h(j\omega)]. \qquad (17.77)$$

$$\frac{\partial\Phi_f(j\omega)}{\partial K_i}=-[E_3+W(j\omega)N(j\omega)]^{-1}W(j\omega)\frac{\partial N(j\omega)}{\partial K_i}\Phi_f(j\omega). \qquad (17.78)$$

Formulas (17.77) and (17.78) show sequence of the matrix operations in which it is necessary to calculate derivatives of frequency-response curves.

The derivative of the frequency-response curve according to the dynamic parameter is composed of derivatives of actual and imaginary frequency-response curves:

$$\frac{\partial\Phi_h(j\omega)}{\partial K_i}=\frac{\partial P_h(\omega)}{\partial K_i}+j\frac{\partial Q_h(\omega)}{\partial K_i}. \qquad (17.79)$$

According to the form of the frequency-response curves, it is possible to estimate the transition process in an automatic control system [2].

The effect of the dynamic parameters of regulators on the transmission of a controlling signal through the automatic control system is estimated according to the values and signs of the partial derivatives of actual frequency-response curves of a closed loop control system.

Thus, for example, when $[\partial P_{11A}(\omega)/\partial K_i]>0$, in the passband of frequencies the increase in the value of dynamic parameter K_i accelerates the transition process according to pressure in the basic chamber of the engine appearing during supply of the controlling signal to the thrust regulator. In the case where $[\partial P_{11A}(\omega)/\partial K_i]<0$, in the passband of frequencies the increase of value K_i retards the transition process.

The signal controlling thrust of the engine should render minimum effect on the mixture ratio, therefore in the passband of frequencies it is desirable to obtain a minimum value of the modulus of frequency-response curve $|\Phi_{21A}(j\omega)|$ for the fuel mixture ratio according to the thrust change controlling signal.

With a change of values of dynamic parameters of the thrust regulator it is desirable to ensure

$$\frac{\partial}{\partial K_i}|\Phi_{21A}(j\omega)|<0.$$

The effect of change of dynamic parameters of regulators on filtration of external disturbance by the system is estimated according to the character of change in the passband of the frequencies of partial derivatives

$$\frac{\partial}{\partial K_i}|\Phi_{1f}(j\omega)| \quad \text{and} \quad \frac{\partial}{\partial K_i}|\Phi_{2f}(j\omega)|.$$

Improvement of the filtration of external perturbing effect with an increase in value of parameter K_i takes place in the case

$$\frac{\partial}{\partial K_i}|\Phi_{1f}(j\omega)| < 0$$

and

$$\frac{\partial}{\partial K_i}|\Phi_{2f}(j\omega)| < 0.$$

Analogously to this, as partial derivatives of frequency-response curves of control system are calculated according to dynamic parameters of the regulators, there can be calculated partial derivatives of frequency-response curves of the control system according to dynamic parameters of the object of control and also partial derivatives according to design parameters of the object of control and of the regulators.

These partial derivatives show the effect of change of design parameters of the object of control and of the regulators on frequency-response curves of the control system.

17.6. Selection of Dynamic Parameters of Regulators with Prescribed Technical Conditions for an Automatic Control System

In the selection of dynamic parameters of regulators it is necessary to ensure fulfillment of a number of requirements imposed upon the system. These requirements, in considerable measure, depend upon the mission and conditions of combat employment of the flight vehicle, and are formulated in technical conditions on the automatic control system of the engine.

One of the important requirements imposed upon the control system is obtaining the required quality of the transition process according to the basic variable values of the engine during feed of the control controlling signal to the inlet of the system. On the change of certain variable values during the transition process there can be put limitations.

The automatic control system of a liquid propellant rocket engine can include several regulators mutually connected among themselves through the object of control. This connection is reflected in the transfer matrix of the object of control.

In the strict formulation of the problem of synthesis of automatic control system there is included selection of optimum structure and optimum parameters of all regulators, taking into account their mutual effect. The solution of this problem is connected with considerable fundamental and computational difficulties. Realization of an optimum system found by theoretical means can be connected with technical difficulties and in many cases can be inexpedient.

Certain authors recommend a practical means of solving the problem of synthesis occurring in the selection of a number of technically expedient structures of the system and determination of the dynamic parameters of each of the structures according to the criterion of optimality corresponding to the mission and operating conditions of the system. A comparison of variants makes it possible to select from among them the one which in best degree satisfies the totality of requirements imposed upon the systems. This method leads to considerable reduction of computational work and rapidly provides a practically acceptable solution. In this study such a means of solution is taken as basic.

Solution of the problem of synthesis of an automatic control system can be expediently performed in two stages.

In the first stage, on the basis of analysis of dynamic properties of a concrete object of control there are performed a number of simplifying assumptions essentially facilitating the solution of the problem. In so doing, values of dynamic parameters of regulators are determined in first approximation.

Investigation of a liquid propellant rocket engine of open circuits without afterburning of gas after the turbine shows that the time constant of the turbopump assembly essentially exceeds in

value the time constants of other dynamic sections and the time lag in the basic chamber and gas generator. As a simplifying assumption in the first stage of solution of the problem of synthesis it is possible to disregard inertness of all sections, except the turbopump assembly, and the lags in the basic chamber and gas generator. The object of control, on the whole, will thus constitute a link of the first order.

For a liquid propellant rocket engine without afterburning, having regulating control of thrust on the feed line by the fuel component of the gas generator, shifting of this regulating element renders a weak influence on the fuel mixture ratio in comparison with the shift of the element regulating this ratio. This is connected with the special selection of characteristics of pumps and hydraulic main lines in the designing of the engine. In first approximation, effect of shift of the regulating element of the thrust regulator on mixture ratio can be disregarded and to consider the operation of the mixture ratio regulator independently from the operation of the thrust regulator.

With the assumptions mentioned the automatic control system of a liquid propellant rocket engine is broken down into several independent systems, each of which consists of an object of control of the first order and one regulator. Selection of dynamic parameters of regulators for first approximation in this case constitutes a very simple problem.

In the second stage of solution of problem, the simplifying assumptions mentioned above are not made, and the values of dynamic parameters of the regulators are defined more accurately during joint consideration of the whole control system, taking into account the mutual effect of the regulators.

Such a solution of the problem of synthesis of the system in two stages leads to a considerable reduction in computational work. In the transition from the first stage of solution of problem to the second, changes of parameters of regulators are small compared with their absolute values, and the transfer function of control system

on second stage of solution of problem can be represented in the form of linearized dependences on increase of the dynamic parameters of the regulators. This makes it possible to easily find these increases which must be added to values of parameters found in the first stage of solution for optimization of the automatic control system in conformity with the accepted criteria.

To estimate the quality of transition processes appearing in a control system during supply to the input of the system of controlling signals in the form of a single step function, wide use is made [24] of integral estimates

$$J_0=\int_0^\infty [x(t)]^2\,dt; \tag{17.80}$$

$$J_1=\int_0^\infty \left[x^2(t)+\tau^2\left(\frac{dx}{dt}\right)^2\right]dt \tag{17.81}$$

and certain other integral estimates.

In formulas (17.80) and (17.81) dependence $x(t)$ constitutes a transition component of error:

$$x(t)=h(\infty)-h(t),$$

where $h(\infty)$ – value of variable magnitude after termination of the transition process; $h(t)$ – transfer function of the system.

A minimum of integral estimates J_0 or J_1 under the condition of limitation of a number of values characterizing engine operating mode during the transition process is frequently used as a criterion in the synthesis of an automatic control system.

The transition component of error and its time derivative are expressed as an actual frequency-response curve of a closed-loop control system in the form of integral ratios:

$$x_1(t)=\frac{2}{\pi}\int_0^\infty \frac{\Phi_{11}(0)-P_{11}(\omega)}{\omega}\sin\omega t\cdot d\omega; \tag{17.82}$$

$$\frac{dx_1(t)}{dt}=-\frac{2}{\pi}\int_0^\infty P_{11}(\omega)\cos\omega t\cdot d\omega, \tag{17.83}$$

where $P_{11}(\omega)$ – actual frequency-response curve of a closed system for variable value $x_1(t)$ according to controlling signal h_1; $\Phi_{11}(0)$ – static amplification factor of a closed-loop system.

Integral estimates of the quality of transition process can be expressed as frequency-response curves of the system by means of Lyapunov-Parseval formulas [8]:

$$\int_0^\infty [x_1(t)]^2 dt = \frac{2}{\pi}\int_0^\infty \left[\frac{\Phi_{11}(0)-P_{11}(\omega)}{\omega}\right]^2 d\omega; \qquad (17.84)$$

$$\int_0^\infty \left[x_1^2(t)+\tau^2\left(\frac{dx_1}{dt}\right)^2\right] dt =$$

$$= \frac{2}{\pi}\int_0^\infty \left\{\left[\frac{\Phi_{11}(0)-P_{11}(\omega)}{\omega}\right]^2+\tau^2[P_{11}(\omega)]^2\right\} d\omega. \qquad (17.85)$$

The transfer function of a closed-loop control system in a wide range of values of dynamic parameters of the regulators, as a rule, is a continuous function of these parameters and allows differentiation by it

$$\Phi_{11}(p)=\Phi_{11}(p, K_i),$$

where $K_i(i=1, 2,\ldots l)$ – dynamic parameters of regulators.

Integral estimates of the quality of transition process here also constitute continuous functions of dynamic parameters of the regulators.

For small increases of dynamic parameters δK_i, the increase of integral estimate δJ_0 can be represented in the form of a linearized dependence

$$\delta J_0 = \sum_{i=1}^{l}\left(\frac{\partial J_0}{\partial K_i}\right)_0 \delta K_i; \qquad (17.86)$$

here $\left(\frac{\partial J_0}{\partial K_i}\right)_0$ – the value of the partial derivative of integral estimate according to dynamic parameter K_i with initial values of dynamic parameters.

Analogously, an increase of integral estimate can be recorded δJ_1.

Differentiating equality (17.84) according to dynamic parameter K_i, we obtain

$$\frac{\partial J_0}{\partial K_i} = \frac{4}{\pi}\left\{\frac{\partial \Phi_{11}(0)}{\partial K_i}\int_0^\infty \frac{\Phi_{11}(0)-P_{11}(\omega)}{\omega^2}d\omega - \right.$$

$$\left. -\int_0^\infty \frac{\Phi_{11}(0)-P_{11}(\omega)}{\omega^2}\cdot\frac{\partial P_{11}(\omega)}{\partial K_i}d\omega\right\}. \qquad (17.87)$$

It is easy to prove that both integrals in the right part of equality (17.87) are convergent.

Partial derivatives of frequency-response curves according to dynamic parameters of regulators are determined by the method expounded in § 5.17.

Integral estimates J_0 and J_1 in the case examined are functions of dynamic parameters $J_0(K_i)$ and $J_1(K_i)$. Approximation to minimum of functions $J_0(K_i)$ and $J_1(K_i)$ with the employment of linearized dependences (17.86) can be very effectively carried out, using the method of steepest descent [42].

The relationship between increases δK_i in each approximation here are taken so that vector $\overline{\delta K}$, the components of which are $\delta K_1, \delta K_2$, etc., coincides in direction with the vector of gradient of function $J_0(K_i)$ or $J_1(K_i)$.

For first approximation there are calculated by formula (17.87) values of partial derivatives $(\partial J_0/\partial K_i)_0$ with initial values of dynamic parameters of the regulators $(K_i)_0$, obtained in the first stage of solution of the problem of synthesis of the system.

In certain cases, during synthesis of a system of automatic regulating there occurs a given specific transition process, which is considered optimum, and there is raised the problem of creating a regulator ensuring realization of this process. Such a problem can be solved by linearization of the integral estimate of the

transition process relative to small variations in the dynamic parameters of the regulators.

In the first stage of solution, analogously to the problem examined above, with very simplifying assumptions, we find the values of dynamic parameters of the regulators of first approximation. In the second stage of solution, values of the dynamic parameters are defined more accurately.

In the graph in Fig. 17.5, the given optimum transition process is designated as $\varphi(t)$. The transition process obtained with certain values of dynamic parameters of the regulators is designated as $x(t)$. Approximation to optimum transition process is carried out by minimization of integral error of the transition process.

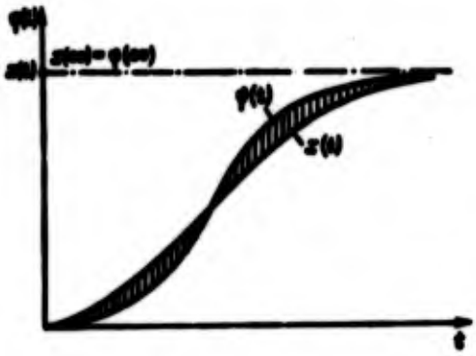

Fig. 17.5. Synthesizing an automatic control system.

Transition component of error of the optimum process is designated as

$$\varepsilon_\varphi(t)=\varphi(\infty)-\varphi(t); \tag{17.88}$$

transition component of error of the process $x(t)$ is designated as

$$\varepsilon_x(t)=x(\infty)-x(t). \tag{17.89}$$

Relative error of approximation to optimum transition process is equal to

$$\varepsilon(t)=\frac{\varepsilon_\varphi(t)}{\varphi(\infty)}-\frac{\varepsilon_x(t)}{x(\infty)}. \tag{17.90}$$

The frequency-response curve of optimum system $\Phi_0(j\omega)$ corresponds to optimum process.

Transition component of error of optimum system can be expressed as a real frequency-response curve of optimum system:

$$\varepsilon_0(t)=\frac{2}{\pi}\int_0^\infty \frac{P_0(0)-P_0(\omega)}{\omega}\sin\omega t\cdot d\omega, \qquad (17.91)$$

and the transition component of error $\varepsilon_x(t)$ – as real frequency-response curve of a synthesized system $P_x(\omega)$, realizing transition process $x(t)$:

$$\varepsilon_x(t)=\frac{2}{\pi}\int_0^\infty \frac{P_x(0)-P_x(\omega)}{\omega}\sin\omega t\cdot d\omega. \qquad (17.92)$$

Taking into account equations (17.90), (17.91)- and (17.92), we record integral relationship for relative error of approximation to optimum transition process:

$$\varepsilon(t)=\frac{2}{\pi}\int_0^\infty\left[\frac{P_0(0)-P_0(\omega)}{\varphi(\infty)}-\frac{P_x(0)-P_x(\omega)}{x(\infty)}\right]\frac{\sin\omega t}{\omega}d\omega. \qquad (17.93)$$

For the controlling signal of the unit step function type

$$x(\infty)=P_x(0);\quad \varphi(\infty)=P_0(0)$$

and, consequently:

$$\varepsilon(t)=\frac{2}{\pi}\int_0^\infty[\overline{P_x(\omega)}-\overline{P_0(\omega)}]\frac{\sin\omega t}{\omega}d\omega, \qquad (17.94)$$

where there is designated

$$\overline{P_x(\omega)}=\frac{P_x(\omega)}{P_x(0)} \quad \text{and} \quad \overline{P_0(\omega)}=\frac{P_0(\omega)}{P_0(0)}.$$

Integral estimate of relative error of approximation to optimum transition process equals

$$J_\varepsilon=\int_0^\infty[\varepsilon(t)]^2\,dt. \qquad (17.95)$$

Applying in conformity with relative error of approximation (17.94) the Lyapunov-Parseval formula, we obtain the expression of integral estimate as real frequency-response curves:

$$J_0 = \frac{2}{\pi}\int_0^\infty [\overline{P_д(\omega)} - \overline{P_э(\omega)}]^2 \frac{d\omega}{\omega^2}. \qquad (17.96)$$

Along with the frequency responses of a system, integral estimate J_0 for a stable system is a continuous function of dynamic parameters of the regulators in the environment of their nominal values and allows differentiation with respect to these parameters.

$$\frac{\partial J_0}{\partial K_i} = \frac{4}{\pi}\int_0^\infty [\overline{P_д(\omega)} - \overline{P_э(\omega)}] \frac{\partial \overline{P_д(\omega)}}{\partial K_i} \frac{d\omega}{\omega^2}, \qquad (17.97)$$

where

$$\frac{\partial \overline{P_д(\omega)}}{\partial K_i} = \frac{1}{P_д(0)} \frac{\partial P_д(\omega)}{\partial K_i} - \frac{P_д(\omega)}{P_д^2(0)} \frac{\partial P_д(0)}{\partial K_i}. \qquad (17.98)$$

Variation of integral estimate δJ_0 with small deviations of dynamic parameters of the regulators can be represented in the form of linearized dependence on variations of parameters

$$\delta J_0 = \sum_{i=1}^{l} \left(\frac{\partial J_0}{\partial K_i}\right)_0 \delta K_i. \qquad (17.99)$$

Values of partial derivatives of integral estimate according to dynamic parameters of regulators are calculated by formula (17.97).

Approximation to minimum of integral estimate $J_0(K_i)$ is expediently carried out with help of dependence (17.99) according to method of steepest descent [42]. In so doing, between increases of dynamic parameters of the regulators of first approximation there must be following relationship:

$$\frac{(\delta K_1)_1}{\left(\frac{\partial J_0}{\partial K_1}\right)_0} = \frac{(\delta K_2)_1}{\left(\frac{\partial J_0}{\partial K_2}\right)_0} = \ldots = \frac{(\delta K_l)_1}{\left(\frac{\partial J_0}{\partial K_l}\right)_0} = B_1. \qquad (17.100)$$

As was shown above, the initial values of dynamic parameters of the regulators, from which is conducted approximation to optimum values, we obtain fulfilling approximate calculation with essential simplifications. To the initial values of dynamic parameters $(K_i)_0$ there corresponds the initial value of integral estimate $(J_0)_0$ calculated by formula (17.96).

Variations of dynamic parameters of first approximation are expediently taken in such a way that the variation of integral estimate of relative error, in highest possible measure, will compensate its initial integral estimate. The condition of full compensation of initial integral appraisal will be recorded in the following way:

$$\Delta J_0 = -(J_0)_0. \tag{17.101}$$

Solving jointly equations (17.99), (17.100), and (17.101) we find the value of the coefficient needed for realization of compensation

$$B_1 = -\frac{(J_0)_0}{\sum_{i=1}^{l}\left(\frac{\partial J_0}{\partial K_i}\right)_0^2} \tag{17.102}$$

and according to the relationship (17.100), we determine variation of dynamic parameters of regulators for first approximation.

17.7. Calculating the Accuracy of Automatic Control Systems

Very stringent requirements with respect to accuracy are imposed on automatic control systems of a liquid propellant rocket engine. One of the important factors affecting accuracy of these systems is accuracy in the manufacture of elements of construction of the engine and the regulators, and also accuracy in adjustment of separate units of the engine to assigned characteristics.

Elements of construction are manufactured with defined technological tolerances. By virtue of this, static and dynamic characteristics of the elementary sections of the system and characteristics of the system on the whole constitute random functions, the scattering of possible realization of which depends on technological and adjustment tolerances.

In the investigation of static accuracy of automatic control systems there is posed the problem of determining maximum possible errors of controlling values on steady state of operation of the system, depending upon errors in constructional parameters and on the character of the connection between elements of the system.

In studying the dynamic accuracy of a system it is necessary to determine maximum possible errors of frequency-response curves and transition processes depending upon errors of those same design parameters.

To estimate the static accuracy of a system it is necessary to examine the connection between errors of inlet and outlet coordinate and error in static characteristic of the section of the automatic control system.

In Fig. 17.6 there is shown the static characteristic of link with one inlet and one outlet coordinate. The standard static characteristic is designated as $x_2^0(x_1)$ one of the possible realizations of static characteristic as $x_2(x_1)$.

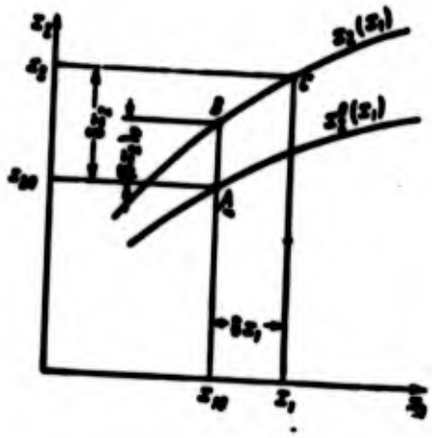

Fig. 17.6. Static characteristic of a link in an automatic control system with random parameters.

Nominal values of inlet and outlet coordinates are designated $x_{1\text{н}}$ and $x_{2\text{н}}$ respectively, errors of inlet and outlet coordinates on steady state – δx_1 and δx_2. Initial error of static characteristic with nominal value of inlet coordinate designated $(\delta x_2)_0$.

As a basic assumption it is accepted that errors of inlet and outlet coordinates are small as compared to their nominal values, but the derivative of error of coordinate according to inlet coordinate constitutes value of higher order of smallness as compared to the value of derivative of nominal static characteristic at point A~

$$\delta x_1 \ll x_{1\text{н}};\ \delta x_2 \ll x_{2\text{н}};\ \frac{d(\delta x_2)}{dx_1} \ll \frac{dx_2^0}{dx_1}.$$

We will record the equation of connection between errors of coordinates and initial error of static characteristic:

$$\delta x_2 = (\delta x_2)_0 + \left(\frac{dx_2}{dx_1}\right)_0 \delta x_1, \qquad (17.103)$$

where $(dx_2/dx_1)_0$ characterizes the slope of static characteristic at point B.

Taking into account that

$$\left(\frac{dx_2}{dx_1}\right)_0 = \left(\frac{dx_2^0}{dx_1}\right)_0 + \left[\frac{d(\delta x_2)}{\delta x_1}\right]_0 \qquad (17.104)$$

and disregarding values of higher order of smallness, we obtain:

$$\delta x_2 = (\delta x_2)_0 + K_{21}\delta x_1, \qquad (17.105)$$

where K_{21} amplification factor of the link.

For a link with several coordinates of system on inlet and with several controlling actions y_j, the equation of connection of errors takes the following form:

$$\delta x_i=(\delta x_i)_0+K_{i1}\delta x_1+\ldots+K_{i,(i-1)}\delta x_{i-1}+$$
$$+K_{i,(i+1)}\delta x_{i+1}+\ldots+K_{in}\delta x_n+\sum_{j=1}^{m}l_{ij}\delta y_j. \qquad (17.106)$$

Equations of connections of errors of coordinates and controlling actions for a control system, having n lines, are recorded in the form of one matrix equation

$$K\delta x=(\delta x)_0+L\delta y, \qquad (17.107)$$

where K – matrix composed of amplification factors of the links; L – matrix of coefficients during controlling actions; δx and δy – columns of errors of coordinates and error of controlling actions; $(\delta x)_0$ – column of initial errors of static characteristics of links.

Matrices K and L have the following form:

$$K=\begin{bmatrix}1 & -K_{12}\ldots-K_{1n}\\ -K_{21} & 1\ldots-K_{2n}\\ \ldots\ldots\ldots\ldots\\ -K_{n1} & -K_{n2}\ldots 1\end{bmatrix};\quad L=\begin{bmatrix}l_{11}\ldots l_{1m}\\ \ldots\ldots\\ l_{n1}\ldots l_{nm}\end{bmatrix}.$$

With small errors of design parameters of the engine and regulators, initial error of static characteristic of each link can be represented in the form of a linearized dependence on errors of design parameters:

$$(\delta x_i)_0=\sum_{j=1}^{r}\left[\frac{\partial(\delta x_i)_0}{\partial l_j}\right]_0\Psi_j. \qquad (17.108)$$

The basic design parameters affecting static characteristics of links for the chamber of a liquid propellant rocket engine are the areas of critical and outlet section of the nozzle, for the centrifugal pump – external diameter of the impeller, width of blade on inlet and outlet, etc.

Let us introduce the designations

$$\left[\frac{\partial(\delta x_i)_0}{\partial l_j}\right]_0 = S_{ij} \tag{17.109}$$

and record for column $(\delta x)_0$ matrix ratio

$$(\delta x)_0 = S\delta l. \tag{17.110}$$

Here S – rectangular matrix, having n rows and r columns; δl – column of errors of design parameters.

Solution of equation (17.107) gives the column of errors of coordinates of the control system on steady state:

$$\delta x = K^{-1}S\delta l + K^{-1}L\delta y. \tag{17.111}$$

If equation (17.107) describes the object of control, then solution (17.111) can be expediently presented in the following form:

$$\delta x = (\delta x)_{00} + K_y\delta y, \tag{17.112}$$

where

$$(\delta x)_{00} = A_{00}\delta l_{00} \tag{17.113}$$

– column of initial errors of static characteristics of the object of control;

$$A_{00} = K^{-1}S \tag{17.114}$$

– matrix of coefficients of influence of errors of design parameters on errors of static characteristics;

$$K_y = K^{-1}L \tag{17.115}$$

– matrix of amplification factors of the object of control.

The equation of the object of control must be examined jointly with equations of the regulators.

From matrix relationship (17.112) we separate those equations which refer to coordinates which are inlets for regulators:

$$\delta x_q = (\delta x_{o6})_q + K_q \delta y, \tag{17.116}$$

where δx_q – column of coordinates of the object, which are inlets for regulators; $(\delta x_{o6})_q$ – column of initial errors of static characteristics for coordinates x_q.

The shortened matrix of coefficients of effect we will designate as A^q_{o6} and, consequently:

$$(\delta x_{o6})_q = A^q_{o6} \delta U_{o6}. \tag{17.117}$$

The equations of connections of errors for regulators are generalized by one matrix relationship

$$\delta y = (\delta y)_0 - K_p \delta x_q, \tag{17.118}$$

where $(\delta y)_0$ – column of initial errors of static characteristics of regulators; K_p – matrix of amplification factors of regulators.

$$K_p = \begin{bmatrix} K^p_{11} \dots K^p_{1m} \\ \dots\dots\dots \\ K^p_{m1} \dots K^p_{mm} \end{bmatrix}.$$

Dependence of the column of initial errors of static characteristics of regulators on column of errors of design and adjustment parameters of the regulators is determined by the matrix of coefficients of effect A_{pn} containing m rows and s columns:

$$(\delta y)_0 = A_p \delta U_p. \tag{17.119}$$

For estimating the error of coordinates of a closed-loop control system, we exclude from equations (17.116) and (17.118) column

$$[E+K_\varphi K_p]\delta x_\varphi=(\delta x_{o6})_\varphi+K_\varphi(\delta y)_0. \tag{17.120}$$

We solve equation (17.120) relative to the column of errors of coordinates on steady state:

$$\delta x_\varphi=[E+K_\varphi K_p]^{-1}\{(\delta x_{o6})_\varphi+K_\varphi(\delta y)_0\}. \tag{17.121}$$

Taking into account equations (17.117) and (17.119), the solution (17.121) we record in the following form:

$$\delta x_\varphi=B_{o6}\delta l_{o6}+B_p\delta l_p. \tag{17.122}$$

In solution (17.122) matrices B_{o6} and B_p are composed of coefficients of effect of errors of design parameters of the object of control and regulators on error of coordinates δx_φ, where

$$B_{o6}=[E+K_\varphi K_p]^{-1}A^\varphi_{o6}; \tag{17.123}$$

$$B_p=[E+K_\varphi K_p]^{-1}K_\varphi A_p. \tag{17.124}$$

All initial design parameters l_{o6} and l_p usually consist of mutually independent random quantities, mathematical expectations of which equal nominal values of the parameters.

Probabilistic characteristics of these random variables are determined by technology and also by operating conditions.

With known dispersions of design and adjustment parameters, relationship (17.122) can be used for calculating the dispersions of errors of coordinates of the control system on steady state of operation. Elements of matrices B_{o6} and B_p characterize the influence of errors of design and adjustment parameters on errors of coordinates of the control system. For concrete cases in examining matrices B_{o6} and B_p, recommendations can be made in regard to change of tolerances.

Amplification factors of the regulators render an essential effect on static errors of adjustable values. For estimating the effect of change of amplification factors of regulators on errors of coordinates of the system there can be used partial derivatives of coefficients of effect of components of matrix (17.123) and (17.124) according to amplification factor K_f of the regulators.

Differentiation of relationships (17.123) and (17.124) according to a certain amplification factor K_f gives matrices of partial derivatives of coefficients of effect in respect to K_f:

$$\frac{\partial B_{\alpha\alpha}}{\partial K_f} = -[E + K_\alpha K_\beta]^{-1} \frac{\partial [E + K_\alpha K_\beta]}{\partial K_f} B_{\alpha\alpha}; \qquad (17.125)$$

$$\frac{\partial B_{\beta}}{\partial K_f} = -[E + K_\alpha K_\beta]^{-1} \frac{\partial [E + K_\alpha K_\beta]}{\partial K_f} B_{\beta}. \qquad (17.126)$$

According to relationship (17.122), error of the i-th coordinate of system is equal to

$$\delta x_i = \sum_{j=1}^{r} (B_{ij} \delta l_j)_{\alpha\alpha} + \sum_{j=1}^{s} (B_{ij} \delta l_j)_{\beta}. \qquad (17.127)$$

Dispersion of error is determined by the formula

$$D[\delta x_i] = \sum_{j=1}^{r} [B_{ij}^2 D[\delta l_j]]_{\alpha\alpha} + \sum_{j=1}^{s} [B_{ij}^2 D[\delta l_j]]_{\beta}, \qquad (17.128)$$

where $D[\delta l_j]$ – dispersion of design parameters and adjustment parameters determined in conformity with tolerances.

Differentiating expression (17.128) by the amplification factor of any of the regulators K_f, we obtain

$$\left\{\frac{\partial}{\partial K_f} D[\delta x_i]\right\}_0 = A_{if} = 2 \sum_{j=1}^{r} \left\{B_{ij} \left(\frac{\partial B_{ij}}{\partial K_f}\right)_0 D[\delta l_j]\right\}_{\alpha\alpha} +$$

$$+ 2 \sum_{j=1}^{s} \left\{B_{ij} \left(\frac{\partial B_{ij}}{\partial K_f}\right)_0 D[\delta l_j]\right\}_{\beta}. \qquad (17.129)$$

In formula (17.129) $(\partial B_{ij}/\partial K_j)_0$ represents elements of i-th rows of matrices (17.125) and (17.126). Coefficients A_{ij} characterize the effect of change of amplification factors of regulators on the dispersion of adjustable value x_i. For a decrease of dispersion of adjustable value, it is expedient to change, in the first place, those amplification facotrs with which coefficients of effect A_{ij} are large.

Change of dispersion of adjustable value with a change of amplification factors of regulators ΔK_j can be approximately estimated by the formula

$$\Delta D[\delta x_i] = \sum_{j=1}^{k} A_{ij} \Delta K_j. \qquad (17.130)$$

where k – total number of variable amplification factors.

Calculations for estimating the static accuracy of automatic control systems include, as basic calculation operations, inversion of matrices and multiplication of matrices. These operations are easily accomplished with help of electronic digital computers on standard programs.

As was shown above, in the study of dynamic accuracy of automatic control systems the problem arises of estimating the dispersions of frequency-response curves and transition processes depending upon dispersions of design and adjustment parameters of the object of control and of the regulators.

Each frequency-response curve of the system or object of automatic control can be represented in the form of the sum of the nominal frequency-response curve and its random component, caused by scattering of values of design and adjustment parameters:

$$W(j\omega) = W_0(j\omega) + \delta W(j\omega). \qquad (17.131)$$

The random component of frequency-response curve $\delta W(j\omega)$ depends on the scattering of values of dynamic parameters of the links. For the object of automatic control, it is necessary to consider scattering of all dynamic parameters entering into equations (16.52).

If the errors of dynamic parameters are small as compared to their nominal values, then the random component of the frequency-response curve can be represented in the form of a linearized dependence on errors of parameters:

$$\delta W(j\omega)=\sum_{j=1}^{s}\frac{\partial W(j\omega)}{\partial K_j}\delta K_j. \qquad (17.132)$$

In formula (17.132) there are designated as K_j all the dynamic parameters of the system, i.e., amplification factors, time constants, and time lags.

For production of partial derivatives $\partial W(j\omega)/\partial K_j$; for object of control, we will differentiate matrix equation (16.54) by the dynamic parameter found on the i-th row and in the j-th column of the matrix $A(p)$:

$$A(p)\frac{\partial W(p)}{\partial K_{ij}}+\frac{\partial A(p)}{\partial K_{ij}}W(p)=0. \qquad (17.133)$$

In differentiation we assume that the frequency-response curves in the vicinity of nominal value of parameter K_{ij} are continuous functions of this parameter. Solving equation (17.133), we obtain a matrix of partial derivatives:

$$\frac{\partial W(p)}{\partial K_{ij}}=-A^{-1}(p)\frac{\partial A(p)}{\partial K_{ij}}W(p), \qquad (17.134)$$

Matrix $\partial A(p)/\partial K_{ij}$ in the case of differentiation with respect to the amplification factor has only one nonzero element, equal to unity, on the i-th row in the j-th column:

$$\frac{\partial A(p)}{\partial K_{ij}}=\begin{bmatrix}0&\dots&0\\ \vdots&&\vdots\\ 0&\dots&1_{ij}&\dots&0\\ \vdots&&\vdots\\ 0&\dots&0\end{bmatrix}. \qquad (17.135)$$

In case of differentiation of a characteristic matrix according to time constant and time lag of the i-th link respectively we obtain

$$\frac{\partial A(p)}{\partial T_i} = p e^{-p\tau_i} \begin{bmatrix} 0 & \dots & 0 \\ \dots & \dots & \dots \\ 0 & \dots & 1_{ij} \dots 0 \\ \dots & \dots & \dots \\ 0 & \dots & 0 \end{bmatrix}; \qquad (17.136)$$

$$\frac{\partial A(p)}{\partial \tau_i} = (T_i p + 1) p e^{-p\tau_i} \begin{bmatrix} 0 & \dots & 0 \\ \dots & \dots & \dots \\ 0 & \dots & 1_{ij} \dots 0 \\ \dots & \dots & \dots \\ 0 & \dots & 0 \end{bmatrix}. \qquad (17.137)$$

The matrix, inverse to the characteristic matrix of the system, is designated

$$A^{-1}(j\omega) = C(j\omega) = \begin{bmatrix} C_{11}(j\omega) \dots C_{1n}(j\omega) \\ \dots \dots \dots \dots \\ C_{n1}(j\omega) \dots C_{nn}(j\omega) \end{bmatrix}. \qquad (17.138)$$

Performing matrix conversions according to equation (17.134), we obtain a matrix of partial derivatives in expanded form:

$$\frac{\partial W(j\omega)}{\partial K_{ij}} = -\begin{bmatrix} C_{1i}(j\omega) W_{j1}(j\omega) \dots C_{1i}(j\omega) W_{jm}(j\omega) \\ C_{2i}(j\omega) W_{j1}(j\omega) \dots C_{2i}(j\omega) W_{jm}(j\omega) \\ \dots \dots \dots \dots \\ C_{ni}(j\omega) W_{j1}(j\omega) \dots C_{ni}(j\omega) W_{jm}(j\omega) \end{bmatrix}. \qquad (17.139)$$

From consideration of matrix (17.139) it follows that the derivative of the frequency-response curve found in matrix $W(j\omega)$ on the p-th row and in the t-th column in respect to amplification factor K_{ij} equal to

$$\frac{\partial W_{pt}(j\omega)}{\partial K_{ij}} = C_{pi}(j\omega) W_{jt}(j\omega). \qquad (17.140)$$

Derivative frequency-response curves according to time constant and time lag of the i-th link respectively are equal, taking into account equalities (17.136) and (17.137), to

$$\frac{\partial W_{pl}(j\omega)}{\partial T_i} = j\omega e^{j\omega\tau_i} C_{pl}(j\omega) W_{ii}(j\omega); \qquad (17.141)$$

$$\frac{\partial W_{pl}(j\omega)}{\partial \tau_i} = j\omega e^{j\omega\tau_i} (T_i j\omega + 1) C_{pl}(j\omega) W_{ii}(j\omega). \qquad (17.142)$$

As can be seen by formulas (17.140), (17.141), and (17.142) all derivatives are obtained by the simple operation of multiplication of frequency-response curves.

The random component of the frequency-response curve (17.132) is composed of random components of real and imaginary frequency-response curves:

$$\delta W(j\omega) = \sum_{j=1}^{s} \left[\frac{\partial P(\omega)}{\partial K_j} + j \frac{\partial Q(\omega)}{\partial K_j} \right] \delta K_j; \qquad (17.143)$$

$$\delta P(\omega) = \sum_{j=1}^{s} \frac{\partial P(\omega)}{\partial K_j} \delta K_j; \qquad (17.144)$$

$$\delta Q(\omega) = \sum_{j=1}^{s} \frac{\partial Q(\omega)}{\partial K_j} \delta K_j. \qquad (17.145)$$

Resolutions of random functions (17.143), (17.144), and (17.145) are not canonical [42], since random variables δK_j depend on initial design and adjustment parameters, can be interdependent. To use these resolutions for direct calculation of dispersions of frequency-response curves is not feasible.

Transition to canonical resolutions of frequency-response curves will be carried out by replacement of random variables δK_j by a system of mutually independent random quantities δl_i consisting of errors of design parameters and errors of adjustment. Dispersions of random variables δl are determined by technological tolerances in the manufacture of parts and tolerances in adjustment of objects of control and regulators.

Dynamic parameters of the links depend on design parameters l_i:

$$K_j = K_j(l_1, \ldots, l_p). \tag{17.146}$$

A small error of dynamic parameter K_j by means of linearization of equation (17.146) can be represented depending upon small errors of design parameters and on errors of adjustment:

$$\delta K_j = \sum_{i=1}^{p} \left(\frac{\partial K_j}{\partial l_i}\right)_0 \delta l_i. \tag{17.147}$$

We will designate the coefficients of effect of errors of design parameters as

$$\left(\frac{\partial K_j}{\partial l_i}\right)_0 = H_{ji}$$

and we will record totality of equations of form (17.147) by one matrix equation

$$\delta K = H \delta l, \tag{17.148}$$

where δK – column of errors of dynamic parameters of links;
δl – column of errors of design parameters and errors of adjustment;

$$H = \begin{bmatrix} H_{11} \ldots H_{1p} \\ \ldots\ldots\ldots \\ H_{q1} \ldots H_{qp} \end{bmatrix} \tag{17.149}$$

– rectangular matrix of coefficients of effect.

Relationship (17.148) we will use for transition from resolutions (17.144) and (17.145) to canonical resolutions of errors of frequency-response curves.

Substituting linearized dependence (17.147) in resolutions (17.144) and (17.145) and changing the order of summation, we obtain

$$\delta P(\omega)=\sum_{q=1}^{r}\frac{\partial P(\omega)}{\partial u_q}u_q; \qquad (17.150)$$

$$\delta Q(\omega)=\sum_{q=1}^{r}\frac{\partial Q(\omega)}{\partial u_q}u_q. \qquad (17.151)$$

For calculation of nonrandom coordinate functions entering into canonical resolutions (17.150) and (17.151), we will obtain the formulas

$$\frac{\partial P(\omega)}{\partial u_q}=\sum_{j=1}^{s}\frac{\partial P(\omega)}{\partial K_j}H_{jq} \qquad (17.152)$$

and

$$\frac{\partial Q(\omega)}{\partial u_q}=\sum_{j=1}^{s}\frac{\partial Q(\omega)}{\partial K_j}H_{jq}, \qquad (17.153)$$

where H_{jq} – elements of the q-th column of matrix H.

Using canonical resolutions (17.150) and (17.151), it is possible to calculate dispersion of frequency-response curves and to estimate the field in which there will be disposed possible realizations of frequency-response curves for different models of the system or object of control.

If errors of design parameters are distributed according to the normal law, then for estimation of the possible field of realization of frequency-response curves, a band will serve near the nominal frequency-response curve with a width of six root-mean-square deviations of frequency-response curve error.

On the graph in Fig. 17.7 there is shown schematically a real frequency-response curve of a control system, the dynamic parameters of which are random variables. The nominal frequency-response curve, constituting a mathematical expectation of random function, is designated as $P_0(\omega)$; the root-mean-square deviation is designated as $\sigma[P(\omega)]$. The possible band of realization of the frequency-response curve on the graph is shaded.

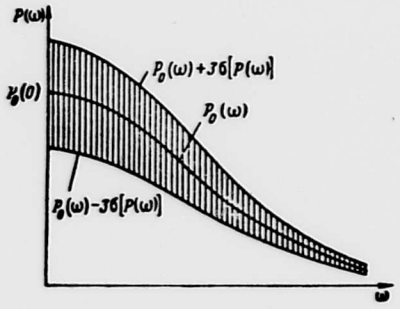

Fig. 17.7. Band of possible realization of a real frequency-response curve of an automatic control system.

In that case when there are separately assigned canonical resolutions of frequency-response curves of an object of control and of the regulators it is easy to obtain canonical resolutions of frequency-response curves of a closed-loop system.

The matrix of transfer functions of a closed-loop control system is expressed through matrix (17.66) of transfer functions of the object of control and of the regulators

$$\Phi_{\lambda}(p)=[E+W(p)N(p)]^{-1}W(p)N(p)K_{\lambda}.$$

The matrix of small errors of transfer functions of closed-loop system, obtained with variation of matrix (17.66) equals

$$\delta\Phi_{\lambda}(p)=[E+W_0(p)N_0(p)]^{-1}\{W_0(p)\delta N(p)+ +\delta W(p)N_0(p)\}[E-\Phi_{\lambda 0}(p)]. \qquad (17.154)$$

After substitution in formula (17.154) of matrices of canonical resolutions of errors of transfer functions of the object of control

$$\delta W(p)=\sum_{q=1}^{r}\frac{\partial W(p)}{\partial l_q}\delta l_q \qquad (17.155)$$

and of the regulators

$$\delta N(p)=\sum_{s=1}^{g}\frac{\partial N(p)}{\partial l_s}\delta l_s \qquad (17.156)$$

we obtain a matrix of canonical resolution of errors of transfer functions of a closed-loop control system:

$$\delta\Phi_h(p)=\sum_{q=1}^{r}G_q(p)\delta l_q+\sum_{s=1}^{g}F_s(p)\delta l_s. \qquad (17.157)$$

In canonical resolution (17.157) the matrix of nonrandom coordinate functions are equal respectively to

$$G_q(p)=[E+W_0(p)N_0(p)]^{-1}\frac{\partial W(p)}{\partial l_q}N_0(p)[E-\Phi_{h0}(p)]; \qquad (17.158)$$

$$F_s(p)=[E+W_0(p)N_0(p)]^{-1}W_0(p)\frac{\partial N(r)}{\partial l_s}[E-\Phi_{h0}(p)]. \qquad (17.159)$$

From the canonical resolutions of transfer functions it is easy to proceed to canonical resolutions of frequency-response curves.

The effect of change of amplification factors of the regulators on error of frequency-response curves can be estimated by means of partial derivatives of coordinate functions according to amplification factors K_f:

$$\frac{\partial G_q(j\omega)}{\partial K_f} \quad \text{and} \quad \frac{\partial F_s(j\omega)}{\partial K_f},$$

which are obtained with differentiation matrices (17.158) and (17.159).

Analogously to that which was done for frequency-response curves canonical resolutions of transfer function for the i-th coordinate of the system can be obtained:

$$\delta x_i(t)=\sum_{q=1}^{r}\frac{\partial x_i(t)}{\partial l_q}\delta l_q. \qquad (17.160)$$

Knowing the coordinate functions for errors of actual frequency-response curves $\partial P_i(\omega)/\partial l_q$, and using the known integral relationship

$$x_i(t)=\frac{2}{\pi}\int_0^{\infty}\frac{P_i(\omega)}{\omega}\sin\omega t\cdot d\omega,$$

we obtain the coordinate functions for canonical resolution (17.160):

$$\frac{\partial x_i(t)}{\partial l_q} = \frac{2}{\pi}\int_0^\infty \frac{\partial P_i(\omega)}{\partial l_q}\frac{\sin \omega t}{\omega}\,d\omega. \qquad (17.161)$$

According to equality (17.160), the dispersion of transfer function is equal to

$$D[x_i(t)] = \sum_{q=1}^{r}\left[\frac{\partial x_i(t)}{\partial l_q}\right]^2 D(l_q). \qquad (17.162)$$

After calculation of dispersion by formula (17.162) and determination of the root-mean-square deviation

$$\sigma[x_i(t)] = \sqrt{D[x_i(t)]}$$

it is possible to construct a field of possible realizations of transfer function of the system.

For a case of normal distribution of errors of initial design parameters, the maximum possible deviation of transfer function from nominal value can be taken as $\pm 3\sigma[x_i(t)]$.

On the graph in Fig. 17.8, nominal transfer function of the control system is designated as $x_{i0}(t)$, root-mean-square deviation of error of transfer function – $\sigma[x_i(t)]$. If realizations of transfer function can fall outside the limits set by technical conditions, then it is necessary to reconsider the tolerances on design parameters or to change certain amplification factors of the regulators.

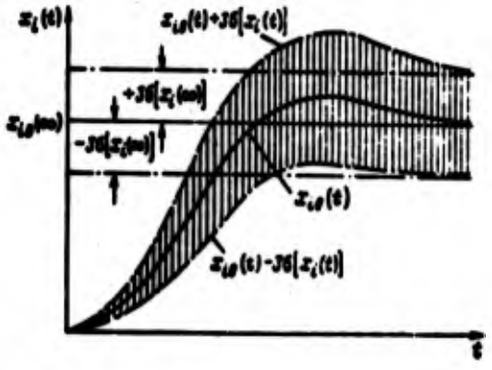

Fig. 17.8. Band of possible realizations of transfer function of an automatic control system.

C H A P T E R XVIII

CONSTRUCTION, STRENGTH OF ELEMENTS, AND CONTROL OF SOLID PROPELLANT ROCKET ENGINES

Solid-propellant rocket engines (RDTT) are used as propulsion systems of flight vehicles of different types, and their construction, to a considerable degree, is determined by the specific purpose of the propulsion system.

Boosters are intended for the creation of supplementary thrust during takeoff of the flight vehicle with a basic propulsion system of another type, for example, an aircraft with turbojet engines or a winged missile with a turbojet engine or ramjet engine, and also for lift off of rockets with a liquid propellant rocket engine. The basic construction requirements of a booster are simplicity and high chamber strength, which in the process of operation does not have to be subjected to permanent deformations and does not have to suffer damages of the walls from overheating.

For boosters, a characteristic is short operating time, on the order of a few seconds with relatively great thrust. As a rule, boosters are not equipped with auxiliary devices for thrust control or change of its direction in flight and cutoff at a given instant.

Basic, or sustainer, engines operating on solid fuel are used in ballistic and surface-to-air rockets, and also in guided and unguided missiles. The engines of objects of mass assignment

(surface-to-air rocket and missiles) also usually must be very simple structurally. Engines of ballistic missiles and space flight vehicles are distinguished by their large dimensions and the presence of several auxiliary devices. Such devices are the control elements and attachments for cutoff of the engine, i.e., shutting it off at a prescribed instant. Sustainers operate for a prolonged time.

The RDTT are used also as auxiliary engines. They are used both as steering engine of powerful rockets and as engines for stabilization and trajectory control of space flight vehicles, as braking and recovery engines of spaceships and as engines for soft landing of spaceships. The features of such engines are necessity for high reliability of switching on and cutoff, and capability of thrust control and restart.

The construction of the charge is determined by its basic method of manufacture and form. The basic elements of the fuel charge are the fuel proper and, in a number of cases, the shielding intended to protect individual surfaces of charge from burning so that in process of operation the burning of charge will be changed in accordance with a prescribed law.

In certain RDTT designs heat shielding coverings are used which are located between the lateral surface of the charge and the walls of the combustion chamber. Heat shielding coverings can be applied to the front and rear faces of the engine and also on the internal surface of the nozzle.

Weight efficiency of an RDTT is estimated by relative weight of the construction $\bar{G}_к = G_к/(G_к+G_т)$, where $G_к$ — weight of the construction and $G_т$ — propellant weight. For the modern RDTT, $G_к$ = 0.05-0.2.

18.1. Structure of Elements of RDTT Chambers

The structural diagram of RDTT and the structure of its basic elements is determined by the purpose, form, construction, and

method of manufacturing the fuel charge, the method of control and cutoff of engine thrust, and duration of operation.

One of the most important factors affecting the operating conditions of the chamber and its construction is the method of accomodating the charge. There are two basic types of charges: inserted and applied. Face charges occupy an intermediate position.

The inserted charge (Fig. 18.1) is placed in the chamber in such a way that between its external surface and the case of the combustion chamber there is clearance, in which hot gases flow along the wall of the combustion chamber. If the external surface of the charge is not armored, then in the clearance mentioned there also occurs combustion of the fuel. In structures where the external surface of the charge is armored, a relatively small quantity of gases flow via the clearance. Consequently, in structures with an inserted charge, if sealing is not placed at the ends, during all the time the engine is operating, the walls of the combustion chamber will be directly washed by hot gases and heat shielding covering will be required. To retain the charge inside the combustion chamber, it is necessary to place a diaphragm or other supporting device.

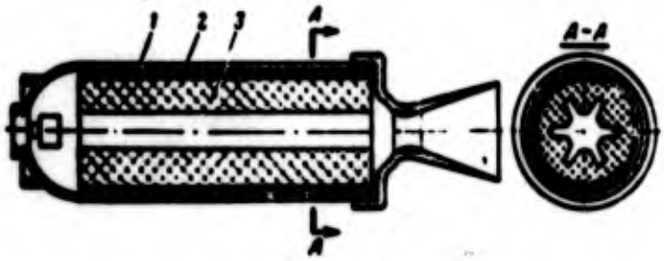

Fig. 18.1. Diagram of an RDTT with inserted charge: 1 — armoring; 2 — combustion chamber case; 3 — charge.

An applied charge (Fig. 18.2) is characterized by the fact that between the charge and the chamber case there is no clearance. The charge can be either poured directly into the combustion chamber, or be densely set in it. Combustion of the charge occurs along

the surface of a central channel. The hot gases make contact with the walls of only the front and rear faces as the charge burns out. If the applied charge does not occupy volume of the chamber fully, then hot gases during operation of the engine make contact with the walls of front and rear faces. Structures with closed charges, to a considerable degree, are protected from the action of hot gases by the fuel itself, and there is required a relatively thin heat-insulating covering. With solid filling of the chamber by the fuel the setting of diaphragms is not required.

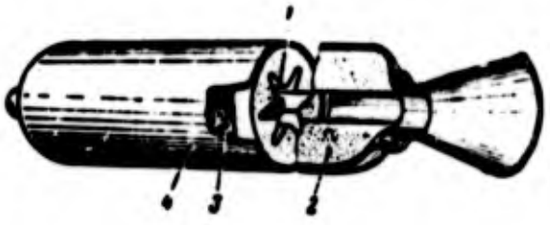

Fig. 18.2. Diagram of an RDTT with applied charge: 1 – igniter; 2 – charge; 3 – adhesive layer; 4 – chamber case.

In an engine with a face charge (Fig. 18.3), as the fuel burns out, the surface of the walls of the chamber, washed by hot gases, is increased. Therefore, in spite of the fact that in the initial moment of operation of the engine the walls of the combustion chamber are protected by the charge, it is necessary to use heat shielding coverings over the entire surface of the chamber of the engine. For fixation of charge in the chamber, fastening it to the forward diaphragm is employed.

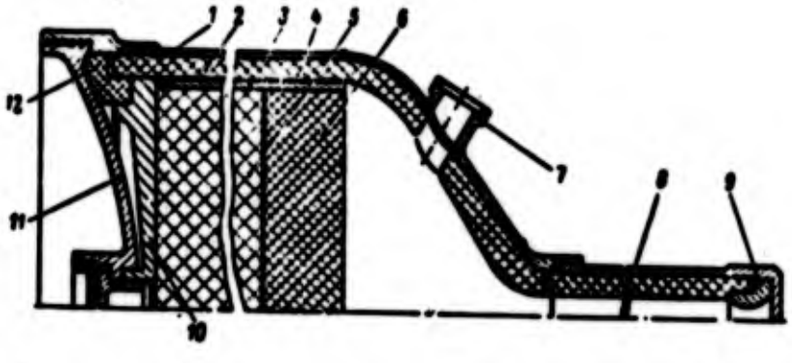

Fig. 18.3. Diagram of an engine with face charge: 1 – case; 2 – thermal insulation; 3 – aluminum tape; 4 – armoring; 5, 6 – sustainer and starting charges; 7 – igniter socket; 8 – extension pipe; 9 – nozzle; 10 – forward diaphragm; 11 – front face; 12 – lining.

The basic supporting member of the chamber is the case of the combustion chamber. Cases are cast, stamped, machined, welded, and wound. As materials for the cases of combustion chambers use is made of low-carbon or low-alloy easily welded steels, cold-rolled steels with controlled location of fibers, light aluminum or magnesium alloys, and fiberglass.

Cast cases are usually made thick-walled and as a unit with the front face or part of it. Their advantage over other case constructions is simplicity in manufacture; the basic disadvantage – great weight. They are used more frequently for restartable boosters. For protection from overheating and to permit repeated use, cast cases are supplied with reliable heat shielding devices.

Cast casings made of light alloys are used in low-thrust engines (for missiles) or in auxiliary engines. After casting subsequent machining of the internal surface is possible, especially with tight pitting of the charge in the casing.

Thin-walled casings of combustion chambers made of steel with small diameters can be prepared simultaneously with the end by deep stamping (drawing). Thin-walled cases of large diameter are made by stamping into separate sections with subsequent welding. After welding, in order to decrease wall thickness variation and to obtain the prescribed internal diameter there is performed additional machining, more frequently rolling. In so doing the material of the walls and welded seam is strengthened. For such constructions $\sigma_в$ = 150-170 kgf/mm^2, whereas for cast chambers $\sigma_в$ = 50-60 kgf/mm^2. As a rule, thin-walled stamped and welded bodies are used with closed charges, while open charges have heat shielding.

Wound cases are made from steel tape or fiberglass. The strength of steel cold-rolled tape with controlled location of fibers is 2-4 times greater than the strength of sheet steel. The tape used is from 0.1-0.3 mm thick with width up to 0.5 m. The tape is wound on a special frame in layers at an angle of 45° to the generating line in forward and reverse directions. The number of layers can attain 20 and more. Individual layers are spot welded to each other.

The fiberglass ones are made on a base of epoxy or phenolic resin and work only on tension. Winding is produced for separate filaments or tapes of fibre with the direction of the fibers at an angle to the generating line. After winding on the frame, the material is impregnated with resin and goes through polymerization under pressure and at high temperature. Fiberglass has $\sigma_в$ = 140-175 kgf/mm^2 (up to 500 kgf/mm^2 with quartz fibers of 0.01 mm diameter) At a temperature of 250°C, fiberglass has $\sigma_в$ = 40-60 kgf/mm^2 (up to 100 kgf/mm^2 – fiberglass made of quartz fibers). Fiberglass cases basically are used with applied charges.

In the majority of designs the front faces are made separate from the combustion chamber. The faces have spherical form with external convexity. In individual designs for reduction of engine length, the face can be internally concave (see Fig. 18.3). Machined faces for ease of manufacture sometimes have conical form. Flat faces, due to low rigidity are used only on engines with small diameter of chamber. In the case of using a chamber made of fiberglass, the face can also be made of multilayer fiberglass by stamping. In this way the weight of the face as compared to steel can be decreased 30-40%.

On the front face, usually in central opening, an igniting device is located. Around the periphery of the front face, if the engine has a cutoff system, there are located the reverse thrust nozzles. To the front face there can be fastened the following stage of the rocket, the nose cone, or fairing. The lugs for mounting the engine to the flight vehicle are also located on the front face. To increase the rigidity of the forward face loaded with great gas forces, it is possible to have reinforcing ribs on the front surface.

The rear face and nozzle usually constitute a single subassembly (see Fig. 18.1). On the rear face one or several basic nozzles ca can be located, and also auxiliary nozzles and windows for thrust and sharp reduction of pressure at the time of cutoff. With high gas pressures in the combustion chamber several basic nozzles are used. In this case, the longitudinal dimensions of engine are made

shorter than in the case of one central basic nozzle. With pressures in the combustion chamber on the order of 50 kgf/cm^2 and lower, it is more expedient to use one central basic nozzle.

Nozzles are made fixed and swiveling. The latter are used for vector control of engine thrust. Fixed nozzles in most cases have axes parallel to the axis of the engine. In certain designs of boosters, for creation of thrust component in the direction of lift of winged flight vehicles the nozzle is set at a certain angle to the axis of the engine.

Fixed nozzles can be adjustable and nonadjustable. Adjustable nozzles are distinguished from nonadjustable by the fact that they have a device to change the area of critical section. Adjustable nozzles are subdivided into preadjustable and continuously adjustable. Continuously adjustable nozzles are supplied with automatically working devices to change the area of critical section. In preadjusted nozzles, the device for change of throat area is set in its assigned position before the start and remains constant during the entire time of operation of the engine.

Nozzles are made by machining, can be welded, and compound.

Machined nozzles (Fig. 18.4a) are usually used on engines of low thrust. They are rather massive and can operate for a short time without thermal insulation. For preventing an increase of throat area due to erosion of material, the critical section is made in the form of cylindrical section, length of which is not less than 3-5 mm. This cylindrical surface is finished with high accuracy. Machined nozzles are screwed into openings on the rear face.

The simplest in construction are the welded conical nozzles shown in Fig. 18.4b and c. The thin-walled outlet part of the nozzle can be welded to the machined massive central part which is screwed into the rear face of the chamber. After welding, the internal part of the nozzle undergoes machining. A conical nozzle

welded from several sections can be screwed into a special duct, welded into the rear face of the chamber. In the design shown in Fig. 18.4c, the nozzle is set at a certain angle to the axis of the chamber. The use of a threaded joint is convenient because of the fact that the engine can be fitted with a set of interchangeable nozzles with different critical throat diameters. Interchangeable nozzles, as will be shown below, are used for adjustment of the engine.

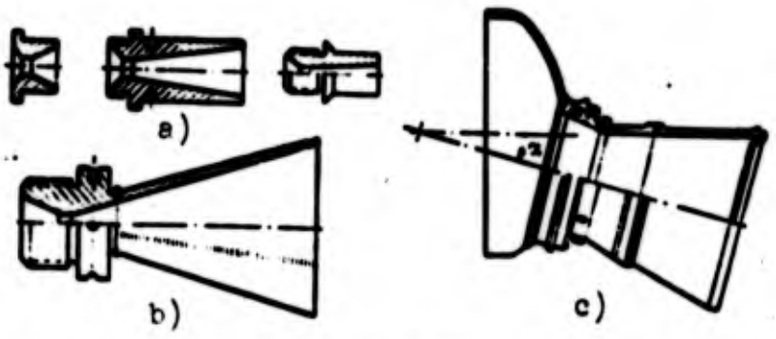

Fig. 18.4. Nozzles of RDTT: a) machined; b) welded conical axisymmetrical; c) welded, set at an angle to the axis of the chamber.

Examples of the designs of shaped welded nozzles are shown in Fig. 18.5. With a relatively small diameter of the combustion chamber, the nozzle can be made as a unit with the rear face of the chamber (Fig. 18.5b). Such a construction is convenient in the case of installation of charge from the nozzle side and in the presence of one central nozzle. In multinozzle engines and engines with large diameter of the combustion chamber it is more expedient to have a nozzle with the inlet part welded or attached by a screw thread in the rear massive face (Fig. 18.5a). The most heat stressed part of the nozzle, at the critical section, can be made from heat-resistant and refractory material (see Fig. 18.5b) or can have insertable insert, for example, one made of graphite (see Fig. 18.5a) or a multilayer one.

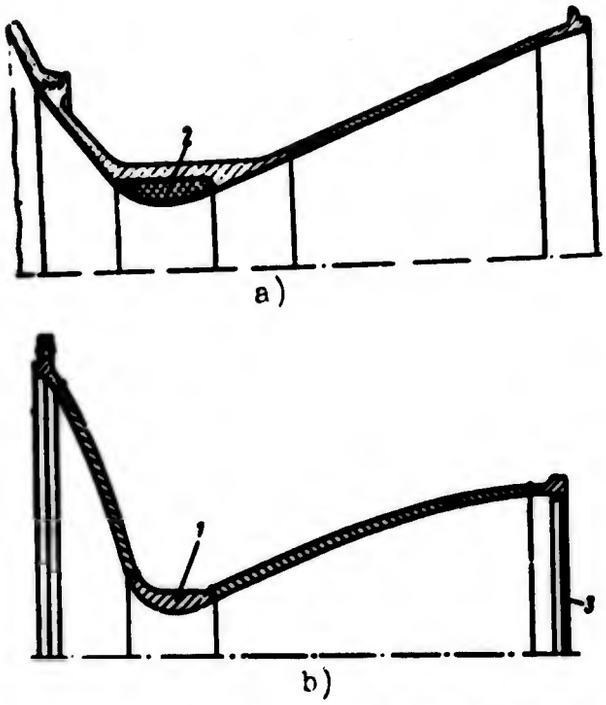

Fig. 18.5. Profiled welded nozzles:
a) screwed into the rear face;
b) made as a unit with the rear face;
1 – insert of refractory material;
2 – graphite insert; 3 – plug.

Compound nozzles (Fig. 18.6) are used in those cases when it is necessary for adjusting the engine to replacable inserts 1 in the throat of the nozzle. In engines with low thrust and with small expansion area ratio (Fig. 18.6a), the insert will form the divergent section of the nozzle. In the design shown in Fig. 18.6b, the insert is set in a hollow of narrowing part of nozzle and is bead pressed on the flange of the divergent section of the nozzle. In the throat of the nozzle there can be located a special inset with the insert, which it is possible to replace separately, leaving with different diameters of insert the same outlet part of the nozzle (Fig. 18.6c). In all the constructions shown, the nozzle does not need to have a special heat shielding coating. An example of the design of a compound nozzle with thick heat-insulating covering and inset with the insert is shown in Fig. 18.6d.

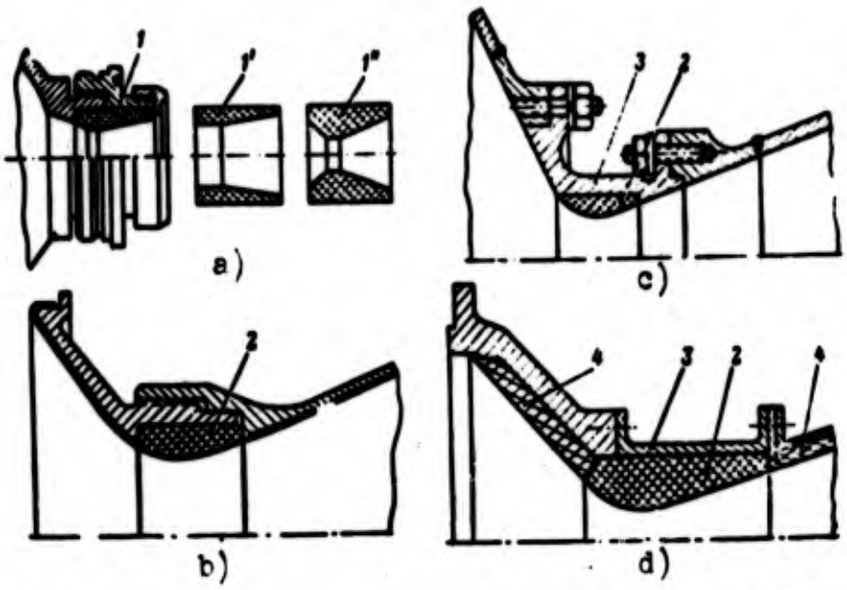

Fig. 18.6. Compound nozzles: a) with insert carried out as a unit with the divergent section of the nozzle; b) with removable insert; c, d) with inset; 1 – insert carried out as a unit with the divergent part (for normal temperature of charge); 1', 1" – the same for a charge with high temperature ("summer") and low temperature ("winter") respectively; 2 – removable insert; 3 – inset; 4 – heat-insulating covering.

The swiveling nozzles (Fig. 18.7) are usually compound. The construction of swiveling nozzles make it possible to deflect nozzle in any direction (Fig. 18.7a, b, c) or only in one plane (Fig. 18.7d). The capability of turning the nozzle is attained by placing a joint in the throat of the nozzle. The articulated joint should ensure free turning under conditions of variable heating of the joined parts in the process of operation and reliable sealing against breakthrough of gases. The simplest articulated joint shown in Fig. 18.7a, has a disadvantage in that its friction surfaces transmit considerable axial forces. To lessen friction the joint is covered graphite lubricant. With nonuniform heating of separate parts of the articulated joint and relatively small clearance wedging of the joint is possible. A more successful design is the one with a universal joint (Fig. 18.7b, c). The universal joint formed by ring 4, joined by pins 5 with the central joint and the case is a supporting member. Friction surfaces of

the central joint are unloaded and the probability of their wedging is less. The size of the clearances in the central joint can be increased, and the layer of lubricant can be thicker. The need for lubrication of the central joint becomes superfluous if, as in the design shown in Fig. 18.7c, both parts of the central joint 2 and 3 are made from graphite. A deficiency in the articulated joints examined in their poor airtightness. Reliable sealing of the articulated joint is attained by the use of bellows (Fig. 18.7d), one end of which is fastened to the movable part of the nozzle, while the other – to the case of the combustion chamber. The bellows is subjected from within to the action of high pressure. In order to prevent distention of the bellows, steel rings 7 are set in its cavities. A convenience in the use of a bellows seal also lies in the fact that friction occurs in parts which are relatively slightly heated.

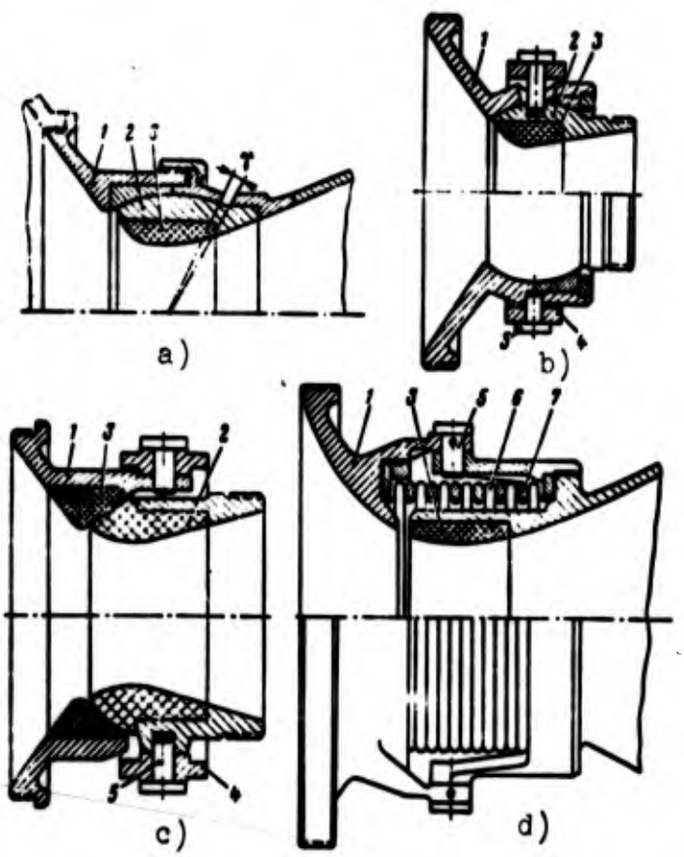

Fig. 18.7. Swiveling nozzles: a) with central joint; b, c) with universal joint; d) with bellows; 1 – base of nozzle; 2 – spherical tip of the nozzle; 3 – insert; 4 – universal joint ring; 5 – axis-pin; 6 – bellows; 7 – protective ring of the bellows; γ – angle of nozzle rotation.

The throat area is usually regulated by shift along the axis of nozzle of central profiled body. For an adjustable nozzle (Fig. 18.8a), before starting the central body can be shifted along bushing 1, by rolling on screw 3. On screw marks inscribed, determining value of throat area.

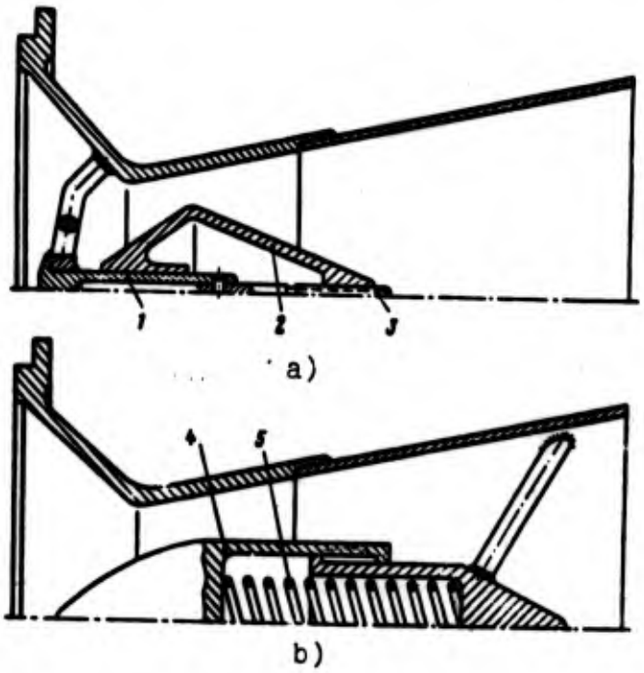

Fig. 18.8. Variable-area nozzles: a) a) preadjusted; b) self-adjusting; 1 – bushing; 2 – central body; 3 – screw; 4 – mushroom; 5 – spring.

The central body can be moved automatically; in such a nozzle (Fig. 18.8b) mushroom 4, on the one hand, is under the impact of gas pressure forces, and on the other – the force of spring 5. The spring is calibrated in such a way that with an increase in the pressure in the combustion chamber greater than prescribed, the mushroom moves back, increasing the throat area, which leads to reduction of pressure. A deficiency in the self-adjusting nozzle is low accuracy in maintaining assigned pressure of gases in the combustion chamber. Shift of the mushroom can be carried out compulsorily with the help of a special servomotor controlled by a regulator. In this case, throat area can be changed in accordance with any accepted law of control.

For protection of the fuel charge from moisture and for creation of increased pressure at the time of ignition, in the nozzle exit section plug 3 is set (Fig. 18.5b). The plug can be fastened by a bolt or be soldered to the wall of the nozzle. With an increase in pressure of gases in the process of starting, the plug is driven from the nozzle.

In order to cut off an RDTT it is necessary either to extinguish the charge or to create counter thrust. Extinguishing is achieved by rapid discharge of pressure in the chamber by increasing the throat area or even by separation of the rear face. During a sharp drop in pressure, in the combustion chamber there appears shock wave of rarefaction, extinguishing the charge.

In nozzles with central body, cutoff can be produced instantaneously by separation of the central body by a special explosive mechanism. Such method is unreliable in view of possible failure of the mechanism located in a zone with high temperature; separation is more reliable with an explosive mechanism of the whole nozzle or rear face of the chamber. The gases filling the combustion chamber and in the first moment of having pressure close to operating, with opening of the rear face flow out, creating thrust equal to the product of pressure on the area of cross section of the chamber. Here a short-term augmentation of engine thrust by a few times is possible. For elimination of this pulse instantly, the windows located on the lateral surface of the engine open with help of the explosive mechanism.

Creation of counter thrust is achieved at the time of cutoff by opening the counter thrust nozzles located on the front or rear face in such a manner that their thrust is directed against the nozzle thrust. It is most convenient to place the counter thrust nozzles on the front face of the engine. With the opening of the counter thrust nozzles there is a simultaneous effect of pressure drop in combustion chamber, leading to the extinguishing of the charge.

Counter thrust nozzles (Fig. 18.9) are fitted with plugs. At the time of engine cutoff the plug must be ejected. Ejection of the plug can be carried out by destruct of the retaining bolt. For heat shielding of the counter thrust nozzle, the plug and the bolt, the internal cavity of the nozzle from the side of the combustion chamber can be filled with a plastic heat-insulating substance.

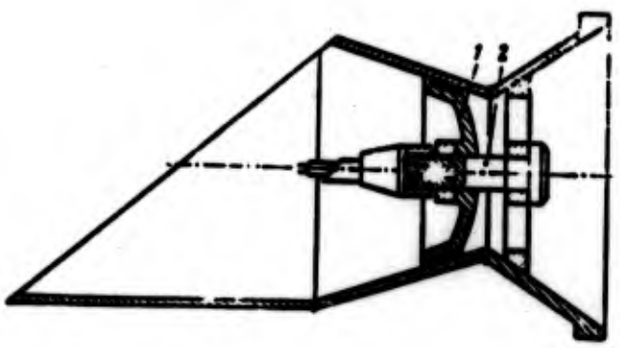

Fig. 18.9. Counter thrust nozzle:
1 – plug; 2 – explosive bolt.

The diaphragms holding the charge, are made by casting or are welded. The rear diaphragm, loaded by considerable forces, should be massive and rigid. Rear diaphragms (Fig. 18.10) for single-grain charges are simple in construction. With a multigrain charge the diaphragm has frequently spaced crosspieces. Fastened charges of lateral combustion are usually bonded to the case of the chamber, but sometimes also are supported by diaphragms, partially absorbing axial forces having an effect on the charge in flight.

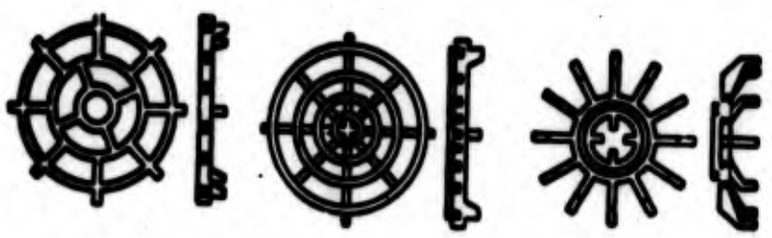

Fig. 18.10. Rear diaphragms.

Heat shielding coatings are of great importance in ensuring efficiency of combustion chambers and faces of the engine. They are divided into sprayed on, smeared on and sheet and enamel.

Sprayed on coatings have relatively small thickness (0.1-0.5 mm). The coating material used is aluminum oxide or zirconium dioxide. Spraying is performed by flame or plasma methods. For best bonding with the surface of the walls the coatings are applied on an underlayer of chromium or nickel up to 0.1 mm in thickness. Ceramic coating of aluminum oxide can be used at temperatures on the order of 1800-2000°C and tolerates prolonged operation of the engine (up to 10 min). Zirconium dioxide tolerates temperature up to 2300-2500°C. For short-term operation, both types of coatings tolerate temperatures up to 3000-3500°C. A disadvantage of ceramic coatings is cracking and crumbling with considerable deformations of the parts to which they are applied. It has been determined that coatings are preserved during deformations of parts, corresponding to yield point of the coating materials.

Heat-insulating coatings of the smeared on type are applied to the parts to be protected in thick layers (up to 10-15 mm thick). The composition of the coating includes asbestos, powdered mica, or oxides of metals and a gluing substance. As heat-resistant metal oxides there are used oxides of aluminum, zirconium, and chromium. For a binder there are used soluble glass or resins (phenol, epoxy, siliconorganic, and others). When applying the coating directly to the wall of the chamber, it will durably hold as long as temperature of the wall is lower than the temperature of destruction of the binder. For example, a coating on a bakelite binder does not crumble up to a wall temperature of 500-600°C. With the necessity of ensuring stability of the coating at higher temperatures, it is applied to a metallic grid, preliminarily fastened to the walls of the chamber.

The simplest are the sheet coverings made of glass laminate, asbestos phenol plastic, glass-phenol-silicon plastic and other heat-resistant plastics glued onto the surface of the walls.

With a thickness of coating of 6 mm, the temperature of the wall does not rise higher than 60-90°C after 5 seconds of operation of the engine and not higher than 300°C after 6-8 minutes with a thickness of coating of about 15 mm.

In restartable engines, thermal insulation is maintained and protected by casings made of thin sheet steel.

Heat-resistant enamels are used for protecting the surface of the wall from oxidation; the heat shielding properties of enamels are relatively low.

For lowering thermal stress of parts of nozzles, they are made of materials with high thermal conductivity, and at high temperatures of gases – from materials having a high melting point – molybdenum, graphite, heat-resistant alloys based on molybdenum, tungsten, and copper. Application of the materials mentioned does not exclude the necessity for protective coverings.

Graphite parts of the nozzle are protected by a layer of silicon carbide (silicon impregnated graphite) or are made entirely from silicon impregnated graphite. Graphite nozzles are covered also by a layer of tungsten applied by plasma spraying (Fig. 18.11a). Such a nozzle works reliably up to gas temperatures of not over 3000°C. For inserts they use pyrolytic graphite (pyrographite) which has different structural orientation determining the anisotropism of its properties. For example, in the construction shown in Fig. 18.11a, insert 7 made of pyrographite serves as a heat conductor in a radial direction, and inserts 2 – as heat insulators.

Nozzles of plastic can be used with coatings (Fig. 18.11b) and without coating. The possibility of using plastic nozzles without special heat-insulating coatings is explained by the formation of a heat shielding film in process of operation of the engine. In the first seconds of operation of the engine, certain materials, for example, glass laminate, burn intensively, and then burning out is inhibited and becomes quite insignificant. The carbonized surface of the plastic prevents burning out, protecting subsequent layers of

the material from destruction. Certain plastics during heating begin to evaporate without fusion giving off a large quantity of gases. In so doing there will be formed a porous residue with poor thermal conduction. Such plastics, forming a heat-resistant porous deposit, are promising materials for use in the form of nozzle insets.

Fig. 18.11. Combined thermal insulation of nozzles: 1 – tungsten coating; 2 – insert made of pyrographite; 3 – steel shell; 4 – thermal insulation coatings; 5, 6 – graphite inserts; 7 – ring made of pyrographite; 8 – glass laminate shell; 9 – direction of layers of coating.

Separate elements of the chamber, the front and rear face and the section of the case of the combustion chamber are joined by threading, flanges, collars, and expanding. Threaded connections are used usually with cast or welded thick-walled constructions in engines with relatively small dimensions. Flanged joints on bolts (Fig. 18.12a) are used for joining separate sections of combustion chambers and faces with combustion chambers in the manufacture of these parts from both metallic and also nonmetallic materials. In the latter case, the flanges are made of steel or heat-resistant alloys, and the nonmetallic bodies, in turn, are fastened to the flanges or are wound in grooves on the shelf of the flanges. Such joints are called combined flanged joints. In Fig. 18.12b, c, there are shown combined flanged joints with the use of collars and radial pins. In certain constructions use is made of a joint with shaped locking rods, entering the grooves of a shaped lock (Fig. 18.12d). An example of a rolled in connection of the face with the case of the combustion chamber is shown in Fig. 18.12e. Securing the face in an

axial direction on the one hand is carried out by a stop in ring 9, welded to the case of the combustion chamber, and in the other – in a rolled bead of the case of the combustion chamber. A sealing ring is inserted for airtightness of the connection.

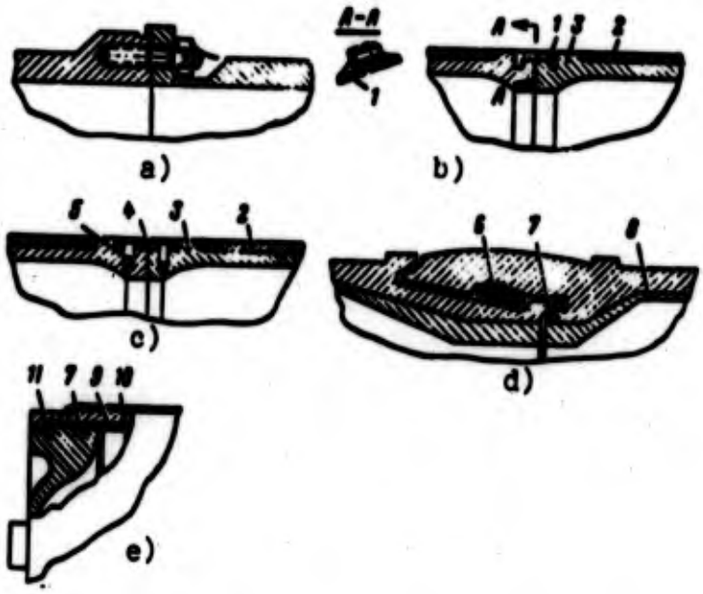

Fig. 18.12. Types of connections of subassemblies of RDTT chambers: a) bolt; b) connection by collar; c) on radial pins; d) with a locking rod; e) rolled in; 1 – collar; 2 – glass laminate bodies; 3 – flanges; 4 – ring; 5 – radial pins; 6 – locking rod; 7 – sealing ring; 8 – heat shielding coating; 9 – thrust collar; 10 – case of the combustion chamber; 11 – face.

In many constructions it is necessary to carry out the joining of ceramic parts with metallic or plastic parts. In view of the different coefficients of linear expansion of these materials the joint should be elastic. Types of similar elastic joints are shown in Fig. 18.13.

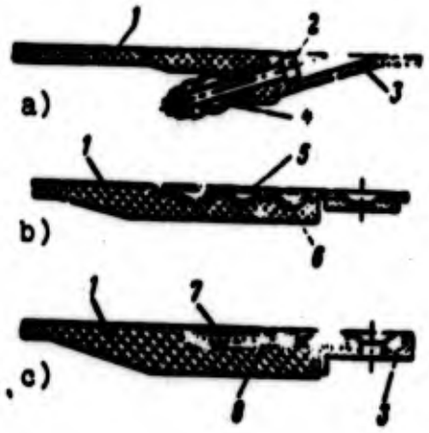

Fig. 18.13. Types of elastic joints between ceramic parts and metals and plastics: a) bolted; b) with grooves; c) winding. 1 – ceramic parts; 2 – bolt; 3 – metallic case; 4 – tubular spring; 5 – stretched metallic sheet; 6 – compressed sheet; 7 – winding with wire or fiberglass tightening; 8 – plastic, set with tightening.

18.2. Designs of Fuel Charges and Igniters

Fuel charges are made by monolithic, sectional, block, and compound (combined).

Monolithic charges (Fig. 18.14) are cast either directly into the chamber of the engine or separately. After casting the charges are polymerized and harden. The necessary form of the channel of the charge is obtained by setting profiled rods in the casting mold and extracting them after solidification of the charge. The advantages of casting separately from the chamber of the engine lie in the possibility of accurately maintaining the weight, form, and dimensions of the charge. With the use of inset charges, the cast fuel grain is placed on packings or is bonded to the case of the combustion chamber. Polymeric bonding substances are applied by direct pouring into a revolving body or are sprayed on the wall in liquid form. Disadvantages of extrachamber casting consist of difficulties in loading the engine and transportation of grains to the place of installation.

For monolithic charges fuel must be used which has great plasticity, comparatively high tensile strength, little shrinkage during polymerization and solidification, and good adhesion to the case. Only separate grades of fuels, to a sufficient degree, satisfy all the enumerated requirements.

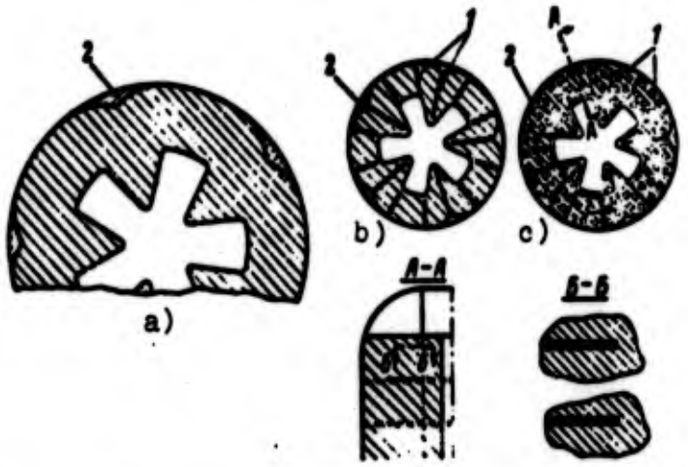

Fig. 18.14. Monolithic fuel charges: a) without reinforcements; b) with longitudinal reinforcing plates; c) with longitudinal and transverse plates. 1 – support plates; 2 – filler.

A deficiency in monolithic charges is the possibility of the appearance of internal cracks in them. The cracks appear due to storage at variable temperatures, and from the action on the charge of internal pressure and forces of inertia during operation of the engine. Due to the causes mentioned in the mass of the fuel there appear internal stresses. Concentration of stresses in separate places in charges with a complex form of internal channel (for example, in star shaped charges) leads to the appearance of cracks. Cracks can also be formed in process of manufacture of grains from fuels with low plasticity. For preventing the possibility of appearance of abnormal combustion or explosion of a charge with cracks, after manufacture, and whenever possible before starting, the charge undergoes control (by X-ray, ultrasonics, and so forth). In monolithic charges, in order to decrease settling due to the action of its own weight, use is made of reinforcing longitudinal and transverse support plates 1 (Fig. 18.14b, c). The plates are made of reinforced rubber, plastic, and other similar materials which burn together with the charge.

To eliminate or decrease the weight of unburned residue (and consequently the weight of the engine) the nonburning particles 2 (Fig. 18.14) of internal combustion charges are replaced by phenoplast or other light materials.

For excluding a concentration of stresses in acute angles of charges, which are inevitable with monolithic construction, there is a conversion to sectional charges (Fig. 18.15). In this case, before casting partitions are placed in the case, dividing the charge into separate sections. The clearances between the partitions, allowing sections to be freely deformed, can be filled with a rubber-like mass. In order that there would be no need in rounding the acute angles in the channels, the partitions are placed in the apexes of the channels. In so doing, as one may see from Fig. 18.15, the nonburning residue of fuel is reduced or eliminated.

Fig. 18.15. Sectional fuel charges: a) five-sectional; b) ten-sectional; c) five-sectional with longitudinal and transverse support plates; 1 – support plates.

Further simplification in the construction and technology of manufacture of charges is provided by the transition to compound (combined) charges. These charges (Fig. 18.16) are made up of several elements which are poured or milled each one separately. The shape of the elements can be selected so that from different combinations of elements charges of different dimension and different shape are assembled. These standardized elements are called moduli. Besides the evident advantages of modulated elements, compound charges are more easily transportable than monolithic and block, they can be manufactured with high accuracy, with good control, and few rejects.

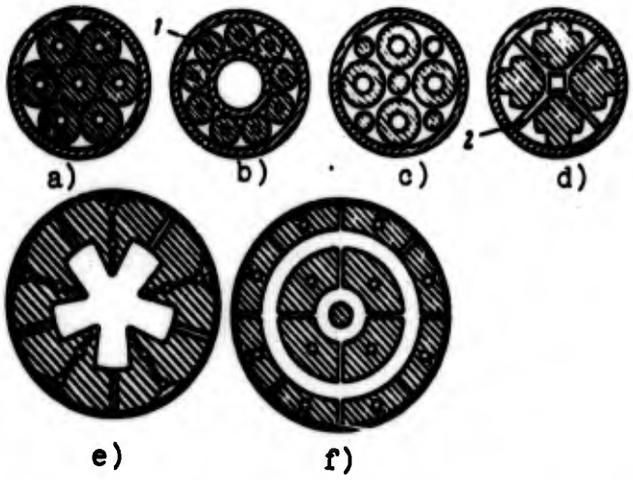

Fig. 18.16. Compound (combined) fuel charges: a) with seven tubular grains; b) with nine cylindrical grains; c) mixed tubular-cylindrical; d) four-grain cruciform; e) from five moduli; f) from thirteen moduli; 1 – fixing rods; 2 – partition.

Moduli of compound charges are bonded to the wall of the case or are attached by special elements. In most cases they are cast with the necessary supporting fittings, rods, plates, etc.

The simplest modular charges include multigrain tubular or cylindrical charges, freely inserted in the combustion chamber.

For compound charges, fuels can be used with somewhat poorer mechanical properties than for monolithic and block charges. Deficiencies of compound charges include a certain loading of the structure by the fastening fittings. Bonding of compound charges is not always possible.

For armoring the surfaces of the charge on which combustion should not occur, there is used acetate or ethylcellulose with charges made of double-base fuels, and with mixed fuels on a polysulfide combustible – synthetic rubber in a mixture with gas black, plasticizers and vulcanizing additives. This mixture is rolled into sheets which are vulcanized under pressure together with the fuel charge at a temperature near 90°C.

Igniters, as was shown, are necessary for RDTT for the purpose of ensuring the combustion process of the basic fuel. The quantity of heat given off by the igniters after the short starting period should be sufficient to increase the surface temperature of the fuel to a value with which there begins a stable process of decomposition, gasification of fuel, and ignition of products of gasification with formation of a zone of combustion. It is necessary to consider also in the initial period the increased thermal losses due to cold surfaces. The quantity of gases forming from the charge of the igniter should be sufficient to increase pressure in the chamber to the minimum value with which process of combustion of the basic fuel can be stable. The thermal power of the igniter, as location, and structural shape depend on form of the combustion surface of the basic fuel and the construction of the engine, and also on the altitude at which it is proposed to start the RDTT. For an RDTT, started at high altitudes, it is necessary to see to it that pressure in the chamber is raised more easily and rapidly; for this purpose are fitted in the nozzles the special diaphragms mentioned earlier.

For double-base fuels and relatively small dimensions of fuel charges (grains), the weight of powder igniter is less than 0.01 the weight of the basic fuel.

As fuels for igniters, they use black powder, double-base fuels, compound fuels based on ammonium perchlorate and other oxidizers, compound fuels with addition of aluminum, and others. Frequently two fuels are used: black powder for the initial explosion and some other fuel as the basic source of heat for ignition of charge in the engine.

Ignition of the igniter fuels is produced by means of an electric current. The ignition time delay of the basic fuel of an RDTT amounts to 0.01-0.35 seconds, and in a large engine - somewhat longer. Combustion time of the igniter charge and its gas temperature play a large role in the reliability of starting an RDTT.

Igniters are placed on the front face, in the nozzle, and in the channel of the charge. With a low power of the igniter, its installation on the front face or in the nozzle does not make it possible to obtain reliable and fast starting of the engine, especially with a relatively long channel in the charge. Very effective in such cases are igniters which are powerful and long working or placed directly in the channel of the charge of the engine. The most profitable are the igniters passing hot gases directly onto the whole burning surface of the charge or onto a considerable part of it, which is possible when the igniter is located in the channel of the RDTT charge.

In a number of cases, to increase the reliability of starting the engine, it is expedient to use several igniters working in parallel, having separate electric systems for switching on.

According to their structure, igniters are divided into igniter charges, igniter chambers, gas generators, tubular, rolled, and corded igniters.

Igniter charges consist of a pyrotechnic charge enclosed in a readily burning or permeable sealing, and a device for ignition. The simplest such device is cartridge igniter (Fig. 18.17). Main part is cartridge 6, having a portion of inflammable powder pulp 7 used for ignition of the pyrocharge. In the powder pulp there is inserted an incandescent filament 8, connected with current-conducting electrodes 4. At ignition of the charge of the cartridge igniter membrane 10 breaks through and gases ignite the pyrotechnic charge of the igniter. The pyrotechnic charge can be enclosed in a plastic container (Fig. 18.17c). Wire frame is filled with plastic. The igniter charges are usually used for starting engines of relatively low thrust. The igniter charges are placed on the front face of the chamber, and in the case of installing several charges, some of them can be placed on the rear face.

Igniter chambers and gas generators possess greater power than ignite charges.

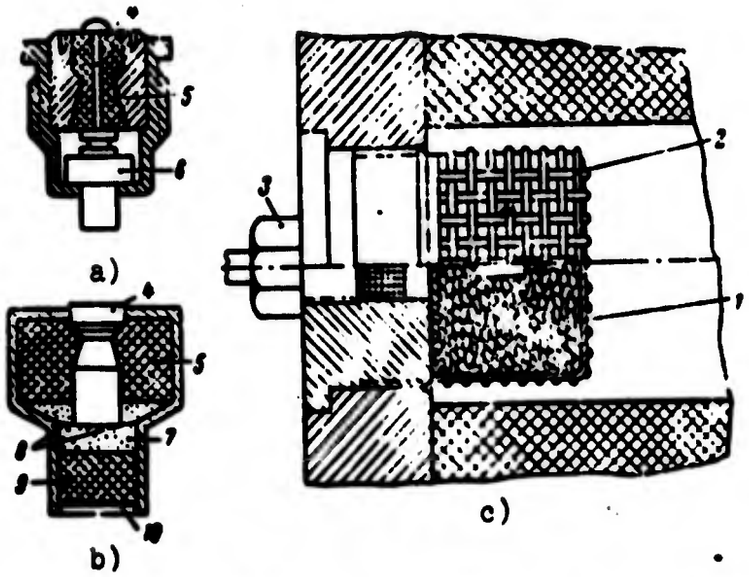

Fig. 18.17. Igniter charges: a) cartridge igniter; b) powder charge; c) basket igniter; 1 – pyrotechnic charge; 2 – wire basket; 3 – cartridge igniter; 4 – current-conducting electrodes; 5 – insulators; 6 – cartridge in holder; 7 – powder pulp; 8 – incandescent filament; 9 – pyrocharge of cartridge; 10 – membrane.

Igniter chambers consist of a little solid-propellant motor with a nozzle (Fig. 18.18b) or perforated nozzle cap (Fig. 18.18a). The igniter chamber has a basic charge of high-calorie fuel and its own igniter, separated by a burn-through diaphragm. Igniter chambers are placed on the front face or in the nozzle of the engine. The location of the igniter chamber in the nozzle of the basic engine permits rapid raising of pressure in the basic chamber, which is promoted by plastic plug 5.

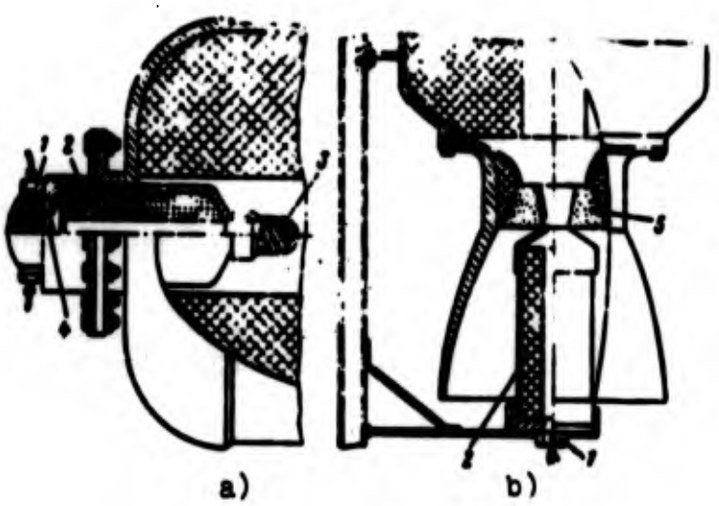

Fig. 18.18. Igniter chambers: a) set on front face; b) set in the nozzle; 1 – igniter; 2 – basic charge of the igniter chamber; 3 – perforated nozzle caps; 4 – diaphragm; 5 – plastic plug.

The gas generator igniter (Fig. 18.19) has the fuel charge placed in a wire frame and a starting igniter with fuse and a portion of black powder. The reliability of operation of an igniter of such diagram is promoted by the installation of charge 3 which consists of inflammable fuel burning at the initial moment of ignition. Basic charge 2 burns for a more prolonged time and ensures the necessary parameters in the process of ignition of the basic charge of the engine. The gas generator igniter is lighter and structurally simpler than an igniter chamber. It can be made the length of the chamber and furnish gas to a large part of the surface of the main charge of the engine.

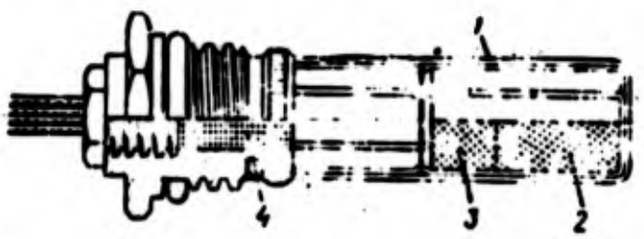

Fig. 18.19. Gas generator igniter:
1 – wire frame; 2 – basic igniter charge; 3 – inflammable charge;
4 – portion of black powder.

Tubular igniters (Fig. 18.20) are made rather long, sometimes as long as the charge, and are placed in the channel of the charge. Main part of this igniter is a performated tube made of plastic or pressed paper. Inside the tube there can be placed a pyrotechnic compound (Fig. 18.20a), and simultaneously it can serve as a mandrel on which is wound the base layer with the pyrotechnic compound (Fig. 18.20b). The tube can be wound with plastic tape for protection of the pyrotechnic compound.

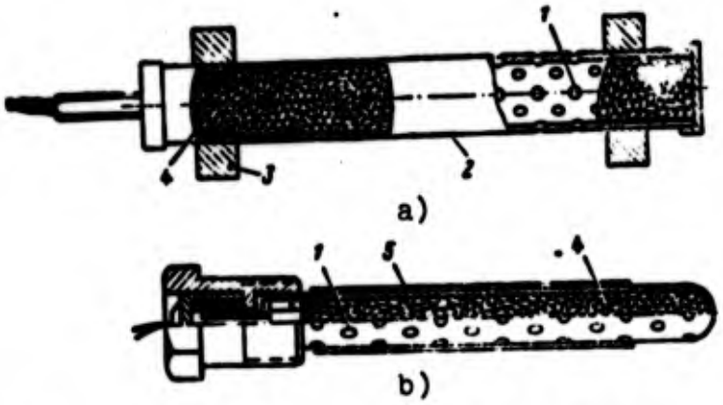

Fig. 18.20. Tubular igniters: a) coarse-grained filler, b) with filler and base layer; 1 – perforated tube; 2 – plastic winding of the tube; 3 – rubber stops; 4 – pyrotechnic compound; 5 – base layer with pyrotechnic compound.

Roll igniters consist of sheets of pyrotechnic compound, which are reeled either on the perforated tube, or on the mandrel 6 (Fig. 18.21). In the latter case, an electric detonator is placed inside the mandrel.

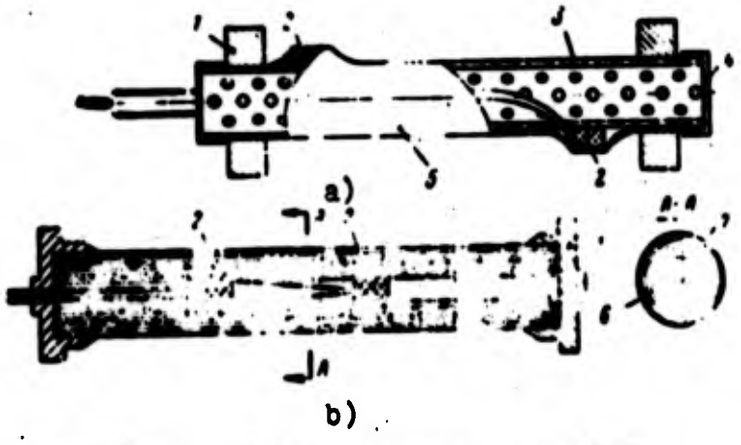

Fig. 18.21. Roll igniters: a) with perforated tube; b) with mandrel; 1 – rubber stops; 2 – electric detonators; 3 – perforated tube; 4 – plug; 5 – sheet of pyrotechnic compound; 6 – central mandrel; 7 – roll sheet with pyrotechnic compound.

A corded igniter has detonating or quick-burning pyrotechnic cord, or explosive wire (Fig. 18.22a), which is wound on a plastic tube located in the channel of the change. For switching on the igniter a low energy detonator is used 3. In the case of using a charge with several longitudinal channels, for reliability of ignition there is a corded igniter, passed in the form of rings or loops in holes and channels of similar charges (Fig. 18.22b).

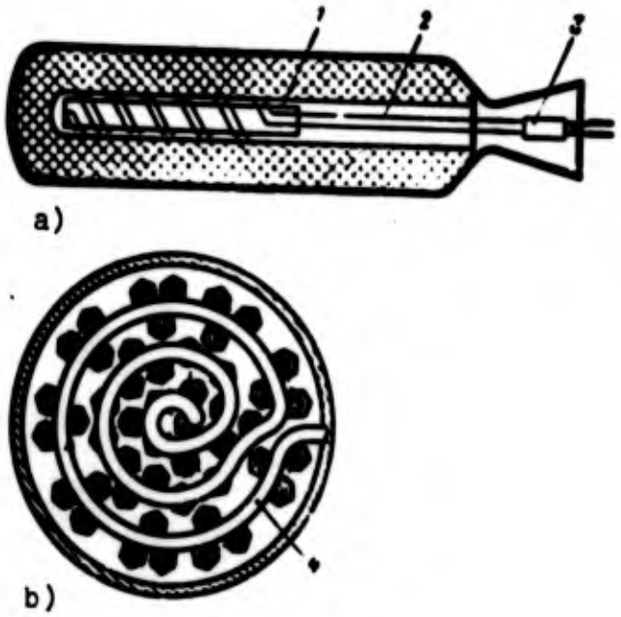

Fig. 18.22. Corded igniters:
a) made of explosive wire;
b) made of pyrotechnic cord;
1 – plastic tube; 2 – detonating cord; 3 – low energy detonator;
4 – pyrotechnic cord.

18.3. Strength of RDTT Chambers

During the operation of the RDTT and acceleration of the flight vehicle, on the chamber, besides gas forces, there act considerable forces of inertia of the contained fuel charge, directed along the axis of the engine. In curvilinear flight there also act forces of inertia perpendicular to the axis of the engine but they usually are small and we will disregard them.

The force of inertia acting along the axis of the fuel charge,

$$P_j = \frac{G_2}{g} j = G_2 n_y = p \frac{G_2}{G_k},$$

where $G_з$ – weight of the whole charge; j – longitudinal acceleration of the flight vehicle; n_x – longitudinal overload; $G_л$ – total weight of the flight vehicle; P – thrust of the engine.

The force of inertia of fuel charge is maximum at the beginning of operation of the engine when the weight of the charge is equal to the total weight of fuel, and decreases as the fuel burns out. The force of inertia is directed backward and strives to shift the charge in the direction of the nozzle. For absorption of this force, the charge must be fastened to the case of the engine or it must be neutralized by the forces of pressure of gases on the face of the fuel charge.

Gas forces act on the charge and elements of the chamber. Let us consider the load of a lateral burning charge, freely inserted in the combustion chamber and resting on the rear diaphragm, and the diagram of distribution of pressure of gases along the length of the charge (Fig. 18.23a). Pressure at the rear end of the charge p_2 due to losses in channel is less than pressure p_1 for the front end. If one were to not consider more comprehensively the compression of the charge, then in section II, the fuel charge is compressed by axial force $P_т$ due to pressure drop

$$P_т = (p_1 - p_2) F_з$$

where $F_з$ – end area of the charge.

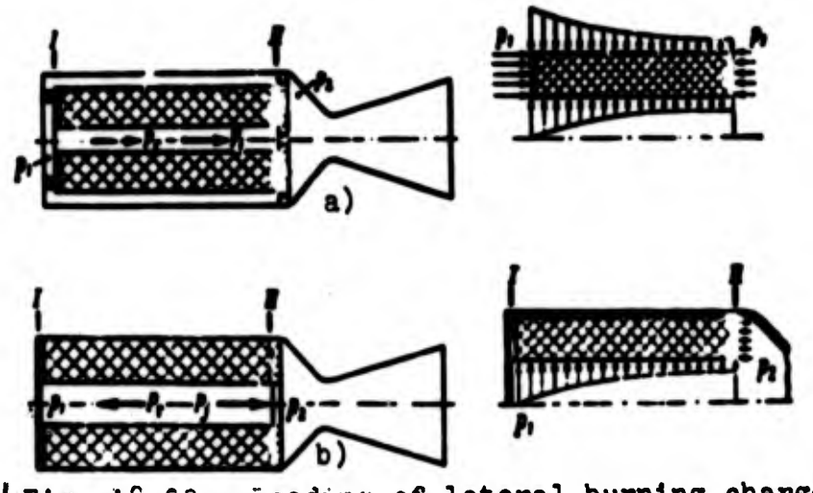

Fig. 18.23. Loading of lateral burning charges: a) freely inserted; b) bonded.

Force P_r acts on the rear diaphragm of the engine; it is maximum at the beginning of combustion of the charge when pressure drop and end area of charge are maximum.

Thus, the rear diaphragm absorbs force $P_д$, compressing the charge in section II and equal to the sum of the gas and inertial forces:

$$P_д=(p_1-p_2)F_1+P\frac{\omega_3}{\omega_д}.$$

This force is maximum at the beginning of combustion and decreases to zero at the conclusion of operation of engine.

The total action of axial and lateral compression of charge leads to buckling of the fuel in the channel. Maximum buckling of charge is at its rear end. Rubber-like mixture fuels have small elastic modulus, and for such fuels buckling can lead to considerable reduction in area of cross section of channel, especially at the moment of start. In so doing, pressure increases in the combustion chamber as compared to that calculated. With very great deformation of the charge, the initial increase of pressure in the combustion chamber leads to an increase in the combustion rate of fuel, increase of gas generation, and due to this - to further increase in pressure in the combustion chamber. In individual cases this process of increase in pressure can lead to destruction of the combustion chamber or explosion of the engine.

The possibility of narrowing of channel due to compression of the charge and increase of pressure in the combustion chamber must be considered during calculation on the strength of the charge and the combustion chamber. Measures to contend with bucklings of the charge are reinforcing of the charges or making the charges from separate lengthwise sections separated by rigid partitions attached to the case.

When the fuel charge is bonded to the walls of the combustion chamber and rests against the front face (Fig. 18.23b), then the force of gas pressure acts only on the rear face of the charge, pressing it

to the front face, and counteracts the force of inertia directed backward. The value of this force

$$P_{\text{п}} = p_{\text{п}} F_{\text{п}}$$

With identical end area compression of a charge of similar construction is greater than in the case of a freely inserted charge. It is possible to decrease the force compressing the charge, by using a construction in which the charge is poured into the combustion chamber so that it tightly adjoins both front and also rear faces.

A characteristic of load on the walls of RDTT chambers is the fact that during operation of the engine, part of load is absorbed and transmitted by the fuel charge. During burnout, the role of charge in transmission of forces gradually decreases. At the end of operation of the engine, the RDTT combustion chamber is loaded by forces of evenly distributed gas pressure, just as the chamber of a liquid propellant rocket engine. Determination of circumferential and axial linear loads in this case is produced by the formulas given in Chapter XIII.

The combustion chamber of an RDTT with inset charge is loaded varying along the length of the chamber and according to time of operation by gas pressure and axial force $P_{\text{п}}$ acting on the rear diaphragm. The calculation case for a combustion chamber with a bonded lateral burning charge is the end of operation of the engine when the case is loaded with pressure of gases in the combustion chamber.

In Fig. 18.24 diagrams are given of axial forces X, having effect on the wall of the chamber when using inset and bonded charges. Dot-dash lines show the diagrams of axial forces at the initial moment of operation of the engine under flight conditions; besides the gas forces, the force of inertia of the fuel charge is acting. Solid lines show the diagrams of axial forces appearing during operation on the test stand due to the action of the forces of gas pressure.

The dotted lines correspond to the loading of the engine at the end of combustion of the charge when the force of inertia of charge is equal to zero.

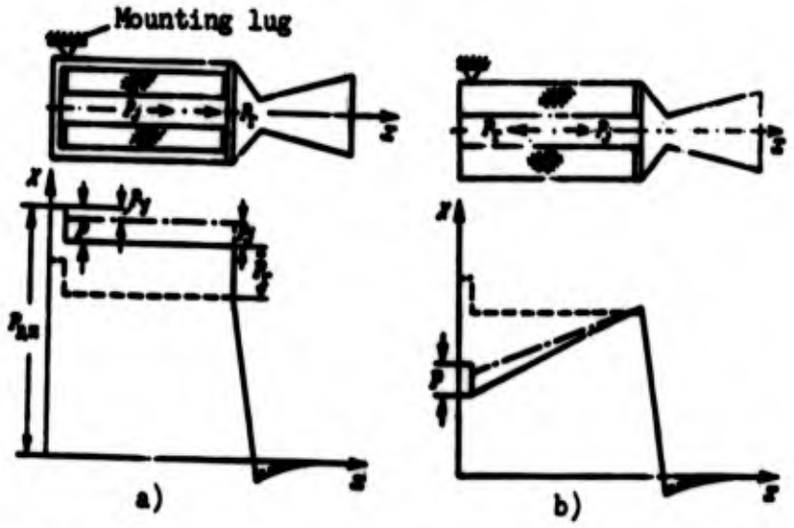

Fig. 18.24. Diagrams of axial forces: a) with open charge; b) with bonded charge.

Since all the mass of the fuel is enclosed inside the engine, at the time of its switch on and beginning of motion of the flight vehicle the thrust is balanced by forces of inertia of the fuel and the mass of the actual engine, and the mounting lugs of engine are loaded by the difference of these forces

$$P_y = P - P_j.$$

As the fuel burns out the forces of inertia of the charge decrease, and the loads transmitted to the mounting lugs are increased. At the end of combustion a force acts on the mounting lugs equal to the difference between thrust and the force of inertia of mass of the actual engine. During operation on the test stand, the mounting lugs are loaded by the full thrust of the RDTT

On the front face of the chamber of the engine axial force $P_{дн} = p_1 F$ act, where p_1 – pressure of gases at the face, F – area of cross section of the chamber. This force causes extension of the walls of the chamber on a section from the face to the mounting lug

of the engine. The right mounting lugs (see Fig. 18.24a) of the wall of the chamber are loaded by axial force $P_{\text{п}} = P_{\text{дн}} - P_{\text{у}} = p_1 F_1 - (P - P_1)$. The part of the wall lying by the right rear end of the charge is loaded by axial force appearing due to pressure of gases on the inlet and outlet part of the nozzle. Force $P_{\text{п}}$ causes additional extension of the walls of the case of the chamber, constant for an RDTT with open charge.

The approximate character of the loading of the walls and face of an engine with bonded charge is shown in Fig. 18.24b. The force of gas pressure on the rear face and the force of inertia of the charge being transmitted to the walls of the chamber through the adhesive joint evenly load the wall from a section corresponding to the rear of the charge to the front face. In the calculation case of loading of walls one should consider the end of combustion; the diagram of axial forces for this case is shown by a dotted line.

Maximum design pressure of gases in the combustion chamber can differ from that accepted in the thermodynamic calculation of pressure $p_{\text{к}}$. In the calculation on strength one should consider the possible increase of pressure in combustion chamber as compared to that calculated due to a number of factors. The number of such basic factors includes:

- deviation of temperature of the charge from the calculated, assumed, or measured initial temperature;

- deviation of actual throat area section of the nozzle from that calculated for obtaining a prescribed pressure in the chamber:

- deviation of form and dimensions of the charge from the calculated;

- deviation of the physical chemistry properties of fuel of different batches

– deviation in characteristics of the igniter from the calculated;

– static and dynamic errors in the automatic control system of the engine (if there is one).

Maximum design pressure in the combustion chamber can be determined by the formula

$$p_{max} = p_r \prod_{i=1}^{i=n} (1 + k_i), \qquad (18.1)$$

where p_r – design pressure of gases in the combustion chamber; Π – sign of the product; k_i – coefficient, considering the deviation of actual pressure from the calculated, induced by one of the above-mentioned factors.

For an unregulated RDTT, design pressure p_r is taken as equal to pressure of gases at highest possible temperature of fuel charge under operating conditions. In case of an adjustable RDTT, including having only prelaunch adjustment of the throat area, for calculation there is taken the nominal value of pressure during the program of adjustment, constructed according to the principle of maintaining constant pressure in the chamber, or maximum pressure, if program of adjustment provides for maintaining constant thrust.

It must be expected that scattering of pressures in the combustion chamber during action of the above-indicated factors will be greater for RDTT of jet missiles and less for aviation and rocket RDTT which have rigid tolerances on dimensions of the engine, its charge, and fuel combustion rate. For approximate calculations, when the effect of separate deflections in the properties of fuel, dimensions of the engine and charge, etc., on pressure in the combustion chamber is unknown, instead of determining design pressure by formula (18.1) it is possible to take $p_{max} = 1.4 p_r$ for RDTT jet missiles and $p_{max} = 1.2\ p_r$ for other RDTT. With such pressure there are determined circumferential and axial linear stresses P_y and P_x and there is performed the calculation on strength of the wall of the engine at average temperature at the end of heating. Average temperature of

the wall at the end of heating is determined by the method expounded in [17].

The safety factor for the wall of an RDTT chamber is estimated by yield point $k_т = \sigma_т/\sigma_i > 1.0 - 1.1$ where $\sigma_т$ – yield point of the material of the wall at its assigned average temperature; σ_i – intensity of stresses characterizing plane stress of the wall is determined by formula (13.10).

18.4. Adjustment and Control of RDTT

Basic problems of control of RDTT emanate from requirements of ballistics and control system of the flight vehicle among conditions of ensuring optimum conditions of flight there can be selected the law of change of thrust according to time of operation of the engine. In certain cases, the program of change of thrust can be designated and from other conditions, for example: limitation of overload and speed of flight, maintenance of prescribed coordinates of trajectory, capability of maneuver of a guided missile, surmounting the enemy's defense system, etc. Change of thrust or its direction become necessary to ensure stability, stabilization, or orientation of the flight vehicle. For these purposes during operation of an RDTT there must be ensured:

- change of thrust in time according to a prescribed program;

- elimination of deviation of thrust from a prescribed value;

- control of thrust vector in direction.

Fulfillment of the first problem is carried out either only by adjusting the engine or by adjustment and subsequent control in the process of operation. The second and third problems are solved only with the help of control systems.

The simplest method of ensuring flow of thrust in time according to a prescribed program is by adjustment of the engine. Adjustment consists of a wide complex of structural, finishing, technological and

operational measures, which in full volume or partially (depending upon the special purpose of the engine and tactical technical requirements) are performed on each engine, independently of whether the engine has an automatic control system or not, and consists of a single process from the designing of the engine up to its operation, including storage of the engine and the period directly prior to use.

Included in the number of basic structural and finishing measures undertaken for adjusting the engine are profiling of the charge, correction of the shape of the charge, finishing of the igniter and the nozzle block.

Profiling of the charge is included in selection of its basic geometric dimensions ensuring the change of combustion surface according to time of operation. In accordance with the accepted law of change of thrust in time, i.e., program of control, and the calculation assumed as the basis of programs of change of other parameters of the engine, for example, pressure in the combustion chamber, throat area, etc., one can determine change of surface combustion according to time and then so to select the form of charge in order to satisfy the selected law $F_{гор}=F_{гор}(\tau)$, where $F_{гор}$ – surface area of combustion, τ – time of engine operation. To the basis of calculation there are also added the assumed characteristics of igniter, and consequently also the defined law of outlet of the engine in operation.

In process of test stand and flight tests, in a number of cases, there may be revealed separate deviations from the assumed program of thrust by virtue of the action of unforeseen factors. With certain forms of charge, the most simple method of dealing with the indicated deviations is to correct the shape of the charge. In the correction, the current combustion surface in specified moments of operation of the engine is increased or decreased. Therefore, it is desirable to employ such forms of charges as will allow, changing only the initial form of the charge to exert an effect in the needed direction on the

law $F_{пор} = F_{пор}(t)$. As an example of such form of charge it is possible to point out the tubular grain with grooves. Such a charge can have the combustion surface on the ends, the sides, and on the outside of its slotted part. Changing the depth and width of the grooves and the thickness of the combustion arch in separate sections of the slotted part, it is possible to very effectively change the law of combustion without changing the overall pulse and weight of the charge.

In those cases when noticeable deviations from the program of control have their causes in uncalculated characteristics of the igniter or nozzle, there is performed their finishing. Finishing of the igniter can consist in changing the size of the igniter charge, its location, and sometimes by transition to another type of igniter. Finishing of the igniter permits correcting basically the initial section of engine performance.

During operation of the engine, due to temperature expansion, burning out of material or heat-insulating covering of nozzle, and in certain cases, due to precipitation of metal oxides on its surface (when burning fuels containing metallic additives) the engine performance can deviate from the calculation. For adjusting the engine, finishing of the nozzle is required which can consist in selection of another initial value of throat area, changing the nozzle material, the heat-insulating covering, the form of nozzle, thickness of protective coatings, the method of their application, etc.

In process of finishing, in most cases certain technological requirements are revealed. There are determined possible fields of tolerances on dimensions of the charge, combustion chamber, igniter, nozzle, diaphragms, etc. Determination is made of the influence of fuel composition and its structure on the combustion rate of the charge, and the mechanical properties of the fuel – on possible narrowing of the channel and erosional burning out. As a result of investigations technical requirements are produced for accuracy in manufacture of different elements of the engine and specifications of the fuel. Also standard methods of control of parameters can be produced.

After termination of these stages it is possible to speak about the fact that engine is built according to an assigned program, i.e., with specified probability there is maintained in a defined field of allowances a designated program, if all dimensions of the engine and its charge, and also the physical chemical properties of the fuel lie within limits of established probable deviations.

In period of operating the engine, appropriate measures have to be taken so that adjustment of the engine does not change. Such measures can be, for example, specified condition of storage and transportation. Storage should, in a number of cases, be such that the temperature of the charge will remain practically constant, or its variation will not exceed specified limits. If no provision is made for maintenance of rated temperature, then it is possible to carry out an additional adjustment operation before starting – installing on the engine a changeable nozzle corresponding to the temperature of the charge, or adjustment of the throat area having a central body.

Transportation of charge in violation of the rules can lead to the appearance of cracks in the charge or to other impermissible defects.

The initial concept of an RDTT as the simplest propulsion system, easy to control and adjust, has undergone considerable changes both because of expansion of the sphere of application of the RDTT, and also because of more rigid requirements for stability of thrust, which outstrip the progress in development of solid fuels with minimum deviations from the standard law of combustion. Application solely of adjustment does not solve for many types of flight vehicles all their problems of control. This pertains, in the first place, to elimination of probable deviations in thrust, and also to cases when the program of change of thrust according to time provides for control according to a defined law of some parameter of the engine. Such problems can be solved only by the presence of a control system. It is obvious that an automatic regulator which is, like the engine, a link in the control system, will be subject to adjustment analogous to the adjustment of the engine.

At present, the problem of automatic control of an RDTT has been developed to a considerably lesser degree than the problem of automatic control of the liquid-propellant rocket engine. This is explained by the relative novelty of the problem and the difficulties of controlling combustion of a solid fuel.

It is possible to distinguish the following basic regions of automatic control systems. Automatic control systems, according to principle of action, are subdivided into control systems by intra-engine parameters and by external conditions.

Control systems by intraengine parameters are autonomous, i.e., are not connected directly with the flight vehicle. Their program of operation is the initial one for ballistic design. Exact maintenance by a control system of an assigned program conditions the accuracy (taking into account possible scattering of parameters of aircraft) flight trajectory.

The most studied control systems by intraengine parameters are systems of pressure stabilization in the combustion chamber.

In a system of pressure stabilization, the variable value is pressure in the combustion chamber. The regulating factor – usually throat area $F_{кр}$. Consequently, the actuating element of the control system must exert influence on $F_{кр}$. Pressure in the combustion chamber and throat area are connected by a simple dependence: increasing $F_{кр}$ leads to a decrease of pressure $p_к$, and conversely.

The simplest system of controlling pressure in the combustion chamber is the above-described self-controlled nozzle. To decrease statism, systems of indirect control are used with isodromic feedback. Such systems, according to the method of influence on $F_{кр}$ are subdivided into mechanical and hydro- or gas-dynamic.

Mechanical systems for control of throat area have actuators with axial shift or rotation. It is possible to change $F_{кр}$ by means of axial shift of the central body or the external shell of the nozzle.

Rotating actuators consist of valve devices, varying during rotation of section of the holes in a diaphragm located in the narrowing of the nozzle. Mechanical control systems have an inherent common deficiency - low reliability during operation under conditions of high temperatures and gas erosion.

Hydro- and gas-dynamic systems for control of $F_{кр}$ do not have moving parts located in the gas flow in the nozzle. Their principle of action is based on introduction into the nozzle near the critical section through annular slots or row of holes of certain quantities of gas or liquid. In so doing there occurs compression of the basic flow of gases, and in the critical section, which is equivalent to decreasing its effective area. By changing the quantity of liquid or gas being introduced, it is possible to regulate the effective area of critical section of the nozzle without changing its geometry. It must be noted that with such method of control it is possible to reliably protect the critical section of nozzle against burning out. Gases for inlet to the critical section can be drawn off directly from the combustion chamber, which does not require expenditures of the working substance on controlling the engine. With hydrodynamic control connected with additional consumption of the working substance, it is possible to use a chemically active liquid which enters into reaction with gases in the divergent section of the nozzle.

The basic deficiency of the gas- and hydrodynamic method is the limited range of change of $F_{кр}$, which is conditioned by the expediency of putting in the nozzle only relatively small quantities of working substance, on the order of 1-2% of the gas consumption.

Systems of control by external conditions are closed. They include the flight vehicle as the object of control and the engine and regulator as links in the system. As a variable value for such a system there is taken the parameter determining to the greatest degree the program of flight of the flight vehicle. Most frequently the variable value selected is acceleration of the flight vehicle j. As regulating factor then there is used thrust P of the engine. The thrust regulator included in the system is adjusted according to a prescribed program $j=j(\tau)$ If, at a certain instant there occurs a

deviation from the given value of acceleration, the regulator will pass a signal to the actuating mechanism of the engine, which should lead to a corresponding change of thrust. The effect of the regulator is terminated after elimination of the deviation of acceleration from that assigned by tne program. Thus, the engine as a link of control system has an inlet coordinate of thrust P. The inlet influence on the engine depends on the method accepted for change of thrust, connected with process of outflow of gases or with a process of gas generation.

The simplest example of use of influence on the process of outflow is control by means of gas-bleeding device (Fig. 18.25). The gas-bleeding device consists of a row of holes symmetrically located behind the critical section of the nozzle. Area of the drain holes can be changed. Closing or opening of the holes is not accompanied by change of parameters of the gas in the combustion chamber of the engine, but only quantity of gases passing from the nozzle in an axial direction is changed. Symmetric tapping of gas from the nozzle through holes in a radial direction does not create thrust or its lateral component. In such a system there is possible asymmetric lateral tap of gases, which will make it possible to obtain a lateral component of thrust and to use it for controlling the flight vehicle. Questions, connected with the calculation of gas-bleeding devices, are expounded in detail in [38]. A deficiency of a similar control system is loss of total impulse.

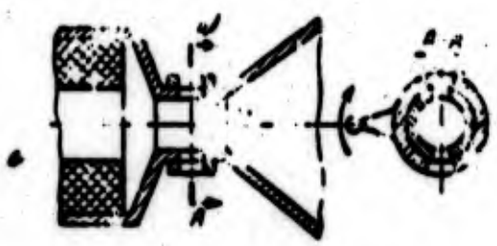

Fig. 18.25. Diagram of a gas-bleeding device.

Systems which have an effect on the process of gas generation are somewhat complicated. One such system – with control of pressure in the combustion chamber – was examined above. The thrust regulator exerts influence on the throat area, there are changes of pressure in the combustion chamber, combustion rate of the fuel and, in final analysis, thrust of the engine. This system has the above-indicated inherent deficiencies of systems with mechanical or hydro- and gas-dynamic effect on throat area.

It is relatively simple to exert influence on the process of gas generation in a solid propellant hybrid engine (see Figs. 5.17, 5.18 and 18.26). The charge of the engine (Fig. 18.26) consists of two grains: of fuel enriched by combustible 1 and of oxidizer 3. Each grain is enclosed in its own combustion chamber, between which is set regulating valve 2. At starting of the engine at first grain 1 ignites. Products of incomplete combustion, enter the combustion chamber through valve 2 with the grain from the oxidizer, where their combustion occurs. Thrust control is carried out by means of valve 2. Closing the valve, for example, leads to an increase of pressure in the chamber with the grain enriched by the combustible; gas generation is increased and more gas enters the chamber with the oxidizer, where there is increased pressure and temperature, the flow rate of gases grows, which leads to augmentation of engine thrust; it is possible, conversely, to decrease thrust by opening the valve. According to some data [38] it is possible to obtain considerable range of change of thrust without essential lowering of unit pulse (for example, threefold change of thrust with average unit pulse equal to 93% of maximum computed value).

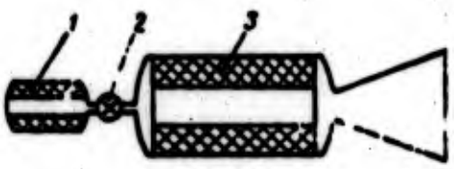

Fig. 18.26. Diagram of a hybrid engine: 1 – grain enriched by combustible; 2 – regulating valve; 3 – oxidizer.

The necessity of having two chambers can be considered a deficiency of such a diagram. The reliability of the regulating valve is low, but in view of the relatively low temperature of gases going through it – not less than for a nozzle with adjustable throat section.

Most widely developed are the methods of controlling thrust vector, for which, besides swiveling nozzles described earlier, there are used mechanical and gas-dynamic deflection of the jet and creation of artificial trim of thrust in a multinozzle installation.

Mechanical deflection of the jet is attained by placing laminar or annular gas vanes in the gas flow. The laminar vanes are always in the flow of gases and cause great drag losses, which leads to an essential loss of pulse. The material of the vanes burns intensively during the flow of gases around them. The erosion of the vanes promotes the possible content of solid particles in the products of combustion.

To a considerable degree, annular jet vanes consisting of cylindrical caps rotated around a lateral axis are free from these deficiencies. At a signal from the control system, a servomechanism turns the vane and introduces it into the flow, deflecting the stream of gases emanating from the nozzle. In the absence of a control signal, the annular vane is not subjected to the action of hot gases and does not cause additional drag. For controlling thrust vector in two planes there can be used an annular vane fastened by hinges to four symmetrically located rods of servomotors which are controlled separately.

Gas-dynamic deflection of the jet is possible by means of tapping the gas or evaporating liquid in the supersonic part of the nozzle (Fig. 18.27). The introduced working substance deflects the gas flow by means of formation in the nozzle of an oblique shock wave, behind which is disposed a region of increased pressure encompassing a certain sector of the internal surface of the nozzle [38]. Usually,

four feeders evenly located around the circumference are used. In so doing this lateral force appears due to the difference of pressure on diametrically opposite sections of the internal surface of the nozzle. If gas is used as the working substance, it is possible to take it from the combustion chamber. As a working fluid it is possible to use freon, nitric acid, or liquid nitrogen. The quantity of working substance passed to each sector of the nozzle can be regulated.

Fig. 18.27. Gas-dynamic deflection of the jet.

(Graphic not Reproducible)

Artificial trim of multinozzle propulsion system is created by choking of one or a pair of symmetrically located nozzles. For choking there are used moving central bodies. Such devices are examined in detail in [38]. An advantage of such a system is the possibility of doing without additional regulating devices, inasmuch as for deflection of thrust vector, the same elements of construction are used as for control of the engine. A disadvantage lies in the necessity of installation of the nozzles at a certain angle to the axis of the engine, which causes constant losses of thrust.

BIBLIOGRAPHY

1. Avduyevskiy V. S. Danilov Yu. I., Osiovy teploperedachi v aviatsionnoy i raketnoy tekhnike (Fundamentals of heat transfer in aviation and rocket technology) Oborongiz, 1960.

2. Ayzerman M. A., Lektsii po teorii avtomaticheskogo regulirovaniya (Lectures on the theory of automatic control), Fizmatgiz, 1958.

3. Alemasov V. Ye., Teoriya raketnykh dvigateley (Theory of rocket engines), Oborongiz, 1962.

4. Barrer M. et al. Raketnyye dvigateli (Rocket engines), Oborongiz 1962.

5. Barrer M. et al., Dvizheniye raket (Rocket motion), IL, 1959.

6. Bassard R. De Lauer R., Raketa s atomnym dvigatelem (A rocket with an atomic engine) IL, 1959.

7. Beledzh, Zhidkostnyye reaktnvnyye dvigateli dlya perspektivnykh raket-nositeley (Liquid propellant jet engines for future launching rockets) VRD, 1965, No. 2.

8. Blokh Z. Sh., Perekhodnyye protsessy v lineynykh sistemakh avtomatiche skogo regulirovaniya (Transition processes in linear automatic control systems), Fizmatgiz, 1961.

9. Breslavskiy O. Ye.. Sobstvennyye kolebaniya krugovoy tsilindricheskoy obolochki, nakhodyashcheysya pod deystviyem gidrostaticheskogo davleniya (Natural vibrations of a circular cylindrical shell under the impact of hydrostatic pressure), Izvestiya AN SSSR, OTN, 1956, No. 12.

10. Bodner V. A., Avtomatika aviatsionnykh dvigateley (Automatics of aircraft engines). Oborongiz, 1956.

11. Vandenkerkkhove Zh., Erozionnoye goreniye kolloidal'nykh topliv (Erosional combustion of colloidal fuels), VRT, 1959, No. 3.

12. Vandenkerkkhove Zh., Posledniye dostizheniya v konstruirovanii shashek tverdogo raketnogo topliva (Latest achievements in designing grains of solid rocket propellant), VRT, 1960, No. 2.

13. Shevyakov A. A., Avtomatika aviatsionnykh i raketnykh silovykh ustanovok (Automatics of aviation and rocket propulsion systems), izd-vo "Mashinostroyeniye", 1965.

14. Gleston S. i Edlund M., Osnovy teorii yadernykh reaktorov (Fundamentals of theory of nuclear reactors) IL, 1954.

15. Gurov A. F., Raschety na prochnost' i kolebaniya v rakegnykh dvigatelyakh (Calculations of strength and vibrations of rocket engines) Izd. "Mashinostroyeniye", 1966.

16. Zhidkiye i tverdyye raketnyye topliva (Liquid and solid rocket propellants). Collection perevodov, IL, 1954.

17. Zarubin V. S., Temperaturnyye polya v konstruktsii letatel'nykh apparatov (Temperature fields in flight vehicle structures), izd. "Mashinostroyeniye", 1966.

18. Zel'dovich Ya. B. et al., Impul's reaktivnoy sily porokhovykh raket (Pulse jet solid propellant rocket propulsion systems), Oborongiz, 1963.

19. Issledovaniye raketnykh dvigateley na zhidkom toplive (Study of liquid propellant rocket engines), Collection perevodov, Izd. [Mir], 1964.

20. Issledovaniye raketnykh dvigateley na tverdom toplive (Study of solid propellant rocket engines), Collection perevodov, IL, 1963.

21. Kvasnikov A. V., Teoriya zhidkostnykh raketnykh dvigateley (Theory of liquid propellant rocket engines) Sudpromgiz 1959.

22. Kligel' I. Ya. Techeniye smesi gaza s chastitsami v sople (Flow of a mixture of gas with particles in a nozzle) VRT, 1965, No. 10.

23. Kokichev A. I., Uplotnyayutsiye ustroystva v mashinostroyenii (Sealing devices in machine building), Mashgiz, 1962.

24. Krasovskiy A. A., Pospelo, G. S. Osnovy avtomatiki i tekhnicheskoy kibernetiki (Fundamentals of automatics and technical cybernetics), Gosznergoizdat, 1962.

25. Kutateladze S. S. Osnovy ucheniya o teploobmene (Fundamentals of teaching heat exchange). Mashgiz, 1962.

26. Kutateladze S. S., Borishanskiy V. M. Spravochnik po teploperedache, (Handbook on heat exchange), Gosznergoizdat, 1958.

27. Krokko L., Chzhen-Sin'-I. Teoriya neustoychivogo goreniya v zhidkostnykh raketnykh dvigatelyakh (Theory of unstable combustion in liquid propellant rocket engines), IL, 1958.

28. Lomakin A. A., Tsentrobezhnyye i propellernyye nasosy (Rotary and propeller pumps), Mashgiz, 1950.

29. Mel'kumov . M. et al., Teoriya zhidkostno-reaktivnykh dvigateley (Theory of liquid-jet engines). Izd. VVIA, 1956.

30. Melik-Pashayev N. I., Vodorodnyye ZhRD (Hydrogen ZhRD), "Aviatsiya i kosmo navtika", 1965, No.

31. Melik-Pashayev N. I., Raschet konvektivnogo teploobmena pri sverkhkriticheskom davlenii (Designing a convection heat exchange with supercritical pressure), "Teplofizika vysokikh temperatur". 1966, No. 6.

32. Moshkin Ye. K., Dinamicheskiye protsessy v ZhRD (Dynamic processes in ZhRD), izd vo "Mashino stroyeniye", 1965.

33. Merrey R., Fizika yadernykh reaktorov (Physics of nuclear reactors), Atomizdat, 1959.

34. Merfi i Osborn, Issledovaniye prodol'noy neustoychivosti v kamerakh sgoraniya raketnykh dvigateley (Study of longitudinal instability in combustion chambers of rocket engines) VRT, 1966, No. 2.

35. Nakhbar V., Grin L., Analiz [word missing] tsennoy modeli rezonansnogogo reniya tverdogo topliva (Analysis of a [word missing] model of resonance combustion of solid fuel), VRT, 1960, No. 3.

36. Neymark Yu. I., Ob opredelennon znacheniy parametrov, pri kotorykh sistema avtomaticheskogo regulirovgniya ustoychiva (Determining values of parameters with which an automatic control system is stable), "Avtomatika i telemekhanika", 1948, No. 3.

37. Ovsyannikov B. V., Teoriya i raschet nasosov ZhRD (Theory and design of ZhRD pumps), Oborongiz, 1960.

38. Orlov B. V., Mazing G. Yu., Termodinamicheskiye i ballisticheskive osnovy proyektirovaniya raketnykh dvigateley na tverdom toplive (Thermodynamic and ballistic fundamentals of design of rocket engines operating on a solid propellant), izd-vo "Mashinostroyeniye", 1964.

39. Paushkin Ya. M., Khimicheskiy sostav i svoystva reaktivnyk topliv (Chemical composition and properties of jet fuels). AN SSSR, 1962.

40. Petrov P. A., Yadernyye energeticheskiye ustanovki (Nuclear power plants), Gosenergoizdat, 1958.

41. Pirs. Nekotoryye metody regulirovaniya tyagi raketnykh dvigateley na tverdom toplive (Some methods of thrust control of rocket engines operating on solid fuel), VRT, 1962, No. 6.

42. Pugachev V. S., Teoriya sluchaynykh funktsiy i yeye primeneniye k zadacham avtomaticheskogo upravleniya (Theory of random functions and its application to problems of automatic control), Fizmatgiz, 1962.

43. Reznikov M. Ye., Abiatsionnyye i raketnyye topliva i smazochnyye materialy (Aviation and rocket fuels and lubricating materials), Voyenizdat, 1960.

44. Satton D., Raketnyye dvigateli (Rocket engines), IL, 1952.

45. Serebryakov M. Ye., Vnutrennyaya ballistika stvol'nykh sistem i porokhovykh raket (Internal ballistics of tubular systems and solid propellant rockets), Oborongiz, 1962.

46. Silant'yev A. I., Tverdyye raketnyye topliva (Rocket solid propellants), Voyenizdat, 1964.

47. Sinyarev G. B., Dobrovol'skiy M. V., Zhidkostnyye raketnyye dvigateli (Liquid propellant rocket engines), Oborongiz, 1957.

48. Stefenson R., Vvedeniye v yadernuyu tekhniku (Introduction to nuclear engineering), IL, 1956.

49. Turbulentnyye techeniya i teploperedacha (Turbulent flows and heat transfer), Collection edited by Lin' Tszya-Tszyao, IL, 1963.

50. Uimpress R., Vnutrennyaya ballistika porokhovykh raket (Internal ballistics of solid propellant rockets), IL, 1952.

51. Uayett O., Kharakteristiki raket s atomnym dvigatelem (Characteristics of rockets with an atomic engine), VRG, 1960, No. 6.

52. Feodos'yev V. I., Sinyarev G. B., Vvedeniye v raketnuyu tekhniku (Introduction to rocket technology), Oborongiz, 1960.

53. Feodos'yev V. I., Prochnost' teplonapryazhennykh uzlov zhidkostnykh raketnykh dvigateley (Strength of thermal stressed subassemblies of liquid propellant rocket engines), Oborongiz, 1965.

54. Khart, Makklyur. Neustoychivost' goreniya, vzaimodeystviya akusticheskikh voln s poverkhnost'yu goreniya tverdogo raketnogo topliva (Combustion instability; interaction of acoustic waves with the combustion surface of a solid rocket fuel), VRT, 1960, No. 2.

55. Khendriks et al. Sootnosheniye dlya koeffitsiyenta teplootdachi k vodorodu pri kipenii i pri sverkhkriticheskom davlenii (A ratio for coefficient of heat transfer to hydrogen during boiling and at supercritical pressure). "Raketnaya tekhnika", 1962, No. 2.

56. Tsukrov M., Osborn I., Eksperimental'noye issledovaniye vysokochastotnogo vibratsionnogo goreniya (Experimental investigation of high-frequency vibration combustion), VRT, 1959, No. 4.

57. Chinayev P. I., Mnogokonturnyye sistemy (Multicircuit systems), Izv. AN USSR, 1961.

58. Shaulov Yu. Kh. i Lerner M. O., Goreniye v zhidkostnykh raketnykh dvigatelyakh (Combustion in liquid propellant rocket engines), Oborongiz, 1961.

59. Bartz D. R., Jet Propulsion, 1957, No. 1.

60. McCormick, Space Aeronautics, 1963, No. 3.

DATA HANDLING PAGE

01-ACCESSION NO.	02-DOCUMENT LOC	20-TOPIC TAGS
TM9501901		solid rocket engine, rocket engine control system, rocket engine cooling, liquid rocket fuel, combustion chamber, nuclear propulsion, chemical propulsion, nozzle flow, thermodynamic calculation, combustion rate

03-TITLE	47-SUBJECT AREA
ROCKET ENGINES -U-	01, 18, 21, 20

42-AUTHOR CO-AUTHORS	10-DATE OF INFO
MEL'KUMOV, T. M. ; 16-MELIK-PASHAYEV, N. I. 16-CHISTYAKOV, P. G. ; 16-SHIUKOV, A. G.	-----68

43-SOURCE	09-DOCUMENT NO.
RAKETNYYE DVIGATELI, MOSCOW IZD-VO MASHINOSTROYENIYE (RUSSIAN)	FTD-MT-24-290-69
	08-PROJECT NO. 60401

63-SECURITY AND DOWNGRADING INFORMATION	64-CONTROL MARKINGS	65-HEADER CLASN
UNCL. 0	NONE	UNCL

76-REEL/FRAME NO.	77-SUPERSEDES	78-CHANGES	40-GEOGRAPHICAL AREA	NO. OF PAGES
1890 1663			UR	620

CONTRACT NO.	X REF ACC. NO.	PUBLISHING DATE	TYPE PRODUCT	REVISION FREQ
	65-	94-	TRANSLATION	NONE

STEP NO.
02-UR/0000/68/000/000/0001/0511

ABSTRACT

(U) The book discusses fundamental problems in the theory and construction of liquid and solid rocket engines. Problems pertaining to the strength of liquid rocket engines [LRE] and solid rocket engines [SRE] are discussed; guidance and automatic control systems of rocket engines [RE] are analyzed, and types of process instability appearing in rocket engines are considered. Material published in the foreign and Soviet literature is used as a basis for information given on RE designs, fuels, cooling systems, turbupump units, gas generators, and applications of nuclear energy in rocket engines. The book is designed for engineers working in the aviation industry and students and graduate students attending higher aviation educational institutions. Orig. art. has: 30 tables, 307 illustrations, and 61 bibliographic references.

CORRECTED COPY

FTD-MT- 24-290-69

EDITED MACHINE TRANSLATION

ROCKET ENGINES

By: T. M. Mel'kumov, N. I. Melik-Pashayev,
P. G. Chistyakov and A. G. Shiukov

English pages: Cover to 620

SOURCE: Raketnyye Dvigateli. 1968, pp. 1-511.

This document is a Mark II machine aided translation post-edited for technical accuracy by:
Charles T. Ostertag and Francis T. Russell.

Insert: Chapters I-VI, pages 1-158, FTD-HT-23-1531-68.

PREPARED BY:

TRANSLATION DIVISION
FOREIGN TECHNOLOGY DIVISION
WP-AFB, OHIO.

FTD-MT- 24-290-69

Date 5 Dec 1969